上海市医学真菌分子生物学重点实验室建设总结报告

上海市医学真菌分子生物学重点实验室

Shanghai Key Laboratory of Molecular Medical Mycology

2018年12月

院士致辞

回顾一年来上海市医学真菌分子生物学重点实验室的工作，我们在论文发表、科研项目、人才梯队建设、国内外合作交流、运行管理等方面都取得了不错的成绩。实验室瞄准国家“一带一路”、“军民融合”等重大战略和议题，关注国际学术前沿，紧密结合人民卫生健康的需要，在全球真菌病的流行病学、临床真菌病的早期诊断、医学真菌系统进化与菌种保藏研究、重要病原真菌与宿主相互作用等多方面稳步推进。在承接国家重大课题方面，我们承担了国家传染病重大专项《“海上丝绸之路”重要病原体的威胁感知和监测预警》以及工程院咨询项目《我国及“一带一路”沿线国家真菌病联合防控策略研究》，旨在阐明“海上丝绸之路”沿线重要真菌病，尤其是“超级真菌”的流行情况，揭示相关海域真菌生物多样性组成，建立适用于当地卫生条件的诊断方法，并为我国“一带一路”沿线相关性真菌病输入性感染提供理论依据和防控策略。同时我们的国自然重大国际合作课题《中国人群高发的难治性暗色真菌感染的生态学和进化起源研究》正在顺利推进，发表了一系列的成果。

逐渐形成了一支以院士以及领军人才作为优秀学科带头人的研究队伍，凝聚了一批具有发展潜力的中青年学术人才。不仅与国内外一流研究机构开展了高效务实的合作交流，而且利用我国在真菌领域的科研优势，逐步影响、提高“一带一路”沿线国家真菌病防控能力。与国内外多家单位联合，建立多个院士工作站和长期合作点，实行优势互补、资源共享，加强研究项目，建立公共研发平台，为包括延安、哈尔滨、邯郸、南昌、杭州、广州、苏州等在内的全国广大学者提供研究场地。

在海军首长、上海市科委、大学领导、医院领导的关心和支持下，以及实验室全体成员的不懈努力下，我们的2018收获满满。同时，我们又将站在以实现自身跨越为目标的新起点，抓住现有的发展契机，发挥自身科研优势，力争在医学真菌学前沿的探索中取得更多系统性原创成果，圆满完成各项科研、临床和政治任务。

在生命科学和生物技术快速发展的新形势下，机遇与挑战并存，实验室的发展建设任重道远，愿团队人员弘扬“探索、奉献、包容、进取”的精神，为理想，追求不断、矢志不渝；为事业，百折不挠、坚韧不拔的态度，扎实工作、团结合作，潜心科研，一起推动实验室各项工作迈向新的台阶！

中国工程院院士

2018年12月21日

参与年报编写的人员名单

总策划：

廖万清

执行编辑：

潘炜华

主要编写人员：

方文捷、杜明威

参与编写人员：

姜伟伟、扈东营、邓宇晨、张蕾、张克明、

洪南、刘伊诺、李　航、朱信霖、陈丽琳

目录

一、实验室基本情况

上海市医学真菌分子生物学重点实验室简介

上海市医学真菌分子生物学重点实验室项目2010年5月经上海市科委批准立项依托上海长征医院建设，2年来共投入建设经费约400万元，2012年12月通过上海市科委检查验收，并于2014年和2016年两次通过实验室评估，获上海市科委滚动支持。现任实验室主任为中国工程院院士廖万清，学术委员会主任为中国工程院院士陈洪铎。

本实验室依托海军军医大学皮肤病与真菌病研究所和长征医院皮肤科建设，在医学真菌学基础与临床研究方面基础深厚。40多年来，廖万清院士领衔的学术团队主要从事隐球菌及隐球菌病的研究，创建了我国第一个隐球菌专业实验室，对隐球菌的分类及系统进化、毒力因子及其调控机制、与宿主相互作用及临床治疗方案等领域的进行了系统、深入的研究，部分研究成果达国际先进水平。

目前，在上海市科委及长征医院各级领导的关心、指导下，实验室整体建设呈现出快速发展的强劲趋势，拥有团结协作、充满生机的工作氛围和浓郁踏实的学术风气，以研究项目为牵引，与美国杜克大学、霍普金斯医学院、NIH、荷兰CBS真菌多态性研究中心等国际著名医学真菌研究机构开展了多个务实高效的国际合作研究，产生的一批如隐球菌毒力调控的分子机制研究、亚洲范围内新生隐球菌临床株特定基因型与耐药趋势的关系、暗色真菌系统进化研究、病原真菌药物敏感性流行病学调查等重要研究成果，在国内外医学真菌学研究领域产生了较大影响。近几年，实验室各项目组成员在New England Journal of Medicine、Clinical Infectious Disease、Frontiers in Immunology、Plos Neglected Tropical Diseases、Journal of Antimicrobial Chemotherapy、Antimicrobial Agents and Chemotherapy、Emerging Microbes & Infections等相关领域顶级期刊发表多篇文章。

实验室拥有中国工程院院士1人，博士生导师4人，硕士生导师2人，固定研究人员28人，汇聚了包括从荷兰皇家科学院、意大利米兰大学、美国杜克大学、霍普金斯医学院、NIH、加州大学等归国中青年学术骨干，学科背景优势互补、科研思路活跃，已基本形成具有一支国际水平、以中青年研究骨干为主体的学术团队。

实验室主要研究方向为重要病原真菌的毒力及其与宿主相互作用、分子流病及系统发育、

我国病原真菌菌株保藏、耐药趋势监测及分子鉴定等。具有国际水平的以基因枪、MALDI-TOF MS，实时荧光定量 PCR 等仪器为核心的病原真菌基因组学研究技术平台完全能够胜任真菌培养、细胞分离培养、临床样本收集、分子生物学操作等研究工作。目前，实验室承担了多项省部级课题，现有科研经费达 2234.18 万元。

实验室秉承“开放、流动、联合、竞争”的运行机制，依托上海长征医院皮肤科和隐球菌专业实验室的临床和科研优势，加强与国内外科研机构的交流合作，通过实验室门户网站 www.shmedmyco.com 向社会公开招标。

实验室自成立到现在，已经逐步走向正轨。为了记录实验室的发展历程，更好的弘扬实验室文化，延续既往优良传统，我们编辑了这本 2018 年实验室年报，以记载实验室年度教学科研及学科人才建设情况，同时也为后人留下实验室可以查阅的历史资料。

实验室的发展和成长，离不开校院党委、上海市科委及卫计委各级领导对我们的关心和帮助，也凝聚着实验室每个成员的心血和汗水。在此我向曾经为实验室建设与发展做出贡献的所有人表示衷心的感谢！

实验室基本信息

实验室中文名称：上海市医学真菌分子生物学重点实验室

实验室英文名称：Shanghai Key Laboratory of Molecular Medical Mycology

门户网站：www.shmedmyco.com

微信公众号：上海医学真菌分子生物重点实验室

依托单位：上海长征医院

实验室主任：廖万清

实验室学术委员会主任：陈洪铎

现有固定人员 32 名，其中中国工程院院士 1 人、高级职称 4 人，中级职称 9 人，技术员 4 人，编辑 3 人，护士 5 名等。在读博士研究生 3 人、硕士研究生 10 人。

实验室现拥有细胞培养室、DNA 提取室、真菌培养室等实验场所，用于完成真菌的分子生物学鉴定、真菌功能基因组学、真菌与宿主相互作用等研究。配备莱卡荧光显微镜、高压气体基因枪、实时荧光定量 PCR 仪、核酸蛋白测定仪、冷冻干燥机、凝胶成像系统、全自动酶标仪等仪器设备。实验室规章制度健全，管理规范，运行有序，具备承担国家重大科研任务和开放研究平台的科技支撑条件。

研究方向和内容

为满足我国医学真菌领域临床实践和基础研究的需要，实验室研究方向主要分为一下三个方向：

（一） 重要病原真菌与宿主细胞的相互作用；

瞄准致病真菌与宿主相互作用这一前沿研究领域，开展针对真菌功能基因组学和宿主抵御真菌侵袭的分子与细胞机制研究，阐明各种医学真菌致病机制，为未来临床诊治寻找合适靶点。目前，实验室的研究重点是新型隐球菌毒力调控的分子与细胞机制研究和重要致病真菌逃逸宿主免疫的机制及信号通路研究。该研究方向目前已获国家重点基础研究发展计划（“973”计划）《重要侵袭性致病真菌与宿主相互作用的分子与细胞机制研究》的支持和多项自然基金重点、面上、青年项目支持。

（二） 临床真菌病分子生物学早期快速诊断；

依托围绕目前临床真菌病患者诊治需要，将分子生物学方法用于临床真菌病诊断，做到真菌病的早诊早治。实验室研究人员通过研发真菌特异性抗体和新型分子生物学诊断方法，努力提高真菌病患者早期诊断的敏感性和特异性。同时，收集临床真菌菌株建成菌种库，为后续科学研究做基础。该研究方向目前已获国家卫生部科技重大专项课题《侵袭性真菌感染现代早期诊断技术体系的研究》、《海上丝绸之路沿线真菌病防控》等重大课题的支持。

（三） 医学真菌系统进化与菌种保藏研究

针对目前全国范围内收集的医学真菌临床菌株和环境菌株进行系统进化学研究，将其与国外流行地区分离菌株和标准菌株对比，初步探讨我国不同地区真菌流行趋势和原因，并探索真菌基因分型与抗真菌药物敏感性之间的关系。实验室现正在进行中国格特隐球菌致病菌株和环境菌株系统进化研究和暗色真菌系统发育学研究，该项研究已获国家自然科学基金国际重大合作课题以及国自然青年项目支持。

为了更好的开展医学真菌保藏工作，实验室采取冷冻干燥法、沙土保藏法、生理盐水甘油等多种国际流行菌种保藏方法保藏病原真菌，并已采购冷冻干燥机、液氮冻结菌种保藏库和-80℃超低温冰箱保藏各种临床分离株和环境株。现已保藏冷冻干燥菌种 1200 余株，包括从意大利、荷兰、美国和比利时等国家引进的隐球菌标准菌株，生理盐水甘油保存菌株 300 余株，日常斜面移种菌株 300 余株，菌种资源多样性高、新资源丰富，包括标准株、临床株

和环境分离株。菌种类型包括隐球菌、曲霉、念珠菌、暗色真菌、皮肤癣菌等常见及罕见致病真菌。在实验室建设期间，研究团队新发现 3 种新的致病真菌也保藏其中。同时，真菌保藏中心秉承互惠共享的原则，与上海和其他省市大型医院保持合作，进行菌种鉴定、药敏和保藏工作，为我国病原真菌研究工作提供坚实保证。实验室拟建成现代化的、亚洲一流的中国上海真菌保藏中心（Shanghai Center of Mycology Collection, SCMC）和上海疑难真菌菌种鉴定质控中心，与世界真菌保藏中心美国 ATCC、荷兰 CBS、比利时 BCCM 等国际一流保藏中心接轨。

实验室运行和管理

本实验室依托上海长征医院皮肤科建设，在原有第二军医大学皮肤病与真菌病研究所和中国科学院隐球菌专业实验室基础上筹建上海市医学真菌分子生物学重点实验室，其中包括医学真菌分子生物学实验室、真菌病理实验室和医学真菌临床检验室三部分组成，涵盖医学真菌病研究的基础、病理、临床和检验四个方面。实验室运行管理实行实验室主任负责制和岗位责任制，实验室设主任一名。由实验室主任提名，聘任实验室副主任，主管技师，学术秘书和行政秘书等。学术委员会是实验室的学术指导机构，主要任务是审议实验室的目标、任务和研究方向，审议实验室的重大活动、年度工作等。实验室工作人员包括：实验室固定研究人员、客座人员、实验技术人员和管理人员。实验室聘请中国医科大学陈洪铎院士（图14）、荷兰皇家科学院真菌生物多样性研究中心 Sybren de Hoog 教授、荷兰真菌生物多样性研究中心 Teun Boekhout 教授和美国杜克大学 John Perfect 教授为实验室客座教授。

实验室实行“开放、流动、联合、竞争”的运行机制，建设依照“边建设、边研究、边开放”的原则，课题向国内学者公开招标，吸引其他院校学者到实验室作访问学者，邀请国内外知名学者到实验室进行学术交流，派送学术骨干到国外科研机构开展科学研究。现已有军事医学科学院、交通大学附属新华医院等单位学者在本实验室进行研究工作。实验室从实际出发、统筹规划、合理设置，做到建筑设施、仪器设备、技术队伍和科学管理协调发展，提高投资效益，充分保证科研项目和企业合作实施，全面培养和造就高层次医学真菌学人才。

实验室人员结构

实验室主任、副主任和学术委员会主任

主治医师

院士秘书、助理

助教

技术人员

《中国真菌学杂志》编辑团队

护士

研究生：


张蕾（博士）


伊九（博士）


洪南（博士）


姜伟伟


王一霖


滕亮


姚国泰


扈东营


雷岩


张克明


邓宇晨


朱信霖


陈丽琳

客座教授


荷兰皇家科学院真菌多样性研究中心
Teun Boekhout


荷兰皇家科学院真菌多样性研究中心
Sybren de Hoog


美国杜克大学
John Perfect

平台建设和新增设备

在上海长征医院皮肤科隐球菌专业实验室和第二军医大学皮肤病与真菌病研究所现有研究设备基础上，逐步添置基因组学相关关键研究设备和菌种保藏设备，培养相关实验技师，现已完成病原真菌基因组学公共研究技术平台和真菌保藏库的建设工作。医学真菌分子生物学重点实验室现有各类仪器设备 32 台，包括微生物快速动态检测系统、冷冻干燥机、基因枪、Real-time PCR 等贵重仪器（详见表 1），这为继续深入研究新生隐球菌、白念珠菌、烟曲霉等目前对我国人民健康威胁最大的病原真菌分子致病机制提供基础支撑。

表 1　部分仪器设备一览表

序号	仪器名称	型号	数量	品牌
1	实时荧光定量 PCR	ABI Prism 7900	1	美国
2	核酸蛋白测定仪	EPOCH	1	美国
3	普通 PCR 仪	ABI 2720	2	美国
4	生物安全柜	Hfsafe-1200A2	2	国产
5	生物安全柜	Hfsafe-1500TE	1	国产
6	超低温冰箱	HFH686 立式	1	美国
7	超低温冰箱	DW-40L508	1	海尔
8	超低温冰箱	DW-40L188	1	海尔
9	凝胶成像系统	TANON2500	1	国产
10	奥林巴斯显微照相系统		1	进口
11	高速冷冻离心机		1	进口
12	制冰机		1	国产
13	电热恒温鼓风干燥箱	DHG-9070A	1	国产
14	三孔电热恒温水槽	DK-8D	1	国产
15	低速大容量离心机	TD5M	1	国产
16	霉菌培养箱	MJ-250-1	1	国产
17	隔水培养箱	GHP-9080	1	国产
18	台式基因枪系统	PDS-1000	1	美国
19	低速自动平衡离心机	TDZ4A-WS	1	湖南湘仪

序号	仪器名称	型号	数量	品牌
20	纯水仪	MILI-Q CENTURY	1	国厂和泰
21	微生物快速动态检测系统	MB-80	1	北京金山川
22	（附带 T02 智能恒温仪）		1	
23	电子天平	BT125D	2	赛多利斯
24	冷冻干燥机		1	美国
25	医用冷藏、冻箱	HYCD-205	1	海尔
26	通风柜	1.2 米	1	国产
27	二氧化碳培养箱	MCO-15AC	1	日本
28	三洋全自动消毒锅	MLS-3750	1	日本
29	药品保存箱	HYC-360	1	海尔
30	药品保存箱	HYC-326A	1	海尔

研究所新增设备一台：禾信 CM-1600 MALDI-TOF MS 微生物鉴定系统。由广州禾信质谱提供以用于科学研究。

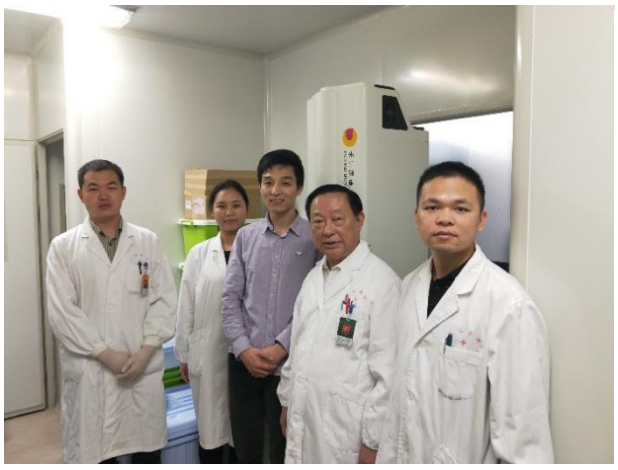

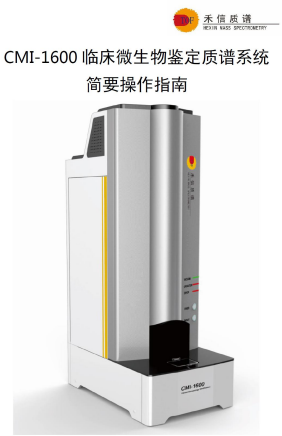

二、2018年度文章、基金、奖项等成果

论文发表、授权发明专利

第一和通讯（含并列）发表或接受12篇，IF>3累计6篇。授权发明3项，新型1项。

1、 Arastehfar A, Fang W, Pan W, Lackner M, Liao W, Badiee P, Zomorodian K, Badali H, Hagen F, Lass-Flörl C, Boekhout T. YEAST PANEL multiplex PCR for identification of clinically important yeast species: stepwise diagnostic strategy, useful for developing countries. Diagn Microbiol Infect Dis. 2018 Sep 21. pii: S0732-8893(18)30381-X. doi: 10.1016/j.diagmicrobio.2018.09.007. [Epub ahead of print] PubMed PMID: 30377018. 【IF=2.3】

2、 Hong N, Chen M, Xu N, Al-Hatmi AMS, Zhang C, Pan WH, Hagen F, Boekhout T, Xu J, Zou XB, Liao WQ. Genotypic diversity and antifungal susceptibility of Cryptococcus neoformans isolates from paediatric patients in China. Mycoses. 2018 Oct 19. doi: 10.1111/myc.12863. [Epub ahead of print] PubMed PMID: 30341799. 【IF=2.793】

3、 Arastehfar A, Fang W, Pan W, Liao W, Yan L, Boekhout T. Identification of nine cryptic species of Candida albicans, C. glabrata, and C. parapsilosis complexes using one-step multiplex PCR. BMC Infect Dis. 2018 Sep 25;18(1):480. doi: 10.1186/s12879-018-3381-5. PubMed PMID: 30253748; PubMed Central PMCID: PMC6156947. 【IF=2.62】

4、 Tang L, Fang W, Lin J, Li J, Wu W, Xu J. Vitamin D protects human melanocytes against oxidative damage by activation of Wnt/β-catenin signaling. Lab Invest. 2018 Dec;98(12):1527-1537. doi: 10.1038/s41374-018-0126-4. Epub 2018 Sep 11. PubMed PMID: 30206310. 【IF=4.2】

5、 Fang W, Wang G, Tang L, Su H, Chen H, Liao W, Xu J. Hydrogen gas inhalation protects against cutaneous ischaemia/reperfusion injury in a mouse model of pressure ulcer. J Cell Mol Med. 2018 Sep;22(9):4243-4252. doi: 10.1111/jcmm.13704. Epub 2018 Jun 19. PubMed PMID: 29921037; PubMed Central PMCID: PMC6111801. 【IF=4.3】

6、 Arastehfar A, Fang W, Badali H, Vaezi A, Jiang W, Liao W, Pan W, Hagen F, Boekhout T. Low-Cost Tetraplex PCR for the Global Spreading Multi-Drug Resistant Fungus, Candida auris and Its Phylogenetic Relatives. Front Microbiol. 2018 May 29;9:1119. doi: 10.3389/fmicb.2018.01119. eCollection 2018. PubMed PMID: 29896181; PubMed Central PMCID: PMC5987591. 【IF=4.019】

7、 Sang J, Yang Y, Fan Y, Wang G, Yi J, Fang W, Pan W, Xu J, Liao W. Isolated iliac cryptococcosis in an immunocompetent patient. PLoS Negl Trop Dis. 2018 Mar 29;12(3):e0006206. doi: 10.1371/journal.pntd.0006206. eCollection 2018 Mar. PubMed PMID: 29596420; PubMed Central PMCID: PMC5875738. 【IF=4.3】

8、 Deng S, Lei W, de Hoog GS, Yang L, Vitale RG, Rafati H, Seyedmousavi M, Tolooe A, van der Lee H, Liao W, Verweij PE, Seyedmousavi S. Combination of Amphotericin B and Terbinafine against Melanized Fungi Associated with Chromoblastomycosis. Antimicrob Agents Chemother. 2018 May 25;62(6). pii: e00270-18. doi: 10.1128/AAC.00270-18. Print 2018 Jun. PubMed PMID: 29581111; PubMed Central PMCID: PMC5971613. 【IF=4.2】

9、 Chen M, Xu Y, Hong N, Yang Y, Lei W, Du L, Zhao J, Lei X, Xiong L, Cai L, Xu H, Pan W, Liao W. Epidemiology of fungal infections in China. Front Med. 2018 Feb;12(1):58-75. doi: 10.1007/s11684-017-0601-0. Epub 2018 Jan 11. Review. PubMed PMID: 29380297. 【IF=2.0】

10、 Chen M, Kondori N, Deng S, Gerrits van den Ende AHG, Lackner M, Liao W, de Hoog GS. Direct detection of Exophiala and Scedosporium species in sputa of patients with cystic fibrosis. Med Mycol. 2018 Aug 1;56(6):695-702. doi: 10.1093/mmy/myx108. PubMed PMID: 29228273. 【IF=2.799】

11、 Novel multiplex qPCR approach for direct detection of Candida auris and its relatives in spiked serum samples. Amir Arastehfar,1, Wenjie Fang‡, Farnaz Daneshnia, Abdullah M S Al-Hatmi, Wanqing Liao, Weihua Pan*, Ziauddin Khan, Suhail Ahmad, Katharina Rosam, Michaela Lackner, Cornelia Lass-Flo¨ rl, Ferry Hagen & Teun Boekhout *Future Microbiology* in press 【IF=3.19】

12、 Unequivocal identification of an underestimated opportunistic yeast species, Cyberlindnera fabianii, and its close relatives using a dual-function

PCR and literature review of published cases Amir Arastehfar, Wenjie Fang, Abdullah M. S. Al-Hatmi, Mohammad Hosein Afsarian, Farnaz Daneshnia, Mina Bakhtiari, Sara Khanjari Sadati, Hamid Badali, Sadegh Khodavaysi, Ferry Hagen, Wanqing Liao, Weihua Pan*, Kamiar Zomorodian6* and Teun Boekhout. *Medical Mycology* 【IF=2.799】

隐球菌活力检测试剂盒及检测方法z1.201310627949.X(发明授权）

一种用于核酸扩增的酵母样真菌总DNA无仪器提取方法z1.201610114856.0(发明授权）

一种异丙基胺代氮唑类抗真菌化合物及其制备方法和应用z1.201610007802.4(发明授权）

一种拇外翻矫正鞋201721864805.6（新型授权）

新增以及在研基金及项目（总经费 2234.18 万）

序号	课题名称	负责人	起止时间	经费（万元）	项目来源
1*	“海上丝绸之路”重要病原体的威胁感知和监测预警	廖万清	2018.01-2020.12	1104.18	国家科技部
2*	我国及“一带一路”沿线国家真菌病联合防控策略研究	廖万清	2018.12-2020.12	100	中国工程院
3*	长征医院“金字塔工程”——国家优青后备人才	方文捷	2018-2021	30	长征医院
4	中国人群高发的难治性暗色真菌感染的生态学和进化起源研究	廖万清	2018.01-2022.12	232	国家自然科学基金
5	circ_0091746 以内源性竞争 RNA 方式结合 miR-6848-5p 在巨噬细胞抗新生隐球菌感染 M1/M2 极化中的作用及调控机制	潘炜华	2018.01-2021.12	65	国家自然科学基金
6	GM-CSF、TF 在我国非 HIV 感染隐球菌性脑	陈江汉	2018.01-2021.12	53	国家自然科学基金

	膜炎患者发病中的作用及机制研究				
7	上海市真菌病与自身免疫性疾病临床医学中心建设	廖万清	2017.07-2020.06	325	上海市卫计委
8	上海市领军人才	潘炜华	2017-2020	40	上海市科委
9	上海市科委扬帆计划	张 超	2017.05-2020.05	20	上海市科委
10	已糖载体蛋白家族对新生隐球菌体内荚膜动态变化的调控机制	廖万清	20151.1.至2018.12.31	80	国家自然科学基金
11	医学真菌生物样本库质量控制体系构建研究	廖万清	2016-8-31 至2019-7-31	20	上海市科委技术标准专项
12	上海市医学真菌分子生物学重点实验室	廖万清	2017-2020	150	上海市科委重点实验室
13	用于酵母感染核酸诊断的两项 DNA 提取试剂盒的研发和产业化	方文捷	2016-2018	5	上海长征医院
14	烟曲霉耐药基因突变检测试剂盒研发与新型临床精准诊断策略探索和验证	方文捷	2017-2019	10	海军军医大学

*2018 年新立项课题

重要新立项课题介绍

1、“海上丝绸之路”重要病原体的威胁感知和监测预警

研究首先在“海上丝绸之路”沿线国家和地区建立传染病病原体联防联控监测体系，结合当地传染病流行情况，有针对性开展重要传染病病原监测，建立的网络实验室监测预警体

系可应用于“一带一路”沿线相关国家和地区、口岸检疫系统等，也是实现我国应对美国 " 空海一体战 " 制定的军事战略的重要保障。同时，形成有较强实用性的研究成果，将建立一套病原体的快速检测技术、溯源数据库、研制出一些小型、实用技术设备和一系列简便、快速的诊断试剂和诊疗产品，包括从现场用的简便快速检测方法到普通实验室用的快速敏感检测方法和对多种病原高通量的检测方法、以及各种相应诊断试剂和诊疗产品，形成一个多层面病原体快速检测技术和处置技术体系。这些技术方法、小型设备、诊断试剂和诊疗产品适用于重大疫情暴发流行的检测。课题开发和集成基因组学、蛋白质组学、生物芯片、生物信息学、分子病原学等前沿生物技术，建立实用性的未知病原体的高通量的快速鉴别和溯源技术，可用于新发、突发传染病病原体的综合检测和鉴定，以及应急处置的对应产品。对传染病流行病学风险评估分析可以获得相关病原体的特征信息，为进一步的特异性检测及鉴别打下基础。

任务研究内容：阐明“海上丝绸之路”沿线重点真菌病流行情况，揭示相关海域真菌生物多样性组成，建立适用于当地卫生条件的诊断方法。

考核指标：1.完成 1000 例流行病学调查，30 次海域多样性调查，建立 40 株菌的基因序列库包含 50 个以上海域地点的微生物宏基因组数据库，包含 300 个菌株可培养微生物数据库；2.多重 PCR 快速诊断体系 4-5 套，在 2-4 小时以内可以诊断 20 个高致病菌种；建立微流控平台，；建立首个近红外荧光探针平台；申请国家发明专利 7-10 项。

2、我国及“一带一路”沿线国家真菌病联合防控策略研究

“一带一路”倡议涉及 100 多个国家，覆盖约 44 亿人口，拟构建世界跨度最长、最具发展潜力的经济走廊。近年来，一些烈性真菌病借由“海上丝绸之路”向沿线国家扩散，而且主要是由“一带一路”国家传入我国为主。比如近年来新发的多重耐药“超级真菌”(Candida auris,耳念珠菌）死亡率高达 60%以上。耳念珠菌已在全球 30 个国家出现过感染病例或局部爆发流行，其中 60%以上分布于我国“一带一路”沿线，对我国存在较大的输入性传播风险。我国同一带一路国家在真菌病防控方面的联合研究，具有一定的滞后性和急迫性。我国同相关国家至今未在本领域内建立成熟的合作模式和网络，缺乏合作互信。因此无法对潜在的高致病真菌病爆发流行进行联合预警和防控。

基于此，本项目拟从以下三个方面，组织调研和策略研究：

（一）国门及“一带一路”沿线病原真菌生物样本库构建策略研究：进行调研国门及“一

带一路”沿线病原真菌生物样本库构建水平；提出国门及“一带一路”沿线真菌病专病登记平台和生物样本库平台构建策略。

（二）我国及“一带一路”沿线国家真菌病研究机构跨国合作模式探索：进行我国及“一带一路”沿线国家真菌病研发实力和跨国合作现状调研；提出“一带一路”真菌病防控联合实验室建设策略。

（三）面向我国及“一带一路”沿线国家的适应性真菌病防控技术研发策略：进行适应性真菌病防控技术联合研发模式调研和理论创新；提出真菌病防控国产技术在“一带一路”沿线国家推广策略。

本课题将形成我国及“一带一路”沿线国家真菌病联合防控咨询报告，拟报送工程院医药卫生学部办公室以及国务院卫生健康委员会，为我国“一带一路”沿线相关性真菌病输入性感染提供理论依据和防控策略。

结题基金（工程院咨询课题顺利结题）

中国工程院院士咨询项目是国家高端智库为国家建言献策重要组成之一，2018年11月29日下午14:30-16:00，中国工程院咨询课题《我国抗真菌药物研发策略国内外对比研究》项目组在上海市医学真菌分子生物学重点实验室会议室召开了项目结题报告会。参加此次项目结题会的工程院领导和专家有：工程院三局易建局长、三局医药卫生学部办公室副调研员赵西路、长征医院徐正梅副院长、田诗音助理、廖万清院士、昆明医科大学第二附属医院邓丹琪副院长、郭芸教授、上海市第一人民医院施伟民主任、上海市新华医院姚志荣主任、军事科学院军事医学研究院杨英副研究员、海军军医大学海军医学系戚中田教授、海军军医大学药学院盛春泉副院长、潘炜华教授以及各技术骨干。

会议由会议主席戚中田教授主持。廖院士首先代表项目组向会议介绍了《我国抗真菌药物研发策略国内外对比研究》项目的研究背景、总体设计及课题设置等基本情况，邓丹琪教授、杨英教授、方伟博士等分别汇报了各子课题的研究目标、研究内容、研究进展与结果、财务收支等情况。项目的主要内容涉及我国真菌感染病原谱的流行规律、现有药物再利用以及我国海洋与中草药抗真菌药物研发策略评估四个方面。会议期间，各位专家主要对本项目的研究意义、设计思路和研究成果等进行了积极讨论，一致同意该项目按计划顺利结题。

经过讨论，与会专家在以下方面达成共识：

（一）真菌感染是危害人类生命健康与生活质量的重要疾病。我国真菌病原谱流行趋势及耐药现象与国际报道相近，但部分真菌在特定区域呈局部流行态势。应加强区域性流行真菌和新发耐药性真菌的诊断和监测。

（二）抗真菌药物研发总体数量偏少，高水平研究缺乏，但近5年来的研究数量与质量较之前有所提高。

（三）我国在现有药物再利用研究方面与国际同步，但较欧美发达国家的研究质量与转化应用尚有一定差距。我国在海洋抗真菌药物研发方面处国际先进地位，应紧密结合国家海洋强国战略的需求，加大研究投入。

（四）充分发挥祖国中医药宝库的优势资源，可作为真菌病高危人群的预防用药研发方向之一。

（五）我国抗真菌药物研发尚处于初级阶段，下一步应在项目资助力度、多学科合作、转化应用等方面加大投入。由于我国及“一带一路”沿线国家社会和医疗的需要，应加强具有自主知识产权的抗真菌新药研发。

科技奖励

序号	获奖项目名称	获奖等级	获奖时间	级别	完成人	完成单位
1	戴芳澜科技进步奖——终身成就奖	无	2018	省部级	第一	第一
2	医学科普卓越成就奖	无	2018	省部级	第一	第一
3	上海医学发展终身成就奖名单	无	2018	省部级	第一	第一
4	“戴芳澜”科技进步奖——优秀博士生奖	无	2018	省部级	第一	第一
5	海军军医大学优秀博士毕业生学金	一等奖	2018	校级	第一	第一
6	中华医学会皮肤性病学分会优秀研究生	三等奖	2018	省部级	第一	第一
7	上海市医学会皮肤性	三等奖	2018	省部级	第一	第一

	病学分会年度SCI论文奖					
8	上海市医学会皮肤性病学分会年度SCI论文奖	优胜奖	2018	省部级	第一	第一

三、2018 年度人才培养与对外交流情况

一、研究生培养

2018年有2名博士，4名硕士顺利通过毕业论文答辩并获得学位。

2018年毕业研究生名单：方文捷（博士）、金怡（博士）、　　、徐媛、林文婷、高睿。

二、出国留学

2018年在国外交流人员2名，已回国2名。

方文捷博士在荷兰CBS访学、张蕾博士赴美国约翰.霍普金斯大学留学深造，均已回国。

WESTERDIJK FUNGAL BIO DIVERSITY INSTITUTE

JOHNS HOPKINS UNIVERSITY

三、出国参会

1、廖万清院士，潘炜华教授 6 月 30 日参加 20th Congresses of the International Society for Human and Animal Mycology （ISHAM）大会

2、5 月 19 日，廖万清院士参加世界华人医师协会理事会换届大会

四、外国专家来访

一）荷兰皇家科学院 Teun Boekhout 教授来访

Teun 教授为上海市医学真菌分子生物学重点实验室客座教授，荷兰皇家科学院真菌多样性中心酵母组组长。今年 5 月 2 日，Teun 教授与其爱人 Chen Shuhui Tan 博士受邀来我研究所针对菌种保藏和管理、MALDI-TOF MS 质谱建库话题进行交流探讨，全程由方文捷博士担任实时翻译。会议期间陈敏博士分享了他多年来在隐球菌领域的工作。

'Preservation of Micro-organisms and Collection Management'

保存微生物和收集管理'

Dr. Shuhui Tan i.c.w. Dr. Chen Min, Prof. Dr. Teun Boekhout, ...

Shanghai Key Laboratory of Molecular Medical Mycology, Shanghai Institute of Medical Mycology, Changzheng Hospital, Second Military Medical University, Shanghai, China

地点长征医院真菌研究所

May 1 2018

2018 年 5 月 1 日

Lab visit and short talk with lab members

实验室访问和与实验室成员进行简短交谈

May 2 2018

2018 年 5 月 2 日

9.30 9.45 Welcome, and Introduction of Shanghai Lab Prof. Liao 廖医生

欢迎，并介绍上海实验室

9.45-10.05 Choice of preservation methods. Dr. Shuhui Tan 谈博士

保存方法的选择.

Agar, semi permanent, e.g. in silica, layered by mineral oil etc., cryopreservation, freeze-drying etc.), including cost aspects, kind of organisms, objectives.

10.05 10.15 Coffee break

咖啡时间

10.15-11:00 Theoretical basis preservation micro-organisms (PART I), Dr. Shuhui Tan

理论基础保存微生物

Including: How to avoid intracellular freezing damage (including video freeze-drying microscopy)

How to freeze and dry mico-organisms without damaging membranes and proteins

Design of freeze-drying and cryopreservation protocols

Choice of stabilizers

11.00-12.00 Lunch

午餐

12.00-14.20 rest (we can go and travel around)

午休

14.20-15:05 Theoretical basis preservation micro-organisms (PART II), Dr. Shuhui Tan

理论基础保存微生物第二部分

Including: How to avoid intracellular freezing damage (including video freeze-drying microscopy)

How to freeze and dry mico-organisms without damaging membranes and proteins

Design of freeze-drying and cryopreservation protocols

Choice of stabilizers

15:05-15:25 Analytical tools for screening of stabilizers 用于筛选稳定剂的分析工具 Dr. Shuhui Tan

15:25-15:35 Administration, bioinformatics

管理，生物信息学

Including stock control, naming/taxonomy and related issues (molecular data, physiology etc.) Dr. Shuhui Tan

15:25-15.40 Discussion on preservation and collection management

讨论保存和收集管理

15.40 -16.00 中国隐球酵母床 Dr. Chen Min

16.00-16.10 Tea

茶歇

16.10-16.50 Yeast biology and identification (MALDI TOF?) Prof. Dr. Teun Boekhout

酵母生物学和鉴定

16.50-17.00 General discussion 总结讨论

May 3 2018

2018 年 5 月 3 日

Practical training by Tan Shuhui for the whole day

谭淑慧全天实习训练

会议日程

会议嘉宾合影

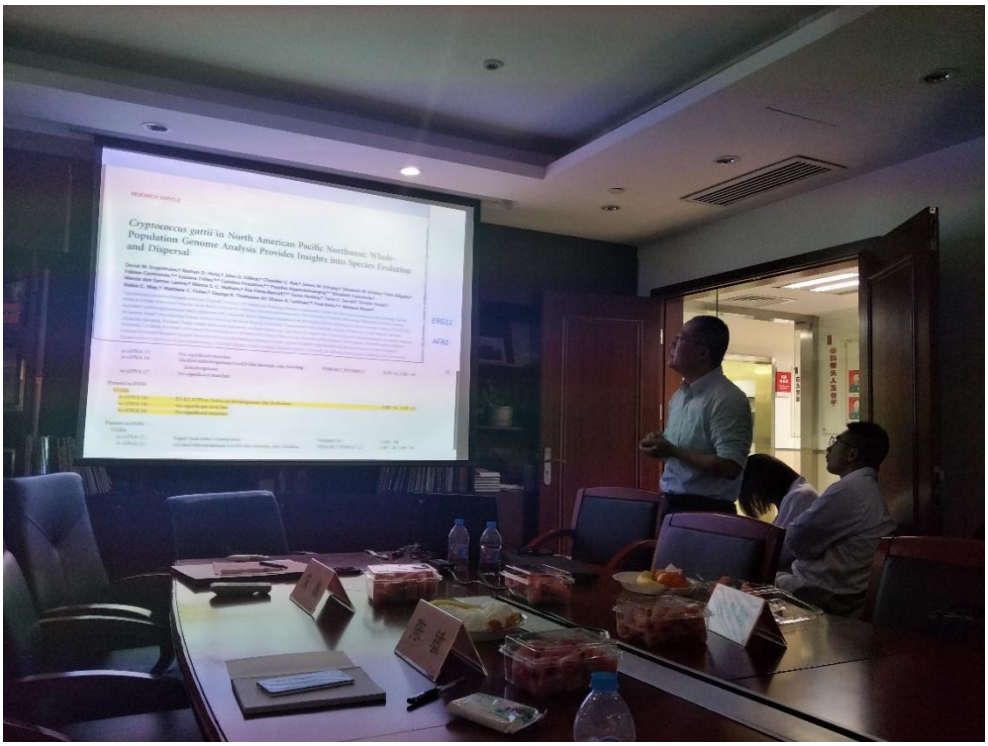

陈敏博士分享了他多年来在隐球菌领域的工作

二）徐建平受廖万清院士邀请来华作报告

2018 年 06 月 12 日受廖院士和陈敏医师邀请加拿大麦克马斯特大学（McMaster University）生物系的徐建平教授来华做了题为“Malenin variation in *Cryptococcus neoformans*”的学术报告，我研究所主要骨干和研究生参加报告会。

徐建平教授为加拿大麦克马斯特大学终身教授。兼任麦克马斯特大学华人教授会会长，国际重要杂志 Mycoses(真菌病害)主编，Mycopathologia (真菌病理学)、Mycology(真菌学)

副主编，国家自然科学基金重大项目海外评审专家，清华大学、中国科学院微生物所和植物所客座教授，云南省高端引进人才。2000 年在 Duke University 完成博士后，以助理教授身份加入 McMaster University 的生物系，长期从事真菌的种群遗传学研究。

五、实验室开放课题情况

序号	服务资源名称	服务描述	服务范围	开放课题负责人
1	实验室平台对外开放	为梅县人民医院提供研究平台	提供实验仪器、技术	张东兴
2	实验平台对外开放	为粤东医院提供研究平台	提供实验仪器、技术	郑跃
3	实验平台对外开放	为梅州嘉应医学院提供研究平台	提供实验仪器和技术支持	肖光文
4	菌株共享	为梅州嘉应医学院提供标准菌株	菌株提供	徐美兰
5	菌株共享	高新区人民医院提供菌株	菌株提供	邓淑文

七、外来研究人员情况

2018 年共有　10　人来我研究所，进行长期或者短期的研究工作，分别为：高磊（哈尔滨医科大学　副主任）、李航（江西胸科医院　研究生）、李帅（延安市人民医院　检验医师）、马涛（延安市人民医院　皮肤科医生）、李改静（河北工程大学附属医院　皮肤科医生）、姜如金（余杭区人民医院检验医师）、杨金（复旦大学附属华山医院研究生）曾炫皓（复旦大学附属华山医院　　研究生）、王鹏磊（广东呼吸病研究所 研究生）、陈晓菲（江苏省高新区人民医院 检验医师）

八、院所互访

一）廖院士参加卫生部免疫皮肤病学重点实验室年会

2018 年 10 月 12 日廖院士参加卫生部免疫皮肤病学重点实验室年会。

卫生部免疫皮肤病学重点实验室、教育部免疫皮肤病学重点实验室、辽宁省皮肤病重点实验室、辽宁省免疫皮肤病学重点实验室、辽宁省免疫性皮肤病诊疗技术工程实验室学术委员会会议在中国医科大学附属第一医院举行。学术委员会由包括廖万清院士在内的四位院士、三位长江学者及五位业内专家组成。会议由学术委员会主任委员王正国院士主持。

会上，中国医科大学闻德亮校长等致辞。实验室常务副主任肖汀教授汇报免疫皮肤病学实验室年度进展概况，陈洪铎院士作补充介绍。学术委员会委员认真听取了汇报，委员们逐个发表意见及建议，梳理了本实验室的工作进展，肯定了实验室一年的工作成绩。对实验室申报和开展更多重大研究项目、高层次人才队伍建设、实验室的较高层次发展方面提出殷切希望。学术委员会的意见顺利通过表决，也得到与会各级领导的认可和重视。

二）钟南山院士团队——叶枫主任来访

2018 年 8 月 30 日，钟南山院士团队叶枫教授、李征途博士、王鹏磊医师来访，分享了该团队在肺隐球菌病诊治和基础研究方面的经验和成果。

李征途博士汇报科研进展

廖万清院士点评

参会人员合影

三）廖万清院士访问东北大学丁辰教授课题组

10 月 12 日，中国工程院院士廖万清访问东北大学丁辰教授课题组，参观了生命科学与健康学院实验室并与生命学院青年教师、学生代表进行座谈。校总会计师芦延华出席座谈会。

芦延华介绍了生命学院的发展历程、基本情况和科学研究情况，希望廖万清院士能够对生命学院的实验室建设、青年人才培养和学术科研提出指导意见。

廖万清院士分享了个人的科研经历，表达了对中国共产党培养、支持的感激之情，希望学院青年教师和学生积极投身科研，为国家发展建设贡献力量，并表示愿意支持学校、学院的发展建设，期待更多合作。

廖万清院士同丁辰教授课题组合影

廖万清院士赠与丁辰教授专著《现代真菌病学》

四）2018 年 11 月 26 日廖万清院士、Sybren de Hoog 教授受邀访问贵阳医学院

2018 年 11 月 26 日，贵州省医疗卫生援黔专家团专家、中国工程院院士、海军军医大学上海长征医院皮肤性病与真菌病研究所所长廖万清教授，荷兰奈梅亨大学 Sybren de Hoog 教授一行莅临贵阳医学院开展学术交流和访问，校党委书记林昌虎代表学校对廖院士、Sybren de Hoog 教授一行的到来表示热烈欢迎。

林昌虎介绍了学校在人才培养、科学研究、服务社会、对外交流与合作等方面工作，并感谢廖万清院士多年来对我校学科建设、人才培养、重点实验室评估、科技成果、项目申报、

人才基地建设等各方面做出的巨大支持，并希望廖院士能继续关心学校发展和健康贵州的建设。廖院士对林书记的热情接待表示感谢，他指出，贵州医科大学教育科研工作在学校党委行政领导的全力推动下取得了日新月异的进步，每次来到学校都能感受到学校全体员工奋发拼搏、克服困难、积极向上的精神风貌，他将一如既往支持推动学校及医院工作，希望贵州百姓的健康生活质量得到提高。

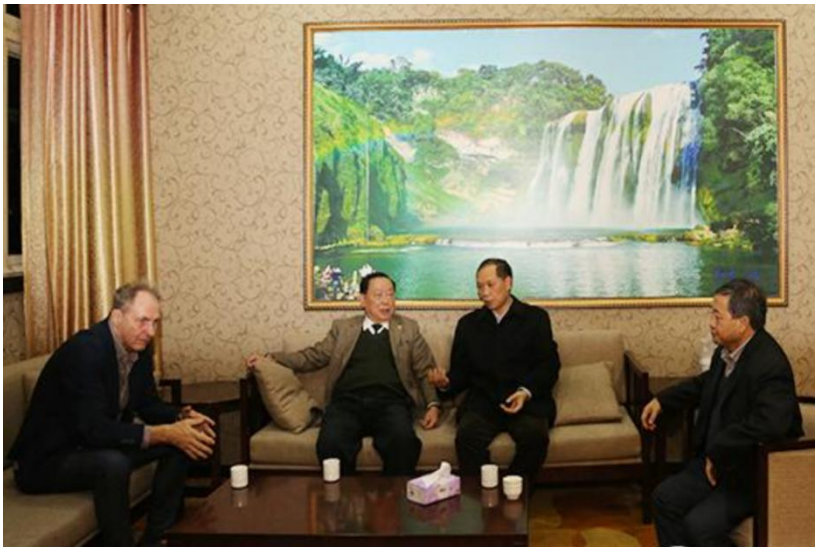

廖万清院士、Sybren de Hoog 教授还参加了 11 月 27 日由贵州医科大学承办的 2018 年贵州省微生物学会学术年会暨贵州省医学会微生物与免疫学分会年会。

五）2018 年 11 月 27 日廖万清院士参加贵州省微生物学会学术年会暨贵州省医学会微生物与免疫学分会年会

11 月 27 至 28 日，2018 年贵州省微生物学会学术年会暨贵州省医学会微生物与免疫学分会年会召开。大会主席、贵州省医学会会长杨克勤，贵州省医学会秘书长甘梁福，大会主席、贵州省微生物学会理事长刘作易，贵州省卫健委副主任杨洪，贵州省科协副主席刘炳银等领导莅临会议指导；贵州医科大学校长梁贵友出席会议；会议由贵州省微生物学会常务副理事长康颖倩及贵州省医学会微免分会主任委员黄山主持。

会上，廖万清院士对贵州省近年来在医疗卫生及科研教育等方面的进步给予了肯定，他心系贵州，热爱贵州，在今后将一如既往不遗余力支持贵州的发展。

杨洪代表贵州省卫健委对医疗卫生援黔院士专家团专家廖万清院士对我省健康贵州建设工作的支持表示感谢，并希望通过学术会议的交流，能全面提高我省微生物的研究水平，为临床医学发挥更大的作用。

会议邀请了中国工程院院士、海军军医大学廖万清教授，荷兰奈梅亨大学 Sybren de Hoog 教授，上海交通大学基础医学院副院长郭晓奎教授作为本次大会的主旨演讲特邀嘉宾，此外还有来自贵州省内各地的 20 位专家学者分别在以医学微生物及微生物生态健康为主题的两个会场进行了精彩的学术

报告。会议期间还设置了墙报（Poster）形式展示研究成果，经过大会评审委员会的严格评选，共评选出优秀学术海报一等奖 2 名、二等奖 5 名、三等奖 7 名，并颁发了荣誉证书及奖金。

感谢状

尊敬的 廖万清 院士：

感谢莅临“2018年贵州省微生物学会学术年会暨贵州省医学会微生物与免疫学分会年会”，并作精彩主旨演讲，会誉增辉，我们受益良多，敬呈此状，仅表谢忱。

贵州省微生物学会（代章）

贵州省医学会

2018年11月27日

四、2018年度重要学术活动情况

成立两个专业学会分会

一）中国整合医学会皮肤病学分会在西安成立，实验室副主任潘炜华教授担任主委

21世纪，医学进入了从生物医学模式向现代医学模式转变、从科学医学时代向整合医学时代发展的历史时期。生物医学模式把心身整体的人体机械地分解成各种器官、组织、细胞与分子，导致临床科室越分越细，让病人成了器官、疾病成了症状，引起很多临床问题。整合医学还器官为病人、还症状为疾病，实现心身并重、中西医并举、防治并行、医养并进、人病同治，让医疗回归人文。整合医学是全方位、全周期保障人类健康的新思维、新的医学观；是未来医学发展的必然方向；是生物医学模式向现代医学模式转变的必由之路；是健康中国战略的重大理论支撑；是全力推进医疗供给侧改革、全方位改善医疗服务质量的重要保证。整合医学将引领医学走向新的时代。

2018中国整合医学大会“整合皮肤病学论坛”4月29日在西安陕西召开。该大会由整合皮肤病专业委员会（筹）、上海医学真菌分子生物学重点实验室、西京医院皮肤科联合承办。论坛主席为本重点实验室副所长、中国整合医学会皮肤分会主任委员潘炜华教授。执行主席为西京皮肤医院副院长李春英教授。论坛名誉主席为工程院陈洪铎院士、廖万清院士。

会议由我院潘炜华教授和西京皮肤病医院副长
李春英教授共同主持

主任委员潘炜华教授主持论坛开幕式，并作皮肤病专业委员会筹备工作报告

名誉主席廖万清院士发言

名誉主席陈洪铎院士作报告：《我们对朗格汉斯细胞的研究》

复旦大学皮肤研究所所长、教育部皮肤病学重点实验室主任、美国皮肤科协会国际名誉会士张学军教授作报告：《银屑病的整合医学》

空军军医大学西京皮肤医院院长、全军皮肤研究所所长、中国皮肤科医师协会候任会长王刚教授作报告：《皮肤屏障与皮肤病及系统炎症》

交大医学院皮肤病研究所所长、新华医院皮肤科主任、上海市领军人才姚志荣教授作报告：《特应性皮炎与整合医学》

中华医学会皮肤性病学会候任主委、中南大学皮肤性病研究所所长、湘雅二医院皮肤科主任陆前进教授作报告：《表观遗传调控与复杂性皮肤病》

广东医学会皮肤病学分会前任主委、中华医学会皮肤病学分会常委委员赖维教授作报告《整合医学理念在皮肤病 诊疗实践中应用的思考》

会场气氛活跃

与会嘉宾合影

二）廖万清院士领衔，世界华人皮肤科医师协会成立

世界华人皮肤科医师协会成立大会日前在中国青岛召开。世界华人医师协会会长、中国医师协会长张雁灵、理事长石丽英，中国工程院陈洪铎院士、廖万清院士等出席会议。世界华人皮肤科医师协会全体委员参加会议。海军军医大学长征医院张殿勇院长亲临会场并做重要指示。

张雁灵会长代表中国医师协会、世界华人医师协会向世界华人皮肤科医师协会成立，以及世界华人皮肤科医师协会新当选的荣誉会长陈洪铎院士，会长廖万清院士、副会长潘炜华、周幼文等 13 位副会长，以及常委、委员表示热烈祝贺。他指出，皮肤科医师协会的成立，标志着世界华人皮肤科医师有了自己的国际组织，有了一个共同合作交流的大平台，有了皮肤科病华人医师的家。

张殿勇院长首先代表海军军医大学长征医院，向来自世界各国的华人医师，来自全国各地的各位皮肤科同仁表示最热烈的欢迎。他指出廖万清院士作为世界华人皮肤科协会的首任会长，为协会的成立和本次大会的召开做了大量的工作；世界华人皮肤科医师协会的成立，为华人皮肤科专家的交流合作提供了一个非常好的学术平台，唯有沟通才能发展，唯有开放才能进步！

张殿勇院长致辞

首任会长廖万清院士致辞

长征医院潘炜华教授作大会报告

世界华人皮肤科医师协会将在廖万清院士的带领下，在副会长、各位委员的努力下，打造有影响的皮肤病国际组织，为世界人民健康，也为中国人民健康，特别是皮肤科疾病的预防和治疗作出贡献。

“一带一路”真菌病防控相关工作

一）我实验室牵头举办“一带一路”中国-伊朗念珠菌血症多中心研究

“海上丝绸之路”沿线侵袭性真菌病调查由廖院士牵头，潘炜华教授负责课题设计，方文捷秘书负责联系海外专家，组建团队以及项目具体实施的细节工作。通过多方走访、多轮越洋视频电话会议，在今年年初，我研究所完成国际团队组建，目前参与方包括阿姆斯特丹大学（临床统计支持）、荷兰皇家科学院（致病菌种分子流行病学支持）、西班牙 CANDIPOP 团队（提供研究方案供参考）、阿曼卫生部医院以及伊朗的德黑兰大学、伊朗大学、设拉子大学、萨里大学、马什哈德大学等的一批顶尖真菌病专家。天津丹娜生物科技有限公司为我研究所”院士工作站“单位，在课题的实施中给我们经费以及技术等支持，同时通过课题，也帮助其他打开一带一路市场。

伊朗在一带一路中占据支点地位，“丝绸之路经济带”和“海上丝绸之路”的交汇点。伊朗周边国家，比如阿曼、土耳其、科威特、阿拉伯联合酋长国等均发现了超级真菌的暴发流行，但是伊朗尚未明确该疾病疫情。故将伊朗作为我们课题的第一站，旨在揭示耳道念珠菌在内的念珠菌流行病学情况。

根据工作日程安排，2018 年 4 月 10 日按计划在德黑兰的德黑兰大学（伊朗排名第一）牵头召开“中国-伊朗念珠菌血症多中心研究”第一次会议，我研究所代表邓淑文教授、丹娜生物代表孙景阳老师、伊朗多个大学的代表均到场参加此次跨国会议，会议由 Aimr 博士主持。此研究项目将根据国家“一带一路”的部署进行，依托“一带一路真菌病工作组”、“伊朗真菌病工作组”推进，是伊朗第一个念珠菌血症多中心研究项目，为伊朗的念珠菌病的发病率、致病菌株、耐药性以及血清学技术的临床价值提供大数据。具体确定研究方案内容、进入监测网络的医院、合作方权责、方案具体实施流程、时间点、最后签订跨国研究合

同。伊朗中心包括：伊朗大学、德黑兰大学、设拉子大学、马什哈德大学、马赞德兰大学、伊斯法罕大学，涵盖伊朗全国，同时，超 22 家医院参与监测网络，覆盖伊朗东、南、西、北以及中部，将为伊朗真菌病流行病学提供临床参考依据。

本项目将在一年内结束。通过该项目，我们将训练两国科研团队、发表一系列高水平成果、提升两国真菌病诊断率和治愈率、增进国际友谊。

有 22 家医院进入我们部署的监测网络

廖万清院士、潘炜华教授、方文捷秘书作为中方代表，签署国际合作协议

邓淑文教授作为研究所代表，参加此次会议

会议现场

邓淑文教授同与会嘉宾合影，参观大学实验室

二）上海海洋大学王永杰教授课题组肖劲洲博士一行来访商讨“海上丝绸之路”传染病防控课题合作

7月4日，上海海洋大学王永杰教授课题组肖劲洲博士一行参观访问了我研究所，并就未来双方在“海上丝绸之路重大传染病防控”等课题的合作内容和方式进行了深入探讨。

廖万清院士课题组成员带领肖博士一行六人参观了分子生物学实验室、真菌保藏中心以及真菌培养室等实验室功能区块。肖博士对我研究所的建设、管理和近年来取得的成果给予了高度的评价，表示下一步将进一步加强与廖院士课题组的合作交流，深入探索双方团队人才发展、培训、使用等方面的新型合作模式。

随后，廖院士团队和肖博士一行就“一带一路”沿线海洋真菌多样性测序、宏基因组分析等具体课题进行了深入会谈。双方就目前各自课题开展中的遇到的问题进行了交流和解答，并在具体的合作模式、成果共享形式等方面达成共识。

海上丝绸之路自秦汉时期开通以来，一直是沟通东西方经济文化交流的重要桥梁。近年来，“一带一路”在卫生领域的合作也逐步深化，各国在卫生政策、医学科研、人才培养、医药贸易等方面交流的广度深度不断拓展，传染病防控、慢病监测、卫生应急、妇幼健康、抗菌药物耐药、传统医药等领域合作惠及更多民众。我国政府一直希望通过共同努力，促进与“一带一路”沿线国家等重点合作伙伴开展合作，携手打造“健康丝绸之路”。“一带一路”伟大战略中“21 世纪海上丝绸之路”为我国海洋相关力量走向远洋，走向深

蓝提出了新的要求。如何提供有力的卫生安全保障是目前我国深蓝计划的重中之重，其中由致病微生物引起的传染性疾病是健康威胁的重大隐患。

受国家科技部委托，我研究所2018年获批“国家科技重大专项课题：《海上丝绸之路及国门输入重要传染病军民融合防控技术研究》（2018ZX10101003；1200万）。该独立子课题由廖万清院士牵头，也是自2013年潘炜华教授牵头国家科技重大专项后，我所第二次牵头该类项目。

鉴于重要病原体产生的健康危害及对一带一路战略的重大影响，对一带一路相关海域、地域和港口的重要病原体建立威胁感知系统并针对性进行防控关键技术研究十分紧迫。通过重点收集和整合“海上丝绸之路”沿岸国家疾病流行数据，对重要病原体进行采样分析，高通量检测鉴定，建立基于地理信息系统的传染病监测预警数据库，绘制传染病地理图谱，研究时空分布特征，形成能够集成疾病防控、监测预警于一体的“传染病医学地理信息预警系统”。对于可能导致严重传染性疾病的病原菌建立快速检测平台，为疾病发生时的快速诊断和及时救治提供依据，并为今后进一步向相关海域、港口开展工作建立成熟的组织、技术模式。

在4月10日，我研究所牵头在伊朗首都德黑兰成功召开中伊真菌病防控第一次国际会议。此次同上海海洋大学达成合作，是我研究所在一带一路课题上的又一项重大进展。

三）“一带一路”免疫缺陷与真菌感染研究进展国际研讨会廖万清院士做重要报告

2018 年 08 月 18 日“一带一路”免疫缺陷与真菌感染研究进展国际研讨会在上海举行。本次大会由上海市公共卫生临床中心、上海市医学会检验医学分会临床微生物学组和上海医药行业协会共同主办。该研讨会聚集了中国工程院院士、医学真菌病学专家廖万清、复旦大学附属华山医院终身教授翁心华、传染病专家卢洪洲、肾移植专家朱同玉等近 300 位国内外真菌学相关领域专家学者，就如何解决侵袭性真菌感染临床诊治中面临的实际问题交流讨论。

近年来，免疫缺陷疾病，尤其是 HIV 感染，器官移植和恶性肿瘤等的发病率呈上升趋势；与此同时，侵袭性真菌感染的发病率和病死率不断升高而成为影响公众健康的重要公共卫生问题。“一带一路”免疫缺陷与真菌感染研究进展国际研讨会与会专家一致认为，真菌感染的诊治已经成为国内外学者关注的热点和重点。同时，侵袭性真菌感染的早期诊断、合理用药是治疗疾病和抢救生命的关键。

中国工程院院士、医学真菌病学专家廖万清做了大会致辞

大会致辞后，廖院士做了专题报告：一带一路沿线真菌病的防控。他指出，如何提供有力的卫生安全保障是目前中国深蓝计划的重中之重，其中致病微生物引起的传染性疾病是健康威胁的重大隐患。感染性疾病病原的发现、鉴定和标准化的诊疗方式，一直是临床救治和诊断实验室面临的难点问题，关系到患者能否及时鉴别诊断、及时隔离和及时救治。而建立高通量、快速、准确、高性价比的病原体鉴定方法是感染性疾病诊疗的基础。

四）廖万清院士担任一带一路热带医学联盟成立大会主席，并发表作演讲

2018 年 10 月 19 日廖万清院士受邀担任“一带一路”热带医学联盟成立大会暨首届热带医学论坛主席，发表题为《“海上丝绸之路”沿线国家重要真菌病防控》的主题报告。

大会开幕

廖万清院士接受中央电视台参访

五）同伊朗和柬埔寨相关研究所签订国际联合实验室协议

Agreement on Establishment of
China-Iran International Joint Laboratory
for Fungal Diseases Prevention and Control
关于建立“中伊重要真菌病防控国际联合实验室”的协议

Background

背景

Century Maritime Silk Road. It is aimed at building a trade and infrastructure network connecting Asia with Europe and Africa along the ancient trade routes. To guarantee the health of Chinese travelers and also local people in the countries alongside the "the Belt and Road", Chinese government is interested in understanding the epidemiology of infectious diseases overseas, evaluating the risk of imported infectious diseases, and step up health cooperation under the framework of the China-proposed Belt and Road Initiative. People has been fighting against invasive and superficial fungal infections for thousands of years, recently fungal infections present new trend of epidemic, and certain pathogens, such as *Candida auris*, have become global issues. Herein, forming a framework for international cooperation is urgent and helpful for preventing, detecting and treating fungal diseases in the new era. Under this situation, we aim to launch a "**China-Iran International Joint Laboratory for Fungal Diseases Prevention and Control**".

习近平主席 2013 提出的“一带一路”倡议，即“丝绸之路经济带”和“二十一世纪海上丝绸之路的建设”，其目的在于建立亚欧非大陆间的贸易和基础设施合作网络。为保障我国出国人员和“一带一路”沿线国家的人民健康安全，我国政府致力于了解国外传染病的流行情况，评估输入性传染病的风险，以及在“一带一路”框架下稳步推进卫生层面的合作。几千年以来，人类一直同真菌病做斗阵，近年来真菌感染呈现出新的流行趋势，某些病原菌如耳道念珠菌的暴发流行已成为全球性问题。鉴于此，建立真菌病预防、检测和诊治的国际框架极具意义。因此我们建立“中伊国际真菌病防治国际联合实验室”。

Parties and Signing Place

协议双方和签订地点

This agreement is signed by Wanqing Liao and Sadegh Khodavaysi and between [Shanghai Key Laboratory of Molecular Medical Mycology, Shanghai Changzheng hospital] and [Tehran University of Medical Sciences] in Shanghai, China, and Tehran, Iran, for the establishment of International Joint Laboratory on for Fungal Diseases Prevention and Control.

本协议由廖万清院士和 Sadegh Khodavaysi 教授分别代表上海医学真菌分子生物学重点实验室（长征医院）和 Tehran University of Medical Sciences，于上海和德黑兰签署，旨在建立“中伊重要真菌病防控国际联合实验室”。

1

Signatures
落款

Signed by **Wanqing Liao**
on behalf of ***Shanghai Key Laboratory of Molecular Medical Mycology, Shanghai Changzheng hospital***
Position: director
Contact info: liaowanqing@sohu.com
Signatures
Signing place
Signing date 2018.8.16

Signed by **Sadegh Khodavaysi**
On behalf of ***Tehran University of Medical Sciences***
Position: director
Contact info: sadegh_7392008@yahoo.com
Signatures
Signing place
Signing date 1.8.2018

5

中国伊朗国际联合实验室协议

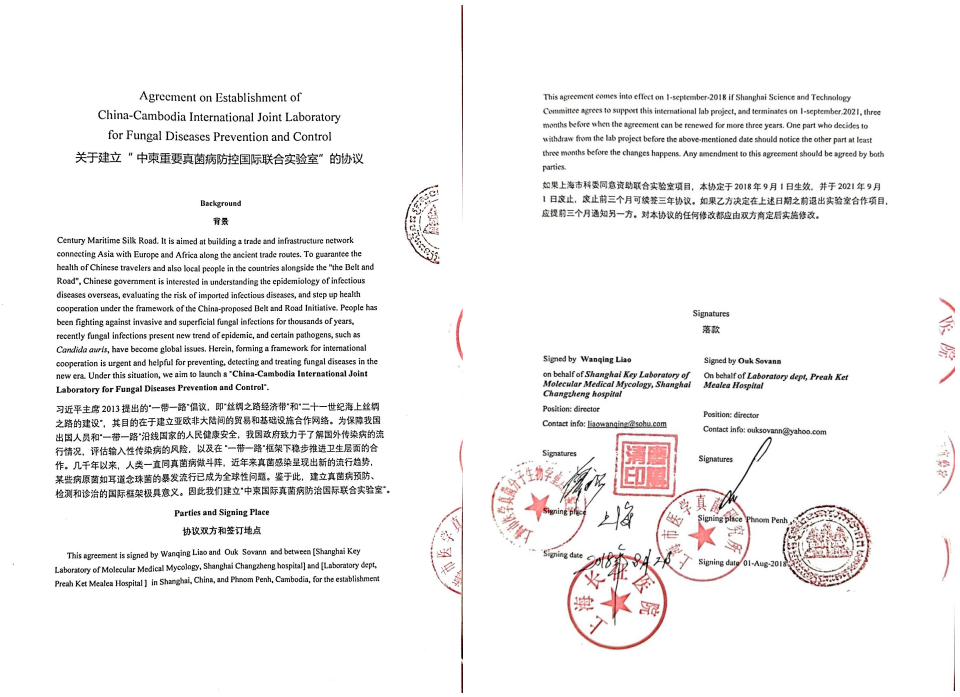

Agreement on Establishment of
China-Cambodia International Joint Laboratory
for Fungal Diseases Prevention and Control
关于建立“中柬重要真菌病防控国际联合实验室”的协议

Background

背景

Century Maritime Silk Road. It is aimed at building a trade and infrastructure network connecting Asia with Europe and Africa along the ancient trade routes. To guarantee the health of Chinese travelers and also local people in the countries alongside the "the Belt and Road", Chinese government is interested in understanding the epidemiology of infectious diseases overseas, evaluating the risk of imported infectious diseases, and step up health cooperation under the framework of the China-proposed Belt and Road Initiative. People has been fighting against invasive and superficial fungal infections for thousands of years, recently fungal infections present new trend of epidemic, and certain pathogens, such as *Candida auris*, have become global issues. Herein, forming a framework for international cooperation is urgent and helpful for preventing, detecting and treating fungal diseases in the new era. Under this situation, we aim to launch a "**China-Cambodia International Joint Laboratory for Fungal Diseases Prevention and Control**".

习近平主席 2013 提出的“一带一路”倡议，即“丝绸之路经济带”和“二十一世纪海上丝绸之路的建设”，其目的在于建立亚欧非大陆间的贸易和基础设施合作网络。为保障我国出国人员和“一带一路”沿线国家的人民健康安全，我国政府致力于了解国外传染病的流行情况，评估输入性传染病的风险，以及在“一带一路”框架下稳步推进卫生层面的合作。几千年以来，人类一直同真菌病做斗阵，近年来真菌感染呈现出新的流行趋势，某些病原菌如耳道念珠菌的暴发流行已成为全球性问题。鉴于此，建立真菌病预防、检测和诊治的国际框架极具意义。因此我们建立“中柬国际真菌病防治国际联合实验室”。

Parties and Signing Place

协议双方和签订地点

This agreement is signed by Wanqing Liao and Ouk Sovann and between [Shanghai Key Laboratory of Molecular Medical Mycology, Shanghai Changzheng hospital] and [Laboratory dept, Preah Ket Mealea Hospital] in Shanghai, China, and Phnom Penh, Cambodia, for the establishment

This agreement comes into effect on 1-september-2018 if Shanghai Science and Technology Committee agrees to support this international lab project, and terminates on 1-september 2021, three months before when the agreement can be renewed for more three years. One part who decides to withdraw from the lab project before the above-mentioned date should notice the other part at least three months before the changes happens. Any amendment to this agreement should be agreed by both parties.

如果上海市科委同意资助联合实验室项目，本协定于 2018 年 9 月 1 日生效，并于 2021 年 9 月 1 日废止，废止前三个月可续签三年协议。如果乙方决定在上述日期之前退出实验室合作项目，应提前三个月通知另一方。对本协议的任何修改都应由双方商定后实施修改。

Signatures
落款

Signed by **Wanqing Liao**
on behalf of ***Shanghai Key Laboratory of Molecular Medical Mycology, Shanghai Changzheng hospital***
Position: director
Contact info: liaowanqing@sohu.com
Signatures
Signing place
Signing date 2018.8.16

Signed by **Ouk Sovann**
On behalf of ***Laboratory dept, Preah Ket Mealea Hospital***
Position: director
Contact info: oukssovann@yahoo.com
Signatures
Signing place Phnom Penh
Signing date 01-Aug-2018

中国柬埔寨国际联合实验室协议

Agreement on Joint Research

I. Collaborative Research Title

Epidemiology of Candidemia in Iranian ICU Patients: A Prospective, Nationwide Surveillance Study by *Iranian Working Group of Candidemia* (IWGC) of **Iran** and *One-belt, One-road Working Group on Fungal Diseases* (B&R WGFD) of **China**

Leading Scientists

Party A: **Principal Investigators of *Iranian Working Group of Candidemia* (IWGC)**

Centre one: Javad Najafzadeh (NajafzadehMJ@mums.ac.ir)

Affiliation: Mashhad University of Medical Sciences, Mashhad, Iran

North-Eastern Part of Iran, Mashhad

Invloved Hospitals: Montazerieh hospital, Ghaen hospital, Omid hospital, Imam Reza hospital

Centre two: Kamiar Zomorrodian (zomorodian@sums.ac.ir)

Affiliation: Shiraz University of Medical Sciences

Southern Part of Iran, Shiraz

Invloved Hospitals: Namazi hospital, Faghihi hospital

Centre three: Sadegh Khodavaisy (sadegh_7392008@yahoo.com)

Affiliation: Tehran University of Medical Sciences

Signature for all principal investigators

Sadegh Khodavaysi

Javad Najafzadeh

Maryam Roudbary

Kamiar Zomorodian

Hamid Badali (His student)

Dynamiker Company

Fardavar Azma Iranian Co.

Amir Arastehfar

Teun Boekhout

Frank Cobelens

Corresponding author: **Weihua Pan**

Wanqing Liao

Fang Wenjie

中国伊朗真菌监测项目协议

其他重要学术活动

一）廖万清院士获戴芳澜终身成就奖 方文捷博士获戴芳澜优秀博士生

8 月 11 日上午，中国菌物学会 2018 年学术年会在山东泰安开幕，此次大会以“组学时代的菌物科学”为主题，中国工程院院士、海军军医大学上海长征医院廖万清院士，山东农业大学副校长张然，山东农业大学植保学院院长许永玉，中国菌物学会理事长、中国科学院微生物研究所研究员郭良栋以及 来自全国 200 多个科研院所、高校、企业的近 800 名专家学者出席了开幕式。

大会设立了以我国真菌学创始人——“戴芳澜”教授的名字命名的 “戴芳澜科学技术奖获奖”，该奖是我国真菌研究领域最高奖项。2018 年戴芳澜科学技术奖评审委员会由庄文颖、李玉、白逢彦、边银丙、戴玉成、郭良栋、姜子德、康冀川、刘杏忠、图力古尔、王成树、王源超、席丽艳、张劲松、张克勤、张修国、朱平组成。

开幕式现场

经评审委员会严格评选，决定授予我研究所所长廖万清院士以及中国科学院院士魏江春 2018 年戴芳澜终身成就奖；授予我研究所方文捷等 2018 年戴芳澜优秀研究生奖。同时大会还评选出了 2018 年戴芳澜杰出成就奖和优秀青年奖。我研究所以及其他获奖单位，将再接再厉，为我国以及世界真菌研究事业继续贡献自己的力量。

开幕式现场

廖万清院士在开幕式致辞

廖万清、魏江春院士获 2018 年戴芳澜终身成就奖

廖万清院士在闭幕式发表获奖感言

2018 年戴芳澜优秀研究生获奖代表

廖万清院士和方文捷博士会后合影

戴芳澜（1893 年 05 月 04 日- 1973 年 01 月 03 日）是著名的真菌学家和植物病理学家，中央研究院院士，中国科学院院士。在真菌分类学、真菌形态学、真菌遗传学以及植物病理学等方面作出了突出的贡献。他建立起以遗传为中心的真菌分类体系，确立了中国植物病理学科研系统；对近代真菌学和植物病理学在我国的形成和发展起了开创和奠基的作用。

二）《大众医学》七十周年刊庆活动，廖院士获评医学科普卓越成就奖

2016 年 8 月，习近平总书记在全国卫生与健康大会上提出：没有全民健康，就没有全面小康，要把人民健康放在优先发展的战略地位。党的十九大报告也明确提出实施健康中国战略，为人民群众提供全方位、全周期的健康服务。要实现全民健康的宏伟目标，除了积极

构建完善的医疗保障体系、提高医疗技术水平以外，大力普及健康知识（也就是科学普及工作），提高广大人民群众的健康素养，促使其主动践行健康的生活方式，做到未病先防、有病早治，也是不可或缺的重要工作。为激励医学相关专业人员积极从事医学科普工作，表彰为中国医学科普事业繁荣发展、提升中国人民健康素养的做出突出贡献的专家，以及在医学科普领域成绩卓著的医疗机构，由中华医学会科学普及部等指导，中华医学会科学普及分会、《大众医学》杂志承办的“传播健康 心系大众”医学科普奖评选活动于 2018 年 8 月 3 日正式启动。截至 2018 年 8 月 31 日，组委会共收到个人自荐、机构推荐的参评材料 306 份。

为表彰廖万清院士在大众科普方面的贡献，大众医学特授予廖万清院士“传播健康 心系大众”医学科普奖——卓越成就奖。

“传播健康 心系大众”医学科普奖

获奖通知

尊敬的 廖万清 院士:

为激励医学相关专业人员积极从事医学科普工作，表彰为中国医学科普事业的繁荣发展、提升中国人民健康素养的做出突出贡献的专家，以及在医学科普领域成绩卓著的医疗机构，由中华医学会科学普及部等指导，中华医学会科学普及分会、《大众医学》杂志承办的“传播健康 心系大众”医学科普奖评选活动已圆满结束。

衷心祝贺您在本次医学科普奖评选中获卓越成就奖。颁奖典礼将在“传播健康 心系大众”首届医学科普创新论坛暨《大众医学》杂志创刊七十周年纪念会上举行。诚邀您作为获奖嘉宾参加本次活动（详见邀请函）。

此致

“传播健康 心系大众”医学科普奖评审委员会

2018年11月3日

编辑部

三）廖万清院士、巴里·马歇尔（诺奖得主）、侯云德院士、

钟南山院士任《新发传染病电子杂志》名誉主编，陈竺担任该杂志总顾问

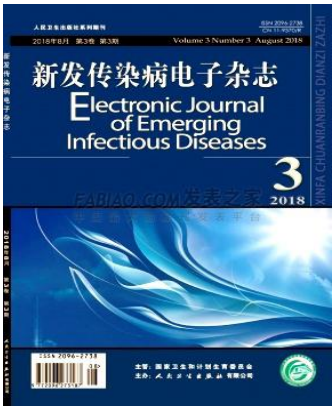

2018年7月14日《新发传染病电子杂志》编委会在深圳召开第一次编委会议。创刊于2016年的《新发传染病电子杂志》由国家卫健委主管、人民卫生出版社主办，该杂志为传播和交流新发传染病新知识、新技术搭建了一个很好的学术共享平台已出版发行7期，杂志以丰富的内容，全新视角引起海内外传染病医学领域极大关注。该杂志创刊填补了我国新发传染病学术交流领域的空白，为处于改革开放前沿的深圳在全国医学系列期刊中取得了一席之地。

据了解,《新发传染病电子杂志》2016年8月获得国家新闻出版广电总局正式批准,于2017年1月落地深圳出版发行，由全国人大常委会副委员长陈竺担任该杂志总顾问，幽门螺杆菌发现者，诺贝尔奖获得者，中国工程院外籍院士巴里·马歇尔；中国工程院院士，呼吸道疾病国家重大实验室主任钟南山；中国工程院院士，重大传染病防控国家重大科技专项技术总师侯云德；中国工程院院士，上海医学真菌分子生物学重点实验室主任廖万清等任名誉主编。

人民卫生出版社总编辑杜贤编审、主编陆普选教授给名誉主编颁发聘书

来自国内外近 100 名流行病医学领域新发传染病防治研究的领军人物、著名专家齐聚一堂，共商办刊大计。侯云德院士，廖万清院士亲临会场祝贺。因故不能到会的钟南山院士，中国工程院外籍院士巴里·马歇尔教授远程视频发言,对杂志的出版发行表示祝贺并提出了希望。

中国工程院院士，上海市医学真菌研究所所长，上海长征医院皮肤病与真菌病研究所所

长廖万清院士担任该杂志的名誉主编并在大会致辞。他首先表示非常荣幸能够担任该杂志的名誉主编，也希望杂志能多刊登中国人自己的最新研究成果，让世界都来关注中国的最新成果。也希望该杂志能成为具有国际影响力的学术期刊。廖万清院士说：医生要勇敢面对新发传染病，100 多年研究史对人类 5000 年历史，是短暂的，杂志为发传染病提供了重要学术交流平台，希望大家认真分析、研究、不断提高研究与学术水平，才能更好做好新发传染病防治工作。

上海长征医院皮肤病与真菌病研究所所长廖万清院士致辞

会者一致认为，该杂志将致力于及时传播新发传染病新技术、新技能和新知识；大力促进新发传染病早预防、早诊断和早治疗；以认真求实、开拓创新为原则,努力打造好这个与国际接轨、先进的学术交流平台，服务于全人类。

新发传染病是指新的、刚出现的或呈现抗药性的传染病，其在人群中的发生在过去不断增加或者有迹象表明在将来其发病有增加的可能。对多数新发传染病，人们目前尚无足够认识。在过去 30 年中，全球发现了 40 余种新发传染病，平均每年至少出现一种。 多重耐药耳道念珠菌、SARS、甲型 H1N1、H5N1、H7N9 人禽流感和中东呼吸综合征等是近 10 年来对人类威胁最大的新发传染病。医务工作者在面对每一次新发传染病到来之际，都会够感到预防控制措施掌握不够，缺乏精准的诊断知识和治疗技术缺憾。通过创办杂志可以广泛传播新发传染病相关防控、诊治知识和新技术，普及和提高广大医务工作者应对新发传染病的水平和能力，利用专业杂志的功能及其特殊性，将新发传染病防控指南、诊

《新发传染病电子杂志》第一届编委合影

疗专家共识及对新发传染病和流行病学研究的科学方法与规范的技术传递到每一位医务人员（包括基层医务工作者）。这对于及时早期预防、早期诊断、及时治疗各种新发传染病，降低病死率有着极其重要的意义。

四）廖万清院士一行人至上海海洋大学实地调研

2018 年 11 月 28 日中国工程院咨询项目《我国抗真菌药物研发策略国内外对比研究》子课题《海洋天然抗真菌药物研发策略的调查与评估》项目组廖万清院士一行人至上海海洋大学实地调研。参加此次实地调研讨论的专家教授有：上海海洋大学海洋生物制药系主任吴文惠教授、包斌副教授、许剑锋副教授、张朝燕副教授、郭锐华讲师、刘宁讲师、马子宾博士、张静怡博士、岳恒博士、长征医院廖万清院士、潘炜华教授、方文捷主治医师、扈东营研究生。

实地调研讨论由上海海洋大学海洋生物制药系主任吴文惠教授主持。廖院士首先代表项目组介绍了《海洋天然抗真菌药物研发策略的调查与评估》课题的研究背景、研究目标和此次实地调研的目的等基本情况，潘炜华教授汇报了课题组前期海洋抗真菌药物研究文献检索和至海军军医大学药学院实地调研的情况。会议期间，各位专家教授主要就海洋天然抗真菌药物研发策略进行了积极讨论，经过讨论，与会专家在以下方面达成共识：

1、海洋微生物具有极其丰富多样的种类，能够生存于低温、缺氧、高压等独特的海洋生态环境中，因而能够产生具有优良生物活性且结构新颖的天然化合物，从海洋生物资源中获取这些化合物具有安全性高、成本低及来源丰富等优点，因此，海洋微生物代谢产物已成为药物创新与新药开发的重要来源。

2、上海海洋大学海洋生物制药系海洋类药物研发主要是从海洋真菌微生物提取具有优良生物活性的天然化合物，包括青霉属、葡萄穗霉、地霉属、短孢霉属等真菌微生物，然后用于心脑血管溶栓、医学工程材料和临床特异性食品等三大领域。目前较大的突破是从海洋真菌微生物长孢葡萄穗霉 FG216 的代谢产物中发现了一种新型纤溶活性小分子化合物 FGFC1，药效学和毒理学研究已证实 FGFC1 是一种安全有效的溶血栓化合物。

3、上海海洋大学海洋生物制药系主要对海水真菌微生物发酵后产生的初级和次级代谢产物进行研究，并未涉及海洋天然抗真菌药物的研发。呼吁国家关注海洋天然抗真菌药物研

发，增加对海洋天然抗真菌药物研发相关课题的支持。

廖万清院士课题组同海洋大学课题组成员合影

五）【汤飞凡论坛】廖万清院士纵论“科研之路”

2018 年 4 月 26 日下午，中国工程院院士、海军军医大学长征医院廖万清教授应邀访问中南大学湘雅二医院做客“汤飞凡”论坛，与医院师生分享了题为《机缘型的科研之路》的学术讲座，讲座由湘雅名医、皮肤性病科主任陆前进教授主持。

廖万清院士创造性提出科学研究大体可分为攻关型科学研究、挑战型科学研究、机缘型科学研究三种类型，结合其数十年的临床科研实践发现，生动分享了格特隐球菌引起脑膜炎、具多育现象米曲霉引起肺曲霉病、小红酵母引起甲真菌病、聚多曲霉致阻塞支气管曲霉病、胶囊青霉引起的肺青霉球等九种新的病原真菌及其新的致病类型被发现的故事，并将这些归属于机缘型科学研究。

廖万清院士提到，作为临床医生，机缘型科学研究不但要有良好的科研素质、深厚扎实的基础知识，并且还要有敏锐的眼光和无边的想象及强大的创造力，要善于从临床工作中发现问题，抓住稍纵即逝的机会以成就科学发现。从科学研究到临床诊疗工作，廖院士的讲座都为每一位与会者提供了宝贵的指导和帮助。

在讲座中，廖万清院士还和与会者进行了深入的交流和探讨，并对提出的问题一一进行详细的解答,师生们表示受益匪浅。

六）廖万清院士参加季德胜先生诞辰 120 周年暨学术研讨活动

我国著名蛇伤专家季德胜先生诞辰 120 周年暨学术研讨活动今天在北京人民大会堂举行。廖万清院士、国医大师和北京、上海、广东等地科研院所、各大医院专家、学者及国家卫健委、江苏南通市政府相关领导近百人出席。

六）廖万清院士受邀参加 2018 第二届中国银屑病大会

2018 年 10 月 26-28 日，中华医学会皮肤性病学分会将联合安徽省医学会在美丽的“大

湖名城，创新高地”安徽省合肥市共同主办第二届“中国银屑病大会”。

中国医科大学附属医院陈洪铎院士、海军医科大学长征医院廖万清院士、复旦大学附属华山医院王侠生教授、国际银屑病协会委员美国密歇根大学 JamesT.Elder 教授、国际银屑病协会委员美国华盛顿大学 AnneBowcock.教授、日本银屑病协会前任主席日本东海大学 AKiraOZAWA 教授、国际皮肤科学会联盟常务理事/国际银屑病协会委员/中华医学会银屑病专业委员会主任委员张学军教授、国际银屑病协会委员/中华医学会银屑病专业委员会副主任委员/浙江大学医学院附属第二医院皮肤科主任郑敏教授等国内外数百位全球顶尖银屑病专家出席。

廖万清院士参与《全国科学技术名词审定委员会
皮肤性病学名词》定稿

七）廖万清院士参加世界温州人大会院士论坛

10 月 29 日，“大健康·新未来”2018 世界温州人大会院士论坛在洞头举行。本次论坛以助力温州全面参与“一带一路”建设，发扬世界温州人精神内涵为主旨，邀请了海内外著名院士和国家级、省部级人才齐聚洞头，聚焦生命科学主题，发挥名家效应，把脉洞头康疗智岛发展方向。

上午八点三十分，开幕式在温州医科大学滨海校区会堂举行，市委常委、统战部部长施艾珠，温州医科大学校长李校堃，洞头区委书记王蛟虎等致辞。温籍科学家、美国文理科学院院士、美国国家科学院院士林海帆以录播视频形式发来致辞。院士论坛主题报告议程，中国科学院院士杨雄里教授、中国工程院院士张心湜教授、中国工程院院士廖万清教授分别就《对脑科学前景的思考》、《如何成为快乐成功的医疗工作人员》、《“海上丝绸之路”沿线国家重要真菌病防控》展开专题报告。

八）廖万清院士受邀参加陆军举办高层次学术交流活动

11 月 8 日至 9 日，陆军举办高层次学术交流活动。活动位于山城重庆陆军军医大学。

陆军高层次学术交流活动会场“高朋”满座，大咖云集。会场共有 20 名军地知名院士，30 名陆军军事医学领域高层次科技人才和科技英才培养对象，90 余名各类型医疗卫生单位专家代表。

廖万清院士同陆军军医大学领导和医务人员合影

廖院士同王云贵校长合影

九）廖万清院士参与中国医师协会年会，并为获奖嘉宾颁奖

中国医师协会皮肤科医师分会年会与 11 月 8 日在广州举办，廖万清受邀参加。11 月 9 日，在广州召开的第十四届中国皮肤科医师年会（2018CDA）暨全国美容皮肤科学大会开幕式上，张会长勉励道：希望 CDA 着力于培养更多的像廖万清、朱学骏、王宝玺、郑志忠、李若瑜、李恒进等一样的高质量人才，这才是 CDA 最大的成功和诚意！”

廖万清院士为 CDA 杰出贡献专家颁奖

院士专访

廖万清院士 | 警惕“超级真菌” 提高实验室鉴定能力

▲《医师报》融媒体记者 张艳萍 陈惠

第二军医大学长征医院皮肤性病与真菌病研究所所长廖万清院士参加了本届CDA年会，他高兴地告诉医师报记者，他是广东人，能够在广州与这么多前辈、老朋友们一起参加皮肤科医师年会，感到非常高兴和激动。同时，他就近年来爆发的“超级真菌”的诊治情况接受了医师报采访。他表示，“超级真菌”危害患者生命，如果全国皮肤科医师一旦发现“超级真菌”，可随时与他联系进行咨询。他的联系邮箱是：liaowanqing@sohu.com

真菌病是大学科之一

廖万清院士表示，皮肤科是大学科，总共有2500余种皮肤疾病，其中真菌性疾病是大学科之一。引起真菌病的致病菌种有400多种，以前认为真菌病是散发的，最近二十多年才发现真菌病也可以爆发流行，比如1999年格特隐球菌在美洲的暴发流行。2016年美国、英国爆发一种叫耳道念珠菌的新型“超级真菌”，当时中国没有；2017年，韩国、巴基斯坦、印度、南非、肯尼亚、科威特、哥伦比亚、委内瑞拉、英国、加拿大和以色列等至少24个国家报告发现了耳道念珠菌感染病例，当时中国没有；2018年，全世界30个国家出现超级真菌爆发，中国有18例。

耳道念珠菌主要引起真菌血症、伤口以及耳部感染，通常对一种或多种主要的抗真菌药物具有耐药性，所以称之为“超级真菌”。“超级真菌”引发的死亡率高达60%~67%，其严重后果已经引起全世界专家重视。目前我国正在开展“一带一路”的建设工作，其顺利推动共建，使沿线国家共同发展，将会产生很好的社会经济效应。但是如何保证“一带一路”成为“健康之路”，需要医疗界共同努力。

诊断与鉴别困难 “超级真菌”常被误诊

“作为皮肤科领域的医务工作者，我们的任务就是帮助沿线国家控制真菌爆发，一旦发现及时防控。要了解超级真菌如何传播，用什么方法防治？目前国内很多地方并没发现，但不表示没有。三天内不明原因发烧、发热、头痛，使用抗生素无效，就要想到有可能是遇到了超级真菌。”廖万清院士说。

据廖万清院士介绍，“超级真菌”主要特点包括：（1）生态源头不清楚，自然环境中目前还分离不到该菌，国际同行推测该菌是近年来进化出来的、能快速地适应并定植于人体的新物种。（2）大部分菌株对目前临床上常用的三大类抗真菌药物均具有耐药性（包括唑类、多烯类和棘白菌素类药物），从而导致治疗失败和60%以上的致死率。（3）诊断和鉴定困难，临床实验室传统的形态和生化诊断方法常常错误地鉴定为其他念珠菌。（4）它能长时间存活于患者和医护人员的皮肤及医院设施表面，从而导致院内爆发性感染。有国外文献报告，超级真菌甚至可以通过体温计在人体间传播。

廖万清院士特别强调，要注意器官移植患者、肿瘤患者、急诊患者等免疫力低下的患者容易被“超级真菌”感染。作为皮肤科医生，如果不认识“超级真菌”，有可能会给患者家属带来无法挽回的损失和痛苦。

因此，廖万清院士呼吁全体皮肤科同仁，要加强宣传与提高实验室鉴定能力，提高警惕，避免漏诊误诊导致死亡。“临床医生对患者的真爱就是，想方设法把患者从死亡的边缘抢救回来，挽救患者生命，解决困扰患者的疾病问题，这也是皮肤科医生的使命与光荣。”

现场报道

（从左到右）陆军军医大学西南医院杨希川教授，中国医学科学院皮肤病医院刘维达教授，CDA会长、中国人民解放军总医院李恒进教授，CDA名誉会长、北京大学第一医院李若瑜教授，优麦医生CEO常江共同参与专场圆桌讨论

首份皮肤科医生在线学习数据报告出炉

医师报讯 11月10日，在第十四届中国皮肤科医师年会互联网在线学习专场上，国内最大的皮肤科医生在线学习平台优麦医生APP发布首份《中国皮肤科医生在线学习数据报告》（简称《报告》）。

《报告》显示，超过90%的皮肤科医生正使用在线学习软件；中青年皮肤科医生是在线学习的活跃人群，从年龄分布看，主力军为30~40岁的群体；晚上6~10点是皮肤科医生在线学习的高峰时间段。

“终身学习是医生的职业特性与需求，广大中青年医生、基层医生的学习需求则更为迫切。”本届年会大会主席、中山大学附属第三医院赖维教授表示，不少基层皮肤科医生身在小城市甚至偏远地区，出远门参加各类会议及学习班的费用有限，而通过同道交流或者书籍资料查阅来获取学术信息又远远不够，借助互联网平台的在线学习方式，大大拓展了广大基层医生获取新知的渠道。

（王勇）

现场报道

“我要上年会－中文演讲比赛”总决赛结果揭晓

上海中山医院申晨、昆明医科大学第二附属医院杨滨宾拔得头魁


总决赛参赛者及专家合影

廖万清院士接受《医师报》采访
呼吁全国同行重视“超级真菌”


惠州厅
惠州厅
2018/11/11 08:29

十）廖万清院士受邀参加 2018 朝阳国际医学大会

2018 年 11 月 17 日廖万清院士受邀参加 2018 朝阳国际医学大会。“2018 朝阳国际医学大会暨首都医科大学附属北京朝阳医院建院 60 周年国际学术研讨会”在北京国际会议中心隆重举办。皮肤分论坛于 11 月 17 日正式召开，这是一次涵盖临床免疫与疾病的基础学科与临床多学科交流的盛会，旨在搭建高水平的学术交流与合作平台，促进学科长远发展。北京朝阳医院皮肤科主任何焱玲担任论坛主席，近 300 名皮肤科医师参加了会议。

本次论坛的主题是皮肤免疫与疾病，探讨皮肤自身免疫性疾病、感染、炎症性皮肤病及肿瘤等免疫相关问题。中国工程院院士、上海长征医院廖万清作为我国在皮肤病学领域功勋

卓著的真菌病学专家，围绕我国一带一路战略，沿着海上丝绸之路流域，进行了真菌感染的流行病学调查。他还对“海上丝绸之路”沿线国家重要真菌病的防控，特殊真菌感染的特点和诊治进行了概述。

此次大会的与会者来自大江南北，从北京、上海，到黑龙江、西安；从山西、内蒙，到苏州、长沙；演讲专家阵容强大，共有 1 位院士、2 位长江学者、3 位“国家杰青”获得者，

代表了当前皮肤科领域和风湿免疫领域的免疫相关性疾病研究方面较高的学术水平；会议内容丰富，从基础研究到临床研究等多个角度、不同层面对皮肤病学和免疫学研究的最新进展进行了较为详细丰富的介绍，是国内临床免疫领域一流水平的对接碰撞。与会专家学者均对此次大会给予了高度评价，认为本次会议学术气氛浓厚、内容新颖丰富，基础与临床联系密切，为国内皮肤免疫及疾病的科研提供了良好的沟通平台，并将有效地推动国内各地区、各中心之间的合作与发展。

与会全体嘉宾合影

五、2018 年度全国院士工作站建设情况

丹娜生物院士专家工作站

一）廖万清院士工作站（丹娜生物）获批全国百家模范院士专家工作站

中国科学技术协会
China Association for Science and Technology

首页 | 全景科协 | 智库 | 学术

当前位置：首页>>新闻>>通知公告>>学术学会

关于2018年模范院士专家工作站名单的公示

发布日期：2018-11-21

根据《关于开展2018年模范院士专家工作站遴选工作的通知》（科协学函企字〔2018〕156号）要求，截至2018年10月31日，全国27个省级科协院士专家工作站建设管理单位推荐了194家候选模范院士专家工作站，其中，院士专家工作站179家，专家工作站12家，院士专家服务中心3家。

依据《模范院士专家工作站遴选办法（试行）》《模范院士专家工作站遴选指标》，中国科协企业创新服务中心对遴选材料进行了形式审查，按照中国科协抽取评审专家相关规定抽取了评审专家，对191家候选模范院士专家工作站进行了网络评审和会议评审。现将通过评审的2018年模范院士专家工作站建站单位名单予以公示，公示期限自发文之日第二天起5个工作日为期。

近日，为充分发挥优秀典型院士专家工作站的引领带动作用，中国科协依据《模范院士专家工作站遴选办法（试行）》、《模范院士专家工作站遴选指标》，通过省部级科协推荐、网络评审和专家会议评审等环节，从全国 5000 余家建站单位中优中选优了一批全国模范院士专家工作站，廖万清院士工作站——丹娜生物成为天津市荣获该项荣誉资质的 3 家建站企业之一。

2018 年模范院士专家工作站名单

（排名不分先后）

序号	地区	院士专家工作站名称
4	天津	丹娜（天津）生物科技有限公司院士专家工作站

在本次评选过程中，评审专家们对丹娜生物院士专家工作站的各项遴选指标给予了很高评价：

- 工作站基础条件良好，建站单位诚信经营、具有良好的社会责任感；工作站保障经费充分，院士专家团队与建站单位联系紧密，“产、学、研”协同效应显著。
- 工作站管理和运行机制规范，制度健全，运行状况良好。
- 工作站在提升企业等建站单位创新能力、促进建站单位创新人才培养与引进、提高建站单位经济效益及社会效益等方面成效突出。
- 进站院士专家对工作站基础条件、运行管理及取得的成效等方面满意度高。

中国科协开展本次遴选工作，主要目的在于引导全国院士专家工作站规范、有序、可持续发展，推动各地工作站提质增效。荣获“全国模范院士专家工作站”是中国科协和天津市科协组织对丹娜生物院士专家工作站几年来整体运营成效的极大肯定。丹娜生物董事长周泽奇表示，公司将进一步提高院士专家工作站的运行质量、加强高水平建设，真正发挥引领带动作用，持续提升工作站服务企业技术创新的能力，用更加完善的联合诊断产品为IFD患者的生命健康提供优质、高效的服务。

二）丹娜生物举办 2018 年院士专家工作站总结报告会

天津滨海新区丹娜生物在生态城举办了 2018 年院士专家工作站总结报告会。会上，中国工程院廖万清院士报告了《“海上丝绸之路”沿线国家重要真菌病防控》国际合作项目所取得的重大进展。 丹娜生物作为这一重大国际合作项目单位之一，在廖万清院士的带领下，与中东地区 22 家重点标杆医院共同开展的“一带一路”念珠菌血症临床诊断技术研究获得了重要的阶段性成果。这充分表明了丹娜生物的侵袭性真菌病早期快速检测核心技术与创新产品具有重要的临床应用价值和很强的国际竞争力。

据介绍，一年以来，在院士专家工作站的带动下，丹娜生物取得了国家级科技型企业、与廖万清院士团队及伊朗22家重点医院共同开展“中国-伊朗念珠菌血症多中心研究”、获批天津市企业人才智力合作项目、G 试验获批天津市中小企业局“专精特新” 产品认定等一系列成就，科研进展迅速。

丹娜生物董事长周泽奇指出，院士专家工作站对丹娜生物的发展和创新研究非常重要，它是吸引人才的高地和智库服务的平台，它对丹娜生物的快速、健康发展具有强大的推动作用。

丹娜生物将进一步加强与廖万清院士团队的全面深入合作，共同解决好 IFD 精准诊疗领域的难题，为有效的改善广谱抗生素不合理利用的现状、不断提高 IFD 患者的检出率和治愈率、减少死亡率提供更加优质高效的服务。

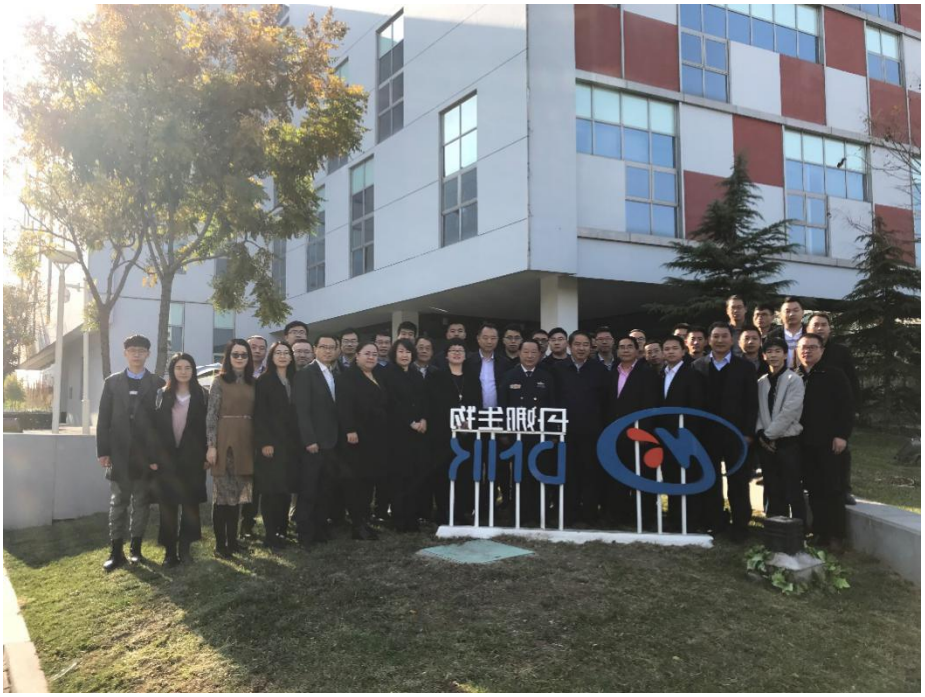

廖万清院士同丹娜全体职工合影

延安市人民医院廖万清院士工作站

廖万清院士专家团队潘炜华教授莅临延安市人民医院指导工作

为进一步深入了解和掌握延安市皮肤科院士专家工作站的建设情况，12 月 22 日，第二军医大学附属上海长征医院皮肤病与真菌病研究所副所长、上海市医学真菌研究所副所长、上海领军人才、廖万清院士专家团队成员潘炜华教授莅临延安市人民医院检查指导皮肤科院士专家工作站工作。市政协副主席、延安市人民医院院长蔺广东出席座谈会并讲话。皮肤科主任熊林、检验科主任曹云、科教科副科长师丽陪同检查。来自科教科、皮肤科、检验科等科室近 20 人参加了座谈会。

当天，潘炜华教授在延安市人民医院检验科培训示教室作了题为《临床真菌感染的检测及诊疗思路》的学术讲座。她分别从基础概念、诊断思路、检测方法与技术、临床应用四个方面进行了深刻阐述，内容丰富实用，使在场人员深感获益匪浅。

培训结束后，潘炜华教授先后走访了工作站办公场所和真菌实验室，她从资金投入、场地建设、人员梯队和实验数据四个方面深入考察，并对医院的全方位投入表示了充分肯定。

“大家一定要做好实验标本的采集和保存工作，尤其是在遇到少见、罕见的标本时，可以及时联系我们并从原始标本里取样寄给我们，通过‘两地实验、一个标本、一个结果’的实验模式共同促进我们真菌实验的发展。”潘教授在检查中强调：“真菌实验的原始标本和实验数据的完整保存，是我们开展科学研究和指导临床实践的基础条件，至关重要。”

座谈会上，潘炜华教授从场地建设、科研课题申报、论文发表等方面做了具体指导。她特别指出，工作站后期的运行要抓住两个重点：一是皮肤科设立浅部真菌实验室，用于浅部真菌的实验和研究，并以此为契机开展相关新技术新业务；二是检验科要充分利用真菌实验室开展好深部真菌的实验、培养和研究工作，要切实做到“从临床实验走向基础研究”，为夯实科研基础走好第一步。

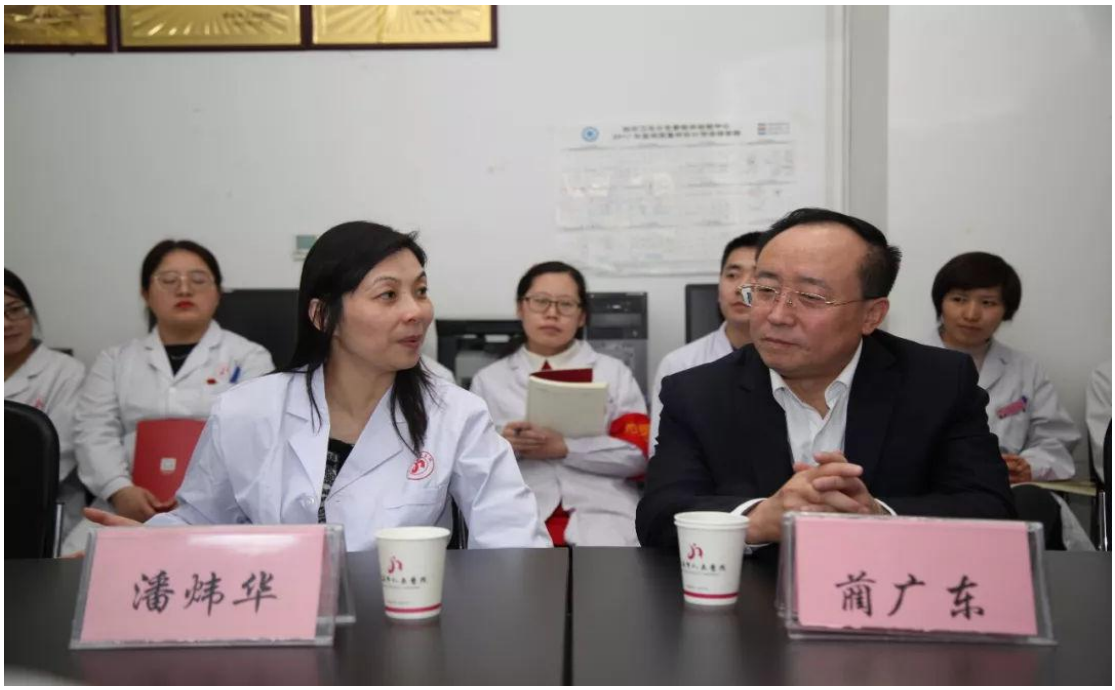

市政协副主席、延安市人民医院院长要求，各相关科室要尽快落实潘炜华教授的具体要求，积极开展新技术新业务，不断提高临床技术水平和科研能力，全力以赴打造陕北首家真菌实验中心。

据悉，延安市人民医院皮肤科院士专家工作站为西北首家皮肤专业院士专家工作站，隶属于陕西省科学技术协会。该工作站设在延安市人民医院皮肤科，其中真菌实验室设在检验科。现阶段，该工作站已经明确了工作职责，并从标本采集、实验研究、科研学术等方面开展相关工作。

江西胸科医院院士工作站

实验室副主任潘炜华教授莅临江西省胸科医院院士工作站视察并指导工作

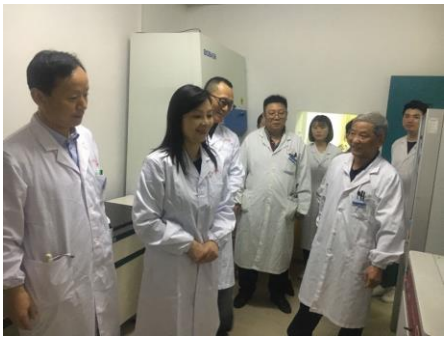

2018 年 10 月 28 日下午，上海长征医院真菌病研究所潘炜华教授莅临院士工作站（省胸科医院致病真菌临床研究及脑脊液实验室）指导工作，这是自我院脑脊液研究室今年 3 月搬迁并扩大装修以来的首次视察。陪同的有江西省胸科医院院长许斌、神经重症医学科主任张齐龙及科室部分成员。

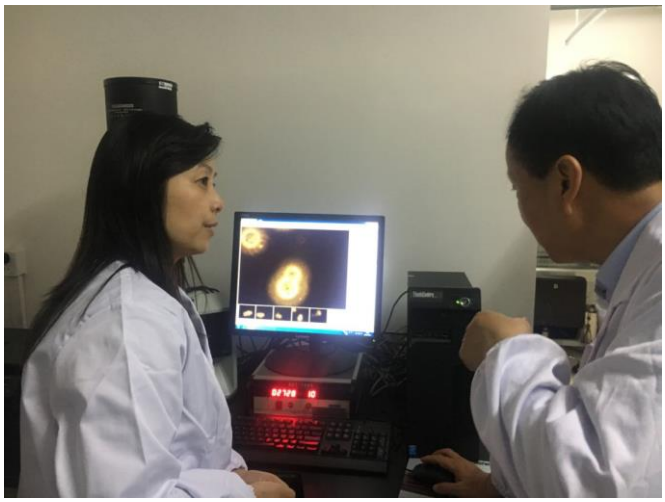

许院长代表江西省胸科医院对潘炜华教授百忙之中莅临本工作站指导工作表示热烈欢迎，同时，对廖万清院士及长征医院院士团队人员给予本工作站诸多的关怀和支持表示衷心的感谢；张齐龙主任向潘炜华教授详细汇报了目前院士工作站主要的工作内容和方向。并就今后如何加强科研合作、推动科研成果转化等进行了深入的探讨和广泛的交流。

潘炜华教授边耐心听取汇报边认真指导各项工作，并对工作站新开展的用超高倍显微镜在暗视野下观察隐球菌给予充分肯定，同时高度赞扬了我院在隐球菌脑膜炎的检出率和救治水平，并表示希望加强交流，相互借鉴经验，促进共同发展。

自 2017 年 12 月我院脑脊液研究室与上海长征医院真菌病研究所廖万清院士签约院士工作站以来，潘炜华教授已多次来江西参加各种学术会议讲学授课。此次莅临指导，对我院进一步凝练工作站建设目标、理清建设思路、设计合理的实验课题等都具有重要启发意义。会后，潘炜华教授还与大家进行亲切的交谈并合影，希望我院能通过工作站的建设不断提高技术水平与服务水平，为病人提供准确快速的诊断和精准有效的治疗，更好地为人民群众健康服务！

粤东医院廖万清院士工作站

一）粤东医院成功举办廖万清院士工作站启动仪式暨第二届粤东皮肤科发展论坛

为进一步促进粤东地区皮肤学科的发展，加强国内的学术交流，粤东医院于 2018 年 2 月 8、9 日举办了廖万清院士工作站启动仪式暨第二届粤东皮肤科发展论坛。本次活动的亮点是廖万清院士工作站落户粤东医院，此外，国内皮肤科学界大伽齐聚粤东，交流讨论皮肤学科发展趋势和最新研究进展，并为皮肤病患者义诊。

2 月 8 日，廖万清院士工作站启动签约仪式在粤东医院门诊大楼六楼会议室举行。上海长征医院廖万清院士的代表陈敏医师，梅县区人民政府副区长管纪城，梅州市科学与技术局副局长熊华、科长梁小向，梅州市卫计局副局长刘水，梅县区人大常委会副主任、梅县区卫计局局长叶世振，梅县区科工商务管理局局长张云龙、副局长何国材和粤东医院领导班子、职能部门代表参加。会上，陈敏医师和粤东医院常务副院长陈燕铭代表双方共同签署了合作建站协议书，并将廖万清院士本人所著的《现代真菌病学》一书赠与医院。随后，陈敏医师、管纪城副区长、熊华副局长、刘水副局长、叶世振局长和陈燕铭常务副院长共同为工作站揭牌。廖万清院士专程拍了一个视频向梅州的乡亲们问好，祝贺院士工作站的启动，并祝愿粤东医院事业发达，越来越兴旺，更好地为广东人民群众服务。通过视频，他和大家分享了他的昨天、今天和明天，他深情地讲到，是党、国家和家乡人民的培养，让他成为了一名中国工程院院士，他的昨天、今天和明天概括起来就是为理想矢志不渝，为事业坚韧不拔。

廖万清院士工作站揭牌

2 月 9 日，由梅州市医学会主办，粤东医院承办的第二届粤东皮肤科发展论坛在粤东医院门诊大楼八楼会议室顺利举办。梅州市卫计局副局长洪霞、梅州市医学会会长张荣在、梅县区卫计局副局长梁碧梅出席大会。廖万清的院士代表潘炜华教授、中华医学会皮肤性病学分会主任委员郑捷教授、中国医师协会皮肤科医师分会会长李恒进教授、中华医学会皮肤性病学分会候任主任委员陆前进教授、中国医师协会皮肤科医师分会副会长刘玮教授、中国医

师协会皮肤科医师分会副会长李利教授、广东省医学会皮肤性病学分会主委曾抗教授、广东省医师协会皮肤科医师分会副主委李其林教授、邓列华教授和陆春教授等国内皮肤科学界大伽齐聚粤东带来了一场国家级学术盛宴，吸引了 200 多名来自梅州、惠州、河源、江门和汕头各级医院的医务人员前来参加。中山大学附属第三医院皮肤科主任赖维教授主持开幕式。学术活动启动仪式上，粤东医院还进行了皮肤科成立的揭牌仪式，市、区领导们、皮肤科学界大伽们和粤东医院党总支书记沈友权共同为粤东医院皮肤科开科揭牌。

廖万清院士工作站签约仪式

9 日下午 3：30-6：30，赖维、曾抗、韩建德、陆春、李其林、邓列华六位教授在门诊大楼四楼皮肤科联袂义诊，帮助广大皮肤病患者摆脱疾病的痛苦。梅州、河源、汕头、惠州等地区的患者慕名前来就诊。专家们耐心地解答每一位群众的疑问,用专业知识细致地为他们诊治。群众们对专家的医疗水平、服务态度纷纷表示满意。据统计,此次专科义诊为 180 多名患者提供了医疗服务,取得了良好的社会效益。

本次活动取得了圆满的成功。廖万清院士工作站这一科研平台落户于粤东医院，将通过联合研究、联合培养科技创新型人才、联合开展高层次学术或技术交流活动等方式，进一步提升粤东医院在皮肤病相关领域的临床诊疗水平和科研能力，更好地服务于社会、服务于患者。

廖万清院士讲话

领导和皮肤科医务人员合影

论坛现场

皮肤科开科揭牌

义诊现场

二）粤东医院举办廖万清院士工作站启动授牌仪式

为了提升广东粤东地区医学真菌领域的研究水平，促进资源共享和合作，2018 年 8 月 24 日，廖万清院士工作站在粤东医院皮肤科正式挂牌。中国工程院院士廖万清，梅县区委书记钟光灵，梅县区政协副主席、粤东医院管理顾问李刚教授，梅县区卫计局局长钟匡仁，粤东医院党总支书记沈友权和中山三院皮肤科赖维教授出席挂牌仪式并为工作站揭牌。

廖万清院士工作站是由梅州市政府推动、以粤东医院为依托，联合进行科学技术研究的高层次科技创新平台。工作站将通过联合研究、联合培养科技创新型人才、联合开展高层次学术或技术交流活动等方式，将粤东医院皮肤科打造成粤东地区乃至广东省一流的皮肤科，为梅州及周边地区的医疗学术及创新提供强有力的支撑。

廖万清院士表示，工作站建成投入使用后，将逐渐完善内部建设，开展有粤东特色的主要包括皮肤癣菌病、孢子丝菌病等皮肤真菌病的研究工作，进一步联合申报省级以上研究课题，建立专业研究人员的真菌研究团队，保持并加强皮肤真菌病方面的诊治优势，推动粤东医院皮肤科诊疗水平达到国内先进水平，真正做到造福百姓。

廖院士作专题讲座，题为：我的昨天、今天和明天

来院期间，廖万清院士一行对粤东医院建设、廖万清院士工作站建设等情况进行了详细考察，并与粤东医院领导班子、相关部门负责人进行座谈。同时，中山三院皮肤科、粤东医院皮肤科联合举办了粤东地区医学真菌高峰论坛暨前沿技术培训班。培训班上，廖万清院士和大家分享了他的昨天、今天和明天，感谢梅县家乡人民的养育之恩，讲述了他的成才之路以及所取得的成就，表达了对真菌研究和医学真菌方面发展的憧憬和希望。随后，上海长征医院潘炜华教授、中山三院赖维教授等就医学真菌临床和基础研究热点，以及抗真菌药物研发的最新成果进行授课。此次培训班吸引了近百名粤闽赣周边地区从事病原真菌的基础研究人员、临床工作者（皮肤科、检验科和血液科等）特地前来参加，是一场难得的学术盛宴。所有与会人员更是非常珍惜本次交流学习的机会，认真听取了专家教授的授课，并对专家的精彩讲述予以热烈掌声。

会后廖万清院士接受梅县电视台的采访

余杭中医院廖万清院士工作站

一）廖万清院士团队到余杭区中医院合作前调研

6 月 8 日，中国工程院院士廖万清技术团队一行 5 人到余杭区中医院进行合作前调研。区政协副主席陈云水、区卫计局局长陆永林、区卫计局党委委员冯天元陪同。

院士技术团队首先来到门诊部，了解医院的整体环境，实地查看皮肤科、检验科两个科室的设备设施，随后双方到会议室就合作事宜进行商谈交流。

院士工作站一旦在余杭落地，将主要开展五方面工作：

- 一是在院士工作站支持下提升区中医院乃至余杭区皮肤科诊疗水平，成为区域皮肤病诊疗中心和全省真菌病的研究高地，造福百姓。

- 二是借助院士工作站品牌招录高层次人才，解决区域内重症皮肤病患者病痛，拓宽皮肤病研究领域，填补我区皮肤病基础研究空白。

- 三是为全区医疗单位开展皮肤科及相关工作人员培训，提升全区皮肤科工作人员临床技能及科研能力。

- 四是发挥院士工作站在真菌病领域的研究优势，成立区域真菌检查和治疗中心，包括深部真菌的诊疗，为全区真菌领域诊疗提供技术科研支撑。

- 五是借助院士工作站号召力，通过举办大型国家级学术交流等活动，提升医院及医院皮肤科影响力，并在周期内成功申报杭州市级重点学科乃至浙江省级重点学科。

座谈交流结束后，廖万清院士还将刚主编出版的《现代真菌学》书籍赠送给了区中医院。

二）中国工程院廖万清院士工作站落户余杭中医院

2018 年 07 月 21 日中国工程院廖万清院士工作站落户余杭区中医院，这是余杭区公立医疗机构引进的首个院士工作站，意味着余杭百姓今后在家门口就能享受到“院士级”专家的医疗服务。副区长许玲娣参加签约仪式。

会议期间，廖万清院士给参会医务人员做了题为“医学真菌研究的前沿和热点”的专题报告。

院士工作站挂牌后，院士团队专家将每两周一次来余杭区中医院坐诊，院士本人每季度到余杭区中医院工作一天，为余杭及周边地区的疑难、重症皮肤病、真菌患者诊疗，帮助提升余杭区中医院及余杭区皮肤病诊疗能力和科研水平，推荐或协助高层次人才招录，促进相关学科建设并成立皮肤病实验室。院士工作站在真菌领域的研究优势将为全区真菌病诊疗提供技术支撑，协助成立区域真菌检查和治疗中心，同时带动检验、重症医学、肿瘤等相关学科的发展，进一步满足余杭市民对优质医疗资源的需求。

嘉兴港区医院廖万清院士工作站

廖万清院士受邀参加“星耀南湖”精英峰会，参加工作站授牌仪式

连续 10 年举办的“星耀南湖”精英峰会，早已成为嘉兴不忘初心、久久为功，打造人才高地，推动创新发展的最好注脚。本届峰会将继续携手浦江创新论坛，紧扣“确立人才引领发展的战略地位”要求，围绕“人才驱动创新、创新引领产业”主题，突出实效性、引领性、高端性、国际性，推进人才与科技、人才与文化的融合发展，搭建人才与企业、项目与资金、产品与市场的对接平台，为打造具有国际化品质的现代化网络型田园城市提供有力人才保障。

市领导为中国工程院廖万清院士和上海市东方医院嘉兴港区医院授牌

在举行授牌、颁证仪式上，嘉兴市人大常委会副主任沈利农先生，嘉兴市政协党组副书记、副主席孙建华先生为院士专家工作站代表授牌。

廖院士团队和嘉兴港区医院谭军副院长合影

河北工程大学附属医院廖万清院士工作站

河北工程大学附属医院廖万清院士工作站揭牌仪式暨皮肤科真菌高峰论坛在邯郸市举行

2018 年 11 月 2 日，河北工程大学附属医院廖万清院士工作站揭牌仪式暨皮肤科真菌高峰论坛在邯郸市举行。廖万清院士、河北省教育厅党组成员、副厅长王廷山、河北工程大学党委书记哈明虎、河北工程大学校长王延吉、邯郸市政府副市长杜树杰、河北省卫计委科教处处长尤殿平、邯郸市科技局局长安凤玲、邯郸市卫生计生委主任周海平、上海长征医院皮肤科潘炜华教授、方文捷秘书、武汉协和医院皮肤科冯爱平教授、河北工程大学副校长、河北工程大学附属医院院长刘志军等参加仪式，河北工程大学附属医院党委书记高红旗主持揭牌仪式。

据了解，河北工程大学附属医院院士工作站将依托上海长征医院皮肤科廖万清院士及其专家团队在临床科研方面的技术优势，在邯郸聚焦一批高端临床、科研及实验室高端人才和创新团队，建立以邯郸市为中心的区域真菌性皮肤病及免疫性皮肤病治疗中心，造福邯郸地区人民。

邯郸市政府副市长杜树杰与廖万清为工作站揭牌

此次成立的院士工作站是河北工程大学附属医院与廖万清院士及其团队合作设立，是由河北省科技厅、省委组织部、省科协联合各主管部门共同发文批准成立的，并纳入省级院士工作站建设序列。工作站设立后，廖万清院士带领他的专家团队在临床科研方面的技术优势，在邯郸聚焦一批高端临床、科研及实验室高端人才和创新团队，建立以邯郸市为中心的区域真菌性皮肤病及免疫性皮肤病治疗中心。

河北工程大學附屬醫院
Affiliated Hospital of Hebei University of Engineering

据悉，河北工程大学附属医院始建于 1970 年，经过 40 多年的风雨春秋，现已发展成为一所集医疗、教学、科研、康复、预防、急救为一体的大型三级甲等综合医院。医院皮肤科是国家级重点专科建设项目，是河北省重点学科，成立了北京市皮肤病专家会诊中心邯郸基地。数十年来，附属医院皮肤科始终薪火传承，初心不忘，从建科初始的一桌、一凳、一室，目前已成为立足邯郸、辐射周边四省的集临床、科研、教学为一体的品牌科室。科室率先在邯郸地区建立了真菌实验室，配备了显微镜，有专门的实验技术人员，开展真菌相关的实验检查，并在上世纪发现了葡萄状佛隆那菌引起皮肤暗色丝孢霉病，此发现属国际首例，填补了世界空白，并获得河北省科技进步二等奖。来自全市 300 余名医务工作者参加仪式。

在皮肤科真菌高峰论坛上，廖万清院士以“‘海上丝绸之路’沿线国家重要真菌防控”为主题，与医务工作者进行了学术交流

上海长征医院潘炜华讲授分别讲授了微生态与真菌性皮肤病、浅表真菌病的诊断与思考学术讲座。

长江润发集团院士专家工作站

廖万清院士参观海南海灵药业

10 月 18 日，长江润发集团院士专家工作站主任、中国工程院院士、世界华人皮肤科医师协会会长、上海长征医院皮肤科教授廖万清一行来我司参观指导。海灵药业执行总裁陆一峰、长江润发集团总裁助理李一青、海灵药业市场总监曹涛热情接待了来访一行。

在公司展厅，陆总向廖院士详细介绍了长江润发集团的发展及我司的现状、规划及发展前景。海灵药业秉承“为大众健康孜孜以求”的愿景，以打造中国领先的健康产业平台为目标，志在为广大临床医师和患者提供更加有效、安全的优质药品。

廖院士在听取了陆总的介绍后，充分认可了海灵药业的优质产品及发展目标。他说，为人民健康服务是中国制药企业的核心责任。廖院士对集团的规模及发展情况表示肯定，对大健康领域的发展也提出许多宝贵意见，并就双方在抗真菌领域的合作进行了深入的探讨。

海灵药业一直以来始终致力于抗感染制剂的研发、生产和销售，是国内细分医药行业领域的龙头企业。2016 年被长江润发并购之后，不断调整和提升发展思路，延伸产品领域，并取得了良好的效果，海灵药业持续保持稳健的发展态势。

雅蒂院士专家工作站

廖万清院士到访雅蒂化妆品集团并达成初步合作意向

2018年7月16日，廖万清院士受邀到访汕头市雅蒂化妆品有限公司。雅蒂公司总经理王泽辉率公司全体管理团队,对廖院士一行的到来表示最热烈的欢迎。

廖院士一行首先依次参观了雅蒂公司的办公场所、产品展厅、实验室以及生产车间,然后宾主双方在总经理室进行座谈。雅蒂公司总经理王泽辉首先为嘉宾们就企业的愿景、使命、科研成果等进行简要的汇报。然后双方就肌肤健康管理行业的发展、科技创新、人才培养等方面进行了热烈、深入的交流,廖院士一一给出了很多前瞻性的指导性意见,整个座谈会现场探讨交流氛围异常浓烈。

大专家.com 院士专家工作站

2018 年 11 月 23 日大专家.com 来访交流吴翀博士一行来访

大专家.com 吴翀博士一行来访，与廖万清院士课题组成员深入讨论了皮肤病 OK 系统的构建、真菌大数据的构架等。廖万清院士亲切接待了吴翀博士一行。

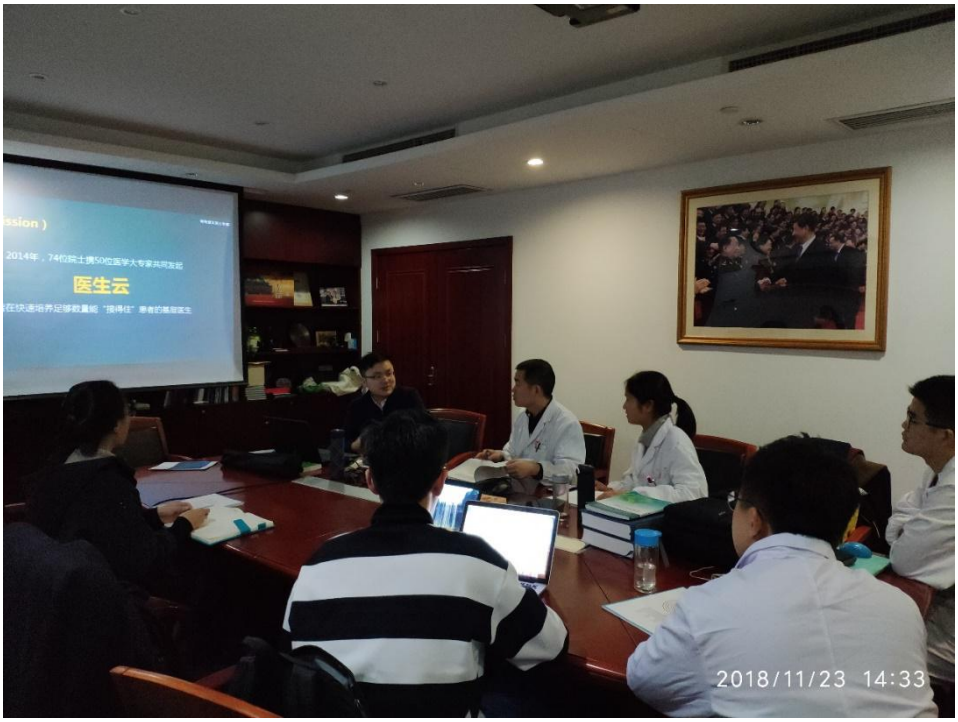

六、2018 年度服务军民情况

一、为军服务

一）朱红梅副教授参加“和谐使命-2018”任务。

2018 年 06 月 29 日海军和平方舟医院船在任务指挥员管柏林、秦威率领下，从浙江舟山某军港解缆起航，赴巴布亚新几内亚、瓦努阿图、斐济、汤加、哥伦比亚、委内瑞拉、格林纳达、多米尼克、安提瓜和巴布达、多米尼加、厄瓜多尔 11 国进行人道主义医疗服务，执行“和谐使命-2018”任务，并应邀赴智利参加其海军成立 200 周年庆典活动。这是该医院船第七次执行“和谐使命”任务。

二）潘炜华教授参加长征医院“移动课堂”

2018 年 12 月上旬，研究所副主任潘炜华教授带队海军军医大学附属长征医院“移动课堂”教学小分队来到上海某部，为舰艇官兵送去了一场健康保健、疾病防治知识讲座并进行了义诊活动。本次活动受到了舰艇全体官兵的一致好评，纷纷称赞专家们的讲座言简意赅，深入浅出、精彩纷呈，讲座内容贴近舰艇训练和生活，科学实用，指导性强。潘炜华教授就湿疹、痤疮、虫咬性皮炎、体癣等舰艇环境下常见皮肤病的治疗和预防展开宣讲，她的授课图文并茂，形象实用。长征医院“移动课堂”巡教项目是贯彻落实习主席、军委、海军和学校党委的决策指示，对标医院党委扩大会议关于“打造海卫特色教学品牌”的具体任务，探索将院校教育与部队训考相结合、医疗服务与教书育人相结合，教学实践与教改研究相结合的海军卫勤医教研工作联动推进的创新模式和方法。“移动课堂”按照“贴近海军、贴近基层、贴近实战”的基本要求，依托舰艇现有卫勤保障与战救装备器材，以海军

舰艇单位卫勤保障力量为主要培训对象，探索面向全体官兵拓展、实现整舰全员覆盖，切实提高受训人员实战技能的有效途径。让舰艇卫勤保障力量“动起来”、让现有列装卫勤装备“活起来”。目前，小分队在东海舰队已展开巡教活动，并取得初步成效。

三三）其他军事任务

2018 年 1 月-2018 年 4 月　　张超参加 2018 年度海军招飞全面检测工作

2018 年 6 月-2018 年 7 月　　张超参加 2018 年度海军招飞定选工作

2018 年 11 月- 2020 年 1 月 张超参加中国驻吉布提保障基地保障任务

2018 年 9 月-2018 年 12 月 潘搏参加南海保障任务

2018 年 12 月-2019 年 2 月 陈敏参加 2018 年度海军招飞工作

2018 年 12 月—2019 年 3 月方伟参加海岛任务

四四）廖万清院士前往八路军一二九师司令部旧址。祭拜革命英烈

2018 年 11 月 02 日廖万清驱车前往河北邯郸涉县，于八路军一二九师司令部旧址祭拜革命英烈。抗日战争时期，涉县是边区根据地的腹心地、首府县，地处华北抗战前哨，为华北抗战战略要地，八路军 129 师在刘伯承、邓小平等师首长率领下，临危受命、东渡黄河、挺进太行，运筹涉县赤岸村，浴血千里太行山，打响了抗日战争中长生口、神头岭、响堂铺和解放战争中上党、平汉等著名战斗、战役，曾有一百一十多个党、政、军、财、文等机关单位在涉县驻扎长达五年之久。

廖万清院士为八路军英烈敬献花圈，并深情鞠躬

二、义诊和其他民间交流

一）廖万清院士为深圳市慢性病防治中心多名疑难皮肤病患者义诊

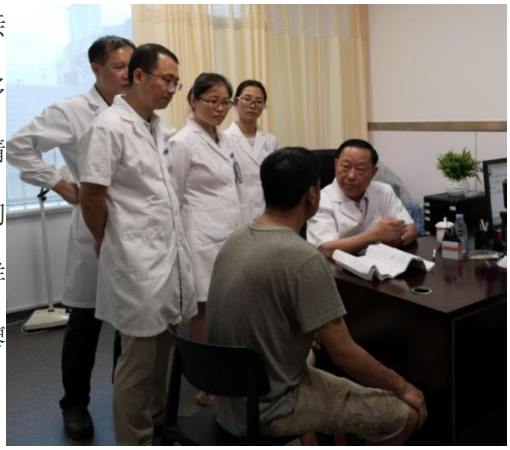

7 月 14 日下午，中国工程院院士廖万清，亲临深圳市慢性病防治中心皮肤病防治研究所为多名疑难皮肤病患者进行会诊。八十岁高龄的廖万清院士认真听取了主管医师汇报的每一例患者，并询问病情，亲自为患者进行全面仔细的体格检查，详细地分析了病情，为下一步治疗给予指导意见。廖院士会诊后，还细心叮嘱患者饮食注意事项。

廖院士表示，深圳市慢性病防治中心就诊环境舒适，中心领导十分重视皮肤病研究所的发展，医护团体强大，积极向上，做到了临床和科研并轨发展，寄望中心医务人员今后继续努力，活到老学到老，通过科学研究解决临床问题，造福广大群众，为理想要孜孜不倦，为事业要坚韧不拔。

廖万清院士参观深圳慢病防治所

廖万清院士深圳慢病防治所皮肤科全体员工合影

二）廖万清院士参加苏州“寒山检验高峰论坛”，并会疑难病例

2018年6月9日，第二届寒山检验医学高峰论坛在高新区人民医院开幕，中国工程院院士廖万清、阮长耿与来自全国各地的顶尖专家、学者600余人汇聚一堂就检验医学的前沿发展进行观点碰撞、智慧交锋。廖万清院士在开幕式上做了大会致辞。

会后，廖万清院士参加了高新区人民医院疑难病例会诊，该患者经院士查房，最终确诊为罕见的地霉属感染病例，最终得到了正确的治疗。

三）廖万清院士入住皮肤宝网络问诊平台，为患者免费诊治

10 月 10 日，皮肤科院士廖万清教授上线皮肤宝在线问诊平台，这是目前国内互联网医疗所有的诊疗平台中首次有院士级别专家入驻。据悉，皮肤宝 APP 在 2016 年 3 月上线，由爱肤宝(上海)信息科技有限公司发布，产品上线以来，开通了医疗“电子处方”、“送药到家”等多项在线服务。

皮肤科医生通过皮肤宝 APP 在线为患者提供皮肤健康及护肤咨询服务，一方面，帮助医

生采集门诊患者病例，线上管理，为皮肤疾病+护理的健康管理进行互联网赋能；另一方面，患者除了能够得到更快捷的诊疗，还能获得更个性化的辅助治疗和护肤建议。同时利用积累的大数据，推出真正有效改善皮肤问题的精准药妆。

廖万清院士为皮肤宝题词：“祝皮肤宝越办越好，造福于民！”

四）廖万清院士抵深为瑞敏皮肤病医院疑难皮肤病患者会诊

今年 80 岁高龄的廖万清院士是皮肤病学专家、医学真菌学专家，他是中国菌物学会医学真菌专业委员会副主任委员、中国医院真菌感染学会副主任委员、中国菌物学会理事、中国中西医结合学会皮肤性病专业委员会常委兼真菌病研究学组主任委员等。多年来，他与深圳瑞敏皮肤科医院形成学术合作，定期来深提供支持。

在当天的会诊中，他为银屑病、黑棘皮病等疑难皮肤病患者进行会诊，前来就诊的患者中不乏治疗多年、病情反复，或者此前一直未能获得明确诊断的病人，甚至还有一位小患者从小受遗传性过敏性湿疹折磨，生长发育严重受到影响，治疗了 10 年也未能治愈。廖万清院士为这些患者提供了治疗方案，并为他们提供了日常生活的健康指导。

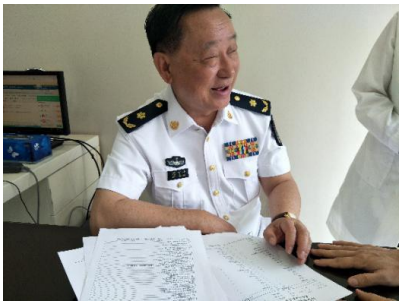

五）廖万清院士参加杨浦区迎重阳、重传统、传美德活动

敬老孝亲庆重阳　墨香雅韵传家风

——廖万清院士参加杨浦区迎重阳、重传统、传美德活动

丹桂正飘香，最美是重阳。2018 年 10 月 15 日上午，在重阳节来临之际，在一段歌声传递中华风韵、一幅长卷描绘灿烂童心、一方花糕承载敬老美德的氛围中，杨浦区文明办和教育局主办的我们的节日“敬老孝亲庆重阳 墨香雅韵传家风”迎重阳、重传统、传美德活动在控江二村小学举行。廖万清院士受到工程院上海中心以及政府邀请参加了此次活动。

1、参加升旗仪式

伴随着悠扬的古风吟唱，升旗仪式正式开始。少先队员行队礼，廖院士敬军礼，相得益彰，灿烂的阳光下闪耀着希望的光芒。升旗仪式之后，廖院士牵手两名中国少年科学院小院士，一起对话交流，一起共话美德。

2、发放证书和颁奖

欢快的乐曲声响起，灵动的非遗传统剪纸舞蹈令人陶醉。为了更好地参与、宣传即将到来的进博会，舞蹈之后为进博会宣传小志愿者们发放了证书，为 2018 年杨浦区中小学生“家风传少年 墨香润心田”家风家训书法作品一等奖获奖者颁奖。

3、参观书法作品展

在小院士们的引导下，廖院士还参观了杨浦区中小学生“家风传少年 墨香润心田”家风家训书法作品展，现场还有学生与书法家泼墨挥毫，分享从“守礼养德”到“家国天下”凝聚智慧的家风祖训，廖院士亲切的与大家分享自己的心得和体会。

4、大小院士面对面

廖院士与小院士们面对面零距离交流，引导他们更好地熟悉家风家训，激励他们感恩于心，回报于行，将严谨的求学问道精神铭记于心。

古人云：年高喜赏登高节，秋老还添不老春。此次活动，通过升旗仪式与书法展示相结合的方式，通过廖院士和小院士对话的方式，通过非遗展示和家长学生互动的方式，多方融合，将中华传统节日赋予新的时代内涵，焕发新的文化活力，进一步弘扬了传统美德，极好地推动杨浦形成孝亲敬老的良好风尚。

六）梅县区委书记钟光灵来访

广东梅县区委书记钟光灵在上海招商引资期间，专程前往长征医院拜访中国工程院院士廖万清，向他介绍了家乡梅县经济社会发展情况，并致以诚挚的问候和美好的祝福。


钟光灵来到廖万清院士位于上海长征医院的办公室，与他促膝交谈，关切询问他的身体和生活情况，并详细介绍家乡梅县近年来在经济、社会、医疗、教育等方面取得的成果，虚心听取他对梅县加快振兴发展的意见建议。钟光灵说，近年来，梅县坚持以习近平新时代中国特色社会主义思想为指导，持续改善民生福祉。特别是在廖院士的直接关心支持下，粤东医院顺利创建三甲医院，该院的皮肤科也成为品牌科室。他诚挚希望廖万清院士更多地关心支持家乡建设，发挥在科研方面的领先技术优势，为梅县培养和引进更多优秀的医技人才。

廖万清对家乡当前加快发展的态势感到由衷高兴，充分肯定了家乡梅县在经济社会特别是医疗、教育、新农村建设等方面取得的成就。他表示，将尽力为梅县经济社会和医疗卫生事业发展贡献自己的一份力量。

会后，钟光灵想院士献上“松口画卷”。有千年历史的松口古镇，是明末以后客家人出南洋的第一站，也是孙中山发动辛亥革命的策源地之一，更被评为广东十大海上丝绸之路文化地理坐标

区人大常委会主任曾庆辉，区委常委、副区长潘雪松等一同拜访。

七、中国真菌学杂志

中国真菌学杂志贯彻党和国家的卫生工作方针政策，主要报道我国真菌学特别是医学真菌学的最新研究进展，内容涉及基础医学与临床医学中的大部分专业，以从事皮肤、感染、血液、呼吸、器官移植、肿瘤、急救、创伤、检验等与真菌感染专业有关的中高级医务人员及从事微生物学、分子生物学及药学等基础研究的研究人员为主要读者群，是真菌学工作者之间交流的窗口和平台。

2018 年《中国真菌学杂志》一共刊发 6 期，录用稿件 107 篇。

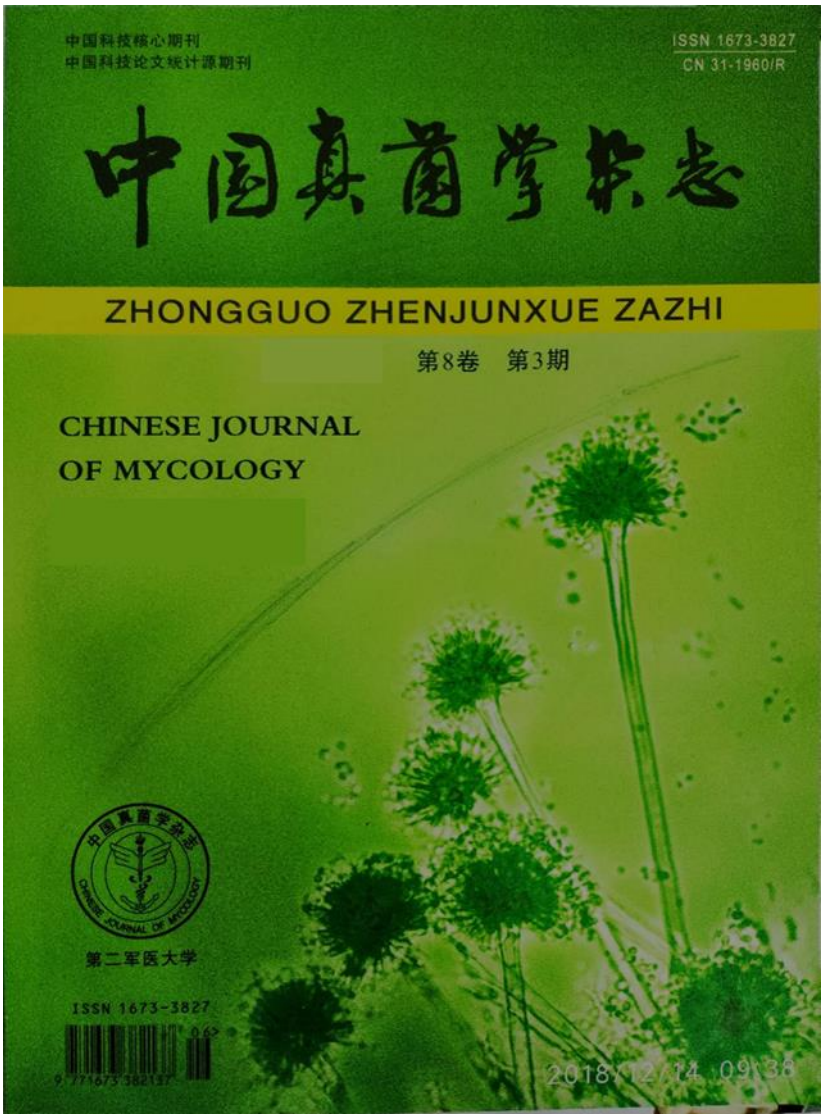

附件：2018年实验室部分SCI文章原文

ISHAM INTERNATIONAL SOCIETY FOR HUMAN AND ANIMAL MYCOLOGY

Medical Mycology, 2018, 56, 695–702
doi: 10.1093/mmy/myx108
Advance Access Publication Date: 8 December 2017
Original Article

Original Article

Direct detection of *Exophiala* and *Scedosporium* species in sputa of patients with cystic fibrosis

Min Chen[1,2,3,*], Nahid Kondori[4], Shuwen Deng[7], A. H. G. Gerrits van den Ende[2], M. Lackner[5], Wanqing Liao[1] and G. S. de Hoog[1,2,3,6,*]

[1]Department of Dermatology, Shanghai Key Laboratory of Molecular Medical Mycology, Shanghai Institute of Medical Mycology, Shanghai Changzheng Hospital, Second Military Medical University, Shanghai, 200003, China, [2]Westerdijk Fungal Biodiversity Institute, Utrecht, The Netherlands, [3]Institute of Biodiversity and Ecosystem Dynamics, University of Amsterdam, Amsterdam, The Netherlands, [4]Department of Infectious Diseases, Sahlgrenska Academy, University of Gothenburg, Sweden, [5]Division of Hygiene and Medical Microbiology, Medical University of Innsbruck, Innsbruck, Austria, [6]Peking University First Hospital, Research Center for Medical Mycology, Beijing, China; Department of Basic Biology, University of Paraná, Curitiba, Brazil and [7]Department of Medical Microbiology, People's Hospital of Suzhou National New & Hi-Tech Industrial Development Zone, Jiangsu, China

*To whom correspondence should be addressed. Min Chen. E-mail: chenmin9611233@163.com
G. S. de Hoog. E-mail: s.hoog@westerdijkinstitute.nl

Received 26 June 2017; Revised 31 August 2017; Accepted 5 October 2017; Editorial Decision 17 September 2017

Abstract

Detection of species of *Exophiala* and *Scedosporium* in the respiratory tracts of cystic fibrosis (CF) patients remains controversial because of highly variable results. The results of our study suggested a significantly higher prevalence and more complex colonization than previously estimated. Approximately 17% (27/162) of clinical sputum samples were found to be positive for *Exophiala dermatitidis* and 30% (49/162) were positive for *Scedosporium apiospermum* / *S. boydii* species complex determined by reverse line blot (RLB) hybridization. In contrast, only 14.2% (23/162) and 1.2% (2/162) of clinical sputa were positive for *E. dermatitidis* and *S. apiospermum* / *S. boydii* species complex when tested by culture, respectively. Molecular detection methods, such as loop-mediated isothermal amplification (LAMP) or reverse line blot (RLB) hybridization, have the potential to become powerful alternatives to selective culture, providing a more realistic understanding on the prevalence of *E. dermatitidis* and *S. apiospermum* / *S. boydii* species complex in the respiratory tract of CF patients.

Key words: *Exophiala dermatitidis*, *Scedosporium*, cystic fibrosis, sputum.

Introduction

Affecting over 70,000 individuals worldwide, cystic fibrosis (CF) is the most common genetically inherited disease among Caucasian populations.[1] CF is caused by mutations in the CF transmembrane conductance regulator (CFTR) protein, which leads to the production of thick and sticky

bronchial mucus that may facilitate microbial accumulation and colonization.[2,3] In addition to bacteria such as *Staphylococcus aureus* and *Pseudomonas aeruginosa*, several fungi colonize the respiratory tracts of CF patients,[3,4] though their prevalence and pathogenicity remain controversial.[5,6] *Aspergillus fumigatus* is the filamentous fungus most commonly isolated from CF patients and is capable of precipitating a chronic allergic inflammatory response or invasive infection after lung transplantation.[4] However, the fungal biota colonizing the lungs of CF patients are more complex and include various non-*Aspergillus* filamentous fungi such as *Scedosporium apiospermum*[7–9] and *Exophiala dermatitidis*.[4,10–12] In the genus *Scedosporium*, *S. apiospermum*, and *S. boydii* have recently been aggregated as the '*S. apiospermum* complex' because of their genetic similarity and the lack of clinical differences observed between sibling species.[13,14]

The black yeast *E. dermatitidis* is another filamentous fungus regularly involved in colonizing the respiratory tract of CF patients.[7–12] Persistent colonization and repeated infection with *E. dermatitidis* or *S. apiospermum* / *S. boydii* may occur in CF patients over decades.[10–12] *Scedosporium* species are resistant to many antifungal agents including amphotericin B.[15] In addition to *Aspergillus* and *Candida*, patients with CF were observed to be colonized by *E. dermatitidis* or *Scedosporium*; however, this may be an artifact because published studies that detected them in combination are scant. In addition, culture only has a limited sensitivity, these species usually remain undetected because they are easily outcompeted by *Aspergillus* and *Candida* species.[15,17] Possible correlations with underlying diseases remain uncertain because of limited amount of data available. An exceptionally high recovery rate of approximately 20% of *E. dermatitidis* was recently reported by incubating sputa on erythritol-chloramphenicol agar (ECA) medium from Sweden, but conventional culture-based diagnosis strategies are hampered by the mucoid consistency of CF sputum or bronchoalveolar lavage (BAL) specimens.[18] Thus, frequencies of accompanying fungi may be underestimated,[12,18] though recent applications of semi-selective media, which inhibit rapidly growing *Aspergillus* and *Candida*, enable fungi with delayed growth to be revealed.[19,20] Detection by culture still requires viable cells in the samples and highly skilled laboratory technicians for successful cultivation.

Molecular techniques have improved detection and thereby our understanding of fungal colonization of the respiratory tracts of CF patients.[21,22] Among these methods, loop-mediated isothermal amplification (LAMP)[21] and reverse line blot (RLB) hybridization[7,21] have shown added value to elucidation of the epidemiology of less common colonizers in the CF patient population.[7,21,22] Molecular detection of *E. dermatitidis* in clinical samples was not conducted frequently to date. Therefore, we compared the detection of *E. dermatitidis*, *S. apiospermum*, and *S. boydii* from CF sputa by two molecular approaches (polymerase chain reaction [PCR]-RLB and LAMP) and culture.[20] The aim of this study is to improve our understanding of the prevalence of *E. dermatitidis*, *S. apiospermum*, and *S. boydii* in the respiratory tracts of CF patients.

Methods

Clinical specimens

Between September and December 2012, a total of 162 sputum specimens from 103 CF patients were collected by the Department of Clinical Microbiology, Sahlgrenska University Hospital, Sweden. Each sample was divided into two portions: one part for the isolation of conventional or semi-selective culture, the other part for molecular detection by PCR-RLB and LAMP assays.

Isolation of fungi from sputum samples by culture

Approximately 1 ml of sputum specimens from each CF patients was routinely cultured on Sabouraud glucose agar (SGA), CHROMagar Candida, maltose agar, and ECA plates. Sputum was liquefied by the addition of pancreatin (10 mg/ml) in a volume ratio of 1/1, vortexed and incubated at 20°C for 5 min prior to culture. Cultures were then incubated at 30°C and examined for fungal growth for up to 20 days. Isolated fungi were identified to the species level using morphological criteria, the ability to grow at present at 42°C and on mycobiotic agar plates supplemented with cycloheximide. A set of reference strains included 46 strains (Table 1) of *E. dermatitidis* and another 22 *Exophiala* species that are taxonomically close to *E. dermatitidis* were obtained from Westerdijk Fungal Biodiversity Institute, Utrecht, The Netherlands, for evaluation of sensitivity and specificity of designed *E. dermatitidis* species-specific primer sets of RLB and LAMP assays according to the previous analysis.[23,24] All reference strains were grown on potato dextrose agar (PDA) at 30°C for 7 days prior to use.

Molecular detection

Genomic DNA from reference strains was extracted using cetyltrimethylammonium bromide (CTAB) as described previously.[14] To extract fungal DNA directly from clinical sputum, a High Pure PCR Template Preparation Kit (Roche Inc., Mannheim, Germany) was used according to

Table 1. Fungal isolates (n = 46) analyzed with PCR-RLB and LAMP assays for detection of *E. dermatitidis.*

Serial number	Strains	Species	Source	PCR-RLB detection	LAMP detection
1	CBS 207.35	*Exophiala dermatitidis*	Clinical strain	+	+
2	CBS 424.67	*Exophiala dermatitidis*	Clinical strain	+	+
3	CBS 632.69	*Exophiala dermatitidis*	Environmental strain	+	+
5	CBS 314.90	*Exophiala dermatitidis*	Environmental strain	+	+
7	CBS 292.49	*Exophiala dermatitidis*	Environmental strain	+	+
8	CBS 109140	*Exophiala dermatitidis*	Environmental strain	+	+
9	CBS 109146	*Exophiala phaeomuriformis*	Environmental strain	-	-
11	CBS 134012	*Exophiala phaeomuriformis*	Environmental strain	-	-
12	CBS 124194	*Exophiala phaeomuriformis*	Environmental strain	-	-
13	CBS 121744	*Exophiala phaeomuriformis*	Environmental strain	-	-
14	CBS 120563	*Exophiala phaeomuriformis*	Clinical strain	-	-
15	CBS 120555	*Exophiala phaeomuriformis*	Environmental strain	-	-
16	CBS 899.68	*Exophiala spinifera*	Clinical strain	-	-
17	CBS 425.92	*Exophiala spinifera*	Environmental strain	-	-
18	CBS 269.28	*Exophiala spinifera*	ND	-	-
19	CBS 668.76	*Exophiala exophialae*	Environmental strain	-	-
20	CBS 507.90	*Exophiala jeanselmei*	Clinical strain	-	-
22	CBS 482.92	*Exophiala angulospora*	Environmental strain	-	-
23	CBS 352.52	*Exophiala bergeri*	Clinical strain	-	-
24	CBS 353.52	*Exophiala bergeri*	Clinical strain	-	-
25	CBS 526.76	*Exophiala bergeri*	Clinical strain	-	-
26	CBS 402.95	*Exophiala mesophila*	Environmental strain	-	-
27	CBS 836.95	*Exophiala mesophila*	Environmental strain	-	-
28	CBS 158.58	*Exophiala castellanii*	Clinical strain	-	-
29	CBS 102400	*Exophiala lecanii-corni*	Environmental strain	-	-
30	CBS 232.39	*Exophiala lecanii-corni*	Clinical strain	-	-
31	CBS 256.92	*Exophiala psychrophila*	ND	-	-
32	CBS 191.87	*Exophiala psychrophila*	ND	-	-
33	CBS 521.82	*Exophiala alcaophila*	Environmental strain	-	-
34	CBS 157.67	*Exophiala salmonis*	ND	-	-
35	CBS 537.73	*Exophiala pisciphila*	Clinical strain	-	-
36	CBS 101610	*Exophiala pisciphila*	Environmental strain	-	-
37	CBS 520.76	*Exophiala moniliae*	ND	-	-
38	CBS 109807	*Exophiala oligosperma*	Clinical strain	-	-
39	CBS 109811	*Exophiala opportunistica*	Environmental strain	-	-
40	CBS 109812	*Exophiala castellanii*	Environmental strain	-	-
41	CBS 115142	*Exophiala cancerae*	Environmental strain	-	-
42	CBS 115831	*Exophiala xenobiotica*	ND	-	-
43	CBS 117641	*Exophiala xenobiotica*	Clinical strain	-	-
44	CBS 118722	*Exophiala alcalophila*	Environmental strain	-	-
45	CBS 119638	*Exophiala heteromorpha*	Environmental strain	-	-
46	CBS 119912	*Exophiala aquamarina*	Clinical strain	-	-

ND, no data; +, positive result; -, negative result.

the manufacturer instructions with two modifications: eight acid-washed glass beads (diameter 10 mm) were separately added into 1 ml of each clinical sample and thoroughly shaken using a MoBio vortex for 10 min, after which proteinase K (40 μl) digestion was performed at 70°C for 1 hour instead of 10 min. The quality of extraction of fungal DNA was quantified using a NanoDrop 2000 spectrophotometer (Thermo Fisher, Wilmington, DE, USA). DNA Samples were stored at −20°C until use. During the period of the molecular detection, we simultaneously collected 1 ml human sputum from one single healthy donor in Utrecht, The Netherlands, which was tested as a negative control. Fungal cells of *S. apiospermum* type strain CBS 116899^T (ranging from 8600 cells/ml to 8.6 cells/ml) and *E. dermatitidis* strain CBS 207.35^T (ranging from 4,800 cells/ml to 4.8 cells/ml) were separately added into sputa from the

Table 2. Primers and probes used in this study.

Primer or probe	Oligonucleotides (5′–3′)	Specificity	Reference
Probes used for PCR-RLB:			
Apio_P	amino-GAGGTAAGTTTTTGGCTAAAGC	*S. apiospermum*	18
Boy_P	amino-CGAGGTAAGTTTTTGGTTCAAA	*S. boydii*	18
PE_P	amino-CTGCTGTCGCTGGGACTAACAAA	*E. dermatitidis*	This study
Primers used for LAMP:			
FIP_SA (F1c+F2)	CAACCGGCCCGTGGCTTTAGCTTGAGCGCATGAGCGTC	*S. apiospermum*	18
BIP_SA (B1c+B2	GTGTCATCCGGCCTCCGTTGTTTGTTGCCCGAAGCCTAT	*S. apiospermum*	18
F3_SA	ATGGCACTTCTGAACTCCAG	*S. apiospermum*	18
B3_SA	GGGCTCGAGATCTACAAGGA	*S. apiospermum*	18
FIP_SB (F1c+F2)	AACCAGCCCGTGGTTTGAACCCTTGAGCGCATGAGCGTT	*S. boydii*	18
BIP_SB (B1c+B2)	GTGTGGTGTCATCCAGCCTCCTTTGTTGCCCGAAGCCTAT	*S. boydii*	18
F3_SB	ATGGCACTTCTGAACTCCAG	*S. boydii*	18
B3_SB	CGAGATCTACAAGGACAGCG	*S. boydii*	18
FIP_ED (F1c+F2)	TCCGCAACCTACTACAGTGAATGGGTCTTCAGCTTGGGTCATTGA	*E. dermatitidis*	This study
BIP_ED (B1c+B2)	TGCAATTGAGACACTTACCAGGCCACGACCATAAAATCAGTAGCGT	*E. dermatitidis*	This study
F3_ED	GGACTTGTACACAGTCTCATCA	*E. dermatitidis*	This study
B3_ED	ATGCGACACAAGCACCAG	*E. dermatitidis*	This study

healthy donor for sensitivity testing in spiked specimens and as positive controls, with 10 times dilution of fungal cells.

PCR-RLB

A primer set for *E. dermatitidis* targeting the *BT2* region of the β-tubulin gene was designed (Table 2). Additionally, the primers developed by Lu et al. were used for *Scedosporium*.[7,21] Two species-specific probes and a species complex specific probe PE_P specific for *Exophiala* species were labeled with C6-amino linker at the 5′ end. All primers and probes were BLAST searched against nucleotide databases available at GenBank and the CBS in-home database, to verify specificity. PCR amplification of *BT2* was performed consisting of 1 × GoTaq Green Master Mix (Promega, Fitchburg, WI, USA), 400 nmol of primers and 2 μl template DNA (100 ng/μl) to 94°C for 5 min, followed by 35 cycles of 94°C for 45 s, 56°C for 45 s, 72°C for 90 s and post-elongation at 72°C for 7 min. Sensitivity tests were repeated twice using 10-fold serial dilutions (ranging from 200 ng/ml to 2 pg/ml) of template DNA extracted from reference strains and spiked sputum specimens (ranging from 4800 fungal cells/ml to 4.8 fungal cells/ml).

LAMP

Assays for detection of *Scedosporium* species were performed as previously described.[7,21] LAMP used in the present study detects *E. dermatitidis* with a combination of the F3, B3, FIP, and BIP primers designed using Primer Explorer V4 software (http://primerexplorer.jp/e/) based on the partial sequence (*BT2*) in the β-tubulin region (GenBank KF928572) of type strain of *E. dermatitidis*, CBS 207.35^T because fragment *BT2* of the β-tubulin gene provided more information than ITS as a target for the identification of *E. dermatitidis* and *Scedosporium* species.[21] The sequences of the primer sets used in this study are listed in Table 2. All LAMP reagents were bought from New England Biolabs (Ipswitch, MA, USA). LAMP reactions were conducted in 25 μl reaction volumes using a PCR machine containing the following reagents: 4 μl each FIP and BIP (10 pmol), 0.5 μl each F3 and B3 (10 pmol), 0.5 μl $MgSO_4$ (80 mM), 2 μl dNTP (5 mM), 4 μl of 5 M betaine (Sigma, Zwijndrecht, The Netherlands), 2.5 μl of 10 × Thermo buffer [20 mM Tris-HCl, pH 8.8, 10 mM KCl, 2 mM $MgSO_4$, 10 mM $(NH_4)_2SO_4$, 0.1% Triton X-100], 1 μl *Bst* DNA polymerase (New England BioLabs), 5 μl double-distilled water (ddH_2O), and 500 pg template DNA (1 μl). The reaction was performed by heating samples to 65°C for 90 min, followed by 85°C for 2 min to terminate the reaction. Similarly, the sensitivity tests were repeated twice using template DNA extracted from reference strains and spiked sputum specimens, respectively.

Statistical analysis

The statistical package for SAS version 9.3 (SAS Institute, Cary, NC, USA) was used to analyze the data. The obtained data were evaluated by percentage ratios. Comparison of percentage ratios yielded by molecular assays was accomplished using the χ^2 test. A P value of less than .05 was considered to be statistically significant.

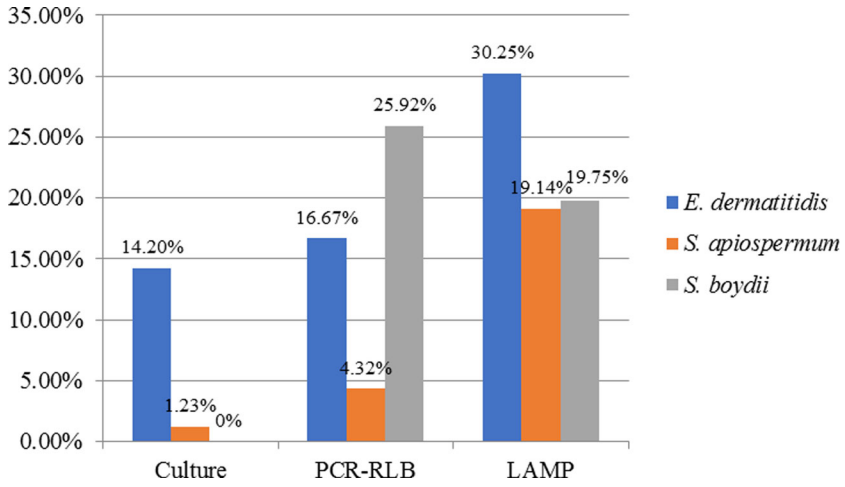

Figure 1. Comparison of results yielded from culture, PCR-RLB and LAMP.

Results

A total of 162 clinical sputum samples were verified for growth of *E. dermatitidis* and *Scedosporium* species. *E. dermatitidis* was detected in 23 sputum samples (14.2%) using selective ECA culture, while *S. apiospermum* / *S. boydii* was detected in two samples (1.2%) using nonselective routine media.

Detection by PCR-RLB

The specificity and sensitivity of the PCR-RLB assay for *S. apiospermum* and *S. boydii* has previously been reported to be 100% and approximately 5.0×10^3 copies of genomic DNA for specificity and sensitivity.[21] Genomic DNA from 46 reference and clinical strains covering each of the main genotypes of *E. dermatitidis* were analyzed to determine the specificity of our newly-designed PCR-RLB assay for *E. dermatitidis* (Table 1). No cross-reaction was observed, including DNA of a sibling species, *E. phaeomuriformis*, CBS 109146. Thus, specificity of the PCR-RLB assay was 100% in our study. The detection limit of PCR-RLB for genomic DNA of *E. dermatitidis* was approximately 1.1×10^3 genomic DNA copies (20 pg) per run. Sensitivity of the PCR-RLB assay was determined using spiked samples, in which concentrations above 4.8×10^3 *E. dermatitidis* spores/ml were positive.

The PCR-RLB assay detected *E. dermatitidis* in approximately 17% of clinical samples (Fig. 1). Among the 23 *E. dermatitidis* culture -positive samples, 21 samples were positive by the PCR-RLB assay. The PCR-RLB assay yielded approximately 30% positive *S. apiospermum* / *S. boydii*, of which 4% were *S. apiospermum* and 26% were *S. boydii*, respectively (Fig. 1). Only one of the two *Scedosporium* culture-positive samples was confirmed to be positive by PCR-RLB assay.

Detection by LAMP

The specificity and sensitivity of the LAMP assay for *S. apiospermum* / *S. boydii* were previously shown to be 100% and approximately 5.0×10^2 copies of genomic DNA, respectively.[21] In this study, no cross-reaction with any of the tested *Exophiala* species was observed after 90 minutes of the LAMP reaction (Table 1). The sensitivity of the LAMP assay was then further evaluated with spiked sputum samples, in which concentrations above 4.8×10^2 *E. dermatitidis* cells/ml were positive.

A total of 162 sputum samples, including two *Scedosporium*-culture positive samples and 23 *E. dermatitidis*-culture positive samples, were analyzed by our LAMP assay. LAMP assay of the DNA extracted from sputa yielded 32% of positive *S. apiospermum* / *S. boydii* samples. Both *Scedosporium* culture-positive samples were confirmed to be positive by LAMP. Additionally, the LAMP assay detected *E. dermatitidis* in 30% of clinical samples, and 49 samples were *E. dermatitidis* positive by LAMP, including the *E. dermatitidis*-culture positive samples.

Comparison of results yielded from culture, PCR-RLB, and LAMP

Of the 162 sputum samples from CF patients, 12 clinical samples were positive by both PCR-RLB and LAMP, whereas five LAMP-negative samples were PCR-RLB positive, 36 PCR-RLB-negative samples were positive with LAMP, and 109 of the total samples were negative by both PCR-RLB and LAMP. For *E. dermatitidis*, 14% of the samples were positive by culture, 17% by PCR-RLB, 30% by LAMP and 14% were positive by both PCR-RLB and LAMP. For *Scedosporium*, LAMP had a higher detection rate (27%) than PCR-RLB ($P < .0001$). Similarly, the

LAMP assay also provided a higher detection rate (30%) for *E. dermatitidis* ($P = .0039$).

Discussion

Previous studies revealed a highly variable prevalence of *Exophiala* and *Scedosporium* species in the respiratory tracts of CF patients (Table 3).[8,12,16,17,25–31] Lack of standardization of the procedures for detection on filamentous fungi in sputum samples from CF patients may be a possible cause for the variable reported data.[31] Moreover, routine processing procedures for isolating filamentous fungi from respiratory sputum samples may underestimate fungal prevalence.[18] Notably, LAMP technology can rapidly and accurately amplify genomic DNA in an isothermal step from partially processed and/or nonprocessed samples in approximately 1 hour without the need for sophisticated equipment and the products can be assessed by the naked eye.[32] The PCR-RLB assay has been used to detect *Scedosporium* species in the respiratory samples of CF patients.[7] Thus, *E. dermatitidis*-specific and *Scedosporium*-specific molecular assays, PCR-RLB and LAMP, and culture assays were used to detect the prevalence of *E. dermatitidis* and *Scedosporium* species in 162 clinical sputa in a double blind experiment.

We noticed that only two samples were positive for *S. apiospermum* / *S. boydii* and 23 samples were positive for *E. dermatitidis* upon culture assay in our study. This may due to cultivation of *Exophiala* by selective medium, and *Scedosporium* culture was nonselective. Some filamentous fungi such as *A. fumigatus* can overlap other fungi such as *Scedosporium* species on non-selective medium because they grow faster than other non-*Aspergillus* fungi that colonize the respiratory tract of CF patients.[4] Generally, our results are similar to the recovery rates reported using comparable media for *Scedosporium* species and *E. dermatitidis*.[10–12,33,34] In contrast, positive recovery rates for *Scedosporium* tend to increase at approximately 15% when the sputum samples processed by benomyl-based media.[33]

In addition to *A. fumigatus*, *E. dermatitidis* and species of the *S. apiospermum* complex are the most frequent molds recovered from respiratory secretions of CF patients, but their recovery rates vary greatly.[18,34,35] With its ability to grow at 37°C, *E. dermatitidis* has a worldwide distribution in hot environments, not only in CF respiratory tracts[10,26,36,37] but also warm indoor environments such as steambaths[38] and dishwashers.[39] Although the significance of *E. dermatitidis* in causing disease in patients with CF remains unclear, this fungus is known to cause severe invasive fungal infections.[40] With selective ECA medium, the prevalence of *E. dermatitidis* ranges from 5% in Germany to 19% in Sweden.[11,12,18] Published recovery rates in Sweden were exceptionally high, around 17–19% by selective culture.[12,37] Our data, which were also from Sweden, showed a high positive rate of 14%, confirming that this detection rate is rather consistent. PCR-RLB and LAMP assays yielded 15 and 30% of *E. dermatitis* detection, respectively, which was significantly higher than culture. The prevalence in Sweden is 2 to almost 20 times higher than in European countries, which is possibly because of differences in indoor conditions. For a better understanding of *E. dermatitidis* prevalence among CF patients, further multi-center epidemiological studies are needed.

Regarding the positive rate for *Scedosporium* species, the results of our molecular assays showed that approximately 10.5% of the CF airway samples were positive for the *S. apiospermum* complex using the PCR-RLB assay, and the positive rate yielded by the LAMP assay was approximately 31.5%. This positive rate for *S. apiospermum* / *S. boydii* was lower than the maximum reported rate of 61.5% that was obtained using PCR-RLB.[7] The high detection rate yielded by LAMP is likely closest to actual value, and LAMP technology would be the most efficient for amplification of target DNA from partially processed and/or non-processed CF specimens.[32] The selective ECA medium yielded a comparatively high positive recovery rate of *E. dermatitidis*, and this figure might be tripled to approach the real prevalence generated by molecular methods. However, LAMP may have a higher risk of false positive results than PCR-RLB, which might be caused by pre-PCR contamination of samples, as the method is highly sensitive. Careful precautions to prevent cross-contamination need to be taken during sample collection, and the methods should be executed using separated rooms and filtered tips. In general, analysis of larger numbers of samples is required to determine their prevalence in clinical samples, and the method should be repeated several times to enable for reliable determination of the presence in a single patient. The recent application of next-generation sequencing (NGS) technology has allowed us to conduct meta-genomic studies,[41] which may provide more comprehensive insight into chronic fungi colonization in airways of CF patients. Finally, we noticed two samples with positive culture results for *E. dermatitidis* were negative upon both PCR-RLB and LAMP assays. The quality of the fungi DNA extracted from respiratory sputum samples is likely poor, and sputa from CF patients might contain PCR inhibiting substances, both of which could influence the performance of the molecular assays.

In summary, current data on the prevalence of *Exophiala* and *Scedosporium* in the respiratory tract of CF patients remains variable and controversial. The results of our comparative detection study suggested a significantly higher prevalence and more complex colonization than previously

Table 3. Overview of *E. dermatitidis* and *Scedosporium* detection in sputum of CF patients.

Time	Geography	Samples (n)	*E. dermatitidis*	*Scedosporium* species	Reference
1991	Germany	121	SGA + CDA: 9%	NA	25
1998	Australia	52	NA	IGS-PCR: 10% (*S. apiospermum* complex)	26
2000	France	128	NA	Culture using filtrate antigens:8.6% (*S. apiospermum* complex)	16
2003	Germany	94	SGA + ECA: 1%	NA	27
2004	Germany	81	ECA: 6.2%	NA	32
2009	Germany	42	NA	SceSel: 14% (*S. apiospermum* complex)	28
2009	Australia, Germany, France, Spain, USA	162	NA	SGA: 14% (*S. prolificans*)	17
2010	Belgium	154	ECA: 5.8%	NA	11
2011	Sweden	97	ECA: 19%	NA	12
2011	France	59	NA	SceSel + PCR-RLB: 61.5% (*S. apiospermum* complex)	7
2013	France	50	NA	SGA + YPGA: 24% (*S. apiospermum* complex)	8
2015	Germany	2346	NA	SceSel: 3.1% (*S. apiospermum* complex)	20
2016	Germany	3186	ECA: 2.8%	SceSel: 2.4% (*S. apiospermum* complex)	30
2017	Sweden	162	SGA, ECA, LAMP, RLB: 17–30%	SGA, LAMP, RLB: 30–39% (*S. apiospermum* complex)	This study

Abbreviations used: CDA, Czapeck Dox Agar; ECA, Erythritol Chloramphenicol Agar; NA, not applied; SGA, Sabouraud's Glucose Agar; SceSel, Scedosporium Select Agar; YPGA, Yeast Peptone Glucose Agar.

estimated. Molecular detection methods such as the LAMP or NGS technology have the potential to become powerful tools that can be used in place of selective culture for to provide a more realistic description of the prevalence of *Exophiala* and *Scedosporium* in the respiratory tracts of CF patients, upon the improvement of the protocols for the extraction of filamentous fungi DNA from clinical specimens.

Acknowledgments

This study was funded in part with the grants from Major National R&D Projects of the National Health Department (2014ZX09J14106-02A), and the National Natural Science Foundation of China (81201269).

Declaration of interest

The authors report no conflicts of interest. The authors alone are responsible for the content and the writing of the paper.

Supplementary material

Supplementary data are available at *MMYCOL* online.

References

1. Bellis G, Cazes MH, Parant A et al. Cystic fibrosis mortality trends in France. *J Cyst Fibros*. 2007; 6: 179–186.
2. Girodon E, Cazeneuve C, Lebargy F et al. CFTR gene mutations in adults with disseminated bronchiectasis. *Eur J Hum Genet*. 1997; 5: 149–155.
3. O'Sullivan BP, Freedman SD. Cystic fibrosis. *Lancet*. 2009; 373: 1891–1904.
4. Lipuma JJ. The changing microbial epidemiology in cystic fibrosis. *Clin Microbiol Rev*. 2010; 23: 299–323.
5. de Vrankrijker AM, Wolfs TF, van der Ent CK. Challenging and emerging pathogens in cystic fibrosis. *Paediatr Respir Rev*. 2010; 11: 246–254.
6. Chotirmall SH, McElvaney NG. Fungi in the cystic fibrosis lung: bystanders or pathogens? *Int J Biochem Cell Biol*. 2014; 52: 161–173.
7. Lu Q, van den Ende AH, de Hoog GS et al. Reverse line blot hybridisation screening of Pseudallescheria/Scedosporium species in patients with cystic fibrosis. *Mycoses*. 2011; 54: 5–11.
8. Zouhair R, Rougeron A, Razafimandimby B, Kobi A, Bouchara JP, Giraud S. Distribution of the different species of the *Pseudallescheria boydii/Scedosporium apiospermum* complex in French patients with cystic fibrosis. *Med Mycol*. 2013; 51: 603–613.
9. Harun A, Blyth CC, Gilgado F, Middleton P, Chen SC, Meyer W. Development and validation of a multiplex PCR for detection of Scedosporium spp. in respiratory tract specimens from patients with cystic fibrosis. *J Clin Microbiol*. 2011; 49: 1508–1512.
10. Haase G, Skopnik H, Kusenbach G. Exophiala dermatitidis infection in cystic fibrosis. *Lancet*. 1990; 336: 188–189.
11. Lebecque P, Leonard A, Huang D et al. *Exophiala* (*Wangiella*) *dermatitidis* and cystic fibrosis: prevalence and risk factors. *Med Mycol*. 2010; 48: S4–9.
12. Kondori N, Gilljam M, Lindblad A, Jonsson B, Moore ER, Wenneras C. High rate of *Exophiala dermatitidis* recovery in the airways of patients with cystic fibrosis is associated with pancreatic insufficiency. *J Clin Microbiol*. 2011; 49: 1004–1009.
13. Cortez KJ, Roilides E, Quiroz-Telles F et al. Infections caused by Scedosporium spp. *Clin Microbiol Rev*. 2008; 21: 157–197.
14. Chen M, Zeng J, De Hoog GS et al. The 'species complex' issue in clinically relevant fungi: a case study in *Scedosporium apiospermum*. *Fungal Biol*. 2016; 120: 137–146.
15. Guarro J, Kantarcioglu AS, Horre R et al. *Scedosporium apiospermum*: changing clinical spectrum of a therapy-refractory opportunist. *Med Mycol*. 2006; 44: 295–327.
16. Cimon B, Carrere J, Vinatier JF, Chazalette JP, Chabasse D, Bouchara JP. Clinical significance of *Scedosporium apiospermum* in patients with cystic fibrosis. *Eur J Clin Microbiol Infect Dis*. 2000; 19 53–56.

17. Rodriguez-Tudela JL, Berenguer J, Guarro J et al. Epidemiology and outcome of *Scedosporium prolificans* infection, a review of 162 cases. *Med Mycol*. 2009; 47: 359–370.
18. Pashley CH, Fairs A, Morley JP et al. Routine processing procedures for isolating filamentous fungi from respiratory sputum samples may underestimate fungal prevalence. *Med Mycol*. 2012; 50: 433–438.
19. Pham T, Giraud S, Schuliar G, Rougeron A, Bouchara JP. Scedo-Select III: a new semi-selective culture medium for detection of the *Scedosporium apiospermum* species complex. *Med Mycol*. 2015; 53: 512–519.
20. Sedlacek L, Graf B, Schwarz C et al. Prevalence of *Scedosporium* species and Lomentospora prolificans in patients with cystic fibrosis in a multicenter trial by use of a selective medium. *J Cyst Fibros*. 2015; 14 237–241.
21. Lu Q, Gerrits van den Ende AH, Bakkers JM et al. Identification of *Pseudallescheria* and *Scedosporium* species by three molecular methods. *J Clin Microbiol*. 2011; 49: 960–967.
22. Lackner M, Klaassen CH, Meis JF, van den Ende AH, de Hoog GS. Molecular identification tools for sibling species of Scedosporium and Pseudallescheria. *Med Mycol*. 2012; 50: 497–508.
23. Hoog GS, Guarro J, Gene J, Figueras MJ. *Atlas of Clinical Fungi, CD-rom* 3rd ed. Utrecht / Reus: CBS-KNAW Fungal Biodiversity Centre/ Universitat Rovirai Virgili, 2009.
24. Najafzadeh MJ, Dolatabadi S, Saradeghi Keisari M, Naseri A, Feng P, de Hoog GS. Detection and identification of opportunistic *Exophiala* species using the rolling circle amplification of ribosomal internal transcribed spacers. *J Microbiol Methods*. 2013; 94: 338–342.
25. Haase G, Skopnik H, Groten T, Kusenbach G, Posselt HG. Long-term fungal cultures from sputum of patients with cystic fibrosis. *Mycoses*. 1991; 34: 373–376.
26. Williamson EC, Speers D, Arthur IH, Harnett G, Ryan G, Inglis TJ. Molecular epidemiology of *Scedosporium apiospermum* infection determined by PCR amplification of ribosomal intergenic spacer sequences in patients with chronic lung disease. *J Clin Microbiol*. 2001; 39: 47–50.
27. Bakare N, Rickerts V, Bargon J, Just-Nubling G. Prevalence of *Aspergillus fumigatus* and other fungal species in the sputum of adult patients with cystic fibrosis. *Mycoses*. 2003; 46: 19–23.
28. Horre R, Marklein G, Siekmeier R, Nidermajer S, Reiffert SM. Selective isolation of *Pseudallescheria* and *Scedosporium* species from respiratory tract specimens of cystic fibrosis patients. *Respiration*. 2009; 77: 320–324.
29. Lackner M, Rezusta A, Villuendas MC, Palacian MP, Meis JF, Klaassen CH. Infection and colonisation due to *Scedosporium* in Northern Spain: an in vitro antifungal susceptibility and molecular epidemiology study of 60 isolates. *Mycoses*. 2011; 54: 12–21.
30. Ziesing S, Suerbaum S, Sedlacek L. Fungal epidemiology and diversity in cystic fibrosis patients over a 5-year period in a national reference center. *Med Mycol*. 2016; 54: 781–786.
31. Borman AM, Palmer MD, Delhaes L et al. Lack of standardization in the procedures for mycological examination of sputum samples from CF patients: a possible cause for variations in the prevalence of filamentous fungi. *Med Mycol*. 2010; 48: S88–97.
32. Kaneko H, Kawana T, Fukushima E, Suzutani T. Tolerance of loop-mediated isothermal amplification to a culture medium and biological substances. *Journal of biochemical and biophysical methods*. 2007; 70: 499–501.
33. Horre R, Schaal KP, Siekmeier R, Sterzik B, de Hoog GS, Schnitzler N. Isolation of fungi, especially Exophiala dermatitidis, in patients suffering from cystic fibrosis: a prospective study. *Respiration*. 2004; 71: 360–366.
34. Burns JL, Emerson J, Stapp JR et al. Microbiology of sputum from patients at cystic fibrosis centers in the United States. *Clin Infect Dis*. 1998; 27: 158–163.
35. Nagano Yuriko, Millar B Cherie et al. Fungal infections in patients with cystic fibrosis. *Rev Med Microbiol*. 2007; 18: 11–16.
36. Kusenbach G, Skopnik H, Haase G, Friedrichs F, Dohmen H. Exophiala dermatitidis pneumonia in cystic fibrosis. *Eur J Pediatr*. 1992; 151: 344–346.
37. Kondori N, Lindblad A, Welinder-Olsson C, Wenneras C, Gilljam M. Development of IgG antibodies to Exophiala dermatitidis is associated with inflammatory responses in patients with cystic fibrosis. *J Cyst Fibros*. 2014; 13: 391–399.
38. Sudhadham M, Prakitsin S, Sivichai S et al. The neurotropic black yeast Exophiala dermatitidis has a possible origin in the tropical rain forest. *Stud Mycol*. 2008; 61: 145–155.
39. Zalar P, Novak M, de Hoog GS, Gunde-Cimerman N. Dishwashers–a man-made ecological niche accommodating human opportunistic fungal pathogens. *Fungal Biol*. 2011; 115: 997–1007.
40. Sood S, Vaid VK, Sharma M, Bhartiya H. Cerebral phaeohyphomycosis by Exophiala dermatitidis. *Indian J Med Microbiol*. 2014; 32: 188–190.
41. Koboldt DC, Steinberg KM, Larson DE, Wilson RK, Mardis ER. The next-generation sequencing revolution and its impact on genomics. *Cell*. 2013; 155: 27–38.

Front. Med. 2018, 12(1): 58–75
https://doi.org/10.1007/s11684-017-0601-0

REVIEW

Epidemiology of fungal infections in China

Min Chen[1,2,*], Yuan Xu[1,2,*], Nan Hong[1,2,*], Yali Yang[1], Wenzhi Lei[1], Lin Du[1], Jingjun Zhao[3], Xia Lei[4], Lin Xiong[5], Langqi Cai[6], Hui Xu[7], Weihua Pan (✉)[1,a], Wanqing Liao (✉)[2,b]

[1] Department of Dermatology, Changzheng Hospital, Second Military Medical University, Shanghai 200003, China; [2] Shanghai Key Laboratory of Molecular Medical Mycology, Changzheng Hospital, Second Military Medical University, Shanghai 200003, China; [3] Department of Dermatology, Tongji Hospital, Tongji University, Shanghai 200442, China; [4] Department of Dermatology, Daping Hospital, Third Military Medical University, Chongqing 400042, China; [5] Department of Dermatology, the People's Hospital of Yan'an, Yan'an 716000, China; [6] Department of Dermatology, the First Affiliated Hospital of Xiamen University, Xiamen 361003, China; [7] Department of Dermatology, Shanghai Ninth People's Hospital, Shanghai Jiao Tong University School of Medicine, Shanghai 200011, China

Abstract **With the increasing number of immunocompromised hosts, the epidemiological characteristics of fungal infections have undergone enormous changes worldwide, including in China. In this paper, we reviewed the existing data on mycosis across China to summarize available epidemiological profiles. We found that the general incidence of superficial fungal infections in China has been stable, but the incidence of tinea capitis has decreased and the transmission route has changed. By contrast, the overall incidence of invasive fungal infections has continued to rise. The occurrence of candidemia caused by *Candida* species other than *C. albicans* and including some uncommon *Candida* species has increased recently in China. Infections caused by *Aspergillus* have also propagated in recent years, particularly with the emergence of azole-resistant *Aspergillus fumigatus*. An increasing trend of cryptococcosis has been noted in China, with *Cryptococcus neoformans* var. *grubii* ST 5 genotype isolates as the predominant pathogen. Retrospective studies have suggested that the epidemiological characteristics of *Pneumocystis* pneumonia in China may be similar to those in other developing countries. Endemic fungal infections, such as sporotrichosis in Northeastern China, must arouse research, diagnostic, and treatment vigilance. Currently, the epidemiological data on mycosis in China are variable and fragmentary. Thus, a nationwide epidemiological research on fungal infections in China is an important need for improving the country's health.**

Keywords fungi; infection; epidemiology; China

Introduction

Fungi are eukaryotic organisms found throughout nature. They emerged about 1.6 million years ago and serve the important function of returning the nutrients removed by plants to the soil [1]. Historically, fungi are major pathogens of plants, rotifers, insects, and amphibians, with a relative few causing infections in humans. However, human modification of natural environments has intensified the dispersal of fungal infections [2]. Global warming has also augmented the prevalence of fungal infections in mammals by its selection of adaptive thermo-tolerant fungal species possessing significant pathogenic potential despite their current nonpathogenicity due to being restricted by mammalian temperatures [3]. To date, approximately 400 fungal species have been reported to be pathogenic to humans, with emerging pathogenic fungal species recorded annually [4].

The patterns of fungal infections are diverse and vary worldwide depending on the fungal species, host immune status, and infection site. For example, superficial fungal infections (SFIs), such as tinea capitis, are closely related to host lifestyle and socioeconomic conditions [5–7], whereas invasive fungal infections (IFIs), such as candidemia, are closely linked to host immune status and fungal species [8]. Since the 1950s, SFIs have steadily declined in incidence globally, especially in fast-developing countries, such as

Received August 12, 2017; accepted October 23, 2017

Correspondence: [a]panweihua@medmail.com.cn;
[b]liaowanqing@smmu.edu.cn

[*]These authors contributed equally to this work and share the first author position.

China, because of improving sanitary conditions [6,7]. By contrast, IFIs have been recognized as an increasing major threat to human health because of the growing prevalence of immunocompromised populations in recent decades [8]. For example, the human immunodeficiency virus (HIV) epidemic in Uganda has dramatically increased the incidence of IFIs that were once considered rare, such as cryptococcosis and disseminated histoplasmosis [9–11].

China, one of the largest countries in the world, is located at the western part of the Pacific Ocean. This country is rich in diversity of geographical environments and microorganisms. As the nation with the world's largest population (1400 million people), China has also reportedly steadily increased in the number of immunocompromised hosts [12,13]. A retrospective research based on single-center autopsy data (3447 cases) in China indicated that the prevalence of IFIs has risen steadily for decades [13]. The drastic socioeconomic lifestyle transformation among Chinese people may have altered the epidemiological characteristics of fungal infections in the country. Nonetheless, epidemiological data on fungal infections in China remain scarce. In the present research, we systematically reviewed the epidemiological data on fungal infections across China to obtain the epidemiological profiles and trends of Chinese fungal infections.

Superficial fungal infections

SFIs are fungal infections limited to the outermost layers of the skin and appendages. These infections are believed to affect approximately 25% of the world's population [5,6,14]. SFIs can be classified by infection site, for example tinea corporis, tinea pedis, tinea cruris, tinea manuum, onychomycosis, tinea capitis, and tinea faciei. The chief causative agents of SFIs are dermatophytes and yeasts. Dermatophytes are a group of filamentous fungi that infect keratin-rich tissues, such as the skin. The geographic distribution of dermatophytes is variable [5,6]. Currently, *Trichophyton rubrum*, *Trichophyton interdigitale*, *Trichophyton tonsurans*, and *Microsporum canis* are the major dermatophyte species globally [15]. Meanwhile, *Malassezia* spp. and *Candida* spp. are the principal yeast pathogens that cause SFIs [5,6]. To date, the majority of epidemiological studies on SFIs in China were conducted in separate disease categories or segmental regions [7]. Consequently, the epidemiological profile of SFIs in China remains thin and fragmented. In this portion of our research, we sought to summarize the epidemiological data on SFIs in China, particularly tinea capitis and onychomycosis.

Previous studies demonstrated that the patterns of SFIs and their chief causative agents vary across the many different geographical regions of China. Tinea corporis and tinea cruris (53.4%; 1682/3152) are the most prevalent types of SFIs in Northern China [16], whereas onychomycosis is the most prevalent in Eastern (55.2%; 5277/9566) and Southern China (28.6%; 199/697) [17,18]. Notably, tinea faciei is the most frequent SFI in Southern China among patients aged below 22 years (median age of 9 years). In Central China, tinea corporis (32.4%; 67/207) is the most prevalent type of SFI, and *T. rubrum* (50.7%; 34/67) is the predominant fungal pathogen [19]. In Northwestern and Northeastern China, tinea pedis (33.1%, 471/1422; 20.0%, 164/818, respectively) is the most prevalent type of SFI, and *T. rubrum* is again the predominant fungal pathogen [20,21]. In Southwestern China, tinea cruris (30.1%; 385/1279) is the most prevalent type of SFI, and *T. rubrum* is the predominant fungal pathogen [22].

In summary, dermatophytes, such as *T. rubrum*, remain as the most common fungal pathogens causing SFIs, especially onychomycosis, tinea pedis, and tinea cruris, in the majority of China. Similar observations were described by investigators in Brazil, America, Sweden, and France [23–26]. Tinea pedis is also the most prevalent type of SFI in Northern China, a finding compatible with previous epidemiological studies from Singapore [27].

Tinea capitis

Tinea capitis, an infection of scalp hair follicles and the surrounding skin caused mainly by dermatophyte fungi [28], is the most common SFI among children of school age, especially in developing countries [7]. From the 1950s through the 1960s, hyperendemic favus, generally a severe form of tinea capitis, was dominant in some provinces of China, such as Hubei, Jiangsu, and Jiangxi [7]. For example, in 1965, the prevalence of favus in Jiangxi reached 3410 per 100 000 [29]. However, after a prevention and treatment project for tinea capitis was initiated successfully in the 1960s, the incidence of favus decreased significantly, down from 1160 per 100 000 in the 1970s to below 1 per 100 000 in the 2000s [7,30–32]. Over time, the prevalence of tinea capitis gradually resurged in some regions of China. For example, in Shanghai, the number of tinea capitis cases increased from 25 cases in 1993 to 105 cases in 2001 [32]. These changes in incidence were probably related to the changing lifestyles of the population. Although finding a nationwide epidemiologic study on tinea capitis in China is difficult, a recent review suggested that anthropophilic fungi overwhelmed the zoophiles across vast regions of China before 1985 and that the dominant species nationwide was *T. schoenleinii* despite the variability of endemic species across different geographic regions [7]. Notably, the predominant etiology switched from *T. schoenleinii* to *T. violaceum* in Europe during 1963–1993, whereas the zoophile *M. canis* increased dramatically since 2000 [33]. Similarly, a shift of etiological agents from anthroponoses to zoonoses also

occurred in contemporary China. Pets became the most likely sources of tinea capitis in modern society, replacing the earlier human-to-human transmission mode [7]. The details are provided in Fig. 1.

Onychomycosis

Onychomycosis is a chronic fungal infection involving the nails, nail bed, nail plate, and matrix. This infection is responsible for almost 50% of all nail diseases [34]. In 2015, Wang *et al*. reported that the dominant form of onychomycosis in China is distal lateral subungual onychomycosis (DLSO: 54%; 531/978), followed by total dystrophy (TD: 24%; 237/978), superficial white onychomycosis (SWO: 16%; 155/978), and proximal subungual onychomycosis (PSO: 6%; 55/978) [35]. The details are provided in Fig. 2. The global prevalence of onychomycosis was estimated to be 5.5% [36], but no accurate data exist about the incidence rate of onychomycosis in China. Onychomycosis can be caused by dermatophytes, non-dermatophyte molds, or yeasts. In China, the pathogenic fungi that cause onychomycosis were found to be most commonly composed of dermatophytes (84.0%; 672/800), followed by yeasts (11.4%; 91/800) and non-dermatophyte molds (4.6%; 37/800) [35]. These observations are consistent with those of some previous reports [6,34,37]. Among the dermatophyte species, *T. rubrum* was dominant (80.9%; 647/800) [35]. These observations are compatible with previous epidemiological studies from China and other countries, such as India and Italy [34,37–40], but different from the findings in Greece, Iran, and Brazil, where yeasts were the predominant agents of onychomycosis [41–43]. These differences may be attributed to the geography, regional climate, or population migration, among other factors, in the regions studied [38]. *C. glabrata* was the most frequently found pathogenic yeasts (16.8%; 135/805) in Guangdong Province [44]. Increasing reports of onychomycosis in China have also implicated a new yeast pathogen as a causative agent. For example, our team reported the first case of onychomycosis caused by *Rhodotorula minuta* in an immunocompetent girl in 2013 [45]. A nationwide epidemiology survey on onychomycosis in China is needed in the future.

Invasive fungal infections

Invasive fungal infections (IFIs) are opportunistic fungal pathogens that infect deep solid organs and/or the bloodstream mainly in immunocompromised patients, such as those with prolonged neutropenia or cancer [8,46]. IFIs are caused primarily by *Candida* spp., *Aspergillus* spp., *Cryptococcus* spp., and others, all of which are distributed universally in the environment [8,47–49]. In general, the epidemiological profile of IFIs is characterized by geographical and temporal variability, with different incidence rates and new emergence incidents revealed over the past 20 years [50]. Notably, two separate single-center autopsy studies conducted in the 2000s showed that the incidence of IFIs increased steadily over time [51,52]. Until recently, the epidemiology of IFIs in China was

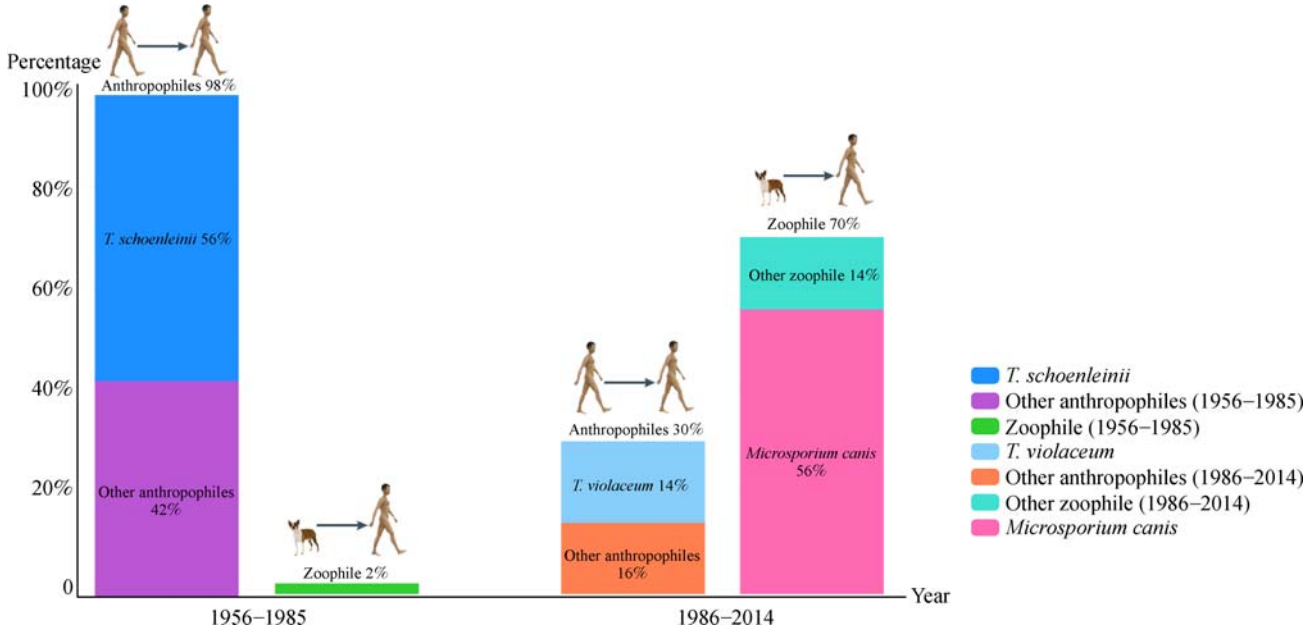

Fig. 1 Dynamic change of fungal etiology of tinea capitis in China.

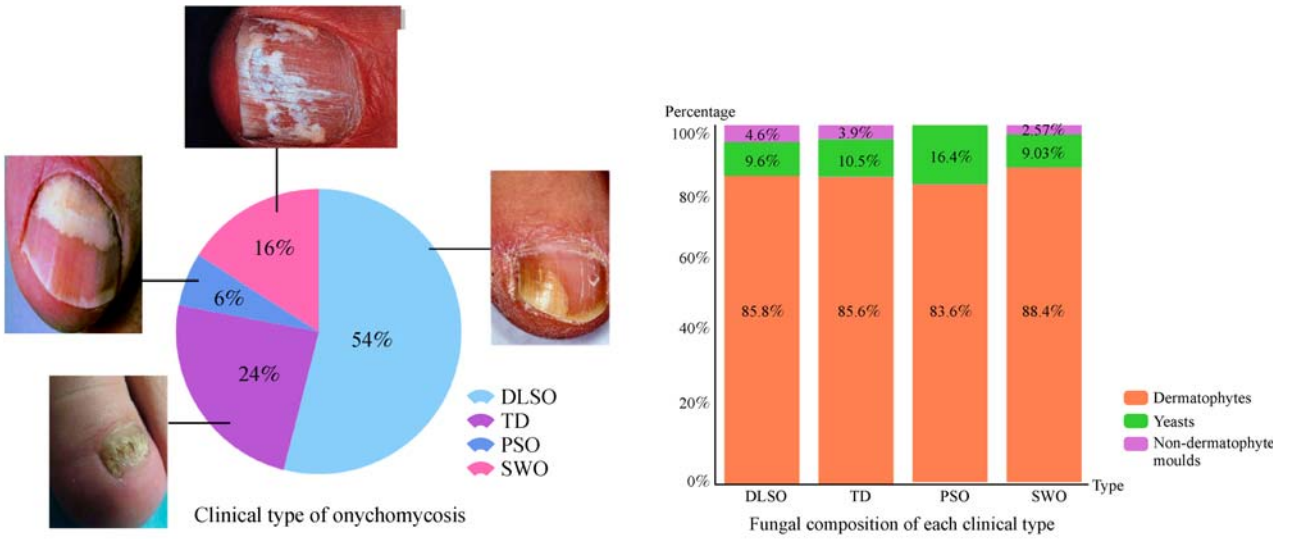

Fig. 2 Clinical type and fungal etiology of onychomycosis in China.

poorly understood because of insufficient and inaccurate data. Epidemiological studies on IFIs were reported mainly in numerous, separate case studies, and most of these studies were written in Chinese [53,54]. Consequently, information about the epidemiology of IFIs in China remains limited. In the following sections, we summarize the epidemiological data of IFIs in China with focus on the five main IFIs caused by *Candida*, *Aspergillus*, *Cryptococcus*, Mucorales, and *Pneumocystis* species.

Invasive candidiasis (IC)

Candida species are important nosocomial yeast pathogens that cause IC, including candidemia. These pathogens may be disseminated to internal organs [8,55,56]. The mortality rates can reach 35%–80% among immunocompromised and other seriously ill patients [57–60], a finding that is similar to the mortality rates reported by several studies (36.6%–60%) of IC in China [56,61–64]. Risk factors for IC include the extensive use of invasive procedures and devices, broad-spectrum antimicrobial agents, advanced life support, and aggressive chemotherapy [62,65]. Improved detection may also have raised the reported number of cases. The risk factors for Chinese patients infected with IC [56] are similar to the factors found by studies of patients from Spain and Canada [66,67], except for some unique risk factors. One such factor was IC caused by *Candida albicans* commonly found in patients with subclavian vein catheters or peritoneal drainage tubes [61]. The details are provided in Fig. 3.

For the past two decades, the incidence of candidemia doubled and currently ranks as the fourth and sixth most

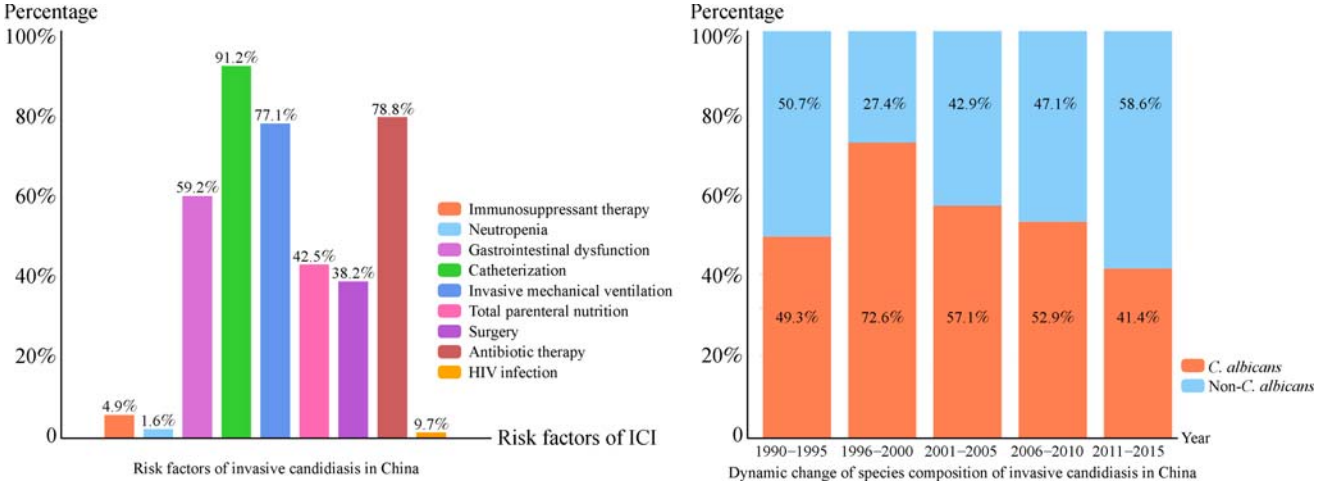

Fig. 3 Risk factors and dynamic change of species composition in invasive candidiasis in China.

common nosocomial bloodstream infection in American and European studies, respectively [68,69]. Notably, the incidence of IC in intensive care units was 0.32% (32 per 1000 admissions) in a multicenter prospective observational study in China from November 2009 to April 2011. This rate was consistent with the global incidence rates of 0.03%–0.5% in hospital-based studies [59].

Although *C. albicans* remains the most common etiological agent worldwide, *Candida* species other than *C. albicans* have been encountered more often than previously reported [8,64,70–76]. In some countries, these species account for increased number of episodes of IC, including candidemia, relative to *C. albicans* [50,56,77–79]. In China, *C. albicans* (40.1%; 156/389) also remains the most common causative agent of IC in recent decades, followed by *C. parapsilosis* (21.3%; 83/389), *C. tropicalis* (17.2%; 67/389), *C. glabrata* (12.9%; 50/389), *C. krusei* (2%; 1/389), and others (8.2%; 32/389) [56,61,78,80,81]. These findings differ slightly from the results based on data of ARTEMIS DISK Global Antifungal Surveillance Program, associated with China from 1997 to 2007, which showed that *C. tropicalis* was the second most common *Candida* species found in IC patients within the Asia-Pacific regions, including China's Taiwan [71,82,83]. Moreover, *C. parapsilosis* was the most common *Candida* isolates from blood in China (33.2%; 107/322) [78].

Significant geographical differences exist in the distribution of *Candida* species involved in IC worldwide. Similarly, variations are present in the distribution among different geographic regions in China [62,84–89]. In general, *C. albicans* is the strain most commonly isolated from candidemia in China, particularly in Southern China, but *C. tropicalis* (28.6%; 38/133) is the most common cause of candidemia in Nanjing [62,84–89].

Recently, uncommon *Candida* species, such as *C. guilliermondii*, *C. rugosa*, *C. quercitrusa*, and *C. auris*, have emerged worldwide, including in China [90–93]. For example, *C. guilliermondii* has been recently reported to cause candidemia in Taibei, Shanghai, and Nanjing and has been proven to be more resistant to both fluconazole (FLU) and voriconazole (VRC) in the Asia-Pacific region than in other regions [62,71,94,95]. More recently, *C. auris* emerged globally as a nosocomial pathogen, which is the multidrug-resistant yeast that exhibits resistance to FLU and shows a markedly variable susceptibility to other azoles, including amphotericin B (AMB) and echinocandins [93,96–98]. To date, IC caused by *C. auris* remains unreported in China, but this new yeast pathogen has been found recently in India and Oman and hence must still be monitored by mycologists [99,100].

In China, the majority of studies on the antifungal susceptibility patterns of *Candida* spp.-associated IC were defined partially in specific regions and/or particular populations [80,86,101–103]. Consequently, results reflecting the distribution and the associated antifungal susceptibility patterns of *Candida* species frequently differed among these studies. Because many non-*albicans* *Candida* spp. are resistant or mildly susceptible to antifungal agents [90–92], the timely and continuous determination of the antifungal susceptibility patterns of these yeasts is required. In the multicenter nationwide China Hospital Invasive Fungal Surveillance Net (CHIF-NET) study, most ($>$ 94%) of the isolates of *C. albicans*, *C. tropicalis*, and *C. parapsilosis* were susceptible to FLU and VRC, although such susceptibility varied with the species [78]. Again, this result was consistent with those of other studies, such as the ARTEMIS DISK Global Antifungal Surveillance Program [56,66,72,87,104]. Notably, 12.2% of the *C. glabrata* isolates were FLU resistant, and 17.8% exhibited a non-wild-type susceptibility to VRC [78].

The China Survey of Candidiasis reported a widespread resistance to itraconazole (ITC) [56]. Only 0.6% *C. albicans* showed susceptibility to ITC, and 96.0% of *C. glabrata* were ITC resistant. No resistance to caspofungin (CFG) was identified in any *Candida* strain isolated from China [56]. Regarding ketoconazole (KTC), the resistance rate was particularly high in *Candida* spp. (61.9%), and almost all isolates were resistant to KTC [62]. AMB and 5-flucytosine (5-FC) remained close to 100% effective against common *Candida* spp. in China, except for *C. krusei* and *C. guilliermondii* (which were only 20% and 71.4% susceptible to 5-FC, respectively) [72,85]. Notably, the resistance to FLU and VRC of *Candida* species other than *C. albicans* in elderly patients was approximately double that of younger patients (30.6% vs. 15.1% and 8.3% vs. 3.8%, respectively). However, the distribution of *Candida* species did not differ between the elderly and younger patients in China [86].

In conclusion, *C. albicans* remains the most common causative agent of IC in China, whereas the number of cases of IC caused by other *Candida* species has increased in the last decade. *C. parapsilosis* is the most common pathogen causing candidemia, but with geographical variation in China. FLU and VRC demonstrated good activity against *C. albicans*, *C. parapsilosis*, and *C. tropicalis* but not against *C. glabrata*. Cross-resistance to both azoles was noted in *C. glabrata* and in uncommon *Candida* strains, such as *C. auris*. Continued surveillance of IC in China is warranted. Details are shown in Fig. 3.

Invasive aspergillosis

Invasive aspergillosis (IA) is a serious opportunistic infection that mainly affects immunocompromised patients, with an extremely high mortality rate ranging between 40% and 90% [105,106]. Inevitably, people inhale

Aspergillus spores or conidia daily; these particles can induce the occurrence of the following four main types of IA: invasive pulmonary aspergillosis (IPA), chronic necrotizing aspergillosis (CNA), allergic bronchopulmonary aspergillosis (ABPA), and aspergilloma [107]. Approximately 60 000 IA cases per year occurred in Europe, whereas more than 160 000 IA patients per year were estimated to have occurred in China, suggesting a heavy burden [108].

In China, the most dominant pattern of aspergillosis is IPA (approximately 15%), followed by ABPA (approximately 4%), CNA (approximately 3%), and aspergilloma (approximately 1%) [107]. IPA is the most severe type of pulmonary aspergillosis, with a high mortality in immunocompromised individuals (39%–100%), especially in patients with malignant hematological disorders, such as neutropenia, or who have undergone hematopoietic stem cell transplantation (HSCT) [109–111]. The mortality rate of IPA in China is similar to the rates found in various countries of Europe, including Italy [50,112].

Previous studies revealed that the overall IA infection rate in China ranged from 0.29%–14% depending on different underlying diseases or conditions [13,110,111,113]. Overall, this rate is similar to the rates exhibited in other countries, such as Italy (0.2%; 13/5561), and in Europe (6.9%; 127/1850) [50,112]. In addition, the lung (71.9%; 1047/1457) is the most frequent site of aspergillosis infection in China [53], followed by sinus infection (18.7%; 273/1457), eye infection (5.0%; 72/1457), and others (4.4%; 64/1457), all of which is consistent with reports from other nations [106,114]. However, the proportion of lung infections in China was lower than noted in an international, multicenter observational study in which lung infections accounted for 94% of the cases [114].

Currently, more than 30 *Aspergillus* species have been implicated in IA, the most common are the following: *A. fumigatus*, *A. flavus*, *A. niger*, *A. terreus*, and *A. nidulans* [115]. In China, *A. fumigatus* was the most commonly isolated *Aspergillus* species (59.3%; 153/258), followed by *A. flavus* (27.5%; 71/258), *A. niger* (5.8%; 15/258), *A. terreus* (2%; 5/258), *A. sydowii* (2%; 5/258), and others (3.4%; 9/258) [53]. These preponderance levels are higher than those found by an Italian study, where *A. fumigatus* accounted for 41.7% (5/12) [50], but lower than those in an international, multicenter observational study and a European study, where *A. fumigatus* accounted for 92.2% (519/563) and 96.1% (98/102), respectively [112,114].

The occurrence of IA caused by *Aspergillus* species other than *A. fumigatus* has increased in China recently [53]. For example, Li *et al*. reported an elevated number of IA cases caused by *A. niger* and *A. tubingensis*, the main black *Aspergillus* species present in clinical and environmental samples in China [116]. Wang *et al*. also found that for patients with HBV-related liver failure, the number of IPA occurrences caused by *A. flavus* (37.9%; 25/66 cases) was greater than that attributed to *A. fumigatus* (27.3%; 18/66 cases) [117].

Since 1997, azole-resistant *A. fumigatus* has been widely identified in clinical isolates from all over the world [118]. Currently, most *A. fumigatus* azole-resistant strains have been associated with mutations of *cyp51A*, followed by TR34/L98H and TR46/Y121F/T289A mutations [118]. In 2011, the ARTEMIS DISK Global Antifungal Surveillance Program first reported that the TR34/L98H mutation can be found in *A. fumigatus* isolates collected in China [115]. Subsequently, Liu *et al.* found that the TR34/L98H mutation (or isolates containing the S297T/F495I mutation) remains the predominant mutation in China and is fairly common in Europe and some other Asian countries [118,119]. Studies in China found that mutations in *A. fumigatus* isolates were the TR34/L98H/S297T/F495I mutation, TR34/L98H mutation, G432A, M220I mutation, and TR46/Y121F/T289A mutation [115,118,120,121]. At present, azole-resistant *A. fumigatus* has spread mainly across Southeastern and Northern China [108]. Until recently, no infection caused by *A. fumigatus* in China has developed the TR/L98H mutation under pressure of triazole therapy, which has proposed that the increase in frequency of this particular mutation in clinical isolates from the Netherlands is driven by the use of azole compounds as fungicides in agricultural practice [115].

In summary, the incidence of IA in China has increased over the past 20 years, with new emerging *Aspergillus* species and azole-resistant *A. fumigatus*. The lung is the most frequent site of IA in China. Molecular methods are essential for the identification of uncommon *Aspergillus* pathogens, such as azole-resistant *Aspergillus* species, in China. Further nationwide surveillance of IA is needed in China.

Cryptococcosis

Cryptococcosis is a life-threatening infection afflicting both immunosuppressed and immunocompetent individuals, which is caused primarily by two sibling basidiomycetous yeasts, *Cryptococcus neoformans* and *Cryptococcus gattii* [122]. In general, *C. neoformans* and *C. gattii* have been further subdivided into several genotypes, such as VN I – VN IV genotypes in *C. neoformans* and VG I – VG IV genotypes in *C. gattii* [12,123,124]. Recent phylogenetic tools have improved our understanding of molecular epidemiological cryptococcosis. In 2009, multilocus sequence typing (MLST) was recommended by the International Society of Human and Animal Mycoses as the preferred method for typing cryptococcal strains [125]. According to research based on the MLST analysis of 305 Chinese clinical *C. neoformans* isolates, sequence type 5 (ST 5) was the predominant sequence type (89.2%) in *C.*

neoformans isolates, followed by ST 31 (6.2%) [126]. The predominance of ST 5 genotype in Chinese clinical *C. neoformans* isolates was also reported by Dou *et al*. (94.9%; 75/79) and Wu *et al*. (82.9%; 34/41) [127]. Actually, ST 5 is the major sequence type in *C. neoformans* isolates from East Asian countries where cryptococcal data were available, including China, Japan, and South Korea [128–130]. However, in Thailand, ST 4 and ST 6 were found to be the major MLST types, whereas ST 93 was dominant in India and Indonesia [128,131]. Recent MLST analysis has indicated that the evolutionary origin of *C. neoformans* var. *grubii* in Thailand is in Africa [131]. The *C. neoformans* var. *grubii* in China was of the same low molecular diversity as the *C. neoformans* var. *grubii* in Thailand. Thus, the *C. neoformans* var. *grubii* in China may have the same evolutionary origin followed by a global expansion and is potentially vector transmitted by avian migration.

In China, cryptococcosis caused by *C. gattii* has been reportedly increasing mostly in patients living in subtropical and tropical regions [132,133]. VG I genotype strains were predominant in Chinese *C. gattii* isolates, whereas the VG IIb genotype strain has been reported in recent studies [134]. The *C. gattii* isolates from China may be distantly related to the highly virulent strain (VG IIa genotype) that caused the outbreaks of cryptococcal infection in western North America. In 2010, the VG IIa genotype strain was reported to have caused infections in Japan, which is adjacent to China [135]. This observation suggests that the VG IIa genotype strain has spread already to the Asia Pacific as a result of international travel and commerce and animal migration. Xue *et al*. [132] stated that if a greater number of laboratories undertook MLST analysis, more cases of *C. gattii* would be diagnosed.

Although an accurate incidence rate of cryptococcosis in China is unavailable, the number of reported cryptococcosis cases in China has increased gradually over the past two decades [12]. A recent survey of invasive yeast infections has indicated that cryptococcosis has become the second most common invasive yeast infection (7.7%) in China [78]. Moreover, meningitis is the most frequent meningoencephalitis in cryptococcosis in China. According to the latest literature review of cryptococcosis in Chinese mailand (1985–2010), central nervous system (CNS) infections occurred in 83.4% (7315/8769) of cryptococcosis patients [136]. A high CNS prevalence involving cryptococcosis was also reported in China's Taiwan (58.9%) and Hong Kong (67.4%) [137,138]. Cryptococcosis is an opportunistic fungal infection because it occurs mainly in immunocompromised populations, such as patients with AIDS, organ transplant recipients, and patients with autoimmune diseases. Notably, a significantly high proportion of cryptococcosis cases have been reported in immunocompetent individuals in China [139–141], which might be the result of a predisposition in the ethnic Chinese population [142]. However, in accordance with a recent meta-analysis of cryptococcosis in China based on 8769 cases in 1032 reports, only 17% of the cases were without identifiable underlying diseases [136]. Therefore, a large-scale epidemiological study is necessary for further understanding of cryptococcosis in China.

Research on environmental *Cryptococcus* strains has been relatively lacking in China. Existing research is either limited in geographic area [143] or lacking the application of the latest molecular typing techniques [144]. Soil enriched with pigeon excreta, decaying wood, and tree detritus such as *Eucalyptus* species and *Laurus* species are ecological niches for *C. neoformans* and *C. gattii*, respectively [144]. Our research group has already isolated *C. gattii* from eucalyptus trees in Yunnan Province (unpublished data). Further high-density sampling of the environmental strain of *Cryptococcus* is needed.

Until today, our understanding on the epidemiological features of *Cryptococcus* and cryptococcosis in China was mainly based on single-center retrospective studies, which cannot reflect the overall prevalence and fungal burden of cryptococcosis in China. The large numbers of reported cryptococcosis in immunocompetent patients but low numbers in immunocompromised hosts in China warrant re-evaluation. Thus, an effective nationwide surveillance of cryptococcosis in China is necessary.

Mucormycosis

Mucormycosis (previously called zygomycosis) is an opportunistic infection caused by fungi belonging to the order Mucorales and the family Mucoraceae [145,146]. *Rhizopus, Mucor*, and *Lichtheimia* (formerly *Absidia*) are the most common genera that cause mucormycosis [147]. With the augmented size of immunocompromised populations, the prevalence of mucormycosis has also increased annually.

In places such as California and Spain, the annual incidence of mucormycosis was 0.43–1.7 cases per 1 million individuals [148–150]. By contrast, the morbidity in China is unclear. A review conducted in 2016 found that the prevalence of diabetes combined with mucormycosis increased in Chinese mainland from 10 cases before 2000 to 28 cases in 2010–2016 [151]. Several researchers reported that the overall mortality rate was 29.4% (126/428)–40.8% (40/98) [151–153], which is similar to the rate reported by non-Chinese sources. For example, the rate for Europe ranged from 23.5% (125/531) to 54.3% (504/929) [145,154,155]. The most frequent pathogen of mucormycosis in China is *Mucor* spp. (54.3%; 19/35), followed by *Rhizopus* spp. (28.6%; 10/35) [152]. These statistics vary from the findings in Europe, where *Rhizopus* spp. accounted for 33.7% (58/172), *Mucor* spp. accounted for 19.2% (33/172), and *Lichtheimia* spp. accounted for 18.6% (32/172) [145].

According to one report external to China [147], the variability of susceptibility to AMB, along with resistance to most other conventional antifungal agents, leads to high mortality. Currently, no large sample studies in China conducted the antifungal susceptibility testing of Mucorales.

Because mucormycosis is an opportunistic infectious disease, patients with underlying diseases are more likely to be infected than healthy individuals [151]. Internationally, mucormycosis is most common in patients with malignant tumors, diabetes, or organ transplants [154]. However, in China, this disease is more common in patients with diabetes, HIV infection, and viral hepatitis and in individuals who are long-term steroid or immunosuppressant users [152]. The close connection of mucormycosis with diabetes is worth noting because China has seen a rising burden of diabetes (92.4 million adults above the age of 20 years) [156].

In China, mucormycosis has occurred mainly on the coast and in humid areas [152]. The most common sites of infection are pulmonary (36.5%; 27/74), followed by rhinocerebral (32.4%; 24/74), skin (10.8%; 8/74), intracranial (6.8%; 5/74), and others (13.5%; 10/74) [151]. This finding is similar to the observations in Europe [145] but differs from the results of an international review that reported the sinus area as the most common site (39%; 359/929) [154].

To date, epidemiological data for this type of mucormycosis are scant in China. Most reports about mucormycosis lack evidence of molecular biological diagnosis. Additional effort should be exerted to identify species by molecular biology, and antifungal susceptibility testing is needed. Mucormycosis and diabetes are closely related; thus, attention must be focused on preventing and controlling diabetes.

Pneumocystis pneumonia

Pneumocystis pneumonia (PCP) is a potentially fatal pulmonary infection that occurs in immunocompromised individuals, especially in AIDS patients with a low CD4 cell count (below 200/mm^3) [157,158]. PCP in humans is only caused by *Pneumocystis jirovecii*, which has recently been reclassified as fungal species [159–163]. Given the widespread use of PCP prophylaxis and highly active antiretroviral therapy, the incidence of PCP has declined significantly in developed countries [164].

However, PCP remains a common opportunistic infection in HIV-infected patients in developing countries, including China [165–167]. The earliest HIV/AIDS-associated PCP case in China was reported in 1985 [167]. From 1985 to 2009, the number of PCP patients afflicted by HIV/AIDS increased dramatically in China, apparently 70.2% (1646/2344) of which were identified along with HIV infection [167]. PCP also affects other immunocompromised patients [168]. In China, the prevalence of *P. jirovecii* colonization in patients with chronic pulmonary diseases is apparently 63.3% (62/98), which is higher than previous reports in North Lebanon (17.3%; 4/23) and Iran (7.9%; 7/89) [169]. However, the incidence of PCP in China is rare among HIV-positive and HIV-negative hosts because all performed epidemiological studies on PCP in China were retrospective studies [170].

The mortality of PCP is diverse among different studies in the world, including China. A retrospective study in Beijing showed that mortality (15.2% vs. 12.4%) did not significantly differ between the PCP cases of HIV-positive and HIV-negative populations [171], which differ from studies in Beijing. Moreover, the mortality of non-HIV–PCP (30%–60%) in other countries, such as Japan, is higher than that of HIV–PCP (11.3%–20%) [157,172–174]. The difference in mortality may be associated with the different genetic backgrounds of *P. jirovecii* and anti-PCP treatment strategy.

Although trimethoprim (TMP)–sulfamethoxazole (SMX) remains the first-line agent for PCP [170], mutations in the dihydrofolate reductase (DHFR) and dihydropteroate synthase (DHPS) genes of *P. jirovecii* with resistance to TMP and SMX, respectively, have progressively emerged [170]. Currently, the prevalence of *P. jirovecii* DHPS and DHFR mutations in HIV-positive patients in China remains low, which is similar to that in other developing countries [175]. Approximately 60% of *P. jirovecii* isolates harbor nucleotide mutations in the DHFR gene in China. The majority ($>$ 90%) of these mutations were synonymous, similar to the data reported in Japan and Thailand [175–177]. Meanwhile, the prevalence of *P. jirovecii* DHPS mutations in China was 12.0% (3/25) [175], which is similar to those reported from other developing countries, such as South Africa (3.8%; 2/53) [178], but lower than those determined from developed countries, such as the United States (40%; 58/145) [179].

In summary, the epidemiological data on PCP are limited in China to date, although the above-mentioned retrospective studies suggested that the epidemiological characteristics of PCP in China are similar to those in other developing countries. A prospective epidemiological survey focused on PCP in China is needed.

Endemic fungal infections

Sporotrichosis

Sporotrichosis is a subcutaneous mycosis caused by several *Sporothrix* species, namely, *S. brasiliensis*, *S. globosa*, *S. mexicana*, and *S. luriei*, besides the classical species *S. schenckii* [180]. Sporotrichosis is globally distributed, but *Sporothrix* species have shown high degrees of endemicity [180]. Given the data in existing

literature, the most endemic regions are China (3299 cases), South Africa (3154 cases), and Brazil (5814 cases) [181]. In China, since sporotrichosis was first found in 1916 [182], the disease has existed nationwide but has been observed mainly in Northeastern China, including Jilin Province, Heilongjiang Province, and Liaoning Province [180,183]. *S. globosa* exhibits a global distribution with nearly identical genotypes, and this species is the only pathogenic *Sporothrix* species that has been reported to date in China [180,183–186]. Such pattern is similar to those found in India and Spain [181].

Although the transmission mode of sporotrichosis remains unclear, trauma may be strongly implicated. Contact with decaying plant material was frequently noted in *S. globosa* and *S. schenckii,* whereas *S. brasiliensis* was significantly associated with transmission by cats [181]. Relative immune impairment and underlying metabolic diseases are important risk factors for sporotrichosis [180].

Sporotrichosis presents as the following three main clinical types: lymphocutaneous, fixed cutaneous, and multifocal or disseminated cutaneous sporotrichosis [187]. Globally, the most common clinical form is lymphocutaneous sporotrichosis, but in China, the fixed cutaneous form is prevalent, followed by the lymphocutaneous form [180,181,187,188]. Classically, sporotrichosis occurs in temperate and subtropical climates of relatively high humidity. By contrast, the climate is relatively cold in the hyperendemic area of Northeastern China, where *S. globosa* is prevalent [181].

As the number of immunocompromised patients rises, the epidemiological monitoring of sporotrichosis is increasingly needed, and research is necessary to indicate whether *S. schenckii* or other *Sporothrix* species exist in China. Additional protective measures should be undertaken to avoid infection during agricultural activities.

Penicilliosis

Penicilliosis is a deep fungal infection caused mainly by the dimorphic fungus *Talaromyces marneffei* (formerly known as *Penicillium marneffei*), a species endemic to Southeast Asia, including some districts in China (e.g., Guangdong, Guangxi, Yunnan, Fujian, Yunnan, and Hong Kong) [189–191]. The organism was discovered in 1956 in bamboo rats [192], and the first natural human case of infection was reported in 1973 [193]. In China, the first case of *T. marneffei* infection was noted in 1984 [194]. After the 1990s, with the prevalence of AIDS in Southeast Asia, the number of patients with *T. marneffei* infection increased rapidly in this area, including Chinese mainland [195,196]. More than 87% of the number of reported *T. marneffei* infections was noted with HIV infection in China [196], and nearly 16% of the patients with AIDS were infected with *T. marneffei* in Guangxi [197]. To date, more than 600 cases of *T. marneffei* infection have been identified in China, with 82% of the cases reported in Guangxi and Guangdong [196,198]. The mortality of *T. marneffei* infection is higher in patients without antifungal therapy (50.6%; 45/89) than in patients with antifungal therapy (24.3%; 138/569) [196]. Cao *et al*. confirmed that the *T. marneffei* isolates from humans are similar to those from infected bamboo rats, and in some cases, the isolates are identical, which parallel the data from Thailand and India [197,199,200]. Although the potential sources of infection are rodent species, particularly bamboo rats, the transmission route of *T. marneffei* to humans remains a mystery [197]. In recent years, *T. marneffei* infection has increasingly impacted immunocompromised patients in Southern China, especially individuals with HIV/AIDS [196]. Additional studies should be conducted to determine the transmission route of *T. marneffei*, and raised attention should be paid to immunocompromised patients, especially those in endemic areas.

Histoplasmosis

Histoplasmosis, caused by the soil-based dimorphic fungus *Histoplasma capsulatum*, is a common endemic mycosis in midwestern United States and in Central America [201]. However, sporadic cases of autochthonous histoplasmosis have been encountered in China, a region traditionally considered non-endemic for *H. capsulatum* [202]. The first case of histoplasmosis in China was reported in 1958 in an individual returning from the USA [203]. Since 1990, 300 cases of histoplasmosis have been reported in China, of which only 17 cases were potentially imported cases [204]. The majority of these cases (75.0%; 225/300) occurred in nine provinces and regions traversed by the Yangtze River. Among these regions, Yunnan Province accounted for more than 27.7% (83/300) of the reported cases of histoplasmosis [204]. Pan *et al*. found that Chinese *H. capsulatum* isolates may have originated from Australia or other continents, such as North America [202].

Underlying diseases associated with histoplasmosis include HIV infection (22.0%; 38/173), diabetes mellitus (10.4%; 18/173), and liver diseases (7.5%; 13/173). Diabetes and malignancy are common in patients with pulmonary infection, but HIV-infected patients are prone to systemic dissemination. This information suggests that the clinical spectrum of histoplasmosis depends on the underlying host immune status [204]. Although histoplasmosis may prefer infecting individuals with underlying illness, research demonstrated that 49.1% (85/173) of patients lack an identifiable underlying disease [204].

At the time of our research, the epidemiology and ecology of *H. capsulatum* in China were unknown. As

Table 1 Recent reports of fungal infections caused by rare fungal species in China

Case	Date	Species	Infective sites	Prognosis	Reference
1	2004	*Arthrographis kalrae*	Eye and sinuses	Blindness	[207]
2	2007	*Prototheca wickerhamii*	Brain	Cured	[208]
3	2010	*Coniosporium epidermidis*	Toes	Cured	[210]
4	2011	*Exophiala asiatica*	Brain	Died	[209]
5	2012	*Filobasidium uniguttulatum*	Brain	Cured	[211]
6	2013	*Pichia fabianii*	Blood	Cured	[212]
7	2013	*Trichophyton tonsurans*	Face	Cured	[213]
8	2013	*Penicillium capsulatum*	Lung	Cured	[214]
9	2013	*Rhinocladiella basitona*	Face	Cured	[215]
10	2014	*Rhodotorula minuta*	Nail	Cured	[45]
11	2014	*Phialemonium curvatum*	Brain	Cured	[216]
12	2015	*Veronaea botryosa*	Cutaneous	Cured	[217]
13	2016	*Bipolaris oryzae*	Corneal	Cured	[218]
14	2017	*Chrysosporium keratinophilum*	Subcutaneous	Cured	[219]

international travel becomes increasingly accessible, *H. capsulatum* may progressively spread globally from China or other endemic countries. A further detailed epidemiologic investigation of *H. capsulatum* is worthwhile.

Coccidioidomycosis

Coccidioidomycosis (CM) is a deep mycotic infection endemic to the Americas [205]. Although China is not a known endemic area for CM, the number of case reports of CM has risen [206]. Since 1958 when the first case was reported, 30 CM cases, of which 27 cases were from Southern China, have been recorded in China. Risk factors for infection include residence in or travel to a CM-endemic region, occupations with high exposure risk, immunocompromising conditions, or other underlying diseases [206]. However, the majority of Chinese patients (80.0%; 24/30) presented with no history of exposure to CM-endemic areas [206]. Since CM has been reported rarely in China, the possible local sources of CM in such region or in other countries remain uncertain.

Rare fungal infections

With the development of molecular diagnosis approaches, the number of case reports on fungal infections caused by rare fungal species has been increasing in China since 2000 [45,207–219]. For example, Pan *et al*. reported a case of meningitis caused by azole- and FLU-resistant *Filobasidium uniguttulatum* in 2012 [211]. Chen *et al*. also published the first case of a fungus ball (*Penicillium capsulatum*) in the left lung of a patient with type 2 diabetes [214]. Fungal infections caused by newly reported species should be monitored in China in the future. The details are provided in Table 1.

Conclusions

We systematically reviewed the epidemiological data of fungal infections across China to understand the related epidemiological profiles and trends. Our analysis demonstrated that the overall incidence of SFIs in China was stable. The overall incidence of IFIs in China continued to increase in both immunocompromised and immunocompetent individuals, with rising numbers caused by *Candida* species besides *C.albicans*, azole-resistant *A. fumigatus*, and *Cryptococcus* species. Moreover, epidemiological studies on mucormycosis and *Pneumocystis* are scarce in China. As regards the endemic fungal infections in China, sporotrichosis, penicilliosis, and histoplasmosis showed obvious regional distribution characteristics with raised number of cases. In addition, the occurrence of fungal infections caused by rare fungal species has augmented in China during the last decade. Considering these findings, we conclude that a nationwide epidemiological research focused on fungal infections in China is direly needed.

Acknowledgements

This study was funded in part by grants from the Severe Infectious Diseases Specific Projects from China's Ministry of Health (No. 2013ZX10004612-7), the 973 Program (Nos. 2013CB531601 and 2013CB531606), and the National Natural Science Foundation of China (No. 81201269).

Compliance with ethics guidelines

Min Chen, Yuan Xu, Nan Hong, Yali Yang, Wenzhi Lei, Lin Du, Jingjun Zhao, Xia Lei, Lin Xiong, Langqi Cai, Hui Xu, Weihua Pan, and Wanqing Liao declare no conflict of interest. This manuscript does not involve a research protocol requiring approval from a relevant institutional review board or ethics committee.

References

1. Wang DY, Kumar S, Hedges SB. Divergence time estimates for the early history of animal phyla and the origin of plants, animals and fungi. Proc Biol Sci 1999; 266(1415): 163–171
2. Fisher MC, Henk DA, Briggs CJ, Brownstein JS, Madoff LC, McCraw SL, Gurr SJ. Emerging fungal threats to animal, plant and ecosystem health. Nature 2012; 484(7393): 186–194
3. Garcia-Solache MA, Casadevall A. Global warming will bring new fungal diseases for mammals. MBio 2010; 1(1): e00061-10
4. Taylor LH, Latham SM, Woolhouse ME. Risk factors for human disease emergence. Philos Trans R Soc Lond B Biol Sci 2001; 356 (1411): 983–989
5. Kaushik N, Pujalte GG, Reese ST. Superficial fungal infections. Prim Care 2015; 42(4): 501–516
6. Ameen M. Epidemiology of superficial fungal infections. Clin Dermatol 2010; 28(2): 197–201
7. Zhan P, Li D, Wang C, Sun J, Geng C, Xiong Z, Seyedmousavi S, Liu W, de Hoog GS. Epidemiological changes in tinea capitis over the sixty years of economic growth in China. Med Mycol 2015; 53 (7): 691–698
8. Miceli MH, Díaz JA, Lee SA. Emerging opportunistic yeast infections. Lancet Infect Dis 2011; 11(2): 142–151
9. Adams P. Cryptococcal meningitis: a blind spot in curbing AIDS. Lancet 2016; 387(10028): 1605–1606
10. Bahr NC, Sarosi GA, Meya DB, Bohjanen PR, Richer SM, Swartzentruber S, Halupnick R, Jarrett D, Wheat LJ, Boulware DR. Seroprevalence of histoplasmosis in Kampala, Uganda. Med Mycol 2016; 54(3): 295–300
11. Parkes-Ratanshi R, Achan B, Kwizera R, Kambugu A, Meya D, Denning DW. Cryptococcal disease and the burden of other fungal diseases in Uganda; Where are the knowledge gaps and how can we fill them? Mycoses 2015; 58(Suppl 5): 85–93
12. Wu SX, Guo NR, Li XF, Liao WQ, Chen M, Zhang QQ, Li CY, Li RY, Bulmer GS, Li DM, Xi LY, Lu S, Liu B, Zheng YC, Ran YP, Kuan YZ. Human pathogenic fungi in China—emerging trends from ongoing national survey for 1986, 1996, and 2006. Mycopathologia 2011; 171(6): 387–393
13. Liao Y, Chen M, Hartmann T, Yang RY, Liao WQ. Epidemiology of opportunistic invasive fungal infections in China: review of literature. Chin Med J (Engl) 2013; 126(2): 361–368
14. Havlickova B, Czaika VA, Friedrich M. Epidemiological trends in skin mycoses worldwide. Mycoses 2008; 51(Suppl 4): 2–15
15. Zhan P, Liu W. The changing face of dermatophytic infections worldwide. Mycopathologia 2017; 182(1-2): 77–86
16. Li GZ, Liu YH, Chen XW. Etiologic analysis of 4000 cases of superficial mycosis in Tianjin region. China J Lepr Skin Dis (Zhongguo Ma Feng Pi Fu Bing Za Zhi) 2010; 26(8): 602 (in Chinese)
17. Cai W, Lu C, Li X, Zhang J, Zhan P, Xi L, Sun J, Yu X. Epidemiology of superficial fungal infections in Guangdong, Southern China: a retrospective study from 2004 to 2014. Mycopathologia 2016; 181(5-6): 387–395
18. Zhu JH, Han DM, Zhao Y, Li L, Zhang QQ. Etiologic analysis of 9566 cases of superficial mycosis in Shanghai region. Chin J Mycol (Zhongguo Zhen Jun Xue Za Zhi) 2016; 11(3): 178–180 (in Chinese)
19. LI LN. Zhang SM, Liu HW, Gao L, Lei DC, Li ZL, Yu HQ, Li JG. Analysis of superficial mycoses and pathogenic fungi in 668 cases. Chin J Derm Venereol (Zhongguo Pi Fu Xing Bing Xue Za Zhi) 2016; 30(3): 259–260 (in Chinese)
20. Ma XN, Zhang H, Han XH, Wang HD, Shi LQ, Ren Y. Clinical analysis of 1422 cases of superficial mycoses in Yan'an Area. Chin J Derm Venereol (Zhongguo Pi Fu Xing Bing Xue Za Zhi) 2016; 30(9): 908–910 (in Chinese)
21. Xu W, Li Y. Clinical analysis of 818 cases of superficial mycosis. Guide China Med (Zhongguo Yi Yao Zhi Nan) 2010; 8(13): 131–132 (in Chinese)
22. Xiong Y, Zhou CJ, Li QJ, Huang XY, Huang YH, Zhong BY, Tang SQ, Dai W, Hao F. Etiologic analysis of 2135 cases of superficial mycosis in Chongqing region. J Clin Dermatol (Lin Chuang Pi Fu Ke Za Zhi) 2008; 37(11): 711–713 (in Chinese)
23. Silva-Rocha WP, de Azevedo MF, Chaves GM. Epidemiology and fungal species distribution of superficial mycoses in Northeast Brazil. J Mycol Med 2017; 27(1): 57–64
24. Foster KW, Ghannoum MA, Elewski BE. Epidemiologic surveillance of cutaneous fungal infection in the United States from 1999 to 2002. J Am Acad Dermatol 2004; 50(5): 748–752
25. Drakensjö IT, Chryssanthou E. Epidemiology of dermatophyte infections in Stockholm, Sweden: a retrospective study from 2005–2009. Med Mycol 2011; 49(5): 484–488
26. Simonnet C, Berger F, Gantier JC. Epidemiology of superficial fungal diseases in French Guiana: a three-year retrospective analysis. Med Mycol 2011; 49(6): 608–611
27. Tan HH. Superficial fungal infections seen at the National Skin Centre, Singapore. Nihon Ishinkin Gakkai Zasshi 2005; 46(2): 77–80
28. Fuller LC, Barton RC, Mohd Mustapa MF, Proudfoot LE, Punjabi SP, Higgins EM. British Association of Dermatologists' guidelines for the management of tinea capitis 2014. Br J Dermatol 2014; 171 (3): 454–463
29. Zhan P, Geng C, Li Z, Jin Y, Jiang Q, Tao L, Luo Y, Xiong Z, Wu S, Li D, Liu W, de Hoog GS. Evolution of tinea capitis in the Nanchang area, Southern China: a 50-year survey (1965–2014). Mycoses 2015; 58(5): 261–266
30. Liu ZS, Fu XQ, Xie SW, Wang Y, Sun JB. Analysis of situation of tinea capitis in Hubei from 1995 to 2000. China J Lepr Skin Dis (Zhongguo Ma Feng Pi Fu Bing Za Zhi) 2003; 14(4): 54–55 (in Chinese)
31. Yu J, Li R, Bulmer G. Current topics of tinea capitis in China. Nihon Ishinkin Gakkai Zasshi 2005; 46(2): 61–66
32. Zhu M, Li L, Wang J, Zhang C, Kang K, Zhang Q. Tinea capitis in Southeastern China: a 16-year survey. Mycopathologia 2010; 169 (4): 235–239
33. Korstanje MJ, Staats CG. Tinea capitis in Northwestern Europe 1963–1993: etiologic agents and their changing prevalence. Int J Dermatol 1994; 33(8): 548–549
34. Sigurgeirsson B, Baran R. The prevalence of onychomycosis in the global population: a literature study. J Eur Acad Dermatol Venereol 2014; 28(11): 1480–1491
35. Wang AP, Yu J, Wan Z, Li FQ, Zeng JS, Liu WD, Zhang QQ, Hao F, Ran YP, Xi LY, Lai W, Li RY. Multi-center epidemiological survey of pathogenic fungi of onychomycosis in China. Chin J Mycol (Zhongguo Zhen Jun Xue Za Zhi) 2015; 10(4): 197–202 (in

Chinese)
36. Gupta AK, Versteeg SG, Shear NH. Onychomycosis in the 21st century: an update on diagnosis, epidemiology, and treatment. J Cutan Med Surg 2017 Jun 1 [Epub ahead of print] https://doi.org/10.1177/1203475417716362
37. Papini M, Piraccini BM, Difonzo E, Brunoro A. Epidemiology of onychomycosis in Italy: prevalence data and risk factor identification. Mycoses 2015; 58(11): 659–664
38. Ribeiro CS, Zaitz C, Framil VM, Ottoboni TS, Tonoli MS, Ribeiro RP. Descriptive study of onychomycosis in a hospital in São Paulo. Braz J Microbiol 2015; 46(2): 485–492
39. Gupta C, Jongman M, Das S, Snehaa K, Bhattacharya SN, Seyedmousavi S, van Diepeningen AD. Genotyping and *in vitro* antifungal susceptibility testing of fusarium isolates from onychomycosis in India. Mycopathologia 2016; 181(7-8): 497–504
40. Segal R, Shemer A, Hochberg M, Keness Y, Shvarzman R, Mandelblat M, Frenkel M, Segal E. Onychomycosis in Israel: epidemiological aspects. Mycoses 2015; 58(3): 133–139
41. Maraki S, Mavromanolaki VE. Epidemiology of onychomycosis in Crete, Greece: a 12-year study. Mycoses 2016; 59(12): 798–802
42. Hashemi SJ, Gerami M, Zibafar E, Daei M, Moazeni M, Nasrollahi A. Onychomycosis in Tehran: mycological study of 504 patients. Mycoses 2010; 53(3): 251–255
43. Souza LK, Fernandes OF, Passos XS, Costa CR, Lemos JA, Silva MR. Epidemiological and mycological data of onychomycosis in Goiania, Brazil. Mycoses 2010; 53(1): 68–71
44. Yin SC, Zhang YQ, Tan YF, Yang JY, Huang HQ, Li H, Lai W. Analysis of pathogenic fungi of 805 cases with onychomycosis. Chin J Mycol (Zhongguo Zhen Jun Xue Za Zhi) 2013; 8(4): 214–216 (in Chinese)
45. Zhou J, Chen M, Chen H, Pan W, Liao W. *Rhodotorula minuta* as onychomycosis agent in a Chinese patient: first report and literature review. Mycoses 2014; 57(3): 191–195
46. Meersseman W, Van Wijngaerden E. Invasive aspergillosis in the ICU: an emerging disease. Intensive Care Med 2007; 33(10): 1679–1681
47. Pappas PG, Alexander BD, Andes DR, Hadley S, Kauffman CA, Freifeld A, Anaissie EJ, Brumble LM, Herwaldt L, Ito J, Kontoyiannis DP, Lyon GM, Marr KA, Morrison VA, Park BJ, Patterson TF, Perl TM, Oster RA, Schuster MG, Walker R, Walsh TJ, Wannemuehler KA, Chiller TM. Invasive fungal infections among organ transplant recipients: results of the Transplant-Associated Infection Surveillance Network (TRANSNET). Clin Infect Dis 2010; 50(8): 1101–1111
48. Gavaldà J, Meije Y, Fortún J, Roilides E, Saliba F, Lortholary O, Muñoz P, Grossi P, Cuenca-Estrella M; ESCMID Study Group for Infections in Compromised Hosts. Invasive fungal infections in solid organ transplant recipients. Clin Microbiol Infect 2014; 20 (Suppl 7): 27–48
49. Brown GD, Denning DW, Gow NA, Levitz SM, Netea MG, White TC. Hidden killers: human fungal infections. Sci Transl Med 2012; 4(165): 165rv13
50. Montagna MT, Caggiano G, Lovero G, De Giglio O, Coretti C, Cuna T, Iatta R, Giglio M, Dalfino L, Bruno F, Puntillo F. Epidemiology of invasive fungal infections in the intensive care unit: results of a multicenter Italian survey (AURORA Project). Infection 2013; 41(3): 645–653
51. Feng WL, Yang J, Xi ZQ, Wang YQ, Zhang RM, Ji Y, Wu Y, Jia XQ. Epidemiologic study on patients with invasive fungal infections. Chin J Epidemiol (Zhonghua Liu Xing Bing Xue Za Zhi) 2009; 30(10): 1043–1046 (in Chinese)
52. Liu ZY, Sheng RY, Li XL, Li TS, Wang AX. Nosocomial fungal infections, analysis of 149 cases. Natl Med J China (Zhonghua Yi Xue Za Zhi) 2003; 83(5): 399–402 (in Chinese)
53. Gao LY, Yu J, Li RY. Epidemiology of aspergillosis in mainland China. Chin J Mycol (Zhongguo Zhen Jun Xue Za Zhi) 2010; 5 (4): 247–251 (in Chinese)
54. Liu YN, She DY, Sun TY, Tong ZH, He B, Xiao Y, He LX, Qu JM, Liu XQ, Li ER, Chen P, Ma ZS, Shi Y, Feng YL, Jiang SJ, Xiong SD, Hu CP. A multicentre retrospective study of pulmonary mycosis clinically proven from 1998 to 2007. Chin J Tubere Respir Dis (Zhonghua Jie He He Hu Xi Za Zhi) 2011; 34(2): 86–90 (in Chinese)
55. Seneviratne CJ, Rajan S, Wong SS, Tsang DN, Lai CK, Samaranayake LP, Jin L. Antifungal susceptibility in serum and virulence determinants of *Candida* bloodstream isolates from Hong Kong. Front Microbiol 2016; 7: 216
56. Guo F, Yang Y, Kang Y, Zang B, Cui W, Qin B, Qin Y, Fang Q, Qin T, Jiang D, Li W, Gu Q, Zhao H, Liu D, Guan X, Li J, Ma X, Yu K, Chan D, Yan J, Tang Y, Liu W, Li R, Qiu H; China-SCAN Team. Invasive candidiasis in intensive care units in China: a multicentre prospective observational study. J Antimicrob Chemother 2013; 68(7): 1660–1668
57. Méan M, Marchetti O, Calandra T. Bench-to-bedside review: *Candida* infections in the intensive care unit. Crit Care 2008; 12 (1): 204
58. Kett DH, Azoulay E, Echeverria PM, Vincent JL; Extended Prevalence of Infection in ICU Study (EPIC II) Group of Investigators. *Candida* bloodstream infections in intensive care units: analysis of the extended prevalence of infection in intensive care unit study. Crit Care Med 2011; 39(4): 665–670
59. Falagas ME, Roussos N, Vardakas KZ. Relative frequency of albicans and the various non-albicans *Candida* spp. among candidemia isolates from inpatients in various parts of the world: a systematic review. Int J Infect Dis 2010; 14(11): e954–e966
60. Horn DL, Neofytos D, Anaissie EJ, Fishman JA, Steinbach WJ, Olyaei AJ, Marr KA, Pfaller MA, Chang CH, Webster KM. Epidemiology and outcomes of candidemia in 2019 patients: data from the prospective antifungal therapy alliance registry. Clin Infect Dis 2009; 48(12): 1695–1703
61. Gong X, Luan T, Wu X, Li G, Qiu H, Kang Y, Qin B, Fang Q, Cui W, Qin Y, Li J, Zang B. Invasive candidiasis in intensive care units in China: Risk factors and prognoses of *Candida albicans* and non-albicans *Candida* infections. Am J Infect Control 2016; 44(5): e59–e63
62. Ma CF, Li FQ, Shi LN, Hu YA, Wang Y, Huang M, Kong QQ. Surveillance study of species distribution, antifungal susceptibility and mortality of nosocomial candidemia in a tertiary care hospital in China. BMC Infect Dis 2013; 13(1): 337
63. Li S, An YZ. Retrospective analysis of invasive fungal infection in surgical intensive care unit. Natl Med J China (Zhonghua Yi Xue Za Zhi) 2010; 90(6): 382–385 (in Chinese)
64. Cao B, Wang H, Wu L, Sun WJ, Li F, Liu YM. Epidemiological study of invasive nosocomial candidiasis in 2 teaching hospitals in

Beijing. Natl Med J China (Zhonghua Yi Xue Za Zhi) 2008; 88 (28): 1970–1973 (in Chinese)

65. Poikonen E, Lyytikäinen O, Anttila VJ, Koivula I, Lumio J, Kotilainen P, Syrjälä H, Ruutu P. Secular trend in candidemia and the use of fluconazole in Finland, 2004–2007. BMC Infect Dis 2010; 10(1): 312
66. Almirante B, Rodríguez D, Park BJ, Cuenca-Estrella M, Planes AM, Almela M, Mensa J, Sanchez F, Ayats J, Gimenez M, Saballs P, Fridkin SK, Morgan J, Rodriguez-Tudela JL, Warnock DW, Pahissa A; Barcelona Candidemia Project Study Group. Epidemiology and predictors of mortality in cases of *Candida* bloodstream infection: results from population-based surveillance, Barcelona, Spain, from 2002 to 2003. J Clin Microbiol 2005; 43 (4): 1829–1835
67. Paphitou NI, Ostrosky-Zeichner L, Rex JH. Rules for identifying patients at increased risk for candidal infections in the surgical intensive care unit: approach to developing practical criteria for systematic use in antifungal prophylaxis trials. Med Mycol 2005; 43(3): 235–243
68. Marchetti O, Bille J, Fluckiger U, Eggimann P, Ruef C, Garbino J, Calandra T, Glauser MP, Täuber MG, Pittet D; Fungal Infection Network of Switzerland. Epidemiology of candidemia in Swiss tertiary care hospitals: secular trends, 1991–2000. Clin Infect Dis 2004; 38(3): 311–320
69. Wisplinghoff H, Bischoff T, Tallent SM, Seifert H, Wenzel RP, Edmond MB. Nosocomial bloodstream infections in US hospitals: analysis of 24,179 cases from a prospective nationwide surveillance study. Clin Infect Dis 2004; 39(3): 309–317
70. González GM, Treviño-Rangel RdeJ, Palma-Nicolás JP, Martínez C, González JG, Ayala J, Caballero A, Morfín-Otero R, Rodríguez-Noriega E, Velarde F, Ascencio EP, Tinoco JC, Vázquez JA, Cano MA, León-Sicairos N, González R, Rincón J, Elías MA, Bonifaz A. Species distribution and antifungal susceptibility of bloodstream fungal isolates in paediatric patients in Mexico: a nationwide surveillance study. J Antimicrob Chemother 2013; 68(12): 2847–2851
71. Pfaller MA, Diekema DJ, Gibbs DL, Newell VA, Ellis D, Tullio V, Rodloff A, Fu W, Ling TA; Global Antifungal Surveillance Group. Results from the ARTEMIS DISK Global Antifungal Surveillance Study, 1997 to 2007: a 10.5-year analysis of susceptibilities of *Candida* species to fluconazole and voriconazole as determined by CLSI standardized disk diffusion. J Clin Microbiol 2010; 48(4): 1366–1377
72. Pu S, Niu S, Zhang C, Xu X, Qin M, Huang S, Zhang L. Epidemiology, antifungal susceptibilities, and risk factors for invasive candidiasis from 2011 to 2013 in a teaching hospital in southwest China. J Microbiol Immunol Infect 2017; 50(1): 97–103
73. Li F, Wu L, Cao B, Zhang Y, Li X, Liu Y. Surveillance of the prevalence, antibiotic susceptibility, and genotypic characterization of invasive candidiasis in a teaching hospital in China between 2006 to 2011. BMC Infect Dis 2013; 13(1): 353
74. Zhang Z, Zhao SL, Pang LJ, Wang H, Liu WY, Yan W. The analysis and survey of 475 strains of fungi from clinical samples. Chin J Lab Med (Zhonghua Jian Yan Yi Xue Za Zhi) 1996; 19(5): 267–269 (in Chinese)
75. Yu J, Li RY, Wang D, Zhao M, Jiang H, Chen W, Wang AP, Wang DL. Analysis on species distribution and risk factors of nosocomial invasive *Candida* infection. China J Lepr Skin Dis (Zhongguo Ma Feng Pi Fu Bing Za Zhi) 2000; 16(4): 211–215 (in Chinese)
76. Wang H, Xu YC, Hsueh PR. Epidemiology of candidemia and antifungal susceptibility in invasive *Candida* species in the Asia-Pacific region. Future Microbiol 2016; 11(11): 1461–1477
77. Nucci M, Queiroz-Telles F, Tobón AM, Restrepo A, Colombo AL. Epidemiology of opportunistic fungal infections in Latin America. Clin Infect Dis 2010; 51(5): 561–570
78. Wang H, Xiao M, Chen SC, Kong F, Sun ZY, Liao K, Lu J, Shao HF, Yan Y, Fan H, Hu ZD, Chu YZ, Hu TS, Ni YX, Zou GL, Xu YC. *In vitro* susceptibilities of yeast species to fluconazole and voriconazole as determined by the 2010 National China Hospital Invasive Fungal Surveillance Net (CHIF-NET) study. J Clin Microbiol 2012; 50(12): 3952–3959
79. Puig-Asensio M, Pemán J, Zaragoza R, Garnacho-Montero J, Martín-Mazuelos E, Cuenca-Estrella M, Almirante B; Prospective Population Study on Candidemia in Spain (CANDIPOP) Project; Hospital Infection Study Group (GEIH); Medical Mycology Study Group (GEMICOMED) of the Spanish Society of Infectious Diseases and Clinical Microbiology (SEIMC); Spanish Network for Research in Infectious Diseases. Impact of therapeutic strategies on the prognosis of candidemia in the ICU. Crit Care Med 2014; 42(6): 1423–1432
80. Wu JQ, Zhu LP, Ou XT, Xu B, Hu XP, Wang X, Weng XH. Epidemiology and risk factors for non-*Candida albicans* candidemia in non-neutropenic patients at a Chinese teaching hospital. Med Mycol 2011; 49(5): 552–555
81. Liu W, Tan J, Sun J, Xu Z, Li M, Yang Q, Shao H, Zhang L, Liu W, Wan Z, Cui W, Zang B, Jiang D, Fang Q, Qin B, Qin T, Li W, Guo F, Liu D, Guan X, Yu K, Qiu H, Li R; China-SCAN team. Invasive candidiasis in intensive care units in China: *in vitro* antifungal susceptibility in the China-SCAN study. J Antimicrob Chemother 2014; 69(1): 162–167
82. Chen TC, Chen YH, Tsai JJ, Peng CF, Lu PL, Chang K, Hsieh HC, Chen TP. Epidemiologic analysis and antifungal susceptibility of *Candida* blood isolates in southern Taiwan. J Microbiol Immunol Infect 2005; 38(3): 200–210
83. Chen PL, Lo HJ, Wu CJ, Lee HC, Chang CM, Lee NY, Wang AH, Lin WL, Ko NY, Lee CC, Ko WC. Species distribution and antifungal susceptibility of blood *Candida* isolates at a tertiary hospital in southern Taiwan, 1999–2006. Mycoses 2011; 54(4): e17–e23
84. Li Y, Du M, Chen LA, Liu Y, Liang Z. Nosocomial bloodstream infection due to *Candida* spp. in China: species distribution, clinical features, and outcomes. Mycopathologia 2016; 181(7-8): 485–495
85. Yang ZT, Wu L, Liu XY, Zhou M, Li J, Wu JY, Cai Y, Mao EQ, Chen EZ, Lortholary O. Epidemiology, species distribution and outcome of nosocomial *Candida* spp. bloodstream infection in Shanghai. BMC Infect Dis 2014; 14(1): 241
86. Wang H, Liu N, Yin M, Han H, Yue J, Zhang F, Shan T, Guo H, Wu D. The epidemiology, antifungal use and risk factors of death in elderly patients with candidemia: a multicentre retrospective study. BMC Infect Dis 2014; 14(1): 609
87. Zhang XB, Yu SJ, Yu JX, Gong YL, Feng W, Sun FJ. Retrospective analysis of epidemiology and prognostic factors for candidemia at a hospital in China, 2000–2009. Jpn J Infect Dis 2012; 65(6): 510–515

88. Yap HY, Kwok KM, Gomersall CD, Fung SC, Lam TC, Leung PN, Hui M, Joynt GM. Epidemiology and outcome of *Candida* bloodstream infection in an intensive care unit in Hong Kong. Hong Kong Med J 2009; 15(4): 255–261
89. Chen PY, Chuang YC, Wang JT, Sheng WH, Yu CJ, Chu CC, Hsueh PR, Chang SC, Chen YC. Comparison of epidemiology and treatment outcome of patients with candidemia at a teaching hospital in Northern Taiwan, in 2002 and 2010. J Microbiol Immunol Infect 2014; 47(2): 95–103
90. Chen SC, Marriott D, Playford EG, Nguyen Q, Ellis D, Meyer W, Sorrell TC, Slavin M; Australian Candidaemia Study. Candidaemia with uncommon *Candida* species: predisposing factors, outcome, antifungal susceptibility, and implications for management. Clin Microbiol Infect 2009; 15(7): 662–669
91. Pfaller MA, Diekema DJ, Colombo AL, Kibbler C, Ng KP, Gibbs DL, Newell VA. *Candida rugosa,* an emerging fungal pathogen with resistance to azoles: geographic and temporal trends from the ARTEMIS DISK antifungal surveillance program. J Clin Microbiol 2006; 44(10): 3578–3582
92. Xiao M, Wang H, Lu J, Chen SC, Kong F, Ma XJ, Xu YC. Three clustered cases of candidemia caused by *Candida quercitrusa* and mycological characteristics of this novel species. J Clin Microbiol 2014; 52(8): 3044–3048
93. Chowdhary A, Sharma C, Meis JF. *Candida auris*: a rapidly emerging cause of hospital-acquired multidrug-resistant fungal infections globally. PLoS Pathog 2017; 13(5): e1006290
94. Wu Z, Liu Y, Feng X, Liu Y, Wang S, Zhu X, Chen Q, Pan S. Candidemia: incidence rates, type of species, and risk factors at a tertiary care academic hospital in China. Int J Infect Dis 2014; 22: 4–8
95. Huang YT, Liu CY, Liao CH, Chung KP, Sheng WH, Hsueh PR. Antifungal susceptibilities of *Candida* isolates causing bloodstream infections at a medical center in Taiwan, 2009–2010. Antimicrob Agents Chemother 2014; 58(7): 3814–3819
96. Chowdhary A, Sharma C, Duggal S, Agarwal K, Prakash A, Singh PK, Jain S, Kathuria S, Randhawa HS, Hagen F, Meis JF. New clonal strain of *Candida auris*, Delhi, India. Emerg Infect Dis 2013; 19(10): 1670–1673
97. Magobo RE, Corcoran C, Seetharam S, Govender NP. *Candida auris*-associated candidemia, South Africa. Emerg Infect Dis 2014; 20(7): 1250–1251
98. Vallabhaneni S, Kallen A, Tsay S, Chow N, Welsh R, Kerins J, Kemble SK, Pacilli M, Black SR, Landon E, Ridgway J, Palmore TN, Zelzany A, Adams EH, Quinn M, Chaturvedi S, Greenko J, Fernandez R, Southwick K, Furuya EY, Calfee DP, Hamula C, Patel G, Barrett P; MSD,Lafaro P, Berkow EL, Moulton-Meissner H, Noble-Wang J, Fagan RP, Jackson BR, Lockhart SR, Litvintseva AP, Chiller TM. Investigation of the first seven reported cases of *Candida auris*, a globally emerging invasive, multidrug-resistant fungus — United States, May 2013–August 2016. MMWR Morb Mortal Wkly Rep 2016; 65(44): 1234–1237
99. Mohsin J, Hagen F, Al-Balushi ZAM, de Hoog GS, Chowdhary A, Meis JF, Al-Hatmi AMS. The first cases of *Candida auris* candidaemia in Oman. Mycoses 2017; 60(9): 569–575
100. Chowdhary A, Anil Kumar V, Sharma C, Prakash A, Agarwal K, Babu R, Dinesh KR, Karim S, Singh SK, Hagen F, Meis JF. Multidrug-resistant endemic clonal strain of *Candida auris* in India. Eur J Clin Microbiol Infect Dis 2014; 33(6): 919–926
101. Wang FJ, Zhang D, Liu ZH, Wu WX, Bai HH, Dong HY. Species distribution and *in vitro* antifungal susceptibility of vulvovaginal *Candida* isolates in China. Chin Med J (Engl) 2016; 129(10): 1161–1165
102. Ding X, Yan D, Sun W, Zeng Z, Su R, Su J. Epidemiology and risk factors for nosocomial non-*Candida albicans* candidemia in adult patients at a tertiary care hospital in North China. Med Mycol 2015; 53(7): 684–690
103. Chen J, Jiang Y, Wei B, Ding Y, Xu S, Qin P, Fu J. Epidemiology of and risk factors for neonatal candidemia at a tertiary care hospital in western China. BMC Infect Dis 2016; 16(1): 700
104. Pfaller MA, Castanheira M, Messer SA, Moet GJ, Jones RN. Echinocandin and triazole antifungal susceptibility profiles for *Candida* spp., *Cryptococcus neoformans*, and *Aspergillus fumigatus*: application of new CLSI clinical breakpoints and epidemiologic cutoff values to characterize resistance in the SENTRY Antimicrobial Surveillance Program (2009). Diagn Microbiol Infect Dis 2011; 69(1): 45–50
105. Montagna MT, Lovero G, Coretti C, Martinelli D, Delia M, De Giglio O, Caira M, Puntillo F, D'Antonio D, Venditti M, Sambri V, Di Bernardo F, Barbui A, Lo Cascio G, Concia E, Mikulska M, Viscoli C, Maximova N, Candoni A, Oliveri S, Lombardi G, Pitzurra L, Sanguinetti M, Masciari R, Santantonio T, Andreoni S, Barchiesi F, Pecile P, Farina C, Viale P, Specchia G, Caggiano G, Pagano L. SIMIFF study: Italian fungal registry of mold infections in hematological and non-hematological patients. Infection 2014; 42(1): 141–151
106. Lin SJ, Schranz J, Teutsch SM. Aspergillosis case-fatality rate: systematic review of the literature. Clin Infect Dis 2001; 32(3): 358–366
107. Zhang S, Wang S, Wan Z, Li R, Yu J. The diagnosis of invasive and noninvasive pulmonary aspergillosis by serum and bronchoalveolar lavage fluid galactomannan assay. Biomed Res Int 2015; 2015: 943691
108. Chen Y, Lu ZY, Jin Y, Han L, Huang LY. Progress of research on azole resistance in *Aspergillus fumigatus*. Chin J Epidemiol (Zhonghua Liu Xing Bing Xue Za Zhi) 2016; 37(12): 1687–1692 (in Chinese)
109. He H, Ding L, Li F, Zhan Q. Clinical features of invasive bronchial-pulmonary aspergillosis in critically ill patients with chronic obstructive respiratory diseases: a prospective study. Crit Care 2011; 15(1): R5
110. Chen J, Yang Q, Huang J, Li L. Clinical findings in 19 cases of invasive pulmonary aspergillosis with liver cirrhosis. Multidiscip Respir Med 2014; 9(1): 1
111. Chen J, Yang Q, Huang J, Li L. Risk factors for invasive pulmonary aspergillosis and hospital mortality in acute-on-chronic liver failure patients: a retrospective-cohort study. Int J Med Sci 2013; 10(12): 1625–1631
112. Meersseman W, Vandecasteele SJ, Wilmer A, Verbeken E, Peetermans WE, Van Wijngaerden E. Invasive aspergillosis in critically ill patients without malignancy. Am J Respir Crit Care Med 2004; 170(6): 621–625
113. Yan X, Li M, Jiang M, Zou LQ, Luo F, Jiang Y. Clinical characteristics of 45 patients with invasive pulmonary aspergillosis: retrospective analysis of 1711 lung cancer cases. Cancer 2009;

115(21): 5018–5025

114. Taccone FS, Van den Abeele AM, Bulpa P, Misset B, Meersseman W, Cardoso T, Paiva JA, Blasco-Navalpotro M, De Laere E, Dimopoulos G, Rello J, Vogelaers D, Blot SI; AspICU Study Investigators. Epidemiology of invasive aspergillosis in critically ill patients: clinical presentation, underlying conditions, and outcomes. Crit Care 2015; 19(1): 7
115. Lockhart SR, Frade JP, Etienne KA, Pfaller MA, Diekema DJ, Balajee SA. Azole resistance in *Aspergillus fumigatus* isolates from the ARTEMIS global surveillance study is primarily due to the TR/L98H mutation in the cyp51A gene. Antimicrob Agents Chemother 2011; 55(9): 4465–4468
116. Li Y, Wan Z, Liu W, Li R. Identification and susceptibility of *Aspergillus* section nigri in china: prevalence of species and paradoxical growth in response to echinocandins. J Clin Microbiol 2015; 53(2): 702–705
117. Wang W, Zhao CY, Zhou JY, Wang YD, Shen C, Zhou DF, Yin HZ. Invasive pulmonary aspergillosis in patients with HBV-related liver failure. Eur J Clin Microbiol Infect Dis 2011; 30(5): 661–667
118. Liu M, Zeng R, Zhang L, Li D, Lv G, Shen Y, Zheng H, Zhang Q, Zhao J, Zheng N, Liu W. Multiple cyp51A-based mechanisms identified in azole-resistant isolates of *Aspergillus fumigatus* from China. Antimicrob Agents Chemother 2015; 59(7): 4321–4325
119. Chen Y, Lu Z, Zhao J, Zou Z, Gong Y, Qu F, Bao Z, Qiu G, Song M, Zhang Q, Liu L, Hu M, Han X, Tian S, Zhao J, Chen F, Zhang C, Sun Y, Verweij PE, Huang L, Han L. Epidemiology and molecular characterizations of azole resistance in clinical and environmental *Aspergillus fumigatus* isolates from China. Antimicrob Agents Chemother 2016; 60(10): 5878–5884
120. Chen J, Li H, Li R, Bu D, Wan Z. Mutations in the cyp51A gene and susceptibility to itraconazole in *Aspergillus fumigatus* serially isolated from a patient with lung aspergilloma. J Antimicrob Chemother 2005; 55(1): 31–37
121. Chen Y, Wang H, Lu Z, Li P, Zhang Q, Jia T, Zhao J, Tian S, Han X, Chen F, Zhang C, Jia X, Huang L, Qu F, Han L. Emergence of TR46/Y121F/T289A in an *Aspergillus fumigatus* isolate from a Chinese patient. Antimicrob Agents Chemother 2015; 59(11): 7148–7150
122. Sloan DJ, Parris V. Cryptococcal meningitis: epidemiology and therapeutic options. Clin Epidemiol 2014; 6: 169–182
123. Gullo FP, Rossi SA, Sardi JdeC, Teodoro VL, Mendes-Giannini MJ, Fusco-Almeida AM. Cryptococcosis: epidemiology, fungal resistance, and new alternatives for treatment. Eur J Clin Microbiol Infect Dis 2013; 32(11): 1377–1391
124. Cogliati M. Global molecular epidemiology of *Cryptococcus neoformans* and *Cryptococcus gattii:* an atlas of the molecular types. Scientifica (Cairo) 2013; 2013: 675213
125. Meyer W, Aanensen DM, Boekhout T, Cogliati M, Diaz MR, Esposto MC, Fisher M, Gilgado F, Hagen F, Kaocharoen S, Litvintseva AP, Mitchell TG, Simwami SP, Trilles L, Viviani MA, Kwon-Chung J. Consensus multi-locus sequence typing scheme for *Cryptococcus neoformans* and *Cryptococcus gattii*. Med Mycol 2009; 47(6): 561–570
126. Fan X, Xiao M, Chen S, Kong F, Dou HT, Wang H, Xiao YL, Kang M, Sun ZY, Hu ZD, Wan Z, Chen SL, Liao K, Chu YZ, Hu TS, Zou GL, Hou X, Zhang L, Zhao YP, Xu YC, Liu ZY. Predominance of *Cryptococcus neoformans* var. *grubii* multilocus sequence type 5 and emergence of isolates with non-wild-type minimum inhibitory concentrations to fluconazole: a multi-centre study in China. Clin Microbiol Infect 2016; 22(10): 887.e1–887.e9
127. Dou HT, Xu YC, Wang HZ, Li TS. Molecular epidemiology of *Cryptococcus neoformans* and *Cryptococcus gattii* in China between 2007 and 2013 using multilocus sequence typing and the DiversiLab system. Eur J Clin Microbiol Infect Dis 2015; 34 (4): 753–762
128. Khayhan K, Hagen F, Pan W, Simwami S, Fisher MC, Wahyuningsih R, Chakrabarti A, Chowdhary A, Ikeda R, Taj-Aldeen SJ, Khan Z, Ip M, Imran D, Sjam R, Sriburee P, Liao W, Chaicumpar K, Vuddhakul V, Meyer W, Trilles L, van Iersel LJ, Meis JF, Klaassen CH, Boekhout T. Geographically structured populations of *Cryptococcus neoformans* variety *grubii* in Asia correlate with HIV status and show a clonal population structure. PLoS One 2013; 8(9): e72222
129. Park SH, Kim M, Joo SI, Hwang SM. Molecular epidemiology of clinical *Cryptococcus neoformans* isolates in Seoul, Korea. Mycobiology 2014; 42(1): 73–78
130. Mihara T, Izumikawa K, Kakeya H, Ngamskulrungroj P, Umeyama T, Takazono T, Tashiro M, Nakamura S, Imamura Y, Miyazaki T, Ohno H, Yamamoto Y, Yanagihara K, Miyzaki Y, Kohno S. Multilocus sequence typing of *Cryptococcus neoformans* in non-HIV associated cryptococcosis in Nagasaki, Japan. Med Mycol 2013; 51(3): 252–260
131. Simwami SP, Khayhan K, Henk DA, Aanensen DM, Boekhout T, Hagen F, Brouwer AE, Harrison TS, Donnelly CA, Fisher MC. Low diversity *Cryptococcus neoformans* variety *grubii* multilocus sequence types from Thailand are consistent with an ancestral African origin. PLoS Pathog 2011; 7(4): e1001343
132. Xue X, Wu H, Wang K, Cao J, Shen D. Cryptococcosis by *Cryptococcus gattii* in China. Lancet Infect Dis 2015; 15(10): 1135–1136
133. Kronstad JW, Attarian R, Cadieux B, Choi J, D'Souza CA, Griffiths EJ, Geddes JM, Hu G, Jung WH, Kretschmer M, Saikia S, Wang J. Expanding fungal pathogenesis: *Cryptococcus* breaks out of the opportunistic box. Nat Rev Microbiol 2011; 9(3): 193–203
134. Feng X, Yao Z, Ren D, Liao W, Wu J. Genotype and mating type analysis of *Cryptococcus neoformans* and *Cryptococcus gattii* isolates from China that mainly originated from non-HIV-infected patients. FEMS Yeast Res 2008; 8(6): 930–938
135. Okamoto K, Hatakeyama S, Itoyama S, Nukui Y, Yoshino Y, Kitazawa T, Yotsuyanagi H, Ikeda R, Sugita T, Koike K. *Cryptococcus gattii* genotype VGIIa infection in man, Japan, 2007. Emerg Infect Dis 2010; 16(7): 1155–1157
136. Yuchong C, Fubin C, Jianghan C, Fenglian W, Nan X, Minghui Y, Yalin S, Zhizhong Z. Cryptococcosis in China (1985–2010): review of cases from Chinese database. Mycopathologia 2012; 173 (5-6): 329–335
137. Lui G, Lee N, Ip M, Choi KW, Tso YK, Lam E, Chau S, Lai R, Cockram CS. Cryptococcosis in apparently immunocompetent patients. QJM 2006; 99(3): 143–151
138. Tseng HK, Liu CP, Ho MW, Lu PL, Lo HJ, Lin YH, Cho WL, Chen YC; Taiwan Infectious Diseases Study Network for Cryptococcosis. Microbiological, epidemiological, and clinical characteristics and outcomes of patients with cryptococcosis in Taiwan, 1997–2010. PLoS One 2013; 8(4): e61921

139. Chen J, Varma A, Diaz MR, Litvintseva AP, Wollenberg KK, Kwon-Chung KJ. *Cryptococcus neoformans* strains and infection in apparently immunocompetent patients, China. Emerg Infect Dis 2008; 14(5): 755–762
140. Chen YY, Lai CH. Nationwide population-based epidemiologic study of cryptococcal meningitis in Taiwan. Neuroepidemiology 2011; 36(2): 79–84
141. Lu CH, Chang WN, Chang HW, Chuang YC. The prognostic factors of cryptococcal meningitis in HIV-negative patients. J Hosp Infect 1999; 42(4): 313–320
142. Fang W, Fa Z, Liao W. Epidemiology of *Cryptococcus* and cryptococcosis in China. Fungal Genet Biol 2015; 78: 7–15
143. Dou H, Wang H, Xie S, Chen X, Xu Z, Xu Y. Molecular characterization of Cryptococcus neoformans isolated from the environment in Beijing, China. Med Mycol 2017; 55(7):737–747
144. Li AS, Pan WH, Wu SX, Hideaki T, Guo NR, Shen YN, Lu GX, Pan RG, Zhu MC, Chen M, Shi WM, Liao WQ. Ecological surveys of the *Cryptococcus* species complex in China. Chin Med J (Engl) 2012; 125(3): 511–516
145. Skiada A, Pagano L, Groll A, Zimmerli S, Dupont B, Lagrou K, Lass-Florl C, Bouza E, Klimko N, Gaustad P, Richardson M, Hamal P, Akova M, Meis JF, Rodriguez-Tudela JL, Roilides E, Mitrousia-Ziouva A, Petrikkos G; European Confederation of Medical Mycology Working Group on Zygomycosis. Zygomycosis in Europe: analysis of 230 cases accrued by the registry of the European Confederation of Medical Mycology (ECMM) Working Group on Zygomycosis between 2005 and 2007. Clin Microbiol Infect 2011; 17(12): 1859–1867
146. Ribes JA, Vanover-Sams CL, Baker DJ. Zygomycetes in human disease. Clin Microbiol Rev 2000; 13(2): 236–301
147. Katragkou A, Walsh TJ, Roilides E. Why is mucormycosis more difficult to cure than more common mycoses? Clin Microbiol Infect 2014; 20(Suppl 6): 74–81
148. Rees JR, Pinner RW, Hajjeh RA, Brandt ME, Reingold AL. The epidemiological features of invasive mycotic infections in the San Francisco Bay area, 1992–1993: results of population-based laboratory active surveillance. Clin Infect Dis 1998; 27(5): 1138–1147
149. Torres-Narbona M, Guinea J, Martínez-Alarcón J, Muñoz P, Gadea I, Bouza E; MYCOMED Zygomycosis Study Group. Impact of zygomycosis on microbiology workload: a survey study in Spain. J Clin Microbiol 2007; 45(6): 2051–2053
150. Bitar D, Van Cauteren D, Lanternier F, Dannaoui E, Che D, Dromer F, Desenclos JC, Lortholary O. Increasing incidence of zygomycosis (mucormycosis), France, 1997–2006. Emerg Infect Dis 2009; 15(9): 1395–1401
151. Zhao JY, Fang W, Yang YL, Pan WH, Liao WQ, Tang YC. Retrospective analysis of diabetes combined with zygomycosis in mainland China: a review of 74 cases. Chin J Mycol (Zhongguo Zhen Jun Xue Za Zhi) 2016; 11(1): 33–36 (in Chinese)
152. Wang SB, Li RY, Yu J. Epidemiology of zygomycosis in mainland China. Chin J Mycol (Zhongguo Zhen Jun Xue Za Zhi) 2013; 8(3): 163–168 (in Chinese)
153. Zhao JY, Wang GZ, Zhang JY, Yang YL, Jia HL, Fang W, Pan WH, Liao WQ. Retrospective analysis of pulmonary zygomycosis in mainland China: a review of 102 cases. Chin J Mycol (Zhongguo Zhen Jun Xue Za Zhi) 2014; 9(3): 150–154 (in Chinese)
154. Roden MM, Zaoutis TE, Buchanan WL, Knudsen TA, Sarkisova TA, Schaufele RL, Sein M, Sein T, Chiou CC, Chu JH, Kontoyiannis DP, Walsh TJ. Epidemiology and outcome of zygomycosis: a review of 929 reported cases. Clin Infect Dis 2005; 41(5): 634–653
155. Cornely OA, Arikan-Akdagli S, Dannaoui E, Groll AH, Lagrou K, Chakrabarti A, Lanternier F, Pagano L, Skiada A, Akova M, Arendrup MC, Boekhout T, Chowdhary A, Cuenca-Estrella M, Freiberger T, Guinea J, Guarro J, de Hoog S, Hope W, Johnson E, Kathuria S, Lackner M, Lass-Flörl C, Lortholary O, Meis JF, Meletiadis J, Muñoz P, Richardson M, Roilides E, Tortorano AM, Ullmann AJ, van Diepeningen A, Verweij P, Petrikkos G; European Society of Clinical Microbiology and Infectious Diseases Fungal Infection Study Group; European Confederation of Medical Mycology. ESCMID and ECMM joint clinical guidelines for the diagnosis and management of mucormycosis 2013. Clin Microbiol Infect 2014; 20(Suppl 3): 5–26
156. Yang W, Lu J, Weng J, Jia W, Ji L, Xiao J, Shan Z, Liu J, Tian H, Ji Q, Zhu D, Ge J, Lin L, Chen L, Guo X, Zhao Z, Li Q, Zhou Z, Shan G, He J; China National Diabetes and Metabolic Disorders Study Group. Prevalence of diabetes among men and women in China. N Engl J Med 2010; 362(12): 1090–1101
157. Thomas CF Jr, Limper AH. *Pneumocystis* pneumonia. N Engl J Med 2004; 350(24): 2487–2498
158. Thomas CF Jr, Limper AH. Current insights into the biology and pathogenesis of *Pneumocystis* pneumonia. Nat Rev Microbiol 2007; 5(4): 298–308
159. Edman JC, Kovacs JA, Masur H, Santi DV, Elwood HJ, Sogin ML. Ribosomal RNA sequence shows *Pneumocystis carinii* to be a member of the fungi. Nature 1988; 334(6182): 519–522
160. Stringer SL, Stringer JR, Blase MA, Walzer PD, Cushion MT. *Pneumocystis carinii:* sequence from ribosomal RNA implies a close relationship with fungi. Exp Parasitol 1989; 68(4): 450–461
161. Gigliotti F, Limper AH, Wright T. *Pneumocystis.* Cold Spring Harb Perspect Med 2014; 4(12): a019828
162. Lu JJ, Lee CH. *Pneumocystis* pneumonia. J Formos Med Assoc 2008; 107(11): 830–842
163. Catherinot E, Lanternier F, Bougnoux ME, Lecuit M, Couderc LJ, Lortholary O. *Pneumocystis jirovecii* pneumonia. Infect Dis Clin North Am 2010; 24(1): 107–138
164. Kaplan JE, Hanson D, Dworkin MS, Frederick T, Bertolli J, Lindegren ML, Holmberg S, Jones JL. Epidemiology of human immunodeficiency virus-associated opportunistic infections in the United States in the era of highly active antiretroviral therapy. Clin Infect Dis 2000; 30(s1 Suppl 1): S5–S14
165. Ruxrungtham K, Brown T, Phanuphak P. HIV/AIDS in Asia. Lancet 2004; 364(9428): 69–82
166. Beck JM, Cushion MT. *Pneumocystis* workshop: 10th anniversary summary. Eukaryot Cell 2009; 8(4): 446–460
167. Wang XL, Wang XL, Wei W, An CL. Retrospective study of *Pneumocystis* pneumonia over half a century in mainland China. J Med Microbiol 2011; 60(Pt 5): 631–638
168. Liu Y, Su L, Jiang SJ, Qu H. Risk factors for mortality from *Pneumocystis carinii* pneumonia (PCP) in non-HIV patients: a meta-analysis. Oncotarget 2017; 8(35): 59729–59739
169. Wang DD, Zheng MQ, Zhang N, An CL. Investigation of

Pneumocystis jirovecii colonization in patients with chronic pulmonary diseases in the People's Republic of China. Int J Chron Obstruct Pulmon Dis 2015; 10: 2079–2085

170. Huang YS, Yang JJ, Lee NY, Chen GJ, Ko WC, Sun HY, Hung CC. Treatment of *Pneumocystis jirovecii* pneumonia in HIV-infected patients: a review. Expert Rev Anti Infect Ther 2017; 15 (9): 873–892
171. Guo F, Chen Y, Yang SL, Xia H, Li XW, Tong ZH. *Pneumocystis* pneumonia in HIV-infected and immunocompromised non-HIV infected patients: a retrospective study of two centers in China. PLoS One 2014; 9(7): e101943
172. Chen M, Tian X, Qin F, Zhou J, Liu J, Wang M, Xu KF. *Pneumocystis* pneumonia in patients with autoimmune diseases: a retrospective study focused on clinical characteristics and prognostic factors related to death. PLoS One 2015; 10(9): e0139144
173. Lemiale V, Debrumetz A, Delannoy A, Alberti C, Azoulay E. Adjunctive steroid in HIV-negative patients with severe *Pneumocystis* pneumonia. Respir Res 2013; 14(1): 87
174. Asai N, Motojima S, Ohkuni Y, Matsunuma R, Nakashima K, Iwasaki T, Nakashita T, Otsuka Y, Kaneko N. Early diagnosis and treatment are crucial for the survival of *Pneumocystis* pneumonia patients without human immunodeficiency virus infection. J Infect Chemother 2012; 18(6): 898–905
175. Deng X, Zhuo L, Lan Y, Dai Z, Chen WS, Cai W, Kovacs JA, Ma L, Tang X. Mutational analysis of *Pneumocystis jirovecii* dihydropteroate synthase and dihydrofolate reductase genes in HIV-infected patients in China. J Clin Microbiol 2014; 52(11): 4017–4019
176. Takahashi T, Endo T, Nakamura T, Sakashitat H, Kimurat K, Ohnishit K, Kitamura Y, Iwamoto A. Dihydrofolate reductase gene polymorphisms in *Pneumocystis carinii* f. sp. *hominis* in Japan. J Med Microbiol 2002; 51(6): 510–515
177. Siripattanapipong S, Leelayoova S, Mungthin M, Worapong J, Tan-Ariya P. Study of DHPS and DHFR genes of *Pneumocystis jirovecii* in Thai HIV-infected patients. Med Mycol 2008; 46(4): 389–392
178. Robberts FJ, Chalkley LJ, Weyer K, Goussard P, Liebowitz LD. Dihydropteroate synthase and novel dihydrofolate reductase gene mutations in strains of *Pneumocystis jirovecii* from South Africa. J Clin Microbiol 2005; 43(3): 1443–1444
179. Kazanjian PH, Fisk D, Armstrong W, Shulin Q, Liwei H, Ke Z, Meshnick S. Increase in prevalence of *Pneumocystis carinii* mutations in patients with AIDS and *P. carinii* pneumonia, in the United States and China. J Infect Dis 2004; 189(9): 1684–1687
180. Zhang Y, Hagen F, Wan Z, Liu Y, Liu Y, Wang Q, de Hoog GS, Li R, Zhang J. Two cases of sporotrichosis of the right upper extremity in right-handed patients with diabetes mellitus. Rev Iberoam Micol 2016; 33(1): 38–42
181. Zhang Y, Hagen F, Stielow B, Rodrigues AM, Samerpitak K, Zhou X, Feng P, Yang L, Chen M, Deng S, Li S, Liao W, Li R, Li F, Meis JF, Guarro J, Teixeira M, Al-Zahrani HS, Pires de Camargo Z, Zhang L, de Hoog GS. Phylogeography and evolutionary patterns in *Sporothrix* spanning more than 14 000 human and animal case reports. Persoonia 2015; 35(1): 1–20
182. Chen YC. Sporotrichosis. Chin J Mycol (Zhongguo Zhen Jun Xue Za Zhi) 2008; 3(4): 233–241 (in Chinese)
183. Liu TT, Zhang K, Zhou X. Molecular identification of *Sporothrix* clinical isolates in China. J Zhejiang Univ Sci B 2014; 15(1): 100–108
184. Yu X, Wan Z, Zhang Z, Li F, Li R, Liu X. Phenotypic and molecular identification of *Sporothrix* isolates of clinical origin in Northeast China. Mycopathologia 2013; 176(1-2): 67–74
185. Zhao MD, Zhou X, Liu TT, Yang ZB. Morphological and physiological comparison of taxa comprising the *Sporothrix schenckii* complex. J Zhejiang Univ Sci B 2015; 16(11): 940–947
186. Marimon R, Cano J, Gené J, Sutton DA, Kawasaki M, Guarro J. Sporothrix brasiliensis, *S. globosa*, and *S. mexicana*, three new *Sporothrix* species of clinical interest. J Clin Microbiol 2007; 45 (10): 3198–3206
187. Mahajan VK. Sporotrichosis: an overview and therapeutic options. Dermatol Res Pract 2014; 2014: 272376
188. Pappas PG, Tellez I, Deep AE, Nolasco D, Holgado W, Bustamante B. Sporotrichosis in Peru: description of an area of hyperendemicity. Clin Infect Dis 2000; 30(1): 65–70
189. Sirisanthana T, Supparatpinyo K. Epidemiology and management of penicilliosis in human immunodeficiency virus-infected patients. Int J Infect Dis 1998; 3(1): 48–53
190. Li HR, Cai SX, Chen YS, Yu ME, Xu NL, Xie BS, Lin M, Hu XL. Comparison of *Talaromyces marneffei* infection in human immunodeficiency virus-positive and human immunodeficiency virus-negative patients from Fujian, China. Chin Med J (Engl) 2016; 129(9): 1059–1065
191. Zheng J, Gui X, Cao Q, Yang R, Yan Y, Deng L, Lio J. A clinical study of acquired immunodeficiency syndrome associated *Penicillium marneffei* infection from a non-endemic area in China. PLoS One 2015; 10(6): e0130376
192. Capponi M, Segretain G, Sureau P. Penicillosis from *Rhizomys sinensis*. Bull Soc Pathol Exot 1956; 49(3): 418–421
193. DiSalvo AF, Fickling AM, Ajello L. Infection caused by *Penicillium marneffei*: description of first natural infection in man. Am J Clin Pathol 1973; 60(2): 259–263
194. Deng ZL. Progressive disseminated penicilliosis caused by *Penicillium marneffei* .J Guangxi Med Col (Gangxi Yi Xue Yuan Xue Bao) 1984; 1(1): 1–4 (in Chinese)
195. Chan JF, Lau SK, Yuen KY, Woo PC. *Talaromyces* (*Penicillium*) *marneffei* infection in non-HIV-infected patients. Emerg Microbes Infect 2016; 5(3): e19
196. Hu Y, Zhang J, Li X, Yang Y, Zhang Y, Ma J, Xi L. *Penicillium marneffei* infection: an emerging disease in mainland China. Mycopathologia 2013; 175(1-2): 57–67
197. Cao C, Liang L, Wang W, Luo H, Huang S, Liu D, Xu J, Henk DA, Fisher MC. Common reservoirs for *Penicillium marneffei* infection in humans and rodents, China. Emerg Infect Dis 2011; 17(2): 209–214
198. Huang X, He G, Lu S, Liang Y, Xi L. Role of *Rhizomys pruinosus* as a natural animal host of *Penicillium marneffei* in Guangdong, China. Microb Biotechnol 2015; 8(4): 659–664
199. Gugnani H, Fisher MC, Paliwal-Johsi A, Vanittanakom N, Singh I, Yadav PS. Role of *Cannomys badius* as a natural animal host of *Penicillium marneffei* in India. J Clin Microbiol 2004; 42(11): 5070–5075
200. Fisher MC, Hanage WP, de Hoog S, Johnson E, Smith MD, White

NJ, Vanittanakom N. Low effective dispersal of asexual genotypes in heterogeneous landscapes by the endemic pathogen *Penicillium marneffei*. PLoS Pathog 2005; 1(2): e20

201. Kauffman CA. Histoplasmosis: a clinical and laboratory update. Clin Microbiol Rev 2007; 20(1): 115–132
202. Wang Y, Pan B, Wu J, Bi X, Liao W, Pan W, Gu J. Detection and phylogenetic characterization of a case of *Histoplasma capsulatum* infection in mainland China. Am J Trop Med Hyg 2014; 90(6): 1180–1183
203. Ge L, Zhou C, Song Z, Zhang Y, Wang L, Zhong B, Hao F. Primary localized histoplasmosis with lesions restricted to the mouth in a Chinese HIV-negative patient. Int J Infect Dis 2010; 14 (Suppl 3): e325–e328
204. Pan B, Chen M, Pan W, Liao W. Histoplasmosis: a new endemic fungal infection in China? Review and analysis of cases. Mycoses 2013; 56(3): 212–221
205. Stevens DA. Coccidioidomycosis. N Engl J Med 1995; 332(16): 1077–1082
206. Wang XL, Wang S, An CL. Mini-review of published reports on coccidioidomycosis in China. Mycopathologia 2015; 180(5-6): 299–303
207. Xi L, Fukushima K, Lu C, Takizawa K, Liao R, Nishimura K. First case of *Arthrographis kalrae* ethmoid sinusitis and ophthalmitis in the People's Republic of China. J Clin Microbiol 2004; 42(10): 4828–4831
208. Zhang QQ, Zhu LP, Weng XH, Li L, Wang JJ. Meningitis due to *Prototheca wickerhamii*: rare case in China. Med Mycol 2007; 45 (1): 85–88
209. Li DM, Li RY, de Hoog GS, Sudhadham M, Wang DL. Fatal *Exophiala* infections in China, with a report of seven cases. Mycoses 2011; 54(4): e136–e142
210. Li DM, Chen XR. A new superficial fungal infection caused by *Coniosporium epidermidis*. J Am Acad Dermatol 2010; 63(4): 725–727
211. Pan W, Liao W, Hagen F, Theelen B, Shi W, Meis JF, Boekhout T. Meningitis caused by *Filobasidium uniguttulatum*: case report and overview of the literature. Mycoses 2012; 55(2): 105–109
212. Wu Y, Wang J, Li W, Jia H, Che J, Lu J, Liu L, Cheng Y. *Pichia fabianii* blood infection in a premature infant in China: case report. BMC Res Notes 2013; 6(1): 77
213. Fu M, Ge Y, Chen W, Feng S, She X, Li X, Liu W. Tinea faciei in a newborn due to *Trichophyton tonsurans*. J Biomed Res 2013; 27 (1): 71–74
214. Chen M, Houbraken J, Pan W, Zhang C, Peng H, Wu L, Xu D, Xiao Y, Wang Z, Liao W. Pulmonary fungus ball caused by *Penicillium capsulatum* in a patient with type 2 diabetes: a case report. BMC Infect Dis 2013; 13(1): 496
215. Cai Q, Lv GX, Jiang YQ, Mei H, Hu SQ, Xu HB, Wu XF, Shen YN, Liu WD. The first case of phaeohyphomycosis caused by *Rhinocladiella basitona* in an immunocompetent child in China. Mycopathologia 2013; 176(1-2): 101–105
216. Zou Y, Bi Y, Bu H, He Y, Guo L, Shi D. Infective meningitis caused by *Phialemonium curvatum*. J Clin Microbiol 2014; 52(8): 3111–3113
217. Zhu CY, Yang YP, Sheng P, Li W, Huang WM, Fan YM. Cutaneous chromoblastomycosis caused by *Veronaea botryosa* in a patient with pemphigus vulgaris and review of published reports. Mycopathologia 2015; 180(1-2): 123–129
218. Wang L, Al-Hatmi AM, Lai X, Peng L, Yang C, Lai H, Li J, Meis JF, de Hoog GS, Zhuo C, Chen M. *Bipolaris oryzae*, a novel fungal opportunist causing keratitis. Diagn Microbiol Infect Dis 2016; 85 (1): 61–65
219. Mijiti J, Pan B, de Hoog S, Horie Y, Matsuzawa T, Yilifan Y, Liu Y, Abliz P, Pan W, Deng D, Guo Y, Zhang P, Liao W, Deng S. Severe chromoblastomycosis-like cutaneous infection caused by *Chrysosporium keratinophilum*. Front Microbiol 2017; 8: 83

Received: 19 January 2018 | Accepted: 25 April 2018

DOI: 10.1111/jcmm.13704

ORIGINAL ARTICLE

WILEY

Hydrogen gas inhalation protects against cutaneous ischaemia/reperfusion injury in a mouse model of pressure ulcer

Wei Fang[1,2,3] | Guizhen Wang[4] | Luyan Tang[1,2] | Huilin Su[1] | Huyan Chen[1] | Wanqing Liao[3] | Jinhua Xu[1,2]

[1]Department of Dermatology, Huashan Hospital, Fudan University, Shanghai, China

[2]The Shanghai Institute of Dermatology, Shanghai, China

[3]Department of Dermatology and Venereology, Changzheng Hospital, Shanghai Key Laboratory of Molecular Medical Mycology, Shanghai, China

[4]Emergency room, Shanghai Tenth People's Hospital of Tongji University, Shanghai, China

Correspondence
Jinhua Xu, Department of Dermatology, Huashan Hospital, Fudan University, Shanghai, China.
Email: xjhhsyy@163.com

Funding information
This study was supported by the Grant of Shanghai Key Medical Discipline for Dermatology (2017ZZ02002), the Grant of Shanghai leading talent project and China Postdoctoral Science Foundation Grant (2016M600286).

Abstract

Pressure ulcer formation depends on various factors among which repetitive ischaemia/reperfusion(I/R) injury plays a vital role. Molecular hydrogen (H_2) was reported to have protective effects on I/R injuries of various internal organs. In this study, we investigated the effects of H_2 inhalation on pressure ulcer and the underlying mechanisms. H_2 inhalation significantly reduced wound area, 8-oxo-dG level (oxidative DNA damage) and cell apoptosis rates in skin lesions. H_2 remarkably decreased ROS accumulation and enhanced antioxidant enzymes activities by up-regulating expression of Nrf2 and its downstream components in wound tissue and/or H_2O_2-treated endothelia. Meanwhile, H_2 inhibited the overexpression of *MCP-1*, *E-selectin*, *P-selectin* and *ICAM-1* in oxidant-induced endothelia and reduced inflammatory cells infiltration and proinflammatory cytokines (TNF-α, IL-1, IL-6 and IL-8) production in the wound. Furthermore, H_2 promoted the expression of pro-healing factors (IL-22, TGF-β, VEGF and IGF1) and inhibited the production of MMP9 in wound tissue in parallel with acceleration of cutaneous collagen synthesis. Taken together, these data indicated that H_2 inhalation suppressed the formation of pressure ulcer in a mouse model. Molecular hydrogen has potentials as a novel and alternative therapy for severe pressure ulcer. The therapeutic effects of molecular hydrogen might be related to its antioxidant, anti-inflammatory, pro-healing actions.

KEYWORDS
hydrogen, inflammation, oxidative stress, pressure ulcer, reperfusion injury, wound healing

1 | INTRODUCTION

Pressure ulcer is a chronic inflammatory dermatosis primarily occurring over bony prominences (such as the sacrum, trochanter and the heels) of senior bedridden patients. Without prompt treatment, pressure ulcer may progress to cellulitis, osteomyelitis, sepsis and even death. Pressure ulcer has become a serious public health problem owing to aging of the population.[1]

There are several hypotheses for the mechanisms underlying chronic pressure ulcer, such as local tissue hypoxia, repetitive ischaemia/reperfusion (I/R), wound bacterial colonization, etc.[2,3] Among these factors, I/R injury is thought to be a principal causative factor.[4,5] Long-time recumbent position interrupts arteriolar capillary blood flow and thus induces local ischaemia in cutaneous tissue with

Wei Fang and Guizhen Wang contributed equally to this work.

prominent bony protrusions. After a change of body position, reperfusion of blood to the ischaemic skin initiates a series of harmful events because of a large increase in reactive oxygen species (ROS).[6] Excessive ROS cause direct damage on lipids, proteins and nucleic acids, leading to cell apoptosis and tissue injury. Meanwhile, these free radicals induce the development of inflammatory responses such as endothelial dysfunction, neutrophil and macrophage infiltration, production of proinflammatory cytokines and, thereafter, tissues necrosis.[6,7] Consistently, several studies demonstrated that skin ulcers induced by cutaneous I/R were inhibited by treatment with antioxidants such as vitamin E, melatonin and deferoxamine.[8-10] Therefore, antioxidant administration may be a good therapeutic strategy for promoting healing of pressure ulcers.

In the past decade, H_2 as a novel medical gas has gained wide attention. In 2007, Ohsawa and colleagues found that H_2 affords neuroprotection against brain I/R injury by selectively neutralizing hydroxyl radicals and peroxynitrite.[11] Later studies demonstrated similar protective effects of hydrogen on I/R injuries of other organs such as liver, heart and intestines.[12-14] The potential mechanisms might be involved in its antioxidant and anti-inflammatory and anti-apoptotic properties.[15] These biological effects further enhanced the potential of H_2 in clinical application of various organ system diseases.[15,16] Moreover, molecular hydrogen displayed high safety in vivo even at high concentration and high pressure, which could effectively reach target tissues and cells by gaseous diffusion but has no effect on physiological variables such as pH, oxygen saturation and blood pressure.[17,18] Taken together, we hypothesized that H_2 could act as an effective treatment for pressure ulcer induced by repeated cutaneous I/R injury.

A recent study reported that hydrogen–water intake promoted wound size reduction and early recovery in 22 elderly in-patients with severe pressure ulcer.[19] However, there has been no experimental evidence of the beneficial effects of molecular hydrogen on I/R-induced pressure ulcer using animal models. This study aimed to determine the possible protective effects of H_2 on pressure ulcer and the underlying mechanisms.

2 | MATERIALS AND METHODS

2.1 | Animals and cells

Female C57BL/6 mice (8 to 12 weeks old) were purchased from Changzhou Cavens Laboratory Animal Ltd. (Changzhou, China). All experiments were approved by the Ethical Committee for Animal Experiments of Fudan University, and strictly carried out in accordance with the approved guidelines. HUVEC cells were purchased from ATCC (Manassan, VA), and maintained in RPMI 1640 containing 10% foetal bovine serum (Thermo Fisher Scientific Inc., Waltham, MA).

2.2 | I/R cycles and analysis

The cutaneous I/R model was established according to previously published reports.[20-22] Briefly, all mice were anaesthetized, and their backs were shaved and cleaned with 75% ethanol. The dorsal skin was gently pulled up and placed between two round ferrite magnetic plates that had a 12-mm diameter and 5-mm thickness (NeoMag Co, Ichikawa, Japan). A single I/R cycle was initiated with a 12-hour period of magnet placement, and followed by a release or rest period of 12 hours. After three I/R cycles, all of the mice developed two circular ulcers separated by a bridge of normal skin. For analysis, each wound site was digitally photographed after wounding, and wound areas were measured on photographs using Image J (version 1.48, NIH, Bethesda, MD) as previously described.[20,23] To assess the effects of hydrogen gas on wound healing, the mice were housed in a specific airtight device producing air mixture including 2% or 75% H_2 and 21%O_2 for one week (6 hours per day) before the beginning of I/R cycles. H_2 treatment was continuously performed until the wounds completely healed. The hydrogen-producing device was provided by Shanghai Asclepius Meditec Co. Ltd (Shanghai, China). Wound sites were digitally photographed at various time-points after wounding, and wound areas were measured on the images using ImageJ software version 1.46r (NIH, Bethesda, MD).

2.3 | Histological and immunohistochemical examinations

The wounds were harvested with a 5-mm rim of unwounded skin tissue from sacrificed mice. Skin samples were fixed in 10% paraformaldehyde and embedded in paraffin. Sections (6 μm) were stained with HE and Masson or processed for subsequent immunostaining. For immunohistochemistry, deparaffinized sections were incubated with 3% H_2O_2 for 5 minutes to block endogenous peroxidase activity. After blocking with 10% foetal bovine serum, sections were stained with primary antibodies of interest followed by secondary Abs. Sections were washed three times with PBS buffer. The colour was developed using DAB substrate-chromogen solution (Biocare Medical). The sections were then counterstained with HE.

2.4 | ROS measurement

ROS levels were measured in wound homogenates using ROS ELISA Kit (J&L Bio., Shanghai, China). For ROS detection in vitro, HUEVC cells were incubated in 2% or 75% H_2 incubator (Shanghai Asclepius Meditec Co. Ltd) for 24 hours and then stimulated with 0.25 mmol/L H_2O_2 (100 mL/well) for 2 hours as previous report.[23] The control group was without H_2 pretreatment. The ROS levels were then examined with dihydroethidium (DHE) (Beyotime, Shanghai, China) according to the manufacturer' protocol. Fluorescent pictures were collected by fluorescence microscope (Olympus IX71), and fluorescence intensity was analysed by Image J software (NIH, Bethesda, MD).

2.5 | CCK8 assay

The rate of cell proliferation was detected using CCK8 assay kit (Beyotime, Shanghai, China). After H_2 preincubation and 0.25 mmol/

L H_2O_2 treatment, 10^4 of HUEVC cells were placed into 96-well plate (200 μL per well) and 20 μL CCK8 was added into each well for 24 hours. The optical density (OD) was read at 450 nm wavelength by ELISA microplate reader (Thermo Multiskan MK3).

2.6 | Apoptosis (TUNEL) assay

Apoptosis assay was carried out in both skin sections and H_2O_2-treated HUEVC cells using terminal deoxynucleotide transferase dUTP nick end labelling (TUNEL) staining kit (Roche Diagnostics, Indianapolis, IN) according to the manufacturer's instructions. Photographs were taken and visualized with inverted fluorescence microscope (Olympus IX71). The number of apoptotic cells was determined by counting TUNEL and Hoechst double positive nuclei in the field as previously described.[23]

2.7 | Quantitative real-time PCR

For real-time PCR, total RNA was isolated from injured skin samples or H_2O_2-treated HUVEC cells using the Rneasy kit (QIAGEN Ltd., Crawley, UK) according to the manufacturer's protocols. First-strand cDNA was synthesized using the SuperScript III First-Strand Synthesis Kit (Invitrogen) according to its protocol. Resulting cDNA was used as template for subsequent real-time PCR using iQ SYBR Green Supermix (Bio-Rad) according to the manufacturer's recommendations. Primers (Table S1) were synthesized by Shanghai Sangon Biotech Co., Ltd (Shanghai, China). Relative expression of PCR products was determined using the $2^{-\Delta\Delta CT}$ method and calculated relative to the control group.

2.8 | Western blot

For protein blotting, total proteins were extracted from homogenized skin tissue using as previously described.[24] Twenty micrograms of proteins was loaded into 8% SDS-PAGE and then transferred onto a polyvinylidene fluoride membrane. After blocking and washing, the membranes were incubated with the indicated primary Abs. The membranes were then incubated with horseradish peroxidase-labelled secondary antibody and developed with the ImmobilonTW Western Chemiluminescent HRP Substrate (Millipore, Billerica, MA). The blots were assessed by Image J software (NIH, Bethesda, MD).

All the antibodies (Abs) and their sources in the study are listed in Table S2.

2.9 | ELISA

Supernatants of mouse wound homogenates or cell culture medium were used for ELISA assay for SOD, GPx, CAT (BioVision), IL-1β, TNF-α, IL-6, IL-8 and IL-22 (eBioscience) according to the manufacturers' recommendation. Total protein in the supernatant was detected with a commercial kit (BCA Protein Assay kit; Pierce, Rockford, IL). The data were expressed as anti-oxidative enzyme (unit/mL) or cytokine (pg/mL)/total protein (mg/mL) for each sample.

2.10 | Statistical analysis

Results were expressed as means ± SEM. Unpaired, two-sided Student's *t* test was performed determine the statistical differences between the sample means using GraphPad Prism 6.0 (La Jolla, CA). $P < .05$ were considered statistically significant.

3 | RESULTS

3.1 | H_2 inhalation protected against cutaneous I/R-induced pressure ulcer formation

To assess the preventive effects of H_2 on the development of cutaneous pressure ulcers after I/R injury in vivo, a decubitus ulcer-like mouse model was constructed as previously described.[20,23] In order to reach fully saturation in cutaneous tissue, 2% or 75% H_2 was inhaled by mice in experimental groups for one week (6 hours per day) before the beginning of I/R cycles according to the discovery of Scottish physiologist John Scott Haldane about the human body and the nature of gases.[25] Wound areas in H_2-treated mice were significantly smaller than those in control mice especially in early stage after I/R cycles (Figure 1). Inhalation of 75% H_2 significantly shortened the wound closure time in pressure ulcer mice. Furthermore, we also observed cleaner wounds and less scratching behaviour in H_2-treated mice than in control group. These results suggested that H_2 inhalation especially at high concentration protected the formation of cutaneous ulcers after I/R cycles.

3.2 | H_2 inhalation altered the histopathological characteristics of pressure ulcer skin after cutaneous I/R

Haematoxylin and eosin (HE) staining showed that H_2 inhalation reduced inflammatory cell infiltration and tissue necrosis in skin wound caused by I/R cycles (Figure S1). Compared with the control group, H_2-treatment groups (especially 75%H_2) displayed notable acceleration and enhancement in dermal collagen synthesis of skin wound (Figure 2). These results suggested that H_2 inhalation alleviated the inflammatory response and promoted the wound healing in pressure ulcer.

3.3 | H_2 inhalation alleviated oxidative DNA damage and suppressed apoptosis in skin tissues after cutaneous I/R

We further evaluated the levels of oxidative DNA damage (8-oxo-dG) and cell apoptosis after cutaneous I/R injury. Immunohistochemical (IHC) analysis showed that three groups had similar levels of 8-oxo-dG staining at 4 days postreperfusion. However, the area and intensity of positive staining in H_2-treated mice were significantly reduced compared to those in control mice and 75% H_2-treated group had lowest level of 8-oxo-dG at 6 and 8 days after reperfusion (Figure S2A). TUNEL analysis showed that wound tissues of

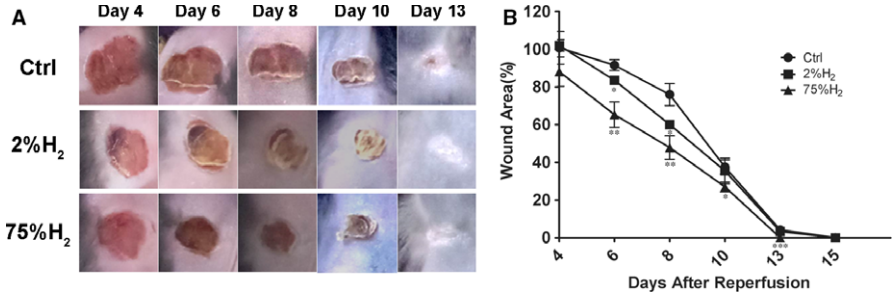

FIGURE 1 H_2 inhalation protected against ulcer formation in cutaneous I/R injury mice model. A, Representative photographs of wounds after cutaneous I/R in control or H_2-treated mice at 4, 6, 8, 10 and 13 days after reperfusion. B, Relative wound area after I/R injury in normal C57BL/6 mice with or without H_2 inhalation (N = 8 for each time point and groups). The ulcer size in control mice at 4 days after reperfusion was assigned a value of 100%. $^*P < .05$; $^{**}P < .01$; $^{***}P < .001$ compared to control

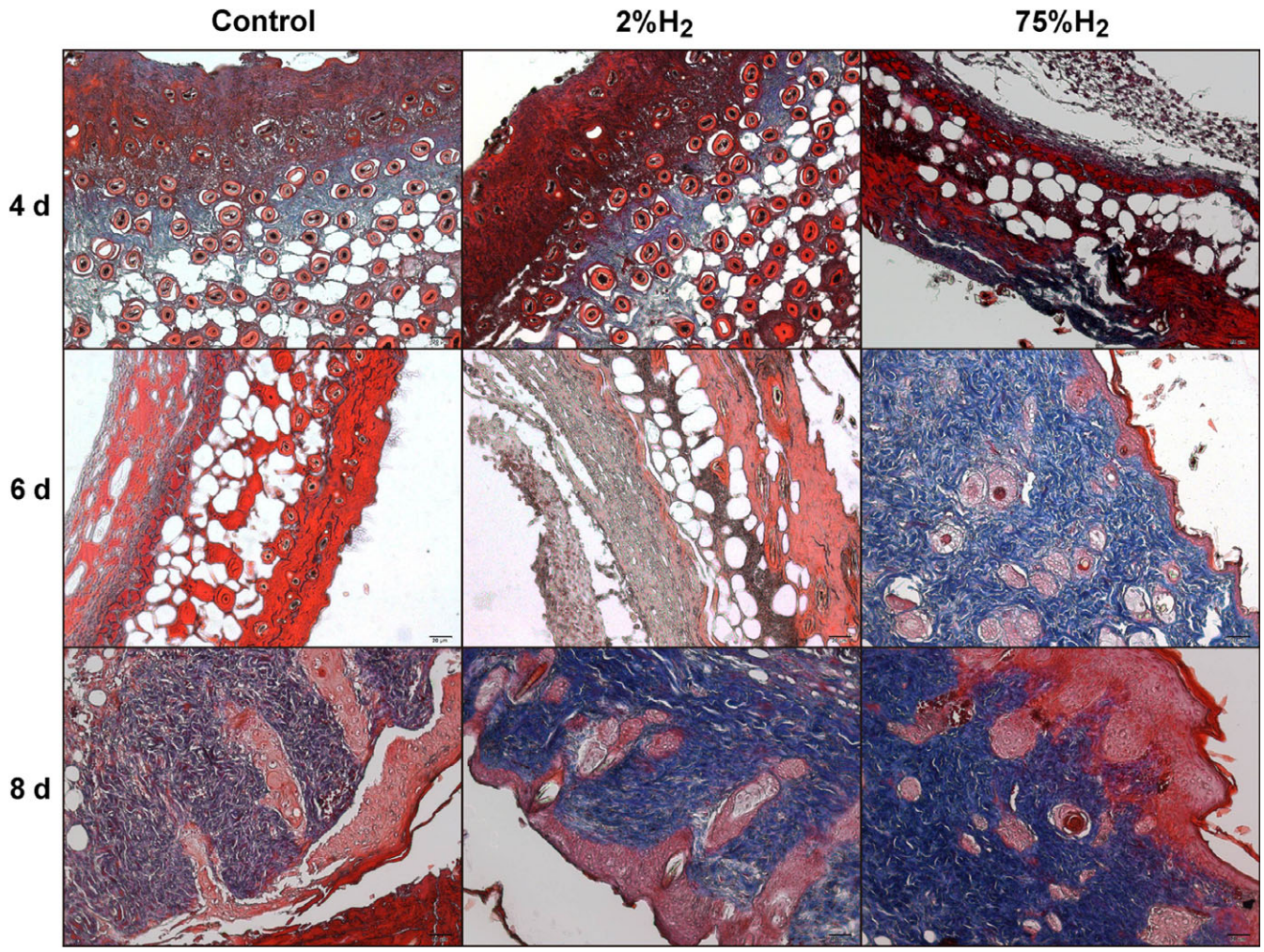

FIGURE 2 H_2 treatment promoted dermal collagen synthesis in skin wound caused by I/R cycles. Skin tissue samples from pressure ulcer mice of each group were fixed and paraffin embedded. The tissue sections were subjected to Masson staining. Representative images from the wound skin tissues are shown. Scale bar, 20 μm

control mice had a large number of apoptotic cells, which was significantly reduced by H_2 inhalation (especially 75% H_2) at day 8 postreperfusion (Figure S2B and Figure 2C). These results suggested that H_2 inhalation could alleviate the oxidative DNA damage and suppress apoptosis of skin tissues, and high-concentration H_2 had optimal protective effect against cutaneous I/R injury.

3.4 | H_2 inhalation reduced ROS accumulation and up-regulated antioxidant enzyme activities in skin tissue after cutaneous I/R

As ROS is essential mediators of reperfusion induced tissue damage,[26-29] we assessed ROS levels and the activities of major

antioxidant enzymes including superoxide dismutase (SOD), catalase (CAT) and glutathione peroxidase (GPx) in the wound tissue at day 6 postreperfusion. H_2 suppressed the ROS accumulation in skin tissue caused by I/R injury ($P < .01$) in a concentration-dependent manner (Figure 3A). Activities of SOD, CAT and GPx in mice inhaled H_2 were significantly higher than in control mice (Figure 3B-D).

3.5 | H_2 activated the NRF2-ARE pathway in skin tissue after cutaneous I/R

We next investigated whether NRF2/ARE antioxidant pathway mediated the inhibition of ROS level of pressure ulcer tissue by H_2. Quantitative real-time PCR analysis showed that H_2 significantly up-regulated the mRNA levels of *NRF2* and its target genes (heme oxygenase-1, *HO-1*; NADH quinone oxidoreductase 1, *NQO1*; aldo-keto reductase, *AKR1C1*) in a concentration-dependent manner in the skin tissue (Figure 4A). Immunoblotting also confirmed the enhanced expression of NRF2-ARE pathway components in the skin tissue of H_2 treatment group (especially 75%) (Figure 4B). These results indicated that H_2 activated the NRF2 pathway in skin lesions after cutaneous I/R.

3.6 | H_2 inhalation inhibited cutaneous I/R-induced inflammation

As proinflammatory cytokines are important for tissue damage during I/R injury, the levels of proinflammatory cytokines in the wounded skin were assessed. At day 6 post-I/R, H_2 treatment significantly reduced the relative mRNA and protein expression of TNF-α, IL-1β, IL-6 and IL-8 in wounded tissue, and their expression was lowest in pressure ulcer mice treated with 75% H_2 (Figure 5A and B). IHC further confirmed that the protein levels of TNF-α, IL-1β, IL-6 and IL-8 in cutaneous I/R injured skin tissue of mice inhaled H2 were substantially lower than those of control mice (Figure 5C). Meanwhile, H_2 treatment significantly up-regulated the expression of IL-22, an essential pro-healing cytokine involved in repair events on different models of epithelial regeneration,[30,31] at both mRNA and protein levels and 75% H_2 treated group displayed the highest level of IL-22 (Figure 5), which was mainly expressed in the dermal layer of perilesional skin tissues in mice treated by H_2 (Figure 5C). These results indicated that hydrogen inhalation reversed proinflammatory effects of skin wound environment after cutaneous I/R.

3.7 | H_2 inhalation modulated the expression of healing-associated molecules in vivo after cutaneous I/R

The metalloprotease MMP9 and pro-healing factors TGF-β, VEGF and IGF-1 play crucial roles during proliferative and remodelling phases of wound healing. To investigate how H_2 improves wound healing in pressure ulcer mice, its effects on expression of aforementioned molecules were analysed by quantitative PCR and immunoblotting. H_2 inhalation significantly decreased the expression level of MMP9 and enhanced the expression of TGF-β1, VEGF and IGF-1 at both mRNA and protein levels in the wound. Mice treated with 75% H_2 had the lowest level of MMP9 and highest expression of pro-healing factors in skin tissue among three groups (Figure 6).

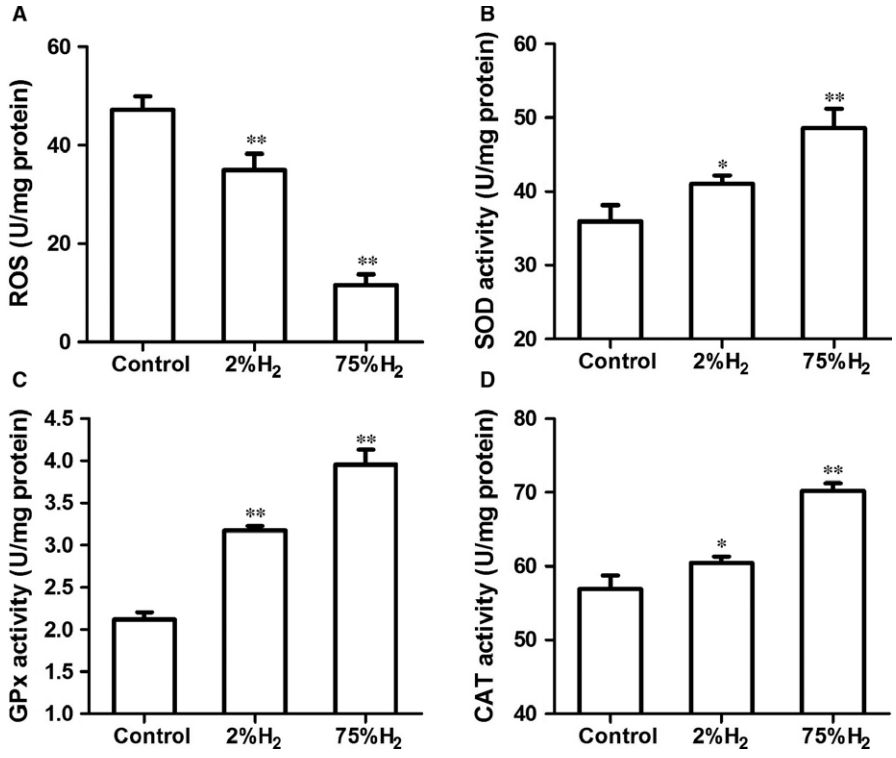

FIGURE 3 H_2 inhalation reduced ROS accumulation and enhanced antioxidant enzyme activities in skin tissue. ELISA assays for detection of ROS production (A) and the activities of SOD (B), GPx (C), and CAT (D). *$P < .05$; **$P < .01$ compared to control

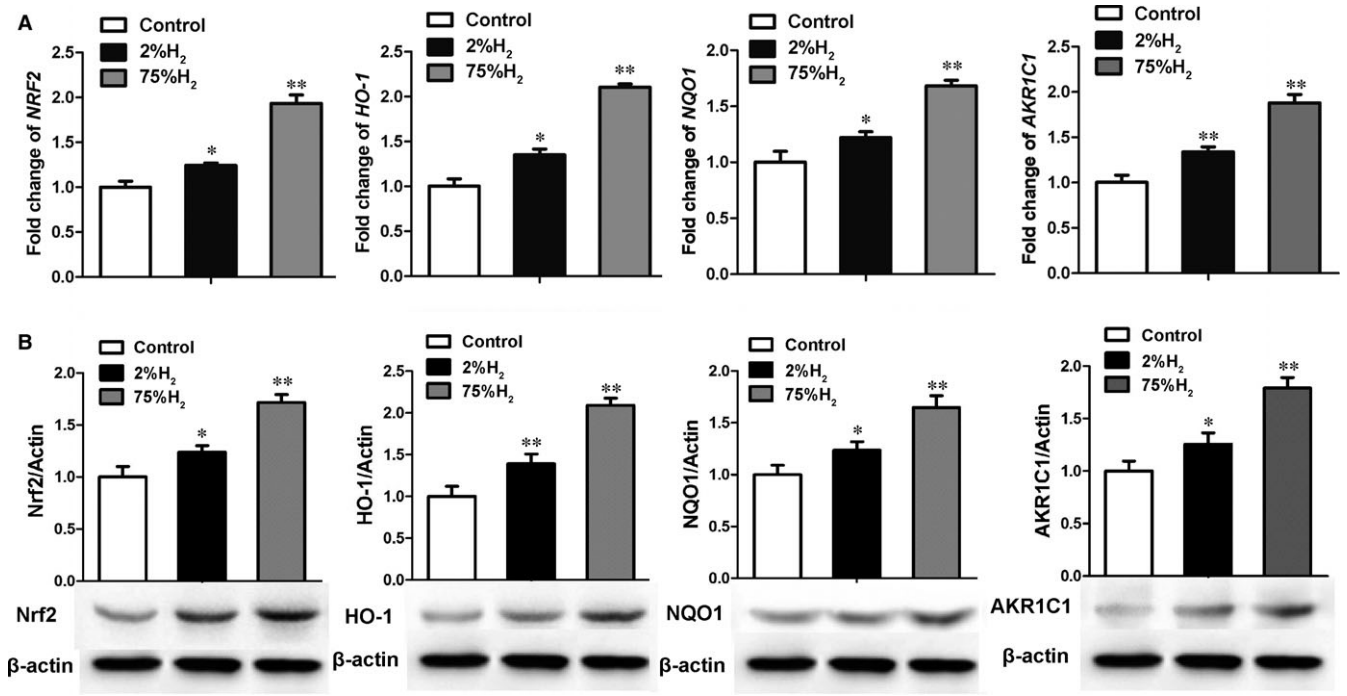

FIGURE 4 Hydrogen activated the NRF2-ARE pathway in wounded tissue. A, The mRNA levels of NRF2, HO-1, NQO1 and AKR1C1 were analysed by quantitative RT-PCR assay. B, Immunoblots of NRF2, HO-1, NQO1, AKR1C1 and β-actin. *$P < .05$; **$P < .01$ compared to control

3.8 | H_2 reversed the adverse effect of H_2O_2 on cell proliferation and apoptosis of vascular endothelia cells

I/R injury is closely associated with microvascular dysfunction, which is largely a consequence of endothelia cell impairment.[7] Thus, we further examine the effects of H_2 on human umbilical vein endothelial cells (HUVECs) against oxidative damage. Preincubation with H_2 for 24 hours significantly relieved the 0.25 mmo/L H_2O_2-induced proliferation inhibition of HUVECs in a concentration-dependent manner ($P < .01$) (Figure S3A). After exposure to 0.25 mmol/L H_2O_2, HUVECs showed a 2.5-folds increase in the apoptosis rate, which was markedly reduced by H_2 pretreatment (especially 75%H_2) ($P < .01$) (Figure S3B and C).

3.9 | H_2 rectified the imbalance of oxidation-reduction system in H_2O_2-treated vascular endothelia cells through the activation of Nrf2/ARE pathway

To further understand the mechanism of H_2-mediated protective effects on endothelial cells during cutaneous I/R, a series of in vitro studies were performed in oxidant-treated HUVECs. H_2O_2 notably up-regulated intracellular ROS production (Figure S4A) and suppressed the expression of various anti-oxidative enzymes (SOD, GPx, and CAT) (Figure S4B-D) in HUVECs, suggesting of a severe disturbance of intracellular oxidation-reduction system. Preincubation with H_2 resulted in a trend towards normalization of both intracellular ROS and anti-oxidative enzyme in H_2O_2-treated HUVECs (Figure S4A-D). Quantitative PCR assay demonstrated that H_2 significantly up-regulated the expression of *NRF2* and its target genes *HO-1*, *AKR1C1* and *NQO1* in HUVECs exposed to H_2O_2 in a concentration-dependent manner (Figure S4E-H). Together, these results suggested that H_2 might maintain intracellular homoeostasis of oxidation-reduction system in vascular endothelial cells through the activation of Nrf2/ARE pathway.

3.10 | H_2 inhibited the expression of several chemokine and adhesion molecules in vascular endothelial cells stimulated by H_2O_2

Endothelial damage is a critical event in the early phase of inflammatory responses induced by cutaneous I/R, which could drive the up-regulation of various chemokines and adhesion molecules and then mediate leucocyte recruit, adhesion and emigration.[7,32] Vascular endothelial cells more than doubled the transcriptional levels of *MCP-1*(monocyte chemoattractant protein-1), *E-selectin*, *P-selectin* and *ICAM-1*(intercellular cell adhesion molecule-1) after H_2O_2 exposure (Figure 7). Pretreatment with H_2 significantly suppressed the elevation of their expression in H_2O_2-exposed HUEVCs ($P < .01$) (Figure 7). The inhibitory effects were positively correlated with H_2 concentration. Our results suggested that H_2 might exert anti-inflammatory effects against cutaneous I/R injury by down-regulating the expression of endothelial chemokines and adhesion molecules.

4 | DISCUSSION

In the present study, we first demonstrated the protective effects of H_2 inhalation on pressure ulcers in a murine model. H_2 treatment significantly reduced the wound area in a concentration-dependent

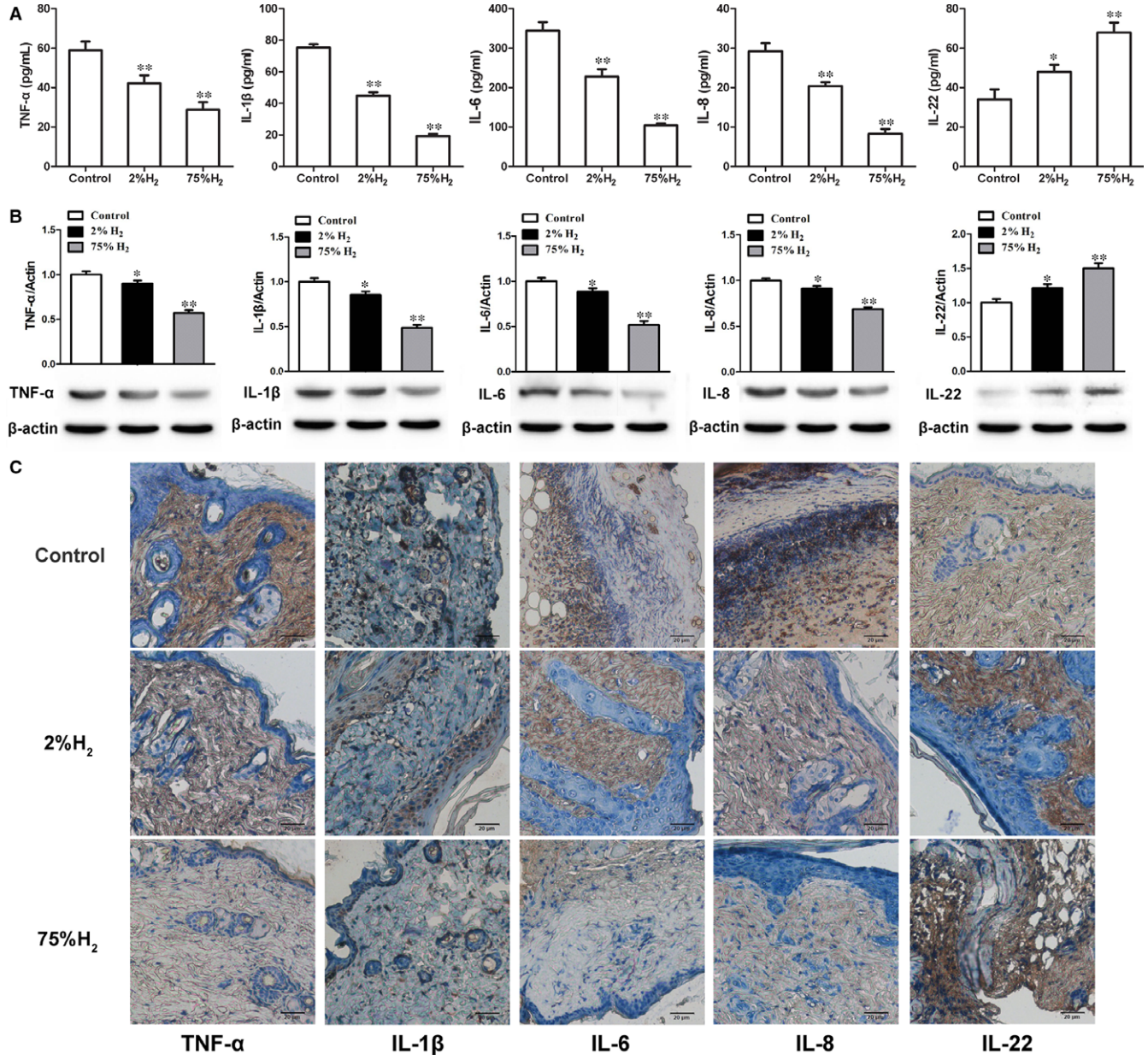

FIGURE 5 Hydrogen altered the expression or production of inflammatory cytokines during IR cycles. A, mRNA expression of TNF-α, IL-1β, IL-6, IL-8 and IL-22 in skin wounds. B, Immunoblot detecting the protein levels of TNF-α, IL-1β, IL-6, IL-8 and IL-22 in wounded skin tissue. C, IHC assessing injured skin TNF-α, IL-1β, IL-6, IL-8 and IL-22 levels. *$P < .05$; **$P < .01$ compared to control

manner in the early phase after cutaneous I/R. The improvement in skin ulcer recovery induced by H_2 was paralleled by significant reductions in oxidative DNA damage, cell apoptosis and acceleration of cutaneous collagen synthesis. This result was consistent with a clinical study that hydrogen–water intake (0.8-1.3 ppm, 600 mL per day) via tube-feeding significantly reduced the wound size in 22 hospitalized patients with pressure ulcer.[19] Theoretically, hydrogen administration through respiratory route displays higher blood concentration and more accessibility for cutaneous lesions than those through gastrointestinal absorption.[15] Therefore, H_2 inhalation has a greater potential to be applied in the prevention and treatment of patients with pressure ulcer.

H_2-mediated protection against pressure ulcers was primarily dependent on its antioxidant property. Oxidative stress plays crucial roles in the initiation and progression phases of cutaneous I/R injury.[3,6,26] In pressure ulcers, blood reperfution after cutaneous ischaemia induced abundant reactive oxygen species (ROS), which could directly damage skin tissue and cause cell apoptosis. These toxic free radicals further aggravated leucocyte infiltration, which in turn triggered more ROS release and thus trapped in a vicious circle. In our study, H_2 treatment remarkably decreased the ROS accumulation and 8-oxo-dG formation (a sensitive biomarker of oxidative DNA damage), and also enhanced the activities of several antioxidant enzymes (such as SOD, GPx and CAT) in wound tissue and/or H_2O_2-treated HUEVCs. The antioxidant ability was positively correlated with its dosage, and high concentration of H_2 was more advantageous in maintaining intracellular

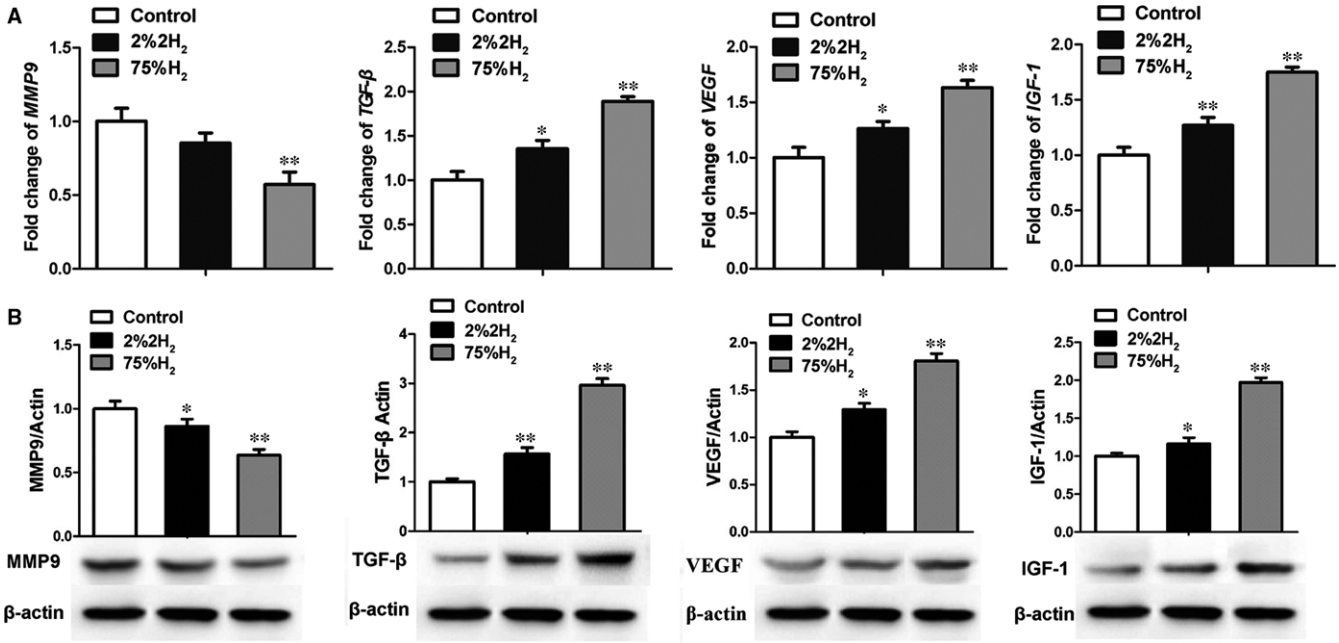

FIGURE 6 Hydrogen modulated the expression of healing-associated molecules in skin wounds. A, mRNA expression of MMP9, TGF-β, VEGF and IGF-1 was analysed by quantitative RT-PCR. B, Immunoblot assessment of MMP9, TGF-β, VEGF and IGF-1 protein levels in wounded skin tissue. *$P < .05$; **$P < .01$ compared to control

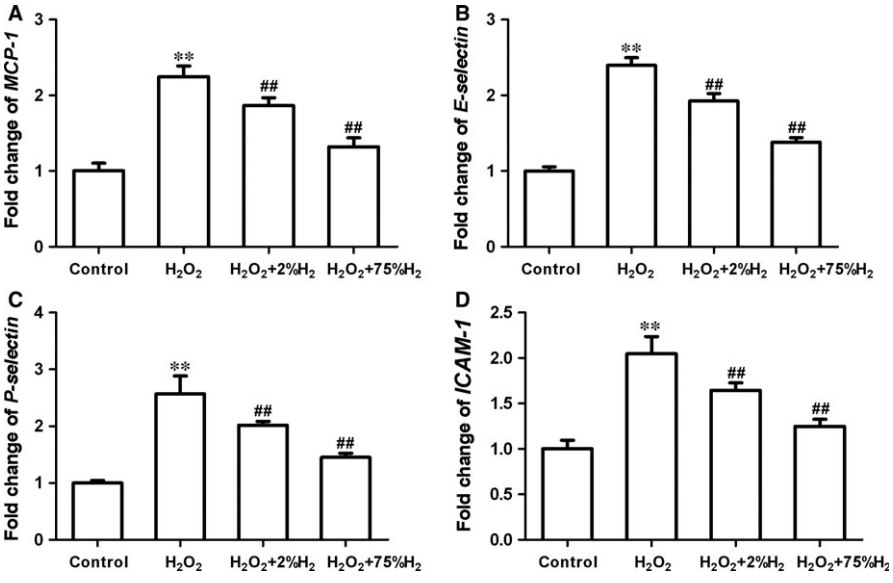

FIGURE 7 Hydrogen decreased the expression of several molecules associated with leucocyte-endothelium in H_2O_2-treated HUEVCs. Quantitative RT-PCR assay of MCP-1 (A), P-selectin (B), E-selectin (C) and ICAM-1(D) in HUEVCs. **$P < .01$, *$P < .05$, compared to the control group; ##$P < .01$, #$P < .05$, compared to H_2O_2-treated group

homoeostasis of oxidation-reduction system in skin tissue after I/R injury.

We also determined the mechanism underlying the antioxidant property of H_2 against cutaneous I/R injury, which was closely associated with the activation of Nrf2/ARE pathway. The transcription factor Nrf2 is essential for regulating the adaptive response to exogenous and endogenous oxidative stresses.[33,34] Under moderate oxidative stress, Nrf2 translocates to the nucleus where it binds to ARE and induces the transcription of downstream antioxidant genes. In our study, H_2 treatment significantly up-regulated the expression of Nrf2 and its downstream targets such as HO-1, NQO1 and AKR1C1 in wound tissue and HUEVCs exposed to H_2O_2. Similar phenomena were also observed in previous studies of other organ I/R injury or other inflammatory diseases.[35-38] Molecular hydrogen could attenuate intestinal injury in wild-type but not NRF2-knockout mice with severe sepsis by regulating HO-1 expression.[37] Therefore, hydrogen might activate the Nrf2/ARE pathway to restore the homoeostasis of cutaneous oxidation-reduction system against I/R injury.

The protective effects of H_2 were also attributed to its potent anti-inflammatory activity. After I/R cycles, plenty of macrophages and neutrophils were accumulated in the treated tissue accompanied by significant production of proinflammatory cytokines, which caused skin injury and necrosis in the wound.[21] In our study, H_2 inhalation attenuated inflammatory cells infiltration and cutaneous

necrosis in the wound induced by I/R injury. Proinflammatory cytokines such as TNF-α, IL-1, IL-6 and IL-8 were decreased while IL-22 was increased in the wounded skin of H_2-treated mice. Distinct from proinflammatory cytokines, IL-22 mediates a crosstalk between immune system and cutaneous cells (such as fibroblasts and keratinocytes) and plays a pro-healing role in wound repairment.[30,39] Our data demonstrated that H_2 reversed the excessive inflammatory response induced by cutaneous I/R injury.

The anti-inflammatory property of hydrogen might be partially attributed to its protection on vascular endothelial cells against oxidative stress. During I/R injury, endothelial damage initiated leucocyte adhesion, recruitment and infiltration by up-regulating the expression of chemokines and adhesion molecules.[6,7,32] Our in vitro assay showed that H_2 treatment significantly alleviated the oxidative injury of endothelial cells and reduced the overexpression of *MCP-1*, *E-selectin*, *P-selectin* and *ICAM-1* in HUEVCs exposed to H_2O_2. MCP-1 is a critical molecule for chemotaxis and activation of macrophage, which is a significant source of proinflammatory cytokines and contributes to I/R injury of skin and other organs.[21,40-42] The adhesion molecules studied here were mainly responsible for leucocyte rolling, localization and adhesion to the endothelium.[43,44] Hence, hydrogen might modulate those molecules associated with leucocyte–endothelium interaction to inhibit subsequent inflammatory reaction caused by cutaneous I/R injury.

In pressure ulcer, the wound sites were constantly in the dynamic pathological alterations of inflammatory injury and tissue repair. Outcome of wound healing process was mainly determined by the presence and concentration of the healing-associated factors such as MMPs, TGF-β, VEGF and IGF1.[45-47] Overproduction or high activity of MMP9 and suppressed expression of TGF-β were identified as indicators of poor healing in skin samples of chronic ulcers.[46,48] In our study, H_2 promoted the expression of pro-healing factors (TGF-β, VEGF and IGF1) and inhibited the production of MMP9 in wound tissue of pressure ulcer, accompanied by acceleration of dermal collagen synthesis. Hence, hydrogen had a wound healing promoting effect against cutaneous I/R injury.

Taken together, the present results indicated that hydrogen suppressed the formation of decubitus ulcers by its antioxidant, anti-inflammatory, pro-healing activities against cutaneous I/R injury. Similar therapeutic effects of hydrogen were also reported in common senile diseases concomitant with decubitus, such as cerebral or myocardial infarctions, COPD, diabetes, hyperlipaemia, malignant tumours.[11,36,49-54] Furthermore, H_2 had no cytotoxicity *in vivo* in human body even at a high concentration.[17] Therefore, hydrogen gas has a great potential for preventing and/or treating pressure ulcer.

There were still some limitations in our study. Firstly, we did not detect the cutaneous hydrogen concentration, which might provide direct evidence to support the dosage-dependent protection of hydrogen gas against cutaneous I/R injury. In addition, the exact mechanisms by which hydrogen modulates oxidative stress, inflammation and wound repair in pressure ulcer were still unclear. More experiments are needed to work out these problems before the clinical trial of H_2 in pressure ulcers.

ACKNOWLEDGEMENTS

We extend our sincerest gratitude to the staff of Shanghai Asclepius Meditec Co., Ltd. for their vital technical support in the hydrogen–oxygen nebulizer device. We also thank Prof. Zhimin Kang of Shanghai Huikang Hydrogen Medical Research Center for technical assistance in study design.

CONFLICT OF INTEREST

The authors have no conflicts of interest to report.

ORCID

Wei Fang http://orcid.org/0000-0002-0749-298X

REFERENCES

1. Gorecki C, Brown JM, Nelson EA, et al. Impact of pressure ulcers on quality of life in older patients: a systematic review. *J Am Geriatr Soc*. 2009;57:1175-1183.
2. Mustoe T. Understanding chronic wounds: a unifying hypothesis on their pathogenesis and implications for therapy. *Am J Surg*. 2004;187:65S-70S.
3. Mustoe TA, O'Shaughnessy K, Kloeters O. Chronic wound pathogenesis and current treatment strategies: a unifying hypothesis. *Plast Reconstr Surg*. 2006;117:35S-41S.
4. Salcido R, Donofrio JC, Fisher SB, et al. Histopathology of pressure ulcers as a result of sequential computer-controlled pressure sessions in a fuzzy rat model. *Adv Wound Care*. 1994;7:23-24, 26, 28 passim.
5. Peirce SM, Skalak TC, Rodeheaver GT. Ischemia-reperfusion injury in chronic pressure ulcer formation: a skin model in the rat. *Wound Repair Regen*. 2000;8:68-76.
6. Eltzschig HK, Collard CD. Vascular ischaemia and reperfusion injury. *Br Med Bull*. 2004;70:71-86.
7. Seal JB, Gewertz BL. Vascular dysfunction in ischemia-reperfusion injury. *Ann Vasc Surg*. 2005;19:572-584.
8. Houwing R, Overgoor M, Kon M, Jansen G, van Asbeck BS, Haalboom JR. Pressure-induced skin lesions in pigs: reperfusion injury and the effects of vitamin E. *J Wound Care*. 2000;9:36-40.
9. Sener G, Sert G, Ozer SA, Arbak S, Gedik N, Ayanoğlu-Dülger G. Melatonin protects against pressure ulcer-induced oxidative injury of the skin and remote organs in rats. *J Pineal Res*. 2006;40:280-287.
10. Duscher D, Neofytou E, Wong VW, et al. Transdermal deferoxamine prevents pressure-induced diabetic ulcers. *Proc Natl Acad Sci U S A*. 2015;112:94-99.
11. Ohsawa I, Ishikawa M, Takahashi K, et al. Hydrogen acts as a therapeutic antioxidant by selectively reducing cytotoxic oxygen radicals. *Nat Med*. 2007;13:688-694.
12. Liu Q, Shen WF, Sun HY, et al. Hydrogen-rich saline protects against liver injury in rats with obstructive jaundice. *Liver Int*. 2010;30:958-968.
13. Sun Q, Kang Z, Cai J, et al. Hydrogen-rich saline protects myocardium against ischemia/reperfusion injury in rats. *Exp Biol Med (Maywood)*. 2009;234:1212-1219.
14. Zheng X, Mao Y, Cai J, et al. Hydrogen-rich saline protects against intestinal ischemia/reperfusion injury in rats. *Free Radic Res*. 2009;43:478-484.
15. Ge L, Yang M, Yang NN, Yin XX, Song WG. Molecular hydrogen: a preventive and therapeutic medical gas for various diseases. *Oncotarget*. 2017;8:102653-102673.

16. Ostojic SM. Molecular hydrogen: an inert gas turns clinically effective. *Ann Med*. 2015;47:301-304.
17. Abraini JH, Gardette-Chauffour MC, Martinez E, Rostain JC, Lemaire C. Psychophysiological reactions in humans during an open sea dive to 500 m with a hydrogen-helium-oxygen mixture. *J Appl Physiol*. 1994;76:1113-1118.
18. Ono H, Nishijima Y, Adachi N, et al. A basic study on molecular hydrogen (H2) inhalation in acute cerebral ischemia patients for safety check with physiological parameters and measurement of blood H2 level. *Med Gas Res*. 2012;2:21.
19. Li Q, Kato S, Matsuoka D, Tanaka H, Miwa N. Hydrogen water intake via tube-feeding for patients with pressure ulcer and its reconstructive effects on normal human skin cells in vitro. *Med Gas Res*. 2013;3:20.
20. Uchiyama A, Yamada K, Perera B, et al. Protective effect of MFG-E8 after cutaneous ischemia-reperfusion injury. *J Invest Dermatol*. 2015;135:1157-1165.
21. Saito Y, Hasegawa M, Fujimoto M, et al. The loss of MCP-1 attenuates cutaneous ischemia-reperfusion injury in a mouse model of pressure ulcer. *J Invest Dermatol*. 2008;128:1838-1851.
22. Stadler I, Zhang RY, Oskoui P, Whittaker MS, Lanzafame RJ. Development of a simple, noninvasive, clinically relevant model of pressure ulcers in the mouse. *J Invest Surg*. 2004;17:221-227.
23. Uchiyama A, Yamada K, Perera B, et al. Protective effect of botulinum toxin A after cutaneous ischemia-reperfusion injury. *Sci Rep*. 2015;5:9072.
24. Long M, de la Vega MR, Wen Q, et al. An essential role of NRF2 in diabetic wound healing. *Diabetes*. 2016;65:780-793.
25. Bove A, Davis J. *Bove and davis' diving medicine* (4th edn.). New York, NY: Saunders; 2003:53-76.
26. Siemionow M, Arslan E. Ischemia/reperfusion injury: a review in relation to free tissue transfers. *Microsurgery*. 2004;24:468-475.
27. Chouchani ET, Pell VR, James AM, et al. A unifying mechanism for mitochondrial superoxide production during ischemia-reperfusion injury. *Cell Metab*. 2016;23:254-263.
28. Minutoli L, Puzzolo D, Rinaldi M, et al. ROS-mediated NLRP3 inflammasome activation in brain, heart, kidney, and testis ischemia/reperfusion injury. *Oxid Med Cell Longev*. 2016;2016:2183026.
29. Granger DN, Kvietys PR. Reperfusion injury and reactive oxygen species: the evolution of a concept. *Redox Biol*. 2015;6:524-551.
30. Avitabile S, Odorisio T, Madonna S, et al. Interleukin-22 promotes wound repair in diabetes by improving keratinocyte pro-healing functions. *J Invest Dermatol*. 2015;135:2862-2870.
31. Pickert G, Neufert C, Leppkes M, et al. STAT3 links IL-22 signaling in intestinal epithelial cells to mucosal wound healing. *J Exp Med*. 2009;206:1465-1472.
32. Toledo-Pereyra LH, Toledo AH, Walsh J, Lopez-Neblina F. Molecular signaling pathways in ischemia/reperfusion. *Exp Clin Transplant*. 2004;2:174-177.
33. Kensler TW, Wakabayashi N, Biswal S. Cell survival responses to environmental stresses via the Keap1-Nrf2-ARE pathway. *Annu Rev Pharmacol Toxicol*. 2007;47:89-116.
34. Jaramillo MC, Zhang DD. The emerging role of the Nrf2-Keap1 signaling pathway in cancer. *Genes Dev*. 2013;27:2179-2191.
35. Yu J, Zhang W, Zhang R, et al. Molecular hydrogen attenuates hypoxia/reoxygenation injury of intrahepatic cholangiocytes by activating Nrf2 expression. *Toxicol Lett*. 2015;238:11-19.
36. Song G, Zong C, Zhang Z, et al. Molecular hydrogen stabilizes atherosclerotic plaque in low-density lipoprotein receptor-knockout mice. *Free Radic Biol Med*. 2015;87:58-68.
37. Yu Y, Yang Y, Bian Y, et al. Hydrogen gas protects against intestinal injury in wild type but not NRF2 knockout mice with severe sepsis by regulating HO-1 and HMGB1 release. *Shock*. 2017;48:364-370.
38. Tamaki N, Orihuela-Campos RC, Fukui M, Ito HO. Hydrogen-rich water intake accelerates oral palatal wound healing via activation of the Nrf2/antioxidant defense pathways in a rat model. *Oxid Med Cell Longev*. 2016;2016:5679040.
39. McGee HM, Schmidt BA, Booth CJ, et al. IL-22 promotes fibroblast-mediated wound repair in the skin. *J Invest Dermatol*. 2012;133:1321-1329.
40. Leonard EJ, Yoshimura T. Human monocyte chemoattractant protein-1 (MCP-1). *Immunol Today*. 1990;11:97-101.
41. Hayasaki T, Kaikita K, Okuma T, et al. CC chemokine receptor-2 deficiency attenuates oxidative stress and infarct size caused by myocardial ischemia-reperfusion in mice. *Circ J*. 2006;70:342-351.
42. Furuichi K, Wada T, Iwata Y, et al. CCR2 signaling contributes to ischemia-reperfusion injury in kidney. *J Am Soc Nephrol*. 2003;14:2503-2515.
43. Sawaya DE, Zibari GB, Minardi A, et al. P-selectin contributes to the initial recruitment of rolling and adherent leukocytes in hepatic venules after ischemia/reperfusion. *Shock*. 1999;12:227-232.
44. Kurose I, Anderson DC, Miyasaka M, et al. Molecular determinants of reperfusion-induced leukocyte adhesion and vascular protein leakage. *Circ Res*. 1994;74:336-343.
45. Ravanti L, Kähäri VM. Matrix metalloproteinases in wound repair (review). *Int J Mol Med*. 2000;6:391-407.
46. Pakyari M, Farrokhi A, Maharlooei MK, Ghahary A. Critical role of transforming growth factor beta in different phases of wound healing. *Adv Wound Care (New Rochelle)*. 2013;2:215-224.
47. Barrientos S, Stojadinovic O, Golinko MS, Brem H, Tomic-Canic M. Growth factors and cytokines in wound healing. *Wound Repair Regen*. 2008;16:585-601.
48. Yager DR, Zhang LY, Liang HX, Diegelmann RF, Cohen IK. Wound fluids from human pressure ulcers contain elevated matrix metalloproteinase levels and activity compared to surgical wound fluids. *J Invest Dermatol*. 1996;107:743-748.
49. Liu SL, Liu K, Sun Q, Liu WW, Tao HY, Sun XJ. Hydrogen therapy may be a novel and effective treatment for COPD. *Front Pharmacol*. 2011;2:19.
50. Kawai D, Takaki A, Nakatsuka A, et al. Hydrogen-rich water prevents progression of nonalcoholic steatohepatitis and accompanying hepatocarcinogenesis in mice. *Hepatology*. 2012;56:912-921.
51. Dole M, Wilson FR, Fife WP. Hyperbaric hydrogen therapy: a possible treatment for cancer. *Science*. 1975;190:152-154.
52. Zong C, Song G, Yao S, et al. Administration of hydrogen-saturated saline decreases plasma low-density lipoprotein cholesterol levels and improves high-density lipoprotein function in high-fat diet-fed hamsters. *Metabolism*. 2012;61:794-800.
53. Hayashida K, Sano M, Ohsawa I, et al. Inhalation of hydrogen gas reduces infarct size in the rat model of myocardial ischemia-reperfusion injury. *Biochem Biophys Res Commun*. 2008;373:30-35.
54. Kamimura N, Nishimaki K, Ohsawa I, Ohta S. Molecular hydrogen improves obesity and diabetes by inducing hepatic FGF21 and stimulating energy metabolism in db/db mice. *Obesity (Silver Spring)*. 2011;19:1396-1403.

SUPPORTING INFORMATION

Additional supporting information may be found online in the Supporting Information section at the end of the article.

How to cite this article: Fang W, Wang G, Tang L, et al. Hydrogen gas inhalation protects against cutaneous ischaemia/reperfusion injury in a mouse model of pressure ulcer. *J Cell Mol Med*. 2018;22:4243–4252. https://doi.org/10.1111/jcmm.13704

AMERICAN SOCIETY FOR MICROBIOLOGY | Applied and Environmental Microbiology®

GENETICS AND MOLECULAR BIOLOGY

Plant Homeodomain Genes Play Important Roles in Cryptococcal Yeast-Hypha Transition

Yunfang Meng,[a,b,c] Yumeng Fan,[b,d] Wanqing Liao,[c] Xiaorong Lin[b,d]

[a]Department of Dermatology, Shandong Provincial Hospital Affiliated with Shandong University, Jinan, China
[b]Department of Biology, Texas A&M University, College Station, Texas, USA
[c]Department of Dermatology and Venereology, Changzheng Hospital, Shanghai, China
[d]Department of Microbiology, University of Georgia, Athens, Georgia, USA

ABSTRACT *Cryptococcus neoformans* is a major opportunistic fungal pathogen. Like many dimorphic fungal pathogens, *C. neoformans* can undergo morphological transition from the yeast form to the hypha form, and its morphotype is tightly linked to its virulence. Although some genetic factors controlling morphogenesis have been identified, little is known about the epigenetic regulation in this process. Proteins with the plant homeodomain (PHD) finger, a structurally conserved domain in eukaryotes, were first identified in plants and are known to be involved in reading and effecting chromatin modification. Here, we investigated the role of the PHD finger family genes in *Cryptococcus* mating and yeast-hypha transition. We found 16 PHD finger domains distributed among 15 genes in the *Cryptococcus* genome, with two genes, *ZNF1*α and *RUM1*α, located in the mating type locus. We deleted these 15 PHD genes and examined the impact of their disruption on cryptococcal morphogenesis. The deletion of five PHD finger genes dramatically affected filamentation. The *rum1*$\alpha\Delta$ and *znf1*$\alpha\Delta$ mutants showed enhanced ability to initiate filamentation but impaired ability to maintain filamentous growth. The *bye1*Δ and the *phd11*Δ mutants exhibited enhanced filamentation, while the *set302*Δ mutants displayed reduced filamentation. Ectopic overexpression of these five genes in the corresponding null mutants partially or completely restored the defect in filamentation. Furthermore, we demonstrated that Phd11, a suppressor of filamentation, regulates the yeast-hypha transition through the known master regulator Znf2. The findings indicate the importance of epigenetic regulation in controlling dimorphic transition in *C. neoformans*.

IMPORTANCE Morphotype is known to have a profound impact on cryptococcal interaction with various hosts, including mammalian hosts. The yeast form of *Cryptococcus neoformans* is considered the virulent form, while its hyphal form is attenuated in mammalian models of cryptococcosis. Although some genetic regulators critical for cryptococcal morphogenesis have been identified, little is known about epigenetic regulation in this process. Given that plant homeodomain (PHD) finger proteins are involved in reading and effecting chromatin modification and their functions are unexplored in *C. neoformans*, we investigated the roles of the 15 PHD finger genes in *Cryptococcus* mating and yeast-hypha transition. Five of them profoundly affect filamentation as either a suppressor or an activator. Phd11, a suppressor of filamentation, regulates this process via Znf2, a known master regulator of morphogenesis. Thus, epigenetic regulation, coupled with genetic regulation, controls this yeast-hypha transition event.

KEYWORDS plant homeodomain (PHD) finger, morphogenesis, pheromone, unisexual development, dimorphism

Received 12 August 2017 **Accepted** 19 February 2018

Accepted manuscript posted online 2 March 2018

Citation Meng Y, Fan Y, Liao W, Lin X. 2018. Plant homeodomain genes play important roles in cryptococcal yeast-hypha transition. Appl Environ Microbiol 84:e01732-17. https://doi.org/10.1128/AEM.01732-17.

Editor Emma R. Master, University of Toronto

Address correspondence to Wanqing Liao, liaowanqing@sohu.com, or Xiaorong Lin, Xiaorong.Lin@uga.edu.

Y.M. and Y.F. contributed equally to this work.

Cryptococcus neoformans is an opportunistic fungal pathogen that claims hundreds of thousands of lives each year globally (1, 2). The fungus can undergo morphological transition from the yeast form to the hypha form. Like many dimorphic fungal pathogens (3, 4), the morphotype of *Cryptococcus* is tightly linked to its virulence (5, 6). To understand the biology and pathology of *Cryptococcus*, some important genetic factors that regulate yeast-hypha transition have been identified. Morphological transition in *Cryptococcus* occurs during unisexual development or during bisexual **a**-α mating (7–9), which is controlled by the pheromone signaling pathway under mating-inducing conditions (10). The HMG domain transcription factor Mat2 is an effector of the pheromone pathway (11). Mat2 activates the zinc finger transcription factor Znf2 under mating-inducing conditions, which ultimately determines the yeast-hypha transition (11). Znf2 is the decision maker in filamentation, and it also bridges morphology and virulence potential in *Cryptococcus* (6, 11, 12).

The mating-type locus of the *Cryptococcus* genome carries many genes that control the mating process (13), including several components of the pheromone pathway, such as the pheromone gene *MF*α/**a** (14, 15), the pheromone receptor gene *STE3*α/**a** (14, 16), *STE20*α/**a**, and elements of the MAPK cascade *STE11*α/**a** and *STE12*α/**a** (9, 17). The mating type locus also harbors the cell identity factor gene *SXI1*α/2**a** (13, 18). Two uncharacterized plant homeodomain (PHD) finger genes, *RUM1* α/**a** and *ZNF1* α/**a**, are also located in the mating type locus (13, 15). The PHD finger was first identified in the plant *Arabidopsis* (19). The highly conserved small PHD fold consists of 50 to 80 amino acid residues and a cross-brace topology in which two zinc atoms are anchored by the Cys4-His-Cys3 motif. PHD finger proteins are important readers of histone modifications and are involved in epigenetic regulation in plants and mammals (20). Although PHD finger proteins are universally distributed in eukaryotes, their biological functions in the fungal kingdom are poorly understood. In another human fungal pathogen, *Candida albicans*, histone modification contributes to the yeast-hypha transition (21), indicating that epigenetic factors can be important in regulating fungal morphogenesis. However, nothing is known about epigenetic regulation of morphogenesis in *Cryptococcus*.

Here, we systematically analyzed the PHD finger genes in the genome of *C. neoformans*. We identified 16 PHD finger domains harbored by 15 genes. We generated and characterized 15 PHD gene knockout mutants and 5 PHD gene overexpression strains. These five selected PHD genes exhibit important roles in filamentation, indicating that some PHD proteins are critical for *Cryptococcus* morphotype transition.

RESULTS

Identification of PHD finger genes in *C. neoformans*. As mentioned in the introduction, two PHD finger genes, *RUM1* and *ZNF1*, are located in the mating type locus. To identify additional putative PHD finger-containing genes, we used the PHD domain sequences from *ZNF1*α as the query sequences in a BLAST search against the genome of *C. neoformans* strain JEC21 (serotype D). Based on the Pfam database, we obtained 16 putative PHD finger domains carried by 15 genes in the genome of JEC21 (Table 1). Corresponding genes also exist in the genome of *C. neoformans* strain H99 (serotype A). The predicted protein sequences of these PHD genes were compared with those of PHD proteins in other eukaryotic species, including budding yeast, fission yeast, mouse, and human. However, these homologues are not conserved with cryptococcal PHD genes except for some conserved domains. The closest homologues of some PHD proteins in *Saccharomyces cerevisiae* that have been previously characterized are provided in Table 1.

Alignment of these PHD finger domain sequences using the DNAMAN software (Lynnon, CA, USA) indicated that they share a feature with the same basic PHD finger topology—two zinc atoms harbored by the Cys4-His-Cys3 motif (Fig. 1A)—as expected based on previous studies (20). The motif scan results revealed additional important domains related to histone modification in Phd11 and Set302 (Fig. 1B). Phd11 carries a MOZ-SAS domain, which may potentially possess lysine acetyltransferase activity (22).

TABLE 1 Fifteen PHD genes in the genomes of JEC21 and H99

Gene name	Gene ID		Homologue in *S. cerevisiae*
	JEC21	H99	
PHD1	CNG02500	CNAG_03329	Pho23
BYE1	CNK01990	CNAG_01859	Bye1
PHD3	CNK01390	CNAG_07532	Yng1
PHD4	CNK00900	CNAG_02604	
PHD5	CNI02340	CNAG_04315	
PHD6	CNG01620	CNAG_03423	
PHD7	CNG01970		
SPP101(PHD8)	CNG01770	CNAG_03406	Spp1
PHD9	CNC00260	CNAG_07967	
PHD11	CNG00240	CNAG_03583	
SET302(PHD12)	CNF04280	CNAG_06591	Set3
RUM1(PHD13)	CND05870	CNAG_07411	
ZNF1(PHD14)	CND05730	—[a]	
PHD15	CND04210	CNAG_01301	Yng2
PHD16	CND03810	CNAG_07430	Cti6

[a]*ZNF1* exists in H99 (13), but there is no annotation of the gene in the current genome database.

Set302 harbors one SET domain, which shows histone methyltransferase activity in *S. cerevisiae* and other organisms (23, 24). The homologue in *Saccharomyces* forms a Set3 complex, which acts as a meiotic-specific repressor of the sporulation genetic program (23). The presence of these motifs in Phd11 and Set302 in *Cryptococcus* suggests that these PHD proteins might act as chromatin modifiers, in addition to chromatin readers.

Different expression patterns of the PHD genes during development. XL280 has been widely used as a reference strain to study morphogenesis, sexual development, and pathogenicity (12, 25–28). It has superior ability to transit from the yeast form to the hypha form (12, 29). We decided to examine if PHD genes are involved in cryptococcal development in the wild-type XL280 strain during vegetative yeast growth in YPD (1% yeast extract, 2% Bacto Peptone, and 2% dextrose) medium and during unisexual development on V8 juice agar medium (30, 31). We first examined their expression patterns by transcriptome sequencing (RNA-Seq) and real-time (RT) PCR.

When the wild-type cells were cultured in YPD medium, the transcript levels of the PHD finger genes were 2^5- to 2^9-fold lower than that of the housekeeping gene *TEF1* (translation elongation factor 1) based on our previous RNA-Seq data (32) (Fig. 2A). The real-time PCR results for the wild-type strain XL280 cultured in YPD liquid medium for 16 h were largely consistent with the pattern observed in the RNA-Seq data (Fig. 2B). The low transcript levels of the PHD finger genes compared to the housekeeping gene *TEF1* are consistent with their potential regulatory roles.

Many morphogenesis factors show development-associated transcription. To examine if the transcript levels of the PHD finger genes change at different cryptococcal development stages under mating-inducing conditions, we analyzed the numbers of fragments per kilobase per million (FPKM) of the PHD genes from our RNA-Seq data obtained from wild-type XL280 cultured alone on YPD medium (yeast growth) and on V8 medium for 24 h (initiation of filamentation), 48 h (filamentation elongation), or 72 h (filamentation and initiation of sporulation). Interestingly, although the transcript levels of PHD finger genes remained low under all the conditions tested, the transcript levels of *BYE1*, *PHD4*, *PHD5*, *PHD11*, *SET302*, *ZNF1*α, and *PHD15* dramatically increased after 24 h to 72 h of culture on V8 medium compared to those in YPD medium, particularly at the later time points (Fig. 3). The transcript levels of *PHD6* and *PHD9* showed significant increases only at the 72-h time point.

We also tested the transcription levels of PHD genes during α-**a** bisexual mating on V8 medium. Here, we cocultured XL280α and its congenic pair strain, XL280**a** (12), on V8 medium for bisexual mating. We found that the transcript levels of the *BYE1*, *PHD4*, *PHD6*, *PHD11*, *SET302*, and *PHD16* genes were increased more than 4-fold after 24 h or

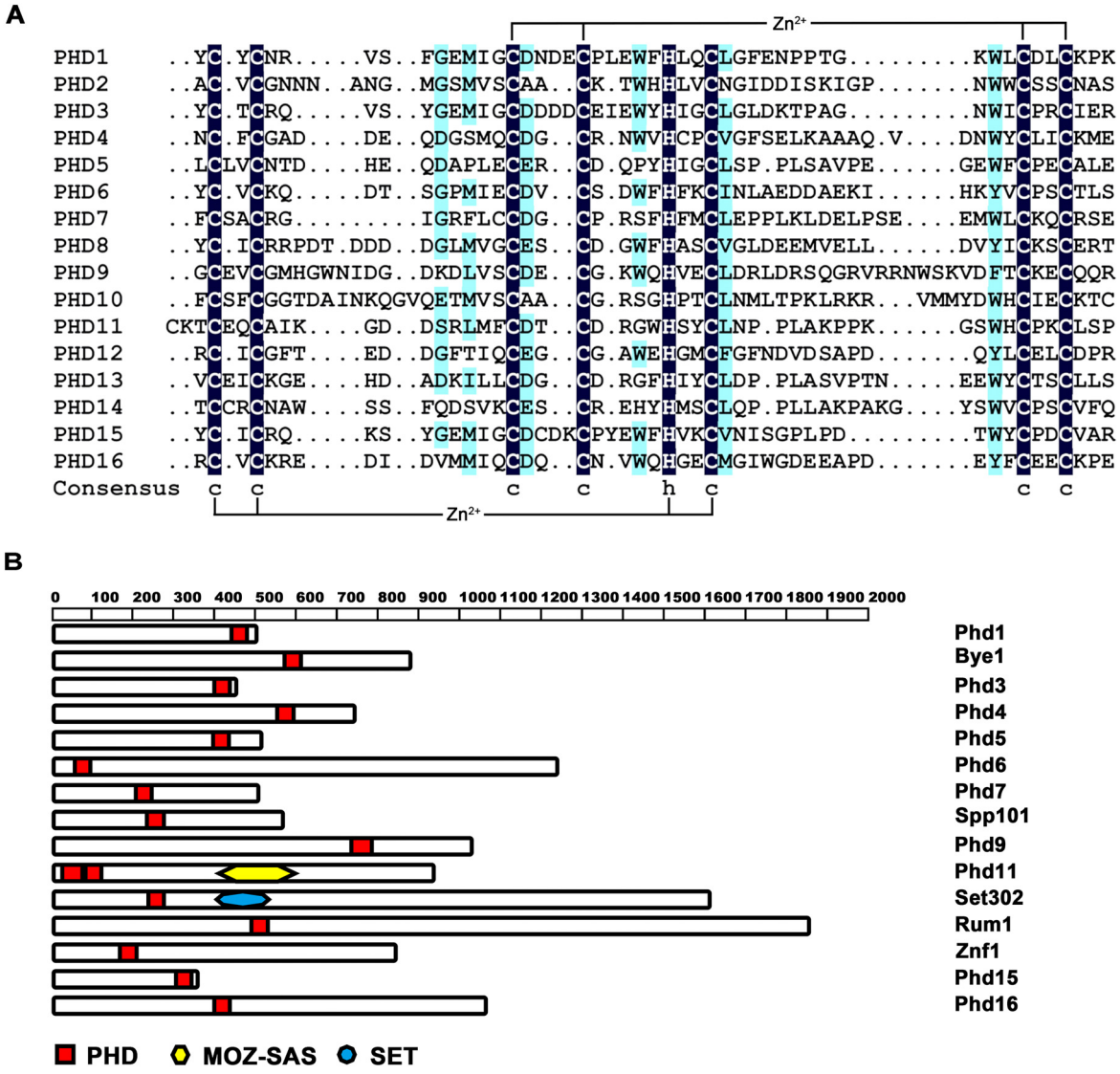

FIG 1 Multiple-sequence alignment for the 16 PHD domains and domain structure of the PHD finger genes in *C. neoformans*. (A) Multiple-sequence alignment analysis of 16 PHD domains in *C. neoformans* showed that they share the same basic topology: two zinc atoms harbored by the Cys4-His-Cys3 motif. Dark blue, residues that are conserved in all PHD fingers. Light blue, residues that are shared in most PHD fingers. (B) PHD finger proteins in *C. neoformans* may contain one or two PHD finger domains. Some harbor other functional domains related to chromatin modifications, such as the MOZ/SAS domain in Phd11 and the SET domain in Set302. The positions of these domains are indicated in the diagram.

48 h during bisexual mating on V8 medium compared to those in YPD medium (Fig. 4). These observations suggest that the expression of the PHD family genes in *C. neoformans* is positively correlated with the filamentation process. In particular, the transcript level of *PHD4* during bisexual mating on V8 medium was dramatically increased compared to that in YPD medium, with a maximum 120-fold increase at the 48-h time point (Fig. 4). Together, both the RNA-Seq and real-time PCR data suggest that PHD genes, particularly *BYE1*, *PHD4*, *PHD6*, *PHD11*, and *SET302*, may play a role in cryptococcal development based on their development-associated expression.

Phenotypical characterization of the PHD gene deletion mutants. To characterize the biological roles of the PHD genes, we deleted the 15 PHD finger genes individually in the XL280 background. Given that *C. neoformans* is a fungal pathogen with well-established virulence traits, we first examined if the deletion of these genes would affect the following traits: thermotolerance, UV sensitivity, capsule production,

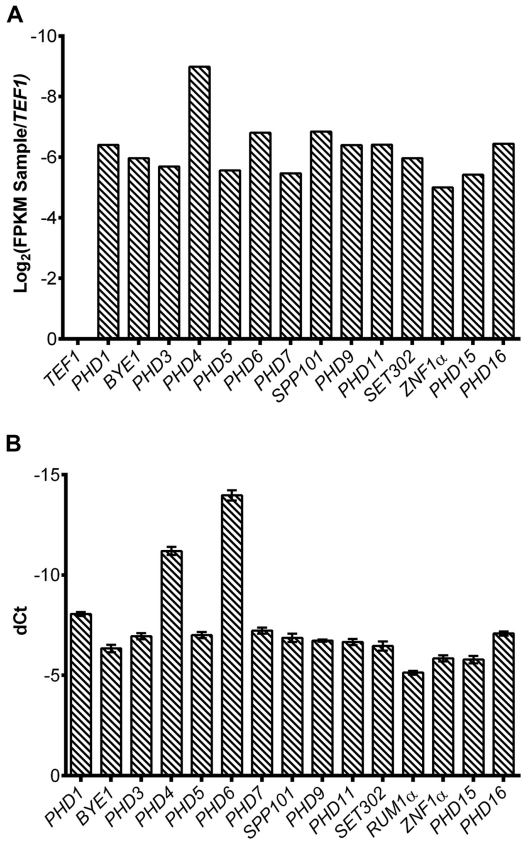

FIG 2 Transcript levels of PHD genes during yeast growth. (A) Transcript levels for all PHD genes are relatively low during vegetative yeast growth in YPD medium based on our RNA-Seq data (32). The FPKM value of the housekeeping gene *TEF1* was used as a reference. *RUM1*α (15) was not included in the RNA-Seq database due to its omission in the current genome annotation file. (B) The transcript level of each PHD finger gene in the wild-type strain XL280 cultured in YPD medium for 16 h was measured by real-time PCR. The transcript level of *TEF1* was used as a reference. The error bars indicate standard deviations. dCt (delta cycle threshold) = C_T (PHD gene) − C_T (*TEF1*).

and melanization. Many fungal species cannot tolerate or grow at mammalian body temperature (33), a prerequisite for systemic infections. Consequently, temperature-sensitive cryptococcal mutants, such as calcineurin mutants or RAM pathway mutants, are often avirulent (34–36). Most of the PHD gene deletion mutants grew well at 30°C, 37°C, or 39°C, similar to the wild type (WT) (Fig. 5A). The *bye1*Δ mutant showed modest growth reduction at 37°C, while the *phd3*Δ and *phd15*Δ mutants showed severe growth defects at both 30°C and 37°C (Fig. 5A). Colonies of the *phd3*Δ and the *phd15*Δ mutants were smaller than those of the wild type even at 30°C, and their growth defects appeared to be much more severe at higher temperatures. At 39°C, there was barely any growth observed in the *phd3*Δ mutant or the *phd15*Δ mutant, and some growth was recovered after temperature downshift from 39°C to 30°C (Fig. 5B). To determine if the smaller colony size was due to a lower growth rate or a smaller cell size at 30°C, we examined the generation time of the *phd3*Δ mutant and its cell size. We did not observe any significant difference in cell size in the *phd3*Δ mutant compared to the wild type (Fig. 5C). As expected, the generation time for the *phd3*Δ mutant was twice as long as that of the wild type at 30°C in YPD liquid culture (Fig. 5D). We also tested the sensitivities of all the PHD finger deletion mutants to UV radiation. Most had sensitivity to UV radiation similar to that of the WT strain (Fig. 6A), with the exception of the *phd3*Δ mutant, which showed increased resistance (Fig. 6A and B). Interestingly, the other slow-growing *phd15*Δ mutant did not show significantly increased resistance to UV radiation, suggesting that Phd3 and Phd15 are not functionally identical. Melanin and capsule production are two other major virulence traits of *Cryptococcus*. All the mutants

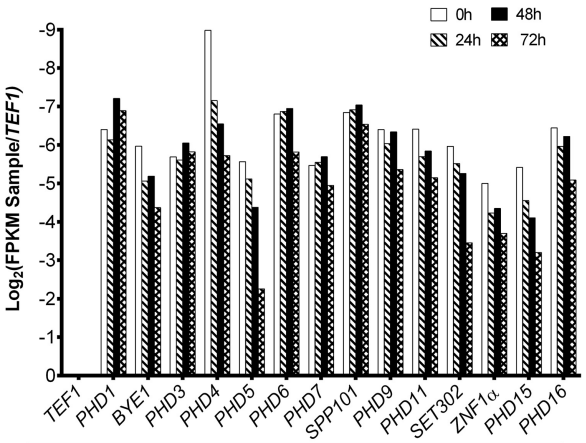

	PHD1	*BYE1*	*PHD3*	*PHD4*	*PHD5*	*PHD6*	*PHD7*
0h vs 24h	ns	**	ns	****	ns	ns	ns
0h vs 48h	**	**	ns	****	****	ns	ns
0h vs 72h	ns	****	ns	****	****	***	ns
	SPP101	*PHD9*	*PHD11*	*SET302*	*ZNF1α*	*PHD15*	*PHD16*
0h vs 24h	ns	ns	*	ns	**	**	ns
0h vs 48h	ns	ns	ns	*	*	****	ns
0h vs 72h	ns	***	****	****	****	****	ns

FIG 3 PHD genes show differential patterns of expression during unisexual mating. Shown are the changes in the transcript levels of PHD genes in the wild-type strain cultured under mating-stimulating conditions (V8 medium) for different times. The overnight culture of the wild type in YPD medium was used as the zero time point. The transcript level of each gene at 24 h, 48 h, and 72 h after inoculation on V8 was compared to that in YPD medium. The FPKMs of *TEF1* at the different time points were used as a reference. Two-way analysis of variance (ANOVA) multicomparison was used for statistical analysis. Statistical significance is shown below (ns, not significant [$P > 0.05$]; *, $P \leq 0.05$; **, $P \leq 0.01$; ***, $P \leq 0.001$; ****, $P \leq 0.0001$).

were capable of producing melanin on L-3,4-dihydroxyphenylalanine (L-DOPA) medium (see Fig. S1A in the supplemental material), and all formed capsule with no apparent defects based on microscopic examination using India ink negative staining (see Fig. S1B in the supplemental material). Thus, it appears that most of the PHD genes are not critical for expressing these classic virulence traits.

Five PHD genes are important for yeast-hypha transition. Besides the classic virulence traits, the morphotype has a profound impact on cryptococcal interactions with various hosts. Filamentation confers on *Cryptococcus* resistance to predation by soil amoebas (37), but filaments are immune stimulatory in a mouse model of cryptococcosis (5, 38). As PHD domain proteins are known to be involved in development in plants and animals (20, 39, 40), we decided to examine their roles in morphogenesis and sexual development in *Cryptococcus*. *C. neoformans* undergoes bisexual mating involving α and **a** cells (no mating type switch) (7, 41), and it can also undergo unisexual development that involves cells of only one mating type (42). During unisexual development, colonies derived from a single cell (and thus a single mating type) can filament and generate meiotic progeny (25, 27, 28, 42).

We first examined these PHD gene deletion mutants for self-filamentation during unisexual development at 48 h and 96 h after inoculation on V8 medium. Filamentation in wild-type XL280 became obvious under a stereoscope at 48 h postinoculation, and filaments were clearly visible as the white fluffy edge of the colony at 96 h postinoculation (Fig. 7). Among the 15 mutants, 5, namely, *bye1*Δ, *phd11*Δ, *set302*Δ, *rum1*αΔ, and *znf1*αΔ, displayed alteration in filamentation (Fig. 7). Reduction in filamentation was also observed in the *phd3*Δ and *phd15*Δ mutants. However, given their growth defects and temperature-sensitive phenotype (Fig. 5), we decided not to focus on these two mutants. The *bye1*Δ and *phd11*Δ mutants showed more robust hyphal growth than the wild type both at 48 h and at 96 h postinoculation (Fig. 7A and B), indicating that Bye1 and Phd11 normally repress filamentation. In contrast, the *set302*Δ mutant exhibited

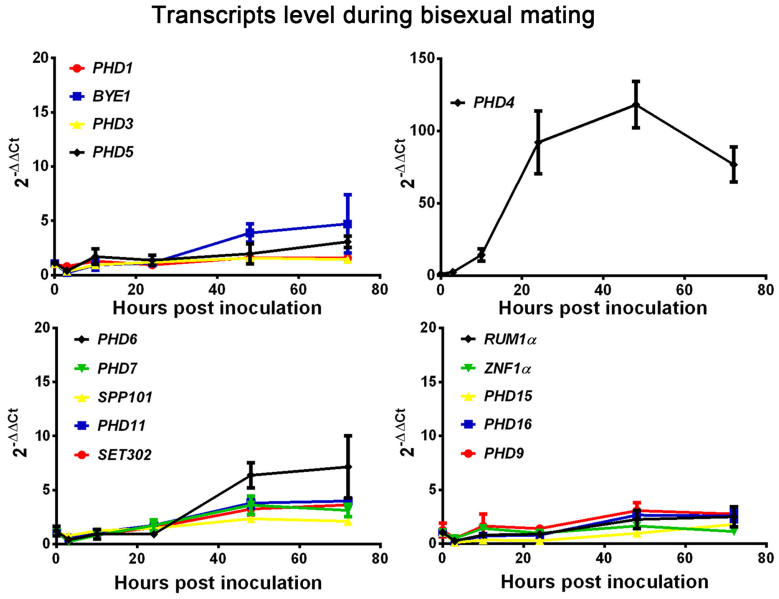

	PHD1	BYE1	PHD3	PHD4	PHD5	PHD6	PHD7	SPP101
0h vs 24h	ns	ns	ns	****	ns	ns	ns	ns
0h vs 48h	ns	*	ns	****	ns	****	*	ns
0h vs 72h	ns	**	ns	****	ns	****	ns	ns
	PHD9	PHD11	SET302	RUM1α	ZNF1α	PHD15	PHD16	
0h vs 24h	ns	ns	ns	ns	ns	ns	ns	
0h vs 48h	*	*	ns	ns	ns	ns	*	
0h vs 72h	ns	**	*	ns	ns	ns	**	

FIG 4 Transcript levels of PHD genes during bisexual mating. The transcript levels of the PHD genes during XL280 **a**-α bisexual mating were measured by real-time PCR at 3 h, 10 h, 24 h, 48 h, and 72 h after inoculation on V8 mating-inducing medium. The transcript level of *TEF1* was used as a reference. Two-way ANOVA multicomparison was used for statistical analysis. The transcript level of each gene at 24 h, 48 h, and 72 h postinoculation on V8 medium was compared to that in YPD medium. Statistical significance is shown below. None of the data at 3 h and 10 h showed significant difference from the 0-h time point. ns, not significant ($P > 0.05$); *, $P \leq 0.05$; **, $P \leq 0.01$; ****, $P \leq 0.0001$. The error bars indicate standard deviations.

drastically reduced filamentation at both time points examined (Fig. 7A and B), suggesting that Set302 is an activator for filamentation. Interestingly, the *rum1*$\alpha\Delta$ and *znf1*$\alpha\Delta$ mutants showed slightly increased robustness in filamentation at 48 h but ended up with shorter filaments than the wild type at 96 h (Fig. 7A and B). This suggests that Rum1 and Znf1 repress the initiation of filamentation but are required for sustained hyphal growth.

Filamentation precedes sporulation in *Cryptococcus*. To examine if the five PHD genes that regulate filamentation also play a role in sporulation, we examined the corresponding gene deletion mutants for their ability to sporulate. The wild-type strain produced basidia with four long chains of spores after 1 week of incubation on V8 medium (see Fig. S2 in the supplemental material). The *set302*Δ mutant rarely yielded spore chains at this point but eventually produced spores after prolonged incubation. This delay in sporulation was likely due to its severely impaired hyphal growth (Fig. 7A and B). All the other mutants were able to produce normal and abundant spore chains (see Fig. S2 in the supplemental material). This result demonstrates that PHD genes were not specifically required for sporulation.

Based on the results obtained with the gene deletion mutants, five PHD genes, namely, *BYE1*, *PHD11*, *SET302*, *RUM1*α, and *ZNF1*α, play important roles in regulating filamentation. To further examine their roles in filamentation, we decided to constitutively express these PHD genes using the promoter of the housekeeping gene *GPD1*. For Phd11, we also fused the fluorescence protein mCherry in frame to its C terminus. We then introduced these PHD gene overexpression constructs ectopically into the corresponding gene deletion mutants. Increased transcript levels of the PHD genes in

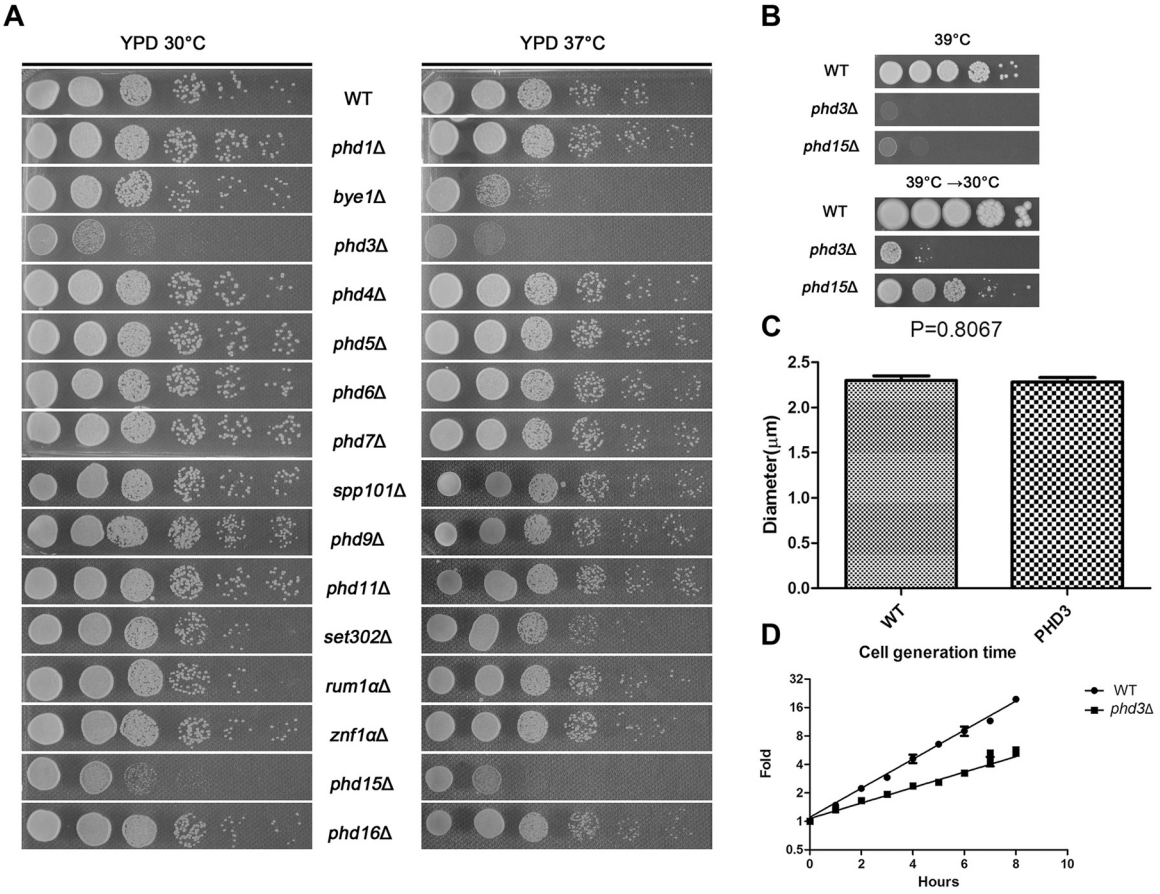

FIG 5 The *phd3*Δ and *phd15*Δ mutants have temperature-dependent growth defects and longer generation times. (A and B) The PHD finger gene deletion mutants and the wild-type strain were cultured on YPD medium at 30°C, 37°C, and 39°C. (C) The cell sizes of the *phd3*Δ and wild-type strains were measured microscopically, and there was no statistically significant difference in cell size. The error bars indicate standard deviations. (D) The generation times of the *phd3*Δ and wild-type strains cultured in YPD liquid medium were examined by plotting changes in the optical density at 600 nm against time.

the transformants were observed based on the real-time PCR results (see Fig. S3 in the supplemental material), indicating that these strains indeed overexpress the corresponding PHD genes compared to the wild type. We then examined self-filamentation of these strains. We found that overexpression of *SET302*, *RUM1*α, and *ZNF1*α led to complete or partial restoration of filamentation in the corresponding *set302*Δ, *rum1*αΔ, and *znf1*αΔ mutants (Fig. 7C). Interestingly, overexpression of *BYE1* and *PHD11* suppressed the overly robust filamentation of the *bye1*Δ and *phd11*Δ mutants (Fig. 7C), corroborating their roles as repressors of filamentation. Collectively, our data indicate that these five PHD genes play important roles in controlling filamentation. The phenotypes of the gene deletion mutants and the gene overexpression strains indicate that Bye1 and Phd11 suppress filamentation while Set302 enhances filamentation. Rum1 and Znf1 suppress the initiation of filamentation, but they are important to sustain filamentous growth.

Impacts on the pheromone and the filamentation genes caused by changes in the PHD finger genes. The evidence presented above reveals the importance of the five PHD genes in regulating filamentation. As mentioned in the introduction, the pheromone pathway is a well-characterized pathway that activates filamentation in *Cryptococcus* under mating-inducing conditions. The transcription factor Mat2 is essential in controlling this pheromone-sensing and response pathway and is required for cell fusion (11). Mat2 then activates Znf2 under mating-inducing conditions (6, 11). Znf2 is the key transcription factor that is required for filamentation under all conditions tested. Deletion of *ZNF2* itself does not abolish the pheromone pathway or cell fusion

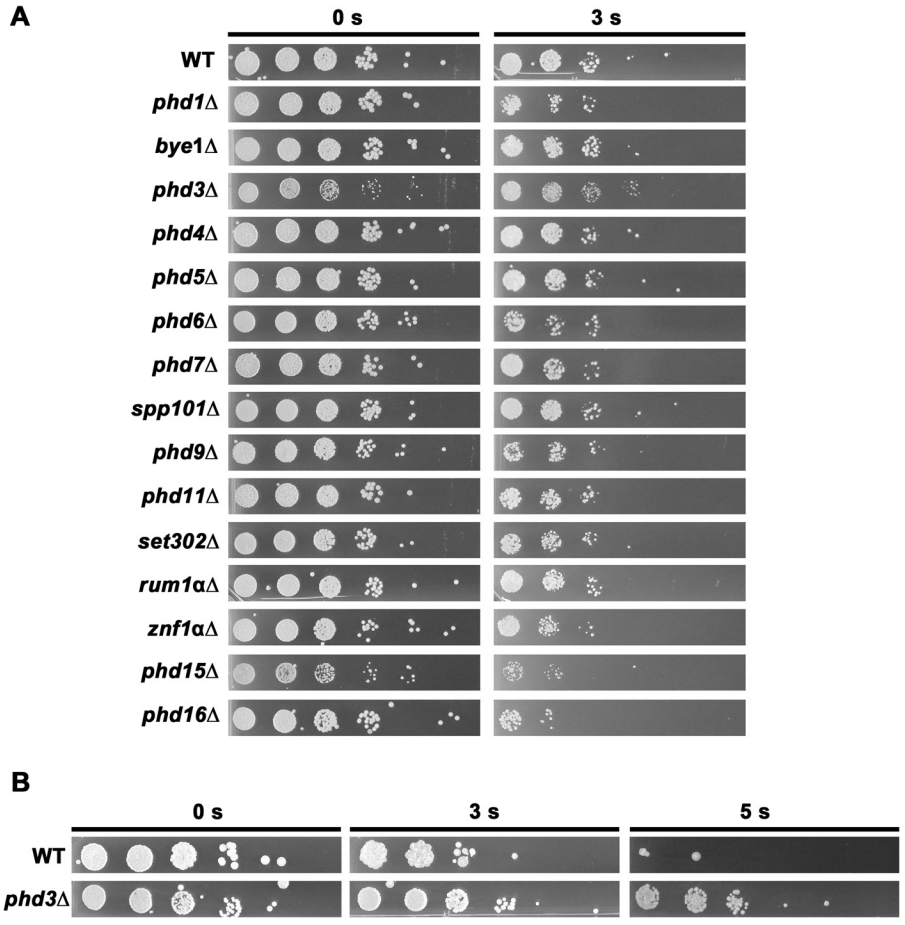

FIG 6 Sensitivity of the PHD gene deletion mutants to UV radiation. (A and B) The wild-type strain, along with all PHD finger gene deletion mutants, was inoculated onto YNB medium and air dried. The cells were then treated with 300 J/m^2 of UV for 0 s, 3 s, and 5 s.

(11). Since the disruption of the PHD finger genes altered filamentation, we speculate that these PHD finger genes may directly or indirectly affect Znf2 via pheromone-dependent or pheromone-independent pathways.

If a mutant cannot sense or respond to pheromones, cell fusion is abolished, as we observed previously for the *mat2*Δ mutant (11). To determine if any of the five PHD finger proteins are essential for cell fusion, the gene deletion mutants in the XL280α background (G418 resistant or NAT resistant) were cocultured with the wild-type **a** mating partner carrying a different drug selection marker on V8 medium. Cell fusion products with two different drug resistance markers were easily recovered from all crosses between the PHD deletion mutants (α) and the wild-type **a** mating partner. In contrast, no fusion products were recovered when the *mat2*Δ mutant was cocultured with a compatible wild-type mating partner, consistent with the essential role of Mat2 in cell fusion. The ability of the PHD mutants to undergo bisexual mating is also supported by the fact that we obtained all the PHD mutants in the mating type **a** background by crossing the mutants in the α mating type with XL280**a** (Table 2). The results indicate that these PHD genes, unlike genes in the pheromone pathway, are not essential for cell fusion.

We further examined the effect of the disruption or overexpression of the PHD genes on the expression of the pheromone pathway controlled by Mat2 and the filamentation pathway controlled by Znf2. Here, we chose to measure the transcript levels of *MF*α and *CFL1*, the respective downstream factors of Mat2 and Znf2. It is known that their transcript levels reflect the activities of the two transcription factors

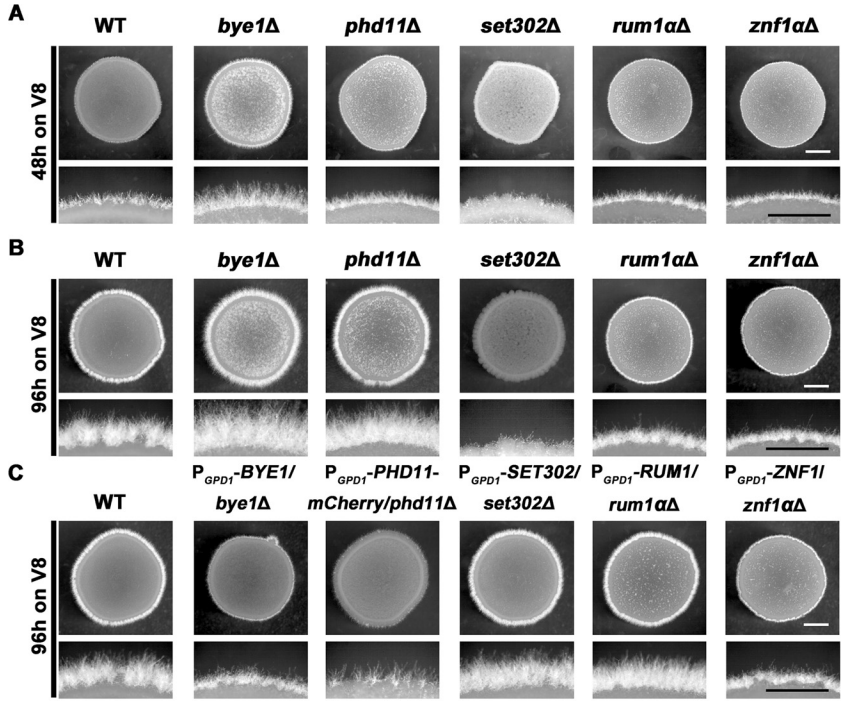

FIG 7 Mutations of the five PHD genes affect self-filamentation. The wild-type, *bye1*Δ, *phd11*Δ, *set302*Δ, *rum1*αΔ, and *znf1*αΔ strains were cultured on V8 agar medium at 22°C for 48 h (A) or 96 h (B and C). The wild type and strains with overexpression of *BYE1*, *PHD11*, *SET302*, *RUM1*α, and *ZNF1*α in the corresponding gene deletion mutant background were cultured on V8 agar medium for 96 h. The upper images show whole colonies, while the lower images show enlarged views of the edges of colonies. Bars, 10 μm (upper panels in white) and 5 μm (lower panels in black).

(6, 11, 29). All the transcript levels in the mutants and the wild-type control were normalized to that of the wild type cultured in YPD medium (Fig. 8; see Fig. S4 in the supplemental material).

Cfl1 is a hypha-specific protein downstream of Znf2, and the transcript level of *CFL1* correlates with filamentation (6, 11, 12, 43). In the *bye1*Δ mutant, the transcript level of *CFL1* was approximately 16-fold higher than that of the wild type (Fig. 8B), consistent with the enhanced filamentation of the *bye1*Δ mutant (Fig. 7A and B). In the *BYE1*^{oe} strain, the pattern was reversed, and the transcript level of *CFL1* was more than 16-fold lower than that of the wild type (Fig. 8E). This is consistent with the decreased filamentation observed in the *BYE1*^{oe} strain (Fig. 7C). Similarly, a higher *CFL1* transcript level ($\sim 2^5$-fold) at the 16-h time point was observed in the *phd11*Δ mutant (Fig. 8A), consistent with the enhanced filamentation of the mutant (Fig. 7A and B). Again, the pattern was reversed, with a much lower *CFL1* transcript level ($>$8-fold reduction) in the *PHD11*^{oe} strain (Fig. 7D), consistent with the reduced filamentation of the *PHD11*^{oe} strain (Fig. 7C). The *rum1*αΔ and the *znf1*αΔ mutants showed increased transcript levels of *CFL1* (about 4- to 8-fold) at the 16-h time point. However, their *CFL1* transcript levels became comparable to that of the wild type at the 24-h time point. This is consistent with our speculation that Rum1 and Znf1 suppress the initiation of hyphal growth but are needed to sustain filamentous growth. The *CFL1* transcript level was about 4-fold lower in the *set302*Δ mutant than that of the wild type at the 24-h time point (Fig. 8B), consistent with its reduced filamentation (Fig. 7A and B). Surprisingly, the *CFL1* transcript level in the *SET302*^{oe} strain was still about 4- to 6-fold lower than that of the wild type, even though the strain showed robust hyphal growth. Overall, the transcript levels of *CFL1* in the PHD gene deletion and gene overexpression strains are largely consistent with their impacts on filamentation.

In contrast to *CFL1*, the *MF*α transcript levels in these PHD gene deletion and overexpression strains were not as predictable. For example, the *set302*Δ and *bye1*Δ

TABLE 2 Strains and plasmids used in this study

Strain or plasmid	Genotype	Source or reference
Strains		
XL280α	Wild type	43
XL280**a**	Wild type	12
YM1	*MAT*α *PHD1*::G418	This study
YM3	*MAT***a** *PHD1*::G418	This study
YM8	*MAT*α *BYE1*::G418	This study
YM10	*MAT*α *PHD3*::G418	This study
YM12	*MAT***a** *PHD3*::G418	This study
YM20	*MAT*α *PHD4*::G418	This study
YM23	*MAT***a** *PHD4*::G418	This study
YM27	*MAT*α *PHD5*::G418	This study
YM28	*MAT* a *PHD5*::G418	This study
YM32	*MAT*α *PHD6*::G418	This study
YM34	*MAT*α *PHD7*::G418	This study
YM38	*MAT***a** *PHD7*::G418	This study
YM42	*MAT*α *PHD8*::G418	This study
YM45	*MAT***a** *PHD8*::G418	This study
YM66	*MAT*α *PHD9*::NAT	This study
YM50	*MAT*α *PHD11*::NAT	This study
YM52	*MAT***a** *PHD11*::NAT	This study
YM60	*MAT*α *SET302*::NAT	This study
YF36	*MAT***a** *SET302*::NAT	This study
YM61	*MAT*α *RUM1*::NAT	This study
YF92	*MAT***a** *RUM1*::NAT	This study
XL571	*MAT*α *ZNF1*::NAT	11
YM69	*MAT***a** *ZNF1*::NAT	This study
YM62	*MAT*α *PHD15*::NAT	This study
YF63	*MAT***a** *PHD15*::NAT	This study
YM63	*MAT*α *PHD16*::NAT	This study
YM64	*MAT***a** *PHD16*::NAT	This study
YM72	*MAT*α P_{GPD1}-*PHD11*-mCherry::NEO	This study
YF58	*MAT*α P_{GPD1}-*SET302*-HYG *SET302*::NAT	This study
YF27	*MAT*α *RUM1*::NAT P_{GPD1}-*RUM1*-HYG	This study
YF30	*MAT*α *ZNF1*::NAT P_{GPD1}-*ZNF1*-HYG	This study
YF159	*MAT*α P_{GPD1}-BYE1-HYG *BYE1*::NEO	This study
XL574	*MAT*α *ZNF2*::NAT	11
YF133	*MAT*α *PHD11*::NAT *ZNF2*::NAT	This study
XX17	*MAT*α *ZNF2*::NAT P_{CTR4}-mcherry-*ZNF2* (G418)	33
LW1	*MAT*α *ZNF2*::NAT P_{GPD1}-*ZNF2*D-NEO	6
YF127	*MAT*α P_{GPD1}-*PHD11*-HYG *ZNF2*::NAT pCTR4-mcherry-*ZNF2* (G418)	This study
XL1348	*MAT*α XL280α $G418^r$	This study
XL1109	*MAT*α XL280α NAT^r	This study
XL1142	*MAT***a** JEC20**a** NAT^r	This study
XL1411	*MAT***a** JEC20**a** $G418^r$	This study
XL942	*MAT*α *MAT2*::NAT	11
Plasmids		
pXL1-PHD11-mcherry	p_{GPD1}-*PHD11*-mCherry-G418	This study
pXL1-SET302	P_{GPD1}-*SET302*-HYG	This study
pXL1-RUM1	P_{GPD1}-*RUM1*-HYG	This study
pXL1-ZNF1	P_{GPD1}-*ZNF1*-HYG	This study
pXL1-PHD11	P_{GPD1}-*PHD11*-HYG	This study
pXL1-BYE1	PGPD1-BYE1-HYG	This study
pPZP-NEO1	pPZP-NEO1	50
pPZP-NATcc	pPZP-NATcc	50

mutants showed opposite phenotypes in term of filamentation, but their *MF*α transcript levels were similar. In the *BYE1*^{oe} strain, the *MF*α level decreased dramatically ($\sim 2^5$-fold changes) at the 16-h and 24-h time points compared to that of the wild type. In the *rum1*$\alpha\Delta$ and *znf1*$\alpha\Delta$ mutants, the *MF*α transcript levels were comparable with that of the wild type, while the transcript level of *MF*α in the *rum1*$\alpha\Delta$ mutant showed only about 2-fold reduction at the 24-h time point. The transcript levels of *MF*α were

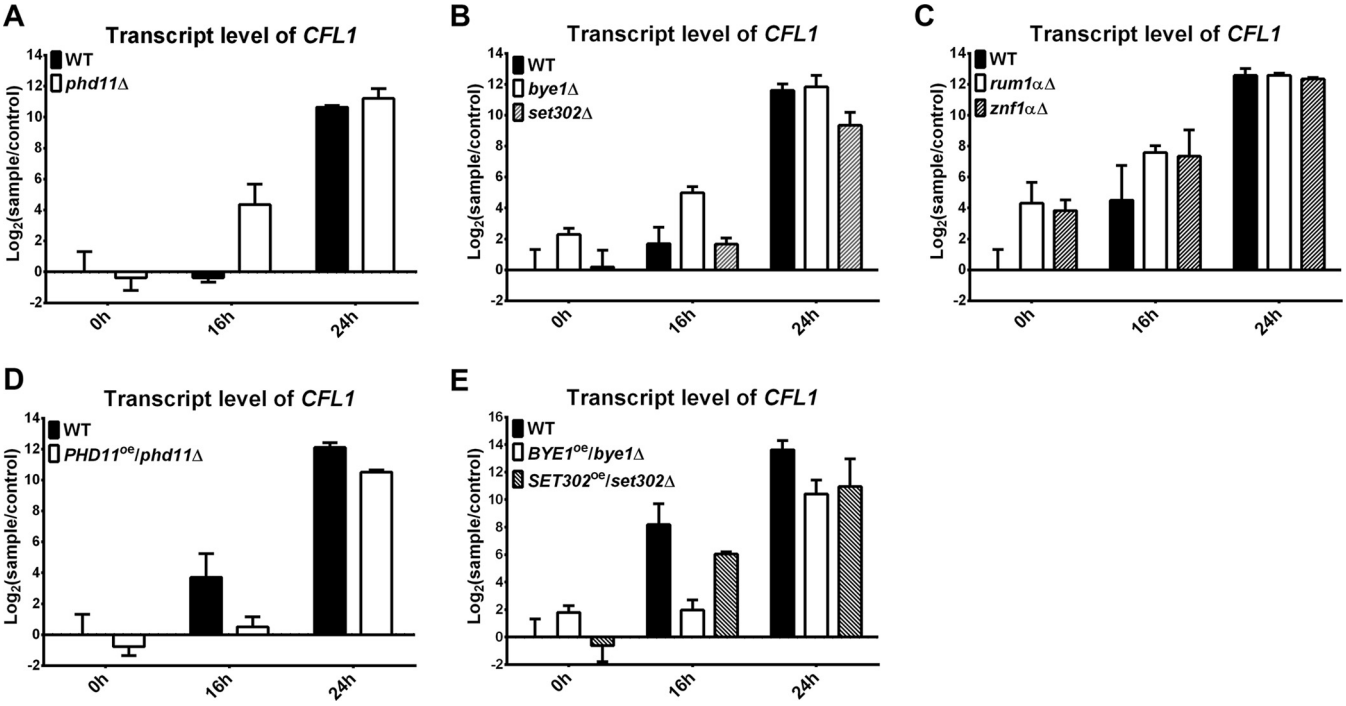

FIG 8 The transcript level of the filamentation marker *CFL1* shows good correlation with the filamentation phenotypes of the PHD gene deletion or overexpression strains. The transcript levels of *CFL1* were measured by real-time PCR in the wild type, the five PHD gene deletion mutants (*bye1*Δ, *phd11*Δ, *set302*Δ, *rum1*αΔ, and *znf1*αΔ), and overexpression strains (*BYE1*^{oe}/*bye1*Δ, *PHD11*^{oe}/*phd11*Δ, and *SET302*^{oe}/*set302*Δ). Overnight cultures of these strains in YPD liquid medium were considered the zero time point. The cells were then cultured on V8 agar medium for 16 h and 24 h. The *CFL1* transcript level in the wild type at the zero time point was used for normalization. The *y* axes show the $\log_2$ changes in the transcript level of *CFL1*. The error bars indicate standard deviations.

significantly different in the *phd11*Δ and *PHD11*^{oe} strains at the 16-h time point (see Fig. S4 in the supplemental material), and the difference became smaller at the later time point. The inconsistency of the *MF*α transcript levels in these strains with the mutant phenotype in filamentation is consistent with the idea that the pheromone pathway is not the major effector of these PHD proteins.

Phd11 functions upstream of Znf2 in regulating filamentation. Although Znf2 is well established in its essential role for hyphal growth (6, 11, 12), the regulatory circuits controlling Znf2, especially factors that suppress filamentation, are unclear. Given the phenotypes of the *PHD11* gene deletion mutant (enhanced filamentation) and the overexpression strain (reduced filamentation) (Fig. 7A to C), Phd11 works as a suppressor of filamentation. Here, we decided to further investigate the relationship between Phd11 and Znf2. First, we examined the impacts of deletion and overexpression of *ZNF2* on the transcript level of *PHD11*. As shown in Fig. 9A, the *PHD11* transcript levels in the wild-type strain, the *znf2*Δ mutant, and the *ZNF2*^{oe} strain were similar regardless of whether cells were cultured in YPD or on V8 medium. This suggests that Znf2 does not affect Phd11 at the transcript level. We then examined the transcript level of *ZNF2* in the wild type, the *phd11*Δ mutant, and the *PHD11*^{oe} strain. As expected, the transcript level of *ZNF2* was low when wild-type cells were cultured in YPD and it was drastically increased ($\sim 2^5$-fold higher) when the wild-type cells were cultured on V8 medium (Fig. 9B). Although the deletion of *PHD11* did not show much impact on the *ZNF2* transcript level, the overexpression of *PHD11* led to a drastically reduced transcript level of *ZNF2* ($>2^6$-fold reduction) on V8 medium when *ZNF2* is normally induced in the wild type. Altogether, Phd11 may act upstream of Znf2 and negatively affect the *ZNF2* transcriptional level.

To further investigate the relationship between *PHD11* and *ZNF2*, we made the *phd11*Δ *znf2*Δ double mutant. The *phd11*Δ single mutant showed enhanced filamentation, while the *znf2*Δ single mutant had filamentation abolished (Fig. 9C). The *phd11*Δ

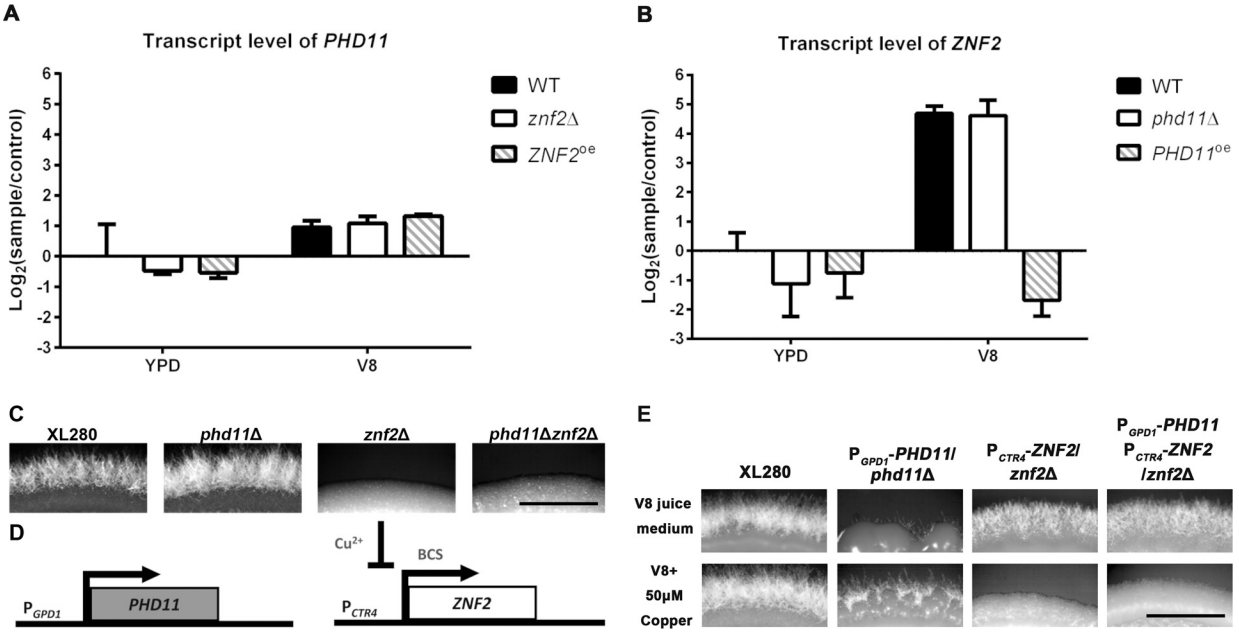

FIG 9 Phd11 functions upstream of the master morphogenesis regulator Znf2. (A) WT, *znf2*Δ, and *ZNF2*^{oe} cells were cultured in YPD liquid medium overnight or on V8 agar medium for 24 h. The transcript levels of *PHD11* were measured by real-time PCR. The *PHD11* transcript level in the WT cultured in YPD medium was used as a reference. (B) WT, *phd11*Δ, and *PHD11*^{oe} cells were cultured in YPD liquid medium overnight or on V8 medium for 16 h. The transcript levels of *ZNF2* were measured by RT-PCR. The *ZNF2* transcript level of the WT cultured in YPD was used as a reference. (C) WT, *phd11*Δ, *znf2*Δ, and *phd11*Δ*znf2*Δ double-mutant cells were cultured on V8 agar medium for 3 days. (D) Diagram of the strain with constitutive expression of *PHD11* driven by the *GPD1* promoter and the inducible expression of *ZNF2* driven by the *CTR4* promoter. The expression of *ZNF2* is induced by copper limitation and suppressed by excess copper. (E) The WT, the P_{GPD1}-*PHD11*/*phd11*Δ strain, the P_{CTR4}-*ZNF2*/*znf2*Δ strain, and the P_{GPD1}-*PHD11*/P_{CTR4}-*ZNF2*/*znf2*Δ strain were cultured on copper-limited V8 juice agar medium (*ZNF2*-inducing condition) and on V8 agar supplemented with 50 μM $CuSO_4$ (*ZNF2*-suppressing condition). The error bars indicate standard deviations.

*znf2*Δ double mutant showed no hyphal growth, similar to the *znf2*Δ single mutant (Fig. 9C). Thus, the deletion of *PHD11*, although it increased filamentation in a wild-type background, failed to confer filamentation on the *znf2*Δ mutant.

To further examine the relationship between Phd11 and Znf2, we constructed a strain with constitutive overexpression of *PHD11* and inducible expression of *ZNF2*. We hypothesized that if Phd11 functions upstream of Znf2, then overexpression of *PHD11* when *ZNF2* is not expressed would recapitulate the *znf2*Δ-like nonfilamentous phenotype. On the other hand, overexpression of the downstream factor *ZNF2* should overcome the suppressive effect of the overexpression of *PHD11* and drive robust filamentation. For this purpose, we had *PHD11* driven by the constitutively active *GPD1* promoter and *ZNF2* by the inducible promoter of the copper transporter gene *CTR4* (Fig. 9D). Because V8 medium itself is slightly copper limiting, the *CTR4* promoter would be activated under these conditions, and consequently, *ZNF2* would be expressed. Indeed, the P_{CTR4}-*ZNF2*/*znf2*Δ strain showed robust hyphal growth on V8 medium (Fig. 9E). The addition of copper to V8 medium suppresses the *CTR4* promoter, and *ZNF2* is not expressed. Consistently, the P_{CTR4}-*ZNF2*/*znf2*Δ strain grew only yeast colonies in the presence of copper (Fig. 9E). When *PHD11* was constitutively overexpressed, the P_{GPD1}-*PHD11*/*phd11*Δ strain showed repressed hyphal growth compared to the wild type (Fig. 9E). When both *PHD11* and *ZNF2* were expressed on V8 medium, the P_{GPD1}-*PHD11*/P_{CTR4}-*ZNF2*/*znf2*Δ strain showed robust hyphal growth, similar to the *ZNF2*^{oe} strain (Fig. 9E). When excess copper ion was added to the V8 medium, the expression of *ZNF2* was suppressed. This resulted in the nonfilamentous phenotype of the P_{GPD1}-*PHD11*/P_{CTR4}-*ZNF2*/*znf2*Δ strain (Fig. 9E), as we predicted. These results again corroborate the essential role of Znf2 in filamentation and demonstrate that Phd11 indeed functions upstream of Znf2 in controlling the yeast-to-hypha morphological change.

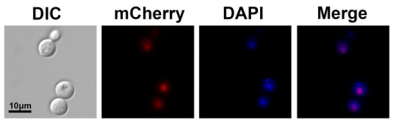

FIG 10 Phd11 is located in the nucleus. The Phd11-mCherry strain was cultured in YPD medium. Cells were fixed and stained with DAPI. DIC, differential inference contrast.

DISCUSSION

The PHD finger is found in many chromatin-remodeling proteins in eukaryotes (20, 39, 40), and their activities could lead to altered gene expression and, consequently, regulate various biological processes. In our study, we systematically deleted PHD finger genes in the environmental opportunistic fungal pathogen *C. neoformans*. We found that *PHD3* and *PHD15* are critical for thermotolerance. Given that growth at mammalian body temperature is a prerequisite for cryptococcal pathogenesis, it would be interesting to identify the effector genes and to investigate their potential impacts on cryptococcal virulence in the future. Interestingly, we identified five PHD genes, namely, *BYE1*, *PHD11*, *SET302*, *RUM1*, and *ZNF1*, that contribute to the yeast-hypha morphological switch in *Cryptococcus*. Accordingly, we found that the deletion or overexpression of these five PHD genes alters the expression of filamentation-related genes. Among the products of the five PHD finger genes, Bye1 and Phd11 work as suppressors of filamentation and Set302 functions as an activator of filamentation. Rum1 and Znf1, two PHD proteins encoded in the *MAT* locus, suppress the initiation of filamentation but are important for maintaining robust hyphal growth. We chose to investigate Set302 and Phd11 further because *set302*Δ and *phd11*Δ strains showed the most dramatic and opposing phenotypes in terms of filamentation. Set302 and Phd11 are predicted to be nuclear proteins due to the presence of a nuclear localization signal (NLS). While attempts to construct mCherry-fused Set302 failed, the generated Phd11-mCherry indeed yielded stable and clear fluorescence that colocalized with DAPI (4′,6-diamidino-2-phenylindole) staining (Fig. 10). The nuclear localization of Phd11 is consistent with its predicted nuclear function as a chromatin reader. Phd11 harbors a predicted histone acetyltransferase MOZ-SAS domain, while Set302 contains a SET domain. The unique domain structures in these two PHD proteins suggest that Phd11 and Set302 may act not only as readers of histone modifications, due to their PHD domains, but also as writers of histone modifications. Further mechanistic studies are warranted to fully understand their modes of action.

MATERIALS AND METHODS

Strains and growth conditions. The strains used in this study are listed in Table 2. All the strains were stored as glycerol stocks at −80°C. For experiments, cells were streaked out from freezer stocks and cultured on YPD medium at 30°C unless otherwise indicated.

Construction of gene deletion mutants and overexpression strains. For gene deletion, we used the method of double-joint PCR as described previously (44). Briefly, two partially overlapping parts of the chosen drug selection marker (NEO, NAT, or HYG) were fused with the 5′ or 3′ flanking region (1 kb) of the open reading frame (ORF) of each gene of interest. The mixture of the pair of fusion products was then introduced into the recipient strain by biolistic transformation as described previously (45). Transformants grown on the drug-selective medium (YPD plus NAT, YPD plus NEO, or YPD plus HYG) were checked for stability, and stable transformants were then screened for homologous replacement events based on diagnostic PCR, as described previously (46). The primers used in generating gene knockout strains and for screening the homologous replacement events are listed in Table 3. For gene overexpression, the ORF of the gene of interest was amplified using the genomic DNA of the wild-type strain XL280 as a template. The resulting amplicons were digested with restriction enzymes FseI and PacI, and the digested products were then inserted into the plasmid pXL1 after the *GPD1* promoter as described previously (6). The resulting plasmids were linearized after restriction enzyme digestion and then introduced into *C. neoformans* cells by biolistic transformation as described previously (45). Transformants grown on the drug-selective medium (YPD plus NAT, YPD plus NEO, or YPD plus HYG) were examined for stability after 5 passages on nonselective medium, and the stable transformants were confirmed by phenotypic assay, diagnostic PCR, or real-time PCR. For the inducible expression system, the construct was generated by the same method except that the amplicon was inserted after the *CTR4* promoter as described previously (6).

TABLE 3 Primers used in this study

Primer no.	Name	Sequence
	M13F	GTAAAACGACGGCCAG
	M13R	AACAGCTATGACCATG
Linlab2091	PHD1-Left Forward	CTACATGTGACACTTACCGTACTG
Linlab2092	PHD1-M13F complement+Left Reverse	CTGGCCGTCGTTTTACCTGGTAGATGAGCGCTATG
Linlab2093	PHD1-M13R complement+Right Forward	GTCATAGCTGTTTCCTGCCTATCCATACCCCTTATAATG
Linlab2094	PHD1-Right Reverse	AAGAATTGGAGGATTTACAAAG
Linlab2095	PHD1-Far left forward	TCGTCTCGAGAGGTAGTTGTC
Linlab2096	BYE1-Left Forward	ACATGCAGCTTTGTGATACG
Linlab2097	BYE1-M13F complement+Left Reverse	CTGGCCGTCGTTTTACAAGCTGTGTCTATCCCGC
Linlab2098	BYE1-M13R complement+Right Forward	GTCATAGCTGTTTCCTGGTATTGTTGCACGTGTTCAGTC
Linlab2099	BYE1-Right Reverse	AGCGCTGTTATTTCTTATCG
Linlab2100	BYE1-Far left forward	ATGCGACTCCACCACTACTAG
Linlab2288	BYE1-Left-forward-nested	CATGGCTTTGTTGCTTCAC
Linlab2101	PHD3-Left Forward	CACGAAAGTATCTTCATTCATTG
Linlab2102	PHD3-M13F complement+Left Reverse	CTGGCCGTCGTTTTACTGTAGGGCGAATTATATGG
Linlab2103	PHD3-M13R complement+Right Forward	GTCATAGCTGTTTCCTGTACTATCGTTACTGGCACATAC
Linlab2104	PHD3-Right Reverse	GAAACTCACTGCCGTAGAGG
Linlab2105	PHD3-Far left forward	GCTACCTCTTTGTCTACTACTGC
Linlab2106	PHD4-Left Forward	CCTATCGATGGAGTAGAGCC
Linlab2107	PHD4-M13F complement+Left Reverse	CTGGCCGTCGTTTTACATTCATGCCCTCGGAGC
Linlab2108	PHD4-M13R complement+Right Forward	GTCATAGCTGTTTCCTGATCCTGCCTTTCTCAATGC
Linlab2109	PHD4-Right Reverse	CATCCATCACACTGCATACTC
Linlab2110	PHD4-Far left forward	GCATCCAGGACAATTACATC
Linlab2225	PHD4-Right reverse2	CGCCTTTCATGACTCTCG
Linlab2289	PHD4-Left-forward-nested	TGTTCAGCCCTTCTCGTG
Linlab2160	PHD5-Left Forward	GGACGAGAGAGAGGACGAG
Linlab2161	PHD5-M13F complement+Left Reverse	CTGGCCGTCGTTTTACAGATGCACCGATGAGCG
Linlab2162	PHD5-M13R complement+Right Forward	GTCATAGCTGTTTCCTGCCATCGGCGTTTGACTG
Linlab2163	PHD5-Right Reverse	ATCCGAGCTGTCGTTGG
Linlab2164	PHD5-Far left forward	CCATCACCTCCGAGCT
Linlab2165	PHD6-Left Forward	AGCAACGCTGGATCTGG
Linlab2166	PHD6-M13F complement+Left Reverse	CTGGCCGTCGTTTTACATACAGCGATGGAAAGTGG
Linlab2167	PHD6-M13R complement+Right Forward	GTCATAGCTGTTTCCTGGTGCATAGGCATATACTTGG
Linlab2168	PHD6-Right Reverse	GGTACCGCCTGCACAAG
Linlab2169	PHD6-Far left forward	TGGAGGTCCTCGAACTCTG
Linlab2348	PHD6-Left Forward-nested	GGCGACAACAGTTGCATAG
Linlab2349	PHD6-Right reverse-nested	TCAGCAGACTCAATCAGCG
Linlab2170	PHD7-Left Forward	AAACGGTATTGATCTTCGC
Linlab2171	PHD7-M13F complement+Left Reverse	CTGGCCGTCGTTTTACACTGATGCGATGTTATGCC
Linlab2172	PHD7-M13R complement+Right Forward	GTCATAGCTGTTTCCTGCGTTCACCGAACTGTACG
Linlab2173	PHD7-Right Reverse	CTGTTGTTGCCAACCCTG
Linlab2174	PHD7-Far left forward	AGAGCCGCTGAGTCCTTC
Linlab2175	PHD8-Left Forward	CGGTCATGGCGTAGAGTC
Linlab2176	PHD8-M13F complement+Left Reverse	CTGGCCGTCGTTTTACAAGACAAGGGCAAAGCG
Linlab2177	PHD8-M13R complement+Right Forward	GTCATAGCTGTTTCCTGGCATGTGCATCTCCTCTCC
Linlab2178	PHD8-Right Reverse	CCCAGAGCCATCTAGCG
Linlab2179	PHD8-Far left forward	AGGCGACTTTCGTGATTG
Linlab2356	PHD9-Left forward-nested	GGCTGCGAAGGACAAAG
Linlab2357	PHD9-Right reverse-nested	TGGCTTCCTGTCACTTGC
Linlab2220	PHD9-Left Forward	CACGAGCACTTGGATGG
Linlab2221	PHD9-M13F complement+Left Reverse	CTGGCCGTCGTTTTACATTGACAACAGGTGGATGC
Linlab2222	PHD9-M13R complement+Right Forward	GTCATAGCTGTTTCCTGCCTCCAGATCCGAGATTG
Linlab2223	PHD9-Right Reverse	AGTTCACTGGGGTGTTGC
Linlab2224	PHD9-Far left forward	GCGAGGAATTTGAACCAG
Linlab2190	PHD11-Left Forward	CATCAAACTCTGCCACAGG
Linlab2191	PHD11-M13F complement+Left Reverse	CTGGCCGTCGTTTTACCGTGTCTCATGCATGGAG
Linlab2192	PHD11-M13R complement+Right Forward	GTCATAGCTGTTTCCTGCAAGTTTCGGGCTTTGG
Linlab2193	PHD11-Right Reverse	GTGGACCGAGGCGAAAG
Linlab2194	PHD11-Far left forward	GGCCGTGAAGCGTGTAG
Linlab2195	SET302-Left Forward	GGTCCGACATTTTCCAGG
Linlab2196	SET302-M13F complement+Left Reverse	CTGGCCGTCGTTTTACATCTACAAGCGGGTCAGG
Linlab2197	SET302-M13R complement+Right Forward	GTCATAGCTGTTTCCTGGCGTTACCGTTGTTGTCC
Linlab2198	SET302-Right Reverse	CCCCTTTTCGCTTTTGC
Linlab2199	SET302-Far left forward	AAGCGTTGGGATCCCAG
Linlab2350	SET302-Left forward-nested	CTCGCTTTCGGGATGAG
Linlab2351	SET302-Right reverse-nested	CAACGGCTTAACCCTGTC

(Continued on next page)

TABLE 3 (Continued)

Primer no.	Name	Sequence
Linlab2200	RUM1-Left Forward	GCCACAACTCGTCCGTG
Linlab2201	RUM1-M13F complement+Left Reverse	CTGGCCGTCGTTTTACAAAGGGAGTGCGTGCTG
Linlab2202	RUM1-M13R complement+Right Forward	GTCATAGCTGTTTCCTGCCTTCCAGATTCGTGAGC
Linlab2203	RUM1-Right Reverse	GAGCTGCTCGATGTACCAC
Linlab2204	RUM1-Far left forward	CGTCACCATCATTTCCG
Linlab2205	ZNF1-Left Forward	AACTCCTGGGCTCAACG
Linlab2206	ZNF1-M13F complement+Left Reverse	CTGGCCGTCGTTTTACTTTGCACAGGGTGACCAG
Linlab2207	ZNF1-M13R complement+Right Forward	GTCATAGCTGTTTCCTGATTCCGGCTGATGCTTC
Linlab2208	ZNF1-Right Reverse	CCAAGCTTGGCAATTCG
Linlab2209	ZNF1-Far left forward	GCAAGCGTTGGCTCAAC
Linlab2210	PHD15-Left Forward	TGTGAAGCCGAGGGACC
Linlab2211	PHD15-M13F complement+Left Reverse	CTGGCCGTCGTTTTACAGATGGATGAGTGGCGG
Linlab2212	PHD15-M13R complement+Right Forward	GTCATAGCTGTTTCCTGGCGAGATGGTTGCTTTTG
Linlab2213	PHD15-Right Reverse	TCCAACCTCCAACACCAC
Linlab2214	PHD15-Far left forward	GCTTCCGGGGATAAACC
Linlab2352	PHD15-Left forward-nested	TGGCTAGAGGAATGGCTG
Linlab2353	PHD15-Right reverse-nested	TGTGTTTTGCGGTGTTGAG
Linlab2354	PHD16-Left forward-nested	CACCGAGTACAGCTGCAAC
Linlab2355	PHD16-Right reverse-nested	GGCGTTCAGACTCCTTTG
Linlab2176	PHD8-M13F complement+Left Reverse	CTGGCCGTCGTTTTACAAGACAAGGGCAAAGCG
Linlab2177	PHD8-M13R complement+Right Forward	GTCATAGCTGTTTCCTGGCATGTGCATCTCCTCTCC
Linlab2178	PHD8-Right Reverse	CCCAGAGCCATCTAGCG
Linlab2179	PHD8-Far left forward	AGGCGACTTTCGTGATTG
Linlab2356	PHD9-Left forward-nested	GGCTGCGAAGGACAAAG
Linlab2357	PHD9-Right reverse-nested	TGGCTTCCTGTCACTTGC
Linlab2220	PHD9-Left Forward	CACGAGCACTTGGATGG
Linlab2221	PHD9-M13F complement+Left Reverse	CTGGCCGTCGTTTTACATTGACAACAGGTGGATGC
Linlab2222	PHD9-M13R complement+Right Forward	GTCATAGCTGTTTCCTGCCTCCAGATCCGAGATTG
Linlab2223	PHD9-Right Reverse	AGTTCACTGGGGTGTTGC
Linlab2224	PHD9-Far left forward	GCGAGGAATTTGAACCAG
Linlab2190	PHD11-Left Forward	CATCAAACTCTGCCACAGG
Linlab2191	PHD11-M13F complement+Left Reverse	CTGGCCGTCGTTTTACCGTGTCTCATGCATGGAG
Linlab2192	PHD11-M13R complement+Right Forward	GTCATAGCTGTTTCCTGCAAGTTTCGGGCTTTGG
Linlab2193	PHD11-Right Reverse	GTGGACCGAGGCGAAAG
Linlab2194	PHD11-Far left forward	GGCCGTGAAGCGTGTAG
Linlab2195	SET302-Left Forward	GGTCCGACATTTTCCAGG
Linlab2196	SET302-M13F complement+Left Reverse	CTGGCCGTCGTTTTACATCTACAAGCGGGTCAGG
Linlab2197	SET302-M13R complement+Right Forward	GTCATAGCTGTTTCCTGGCGTTACCGTTGTTGTCC
Linlab2198	SET302-Right Reverse	CCCCTTTTCGCTTTTGC
Linlab2199	SET302-Far left forward	AAGCGTTGGGATCCCAG
Linlab2350	SET302-Left forward-nested	CTCGCTTTCGGGATGAG
Linlab2351	SET302-Right reverse-nested	CAACGGCTTAACCCTGTC
Linlab2200	RUM1-Left Forward	GCCACAACTCGTCCGTG
Linlab2201	RUM1-M13F complement+Left Reverse	CTGGCCGTCGTTTTACAAAGGGAGTGCGTGCTG
Linlab2202	RUM1-M13R complement+Right Forward	GTCATAGCTGTTTCCTGCCTTCCAGATTCGTGAGC
Linlab2203	RUM1-Right Reverse	GAGCTGCTCGATGTACCAC
Linlab2204	RUM1-Far left forward	CGTCACCATCATTTCCG
Linlab2205	ZNF1-Left Forward	AACTCCTGGGCTCAACG
Linlab2206	ZNF1-M13F complement+Left Reverse	CTGGCCGTCGTTTTACTTTGCACAGGGTGACCAG
Linlab2208	ZNF1-Right Reverse	CCAAGCTTGGCAATTCG
Linlab2207	ZNF1-M13R complement+Right Forward	GTCATAGCTGTTTCCTGATTCCGGCTGATGCTTC
Linlab2209	ZNF1-Far left forward	GCAAGCGTTGGCTCAAC
Linlab2210	PHD15-Left Forward	TGTGAAGCCGAGGGACC
Linlab2211	PHD15-M13F complement+Left Reverse	CTGGCCGTCGTTTTACAGATGGATGAGTGGCGG
Linlab2212	PHD15-M13R complement+Right Forward	GTCATAGCTGTTTCCTGGCGAGATGGTTGCTTTTG
Linlab2213	PHD15-Right Reverse	TCCAACCTCCAACACCAC
Linlab2214	PHD15-Far left forward	GCTTCCGGGGATAAACC
Linlab2352	PHD15-Left forward-nested	TGGCTAGAGGAATGGCTG
Linlab2353	PHD15-Right reverse-nested	TGTGTTTTGCGGTGTTGAG
Linlab2354	PHD16-Left forward-nested	CACCGAGTACAGCTGCAAC
Linlab2355	PHD16-Right reverse-nested	GGCGTTCAGACTCCTTTG
Linlab2215	PHD16-Left Forward	CGATGCTGATTTACCCG
Linlab2216	PHD16-M13F complement+Left Reverse	CTGGCCGTCGTTTTACTGGATGAAGAGTTGCTCG
Linlab2217	PHD16-M13Rcomplement+Right Forward	GTCATAGCTGTTTCCTGCGGGATATCGGGTGTTC
Linlab2218	PHD16-Right Reverse	AGCCTCGGACGATCCTG
Linlab2219	PHD16-Far left forward	GTCTTGGAAGCAACCTCG

(Continued on next page)

TABLE 3 (Continued)

Primer no.	Name	Sequence
Linlab2669	Fse1+PHD11 Left Forward	TGATCTGGCCGGCCGACAGAATCAAACTCTCCATGC
Linlab2724	Asisi+PHD11 Right Reverse	ATATGCGATCGCAACATCATAGTCAATATACTCCTCATC
Linlab3279	Pac1+PHD11Right Reverse	GTTTAATTAATCAAACATCATAGTCAATATACTCC
Linlab2828	FseI+BYE1-LeftForward	TGATCTGGCCGGCCATGGCAGGTCCAGTCATC
Linlab3219	PacI+BYE1-Right Reverse	GTTTAATTAACTATTCCTCCTCCTTTTCTTC
Linlab2901	Fse1+SET302-Left Forward	TGATCTGGCCGGCCAAATGGACACCATCAACC
Linlab3220	PacI+SET302-Right Reverse	GTTTAATTAATTATCCACCTCTCCCACG
Linlab2903	Fse1+RUM1+Left Forward	TGATCTGGCCGGCCAATGCTGCCATCAAGCC
Linlab3137	PacI+RUM1+Right Reverse	GTTTAATTAATTATTGGTTCTCCATAGTAACATC
Linlab2949	Fse1+ZNF1+Left Forward	TGATCTGGCCGGCCATGTGTATGTTTCACTACCTTG
Linlab3138	PacI+ZNF1+Right Reverse	GTTTAATTAACTAATTTTGGTTCTTAAAC
Linlab2405	PHD1-RT-left forward	GCAAGGTGGAAGAAAACTG
Linlab2406	PHD1-RT-right reverse	CGTTATCACAGCCAATCATC
Linlab2787	PHD2-RT-left forward	CCTCGATGGCCTAGTCTAC
Linlab2788	PHD2-RT-right reverse	GAACTCGACCGGATACTACTC
Linlab2407	PHD3-RT-left forward	GTATGCCGAGATGGAGATG
Linlab2408	PHD3-RT-right reverse	TCTTTCGCCTCTCAATACAC
Linlab2789	PHD4-RT-left forward	AGAAAGGGAGCTTTTCGAG
Linlab2790	PHD4-RT-right reverse	CAGCGTCATAAGTTACCAATC
Linlab2791	PHD5-RT-left forward	CTGAAGCTGCCGTCTCTG
Linlab2792	PHD5-RT-right reverse	CTTCTTGCCTGACCCTTG
Linlab2793	PHD6-RT-left forward	CAGAATCGTCAGCAAGAGC
Linlab2794	PHD6-RT-right reverse	CGTTTCCATCCTCCATTG
Linlab2795	PHD7-RT-left forward	GATGCGCAAGAGGTCGT
Linlab2796	PHD7-RT-right reverse	TGTACGTGAGTGAATTTGAGTG
Linlab2629	PHD8-RT-left forward	TGGGAAGCTAGCCTGATC
Linlab2630	PHD8-RT-right-reverse	ATTCTCCTGCAGGCTTTC
Linlab2805	PHD9-RT-left forward	CACTGCTAGATACCCACACC
Linlab2806	PHD9-RT-right reverse	CTGCTGACGAGTGTCTTGC
Linlab2409	PHD11-RT-left forward	ACCTGTCAAGCCTGTTACC
Linlab2410	PHD11-RT-right reverse	CTCCTTCTGCATCGTCATC
Linlab2797	SET302 RT-left forward	CGTTTAGTGGTTCGGGAG
Linlab2798	SET302-RT-right reverse	TCCTCTTGACAATCCCAGAC
Linlab2799	RUM1-RT-left forward	GATTCACGTGAAGGCTCTG
Linlab2800	RUM1-RT-right reverse	CTCCATAGTAACATCTTCATCG
Linlab2821	ZNF1-RT-left forward	CGACGGAACCGTACAATC
Linlab2822	ZNF1-RT-Right reverse	GGCAGAGCAGTCGCAAT
Linlab2801	PHD15-RT-left forward	CACGTCAAATGTGTCAACATC
Linlab2802	PHD15-RT-right reverse	GTTGCCCTTGTCATTTGAG
Linlab2803	PHD16-RT-left forward	CAGGTAAGGGATTGGACG
Linlab2804	PHD16-RT-right reverse	CCTGAGTGATTTCCTCTACCT
Linlab1345	ZNF2-RT-Left Forward	GCCATCTTACCCCTACCATCTAC
Linlab1346	ZNF2-RT-Right Reverse	TGGACATAGGAACGCTGACAAT
Linlab329	TEF1-RT-Left forward	CGTCACCACTGAAGTCAAGT
Linlab330	TEF1-RT-Right Reverse	AGAAGCAGCCTCCATAGG
Linlab1341	CFL1-RT- Left forward	CTCCACTCTCGTGCTCCTGAA
Linlab1342	CFL1-RT-Right Reverse	AGTTCGCTTGCCTTTTCCTTT
Linlab1267	MFα-RT-Left Forward	ATCTTCACCACCTTCACTTCT
Linlab1268	MFα-RT-Right Reverse	CTAGGCGATGACACAAAGG

Construction of mCherry-fused Phd11. The *PHD11* ORF was digested with the restriction enzymes FseI and AsisI and then introduced into the plasmid pXL1-mCherry between the *GPD1* promoter and mCherry in frame (6). Linearized plasmids were introduced into the corresponding *phd11*Δ mutant by biolistic transformation. Stable transformants were examined for the presence of mCherry fluorescence and for the increased transcript level of *PHD11* by real-time PCR. To examine the subcellular localization of Phd11-mCherry, the strain was cultured in liquid YPD at 30°C overnight. The cells were fixed with formaldehyde and stained or not with DAPI as described previously (42). Images were acquired using a Zeiss Imager M2 with an Axiocam 506 camera with Zen 11 software (Carl Zeiss Microscopy). The mCherry signal was visualized using the FL filter set 43 HE Cy3 (Carl Zeiss Microscopy).

Mating and isolation of recombinant progeny. For the self-filamentation assay, the strains were first cultured in YPD liquid medium overnight. Cells were collected, washed with water, and resuspended to achieve a cell density (optical density at 600 nm [OD_{600}]) of 3.0. Then, 5 μl of the cell suspension was spotted onto V8 juice agar (5% V8 juice, 0.5 g/liter KH_2PO_4, 4% agar, pH 7), and the cells were incubated at 22°C in the dark for the indicated time before images of the colonies were taken. For overexpression strains driven by the copper-inducible promoter, cells were maintained and cultured in YPD medium plus 200 μM bovine calf serum (BCS), washed, and resuspended

to achieve a cell density (OD_{600}) of 3.0. The cells were inoculated onto V8 or V8 plus 50 μM BCS agar and then incubated as described above. The filamentation and the fruiting structure produced by unisexual development of each mutant were examined under an Olympus CX41 microscope with a 20× objective after 2 weeks.

For bisexual mating, the α and **a** mating pair in equal cell numbers were mixed and cocultured on V8 juice agar at 22°C in the dark. Bisexual mating was monitored by examining the production of mating hyphae and spores microscopically. Spores were isolated by microdissection. The genotype of the gene of interest (deletion or overexpression) of the dissected progeny was confirmed by diagnostic PCR and by the presence or absence of the selective drug marker. The mating type of the dissected progeny was determined by their ability to mate with reference strains JEC21α and JEC20**a**, as described previously (12). Mendelian segregation of the mating type and the drug marker (gene deletion) was confirmed prior to their use in the subsequent phenotypical analyses.

Cell fusion assays. Cell fusion assays were performed as previously reported (6, 11). Strains were first cultured on YPD solid medium for 2 days. Cells were collected and resuspended in water. The cell concentration was measured by spectrophotometer, and the OD_{600} was adjusted to 3.00. Equal amounts of mating partner cells were mixed, and 5 μl of the mixture was dropped onto V8 juice agar medium (pH 7.0). The *bye1*Δ α mutant and the control wild-type XL280α strain with the G418 resistance marker (XL1348) were cocultured with the wild-type mating partner JEC20**a** marked with NAT^r (XL1142). Similarly, the *phd11*Δα, *set302*Δα, *rum1*αΔ, *znf1*αΔ, and wild-type XL280α strains with the NAT resistance marker (XL1109) were cocultured with the wild-type mating partner JEC20**a** marked with $G418^r$ (XL1411). XL942α (*mat2*::NAT^r) and XL574α (*znf2*::NAT^r) cocultured with JEC20**a** marked with $G418^r$ (XL1411) were used as the negative and positive controls. After 16 h of incubation at 22°C in the dark, colonies were cut off from the plates and suspended in 1 ml water. After 45 s of vortexing, the cells were plated on YPD selective medium with NAT and G418 drugs and examined for growth of the fusion products after 2 days of incubation.

***In vitro* phenotypic assays.** *In vitro* phenotypic assays were performed as reported previously (47, 48). Briefly, cryptococcal strains were cultured in YPD liquid medium at 30°C with shaking overnight and then washed twice with sterile water. All strains were adjusted to the same cell optical density (OD_{600} = 3) and then 10× serially diluted. Then, the serial dilutions of each strain (4 μl) were spotted onto various agar media for phenotypical analyses as described previously (49). To test melanin production, yeast cells were spotted onto L-DOPA medium and incubated at 30°C and 37°C. To characterize the production of capsule, cells were spotted onto RPMI medium and incubated at 37°C with or without 5% CO_2. Capsule was visualized microscopically as a halo surrounding the yeast cell by India ink exclusion. For the temperature sensitivity test, yeast cells were spotted onto YPD medium and incubated at 30°C, 37°C, or 39°C. For the test for susceptibility to UV radiation, cells of different strains at the same concentration were spotted onto yeast nitrogen base (YNB) agar medium and air dried. Then, the cells were exposed to 300 J/m^2 UV radiation for 0 s, 3 s, and 5 s in a UV cross-linker. The treated cells were incubated at 30°C for an additional 2 to 3 days before images of the colonies were taken.

Growth curve and generation time. The *phd3*Δ mutant and wild-type cells were inoculated in YPD liquid medium at the same cell density. Cultures were incubated at 30°C with shaking at 225 rpm. Measurements at OD_{600} with a spectrophotometer (SmartSpec Plus; Bio-Rad) were taken at 1-h intervals. The experiment was carried out with three independent biological replicates. Data analysis was performed with GraphPad software.

RNA purification and quantitative PCR (qPCR) analyses. Strains were cultured in YPD liquid medium at 30°C overnight and washed twice with distilled water. To examine the transcript levels during bisexual mating, equal numbers of cells from the wild-type mating pair XL280α and XL280**a** (OD_{600} = 1) were mixed and spotted onto V8 juice agar medium. The cells were incubated at 22°C in the dark. Cells from the coculture were collected from the V8 medium at 0 h, 3 h, 10 h, 24 h, 48 h, and 72 h after incubation. The 0-h time point was used as a reference. Total RNA samples were collected from three biologically independent replicates for each time point using the PureLink RNA minikit (Life Technology) according to the manufacturer's instructions. Synthesis of the first-strand cDNA was carried out using a Superscript III cDNA synthesis kit (Invitrogen). Real-time PCR was performed using SYBR Fast qPCR master mix (KAPA Biosystems, Wilmington, MA) on a realplex^2 instrument (Eppendorf). The housekeeping gene *TEF1* was used to normalize the gene transcript level as described previously (32). To examine the transcript levels of the genes of interest during unisexual mating, the wild-type XL280α, the gene deletion mutants, and the gene overexpression strains in the mating type α background (OD = 1) were spotted onto V8 juice agar medium. Cells were collected at 0 h, 16 h, 24 h, and 48 h postinoculation. Overnight liquid culture of XL280α in YPD medium was used as a reference. The extraction of total RNAs and synthesis of the first-strand cDNA were carried out using the same procedures described above. The relative levels of transcripts were quantified by real-time PCR as described previously (6, 28). Primers for real-time PCR are included in Table 3.

SUPPLEMENTAL MATERIAL

Supplemental material for this article may be found at https://doi.org/10.1128/AEM.01732-17.

SUPPLEMENTAL FILE 1, PDF file, 0.4 MB.

ACKNOWLEDGMENTS

We thank Lin laboratory members for their helpful suggestions.

This work was supported by the National Institutes of Health (http://www.niaid.nih.gov) (R01AI097599 to X.L.) and by the China Scholarship Council (201306580029 to Y.M.). X.L. holds an Investigator Award in the Pathogenesis of Infectious Disease from the Burroughs Wellcome Fund (http://www.bwfund.org/) (1012445 to X.L.). The funders had no role in study design, data collection and interpretation, or the decision to submit the work for publication.

Y.M., Y.F., and X.L. conceived and designed the experiments; Y.M. and Y.F. performed the experiments; Y.M., Y.F., and X.L. analyzed the data; X.L. contributed reagents/materials/analysis tools; Y.M., Y.F., and X.L. wrote the paper. Y.M., Y.F., W.L., and X.L. edited the paper.

REFERENCES

1. Park BJ, Wannemuehler KA, Marston BJ, Govender N, Pappas PG, Chiller TM. 2009. Estimation of the current global burden of cryptococcal meningitis among persons living with HIV/AIDS. AIDS 23:525–530. https://doi.org/10.1097/QAD.0b013e328322ffac.
2. Rajasingham R, Smith RM, Park BJ, Jarvis JN, Govender NP, Chiller TM, Denning DW, Loyse A, Boulware DR. 2017. Global burden of disease of HIV-associated cryptococcal meningitis: an updated analysis. Lancet Infect Dis 17:873–881. https://doi.org/10.1016/S1473-3099(17)30243-8.
3. Wang L, Lin X. 2012. Morphogenesis in fungal pathogenicity: shape, size, and surface. PLoS Pathog 8:e1003027. https://doi.org/10.1371/journal.ppat.1003027.
4. Sil A, Andrianopoulos A. 2014. Thermally dimorphic human fungal pathogens-polyphyletic pathogens with a convergent pathogenicity trait. Cold Spring Harb Perspect Med 5:a019794. https://doi.org/10.1101/cshperspect.a019794.
5. Zhai B, Wozniak KL, Masso-Silva J, Upadhyay S, Hole C, Rivera A, Wormley FL, Lin X. 2015. Development of protective inflammation and cell-mediated immunity against *Cryptococcus neoformans* after exposure to hyphal mutants. mBio 6:e01433-15. https://doi.org/10.1128/mBio.01433-15.
6. Wang L, Zhai B, Lin X. 2012. The link between morphotype transition and virulence in *Cryptococcus neoformans*. PLoS Pathog 8:e1002765. https://doi.org/10.1371/journal.ppat.1002765.
7. Kwon-Chung KJ. 1976. Morphogenesis of Filobasidiella neoformans, the sexual state of *Cryptococcus neoformans*. Mycologia 68:821–833. https://doi.org/10.2307/3758800.
8. Heitman J. 2010. Evolution of eukaryotic microbial pathogens via covert sexual reproduction. Cell Host Microbe 8:86–99. https://doi.org/10.1016/j.chom.2010.06.011.
9. Idnurm A, Bahn YS, Nielsen K, Lin X, Fraser JA, Heitman J. 2005. Deciphering the model pathogenic fungus *Cryptococcus neoformans*. Nat Rev Microbiol 3:753–764. https://doi.org/10.1038/nrmicro1245.
10. Davidson RC, Nichols CB, Cox GM, Perfect JR, Heitman J. 2003. A MAP kinase cascade composed of cell type specific and non-specific elements controls mating and differentiation of the fungal pathogen *Cryptococcus neoformans*. Mol Microbiol 49:469–485. https://doi.org/10.1046/j.1365-2958.2003.03563.x.
11. Lin X, Jackson JC, Feretzaki M, Xue C, Heitman J. 2010. Transcription factors Mat2 and Znf2 operate cellular circuits orchestrating opposite- and same-sex mating in *Cryptococcus neoformans*. PLoS Genet 6:e1000953. https://doi.org/10.1371/journal.pgen.1000953.
12. Zhai B, Zhu P, Foyle D, Upadhyay S, Idnurm A, Lin X. 2013. Congenic strains of the filamentous form of *Cryptococcus neoformans* for studies of fungal morphogenesis and virulence. Infect Immun 81:2626–2637. https://doi.org/10.1128/IAI.00259-13.
13. Lengeler KB, Fox DS, Fraser JA, Allen A, Forrester K, Dietrich FS, Heitman J. 2002. Mating-type locus of *Cryptococcus neoformans*: a step in the evolution of sex chromosomes. Eukaryot Cell 1:704–718. https://doi.org/10.1128/EC.1.5.704-718.2002.
14. Shen W-C, Davidson RC, Cox GM, Heitman J. 2002. Pheromones stimulate mating and differentiation via paracrine and autocrine signaling in *Cryptococcus neoformans*. Eukaryot Cell 1:366–377. https://doi.org/10.1128/EC.1.3.366-377.2002.
15. Fraser JA, Diezmann S, Subaran RL, Allen A, Lengeler KB, Dietrich FS, Heitman J. 2004. Convergent evolution of chromosomal sex-determining regions in the animal and fungal kingdoms. PLoS Biol 2:e384. https://doi.org/10.1371/journal.pbio.0020384.
16. Chung S, Karos M, Chang YC, Lukszo J, Wickes BL, Kwon-Chung KJ. 2002. Molecular analysis of CPRalpha, a MATalpha-specific pheromone receptor gene of *Cryptococcus neoformans*. Eukaryot Cell 1:432–439. https://doi.org/10.1128/EC.1.3.432-439.2002.
17. Wang L, Lin X. 2011. Mechanisms of unisexual mating in *Cryptococcus neoformans*. Fungal Genet Biol 48:651–660. https://doi.org/10.1016/j.fgb.2011.02.001.
18. Hull CM, Davidson RC, Heitman J. 2002. Cell identity and sexual development in *Cryptococcus neoformans* are controlled by the mating-type-specific homeodomain protein Sxi1α. Genes Dev 16:3046–3060. https://doi.org/10.1101/gad.1041402.
19. Schindler U, Beckmann H, Cashmore AR. 1993. HAT3.1, a novel Arabidopsis homeodomain protein containing a conserved cysteine-rich region. Plant J 4:137–150. https://doi.org/10.1046/j.1365-313X.1993.04010137.x.
20. Sanchez R, Zhou M-M. 2011. The PHD finger: a versatile epigenome reader. Trends Biochem Sci 36:364–372.
21. Kim J, Lee JE, Lee JS. 2015. Histone deacetylase-mediated morphological transition in *Candida albicans*. J Microbiol 53:805–811. https://doi.org/10.1007/s12275-015-5488-3.
22. Dreveny I, Deeves SE, Fulton J, Yue B, Messmer M, Bhattacharya A, Collins HM, Heery DM. 2014. The double PHD finger domain of MOZ/MYST3 induces α-helical structure of the histone H3 tail to facilitate acetylation and methylation sampling and modification. Nucleic Acids Res 42:822–835. https://doi.org/10.1093/nar/gkt931.
23. Pijnappel WW, Schaft D, Roguev A, Shevchenko A, Tekotte H, Wilm M, Rigaut G, Seraphin B, Aasland R, Stewart AF. 2001. The *S. cerevisiae* SET3 complex includes two histone deacetylases, Hos2 and Hst1, and is a meiotic-specific repressor of the sporulation gene program. Genes Dev 15:2991–3004. https://doi.org/10.1101/gad.207401.
24. Hnisz D, Majer O, Frohner IE, Komnenovic V, Kuchler K. 2010. The Set3/Hos2 histone deacetylase complex attenuates cAMP/PKA signaling to regulate morphogenesis and virulence of *Candida albicans*. PLoS Pathog 6:e1000889. https://doi.org/10.1371/journal.ppat.1000889.
25. Lin X, Huang JC, Mitchell TG, Heitman J. 2006. Virulence attributes and hyphal growth of *C. neoformans* are quantitative traits and the *MAT*alpha allele enhances filamentation. PLoS Genet 2:e187. https://doi.org/10.1371/journal.pgen.0020187.
26. Feretzaki M., Hardison SE., Wormley FL., Jr., Heitman J. 2014. *Cryptococcus neoformans* hyperfilamentous strain is hypervirulent in a murine model of cryptococcal meningoencephalitis. PLoS One 9:e104432. https://doi.org/10.1371/journal.pone.0104432.
27. Ni M, Feretzaki M, Li W, Floyd-Averette A, Mieczkowski P, Dietrich FS, Heitman J. 2013. Unisexual and heterosexual meiotic reproduction generate aneuploidy and phenotypic diversity *de novo* in the yeast *Cryptococcus neoformans*. PLoS Biol 11:e1001653. https://doi.org/10.1371/journal.pbio.1001653.
28. Wang L, Tian X, Gyawali R, Upadhyay S, Foyle D, Wang G, Cai JJ, Lin X. 2014. Morphotype transition and sexual reproduction are genetically associated in a ubiquitous environmental pathogen. PLoS Pathog 10:e1004185. https://doi.org/10.1371/journal.ppat.1004185.
29. Gyawali R, Zhao Y, Lin J, Fan Y, Xu X, Upadhyay S, Lin X. 2017. Pheromone

independent unisexual development in *Cryptococcus neoformans*. PLoS Genet 13:e1006772. https://doi.org/10.1371/journal.pgen.1006772.
30. Erke KH. 1976. Light microscopy of basidia, basidiospores, and nuclei in spores and hyphae of *Filobasidiella neoformans* (*Cryptococcus neoformans*). J Bacteriol 128:445–455.
31. Kent CR, Ortiz-Bermudez P, Giles SS, Hull CM. 2008. Formulation of a defined V8 medium for induction of sexual development of *Cryptococcus neoformans*. Appl Environ Microbiol 74:6248–6253. https://doi.org/10.1128/AEM.00970-08.
32. Chacko N, Zhao Y, Yang E, Wang L, Cai JJ, Lin X. 2015. The lncRNA RZE1 controls Cryptococcal morphological transition. PLoS Genet 11:e1005692. https://doi.org/10.1371/journal.pgen.1005692.
33. Bergman A, Casadevall A. 2010. Mammalian endothermy optimally restricts fungi and metabolic costs. mBio 1:e00212-10. https://doi.org/10.1128/mBio.00212-10.
34. Chen Y-L, Lehman VN, Lewit Y, Averette AF, Heitman J. 2013. Calcineurin governs thermotolerance and virulence of *Cryptococcus gattii*. G3 (Bethesda) 3:527–539. https://doi.org/10.1534/g3.112.004242.
35. Walton FJ, Heitman J, Idnurm A. 2006. Conserved elements of the RAM signaling pathway establish cell polarity in the basidiomycete *Cryptococcus neoformans* in a divergent fashion from other fungi. Mol Biol Cell 17:3768–3780. https://doi.org/10.1091/mbc.E06-02-0125.
36. Magditch DA, Liu T-B, Xue C, Idnurm A. 2012. DNA mutations mediate microevolution between host-adapted forms of the pathogenic fungus *Cryptococcus neoformans*. PLoS Pathog 8:e1002936. https://doi.org/10.1371/journal.ppat.1002936.
37. Lin J, Idnurm A, Lin X. 2015. Morphology and its underlying genetic regulation impact the interaction between *Cryptococcus neoformans* and its hosts. Med Mycol 53:493–504. https://doi.org/10.1093/mmy/myv012.
38. Lin X. 2009. *Cryptococcus neoformans*: morphogenesis, infection, and evolution. Infect Genet Evol 9:401–416. https://doi.org/10.1016/j.meegid.2009.01.013.
39. Musselman CA, Kutateladze TG. 2009. PHD fingers: epigenetic effectors and potential drug targets. Mol Interv 9:314–323. https://doi.org/10.1124/mi.9.6.7.
40. Bienz M. 2006. The PHD finger, a nuclear protein-interaction domain. Trends Biochem Sci 31:35–40. https://doi.org/10.1016/j.tibs.2005.11.001.
41. Kwon-Chung KJ. 1975. A new genus, *Filobasidiella*, the perfect state of *Cryptococcus neoformans*. Mycologia 67:1197–1200. https://doi.org/10.2307/3758842.
42. Lin X, Hull CM, Heitman J. 2005. Sexual reproduction between partners of the same mating type in *Cryptococcus neoformans*. Nature 434:1017–1021. https://doi.org/10.1038/nature03448.
43. Gyawali R, Upadhyay S, Way J, Lin X. 2017. A family of secretory proteins is associated with different morphotypes in *Cryptococcus neoformans*. Appl Environ Microbiol 83:e02967-16. https://doi.org/10.1128/AEM.02967-16.
44. Kim MS, Kim SY, Yoon JK, Lee YW, Bahn YS. 2009. An efficient gene-disruption method in *Cryptococcus neoformans* by double-joint PCR with NAT-split markers. Biochem Biophys Res Commun 390:983–988. https://doi.org/10.1016/j.bbrc.2009.10.089.
45. Toffaletti DL, Rude TH, Johnston SA, Durack DT, Perfect JR. 1993. Gene transfer in *Cryptococcus neoformans* by use of biolistic delivery of DNA. J Bacteriol 175:1405–1411. https://doi.org/10.1128/jb.175.5.1405-1411.1993.
46. Lin X, Chacko N, Wang L, Pavuluri Y. 2015. Generation of stable mutants and targeted gene deletion strains in *Cryptococcus neoformans* through electroporation. Med Mycol 53:225–234. https://doi.org/10.1093/mmy/myu083.
47. Lin X, Litvintseva AP, Nielsen K, Patel S, Floyd A, Mitchell TG, Heitman J. 2007. Alpha AD alpha hybrids of *Cryptococcus neoformans*: evidence of same-sex mating in nature and hybrid fitness. PLoS Genet 3:1975–1990. https://doi.org/10.1371/journal.pgen.0030186.
48. Lin X, Patel S, Litvintseva AP, Floyd A, Mitchell TG, Heitman J. 2009. Diploids in the *Cryptococcus neoformans* serotype A population homozygous for the α mating type originate via unisexual mating. PLoS Pathog 5:e1000283. https://doi.org/10.1371/journal.ppat.1000283.
49. Lin X, Nielsen K, Patel S, Heitman J. 2008. Impact of mating type, serotype, and ploidy on the virulence of *Cryptococcus neoformans*. Infect Immun 76:2923–2938. https://doi.org/10.1128/IAI.00168-08.
50. Walton FJ, Idnurm A, Heitman J. 2005. Novel gene functions required for melanization of the human pathogen *Cryptococcus neoformans*. Mol Microbiol 57:1381–1396. https://doi.org/10.1111/j.1365-2958.2005.04779.x.

AMERICAN SOCIETY FOR MICROBIOLOGY | Antimicrobial Agents and Chemotherapy®

PHARMACOLOGY

Combination of Amphotericin B and Terbinafine against Melanized Fungi Associated with Chromoblastomycosis

S. Deng,[a] W. Lei,[b] G. S. de Hoog,[b,c,d,e] L. Yang,[c] R. G. Vitale,[f] H. Rafati,[g] M. Seyedmousavi,[g] A. Tolooe,[g] H. van der Lee,[e] W. Liao,[b] P. E. Verweij,[e] S. Seyedmousavi[e,g,h]*

[a]Department of Medical Microbiology, People's Hospital of Suzhou National New & Hi-Tech Industrial Development Zone, Jiangsu, China

[b]Shanghai Institute of Medical Mycology, Department of Dermatology, Changzheng Hospital, Second Military Medical University, Shanghai, China

[c]Westerdijk Fungal Biodiversity Institute, Utrecht, The Netherlands

[d]Basic Pathology Department, Federal University of Paraná State, Curitiba, Paraná, Brazil

[e]Department of Medical Microbiology, Radboud University Medical Center, and Center of Expertise in Mycology Radboudumc/CWZ, Nijmegen, The Netherlands

[f]CONICET and Ramos Mejia Hospital, Parasitology Unit, Mycology Section, Buenos Aires, Argentina

[g]Center of Excellence for Infection Biology and Antimicrobial Pharmacology, Tehran, Iran

[h]Invasive Fungi Research Center, School of Medicine, Mazandaran University of Medical Sciences, Sari, Iran

ABSTRACT Our *in vitro* studies showed that a combination of amphotericin B and terbinafine had synergistic effects against the majority of melanized fungi associated with chromoblastomycosis (CBM) and similar infections, including those with *Cladophialophora carrionii*, *Cladophialophora arxii*, *Exophiala dermatitidis*, *Exophiala spinifera*, *Fonsecaea monophora*, *Fonsecaea nubica*, *Fonsecaea pedrosoi*, and *Phialophora verrucosa*. This drug combination could provide an option for the treatment of severe or unresponsive cases of CBM, particularly in cases due to species of *Fonsecaea* and *Cladophialophora*.

KEYWORDS combination therapy, amphotericin B, terbinafine, melanized fungi, chromoblastomycosis

Chromoblastomycosis (CBM) is a serious fungal skin disease associated with significant morbidity (1). The disease is characterized histologically by muriform cells that cause chronic inflammation of the skin and subcutaneous tissues (2, 3). The infection leads to excessive proliferation of host tissue, formation of cauliflower-like eruptions on the skin, or hyperkeratosis, or it may exhibit intermediate forms, depending on the type of interaction between host and fungal cells (4, 5). Because of chronicity, the CBM lesions may also undergo neoplastic transformation leading to skin cancer (6). The chronic nature of the infections seems to be due to inadequate innate recognition and subsequent failure to mount protective inflammatory responses (7).

The disease has worldwide distribution, mainly in tropical and subtropical climates (8). Species in humid climates, particularly members of the genus *Fonsecaea* (*F. pedrosoi*, *F. monophora*, and *F. nubica*), are prevalent agents of CBM (9). *Cladophialophora carrionii* is the predominant agent of the disease under arid desert-like climate conditions (10). Sporadic cases of CBM-like infections have also been reported for *Cladophialophora arxii* (11), *Exophiala dermatitidis* (12), *Exophiala spinifera* (13), *Phialophora verrucosa* (14), and *Veronaea botryose* (15), although attribution to this disease category has not been confirmed.

CBM is extremely difficult to treat due to its recalcitrant nature, and there is no consensus regarding the treatment of choice (16). Based on open clinical studies and expert opinions, itraconazole is the first-line recommended therapy for CBM (17),

Received 8 February 2018 **Returned for modification** 2 March 2018 **Accepted** 15 March 2018

Accepted manuscript posted online 26 March 2018

Citation Deng S, Lei W, de Hoog GS, Yang L, Vitale RG, Rafati H, Seyedmousavi M, Tolooe A, van der Lee H, Liao W, Verweij PE, Seyedmousavi S. 2018. Combination of amphotericin B and terbinafine against melanized fungi associated with chromoblastomycosis. Antimicrob Agents Chemother 62:e00270-18. https://doi.org/10.1128/AAC.00270-18.

Address correspondence to S. Seyedmousavi, Seyedmousavi@nih.gov.

* Present address: S. Seyedmousavi, Molecular Microbiology Section, Laboratory of Clinical Immunology and Microbiology, National Institute of Allergy and Infectious Diseases, National Institutes of Health, Bethesda, Maryland, USA.

S.D. and W.L. contributed equally as first author.

followed by terbinafine (18). However, infections by *F. pedrosoi* strains resistant to itraconazole have been reported (19). Cure rates with itraconazole and terbinafine monotherapy may range from 15 to 80%, which on average, is insufficient (20). When possible, the addition of physical therapeutic methods, such as laser and photodynamic therapy, is recommended (21, 22), which is still associated with rather low cure rates and high refractory rates.

Alternative therapeutic strategies employing newer antifungal agents and/or combination of drugs (23–26) might be promising to treat CBM more efficiently. In a recent study, we also demonstrated that amphotericin B in combination with flucytosine may have a role in the treatment of primary cerebral infections caused by other melanized fungi of the order *Chaetothyriales* (27). We therefore sought to investigate the *in vitro* antifungal activity of amphotericin B in combination with terbinafine against a collection of black fungi obtained from patients with CBM.

A collection of 46 isolates of melanized fungi associated with CBM or similar skin infections were studied, including *C. carrionii* ($n = 10$), *C. arxii* ($n = 1$), *Exophiala dermatitidis* ($n = 9$), *E. spinifera* ($n = 3$), *Fonsecaea monophora* ($n = 7$), *F. nubica* ($n = 5$), *F. pedrosoi* ($n = 5$), *Phialophora verrucosa* ($n = 3$), and *Veronaea botryosa* ($n = 3$). The identities of the organisms were confirmed by sequencing of the internal transcribed spacer regions of ribosomal DNA (rDNA), as described previously (28). All isolates were subcultured on malt extract agar (MEA) at 25°C. Conidial suspensions were harvested and suspended in normal saline containing 0.025% Tween 20. Supernatants were adjusted spectrophotometrically at 530-nm wavelengths to optical densities (ODs) that ranged from 0.15 to 0.17 (68 to 71% transmission) for all isolates, except *E. dermatitidis*, whose ODs ranged from 0.09 to 0.13 (80 to 83% transmission), as described previously (27).

Amphotericin B (Sigma-Aldrich, St. Louis, MO, USA) and terbinafine (Novartis, Arnhem, The Netherlands) were obtained as standard pure powders, and serial dilutions were prepared according to the Clinical and Laboratory Standards Institute (CLSI) broth microdilution guidelines (29). Antifungal susceptibility and drug interaction testing were performed by using the broth microdilution checkerboard (2-dimensional, 8-by-12) method (27). The final concentrations of the antifungal agents ranged from 0.125 to 8 μg/ml for amphotericin B and 0.008 to 8 μg/ml for terbinafine. To assess the nature of *in vitro* interactions between amphotericin B and terbinafine, the data obtained were analyzed using nonparametric approaches of the following two no (zero)-interaction theories: Loewe additivity, defined as the fractional inhibitory concentration (FIC), and the Bliss independence (BI) parameter, obtained from response surface analysis (30), as described previously (27). Drug interactions were defined as synergistic if the FIC index was <1, additive if the FIC index was 1, and antagonistic if the FIC index was >1 (31). The BI drug interactions were considered synergistic if ΔE was >0 (positive ΔE), indifferent if ΔE was 0, or antagonistic if ΔE was <0 (negative ΔE) (32). All experiments were performed in three independent replicates on different days. All data analyses were performed by using the software package GraphPad Prism version 5.0 for Windows (GraphPad Software, San Diego, CA, USA). A P value of ≤ 0.05 was considered significant (two-tailed).

The mean (range) MICs were 4.46 (0.125 to >8) μg/ml for amphotericin B across all isolates and 0.86 (0.16 to >8) for terbinafine (Table 1). For the amphotericin B and terbinafine combinations, the geometric mean FIC indices, in increasing order, were 0.41 for *F. monophora* ($\sum$FIC range, 0.25 to 0.5), 0.5 for *E. spinifera* ($\sum$FIC range, 0.25 to 1), 0.63 for *E. dermatitidis* ($\sum$FIC range, 0.25 to 1), 0.7 for *C. carrionii* ($\sum$FIC range, 0.5 to 1), 0.72 for *P. verrucosa* ($\sum$FIC range, 0.5 to 1), 0.76 for *F. nubica* ($\sum$FIC range, 0.25 to 1), 0.76 for *F. pedrosoi* ($\sum$FIC range, 0.5 to 1), and 1 for *C. arxii* ($n = 1$), which indicate synergy and additivity for these strains. However, antagonism was noted in *V. botryosa* isolates, with a mean FIC value of 1.4 ($\sum$FIC range, 1 to 2).

The Bliss independence drug interaction analysis for the amphotericin B and terbinafine combination resulted in a synergistic interaction for 71.74% (33/46) of the strains tested. The degree of synergy was the highest among the *C. carrionii* strains (sum ΔE,

TABLE 1 MIC, FIC indices, and Bliss independence results for the *in vitro* combination of AmB and TBF against melanized fungi associated with chromoblastomycosis

Strain no.	Fungal species	Strain	Source	Origin	MIC (μg/ml)[a]		FIC index	Bliss independence index
					TBF	AmB		
1	*Cladophialophora carrionii*	CBS 131844	Human, chromoblastomycosis	China	0.031	1	0.75	111.3
2		CBS 131854	Human, chromoblastomycosis	Madagascar	0.063	8	0.5	69.24
3		CBS 131833	Human, chromoblastomycosis	China	1	8	1	−4.48
4		CBS 131847	Human, chromoblastomycosis	China	0.031	4	0.5	410.73
5		CBS 160.54	Human, chromoblastomycosis	Australia	0.031	1	0.75	−8.29
6		CBS 859.96	Dry plant debris	Venezuela, arid zone west of Coro	0.016	1	0.75	−40.42
7		CBS 863.96	Dry plant debris	Venezuela, arid zone west of Coro	0.016	2	0.75	6.37
8		CBS 131736	Soil	Venezuela, arid zone west of Coro	0.031	4	0.5	75.15
9		CBS 860.96	Dry plant debris	Venezuela, arid zone west of Coro	0.016	4	0.75	893.89
10		CBS 861.96	Dry plant debris	Venezuela, arid zone west of Coro	0.125	8	1	143.51
11	*Cladophialophora arxii*	CBS 102461	Human, brain abscess	USA	0.5	4	1	90.2
12	*Exophiala dermatitidis*	CBS 120542	Human or animal, stool	Slovenia	0.5	4	0.5	138.26
13		CBS 120562	Human, keratitis	USA	0.5	0.25	1	151.7
14		CBS 120473	Human, brain	USA	0.25	0.5	1	−4,736
15		CBS 424.67	Human, chromoblastomycosis	Germany	0.5	0.125	1	−11.78
16		CBS 550.9	Human, sputum, cystic fibrosis	Germany	0.031	2	1	258.1
17		CBS 126590	Human, sputum, cystic fibrosis	The Netherlands	0.5	1	0.25	89.2
18		CBS 120550	Steam bath	Austria	0.5	2	0.5	133.05
19		CBS 120483	Flying fox's feces	Thailand	0.25	4	0.25	346.03
20		CBS 109138	Hall of sauna complex	The Netherlands	0.5	4	1	−43.35
21	*Exophiala spinifera*	CBS 899.68	Human, nasal granuloma	USA	2	2	1	62.94
22		CBS 269.28	Human, chromoblastomycosis	Unknown	0.5	8	0.5	64.9
23		CBS 194.61	Human, systemic mycosis	India	0.5	>8	0.25	450.11
24	*Fonsecaea monophora*	CBS 117236	Human, brain abscess	USA	0.5	8	0.5	305
25		CBS 269.37	Unknown, chromoblastomycosis	Unknown	0.25	8	0.5	209.7
26		CBS 117238	Unknown, brain	England	5	8	0.25	49.7
27		CBS 122742	Human, chromoblastomycosis	China	0.5	8	0.5	14.98
28		CBS 100430	Human, brain	Africa	0.5	8	0.5	311.02
29		CBS 102229	Decaying vegetable	Piraquara, Paraná, Brazil	0.5	4	0.5	27.6
30		CBS 289.93	Animal, lymph node, aspiration biopsy	The Netherlands	8	8	0.25	526.72
31	*Fonsecaea nubica*	CBS 277.29	Human, chromoblastomycosis	Brazil	1	4	1	154.1
32		CBS 444.62	Human, chromoblastomycosis	Suriname	0.5	8	1	−7.07
33		CBS 122733	Human, chromoblastomycosis	China	0.25	4	1	−69.4
34		CBS 269.64	Human, chromoblastomycosis	Cameroon	0.5	8	0.75	−79.6
35		CBS 125198	Human, chromoblastomycosis	China	0.25	8	0.25	−223.17
36		CBS 127264	Human, chromoblastomycosis	Mexico	1	4	1	−271.7
37	*Fonsecaea pedrosoi*	CBS 102247	Human, chromoblastomycosis	Paraná, Brazil	0.5	4	0.5	123.76
38		CBS 285.47	Human, chromoblastomycosis	Puerto Rico	0.5	4	0.5	298.9
39		CBS 122739	Human, chromoblastomycosis	Mexico	0.5	4	1	114.3
40		CBS 117910	Human, chromoblastomycosis	Venezuela	0.5	4	1	297.27
41		CBS 671.66	Soil	Venezuela	0.5	2	1	64.1
42	*Phialophora verrucosa*	CBS 120349	Plant	China	0.5	4	1	123.76
43		CBS 262.93	Exudate from right hand (human or animal)	Germany	0.016	0.5	0.5	52941
44		CBS 115.89	Disseminated (human or animal)	Libya	0.25	8	0.75	−47.99
45	*Veronaea botryosa*	CBS 122826	Railway tie treated with creosote for 20 years	Brazil	1	4	2	−271.7
46		CBS 121506	Cutaneous lesion, wrist	Japan	>8	2	1	160.1

[a]The final concentration range for TBF was 0.008 to 8 μg/ml, and that for AmB was 0.125 to 8 μg/ml.

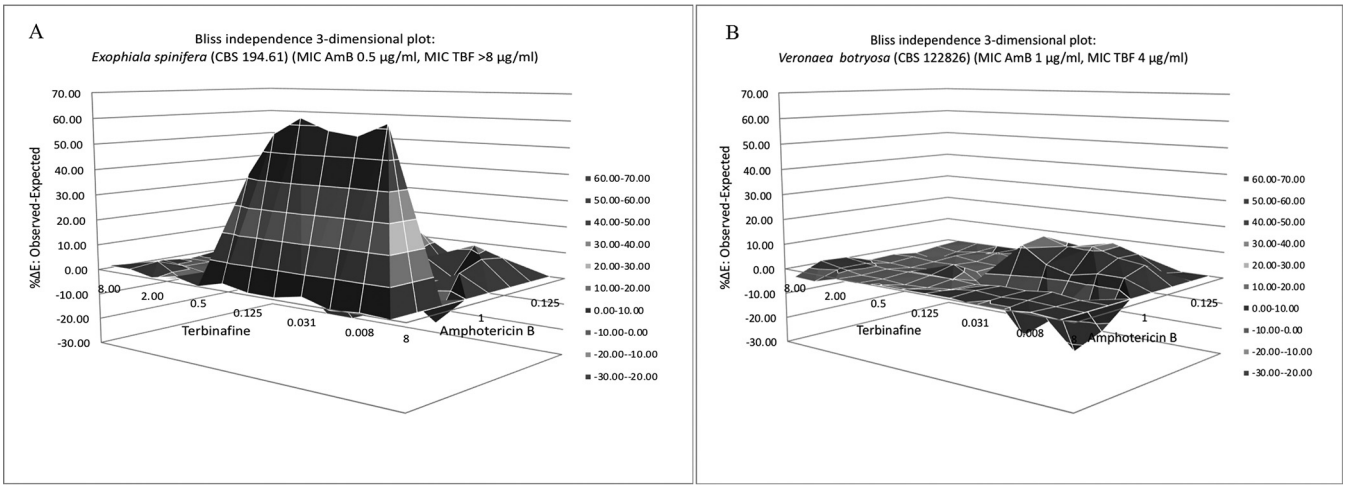

FIG 1 Interaction surfaces obtained from response surface analysis of Bliss independence no-interaction model for *in vitro* combination of amphotericin B (AmB) plus terbinafine (TBF). The *x* and *y* axis represent the efficacy of AmB and TBF, respectively. The *z* axis is the ΔE (%). The 0-plane represents Bliss independent interactions, whereas the volumes above the 0-plane represent statistically significantly synergistic (positive ΔE) interactions. The magnitude of interactions is directly related to ΔE. The different tones in three dimensional plots represent different percentile bands of synergy. The highest level of synergistic interactions was found between 0.25 μg/ml amphotericin B and terbinafine concentrations in the range of 0.008 to 0.5 μg/ml. (A) Synergistic interaction of AmB plus TBF against an *Exophiala spinifera* strain (CBS 194.61) (AmB MIC, 0.5 μg/ml; TBF MIC, >8 μg/ml). The mean ΔE ± standard error of the mean and sum ΔE were 5.36% ± 1.81% and 450.11%, respectively. The highest level of synergistic interactions was found between 0.25 μg/ml amphotericin B and terbinafine concentrations in the range of 0.008 to 0.5 μg/ml. (B) Antagonistic interaction of AmB plus TBF against a *Veronaea botryosa* strain (CBS 122826) (AmB MIC, 1 μg/ml; TBF MIC, 4 μg/ml). The mean ΔE ± standard error of the mean and sum ΔE were −3.23% ± 1.70% and −271.70%, respectively.

1,546%), followed by *F. monophora* (sum ΔE, 1,140%), *F. pedrosoi* (sum ΔE, 775%), *E. spinifera* (sum ΔE, 515%), *P. verrucosa* (sum ΔE, 481%), *E. dermatitidis* (sum ΔE, 449%), and *C. arxii* (sum ΔE, 90%). The strongest synergistic interactions were found at amphotericin B and terbinafine concentration ranges of 0.125 to 0.5 μg/ml and 0.008 to 0.5 μg/ml, respectively. Examples of Bliss independence 3-dimensional plots for the synergistic and antagonistic interactions of amphotericin B and flucytosine are shown in Fig. 1.

Overall, our results show that the amphotericin B and terbinafine combination has synergistic effects against the majority of melanized fungi associated with CBM, including *C. carrionii*, *C. arxii*, *E. dermatitidis*, *E. spinifera*, *F. monophora*, *F. nubica*, *F. pedrosoi*, and *P. verrucosa*. The results of FIC analysis were supported by response surface analysis using a Bliss independence no-interaction model for the isolates tested.

Terbinafine is one of most commonly used antifungal agents in the treatment of patients with CBM (18), due to its high degree of effectiveness and tolerability. In an athymic murine model of CBM caused by *F. pedrosoi*, terbinafine, especially at the highest dose, was able to reduce the inflammatory response to the infection to levels similar to those with azoles (33), although a total cure in patients with CBM remains difficult to achieve (26, 34). On the other hand, various formulations of amphotericin B have been developed and are now available in most countries (35). The compound is nevertheless not recommended as a first-line therapy in chronic infections because of its adverse effects, such as nephrotoxicity, neurotoxicity, hematological side effects, and allergic reactions (36). However, the use of combination therapy can reduce cost- and toxicity-related effects and may prevent the emergence of resistance (35). Combination therapy is also recommended in salvage therapy scenarios for patients with antifungal-resistant and invasive refractory mycoses (37). Few studies have reported data on the efficacy of antifungal combination therapy in the treatment of severe and refractory CBM. Treatment with amphotericin B and a subsequent combination of flucytosine and itraconazole was shown to be effective in a patient with a CBM-like infection caused by *P. verrucosa* (23). Combinations of itraconazole with flucytosine (24, 25) and itracona-

zole with terbinafine have also shown better efficacy than monotherapy for CBM caused by *F. pedrosoi* (26) and *F. monophora* (38). In general, however, combination therapy still is inadequate, requiring long-term therapy at high doses, and treatment failure of CBM remains common. The *in vitro* results obtained in the present study confirmed that terbinafine is active against the majority of strains tested. Of the nine species investigated, *Cladophialophora carrionii* and *Phialophora verrucosa* were more sensitive to terbinafine than species of *Fonsecaea* and *Exophiala*. The three species of *Fonsecaea* showed similar degrees of susceptibility. As in previous reports (39–41), in our study, *E. spinifera* and *V. botryosa* were resistant to terbinafine and amphotericin B when used alone. Although a synergistic interaction was found in a combination setting for *E. spinifera*, the combination of terbinafine and amphotericin B exhibited an indifferent interaction for tested isolates of *Veronaea botryosa*. In the current study, a wide range of amphotericin B MICs (0.125 to >8 μg/ml) was observed for agents of CBM. *Exophiala dermatitidis* and *P. verrucosa* were the species being relatively susceptible, which is in agreement with previous studies (27, 42). When terbinafine and amphotericin B were used in combination, the highest synergy was shown for *F. monophora* and *E. spinifera*, followed by *E. dermatitidis*, *C. carrionii*, *F. nubica*, and *F. pedrosoi.* Our findings agree with those of Daboit et al. (43), demonstrating *in vitro* synergy between amphotericin B and terbinafine for *Fonsecaea* spp., *C. carrionii*, and *P. verrucosa*. Biancalana et al. (44) also reported 96.5% *in vitro* synergy between terbinafine and amphotericin B against clinical isolates obtained from cases of phaeohyphomycosis and CBM, including *F. pedrosoi*, *Curvularia* spp., *Exophiala jeanselmei*, *Alternaria alternata*, *Cladophialophora bantiana*, and *Bipolaris* species. In contrast, Yu et al. (45) did not find an interaction for this combination against agents for CBM.

Overall, the management of CBM is complicated and requires long-term antifungal therapy, surgery, thermotherapy, chemotherapy, or combinations of these (3). Importantly, the clinical experience with posaconazole and voriconazole is limited for CBM. However, the good *in vitro* activities and *in vivo* efficacies of these agents against dematiaceous fungi (46–48), together with the tolerance of the drug in long-term therapies, suggest that further studies are warranted to evaluate the potential use of these drugs for the treatment of CBM.

Collectively, the present study demonstrated that the combination with terbinafine allows a significant reduction in amphotericin B MICs and could be an option for severe or unresponsive cases of CBM, particularly in cases due to *Fonsecaea* and *Cladophialophora* species, and in *E. spinifera*. Our results therefore suggest that a combination of amphotericin B and terbinafine may have a promising role in the treatment of CBM.

ACKNOWLEDGMENTS

P.E.V. has served as a consultant and has received research grants from Astellas, Basilea, Gilead Sciences, Merck, and Pfizer.

We declare no conflicts of interest. We alone are responsible for the content and the writing of the paper.

This study was supported in part by the National Natural Science Foundation of China (grant 81260236), the 973 Program of China (grant 2013CB531601), National Science and Technology Major Projects of China grant 2013ZX10004612, Shanghai Science and Technology Committee grant 14DZ2272900, the Center of Excellence for Infection Biology and Antimicrobial Pharmacology, Tehran, Iran, the Department of Medical Microbiology, Radboudumc, Nijmegen, The Netherlands, and the Westerdijk Fungal Biodiversity Center, Utrecht, The Netherlands.

REFERENCES

1. Queiroz-Telles F, de Hoog S, Santos DW, Salgado CG, Vicente VA, Bonifaz A, Roilides E, Xi L, Azevedo CM, da Silva MB, Pana ZD, Colombo AL, Walsh TJ. 2017. Chromoblastomycosis. Clin Microbiol Rev 30:233–276. https://doi.org/10.1128/CMR.00032-16.
2. Bonifaz A, Carrasco-Gerard E, Saul A. 2001. Chromoblastomycosis: clinical and mycologic experience of 51 cases. Mycoses 44:1–7. https://doi.org/10.1046/j.1439-0507.2001.00613.x.
3. Seyedmousavi S, Netea MG, Mouton JW, Melchers WJG, Verweij PE, de

Hoog GS. 2014. Black yeasts and their filamentous relatives: principles of pathogenesis and host defense. Clin Microbiol Rev 27:527–542. https://doi.org/10.1128/CMR.00093-13.
4. Carrión AL. 1950. Chromoblastomycosis. Ann N Y Acad Sci 50:1255–1282. https://doi.org/10.1111/j.1749-6632.1950.tb39826.x.
5. Carrión AL. 1975. Chromoblastomycosis and related infections: new concepts, differential diagnosis, and nomenclatorial implications. Int J Dermatol 14:27–32. https://doi.org/10.1111/j.1365-4362.1975.tb00074.x.
6. Queiroz-Telles F. 2015. Chromoblastomycosis: a neglected tropical disease. Rev Inst Med Trop Sao Paulo 57(Suppl 19):S46–S50. https://doi.org/10.1590/S0036-46652015000700009.
7. Sousa Mda G, Reid DM, Schweighoffer E, Tybulewicz V, Ruland J, Langhorne J, Yamasaki S, Taylor PR, Almeida SR, Brown GD. 2011. Restoration of pattern recognition receptor costimulation to treat chromoblastomycosis, a chronic fungal infection of the skin. Cell Host Microbe 9:436–443. https://doi.org/10.1016/j.chom.2011.04.005.
8. Gomes RR, Vicente VA, Azevedo CM, Salgado CG, da Silva MB, Queiroz-Telles F, Marques SG, Santos DW, de Andrade TS, Takagi EH, Cruz KS, Fornari G, Hahn RC, Scroferneker ML, Caligine RB, Ramirez-Castrillon M, de Araujo DP, Heidrich D, Colombo AL, de Hoog GS. 2016. Molecular epidemiology of agents of human chromoblastomycosis in Brazil with the description of two novel species. PLoS Negl Trop Dis 10:e0005102. https://doi.org/10.1371/journal.pntd.0005102.
9. Najafzadeh MJ, Sun J, Vicente VA, Klaassen CH, Bonifaz A, Gerrits van den Ende AH, Menken SB, de Hoog GS. 2011. Molecular epidemiology of *Fonsecaea* species. Emerg Infect Dis 17:464–469. https://doi.org/10.3201/eid1703.100555.
10. de Hoog GS, Nishikaku AS, Fernandez-Zeppenfeldt G, Padin-Gonzalez C, Burger E, Badali H, Richard-Yegres N, van den Ende AH. 2007. Molecular analysis and pathogenicity of the *Cladophialophora carrionii* complex, with the description of a novel species. Stud Mycol 58:219–234. https://doi.org/10.3114/sim.2007.58.08.
11. Brischetto A, Kidd S, Baird R. 2015. First reported Australian case of *Cladophilophora arxii*: features consistent with possible primary pulmonary chromoblastomycosis. Am J Trop Med Hyg 92:791–793. https://doi.org/10.4269/ajtmh.14-0711.
12. Matsumoto T, Matsuda T, McGinnis MR, Ajello L. 1993. Clinical and mycological spectra of *Wangiella dermatitidis* infections. Mycoses 36:145–155. https://doi.org/10.1111/j.1439-0507.1993.tb00743.x.
13. Barba-Gómez JF, Mayorga J, McGinnis MR, Gonzalez-Mendoza A. 1992. Chromoblastomycosis caused by *Exophiala spinifera*. J Am Acad Dermatol 26:367–370. https://doi.org/10.1016/0190-9622(92)70058-N.
14. Takeuchi A, Anzawa K, Mochizuki T, Takehara K, Hamaguchi Y. 2015. Chromoblastomycosis caused by *Phialophora verrucosa* on the hand. Eur J Dermatol 25:274–275.
15. Zhu CY, Yang YP, Sheng P, Li W, Huang WM, Fan YM. 2015. Cutaneous chromoblastomycosis caused by *Veronaea botryosa* in a patient with pemphigus vulgaris and review of published reports. Mycopathologia 180:123–129. https://doi.org/10.1007/s11046-015-9887-0.
16. Queiroz-Telles F, Santos DW. 2013. Challenges in the therapy of chromoblastomycosis. Mycopathologia 175:477–488. https://doi.org/10.1007/s11046-013-9648-x.
17. Restrepo A, Gonzalez A, Gomez I, Arango M, de Bedout C. 1988. Treatment of chromoblastomycosis with itraconazole. Ann N Y Acad Sci 544:504–516. https://doi.org/10.1111/j.1749-6632.1988.tb40448.x.
18. Bonifaz A, Saul A, Paredes-Solis V, Araiza J, Fierro-Arias L. 2005. Treatment of chromoblastomycosis with terbinafine: experience with four cases. J Dermatol Treat 16:47–51. https://doi.org/10.1080/09546630410024538.
19. Andrade TS, Castro LG, Nunes RS, Gimenes VM, Cury AE. 2004. Susceptibility of sequential Fonsecaea pedrosoi isolates from chromoblastomycosis patients to antifungal agents. Mycoses 47:216–221. https://doi.org/10.1111/j.1439-0507.2004.00984.x.
20. Queiroz-Telles F, Esterre P, Perez-Blanco M, Vitale RG, Salgado CG, Bonifaz A. 2009. Chromoblastomycosis: an overview of clinical manifestations, diagnosis and treatment. Med Mycol 47:3–15. https://doi.org/10.1080/13693780802538001.
21. Castro LG, Pimentel ER, Lacaz CS. 2003. Treatment of chromomycosis by cryosurgery with liquid nitrogen: 15 years' experience. Int J Dermatol 42:408–412. https://doi.org/10.1046/j.1365-4362.2003.01532.x.
22. Bonifaz A, Martinez-Soto E, Carrasco-Gerard E, Peniche J. 1997. Treatment of chromoblastomycosis with itraconazole, cryosurgery, and a combination of both. Int J Dermatol 36:542–547. https://doi.org/10.1046/j.1365-4362.1997.00085.x.
23. Park SG, Oh SH, Suh SB, Lee KH, Chung KY. 2005. A case of chromoblastomycosis with an unusual clinical manifestation caused by *Phialophora verrucosa* on an unexposed area: treatment with a combination of amphotericin B and 5-flucytosine. Br J Dermatol 152:560–564. https://doi.org/10.1111/j.1365-2133.2005.06424.x.
24. Antonello VS, Appel da Silva MC, Cambruzzi E, Kliemann DA, Santos BR, Queiroz-Telles F. 2010. Treatment of severe chromoblastomycosis with itraconazole and 5-flucytosine association. Rev Inst Med Trop Sao Paulo 52:329–331. https://doi.org/10.1590/S0036-46652010000600008.
25. Paniz-Mondolfi AE, Colella MT, Negrin DC, Aranzazu N, Oliver M, Reyes-Jaimes O, Perez-Alvarez AM. 2008. Extensive chromoblastomycosis caused by *Fonsecaea pedrosoi* successfully treated with a combination of amphotericin B and itraconazole. Med Mycol 46:179–184. https://doi.org/10.1080/13693780701721856.
26. Gupta AK, Taborda PR, Sanzovo AD. 2002. Alternate week and combination itraconazole and terbinafine therapy for chromoblastomycosis caused by *Fonsecaea pedrosoi* in Brazil. Med Mycol 40:529–534. https://doi.org/10.1080/mmy.40.5.529.534.
27. Deng S, Pan W, Liao W, de Hoog GS, Gerrits van den Ende AH, Vitale RG, Rafati H, Ilkit M, Van der Lee AH, Rijs AJ, Verweij PE, Seyedmousavi S. 2016. Combination of amphotericin B and flucytosine against neurotropic species of melanized fungi causing primary cerebral phaeohyphomycosis. Antimicrob Agents Chemother 60:2346–2351. https://doi.org/10.1128/AAC.02526-15.
28. de Hoog GS, Guarro J, Gene J, Figueras MJ. 2009. Atlas of clinical fungi: the ultimate benchtool for diagnostics. Centraalbureau voor Schimmelcultures, KNAW Fungal Biodiversity Center/Universitat Rovira i Virgili, Utrecht, The Netherlands.
29. CLSI. 2008. Reference method for broth dilution antifungal susceptibility testing of filamentous fungi; approved standard, 2nd ed. CLSI document M38-A2. Clinical and laboratory Standards Institute, Wayne, PA.
30. Hindler J. 1995. Antimicrobial susceptibility testing, p 5.18.11–15.18.20. *In* Isenberg HD (ed), Clinical microbiology procedures handbook. ASM Press, Washington, DC.
31. Berenbaum MC. 1978. A method for testing for synergy with any number of agents. J Infect Dis 137:122–130. https://doi.org/10.1093/infdis/137.2.122.
32. Prichard MN, Prichard LE, Shipman C, Jr. 1993. Strategic design and three-dimensional analysis of antiviral drug combinations. Antimicrob Agents Chemother 37:540–545. https://doi.org/10.1128/AAC.37.3.540.
33. Calvo E, Pastor FJ, Mayayo E, Hernandez P, Guarro J. 2011. Antifungal therapy in an athymic murine model of chromoblastomycosis by *Fonsecaea pedrosoi*. Antimicrob Agents Chemother 55:3709–3713. https://doi.org/10.1128/AAC.01662-10.
34. Minotto R, Bernardi CD, Mallmann LF, Edelweiss MI, Scroferneker ML. 2001. Chromoblastomycosis: a review of 100 cases in the state of Rio Grande do Sul, Brazil. J Am Acad Dermatol 44:585–592. https://doi.org/10.1067/mjd.2001.112220.
35. Seyedmousavi S, Rafati H, Ilkit M, Tolooe A, Hedayati MT, Verweij P. 2017. Systemic antifungal agents: current status and projected future developments. Methods Mol Biol 1508:107–139. https://doi.org/10.1007/978-1-4939-6515-1_5.
36. Hamill RJ. 2013. Amphotericin B formulations: a comparative review of efficacy and toxicity. Drugs 73:919–934. https://doi.org/10.1007/s40265-013-0069-4.
37. Seyedmousavi S, Meletiadis J, Melchers WJ, Rijs AJJM, Mouton JW, Verweij PE. 2013. *In vitro* interaction of voriconazole and anidulafungin against triazole-resistant *Aspergillus fumigatus*. Antimicrob Agents Chemother 57:796–803. https://doi.org/10.1128/AAC.00980-12.
38. Zhang JM, Xi LY, Zhang H, Xie Z, Sun JF, Li XQ, Lu S. 2009. Synergistic effects of terbinafine and itraconazole on clinical isolates of *Fonsecaea monophora*. Eur J Dermatol 19:451–455. https://doi.org/10.1684/ejd.2009.0728.
39. Daboit TC, Duquia RP, Magagnin CM, Mendes SD, Castrillon MR, Steglich R, dos Santos IS, Vettorato G, Valente P, Scroferneker ML. 2012. A case of *Exophiala spinifera* infection in southern Brazil: molecular identification and antifungal susceptibility. Med Mycol Case Rep 1:72–75. https://doi.org/10.1016/j.mmcr.2012.08.006.
40. Vitale RG, Perez-Blanco M, De Hoog GS. 2009. *In vitro* activity of antifungal drugs against *Cladophialophora* species associated with human chromoblastomycosis. Med Mycol 47:35–40. https://doi.org/10.1080/13693780802566333.
41. Duarte APM, Pagnocca FC, Baron NC, Melhem MDC, Palmeira GA, de Angelis DD, Attili-Angelis D. 2013. *In vitro* susceptibility of environmental

isolates of *Exophiala dermatitidis* to five antifungal drugs. Mycopathologia 175:455–461. https://doi.org/10.1007/s11046-012-9597-9.
42. Sun Y, Liu W, Wan Z, Wang XH, Li RY. 2011. Antifungal activity of antifungal drugs, as well as drug combinations against *Exophiala dermatitidis*. Mycopathologia 171:111–117. https://doi.org/10.1007/s11046-010-9358-6.
43. Daboit TC, Massotti Magagnin C, Heidrich D, Czekster Antochevis L, Vigolo S, Collares Meirelles L, Alves K, Scroferneker ML. 2014. *In vitro* susceptibility of chromoblastomycosis agents to five antifungal drugs and to the combination of terbinafine and amphotericin B. Mycoses 57:116–120. https://doi.org/10.1111/myc.12111.
44. Biancalana FSC, Lyra L, Schreiber AZ. 2011. *In vitro* evaluation of the type of interaction obtained by the combination of terbinafine and itraconazole, voriconazole, or amphotericin B against dematiaceous molds. Antimicrob Agents Chemother 55:4485–4487. https://doi.org/10.1128/AAC.01015-10.
45. Yu J, Li R, Zhang M, Liu L, Wan Z. 2008. *In vitro* interaction of terbinafine with itraconazole and amphotericin B against fungi causing chromoblastomycosis in China. Med Mycol 46:745–747. https://doi.org/10.1080/13693780802163438.
46. Calvo E, Pastor FJ, Salas V, Mayayo E, Capilla J, Guarro J. 2012. Histopathology and antifungal treatment of experimental murine chromoblastomycosis caused by *Cladophialophora carrionii*. J Antimicrob Chemother 67:666–670. https://doi.org/10.1093/jac/dkr537.
47. Negroni R, Tobon A, Bustamante B, Shikanai-Yasuda MA, Patino H, Restrepo A. 2005. Posaconazole treatment of refractory eumycetoma and chromoblastomycosis. Rev Inst Med Trop Sao Paulo 47:339–346. https://doi.org/10.1590/S0036-46652005000600006.
48. Bonifaz A, Paredes-Solis V, Saul A. 2004. Treating chromoblastomycosis with systemic antifungals. Expert Opin Pharmacother 5:247–254. https://doi.org/10.1517/14656566.5.2.247.

PLOS | NEGLECTED TROPICAL DISEASES

SYMPOSIUM

Isolated iliac cryptococcosis in an immunocompetent patient

Junjun Sang[1,2☯], Yali Yang[1☯], Yibin Fan[3], Guizhen Wang[4], Jiu Yi[1], Wei Fang[1,5]*, Weihua Pan[1]*, Jinhua Xu[5], Wanqing Liao[1]*

1 Shanghai Key Laboratory of Molecular Medical Mycology, Department of Dermatology and Venereology, Changzheng Hospital, Shanghai, China, **2** Department of dermatology, Fuzhou General Hospital, Fuzhou, China, **3** Department of dermatology, Zhejiang Provincial People's Hospital, Hangzhou, Zhejiang, China, **4** Emergency room, Shanghai Tenth People's Hospital of Tongji University, Shanghai, China, **5** Department of Dermatology, Huashan Hospital, Fudan University, Shanghai, China

☯ These authors contributed equally to this work.
* weifang081782@163.com (WF); panweihua@medmail.com.cn (WP); liaowanqing@sohu.com (WL)

Citation: Sang J, Yang Y, Fan Y, Wang G, Yi J, Fang W, et al. (2018) Isolated iliac cryptococcosis in an immunocompetent patient. PLoS Negl Trop Dis 12(3): e0006206. https://doi.org/10.1371/journal.pntd.0006206

Editor: Ángel González, Universidad de Antioquia, COLOMBIA

Published: March 29, 2018

Funding: This study was supported by the National Natural Science Foundation of China (81401651, 81501728, and 81471926), the National Key Basic Research Programs of China (2013CB531601), China Postdoctoral Science Foundation Grant (2016M600286), and Zhejiang Provincial Natural Science Foundation (LQ14H190002). The funders had no role in study design, data collection and analysis, decision to publish, or preparation of the manuscript.

Competing interests: The authors have declared that no competing interests exist.

Introduction

Overview

Cryptococcal osteomyelitis is an infrequent infection that is usually associated with disseminated cryptococcosis or underlying immunocompromised conditions. Here we describe a rare case of isolated iliac cryptococcosis in an immunocompetent patient. Through histological, microbial, and molecular biological examinations, the pathogen was finally identified as *Cryptococcus neoformans* VNI genotype, which likely originated from environmental bird droppings. The clinical isolate was hypomelanized but fully virulent in a mouse infection model. The patient displayed a lower $CD4^+$ T-lymphocyte ratio, reduced serum interferon gamma (IFN-γ) and interleukin 12 (IL-12) levels, and a dysregulated transcriptional profile of blood leukocytes compared with the healthy host. After surgical excision and 34 weeks of antifungal treatment, the patient achieved clinical cure. Our study suggests that cryptococcosis development is closely associated with the interaction of the fungal agent and host immunity. Accurate diagnosis of bone cryptococcosis depends mainly on histological and fungal examinations. A combination of an antifungal agent treatment regimen and surgery are highly effective for resolving bone cryptococcosis.The *C. neoformans* species complex primarily causes opportunistic infections in immunocompromised patients, commonly involving the lungs and central nervous system [1]. Skeletal involvement is infrequent and usually associated with disseminated cryptococcosis or underlying predisposing conditions such as sarcoidosis, tuberculosis, or other systemic disorders [2,3]. We present here a rare case of isolated skeletal cryptococcosis in an immunocompetent host and further discuss the manifestation of the infection from both pathogen and host perspectives by in vitro and in vivo assays. Informed written consent was obtained prior to publication of the case details.

Case report

A previously healthy 46-year-old woman presented with left hip pain of undetermined origin for 2 months. The pain was not alleviated after symptomatic treatment. Physical examination showed slight swelling of the left hip with no broken skin, and the patient presented a limp. There was no obvious spine deformity or muscle atrophy nor tenderness or a mass detected upon palpation. The Patrick sign and ankle or knee jerk reflexes were normal. The patient had no fever, cough, coma, headaches, or weight loss.

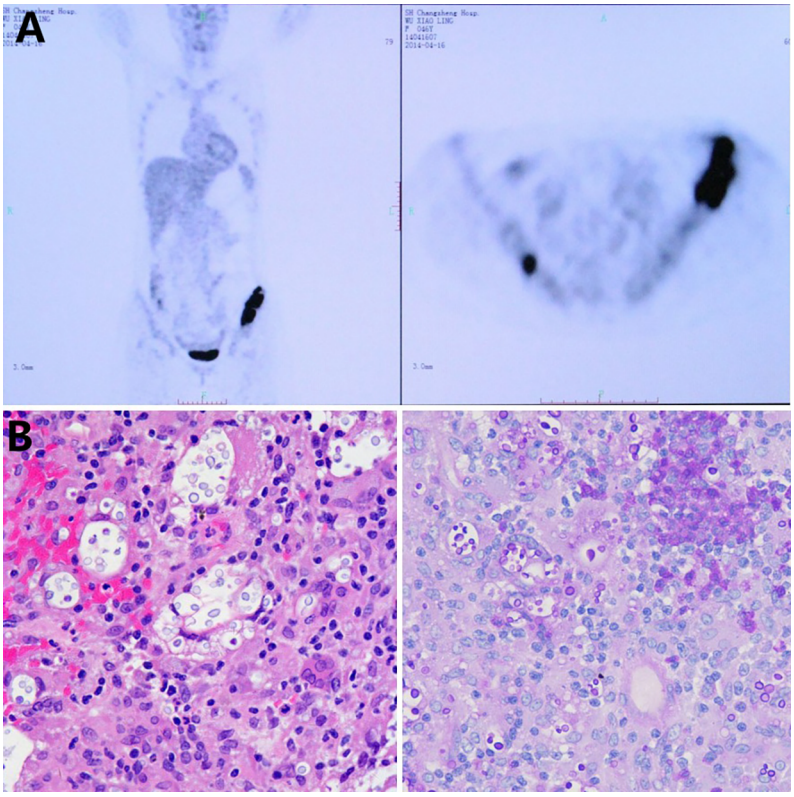

Fig 1. ^{18}FDG-PET/CT scan and histological examination. (A) ^{18}FDG-PET/CT indicated hypermetabolic lesions in the bilateral iliac crest, especially in the left iliac crest. **(B)** Histological examinations (HE stain, left panel; PAS stain, right panel) after left iliac biopsy revealed round yeast cells. HE, hematoxylin and eosin; PAS, periodic acid–Schiff; ^{18}FDG-PET/CT, ^{18}fluorodeoxyglucose positron emission tomography and computed tomography.

https://doi.org/10.1371/journal.pntd.0006206.g001

Most of the laboratory examinations were normal, such as blood biochemistry tests, HIV test, antinuclear antibodies, and tumor markers. The blood profile revealed 79.8% neutrophils (high) and 12.9% lymphocytes (low). CD4 and CD3 counts were further performed, and the results were negative (CD3: 63.6%, normal; CD3 absolute value: 284; CD4: 25.1%, low; CD4 absolute value: 112; CD8: 37.5%, high; CD8 absolute value: 168; CD4/CD8: 0.67%, low). ^{18}fluorodeoxyglucose positron emission tomography and computed tomography (^{18}FDG-PET/CT) indicated hypermetabolic lesions in the bilateral iliac crest, especially in the left iliac crest (Fig 1A). The pulmonary computed tomography (CT) scan demonstrated multiple obsolete bilateral lung lesions (S1 Fig). The patient underwent a left iliac bone biopsy. Microscopic examination and fungal culture displayed abundant small round organisms, which were suspected to be *C. neoformans* based on morphological characteristics and histopathological findings (Fig 1B). The blood cryptococcal antigen test was positive (>1:5,120). The cerebrospinal fluid (CSF) biochemistry and microbial tests were negative.

After excision of skeletal cryptococcosis, treatment with liposomal amphotericin B (4 mg/kg/day) and flucytosine (100 mg/kg/day) was administered for 2 weeks; voriconazole (0.4 g/day) was then administered for 8 weeks. The patient was discharged to her home on oral fluconazole (800 mg/day for 12 weeks) for consolidation, which was then tapered to 400 mg/day for 12 weeks. The serum cryptococcal antigen titers were 1:2,560 after 1 month of treatment, 1:1,280 after 2 months of treatment, and 1:2 at 1 year postdischarge. The pelvic CT findings at 1 year postdischarge suggested clinical cure (S1 Fig).

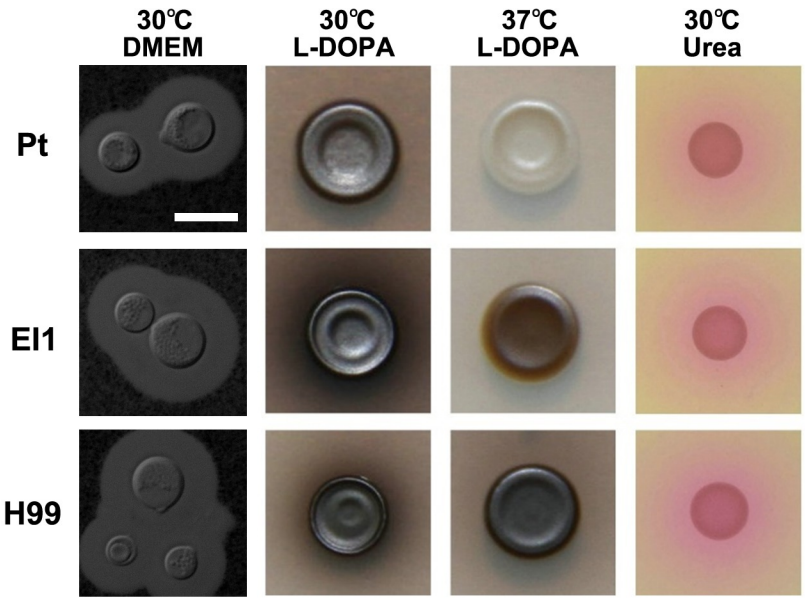

Fig 2. In vitro assay of virulence factors. Different media (DMEM liquid, L-DOPA, and Christiansen's urea agars) were utilized to test the production of major virulence factors (such as capsule, melanin, and urease) in *C. neoformans*. Compared with the hypervirulent strain (H99) or environmental isolate (El1), the clinical isolate (Pt) displayed a significant defect in melanization at host temperature but not in capsule or urease production.

https://doi.org/10.1371/journal.pntd.0006206.g002

We examined her epidemiological history to determine the potential source of exposure to cryptococcosis. Three yeast colonies were finally isolated from 20 samples of wild bird droppings near the patient's residence. The internal transcribed spacer (ITS) sequencing [4] and PCR fingerprinting [5] confirmed that all the clinical and environmental isolates were *C. neoformans* VNI genotype (S2 Fig and S1 Table). In vitro phenotypic assays showed that the clinical isolate exhibited significant hypomelanization at 37˚C but normal production of capsule or urease (Fig 2). Furthermore, the clinical isolate was fully virulent in vivo, although it displayed extended survival in a mouse inhalation model ($P < 0.001$) (Fig 3B) and exhibited a significant reduction in intracellular survival compared with the standard strain (H99) or the environmental isolate (El1) ($P < 0.01$) (Fig 3A).

Cytokine and transcriptional profiles were examined in patient serum samples by ELISA and RNA-seq analysis, respectively. The results revealed a significant reduction of interferon gamma (IFN-γ) ($P < 0.001$) and interleukin 12 (IL-12) ($P < 0.05$) compared with the healthy control groups (S3 Fig). The transcriptional profiles (Gene Expression Omnibus Accession number: GSE108534) showed an enrichment of a primary immunodeficiency phenotype, such as T cell signaling pathways, the hematopoietic cell lineage, the nuclear factor kappa-light-chain-enhancer of activated B cells (NF-κB) signaling pathway, antigen processing and presentation, and natural killer cell-mediated cytotoxicity (S3 Fig). All the materials and methods are provided in S1 Text.

Discussion

Skeletal cryptococcosis is usually secondary to direct inoculation during trauma or hematogenous dissemination [3]. Since the patient had multiple obsolete pulmonary lesions and a high blood cryptococcal antigen titer but no history of trauma, we speculated that the agent originated from primary pulmonary lesions. PCR fingerprinting revealed that all isolates grouped

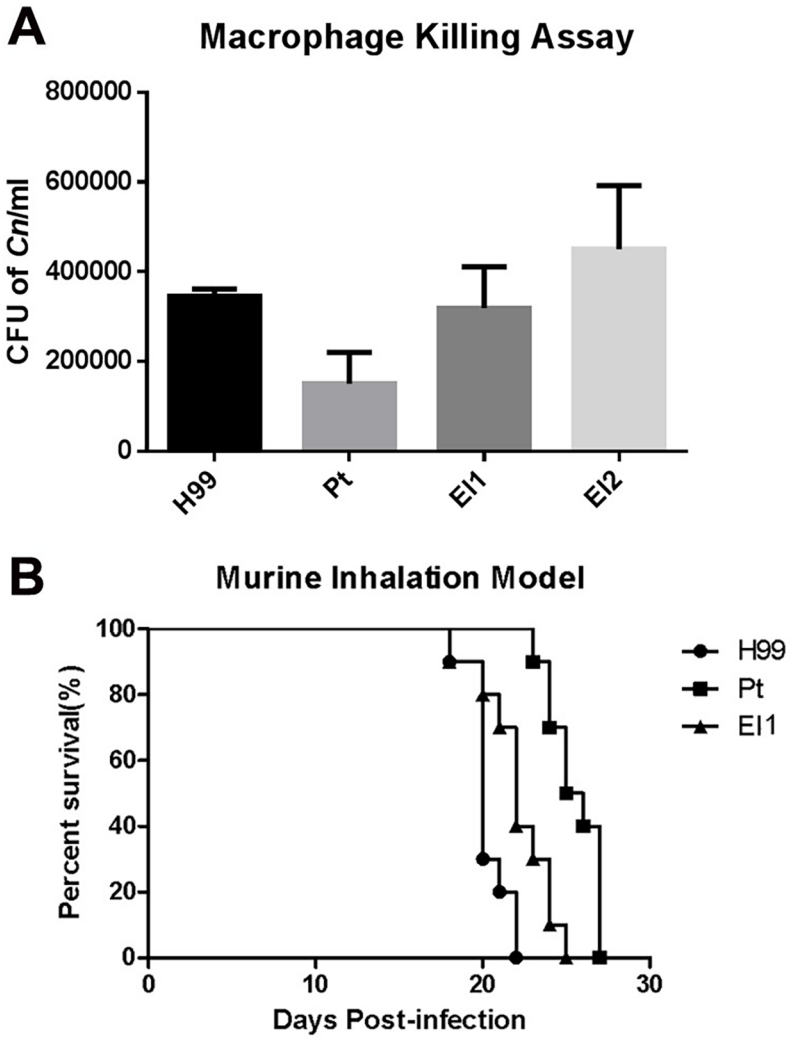

Fig 3. Macrophage killing assay and murine inhalation model. Both macrophage **(A)** ($P < 0.01$) and animal **(B)** ($P < 0.001$) infection experiments displayed attenuated virulence of the clinical isolate compared with the hypervirulent strain H99.

https://doi.org/10.1371/journal.pntd.0006206.g003

into the VNI genotype [6]. Thus, an environmental carrier (bird droppings) of *C. neoformans* might be the ultimate source of skeletal infection in this case.

Pathogenesis and progression of cryptococcosis depends on the interaction between the fungal agent and host immunity. The clinical agent in this study showed complete virulence in vivo and ex vivo, although its virulence was inferior to the standard strain (H99) or environmental isolates, which might be partially attributed to its hypomelanization at host temperature. Several laboratory test indices, such as HIV, autoimmune antibodies, and tumor markers, were normal, and the patient's medical history showed no medical use of steroids or immunosuppressants. The patient displayed a lower $CD4^+$ T-lymphocyte ratio, significantly reduced serum Th1 cytokine (IFN-γ and IL-12) responses, and a dysregulated transcriptional profile of blood leukocytes, as compared with healthy populations. Two potential scenarios may explain this phenomenon. On the one hand, the presence of cryptococcal antigens (such as glucuronoxylomannan) or previously applied anti-inflammatory therapy might cause a slight compromise of host cellular immunity [7,8]. On the other hand, the abnormalities in

immunological indices might originate from host subclinical immune impairment, which remains to be further confirmed.

We reviewed the literature on immunological analyses in apparently normal individuals with cryptococcosis. The *IL12RB1* gene mutation has been reported in pediatric patients with cryptococcal osteomyelitis or disseminated cryptococcosis [9,10]. Several studies have also suggested that genetic polymorphisms of some immune molecules (such as mannose-binding lectin, dectin-2, and Fcγ receptor IIB) are closely associated with cryptococcosis in immunocompetent populations [11,12,13]. All these factors were associated with host immune functions essential for fungal control and containment, such as phagocytic activity and T cell responses [14,15]. Thus, subclinical immune impairment might be a non-negligible factor in apparently healthy patients with cryptococcosis.

The clinical symptoms and radiological findings of skeletal cryptococcosis were nonspecific. A correct diagnosis still relied on histopathological and fungal examinations of lesion specimens. After focal cleaning operations, multiple antifungal agents were sequentially administered, such as liposomal amphotericin B, flucytosine, and azole agents, and the patient achieved clinical cure.

Conclusions

Isolated skeletal cryptococcosis is rare but may occur in healthy individuals after daily exposure to the organism. Herein, the clinical isolate likely originated from environmental bird droppings disseminated from the pulmonary lesion to the hip. The development of cryptococcosis was closely associated with the interaction of the fungal agent and host immunity. Accurate diagnosis of bone cryptococcosis depends mainly on histological and fungal examinations. A combination antifungal agent treatment regimen and surgery were quite effective for resolving bone cryptococcosis.

Ethics statement

This study was approved by the Committee on Ethics of Biomedicine Research, Changzheng Hospital. All subjects gave written informed consent in accordance with the Declaration of Helsinki. The animal experiments were carried out in strict accordance with the recommendations in the Regulations for the Administration of Affairs concerning Experimental Animals of the State Science and Technology Commission (China). The protocol was approved by the Animal Experiment Center of Second Military Medical University.

Supporting information

S1 Text. Materials and methods.
(DOCX)

S1 Fig. CT scans. (A) The pulmonary CT scan on admission showed multiple obsolete lesions in the bilateral upper lobes and lower lobe of the left lung. **(B)** The pelvic CT scan at 1 year post-discharge suggested the infectious lesions had disappeared. CT, computed tomography.
(TIF)

S2 Fig. Molecular-type identification of clinical and environmental isolates by PCR fingerprinting. All isolates were identified as VNI genotype. Pt is the cryptococcal strain isolated from the iliac lesion of the patient. EI denotes environmental isolates from the patient's area of residence.
(TIF)

S3 Fig. Serum cytokine and transcriptional profile analyses. (A) The serum cytokine assay revealed a significant reduction of IFN-γ and IL-12 compared with the control groups. *** means $P < 0.001$. * means $P < 0.05$. **(B)** Bioinformatics analysis of RNA sequencing in the patient serum sample displayed an enrichment of several immunological pathways. IFN-γ, interferon gamma; IL-12, interleukin 12.
(TIF)

S1 Table. Strains used in this study. Pt, cryptococcal strain isolated from the biopsy specimen; EI-1,2,3, cryptococcal strains isolated from bird droppings near the patient's residence. The other strains were provided by our laboratory.
(DOCX)

References

1. Maziarz EK, Perfect JR. Cryptococcosis. Infect Dis Clin North Am. 2016; 30: 179–206. https://doi.org/10.1016/j.idc.2015.10.006 PMID: 26897067
2. Amenta PS, Stead J, Kricun ME. Case report 226: isolated Cryptococcus neoformans osteomyelitis of femur. Skeletal Radiol. 1983. 9(4): 263–5. PMID: 6867777
3. Zhou HX, Lu L, Chu T, et al. Skeletal cryptococcosis from 1977 to 2013. Front Microbiol. 2014; 5: 740. https://doi.org/10.3389/fmicb.2014.00740 PMID: 25642211
4. Feng X, Yao Z, Ren D, Liao W, Wu J. Genotype and mating type analysis of Cryptococcus neoformans and Cryptococcus gattii isolates from China that mainly originated from non-HIV-infected patients. FEMS Yeast Res. 2008. 8(6): 930–8. https://doi.org/10.1111/j.1567-1364.2008.00422.x PMID: 18671745
5. Meyer W, Castaneda A, Jackson S, Huynh M, Castaneda E. Molecular typing of IberoAmerican Cryptococcus neoformans isolates. Emerg Infect Dis. 2003; 9: 189–95. https://doi.org/10.3201/eid0902.020246 PMID: 12603989
6. Fang W., Fa Z., and Liao W. (2015). Epidemiology of Cryptococcus and cryptococcosis in China. *Fungal Genet. Biol.* 78, 7–15. doi: https://doi.org/10.1016/j.fgb.2014.10.017 PMID: 25445309
7. Albuquerque PC, Fonseca FL, Dutra FF, Bozza MT, Frases S, et al. (2014) Cryptococcus neoformans glucuronoxylomannan fractions of different molecular masses are functionally distinct. Future Microbiol 9: 147–161. https://doi.org/10.2217/fmb.13.163 PMID: 24571070
8. Ratzinger F, Haslacher H, Poeppl W, Hoermann G, Kovarik JJ, et al. (2014) Azithromycin suppresses CD4(+) T-cell activation by direct modulation of mTOR activity. Sci Rep 4: 7438. https://doi.org/10.1038/srep07438 PMID: 25500904
9. Rezai M. S., Khotael G., Kheirkhah M., Hedayat T., Geramishoar M., and Mahjoub F. (2008). Cryptococcosis and deficiency of interleukin12r. *Pediatr. Infect. Dis. J.* 27, 673. doi: https://doi.org/10.1097/INF.0b013e318179263a PMID: 18520441
10. Jirapongsananuruk O., Luangwedchakarn V., Niemela J. E., Pacharn P., Visitsunthorn N., Thepthai C., et al. (2012). Cryptococcal osteomyelitis in a child with a novel compound mutation of the IL12RB1 gene. *Asian Pac. J. Allergy Immunol.* 30, 79–82. PMID: 22523911
11. Ou X. T., Wu J. Q., Zhu L. P., Guan M., Xu B., Hu X. P., et al. (2011). Genotypes coding for mannose-binding lectin deficiency correlated with cryptococcal meningitis in HIV-uninfected Chinese patients. *J. Infect. Dis.* 203, 1686–1691. doi: https://doi.org/10.1093/infdis/jir152 PMID: 21592999
12. Hu X. P., Wu J. Q., Zhu L. P., Wang X., Xu B., Wang R. Y., et al. (2012). Association of Fcγ receptor IIB polymorphism with cryptococcal meningitis in HIV-uninfected Chinese patients. *PLoS ONE* 7, e42439. doi: https://doi.org/10.1371/journal.pone.0042439 PMID: 22879986
13. Hu X. P., Wang R. Y., Wang X., Cao Y. H., Chen Y. Q., Zhao H. Z., et al. (2015). Dectin-2 polymorphism associated with pulmonary cryptococcosis in HIV-uninfected Chinese patients. *Med. Mycol.* 53, 810–816. doi: https://doi.org/10.1093/mmy/myv043 PMID: 26129889
14. Heitman J KTR, Kwon-Chung KJ PJR, Casadevall A. Cryptococcus: from human pathogen to model yeast. Washington, DC: ASM Press. 2011.
15. Rohatgi S., and Pirofski L. A. (2015). Host immunity to Cryptococcus neoformans. *Future Microbiol* 10, 565–581. doi: https://doi.org/10.2217/fmb.14.132 PMID: 25865194

Low-Cost Tetraplex PCR for the Global Spreading Multi-Drug Resistant Fungus, Candida auris and Its Phylogenetic Relatives

Article *in* Frontiers in Microbiology · May 2018

DOI: 10.3389/fmicb.2018.01119

CITATIONS
0

READ
1

5 authors, including:

Amir Arastehfar
Westerdijk Fungal Biodiversity Institute
3 PUBLICATIONS **4** CITATIONS
SEE PROFILE

Wenjie Fang
Second Military Medical University, Shanghai
32 PUBLICATIONS **42** CITATIONS
SEE PROFILE

Hamid Badali
Mazandaran University of Medical Sciences, Sari Iran
176 PUBLICATIONS **1,485** CITATIONS
SEE PROFILE

Afsane Vaezi
Mazandaran University of Medical Sciences
21 PUBLICATIONS **97** CITATIONS
SEE PROFILE

frontiers in Microbiology

ORIGINAL RESEARCH
published: 29 May 2018
doi: 10.3389/fmicb.2018.01119

Low-Cost Tetraplex PCR for the Global Spreading Multi-Drug Resistant Fungus, *Candida auris* and Its Phylogenetic Relatives

Amir Arastehfar[1†], Wenjie Fang[1,2,3†], Hamid Badali[4], Afsane Vaezi[5], Weiwei Jiang[2,3], Wanqing Liao[2,3], Weihua Pan[2,3*], Ferry Hagen[1] and Teun Boekhout[1,3,6]*

[1] Westerdijk Fungal Biodiversity Institute, Utrecht, Netherlands, [2] Department of Dermatology, Shanghai Changzheng Hospital, Second Military Medical University, Shanghai, China, [3] Shanghai Key Laboratory of Molecular Medical Mycology, Shanghai Institute of Medical Mycology, Shanghai Changzheng Hospital, Second Military Medical University, Shanghai, China, [4] Department of Medical Mycology/Invasive Fungi Research Center, School of Medicine, Mazandaran University of Medical Sciences, Sari, Iran, [5] Student Research Committee, Mazandaran University of Medical Sciences, Sari, Iran, [6] Institute for Biodiversity and Ecosystem Dynamics, University of Amsterdam, Amsterdam, Netherlands

OPEN ACCESS

Edited by:
Dominique Sanglard, Université de Lausanne, Switzerland

Reviewed by:
Alix Thérèse Coste, Centre Hospitalier Universitaire Vaudois (CHUV), Switzerland
Guillermo Quindós, University of the Basque Country (UPV/EHU), Spain

***Correspondence:**
Weiwei Jiang
jiangxuejiangwei@qq.com
Weihua Pan
panweihua@smmu.edu.cn

† These authors have contributed equally to this work.

Specialty section:
This article was submitted to Infectious Diseases, a section of the journal Frontiers in Microbiology

Received: *23 February 2018*
Accepted: *11 May 2018*
Published: *29 May 2018*

Citation:
Arastehfar A, Fang W, Badali H, Vaezi A, Jiang W, Liao W, Pan W, Hagen F and Boekhout T (2018) Low-Cost Tetraplex PCR for the Global Spreading Multi-Drug Resistant Fungus, Candida auris and Its Phylogenetic Relatives. Front. Microbiol. 9:1119. doi: 10.3389/fmicb.2018.01119

Candida auris, *C. haemulonii*, *C. duobushaemulonii,* and *C. pseudohaemulonii* are closely related and highly multidrug resistant yeast pathogens. The high cost and low accuracy of current diagnostics may underestimate their prevalence, especially in medical resource-limited regions. In this study, we used 172 *C. auris* stains and its relatives and 192 other fungal strains to establish and validate a novel multiplex end-point PCR. A prospective and a retrospective clinical screenings using this assay were further performed in China and Iran respectively. We identified the first isolate of *C. pseudohaemulonii* in China and the first isolate of *C. haemulonii* in Iran from 821 clinical isolates in total, without any false positive. Animal models of *C. auris* and *C. haemulonii* were established for validation. The overall positive rates of the assay for mice blood and tissue were 28.6 and 92.9%, respectively. Compared with previously developed assays, our assay is more available and affordable to the developing countries, and may contribute to a better understanding of the epidemiology of *C. auris* and its relatives in these regions.

Keywords: end-point PCR, *Candida auris*, multi-drug resistance, animal model, clinical validation, molecular diagnosis

INTRODUCTION

The evolving epidemiology of non-*albicans Candida* species and other emerging opportunistic pathogenic yeasts contributes to an increasing morbidity and mortality globally (Miceli et al., 2011; Fang et al., 2017). Among them, *Candida auris* and its medically important relatives in the *Metschnikowiaceae* clade, e.g., *C. haemulonii*, *C. duobushaemulonii,* and *C. pseudohaemulonii*, are well known as highly multidrug resistant pathogens that can lead to both superficial and deep-seated infections (Cendejas-Bueno et al., 2012). *C. auris* appears to be the most notable species at present due to its outbreak potential and high mortality rate (30–50%) (Calvo et al., 2016; de Almeida et al., 2016). After the first isolate from the external ear canal of a Japanese inpatient in 2009, a number of severe *C. auris* cases occurred subsequently in 17 countries from five continents

(Chowdhary et al., 2017; Mohsin et al., 2017; Arauz et al., 2018). Meanwhile, other phylogenetic related species (*C. haemulonii*, *C. duobushaemulonii,* and *C. pseudohaemulonii*) share similar characteristics of *C. auris* and are also emerging worldwide (Sugita et al., 2006; Ramos et al., 2015; Boatto et al., 2016; de Almeida et al., 2016; Fang et al., 2016; Kumar et al., 2016).

Besides the antifungal profile and outbreak characteristics, clinical intervention for *C. auris*, *C. haemulonii*, *C. duobushaemulonii,* and *C. pseudohaemulonii* infections are mainly challenged by diagnostic difficulties. Firstly, the most commonly used identification systems, e.g., VITEK and API-20C AUX, are time-consuming and tend to misidentify *C. auris* as other yeasts, such as *C. haemulonii*, *C. sake*, *C. famata*, *Rhodotorula glutinis*, *Saccharomyces cerevisiae* (Chowdhary et al., 2017). Secondly, more specific diagnostic methods (e.g., sequence-, RT-PCR- and MALDI-TOF MS- based) require high-cost equipment and trained technicians (Girard et al., 2016; Kordalewska et al., 2017). Thirdly, although there are some in-house developed detective systems, such as the updated MALDI-TOF MS library for *C. auris*, there is no FDA approved one that can be used in the clinic till now (Mizusawa et al., 2017).

The high cost, low accuracy and unavailability of current diagnostics tools may underestimate the global prevalence of these pathogens, especially in medically resource-limited regions (such as the Africa and Southeast Asia). Consequently, this may lead to the fact that nearly all the reported cases were from developed countries (such as United States, United Kingdom, and Germany) or medically developed cities in the low-income regions (such as New Delhi, India) (Kumar et al., 2016; Chowdhary et al., 2017; Rudramurthy et al., 2017).

Herein, the aim of our study is to establish a multiplex assay that can identify *C. auris*, *C. haemulonii*, *C. duobushaemulonii,* and *C. pseudohaemulonii*. Simplicity and affordability of our assay allow the researchers in developing countries to exploit our multiplex PCR assay as a robust screening tool.

MATERIALS AND METHODS

Fungal Isolates

Reference strains for the tetraplex PCR validation comprised *C. auris* (n = 138), *C. haemulonii* (n = 26), *C. duobushaemulonii* (n = 6), and *C. pseudohaemulonii* (n = 2) (**Table 1**). Human genomic DNA (Sigma–Aldrich, St. Louis, MO, United States) and 192 other fungal strains ranging from the closest to distant related species were used for specificity testing (**Table 2**). All the samples were obtained from the collection department of Westerdijk Fungal Biodiversity Institute in the form of freeze-dried powder. Subsequently the strains were incubated on Glucose Yeast Extract Peptone Agar plates at 25°C for 48 h, and subsequently pure colonies were confirmed by MALDI-TOF MS (Bruker, Billerica, MA, United States) and LSU sequencing (Vlek et al., 2014; Stielow et al., 2015).

DNA Sample Preparation

DNA extraction from pure colonies of yeast cells was performed using the CTAB method as previously described (Gupta et al., 2004). DNA was purified from blood and tissue (kidney) samples using the animal tissue and blood DNA isolation kit (DENAzist Asia, Mashhad, Iran) according to the manufacturer's instructions.

Primer Design and PCR Amplification

The 26s rDNA sequence were obtained from our own in-house database or from NCBI Nucleotide Database[1] and searched for species-specific and universal regions for primer design. Kordalewska et al. (2017) classified 47 *C. auris* isolates from India, Pakistan, Venezuela, Japan, and South Africa into four clades using Genome-wide SNP-based phylogenetic analyses, which indicated there is high genetic heterogeneity within *C. auris* globally. Considering this and also the large number of new cases after 2016, we designed the primers for *C. auris* by analyzing more isolates from a wider range. For the reverse specific primer for *C. auris*, we analyzed the 26S rDNA sequence of 233 isolates from Kuwait, Japan, Korea, Pakistan, South Africa, Venezuela, India, Malaysia, Israel, United States, and Oman. 137 sequences were done by ourselves and the rest were downloaded from Genbank. By alignment, genetic heterogeneity was easily found in 26S rDNA. Accordingly, a region which is stable within *C. auris*, and specific to other species was chosen for reverse primer. The primer system used in this assay were shown in **Figure 1**, which contained one universal forward primer (Uni-F: 5′-GAACGCACATTGCGCCTTGG-3′) and four species-specific primers (*C. auris*: Au-R, 5′-TCCAAAGGACTTGCCTGCT-3′; *C. duobushaemulonii*: Du-R,

[1]https://www.ncbi.nlm.nih.gov/nuccore/

TABLE 1 | Reference strains used for tetraplex PCR validation.

Species name	Strain code
C. auris (n = 138)	CBS 10913; CBS 12372; CBS 12373; CBS 12766; CBS 12767; CBS 12768; CBS 12769; CBS 12770; CBS 12771; CBS 12772; CBS 12773; CBS 12774; CBS 12775; CBS 12776; CBS 12777; CBS-12874; CBS 12875; CBS 12876; CBS 12877; CBS 12878; CBS 12880; CBS 12881; CBS 12882; CBS 12883; CBS 12884; CBS 12887; CBS 12886; Five clinical stains from Oman; 105 clinical strain for Kuwait
C. haemulonii (n = 26)	CBS 5149; CNM CL4642; CNM CL3458; CNM CL6800; CNM CL7793; CNM CL4640; CNM CL4641; CBS 7801; CBS 5150; CBS 6590; CBS 5468; CBS 7802; CBS 6332; CBS 10968; CBS 10969; CBS 10970; CBS 10971; CBS 10972; CBS 10973; CBS 12439; CBS 6915; CBS 12371; CNM CL7256; CNM CL7462; CNM CL7239T; CNM CL7073
C. duobushaemulonii (n = 6)	CBS 7800; CBS 7799; CBS 9754; CBS 6915; CBS 7798; CNM CL7829P
C. pseudohaemulonii (n = 2)	CBS 10004; CBS 12370

TABLE 2 | Fungal isolates for specificity test.

Species name	Strain code
Candida albicans	CBS 2704; CBS 2691; CBS 2697; CBS 1893; CBS 2712; CBS 5703; CBS 6552; CBS 2689; CBS 2690; CBS 2691; CBS 2695; CBS 2698; CBS 2696; CBS 5137; CBS 2702; CBS 1912; CLF-2; CLF-11; CLF-32; CLF-41; CLF-52; CLF-61; CLF-71; CLF-82; CLF-91; CLF-844; CLF-177; CLF-282; CLF-283; CLF-378; CLF-403; CLF-435; CLF-539; CLF-Llama 1; CLF-Llama 2; CLF-Llama 11
Candida africana	CBS 8781
Candida tropicalis	CBS 2313; CBS 94; CBS 1920; CLF-6; CLF-15; CLF-26; CLF-36; CLF-45; CLF-56; CLF-65; CLF-75; CLF-86
Candida parapsilosis	CBS 11045; CBS 7154; CBS 604; CBS 2197; CBS 2915; CBS 11059; CBS 11920; CBS 8050; CBS 2216; CBS 1954; CBS 2194; CBS 2211; CBS 11043; CBS 11359; CBS 7248; CBS 7156; CBS 10947; CBS 11130; CBS 7157; CBS 8836; CBS 2215; CBS 8181; CBS 12025; CBS 7155; CBS 6318; CBS 2196; CBS 2195; CLF-8; CLF-17; CLF-47; CLF-58; CLF-67; CLF-77; CLF-88; CLF-97
Candida metapsilosis	CBS 10907; CBS 2916; CBS 10747; CBS 11127; CBS 2315
Candida orthopsilosis	CBS 8825; CBS 9894; CBS 9348; CBS 10741; CBS 10906; CBS 11337; CBS 9347; CBS 10743; CBS 2212; CBS 10744; CBS 11698; CBS 10745; CBS 8548
Candida glabrata	CLF-4; CLF-13; CLF-24; CLF-34; CLF-43; CLF-63; CLF-73; CLF-83; CLF-84; CLF-93; CLF-310; CLF-611A; CLF-Llama 3; CLF-Llama 24; CLF-Llama 63
Candida krusei	CBS 5147; CLF-30; CLF-40; CLF-60; CLF-69; CLF-79; CLF-99; CLF-611B
Candida norvegensis	CBS 6564
Pichia cactophila	CBS 6926
Candida lusitaniae	CBS 6936; CLF-19
Candida famata	CBS 767
Candida dubliniensis	CLF-10; CLF-49
Candida guilliermondii	CBS 7099
Candida kefyr	STA#63
Candida sake	CBS 159
Candida rugosa	CBS 613
Candida zeylanoides	CBS 619
Yarrowia lipolytica	CBS 6124
Pichia fermentans	CBS 187
Pichia kluyveri	CBS 188
Pichia membranifaciens	CBS 107
Pseudozyma thailandica	CBS 10006
Kluyveromyces lactis var. lactis	CBS 683
Kluyveromyces marxianus	CBS 712
Kodamaea ohmeri	CBS 5367
Lindnera fabianii	CBS 5640
Lindnera jadinii	CBS 1600
Lodderomyces elongisporus	CBS 2605
Magnusiomyces capitatus	CBS 162.8
Metschnikowia pulcherrima	CBS 5833
Meyerozyma caribbica	CBS 9966
Millerozyma farinosa	CBS 185
Ogataea polymorpha	CBS 4732
Cryptococcus neoformans	CBS 8710; CBS 6885
Cryptococcus deneoformans	CBS6900; CBS10511
Cryptococcus gattii	CBS 7229; CBS 6289
Cryptococcus bacillisporus	CBS 6955; CBS 8755
Cryptococcus deuterogattii	CBS 10514; CBS 7750
Cryptococcus tetragattii	CBS 10101;
Cryptococcus decagattii	CBS 11687
Cryptococcus amylolentus	CBS 6039
Rhodotorula mucilaginosa	CBS 316
Saccharomyces cerevisiae	CBS 1171
Saccharomyces paradoxus	CBS 432
Trichosporon asahii	CBS 2479
Trichosporon inkin	CBS 5585
Debaryomyces nepalensis	CBS 5921
Exophiala dermatitidis	CBS 207.35
Galactomyces candidus	CBS 615.84
Hortaea werneckii	CBS 107.67
Hyphopichia burtonii	CBS 2352; CBS 2532
Torulaspora globosa	CBS 764
Wickerhamomyces anomalus	CBS 5759
Wickerhamomyces onychis	CBS 5587
Zygosaccharomyces rouxii	CBS 732
Schizosaccharomyces pombe	CBS 356
Schizosaccharomyces japonicus	CBS 354
Aspergillus fumigatus	CBS 114.55
Aspergillus flavus	CBS 107.45
Aspergillus niger	CBS 102.12
Aspergillus terreus	CBS 106.25
Aspergillus nidulans	CBS 100.20
Fusarium moniliforme	CBS 130180
Fusarium solani	CBS 101427
Aspergillus versicolor	CBS 106.57
Fusarium oxysporum	CBS 100.97

5′-GTAGACTTCGCTGCGGATATGTTA-3′; C. *haemulonii*: Ha-R, 5′-ATTGCGCCAGCATCCTTATTG-3′; *C. pseudohaemulonii*: Ps-R, 5′-GCACCCGATGCTGACAGTCTAC-3′). Primers were synthesized by Integrated DNA Technologies, Coralville, IA, United States.

A total volume of 50 μl PCR mixture containing 5 μl of buffer, 1.5 mM magnesium chloride, 2.5 units of *Taq* polymerase enzyme (BIO-21040, BioLine Company, London, United Kingdom), 0.2 mM dNTP (BIO-39043, BioLine Company, London, United Kingdom), 5 pM Uni-F primer, 5 pM Du-R, 2 pM Ps-R, 3 pM Au-R, and 10 pM Ha-R, 1 μl template DNA

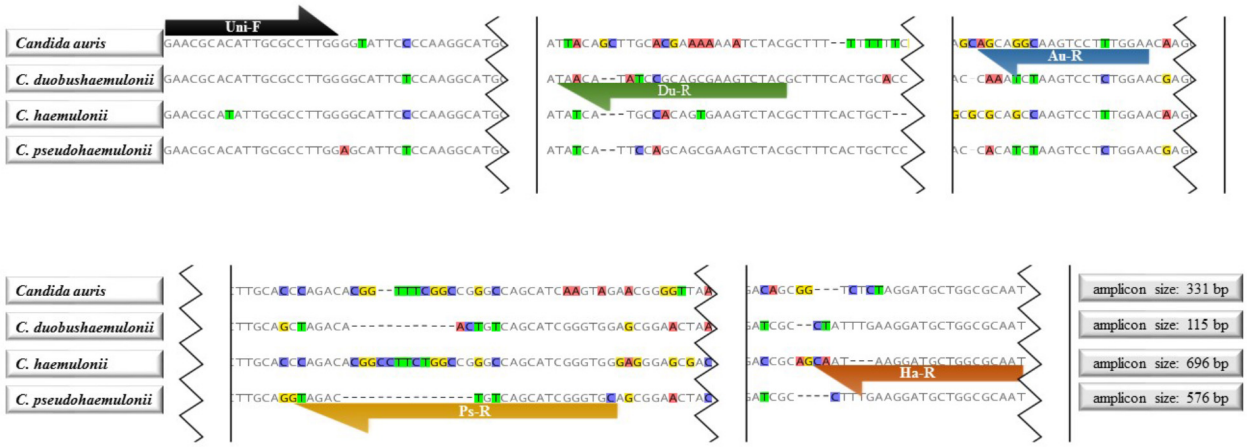

FIGURE 1 | Primer sequences and positions used in the tetraplex PCR. Uni-F: Universal forward primer for *Candida auris*, *C. duobushaemulonii*, *C. haemulonii,* and *C. pseudohaemulonii*; Du-R: *C. duobushaemulonii* specific reverse primer; Au-R: *C. auris* specific reverse primer; Ps-R: *C. pseudohaemulonii* specific reverse primer; Ha-R: *C. haemulonii* specific reverse primer.

or single colony pick (≈1 mm^3), and 38.3 μl Mili-Q water (Millipore Corporation, Billerica, MA, United States) was used for amplification of DNA from target species.

The PCR was performed using a 2720 thermal cycler (Applied Biosystems, Waltham, MA, United States), and the PCR program consisted of 5 min pre-denaturation at 94°C, followed by 35 cycles of 30 s at 94°C, 30 s at 62°C, 30 s at 72°C and 8 min at 72°C as final extension.

Validation via Animal Model

When certain infected human samples are not easily available for diagnostic validation, animal model can be an alternative (Bialek et al., 2001). To evaluate its potential use for infected human blood or tissue, animal models infected by the most important pathogens in *Metschnikowiaceae* clade, i.e., *C. auris* and *C. haemulonii,* were developed for diagnostic purpose. All procedures related to animal experiments were approved by the ethics and research committee of Mazandaran University of Medical Sciences, Sari, Iran.

Candida auris (CBS 10913, type strain), *C. haemulonii* (CBS 5149, type strains) and *C. albicans* (ATCC 29008, control) were cultured twice at 35°C for 48 h on Sabouraud dextrose agar (SDA, Difco). All isolates were subcultured in brain heart infusion broth and incubated at 37°C with shaking at 150 rpm. Supernatants were carefully removed and washed twice in sterile phosphate buffered saline (PBS). After centrifugation, the cells were washed in PBS and a hemocytometer was used to count the yeast cell. The yeast cell concentration was adjusted to an inoculum size of 5×10^5 yeast/ml. The viable counts of isolates were confirmed by 10-fold serially diluting the cell suspension on SDA plates.

Immunocompetent female ICR (CD-1 specific pathogen- free) mice with a mean weight of 22 g (purchased from Royan Institute, Tehran, Iran) were used in the study. Animals were housed at the accredited Animal Experimentation Facility in standard cages, received sterilized food and were monitored daily (Fakhim et al., 2018). Seven mice were allocated into each of the three mice groups infected with *C. auris*. *C. haemulonii* and *C. albicans*. Infection was induced in the mice for each group with an inoculum of 5×10^5 CFU/mouse in a volume of 0.2 ml into the lateral tail vein. No immunosuppressive scheme was used. Mice were checked daily and euthanized when symptoms of disseminated infection were detected. Any animal that had more than one of the criteria including, decreased activity, hunched posture, torticollis or barrel rolling, inability to eat or drink and hypothermia was humanly euthanized by intracardiac puncture under general anesthesia (Conti et al., 2014). Tissue sections were also stained with hematoxylin and eosin (H&E) for microscopic examination. Tissue (kidney) and blood samples were recovered under aseptic conditions. Tissue samples were homogenized in sterile saline and 100 μl of homogenate was cultured on SDA at 35°C to confirm *Candida* infection and determine the colony forming units (CFU) were determine (Fakhim et al., 2018). All yeast cells cultures were identified by our tetraplex PCR. In addition, 100 μl of each EDTA-blood sample was cultured on SDA plates. The rest of the homogenate and blood samples were used for tetraplex PCR test.

Application in Clinical Setting

A single-center prospective clinical screening for *C. auris*, *C. duobushaemulonii*, *C. haemulonii* and *C. pseudohaemulonii* was performed during 2017.05.01 to 2017.11.01 in Shanghai Changzheng Hospital, China. The newly developed multiplex PCR system worked as a supplementary tool to BD BACTEC™ FX40 Instrument (Becton, Dickinson and Company, Franklin Lakes, NJ, United States), CHROMagar™ Candida (CHROMagar Microbiology, Paris, France) and microscopic examination to finding infection cases by the targeted species. In order to further test the specificity of our assay using more clinical isolates, we used a wide range of sample types for screening, including blood, sputum, feces, bronchoalveolar lavage fluid and oral swab. We test all the clinical yeast isolates that are identified by CHROMagar™ Candida as non-*albicans*

Candida species. As soon as the clinical culture is obtained by conventional diagnostic methods, single colony (≈1 mm^3) is tested by this multiplex PCR system. DNA extraction and ITS sequencing are done as well to confirm the accuracy of the assay in the clinical settings as described before (Stielow et al., 2015).

Two hundred and fifty five clinical non-*albicans Candida* isolates (identified by CHROMagar™ Candida) from Mazandaran University of Medical Sciences, Iran, were used as a retrospective screening sample in this study. The isolates were collected from blood, sputum, feces, oral swab and vaginal samples during 2016.1–2017.6. Multiplex PCR were performed, and MALDI-TOF and LSU sequencing were done as well to confirm the accuracy of the assay in the clinical settings (Vlek et al., 2014; Stielow et al., 2015).

All the tests were approved by the ethics and research committees of Shanghai Changzheng Hospital and Mazandaran University of Medical Sciences.

RESULTS

Analytical Validation

Figure 2 showed that four amplicons exhibited major bands that could be differentiated from each other. The gel figure for all the strains of *C. auris* and its relatives tested in this study was shown in **Supplementary Figure S1**. Sequencing results of PCR amplicons were 100% matched with the targeted species. Human genomic DNA and 192 other fungal species were tested, and no cross-reactivity was found (100% specificity).

Animal Model Testing

Figure 3 showed the detailed information of the animal model testing.

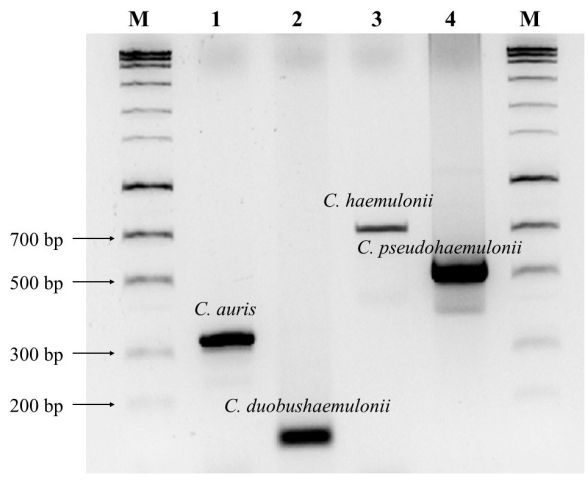

FIGURE 2 | Agarose gel electrophoresis (2% agarose) of PCR amplicons. Lanes 1–4 are *C. auris* (CBS 10913 type, 331 bp), *C. duobushaemulonii* (CBS 7798 type, 115 bp), *C. haemulonii* (CBS 5149 type, 696 bp) and *C. pseudohaemulonii* (CBS 10004 type, 576 bp), respectively. Lane M, HyperLadder™ 100 bp (Bioline, London, United Kingdom).

Application of the tetraplex PCR in blood showed a higher overall positive rate (4 of 14, 28.6%) than blood culture positive rate (1 of 14, 7.1%) in animal models of *C. auris* and *C. haemulonii*. Specifically, three *C. auris* (3/7, on the 3rd, 4th, and 5th day post-infection (PI)) and one *C. haemulonii* (1/7, on the 5th day, PI) infected mice showed positive PCR results from blood, without cross-reactivity in *C. albicans* group (0/7). Culture results were positive only in one blood samples of *C. auris* (1/7, on the 4th day, PI), negative in all *C. haemulonii* infected mice (0/7), and positive in three *C. albicans* infected mice (3/7, on the 3rd, 4th, and 5th day PI), with CFUs ranging from 1 to 6 colonies in 100 μl.

The overall positive PCR rate of mice kidney samples was 92.8% (13/14) among *C. auris* and *C. haemulonii*, without cross-reactivity in *C. albicans* group (0/7). Among the kidney samples from 21 mice examined by culture, 19 were positive due to *C. auris* (7/7), *haemulonii* (6/7), and *C. albicans* (6/7) with CFUs ranging from 8.3×10 to 4.3×10^4 colonies in 100 μl (mean 3.5×10^3 colonies).

Clinical Validation

Applying our assay in a prospective (566 clinical isolates) and a retrospective cohorts (255 clinical isolates), revealed one *C. haemulonii* isolate (S49AF, accession number: KY112738) from Iran and one *C. haemulonii* isolate (SCZ90793, accession number: MG637448), one *C. duobushaemulonii* isolate (SCZ91445, accession number: MG963993) and one *C. pseudohaemulonii* isolate (SCZ90800, accession number: MG242063) from China. Specifically, the Chinese *C. pseudohaemulonii* was isolated from sputum of a 65-year-old male who suffered from lower esophageal resection (Shanghai, China). To our knowledge this the first isolate of C. *pseudohaemulonii* from China. Whereas the Iranian *C. haemulonii* isolate was recovered from toenail sample of a 36-year-old diabetic male in 2016 (Shiraz, Iran), and also was the first *C. haemulonii* isolate from Iran.

DISCUSSION

Achieving a timely and accurate diagnosis of infections caused by *C. auris* and its phylogenetic relatives is of great difficulty in clinical settings (Mizusawa et al., 2017). Nearly all the *C. auris* isolates were misdiagnosed as *C. haemulonii*, *C. sake*, *C. famata*, *Rhodotorula glutinis*, *Saccharomyces cerevisiae* by clinical commercial methods such as Vitek-2 YST ID system, API-20C AUX, AuxaColor 2, BD Phoenix, and MicroScan (Chowdhary et al., 2017). Studies also showed that *C. pseudohaemulonii* failed to be distinguished from *C. haemulonii* by these methods (Kim et al., 2009). All the identifications from the biochemical assays should be confirmed by sequencing. The Centers for Disease Control of America speculated that the unavailability of appropriate diagnostic method underestimate its prevalence in many countries (Sarma and Upadhyay, 2017), which includes medical resource-limited regions. Hence, we developed a novel end-point tetraplex PCR system in a low-cost, rapid and accurate format. This novel assay

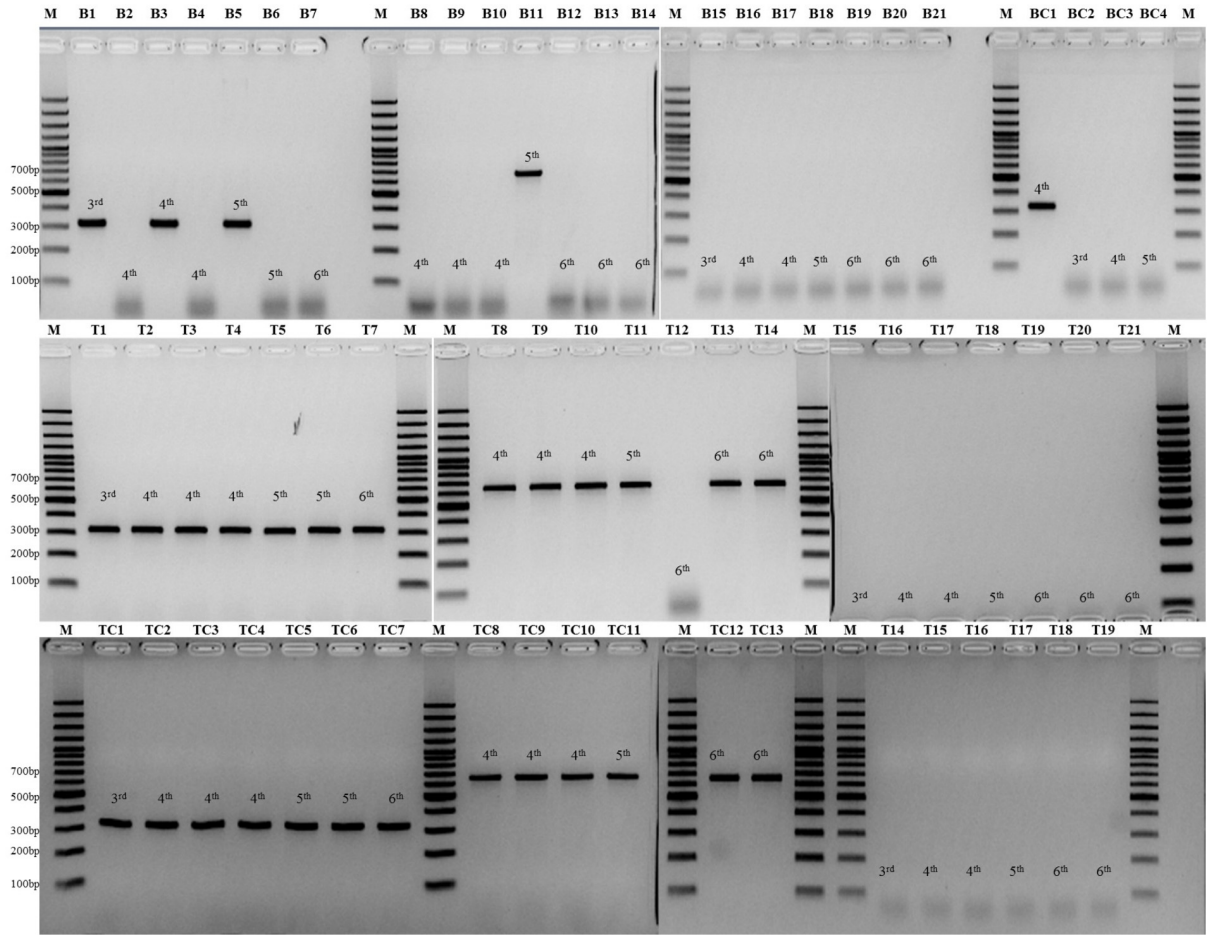

FIGURE 3 | Lanes B1–B7 are PCR results of blood sample from seven mice infected with *C. auris*; Lanes B8-B14 are PCR results of blood sample from seven mice infected with *C. haemulonii*; Lanes B15-B21 are PCR results of blood sample from seven mice infected with *C. albicans*; Lane BC1–4 are PCR results of four cultured strains from blood samples of all the 21 mice; Lanes T1–T7 are PCR results of kidney tissue sample from seven mice infected with *C. auris*; Lanes T8–T14 are PCR results of kidney tissue sample from seven mice infected with *C. haemulonii*; Lanes T15–T21 are PCR results of kidney tissue sample from seven mice infected with *C. albicans*; Lane TC1–7 are PCR results of seven cultured strains from kidney samples of mice infected with *C. auris*; Lane TC8–13 are PCR results of six cultured strains from kidney samples of mice infected with *C. haemulonii*; Lane TC14–19 are PCR results of six cultured strains from kidney samples of mice infected with *C. albicans*; Lane M, GeneRuler 100 bp Plus DNA Ladder (Thermo Fisher, Waltham, MA, United States).

has been validated by a large number of CBS/clinical isolates, diagnostic animal models and clinical application. We hope this assay can help to understand the global clinical impact of *C. auris* and its relatives, especially in the under-served and poor regions.

Our new end-point tetraplex PCR was designed to identify and differentiate the most medically important and related species to *C. auris*. Recently, two real-time PCR based assays for *C. auris* were developed (Kordalewska et al., 2017; Leach et al., 2017). Compared with the real-time PCR method, our end-point PCR is non-automated and labor-intensive. The electrophoresis step of our assay normally required 45 min, which is more time-consuming than real-time PCRs. Additionally, since the nature of end-point PCR, our assay is unable to quantify the fungal load of host. However, the advantages of our assay over theirs are also obvious.

Kordalewska et al. (2017) established the first SYBR Green real-time PCR system for *C. auris*, *C. duobushaemulonii*, *C. haemulonii,* and *C. lusitaniae*; While Leach et al. (2017) developed a probe-based singleplex real-time PCR only for *C. auris*. Considering the high misdiagnostic rate between *C. auris, C. haemulonii*, *C. duobushaemulonii,* and *C. pseudohaemulonii*, and higher resistance of *C. pseudohaemulonii* to AMB than *C. auris, C. haemulonii, C. duobushaemulonii,* and *C. lusitaniae* (Kim et al., 2009; Shin et al., 2012), we used a multiplex strategy for this assay and included *C. pseudohaemulonii* instead of *C. lusitaniae.* Among the selected species, *C. haemulonii* initially was known as a multi-antifungal resistant pathogen since the first case report in 1984, and it can cause outbreaks and infect immunocompetent individuals (Loosova et al., 2001; Khan et al., 2007). Subsequently, *C. haemulonii* was recognized as a complex species and reclassified as *C. haemulonii, C. duobushaemulonii,* and *C. haemulonii var. vulnera* (Cendejas-Bueno et al., 2012). *C. auris* and *C. pseudohaemulonii* were described in 2009 and

2006, respectively. Both of them were multi-antifungal resistant pathogens and the latter is spreading across the world at an accelerated pace (Sugita et al., 2006; Chowdhary et al., 2017). Correct species-level identification for the four species is needed due to the clinical importance and heterogeneity in terms of taxonomy, spreading prevalence and antifungal susceptibility profile.

Our multiplex PCR system is the first assay for *C. auris* that has been validated by animal model testing. The overall PCR positive rates of mice blood and tissue were 28.6 and 92.9%, respectively, which showed slightly higher performance than culture based identification. And PCR/culture from tissue samples showed higher value than those from blood for diagnosing infections caused by these pathogens. Moreover, our new assay is much faster than culture based identification. PCR directly from tissue/blood only requires 3 h from sample preparation to result read-out; while culture based identification is more time-consuming (normally 1–3 days).

Our new assay is also featured by its low cost and potential to be used in medical resource-limited settings. Due to the poor economic condition, lack of basic medical facilities and the relatively poor population health, the developing countries were reported to have a much higher risk of infections than the developed ones (Pittet et al., 2008). Among the 17 countries reported with *C. auris* prevalence, seven are the developing ones (Oman, Venezuela, Colombia, South Africa, Kenya, Pakistan, and India). Considering this, our new assay was established to help to extend the global knowledge of the epidemiology of these important and emerging pathogens, especially for medical resource-limited countries. Compared with MALDI-TOF and real-time PCR cycler, end-point PCR cycler used in this assay is more portable and much cheaper ($130–$4,000 per cycler) (Wong et al., 2015). For clinical validation, we used isolates from two clinical settings that can represent different situations of medical care in developing countries (Shanghai, China and Sari, Iran). In Shanghai, specific diagnostic tools such as MALDI-TOF and sequencing are available to most hospitals. However, since China is a developing country, there are still a large number of patients that cannot afford these tests. While in Iran, to our knowledge, there is no MALDI-TOF and sequencing machine. There was only one epidemiology study related to *C. haemulonii* and *C. duobushaemulonii* in China and no epidemiology data is available in Iran (Hou et al., 2016). Hence, we hold the prevalence of *C. auris* and its close related relatives are underestimated due to the lack of low-cost and accurate assays in both countries. By using this assay, we successfully found the first clinical isolates of *C. haemulonii* in Iran and first clinical isolates of *C. pseudohaemulonii* in China. However, no *C. auris* isolate was found in both cohorts.

CONCLUSION

The novel end-point tetraplex PCR for *C. auris* and its phylogenetic relatives is rapid and 100% specific. Clinical validation and animal model testing further proved its clinical performance. This assay only requires the simple devices of end-point PCR cycler and electrophoresis instrument, showing its availability and affordability to most of the developing countries, and can contribute to a better understanding of the clinical occurrence of *C. auris* and its relatives.

ETHICS STATEMENT

This study was carried out in accordance with the recommendations of Guide for the Care and Use of Laboratory Animals, committee of the Update of the Guide of the Care and Use of Laboratory Animals. The protocol was approved by the Ethics and Research Committee of Mazandaran University of Medical Sciences, Sari, Iran (No. 2321).

AUTHOR CONTRIBUTIONS

AA and WF participated in primer design, PCR optimization, data collection, and drafted the manuscript. WP, FH, and TB participated in designing this study and revising the manuscript. HB and AV participated in animal model testing and collecting Iranian clinical isolates. WJ participated in clinical validation in China. All authors contributed to the writing of the final manuscript.

FUNDING

This work was supported by the Major National R&D Projects of the National Health Department (2018ZX10101003), European Union's Horizon 2020 research and innovation program under the Marie Sklodowska-Curie grant agreement No. 642095, National Natural Science Foundation of China (31770161), Shanghai Science and Technology Committee (Grant Nos. 14DZ2272900 and 14495800500).

SUPPLEMENTARY MATERIAL

The Supplementary Material for this article can be found online at: https://www.frontiersin.org/articles/10.3389/fmicb.2018.01119/full#supplementary-material

FIGURE S1 | Gel figure for all the strains of *C. auris* and its relatives tested in this study.

REFERENCES

Araúz, A. B., Caceres, D. H., Santiago, E., Armstrong, P., Arosemena, S., Ramos, C., et al. (2018). Isolation of *Candida auris* from 9 patients in Central America: importance of accurate diagnosis and susceptibility testing. *Mycoses* 61, 44–47. doi: 10.1111/myc.12709

Bialek, R., Fischer, J., Feucht, A., Najvar, L. K., Dietz, K., Knobloch, J., et al. (2001). Diagnosis and monitoring of murine histoplasmosis by a nested

PCR assay. *J. Clin. Microbiol.* 39, 1506–1509. doi: 10.1128/jcm.39.4.1506-1509.2001

Boatto, H. F., Cavalcanti, S. D., Del Negro, G. M., Girao, M. J., Francisco, E. C., Ishida, K., et al. (2016). *Candida duobushaemulonii*: an emerging rare pathogenic yeast isolated from recurrent vulvovaginal candidiasis in Brazil. *Mem. Inst. Oswaldo Cruz* 111, 407–410. doi: 10.1590/0074-02760160166

Calvo, B., Melo, A. S., Perozo-Mena, A., Hernandez, M., Francisco, E. C., Hagen, F., et al. (2016). First report of *Candida auris* in America: clinical and microbiological aspects of 18 episodes of candidemia. *J. Infect.* 73, 369–374. doi: 10.1016/j.jinf.2016.07.008

Cendejas-Bueno, E., Kolecka, A., Alastruey-Izquierdo, A., Theelen, B., Groenewald, M., Kostrzewa, M., et al. (2012). Reclassification of the *Candida haemulonii* complex as *Candida haemulonii* (*C. haemulonii* group I), *C. duobushaemulonii* sp. nov. (*C. haemulonii* group II), and *C. haemulonii* var. *vulnera* var. nov.: three multiresistant human pathogenic yeasts. *J. Clin. Microbiol.* 50, 3641–3651. doi: 10.1128/JCM.02248-12

Chowdhary, A., Sharma, C., and Meis, J. F. (2017). *Candida auris*: a rapidly emerging cause of hospital-acquired multidrug-resistant fungal infections globally. *PLoS Pathog.* 13:e1006290. doi: 10.1371/journal.ppat.1006290

Conti, H. R., Huppler, A. R., Whibley, N., and Gaffen, S. L. (2014). Animal models for candidiasis. *Curr. Protoc. Immunol.* 105, 11–17. doi: 10.1002/0471142735.im1906s105

de Almeida, J. N. Jr., Assy, J. G., Levin, A. S., Del Negro, G. M., Giudice, M. C., Tringoni, M. P., et al. (2016). *Candida haemulonii* complex species. *Emerg. Infect. Dis.* 22, 561–563. doi: 10.3201/eid2203.151610

Fakhim, H., Vaezi, A., Dannaoui, E., Chowdhary, A., Nasiry, D., Faeli, L., et al. (2018). Comparative virulence of *Candida auris* with *Candida haemulonii*, *Candida glabrata* and *Candida albicans* in a murine model. *Mycoses* 61, 377–382. doi: 10.1111/myc.12754

Fang, S. Y., Wei, K. C., Chen, W. C., Lee, S. J., Yang, K. C., Wu, C. S., et al. (2016). Primary deep cutaneous candidiasis caused by *Candida duobushaemulonii* in a 68-year-old man: the first case report and literature review. *Mycoses* doi: 10.1111/myc.12540 [Epub ahead of print].

Fang, W., Zhang, L., Liu, J., Denning, D. W., Hagen, F., Jiang, W., et al. (2017). Tuberculosis/cryptococcosis co-infection in China between 1965 and 2016. *Emerg. Microbes Infect.* 6:e73. doi: 10.1038/emi.2017.61

Girard, V., Mailler, S., Chetry, M., Vidal, C., Durand, G., van Belkum, A., et al. (2016). Identification and typing of the emerging pathogen *Candida auris* by matrix-assisted laser desorption/ionisation time of flight mass spectrometry. *Mycoses* 59, 535–538. doi: 10.1111/myc.12519

Gupta, A. K., Boekhout, T., Theelen, B., Summerbell, R., and Batra, R. (2004). Identification and typing of *Malassezia* species by amplified fragment length polymorphism and sequence analyses of the internal transcribed spacer and large-subunit regions of ribosomal DNA. *J. Clin. Microbiol.* 42, 4253–4260. doi: 10.1128/JCM.42.9.4253-4260.2004

Hou, X., Xiao, M., Chen, S. C., Wang, H., Cheng, J. W., Chen, X. X., et al. (2016). Identification and antifungal susceptibility profiles of *Candida haemulonii* species complex clinical isolates from a multicenter study in China. *J. Clin. Microbiol.* 54, 2676–2680. doi: 10.1128/jcm.01492-16

Khan, Z. U., Al-Sweih, N. A., Ahmad, S., Al-Kazemi, N., Khan, S., Joseph, L., et al. (2007). Outbreak of fungemia among neonates caused by *Candida haemulonii* resistant to amphotericin B, itraconazole, and fluconazole. *J. Clin. Microbiol.* 45, 2025–2027. doi: 10.1128/JCM.00222-07

Kim, M. N., Shin, J. H., Sung, H., Lee, K., Kim, E. C., Ryoo, N., et al. (2009). *Candida haemulonii* and closely related species at 5 university hospitals in Korea: identification, antifungal susceptibility, and clinical features. *Clin. Infect. Dis.* 48, e57–e61. doi: 10.1086/597108

Kordalewska, M., Zhao, Y., Lockhart, S. R., Chowdhary, A., Berrio, I., and Perlin, D. S. (2017). Rapid and accurate molecular identification of the emerging multidrug resistant pathogen *Candida auris*. *J. Clin. Microbiol.* 55, 2445–2452. doi: 10.1128/JCM.00630-17

Kumar, A., Prakash, A., Singh, A., Kumar, H., Hagen, F., Meis, J. F., et al. (2016). *Candida haemulonii* species complex: an emerging species in India and its genetic diversity assessed with multilocus sequence and amplified fragment-length polymorphism analyses. *Emerg. Microbes Infect.* 5:e49. doi: 10.1038/emi.2016.49

Leach, L., Zhu, Y., and Chaturvedi, S. (2017). Development and validation of a real-time PCR assay for rapid detection of *Candida auris* from surveillance samples. *J. Clin. Microbiol.* 56:e01223-17. doi: 10.1128/jcm.01223-17

Loosova, G., Jindrak, L., and Kopacek, P. (2001). Mortality caused by experimental infection with the yeast *Candida haemulonii* in the adults of *Ornithodoros moubata* (Acarina: argasidae). *Folia Parasitol.* 48, 149–153. doi: 10.14411/fp.2001.023

Miceli, M. H., Diaz, J. A., and Lee, S. A. (2011). Emerging opportunistic yeast infections. *Lancet Infect. Dis.* 11, 142–151. doi: 10.1016/S1473-3099(10)70218-8

Mizusawa, M., Miller, H., Green, R., Lee, R., Durante, M., Perkins, R., et al. (2017). Can multidrug-resistant *Candida auris* be reliably identified in clinical microbiology laboratories? *J. Clin. Microbiol.* 55, 638–640. doi: 10.1128/jcm.02202-16

Mohsin, J., Hagen, F., Al-Balushi, Z. A. M., de Hoog, G. S., Chowdhary, A., Meis, J. F., et al. (2017). The first cases of *Candida auris* candidaemia in Oman. *Mycoses* 60, 569–575. doi: 10.1111/myc.12647

Pittet, D., Allegranzi, B., Storr, J., Bagheri Nejad, S., Dziekan, G., Leotsakos, A., et al. (2008). Infection control as a major world health organization priority for developing countries. *J. Hosp. Infect.* 68, 285–292. doi: 10.1016/j.jhin.2007.12.013

Ramos, L. S., Figueiredo-Carvalho, M. H., Barbedo, L. S., Ziccardi, M., Chaves, A. L., Zancope-Oliveira, R. M., et al. (2015). *Candida haemulonii* complex: species identification and antifungal susceptibility profiles of clinical isolates from Brazil. *J. Antimicrob. Chemother.* 70, 111–115. doi: 10.1093/jac/dku321

Rudramurthy, S. M., Chakrabarti, A., Paul, R. A., Sood, P., Kaur, H., Capoor, M. R., et al. (2017). *Candida auris* candidaemia in Indian ICUs: analysis of risk factors. *J. Antimicrob. Chemother.* 72, 1794–1801. doi: 10.1093/jac/dkx034

Sarma, S., and Upadhyay, S. (2017). Current perspective on emergence, diagnosis and drug resistance in *Candida auris*. *Infect. Drug Resist.* 10, 155–165. doi: 10.2147/idr.s116229

Shin, J. H., Kim, M. N., Jang, S. J., Ju, M. Y., Kim, S. H., Shin, M. G., et al. (2012). Detection of amphotericin B resistance in *Candida haemulonii* and closely related species by use of the Etest, Vitek-2 yeast susceptibility system, and CLSI and EUCAST broth microdilution methods. *J. Clin. Microbiol.* 50, 1852–1855. doi: 10.1128/JCM.06440-11

Stielow, J. B., Levesque, C. A., Seifert, K. A., Meyer, W., Iriny, L., Smits, D., et al. (2015). One fungus, which genes? Development and assessment of universal primers for potential secondary fungal DNA barcodes. *Persoonia* 35, 242–263. doi: 10.3767/003158515x689135

Sugita, T., Takashima, M., Poonwan, N., and Mekha, N. (2006). *Candida pseudohaemulonii* Sp. Nov., an amphotericin B-and azole-resistant yeast species, isolated from the blood of a patient from Thailand. *Microbiol. Immunol.* 50, 469–473. doi: 10.1111/j.1348-0421.2006.tb03816.x

Vlek, A., Kolecka, A., Khayhan, K., Theelen, B., Groenewald, M., Boel, E., et al. (2014). Interlaboratory comparison of sample preparation methods, database expansions, and cutoff values for identification of yeasts by matrix-assisted laser desorption ionization-time of flight mass spectrometry using a yeast test panel. *J. Clin. Microbiol.* 52, 3023–3029. doi: 10.1128/JCM.00563-14

Wong, G., Wong, I., Chan, K., Hsieh, Y., and Wong, S. (2015). A rapid and low-cost PCR thermal cycler for low resource settings. *PLoS One* 10:e0131701. doi: 10.1371/journal.pone.0131701

Conflict of Interest Statement: The authors declare that the research was conducted in the absence of any commercial or financial relationships that could be construed as a potential conflict of interest.

Laboratory Investigation
https://doi.org/10.1038/s41374-018-0126-4

ARTICLE

Vitamin D protects human melanocytes against oxidative damage by activation of Wnt/β-catenin signaling

Luyan Tang[1,2] · Wei Fang[1,3] · Jinran Lin[1,2] · Jian Li[1,2] · Wenyu Wu[1,2] · Jinhua Xu[1,2]

Received: 1 April 2018 / Revised: 6 July 2018 / Accepted: 9 August 2018

Abstract

Vitamin D analogs have been widely utilized for the treatment of vitiligo, but the molecular mechanism underlying their pharmacological effects (especially their antioxidant properties) has not yet been investigated. We evaluated the relationship between serum vitamin D level and oxidative damage severity in vitiligo patients, and investigated the molecular mechanism of vitamin D in protecting melanocytes against oxidative stress. Serum levels of 25-hydroxyvitamin D and malondialdehyde (MDA) were first measured in patients. A variety of in vitro experiments such as intracellular reactive oxygen species (ROS), cellular viability, migration, and apoptotic assays were then performed to detect the effects of vitamin D or β-catenin silencing on H_2O_2-treated melanocytes. Expression of Wnt/β-catenin, Nrf2, apoptotic, and MITF pathways was finally examined using quantitative real-time PCR and western blot. In this study, we initially found that vitamin D insufficiency was closely associated with the severity of oxidative stress in vitiligo patients. Using ex vivo cell models, we further showed that vitamin D positively modulated β-catenin signaling at both translational and posttranslational levels in melanocytes under oxidative stress. Like WNT agonists, vitamin D significantly inhibited ROS accumulation and cell apoptosis in H_2O_2-treated melanocytes and promoted their proliferative and migratory activity, while the protective effects of vitamin D against oxidative stress were abolished by β-catenin silencing in melanocytes. Furthermore, β-catenin deficiency also blocked the activation of Nrf2 and MITF as well as the inhibition of apoptosis induced by vitamin D. Taken together, vitamin D insufficiency was associated with severity of oxidative stress in vitiligo patients. Our work also provides new insights into the mechanism of vitamin D against vitiligo, in which vitamin D protects melanocytes against oxidative stress by activating Wnt/β-catenin signaling.

Introduction

Vitiligo is an acquired skin disease characterized by progressive depigmentation due to localized destruction of epidermal melanocytes. The etiology of vitiligo is still not fully understood, but several factors have been implicated in the melanocyte destruction, such as oxidative stress, autoimmunity, and genetic predisposition [1–4]. Among them, oxidative stress has been attracting increasing attention. It can directly damage lipids and proteins, leading to functional impairment or cell apoptosis of melanocytes, and also initiate the autoimmune response that subsequently mediates melanocyte cytotoxicity 5, 6]. Therefore, antioxidant treatment has become a promising therapeutic direction for vitiligo.

Vitamin D exerts potent physiological and pharmacological actions through its nuclear receptor (VDR) in various cell types, and thus it has great potential for treating a

These authors contributed equally: Luyan Tang, Wei Fang

Electronic supplementary material The online version of this article (https://doi.org/10.1038/s41374-018-0126-4) contains supplementary material, which is available to authorized users.

✉ Wenyu Wu
wuwenyu@medmail.com.cn

✉ Jinhua Xu
xjhhsyy@163.com

[1] Department of Dermatology, Huashan Hospital, Fudan University, Shanghai, China

[2] The Shanghai Institute of Dermatology, Shanghai, China

[3] Shanghai Key Laboratory of Molecular Medical Mycology, Department of Dermatology and Venereology, Changzheng Hospital, Second Military Medical University, Shanghai, China

Published online: 11 September 2018

variety of diseases such as osteoporosis, cancer, and autoimmune diseases [7]. Vitamin D analogs (particularly calcipotriol and tacalcitol) have been widely utilized as topical therapeutic agents in vitiligo [8, 9]. In addition, serum vitamin D insufficiency and VDR gene polymorphisms were also reported in vitiligo patients, further highlighting the significance of vitamin D against vitiligo [10–12]. The multipronged effect of vitamin D analogs against vitiligo has been confirmed in several studies. For example, vitamin D compounds can modulate the proliferation, differentiation, migration, and apoptosis of melanocytes, and influence the local immune response by regulating T cell activation in vitiligo [8, 13–15]. A recently proposed mechanism involving the pharmacological action of vitamin D against vitiligo is based on its antioxidant properties since oxidative stress is crucial during the onset and progression of vitiligo [16, 17]. However, the molecular mechanism by which vitamin D protects human melanocytes against oxidative damage is still not clear.

Canonical Wnt signaling is a fundamental mechanism that governs cell proliferation, differentiation, and apoptosis by regulating the amount of the transcriptional coactivator β-catenin [18–20]. In the absence of Wnt signaling, cytoplasmic β-catenin is constitutively degraded via destruction of the Axin complex. When Wnt binds to Frizzled receptor (Fz) and its co-receptor (LRP6 or LRP5), Wnt/β-catenin signaling is activated. Formation of the Wnt–Fz–LRP6 complex together with recruitment of the scaffolding protein Dishevelled (Dvl) further mediates the disassembly of the destruction complex, and thus the stabilization of β-catenin, which accumulates and travels to the nucleus and activates target gene expression. β-catenin stabilization is negatively associated with the activity of glycogen synthase kinase 3β (GSK3β), which is an essential component of the destruction complex [20]. Recently, some studies have found that Wnt/β-catenin signaling is inhibited in H_2O_2-treated keratinocytes and melanocytes, while Wnt agonists trigger melanocyte differentiation and melanogenesis in vitiligo [21, 22]. In addition, Wnt/β-catenin pathway has also been shown to be responsible for the protection of vitamin D against oxidative stress in other types of cells such as osteoblasts and nephrocytes [23, 24]. Thus, we hypothesized that vitamin D protects human melanocytes from oxidative stress by activating Wnt/β-catenin signaling.

Materials and methods

Patient and control specimens

After obtaining informed written consent, blood samples were collected from 53 vitiligo patients with non-segmental disease (29 men and 24 women; 37 active and 16 stable; age range, 11–57 years; mean age, 30 years) and from 23 healthy controls (10 men and 13 women; age range, 18–60 years; mean age, 33 years). The lesional area in all vitiligo patients was more than 3% of the body area. None of the patients underwent any systemic or topical treatment 3 months before the blood samples were obtained. This study was approved by the local ethics committee of Huashan Hospital and performed in strict compliance with the principles of the Declaration of Helsinki.

Serum MDA and vitamin D measurement

Serum MDA levels were tested using the thiobarbituric acid (TBA) reactive substances assay (Nanjing Jiancheng Bioengineering Institute, Nanjing, China) [25]. MDA is an oxidative degradation product of lipids, which reacts with TBA and then forms red complexes with the absorbent at 532 nm. Serum vitamin D (25-hydroxyvitamin D) was detected using an enzyme-linked immunosorbent assay kit (Groundwork Biotechnology Diagnosticate Ltd, San Diego, CA, USA), according to the manufacturer's protocol. The 25-hydroxyvitamin D levels were divided into 'sufficiency' (>75 nmol/L), 'insufficiency' (≥25 nmol/L but <75 nmol/L), and 'deficiency' (<25 nmol/L) as previously reported [26].

Cell culture and treatment

The immortalized human epidermal melanocyte cell lines PIG1 (normal melanocytes) and PIG3V (vitiligo melanocytes) were gifts from Dr. Caroline Le Poole (Loyola University Chicago, Maywood, IL) and cultured in Medium 254 (Cascade Biologics/Invitrogen, Portland, OR, USA) supplemented with human melanocyte growth supplement (Cascade Biologics/Invitrogen), 5% fetal bovine serum (Invitrogen, CA, USA), and penicillin–streptomycin antibiotic mix (Invitrogen) at 37 °C in the presence of 5% CO_2 [27]. Melanocytes were pretreated with 1 nM 1,25-dihydroxyvitamin D3 (D1530, Sigma) or 40 μM SKL2001 (S8230, Selleck, USA) for 24 h as in previous studies [21, 28]. Oxidative stress was then induced by addition of 0.5 mM H_2O_2 (Sigma) for another 24 h.

Determination of cell viability by the CCK-8 assay

Cell viability was measured using the CCK-8 assay (Cell Counting Kit-8; Beyotime Institute of Biotechnology, Haimen, China) to count living cells following the manufacturer's protocol. PIG1 or PIG3V cells were seeded into 96-well plates (3×10^3 cells per well) in quadruplicate. After treatment with the indicated agents, 10 μL of CCK-8

reagent was added to 90 μL medium and incubated for 90 min at 37 °C. Cell viability was determined by monitoring the color change using an ELISA plate reader (Bio-Rad, Hercules, CA, USA) at an absorbance of 450 nm.

Apoptosis detection by Annexin V-FITC

Melanocytes were cultured in six-well plates at a density of 1.2×10^6 cells for PIG1 and 0.8×10^6 cells for PIG3V. Cell apoptosis was evaluated using the Annexin V-FITC Apoptosis Detection Kit (MaiBio, Shanghai, China). FITC fluorescence was detected using a flow cytometer (Beckman Coulter, Miami, USA) and analyzed with the Expo32 software (Beckman Coulter).

Transwell migration assay

Cell migration was evaluated in Transwell cell culture chambers (Costar 3422; Cambridge, MA, USA) as previously described [29]. PIG1 and PIG3V cells were treated with 0.5 mM H_2O_2 for 24 h and then seeded into the top chambers of the Transwell in medium containing 1 nM 1,25-dihydroxyvitamin D3 or 40 μM SKL2001 for 48 h. The bottom chambers of the Transwell were filled with 500 μL 10% FBS supplemented with different treatments. Non-migrating cells on the top surface of the membrane were scraped with a cotton swab, and the cells that had traveled to the bottom side (migrating cells) were fixed with cold 4% paraformaldehyde for 10 min. Migrating cells were stained with 0.1% hexamethyl pararosaniline, imaged with a Nikon microscope, and then quantified by manual counting.

Measurement of intracellular reactive oxygen species (ROS)

Melanocytes were seeded into 96-well plates at a density of 6×10^3 cells for PIG1 and 3×10^3 cells for PIG3V. Following the indicated treatments, intracellular ROS levels were determined using the fluorescent probe H2DCFDA (Thermofisher, MA, USA) according to the manufacturer's protocol.

RNA isolation and quantitative real-time PCR

Total RNA was isolated using TRIzol reagent (Invitrogen) and then reverse-transcribed into cDNA using the SuperScript III First-Strand Synthesis Kit (Invitrogen). Subsequent real-time PCR was performed using iQ SYBR Green Supermix (Bio-Rad) per the manufacturer's recommendations. Primers (Supplementary Material, Table S1) were synthesized by Shanghai Sangon Biotech Co., Ltd (Shanghai, China).

Western blot analysis

Nuclear-cytoplasmic fractionation was carried out using the NE-PER Nuclear and Cytoplasmic Extraction Reagents kit (Thermo Fisher Scientific, USA). Proteins were extracted from cells after the indicated treatment and quantified using the BCA protein assay kit (Pierce, Rockford, IL, USA). Equal amounts of proteins were loaded into 8% SDS-PAGE and then transferred onto a polyvinylidene fluoride membrane (Millipore, Billerica, MA, USA). After blocking and washing, the membranes were incubated with the indicated primary Abs and then with horseradish peroxidase-labeled secondary antibody. The blots were assessed using ImageJ software (NIH, Bethesda, MD). All antibodies (Abs) and their sources are listed in Table S2.

RNA interference

The siRNA for beta-catenin (Supplementary Material, Table S1) was purchased from Genepharm technology, China. Melanocyte cells were seeded at 2×10^5 cells per well for 24 h before transfection. Cells were transfected with beta-catenin siRNA and an irrelevant siRNA control at 50 nM (GenePharma, China) with LipofectamineTM 2000 (Invitrogen, Carlsbad, USA) following the manufacturer's protocol.

Statistical analyses

The data represent the mean ± SD of at least three independent experiments. All statistical analyses were performed using the GraphPad Prism version 5.0 software (GraphPad Software, San Diego, CA, USA). Dual comparisons were carried out with the two-tailed Student's unpaired *t* test. Groups of three or more were analyzed by one-way analysis of variance (ANOVA) with Dunnett's post-tests. The Pearson correlation coefficient was calculated to examine the association between serum MDA and vitamin D levels. P values < 0.05 were considered statistically significant.

Results

Decreased serum vitamin D levels correlated with increased serum MDA in vitiligo patients

Malondialdehyde (MDA) is a specific indicator of lipid peroxidation, reflecting the extent of oxidative damage in vitiligo patients. To investigate the possible role of Vitamin D in the pathogenesis of vitiligo, serum levels of vitamin D and MDA were first tested in 53 patients with non-segmental vitiligo (lesional area ≥ 3%) and 23 healthy

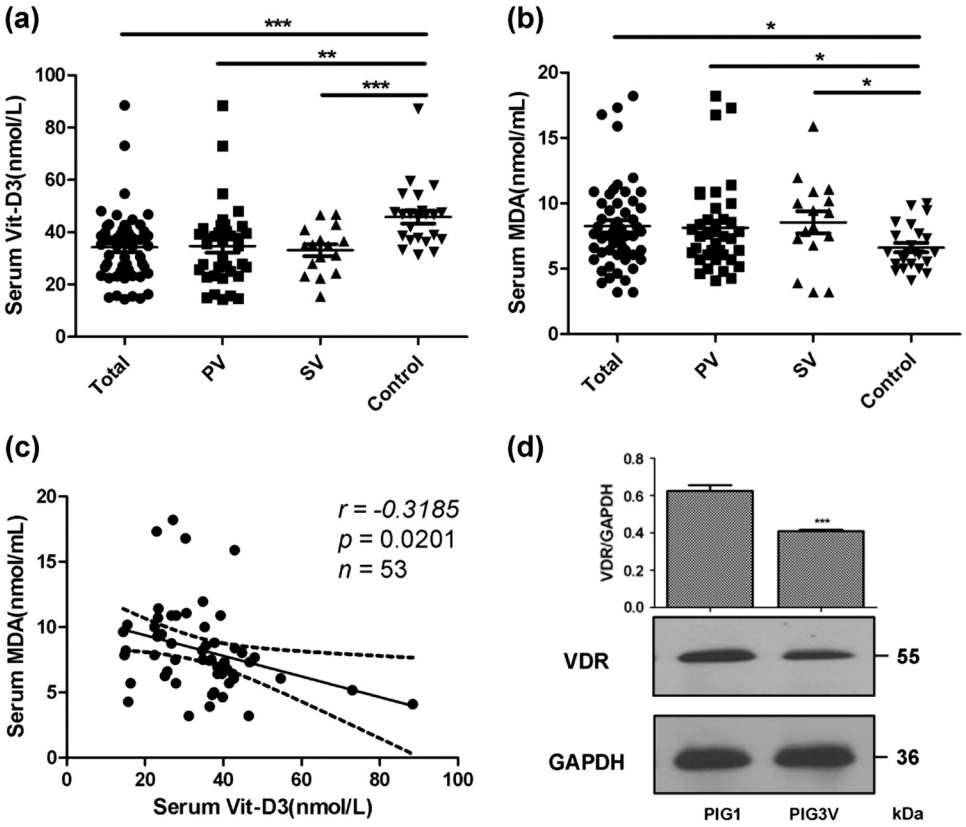

Fig. 1 Serum vitamin D insufficiency or decreased VDR expression was associated with vitiligo pathogenesis. **a** Decreased serum vitamin D levels and (**b**) increased serum MDA levels in patients with vitiligo. Ctrl healthy controls, PV progressive vitiligo, SV stable vitiligo, Total total patients. **c** Association between serum vitamin D and MDA levels. Serum vitamin D levels were inversely correlated with serum MDA levels in vitiligo patients ($r = -0.3185$, $p = 0.0201$, $n = 53$, Spearman's correlation test). The solid line represents the regression line. **d** Vitiligo melanocytes showed lower expression of vitamin D receptor (VDR) than normal melanocytes. $^{*}P < 0.05$, $^{**}P < 0.01$, $^{***}P < 0.001$

control subjects by using ELISA. Median serum MDA levels were significantly higher in the patients with vitiligo (8.02 ± 3.22 nmol/mL) than in healthy controls (6.54 ± 1.68 nmol/mL) (Fig. 1a). However, the overall level of serum vitamin D in vitiligo patients (34.23 ± 13.57 nmol/L) was clearly lower than that in healthy controls (45.80 ± 12.01 nmol/L; Fig. 1b). The rate of vitamin D deficiency was 24.5% in vitiligo patients as compared with none in healthy controls. Moreover, we also assessed the relationship between serum vitamin D levels and MDA levels in vitiligo patients. Statistical analysis suggested that the level of serum vitamin D was inversely correlated with that of serum MDA in vitiligo patients ($r = -0.3185$, $P = 0.0201$, $n = 53$; Fig. 1c).

Since vitamin D exerted pleiotropic biological effects on the growth and differentiation of cutaneous cells via the nuclear vitamin D receptor (VDR) [30], we further assessed the expression of VDR in both normal (PIG1) and vitiligo melanocytes (PIG3V). Protein blotting showed that the protein level of VDR was significantly lower in PIG3V than PIG1 ($P < 0.001$; Fig. 1d). Taken together, these results indicated that serum vitamin D insufficiency and functional impairment was involved in vitiligo pathogenesis, which might be associated with oxidative damage in melanocytes.

Vitamin D activated the WNT/β-catenin pathway in human melanocytes under oxidative stress

Since the β-catenin pathway was involved in the protection of vitamin D against various skin diseases [30, 31], we next evaluated the effect of vitamin D on the expression of β-catenin pathway components in both normal and vitiligo melanocytes. A concentration of 1 nM vitamin D (1,25-dihydroxyvitamin D3) was selected for dosing according to our previous study, using the Wnt agonist SKL2001 (40 μM) as a positive control [21, 28, 32]. Melanocytes were pretreated with vitamin D or SKL2001 and then challenged with 0.5 mM H_2O_2 for 24 h. As shown in Fig. 2, 0.5 mM H_2O_2 significantly downregulated the expression of β-catenin and its downstream effector CDH3 at both mRNA and protein levels in both PIG1 and PIG3V cells. Vitamin D partially reversed the inhibitory effect of oxidative stress on the expression of β-catenin in both H_2O_2-treated PIG1 and PIG3V, similarly to SKL2001 (Fig. 2a-d). We further showed that vitamin D significantly enhanced the nuclear/cytosolic ratio of β-catenin in these two melanocytes with or without oxidative stress. Consistently, vitamin D also induced a significant enhancement of CDH3 expression at both mRNA and protein levels in both PIG1 and PIG3V under oxidative stress, demonstrating the functional

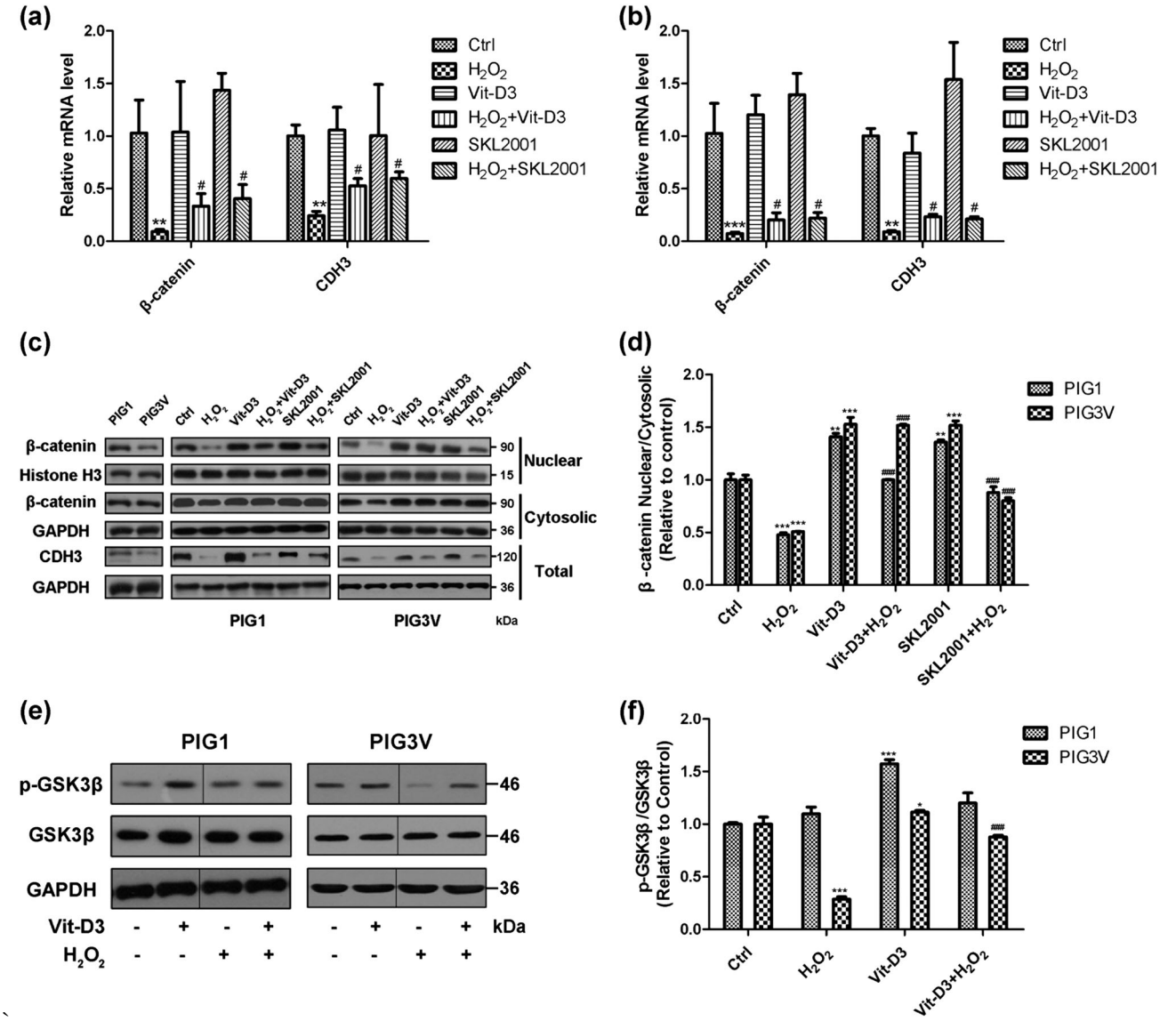

Fig. 2 Vitamin D promoted the activation of Wnt/β-catenin signaling in H_2O_2-treated melanocytes. Melanocytes were exposed to 1 nM vitamin D or 40 μM SKL2001 for 24 h and then further treated with 0.5 mmol/L H_2O_2 for another 24 h. β-catenin and CDH3 mRNA levels were analyzed by quantitative real-time PCR in PIG1 (**a**) and PIG3V (**b**). **c** Western blots of nuclear and cytoplasmic fractions of β-catenin and total CDH3. **d** The ratio of nuclear/cytosolic of β-catenin was calculated by densitometry analysis. (**e**) Western blots of total GSK3β and phosphorylated GSK3β at Ser9. **f** The ratio of p-GSK3β (Ser9)/GSK3β was analyzed by densitometry analysis. $^{*}P < 0.05$, $^{**}P < 0.01$, $^{***}P < 0.001$, compared with the control group; $^{\#}P < 0.05$, $^{\#\#}P < 0.01$, $^{\#\#\#}P < 0.001$, compared with the H_2O_2 group

activation of β-catenin. Therefore, vitamin D might promote nuclear translocation and transcriptional activity of β-catenin in human melanocytes under oxidative stress.

GSK3β is an important negative regulator of β-catenin signaling, and the stabilization of β-catenin is directly proportional to GSK3β phosphorylation at Ser9 [18, 20]. As shown in Fig. 2e, f, vitamin D markedly increased the ratio of p-GSK3β (Ser9)/GSK3β in melanocytes even without H_2O_2 treatment, indicating that vitamin D might induce GSK3β phosphorylation on Ser9 and thus promote GSK3β inactivation and nuclear translocation of β-catenin. Taken together, vitamin D activated WNT/β-catenin signaling in both normal and vitiligo melanocytes against oxidative stress.

Vitamin D ameliorates H_2O_2-induced oxidative damage in human melanocytes similar to Wnt agonist

To further assess the protective effects of vitamin D against vitiligo, a series of in vitro assays were performed in both normal and vitiligo melanocytes. As shown in Fig. 3a, H_2O_2

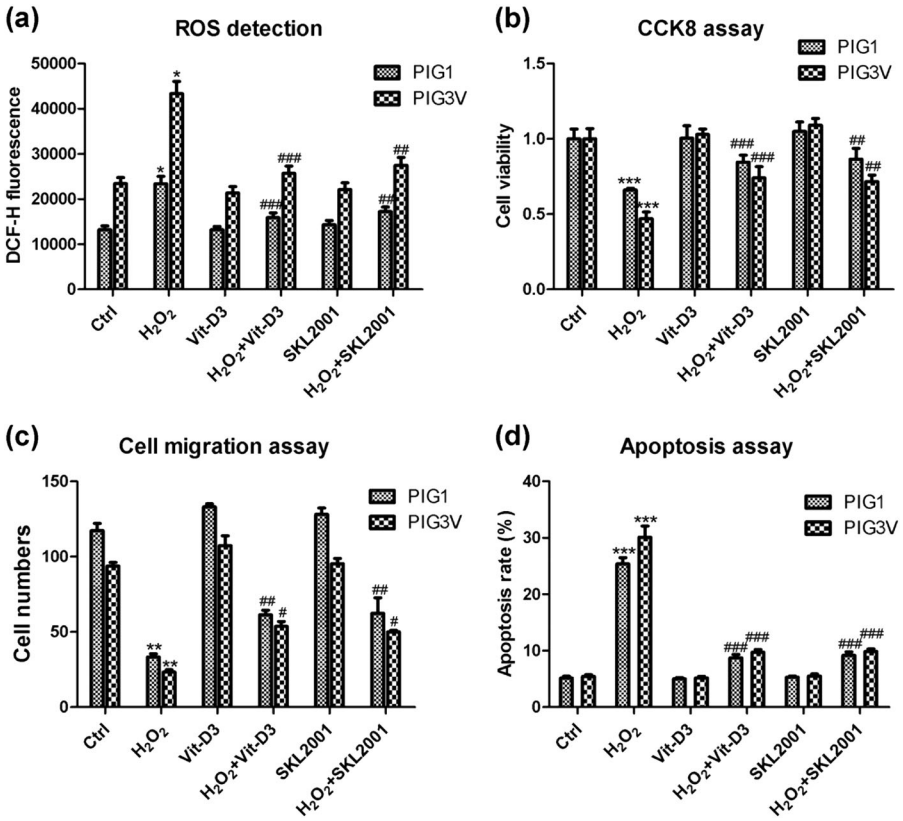

Fig. 3 Vitamin D attenuated H_2O_2-induced oxidative damage in human melanocytes similarly to Wnt agonist. **a** Measurement of intracellular ROS. **b** Cell viability determination by the CCK-8 assay. **c** Cell migration assay. **d** Cell apoptosis assay. $^{*}P < 0.05$, $^{**}P < 0.01$, $^{***}P < 0.001$, compared with the control group; $^{\#}P < 0.05$, $^{\#\#}P < 0.01$, $^{\#\#\#}P < 0.001$, compared with the H_2O_2 group

treatment significantly increased intracellular ROS production in human melanocytes, especially PIG3V. Nevertheless, pretreatment with vitamin D or SKL2001 attenuated H_2O_2-induced ROS accumulation. Moreover, CCK8 and Transwell assays further revealed that either vitamin D or SKL2001 dramatically increased the cell viability and migratory rates of H_2O_2-treated melanocytes (Fig. 3b, c, Fig. S1). Similarly to previous studies, we also found that H_2O_2 exposure increased the apoptotic rates of PIG1 and PIG3V approximately five- to six-fold, whereas pretreatment with vitamin D or SKL2001 markedly reduced melanocytes apoptosis by 66–70% (Fig. 3d, Fig. S2). Although vitiligo melanocytes were more susceptible to oxidative stress than normal ones, vitamin D displayed potent protective effects on the proliferation, migration, and apoptosis of PIG3V similarly to those on PIG1. Taken together, these results indicated that vitamin D could reverse H_2O_2-induced oxidative damage of human melanocytes similar to the WNT agonist.

β-catenin silencing abolished the protective effect of Vitamin D on melanocytes against oxidative stress

To test whether the WNT/β-catenin pathway is required for the effects of vitamin D protecting melanocytes against oxidative stress, we used a specific short interfering RNA (siRNA) to downregulate the expression of β-catenin. Quantitative real-time PCR and immunoblotting showed significant changes in β-catenin mRNA and protein levels after β-catenin siRNA#2 (S2) transfection compared with scrambled siRNA (NC) (Fig. 4a, b). In subsequent experiments, PIG1 and PIG3V cells were pretreated with NC or S2 for phenotypic analyses. β-catenin deficiency markedly abrogated the downregulation of ROS production in vitamin D-treated melanocytes under oxidative stress (Fig. 4c). In addition, vitamin D induced enhancement of the proliferation and migration of H_2O_2-treated melanocytes was also abolished by β-catenin silencing (Fig. 4d, e, Fig. S3). Consistently, β-catenin silencing also neutralized the protection of vitamin D against H_2O_2-induced apoptosis (Fig. 4f, Fig. S4). Both PIG1 and PIG3V cells with β-catenin silencing displayed similar phenotypes in vitro under oxidative stress. These results suggested that β-catenin activation was essential for the protective capacity of vitamin D in melanocytes against oxidative stress.

Vitamin D modulated Nrf2, MITF, and apoptosis pathways by activation of β-catenin in melanocytes

Previous studies have shown that Wnt/β-catenin signaling controls cell proliferation, differentiation, and apoptosis by regulating a large number of target genes [19, 33]. We first examined the alterations of the Nrf2/ARE pathway, which

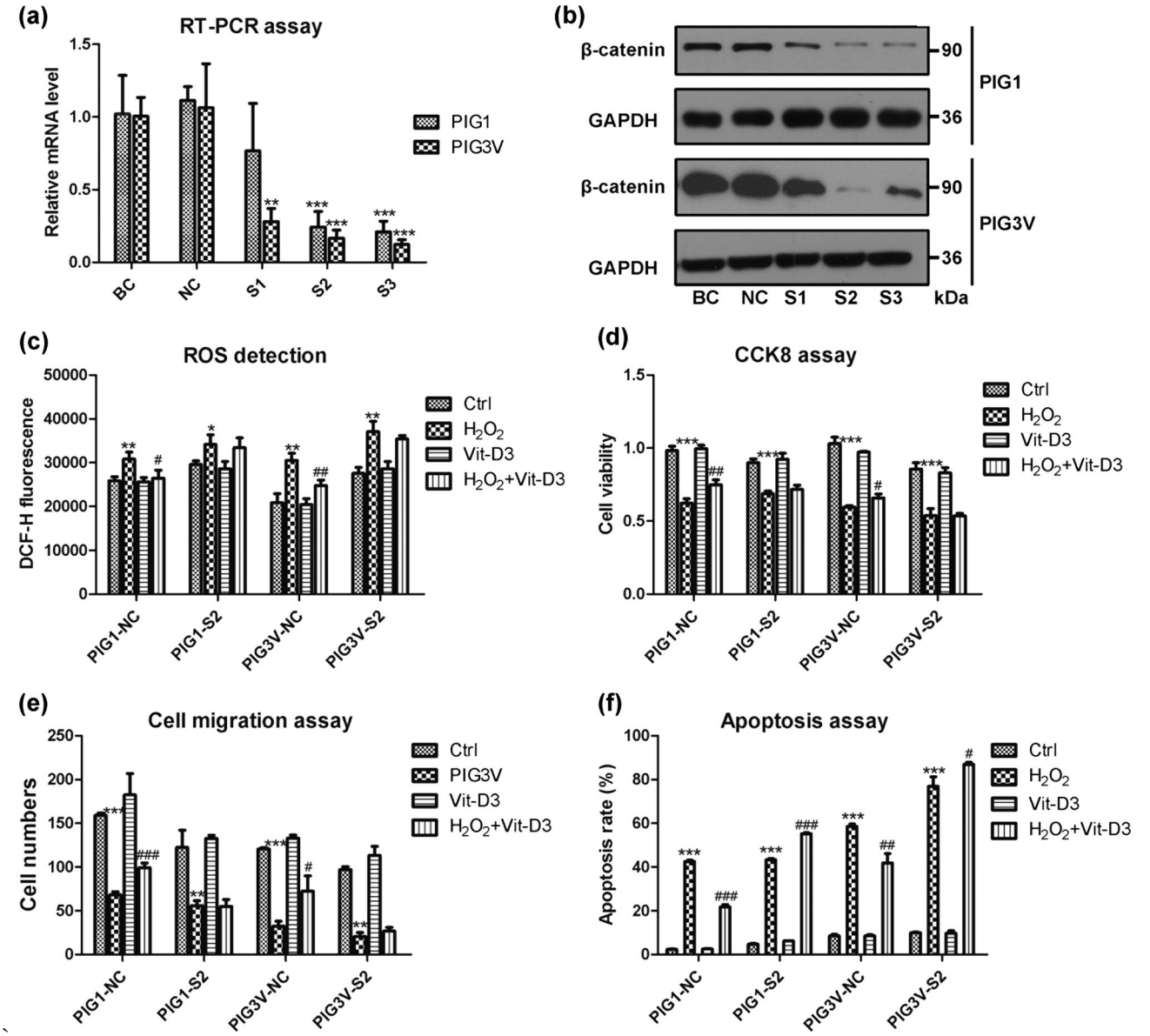

Fig. 4 β-catenin silencing abolished the protection of vitamin D in H_2O_2-treated melanocytes. Quantitative real-time PCR (**a**) and Western blotting (**b**) were carried out to evaluate β-catenin expression in melanocytes transfected with β-catenin siRNA and an irrelevant siRNA control. BC blank control, NC negative control, S1-S3 β-catenin siRNA#1-#3. **c** Measurement of intracellular ROS. **d** Cell viability determination by the CCK-8 assay. **e** Cell migration assay. **f** Cell apoptosis assay. $^{*}P < 0.05$, $^{**}P < 0.01$, $^{***}P < 0.001$, compared with the control group; $^{\#}P < 0.05$, $^{\#\#}P < 0.01$, $^{\#\#\#}P < 0.001$, compared with the H_2O_2 group

is a master regulator that governs the redox balance of melanocytes [27, 34]. We found that H_2O_2 exposure induced a significant decrease in the ratio of nuclear/cytosolic of Nrf2 and the expression of HO-1 in normal melanocytes (Fig. 5a-c). Impairment of the Nrf2/ARE pathway caused by H_2O_2 was markedly reversed by addition of vitamin D, while activation of the Nrf2/ARE pathway induced by vitamin D was further blocked by β-catenin silencing. Therefore, β-catenin pathways mediated the activation of Nrf2 in vitamin D-treated melanocytes against oxidative damage.

Microphthalmia-associated transcription factor (MITF) is an essential transcription factor involved in melanocyte differentiation, migration, and melanogenesis. We found that vitamin D treatment significantly upregulated the protein level of MITF in PIG1 cells with or without β-catenin silencing (Fig. 5a, c). Moreover, vitamin D also notably reversed the inhibitory effect of H_2O_2 on MITF expression,

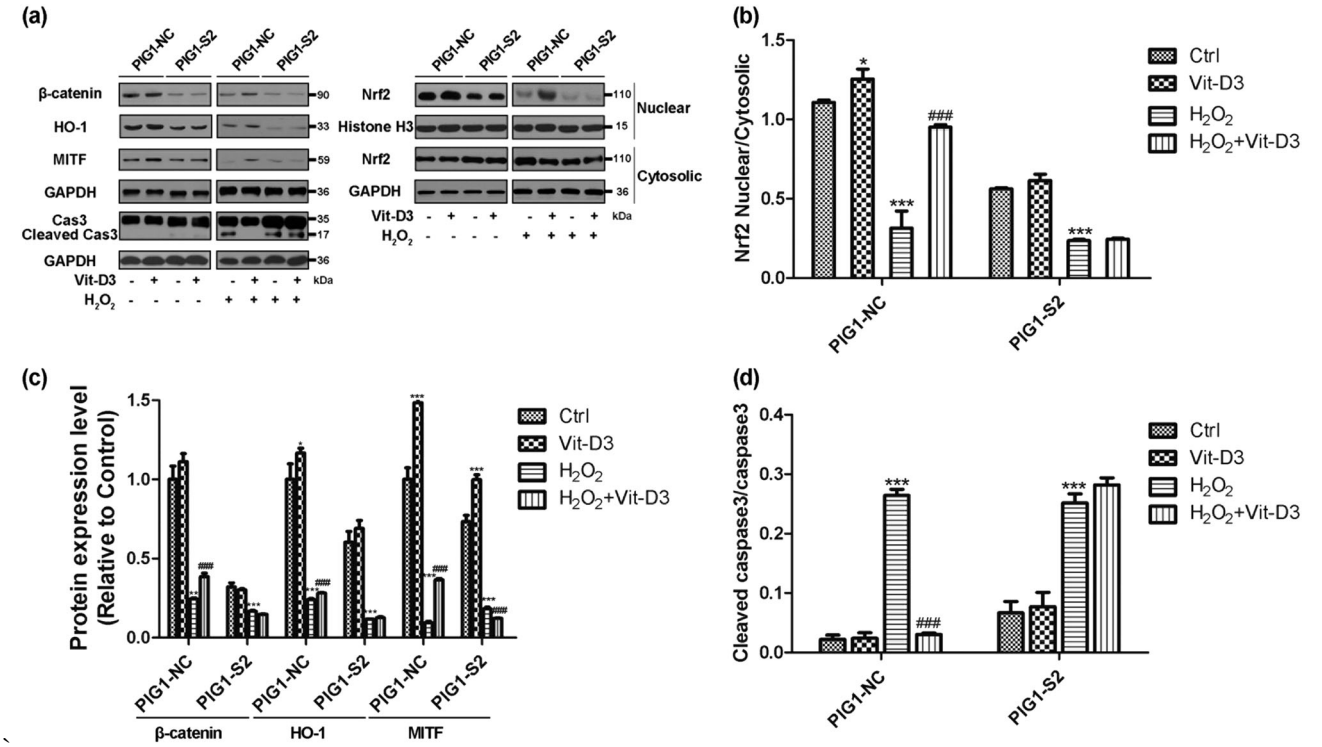

Fig. 5 β-catenin activation was required for vitamin D to modulate Nrf2, MITF, and apoptosis pathways in melanocytes. **a** Western blotting was performed to assess the expression of downstream components in Wnt/β-catenin signaling. The ratio of nuclear/cytosolic of Nrf2 (**b**), total HO-1 and MITF (**c**), and the ratio of cleaved-caspase3/total caspase 3 (**d**) were analyzed by densitometry analysis. $^{*}P < 0.05$, $^{**}P < 0.01$, $^{***}P < 0.001$, compared with the control group; $^{\#}P < 0.05$, $^{\#\#}P < 0.01$, $^{\#\#\#}P < 0.001$, compared with the H_2O_2 group

but the protection of vitamin D was abolished by β-catenin deficiency. The results indicated that vitamin D might positively modulate MITF to promote melanocyte proliferation and migration by activating the β-catenin pathway.

In addition to Nrf2 and MITF, the apoptotic pathway is another important target of the WNT/β-catenin pathway [33]. Thus, expression of caspase 3 and its cleaved form were tested in melanocytes. Consistent with the increased apoptotic rates of melanocytes, H_2O_2 exposure induced a ten-fold upregulation of the ratio of cleaved-caspase3/caspase3 (Fig. 5a, d). Vitamin D treatment remarkably clearly inhibited the upregulation of cleaved caspase 3, while its protective role was further blocked by β-catenin silencing. These results suggested that the β-catenin pathway was required for the anti-apoptotic effect of vitamin D on human melanocytes.

Discussion

Recent evidence indicates that treatment with vitamin D analogs enhances repigmentation in vitiligo, especially in combination with UV light or corticosteroids [8]. However, the molecular mechanisms underlying the pharmacological action of vitamin D compounds against vitiligo have not yet been investigated. In the present study, we revealed a new mechanism of vitamin D as an antioxidative agent for vitiligo treatment. We found that vitamin D protected melanocytes against oxidative damage by activating the WNT/β-catenin pathway. The β-catenin pathway was required for vitamin D to modulate downstream targets such as Nrf2/ARE, MITF, and apoptotic pathways.

Oxidative stress is a critical factor in the onset and progression of vitiligo [1, 2, 6, 27]. Consistent with previous studies [10, 35–37], we found that patients with vitiligo had higher MDA levels and lower vitamin D levels than the healthy control group. Intriguingly, the decreased serum vitamin D level was inversely correlated with serum MDA levels in vitiligo patients, indicative of the potential antioxidant effect of vitamin D. A series of in vitro experiments was conducted and further confirmed that vitamin D attenuated H_2O_2-induced ROS accumulation in human melanocytes and ameliorated the effect of oxidative stress on proliferation, migration, and apoptosis of melanocytes. Furthermore, vitiligo melanocytes displayed a significant decrease in protein levels of VDR compared with normal melanocytes. Our results were highly consistent with

previous studies which revealed that VDR expression was remarkably decreased in the lesional/perilesional skin while repigmentation was accompanied with upregulated VDR expression in vitiligo patients [38, 39]. The VDR gene polymorphisms were also reported to be associated with serum 25-hydroxyvitamin D levels in Chinese patients with generalized vitiligo [12]. Therefore, vitamin D insufficiency or functional impairment of the vitamin D pathway might attenuate the antioxidant capacity of patients and thus represent a risk factor for vitiligo.

It has been reported that vitiligo patients with comorbid autoimmune illness have lower levels of 25-hydroxyvitamin D [11]. The mechanism by which vitamin D modulates autoimmunity is unknown, which might be explained by the following possible reasons. On the one hand, vitamin D has multiple effects on innate and adaptive immune responses by regulating various immune cells in vitro [40]. On the other hand, oxidative stress has been shown to be an important initiate factor in the pathogenesis of various autoimmune diseases [6, 41, 42], and vitamin D ameliorates oxidative damage and thus reduces the incidence and severity of autoimmune responses. The antioxidant property of vitamin D has been validated in various human cells, such as cardiac cells, endothelial cells, gastric epithelial cells, and melanocytes [16, 43–45]. In the present study, we further showed that vitamin D could protect melanocytes against oxidative damage by activating the canonical WNT/β-catenin pathway.

A previous study by Regazzetti et al has demonstrated an inhibition of the WNT/β-catenin pathway in keratinocytes and melanocytes under oxidative stress [21]. Moreover, lesional vitiligo skin is also characterized by downregulated expression of WNT pathway components such as LEF1, CDH2, CDH3. Similarly, in our study, vitiligo melanocytes displayed lower expression of CDH3 (p-cadherin) and nuclear β-catenin than normal melanocytes. Because β-catenin is a transcription factor, nuclear translocation of β-catenin is critical for its dissociation from GSK3β and transcriptional activation of multiple target genes [18, 33]. We further found that in addition to downregulation of CDH3 and β-catenin expression, H_2O_2 also decreased the nuclear/cytosolic ratio of β-catenin in both PIG1 and PIG3V and prevented GSK3β phosphorylation on Ser9 in PIG3V, indicating that oxidative stress inhibited the nuclear translocation of β-catenin. The inhibitory effects on β-catenin signaling induced by H_2O_2 were reversed by addition of vitamin D or WNT agonist (SKL2001). Thus, vitamin D positively modulated β-catenin signaling at both translational and posttranslational levels in melanocytes under oxidative stress.

A previous study has shown that WNT agonist induces the differentiation of resident stem cells into pre-melanocytes in vitiligo lesional skin ex vivo [21]. Our study further highlighted that WNT pathway activation was essential for the antioxidant properties of vitamin D in melanocytes. Like the WNT agonist, vitamin D significantly inhibited ROS accumulation and cell apoptosis in H_2O_2-treated melanocytes, and promoted their proliferative and migratory activity. The protective effects of vitamin D against oxidative stress were abolished by β-catenin silencing in melanocytes. Similar protective effects and mechanisms of vitamin D have been reported in other cells and tissues [23, 24, 46, 47]. For example, activated β-catenin signaling is required for vitamin D to promote osteogenesis in oxidative stress, while inhibition of the WNT pathway is involved in the protection of vitamin D against colorectal tumorigenesis [23, 47]. Thus, vitamin D might utilize different modulatory patterns of the WNT/β-catenin pathway to protect against various diseases.

The transcription factor Nrf2 is a critical regulator of oxidant metabolism in melanocytes, and it is required for the effectiveness of aspirin and simvastatin as novel therapeutic strategies against vitiligo [27, 48–50]. Several studies also revealed that Nrf2 signaling is involved in the protective effects of vitamin D in various disease models [51–53]. Consistently, our results also showed that vitamin D promoted the upregulation of nuclear Nrf2 and its downstream component HO-1 in melanocytes. Furthermore, activation of Nrf2 signaling was completely blocked by β-catenin silencing, indicating that the β-catenin pathway mediated Nrf2 activation in vitamin D-treated melanocytes. Recently, a number of studies have explored the relationship between the Wnt/β-catenin and Nrf2 pathways [54–57]. For example, WNT-3A controls the antioxidant metabolism of hepatocytes by activating Nrf2 in a β-catenin-independent manner, and Nrf2 pathway disruption induces neurogenic impairment in Parkinsonian mice via Wnt/β-catenin dysregulation [54, 57]. Therefore, Wnt/β-catenin signaling has complex interactions with Nrf2 signaling that might be specific to the cell type and disease model. The potential mechanism by which β-catenin activates Nrf2 signaling in melanocytes remains to be further investigated.

In addition to Nrf2 signaling, we also found that MITF and apoptotic pathways were regulated by β-catenin in vitamin D-treated melanocytes. MITF is a central regulator of the differentiation, migration, survival, and melanogenesis of melanocytes [58–60]. Previous studies have shown that MITF is significantly upregulated by WNT/β-catenin pathway activation in both vitiligo lesional skin ex vivo and hair follicle melanocytes in vitro [21, 61]. Consistently, we observed that vitamin D treatment enhanced the expression of MITF in human melanocytes. In our study, however, β-catenin deficiency abolished the upregulation of MITF in melanocytes under oxidative stress, but not in melanocytes without H_2O_2 exposure. A previous study by Watabe et al.

once showed that vitamin D induced MITF expression by stimulating endothelin B receptor signaling [13]. Thus, we speculated that vitamin D could modulate MITF through multiple pathways and Wnt/β-catenin signaling might be crucial for MITF regulation in melanocytes under oxidative stress. These hypotheses remain to be validated in further experiments. We also showed that β-catenin activation was essential for vitamin D to modulate apoptotic pathway in melanocytes. When β-catenin was silenced, vitamin D could not reverse the increase in cleaved caspase 3 expression or apoptotic rates in H_2O_2-treated melanocytes.

In conclusion, our study shows that vitamin D protects human melanocytes against oxidative damage by activation of Wnt/β-catenin signaling, indicating targeting Wnt/β-catenin signaling could be a useful approach to improve treatment of vitiligo. Serum vitamin D insufficiency or functional impairment of the vitamin D pathway might be a risk factor for vitiligo due to impairment of the antioxidant system in vivo. Further studies using vitiligo mice are necessary to confirm the therapeutic potential of systemic administration of vitamin D for vitiligo.

Acknowledgements This study was supported by grants from Municipal Hospital Emerging Frontier Technology United Key Projects (SHDC12016112), the Shanghai Key Medical Discipline for Dermatology (2017ZZ02002), Shanghai leading talent project, and China Postdoctoral Science Foundation (2016M600286). The authors thank Dr. Caroline Le Poole (Loyola University Chicago, Maywood, IL, US) for providing the human melanocyte cell lines PIG1 and PIG3V and Dr. Chunying Li (Xijing Hospital, Fourth Military Medical University, Xi'an, Shaanxi, China) for assisting with the cell transfer. The authors also thank the vitiligo patients and healthy donors for their participation in this study.

Conflict of Interest The authors declare that they have no financial conflict of interest.

References

1. Colucci R, Dragoni F, Moretti S. Oxidative stress and immune system in vitiligo and thyroid diseases. Oxid Med Cell Longev. 2015;2015:631927.
2. Denat L, Kadekaro AL, Marrot L, et al. Melanocytes as instigators and victims of oxidative stress. J Invest Dermatol. 2014;134:1512–8.
3. Speeckaert R, Speeckaert MM, van Geel N. Why treatments do (n't) work in vitiligo: An autoinflammatory perspective. Autoimmun Rev. 2015;14:332–40.
4. Jin Y, Birlea SA, Fain PR, et al. Genome-wide analysis identifies a quantitative trait locus in the MHC class II region associated with generalized vitiligo age of onset. J Invest Dermatol. 2011;131:1308–12.
5. Dell'Anna ML, Ottaviani M, Albanesi V, et al. Membrane lipid alterations as a possible basis for melanocyte degeneration in vitiligo. J Invest Dermatol. 2007;127:1226–33.
6. Li S, Zhu G, Yang Y, et al. Oxidative stress drives CD8+ T-cell skin trafficking in patients with vitiligo through CXCL16 upregulation by activating the unfolded protein response in keratinocytes. *J Allergy Clin Immunol*. 2017;140(1):177–189.
7. Sintov AC, Yarmolinsky L, Dahan A, et al. Pharmacological effects of vitamin D and its analogs: recent developments. Drug Discov Today. 2014;19:1769–74.
8. Birlea SA, Costin GE, Norris DA. New insights on therapy with vitamin D analogs targeting the intracellular pathways that control repigmentation in human vitiligo. Med Res Rev. 2009;29:514–46.
9. Parsad D, Kanwar AJ. Topical vitamin D analogues in the treatment of vitiligo. Pigment Cell Melanoma Res. 2009;22:487–8.
10. Upala S, Sanguankeo A. Low 25-hydroxyvitamin D levels are associated with vitiligo: a systematic review and meta-analysis. Photodermatol Photoimmunol Photomed. 2016;32:181–90.
11. Silverberg JI, Silverberg AI, Malka E, et al. A pilot study assessing the role of 25 hydroxy vitamin D levels in patients with vitiligo vulgaris. J Am Acad Dermatol. 2010;62:937–41.
12. Li K, Shi Q, Yang L, et al. The association of vitamin D receptor gene polymorphisms and serum 25-hydroxyvitamin D levels with generalized vitiligo. Br J Dermatol. 2012;167:815–21.
13. Watabe H, Soma Y, Kawa Y, et al. Differentiation of murine melanocyte precursors induced by 1,25-dihydroxyvitamin D3 is associated with the stimulation of endothelin B receptor expression. J Invest Dermatol. 2002;119:583–9.
14. Birlea SA, Costin GE, Norris DA. Cellular and molecular mechanisms involved in the action of vitamin D analogs targeting vitiligo depigmentation. Curr Drug Targets. 2008;9:345–59.
15. Kawakami T, Ohgushi A, Hirobe T, et al. Effects of 1,25-dihydroxyvitamin D3 on human epidermal melanocytes and melanoblasts. J Dermatol Sci. 2014;76:72–4.
16. Gong Q, Li X, Sun J, et al. The effects of calcipotriol on the dendritic morphology of human melanocytes under oxidative stress and a possible mechanism: is it a mitochondrial protector? J Dermatol Sci. 2015;77:117–24.
17. Li QL, Wu YH, Niu M, et al. Protective effects of tacalcitol against oxidative damage in human epidermal melanocytes. Int J Dermatol. 2017;56:232–8.
18. MacDonald BT, Tamai K, He X. Wnt/beta-catenin signaling: components, mechanisms, and diseases. Dev Cell. 2009;17:9–26.
19. Logan CY, Nusse R. The Wnt signaling pathway in development and disease. Annu Rev Cell Dev Biol. 2004;20:781–810.
20. Kimelman D, Xu W. beta-catenin destruction complex: insights and questions from a structural perspective. Oncogene. 2006;25:7482–91.
21. Regazzetti C, Joly F, Marty C, et al. Transcriptional analysis of vitiligo skin reveals the alteration of WNT pathway: a promising target for repigmenting vitiligo patients. J Invest Dermatol. 2015;135:3105–14.
22. Yamada T, Hasegawa S, Inoue Y, et al. Wnt/beta-catenin and kit signaling sequentially regulate melanocyte stem cell differentiation in UVB-induced epidermal pigmentation. J Invest Dermatol. 2013;133:2753–62.
23. Xiong Y, Zhang Y, Xin N, et al. 1alpha,25-Dihydroxyvitamin D3 promotes osteogenesis by promoting Wnt signaling pathway. J Steroid Biochem Mol Biol. 2017;174:153–60.
24. Guo J, Lu C, Zhang F, et al. VDR activation reduces proteinuria and high-glucose-induced injury of kidneys and podocytes by regulating wnt signaling pathway. Cell Physiol Biochem. 2017;43:39–51.
25. Ohkawa H, Ohishi N, Yagi K. Assay for lipid peroxides in animal tissues by thiobarbituric acid reaction. Anal Biochem. 1979;95:351–8.
26. Xu X, Fu WW, Wu WY. Serum 25-hydroxyvitamin D deficiency in Chinese patients with vitiligo: a case-control study. PLoS ONE. 2012;7:e52778.
27. Jian Z, Li K, Song P, et al. Impaired activation of the Nrf2-ARE signaling pathway undermines H2O2-induced oxidative stress response: a possible mechanism for melanocyte degeneration in vitiligo. J Invest Dermatol. 2014;134:2221–30.

28. Tang Luyan, Fu Wenwen, Zhang Yong, et al. Effect of calcipotriol on melanin synthesis of human melanocytes. Chin J Dermatol. 2009;42:771–3.
29. Lei TC, Vieira WD, Hearing VJ. In vitro migration of melanoblasts requires matrix metalloproteinase-2: implications to vitiligo therapy by photochemotherapy. Pigment Cell Res. 2002;15:426–32.
30. Slominski AT, Janjetovic Z, Kim TK, et al. Novel non-calcemic secosteroids that are produced by human epidermal keratinocytes protect against solar radiation. J Steroid Biochem Mol Biol. 2015;148:52–63.
31. Shah S, Islam MN, Dakshanamurthy S, et al. The molecular basis of vitamin D receptor and beta-catenin crossregulation. Mol Cell. 2006;21:799–809.
32. Gwak J, Hwang SG, Park HS, et al. Small molecule-based disruption of the Axin/beta-catenin protein complex regulates mesenchymal stem cell differentiation. Cell Res. 2012;22:237–47.
33. Vlad A, Rohrs S, Klein-Hitpass L, et al. The first five years of the Wnt targetome. Cell Signal. 2008;20:795–802.
34. Jian Z, Li K, Liu L, et al. Heme oxygenase-1 protects human melanocytes from H_2O_2-induced oxidative stress via the Nrf2-ARE pathway. J Invest Dermatol. 2011;131:1420–7.
35. Ines D, Sonia B, Riadh BM, et al. A comparative study of oxidant-antioxidant status in stable and active vitiligo patients. Arch Dermatol Res. 2006;298:147–52.
36. Khan R, Satyam A, Gupta S, et al. Circulatory levels of antioxidants and lipid peroxidation in Indian patients with generalized and localized vitiligo. Arch Dermatol Res. 2009;301:731–7.
37. Saleh HM, Abdel Fattah NS, Hamza HT. Evaluation of serum 25-hydroxyvitamin D levels in vitiligo patients with and without autoimmune diseases. Photodermatol Photoimmunol Photomed. 2013;29:34–40.
38. Doss RW, El-Rifaie AA, Gohary YM, et al. Vitamin D receptor expression in vitiligo. Indian J Dermatol. 2015;60:544–8.
39. El-Hanbuli HM, Dawoud NM, Mahmoud RH. Narrow-band UVB effects on cutaneous vitamin D receptor expression and serum 25-hydroxyvitamin D in generalized vitiligo. Photodermatol Photoimmunol Photomed. 2018;34:175–83.
40. Adorini L, Penna G. Control of autoimmune diseases by the vitamin D endocrine system. Nat Clin Pract Rheumatol. 2008;4:404–12.
41. Adamczyk B, Adamczyk-Sowa M. New Insights into the role of oxidative stress mechanisms in the pathophysiology and treatment of multiple sclerosis. Oxid Med Cell Longev. 2016;2016:1973834.
42. Harris JE. Cellular stress and innate inflammation in organ-specific autoimmunity: lessons learned from vitiligo. Immunol Rev. 2016;269:11–25.
43. Farhangi MA, Nameni G, Hajiluian G, et al. Cardiac tissue oxidative stress and inflammation after vitamin D administrations in high fat- diet induced obese rats. BMC Cardiovasc Disord. 2017;17:161.
44. Haas MJ, Jafri M, Wehmeier KR, et al. Inhibition of endoplasmic reticulum stress and oxidative stress by vitamin D in endothelial cells. Free Radic Biol Med. 2016;99:1–10.
45. Uberti F, Bardelli C, Morsanuto V, et al. Role of vitamin D3 combined to alginates in preventing acid and oxidative injury in cultured gastric epithelial cells. BMC Gastroenterol. 2016;16:127.
46. Lee H, Bae S, Yoon Y. Anti-adipogenic effects of 1,25-dihydroxyvitamin D3 are mediated by the maintenance of the wingless-type MMTV integration site/beta-catenin pathway. Int J Mol Med. 2012;30:1219–24.
47. Groschel C, Aggarwal A, Tennakoon S, et al. Effect of 1,25-dihydroxyvitamin D3 on the Wnt pathway in non-malignant colonic cells. J Steroid Biochem Mol Biol. 2016;155:224–30. (Pt B)
48. Natarajan VT, Singh A, Kumar AA, et al. Transcriptional upregulation of Nrf2-dependent phase II detoxification genes in the involved epidermis of vitiligo vulgaris. J Invest Dermatol. 2010;130:2781–9.
49. Jian Z, Tang L, Yi X, et al. Aspirin induces Nrf2-mediated transcriptional activation of haem oxygenase-1 in protection of human melanocytes from H_2O_2 -induced oxidative stress. J Cell Mol Med. 2016;20:1307–18.
50. Chang Y, Li S, Guo W, et al. Simvastatin protects human melanocytes from H_2O_2-induced oxidative stress by activating Nrf2. J Invest Dermatol. 2017;137:1286–96.
51. Wang Z, Zhang H, Sun X, et al. The protective role of vitamin D3 in a murine model of asthma via the suppression of TGF-beta/Smad signaling and activation of the Nrf2/HO-1 pathway. Mol Med Rep. 2016;14:2389–96.
52. Nakai K, Fujii H, Kono K, et al. Vitamin D activates the Nrf2-Keap1 antioxidant pathway and ameliorates nephropathy in diabetic rats. Am J Hypertens. 2014;27:586–95.
53. Teixeira TM, da Costa DC, Resende AC, et al. Activation of Nrf2-antioxidant signaling by 1,25-dihydroxycholecalciferol prevents leptin-induced oxidative stress and inflammation in human endothelial cells. J Nutr. 2017;147:506–13.
54. Rada P, Rojo AI, Offergeld A, et al. WNT-3A regulates an Axin1/NRF2 complex that regulates antioxidant metabolism in hepatocytes. Antioxid Redox Signal. 2015;22:555–71.
55. Long MJ, Lin HY, Parvez S, et al. beta-TrCP1 Is a vacillatory regulator of Wnt signaling. Cell Chem Biol. 2017;24:944–957. e947.
56. Manigandan K, Manimaran D, Jayaraj RL, et al. Taxifolin curbs NF-kappaB-mediated Wnt/beta-catenin signaling via up-regulating Nrf2 pathway in experimental colon carcinogenesis. Biochimie. 2015;119:103–12.
57. L'Episcopo F, Tirolo C, Testa N, et al. Aging-induced Nrf2-ARE pathway disruption in the subventricular zone drives neurogenic impairment in parkinsonian mice via PI3K-Wnt/beta-catenin dysregulation. J Neurosci. 2013;33:1462–85.
58. Levy C, Khaled M, Fisher DE. MITF: master regulator of melanocyte development and melanoma oncogene. Trends Mol Med. 2006;12:406–14.
59. Cheli Y, Ohanna M, Ballotti R, et al. Fifteen-year quest for microphthalmia-associated transcription factor target genes. Pigment Cell Melanoma Res. 2010;23:27–40.
60. Seberg HE, Van Otterloo E, Cornell RA. Beyond MITF: Multiple transcription factors directly regulate the cellular phenotype in melanocytes and melanoma. Pigment Cell Melanoma Res. 2017;30:454–66.
61. Guo H, Yang K, Deng F, et al. Wnt3a promotes melanin synthesis of mouse hair follicle melanocytes. Biochem Biophys Res Commun. 2012;420:799–804.

Arastehfar et al. BMC Infectious Diseases (2018) 18:480
https://doi.org/10.1186/s12879-018-3381-5

BMC Infectious Diseases

RESEARCH ARTICLE Open Access

Identification of nine cryptic species of *Candida albicans*, *C. glabrata*, and *C. parapsilosis* complexes using one-step multiplex PCR

Amir Arastehfar[1†], Wenjie Fang[1,2†], Weihua Pan[2*], Wanqing Liao[2], Liang Yan[2] and Teun Boekhout[1,2,3*]

Abstract

Background: *Candida albicans*, *Candida glabrata*, and *Candida parapsilosis* are three prevalent causes of candidiasis, worldwide. These species are considered as nine medically important complex species. Limited knowledge about these newly recognized species prompted us to develop a one-step, multiplex PCR to detect and identify them in clinical settings.

Methods: Primers targeting Hyphal Wall Protein I gene for the *C. albicans, C. dubliniensis, C. africana*, Intergenic Spacer for the *C. glabrata, C. nivariensis, C. bracarensis*, and Intein and ITS rDNA for the *C. parapsilosis, C. orthopsilosis,* and *C. metapsilosis* were designed. Using 168 CBS reference strains and 280 clinical isolates, the specificity and reproducibility of the developed assay were evaluated.

Results: Our developed assay successfully identified and distinguished all the nine species. No cross-reaction with closely- and distantly-related yeast species, *Aspergillus* species and human DNA was observed, resulting in 100% specificity. The ambiguous results obtained by MALDI-TOF for *C. albicans* and *C. africana* were corrected by our 9-plex PCR assay. This assay identified all the cryptic complex species from two test sets from Iran and China, correctly.

Conclusions: Our developed multiplex assay is accurate, specific, cost/time-saving, and works without the tedious DNA extraction steps. It could be integrated into routine clinical laboratories and as a reliable identification tool and has the potential to be implemented into epidemiological studies to broaden the limited knowledge of cryptic species complexes.

Keywords: Cryptic species, *Candida*, Molecular diagnosis, Multiplex PCR

Introduction

Candida albicans, *C. glabrata*, and *C. parapsilosis* were reported to be the three most clinically important *Candida* species [1]. Due to the inclusion of newly designated species through taxonomic studies, these three *Candida* species are now considered cryptic complex species, including *C. albicans*, *C. africana*, and *C. dubliniensis* (as *C. albicans* complex) [2, 3], *C. glabrata*, *C. nivariensis*, and *C. bracarensis* (as *C. glabrata* complex) [4, 5], and *C. parapsilosis*, *C. orthopsilosis*, and *C. metapsilosis* (as *C. parapsilosis* complex) [6]. Despite the fact that for more than a decade these cryptic species have been introduced, still limited knowledge exists on their distribution, pathogenicity, and antifungal susceptibility pattern. Moreover, from an evolutionary standpoint, identification and discrimination of these cryptic species complexes could shed light on pathogenicity acquisition, as Pryszcz et al. (2015) found *C. metapsilosis* as a highly heterozygous opportunistic pathogen arose from a two parental lineages that were not pathogenic [7].

* Correspondence: panweihua@smmu.edu.cn; t.boekhout@westerdijkinstitute.nl
†Amir Arastehfar and Wenjie Fang contributed equally to this work.
[2]Department of Dermatology, Shanghai Key Laboratory of Molecular Medical Mycology, Shanghai Institute of Medical Mycology, Shanghai Changzheng Hospital, Second Military Medical University, Shanghai 200003, China
[1]Westerdijk Fungal Biodiversity Institute, Utrecht 3584, the Netherlands
Full list of author information is available at the end of the article

Biochemical and morphological tests failed to unequivocally identify and differentiate these cryptic species, which is attributed to the presence of similar phenotypic properties among the complexes [8]. Accordingly, various methodologies, including amplified fragment length polymorphism (AFLP) [9], matrix-assisted laser desorption-time of flight (MALDI-TOF) [10], sequencing of ITS rDNA [11] have been used to tackle this problem. Nowadays, due to affordability and the high reproducibility of PCR, myriad aspects of biology have been revolutionized throughout the world [12, 13]. In line with this, identification and differentiation of *Candida albicans*, *Candida glabrata*, and *Candida parapsilosis* complexes representatives through fast and simple conventional PCR by targeting hyphal wall protein 1(HWP1) gene [14], large ribosomal protein 31 (RPL31) gene [15], and vacuolar ATPase (VMA) gene [16], have been addressed. However, the simultaneous detection of all of aforementioned nine medically important cryptic species in a single reaction was not described, previously.

Consequently, the aim of this study was to develop an easy-to-perform, low-cost, highly specific and accurate, multiplex PCR assay capable of differentiation of all these nine medically important *Candida* species, without tedious DNA extraction steps and directly through mixing of pure colonies into the PCR master mix.

Materials and methods

Isolates and growth conditions

Four hundred forty-eight isolates including, 168 reference strains (111 target cryptic strains and 57 non-target strains representing 57 species) from Westerdijk Fungal Biodiversity Institute (Additional file 1: Table S1) and 280 clinical isolates comprising only cryptic species complexes (Table 1) were included. Chinese clinical isolates ($n = 145$) were pooled from a Chinese collection ($n = 1500$), and included cryptic species of *C. glabrata* and *C. parapsilosis* complexes and the Iranian clinical isolates ($n = 135$) included cryptic species complexes of *C. albicans*. Clinical isolates were from different anatomical sites, ranging from nail, sputum, urine and bronchial fluids to blood and were collected from different hospitals in Iran and China (Table 1). CBS reference strains were used for optimization and specificity testing, while clinical isolates used for confirming reproducibility of the developed multiplex PCR assay. Isolates were grown on Glucose Yeast Extract Peptone Agar (Westerdijk Fungal Biodiversity Institute, Utrecht, Netherlands) at 25 °C for 48 h.

DNA extraction

DNA extraction was carried out using CTAB and phenol-chloroform method as described previously [17]. Briefly, a full loop of fresh yeasts colonies was suspended in 700 μL of CTAB buffer followed by bead beating (TissueLyzer II, QIAGEN, Hannover, Germany) for 3 min, 3000 beats/minute. After incubation for 60 min at 55 °C, 700 μL of phenol-chloroform was added. Upon vortexing and centrifugation for 20 min at 14000 rpm, 4 °C, 400 μL of supernatant was added to isopropanol. Finally, upon washing with 70% ethanol and drying the DNA samples on air, the pellets were suspended in Tris-EDTA (10 mM Tris Base, 1 mM EDTA, pH 8.0) buffer. DNA purity and quantity was assessed using NanoDrop and Qubit Broad range kit (Invitrogen) and the quality was evaluated by electrophoretic separation of 5 μl of DNA samples on 1% agarose gel.

Table 1 Clinical isolates utilized for reproducibility and validation testing

Species	Number of Isolates	Origin
Iran ($n = 135$)		
C. albicans	128	Urine, blood
C. africana	3	Vagina
C. dubliniensis	4	Urine
China ($n = 145$)		
C. nivarensis	2	Sputum
C. glabrata	87	Urine, blood, sputum, BALF[a]
C. metapsilosis	20	Sputum
C. orthopsilosis	6	Nail, blood, mouths
C. bracarensis	2	Sputum
C. parapsilosis	28	Urine, blood, nail, sputum

[a]*BALF* bronchoalveolar lavage fluid

Primer design

Target sequences were retrieved from NCBI website (https://blast.ncbi.nlm.nih.gov/Blast.cgi). Primers utilized in this study were all designed by authors, and are listed and depicted in Table 2 and Fig. 1. Primers were selected if 1) lack of cross-reactivity with each other and other non-target species, 2) Compatible PCR product size, 3) compatible in Tm values, and 4) positioned in the most stable part of target loci. Gaps and mismatches with non-target species were located in the 3′ end of primers, hence allow specific amplification of target species. Online free software of Integrated DNA Technology was used to calculate Tm and Delta G of primers (https://eu.idtdna.com/calc/analyzer).Primers were manufactured by Integrated DNA Technology (IDT) Company.

PCR condition

The PCR reaction was optimized in a final volume of 50 μL as follows: 37 μL MiliQ water (Merck Millipore, Billerica, Massachusetts, United States), 5 μL 10X buffer, 1.5 mM $MgCl_2$, 2.5 units of *Taq* enzyme (Bio Taq DNA Polymerase, Biolab), 0.2 mM of mixed dNTP (dNTP mix, 100 Mm, Biolab), *C. albicans* complex primers pair 10 p-mole each one, 5 p-mole for the rest of the primers

Table 2 Sequence of utilized primers in this study

Primer Name	Primer sequences	Annotation
PACF	GCTACCACTTCAGAATCATCATC	Universal forward (PACF) and reverse (PACR) primers for *C. albicans, C. dubliniensis and C. africana*
PACR	AGATCAAGAATGCAGCAATACCAA	
PGCF	TCACTTTCAACTGCTTTCGC	Universal forward primers for *C. glabrata, C. nivariensis* and *C. bracarensis*
GR	TGCGAGTCATGGGCGGAA	Reverse primer only for *C. glabrata*
NR	ACCCCAGAGGCATAAATAGC	Reverse primer only for *C. nivariensis*
BR	GCAACTGGACGAAAGTGC	Reverse primer only for *C. bracarensis*
PF	GCGGAAGGATCATTACAGAATG	Forward (PF) and reverse (PR) primers specifically for *C. parapsilosis*
PR	CTGGCAGGCCCCATATAG	
OMF	GAGAAAGCACGCCTCTTTGC	Universal forward (OMF) and reverse (OMR) primers for *C. orthopsilosis* and *C. metapsilosis*
OMR	TCAGCATTTTGGGCTCTTGC	

(*C. glabrata* and *C. parapsilosis* complex primers), and 1 μL of DNA template.

PCR (2720 Thermal Cycler,, Applied Biosystems, Waltham, Massachusetts, USA) used the following program, pre-denaturation for 5 min at 94 °C, 35 cycles of 94 °C for 30 s, 60 °C for 30 s, 72 °C for 30 s, and final extension at 72 °C for 8 min. PCR products were run on 2% agarose gel for 70 min (8 Volt/cm), stained with GelRed (BioTium Corporation, USA) and visualized using gel documentation with exposure time of 4 s (Gel Doc XR$^+$, BioRad, California, USA). In order to prepare in-house ladders, 10 μL of PCR products from controls (90 μL), 10 μL deionized water, and 20 μL of 10X loading dye were mixed. 15 μL of prepared in-house ladders were utilized as marker to aid in identifying target species (Additional file 2: Figure S1).

Optimization of 9-plex PCR assay using CBS reference strains

After initial successful amplification from CBS 2691 (*C. albicans*), CBS 7987 (*C. dubliniensis*), CBS 8781 (*C. africana*), CBS 138 (*C. glabrata*), CBS 9983 (*C. nivariensis*), CBS 10154 (*C. bracarensis*), CBS 11045 (*C. parapsilosis*), CBS 10906 (*C. orthopsilosis*) and CBS 2916 (*C. metapsilosis*), A panel of 111 CBS reference strains (Additional file 1: Table S1) encompassing only cryptic species of *C. albicans*, *C. glabrata*, *C. parapsilosis* complexes were further tested with our 9-plex PCR.

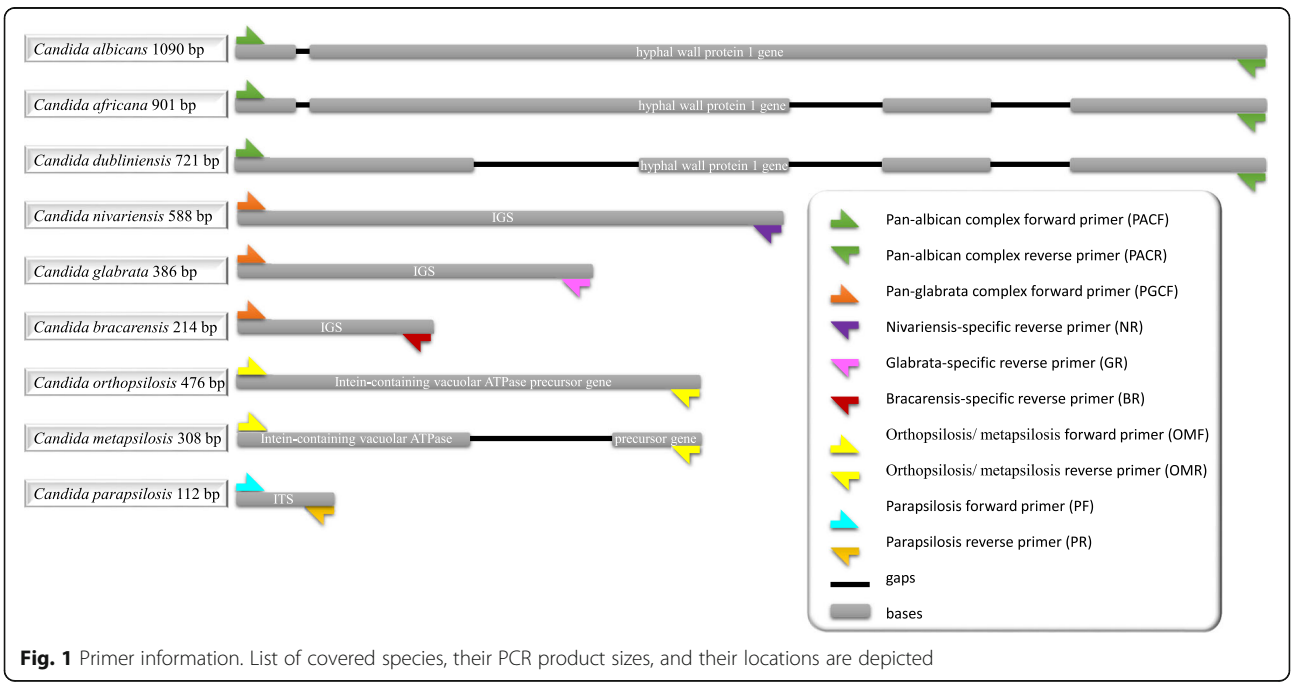

Fig. 1 Primer information. List of covered species, their PCR product sizes, and their locations are depicted

Specificity testing

To evaluate the specificity of the 9-plex PCR assay, 100 DNA samples containing 57 closely- and distantly-related yeast species, *Aspergillus* spp., and human DNA (from blood) and 43 target strains pooled from CBS reference (optimization test set) were prepared in a blinded fashion (blind test set) (Table 1). For preparation of the specificity test set, two technicians were involved. The first technician randomly dispersed DNA samples and serially coded them from one to 100. The second technician subjected the specificity blind test set to the optimized multiplex PCR. The first technician was provided with the results derived from PCR and the consistency of the results was checked with the CBS identity of each strain.

Pure colony testing

In order to eliminate the DNA extraction step and confirm the compatibility of the multiplex assay, single colonies of yeast species derived from the blind test set were subjected to PCR as a template (except for *Rhodotorula mucilaginosa*). Briefly, a single colony (≈ 1 mm^3) was suspended in the prepared PCR master mix (50 μl) as mentioned earlier.

Validation of 9-plex multiplex PCR using clinical isolates

Upon optimization of the multiplex PCR assay using CBS reference strains, specificity and pure colony testing, a panel of clinical isolates (n = 280) (Table 1) prepared in a blind fashion were subjected to the 9-plex assay. One technician performed the LSU sequencing and MALDI-TOF. Upon, identification, the first technician coded the yeast culture plates from 1 to 280, and then a new random number (integer number from 1 to 280) for each plate was generated by SPSS random number generator (version 21, International Business Machines Corp, Armonk, New York, United States) and used as blind test number. The second technician subjected the blind test set to the optimized multiplex PCR. The first technician was provided with the results derived from PCR and the consistency of these results with MALDI-TOF and sequencing were evaluated.

MALDI-TOF

The full extraction method using MALDI-TOF MS (Bruker Biotyper, MicroFlex, LT, Bruker Daltonics, Bremen, Germany) was followed, according to the manufacturer's instructions (https://www.bruker.com/fileadmin/user_upload/8-PDF-Docs/Separations_MassSpectrometry/InstructionForUse/IFU_268711_267615_226413_MALDI_Biotarget_48_Rev1.pdf). Briefly, after suspending of pure colonies in 300 μL of MiliQ water, 900 μL of absolute ethanol was added. After centrifugation step (14,000 rpm, 3 min, room temperature) the supernatant was discarded and another centrifugation step was repeated to totally discard the supernatant. Subsequently, 70% formic acid (Sigma Aldrich, St. Louis, Missouri, United States) was added and upon five minutes incubation at room temperature equal amount of Acetonitrile was added. After a final centrifugation step (14,000 rpm, 3 min, room temperature) 1 μL of clear supernatant was transferred onto the 96-well target plate. Subsequently, 1 μL of matrix was overlaid on the top of air dried samples. Finally, the 96 well target plate was loaded into the MALDI-TOF device.

Sequencing

In order to ensure that the designed primers targeted the right genes, the amplified PCR products were subject to bidirectional dideoxy chain terminated Sanger sequencing using the respective primers. Obtained sequences were subjected to online searching database of NCBI (https://blast.ncbi.nlm.nih.gov/Blast.cgi).

The ribosomal DNA large subunit (LSU) primers including LROR (5′-ACCCGCTGAACTTAAGC-3′) and LR5 (5′-TCCTGAGGGAAACTTCG-3′) were exploited to address the identity of each isolate [18]. Sequences obtained for each isolate was subject to BLAST online database tool (https://blast.ncbi.nlm.nih.gov/Blast.cgi).

Results

Development of 9-plex PCR assay using CBS reference strains

Subjecting 111 CBS reference strains belonging to the species complexes of *C. albicans* (n = 55), *C. glabrata* (n = 28), and *C. parapsilosis* (n = 28) successfully differentiated and identified the nine target species (Fig. 2). Although, the lengths of PCR products were different from those were designed, target species were unequivocally distinguishable from one another (Figs. 1 and 2 and Table 3). In order to prevent misidentifications it is advised to prepare in-house master mixes in large scale by mixing PCR products of target species and storing them at 4 °C for future identification purposes.

Specificity testing using the blind test set

Subjecting 100 DNA samples (containing 66 fungal species) to our 9-plex PCR assay ranging from closely- and distantly-related yeast species, *Aspergillus* spp. resulted in 100% specificity and no cross-reaction with any other fungal species. Additionally, subjecting human DNA to our 9-plex PCR assay, showed no cross-reaction either.

Pure colony testing

Subjecting 105 yeast pure colonies from 61 yeast species pooled from the optimization test set (Additional file 1: Table S1) resulted in successful amplification of all nine target species. No PCR inhibition by cell components was observed, indicating that pure colonies are compatible

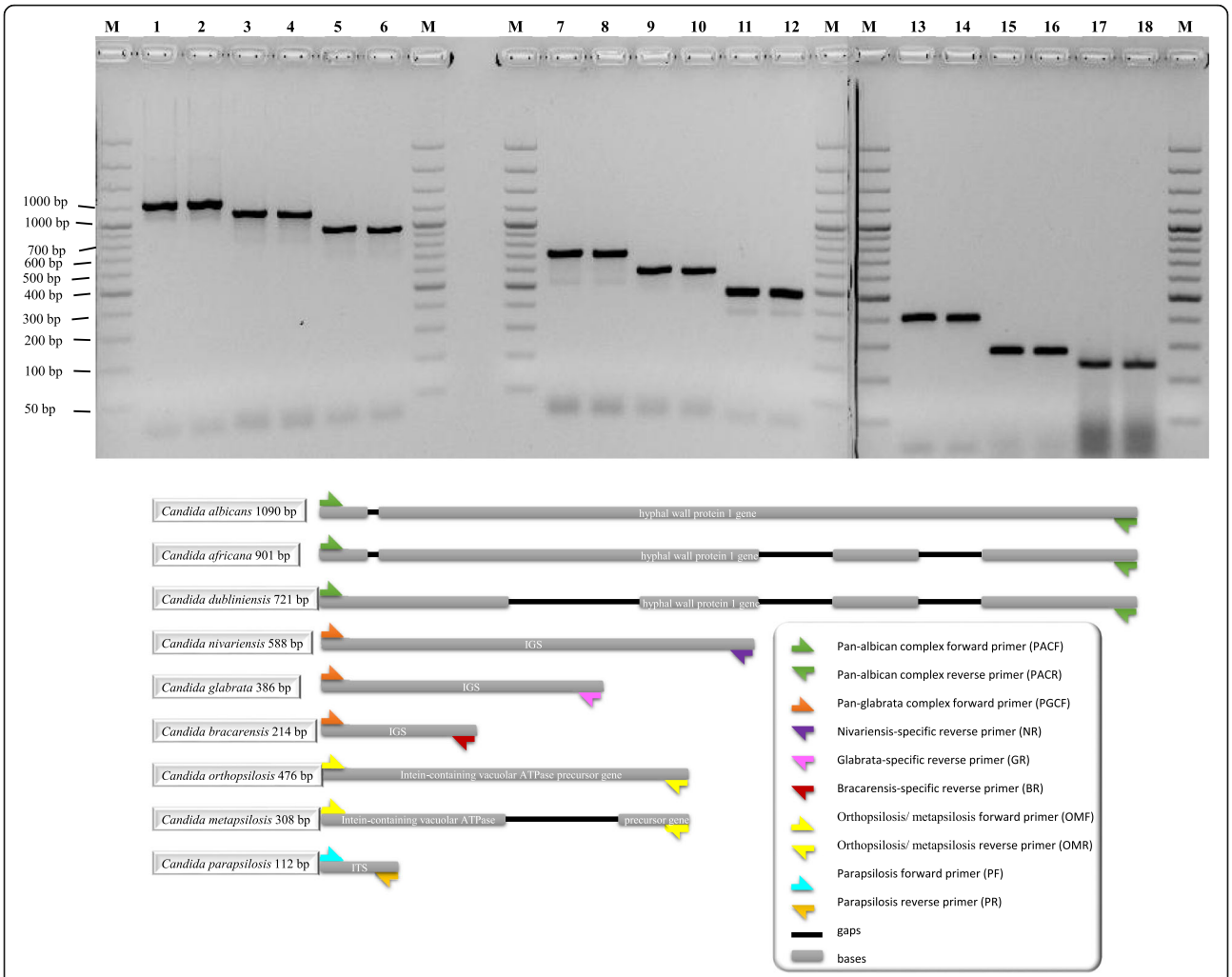

Fig. 2 Amplified PCR products for nine target cryptic species complexes are shown. M. 100 bps Molecular ladder (SM 0324), 1–2 *C. albicans* (1090 bps), 3–4 *C. africana* (901 bps), 5–6 *C. dubliniensis* (721 bps), 7–8 *C. nivariensis* (586 bps), 9–10 *C. orthopsilosis* (476 bps), 11–12 *C. glabrata* (386 bps), 13–14 *C. metapsilosis* (308 bps), 15–16 *C. bracarensis* (214 bps), 17–18 *C. parapsilosis* (112 bps)

with the 9-plex PCR. Compatibility of our 9-plex PCR with pure colony testing allowed decreasing turn-around time from 7 h to 4 h.

Agreement of 9-plex PCR assay with MALDI-TOF MS

Results obtained from our 9-plex PCR for 280 clinical isolates were compared with MALDI-TOF (Table 4). Previously in Westerdijk Fungal Biodiversity Institute, clinically isolated yeast species were identified by MALDI-TOF MS and it showed 98–100% agreement with sequencing [19, 20]. Hence, in this study MALDI-TOF MS along with Sanger sequencing were used as validation tools. Additionally, the spectra for many yeast species utilized in brewery have been added to the MALDI-TOF CBS in-house database. Of 131 strains identified as *C. albicans* using MALDI-TOF MS, our 9-plex PCR assay identified 128 as *C. albicans* and three *as C. africana*. The rest of cryptic species complexes of *C. glabrata* ($n = 91$), and *C. parapsilosis* ($n = 54$) were all identified correctly by MALDI-TOF MS. The overall agreement between MALDI-TOF MS and our 9-plex PCR assay was 98.93%.

Agreement of 9-plex PCR assay with sequencing

Results obtained from our 9-plex PCR was 100% consistent with sequencing of D1/D2 domains of LSU rDNA for 280 clinical strains (Table 4). Cryptic species complexes of *C. parapsilosis* ($n = 54$) and *C. glabrata* ($n = 91$) were all clearly distinguishable using sequencing of respective domain. Despite the fact that, *C. dubliniensis* ($n = 4$) and *C. albicans* ($n = 128$) clearly were distinguishable using sequencing of respective domain, *C. africana* and *C. albicans* showed > 99% similarity, and, hence, making their discrimination at

Table 3 Expected and actual PCR products on gel are shown. Despite of deviation of amplicon sizes in both individual PCR products and home-made ladder containing mixture of PCR products, target species were clearly distinguishable from each other

Target species	Expecetd PCR product size	Actual home-made ladder PCR product sizes on gel (approximately)	Actual indidividual PCR product size on gel (approximately)
Candida albicans	1090 bps	950 bps	1200 bps
Candida africana	901 bps	800 bps	1100 bps
Candida dubliniensis	721 bps	600 bps	950 bps
Candida nivariensis	588 bps	500 bps	700 bps
Candida orthopsilosis	476 bps	> 400 bps	576 bps
Candida glabrata	386 bps	> 350 bps	486 bps
Candida metapsilosis	308 bps	˜280 bps	400 bps
Candida bracarensis	214 bps	˜200 bps	300 bps
Candida parapsilosis	112 bps	100 bps	250 bps

the species level difficult. However, our 9-plex PCR assay clearly discriminated the two closely related species complexes of *C. albicans* and *C. africana*. Consistently, 9-plex PCR assay distinctly identified all of the cryptic species complexes as distinct fragment on the gel. The overall agreement between sequencing of D1/D2 LSU rDNA was 100%.

Discussion

Representatives of the cryptic species of *Candida albicans*, *Candida glabrata*, and *Candida parapsilosis* complexes account for the majority of candidiasis cases [21]. Appropriate identification and differentiation of cryptic species complexes is clinically relevant, as not only there are differences on virulence and antifungal susceptibility patterns among species within the same complex, but also contradictory observations for antifungal susceptibility patterns among different studies have been reported [5, 22–25]. Due to facing these contradictory results along with the limited epidemiological data for cryptic species complexes, the genuine distribution and antifungal susceptibility profiles of these species in different geographical locations remained unclear. Moreover, as antifungal susceptibility profile of cryptic species within the same complex are varied, identification down to the species level is imperative to establish the appropriate antifungal therapy [24, 26, 27]. In line with this, providing epidemiologists and small laboratories with a fast, accurate, specific, and cheap means of identification to disclose the prevalence and antifungal susceptibility profiles of isolates belonging to cryptic *Candida* species. Accordingly, we have developed and validated an inexpensive, reliable, accurate, specific, and user friendly multiplex PCR assays capable of identifying nine cryptic species in one assay.

From different perspectives including, time needed to finish the experiments, required expenses and need of trained technicians our assays is comparable to other PCR-based assay and platforms such as MALDI-TOF.

Application of cryptic species complexes strains isolated in clinical settings with our 9-plex PCR assay and its comparison with results obtained by Sanger sequencing of D1/D2 domain of LSU rDNA, revealed 100% consistency between these techniques. However, due to the high similarity between *C. albicans* and *C. africana* in the sequences of the D1/D2 and ITS rDNA fragments (99.3–100%), distinguishing these two species is difficult

Table 4 Comparison of 9-plex PCR with CBS in-house MALDI-TOF database and sequencing of D1/D2 LSU rDNA

Species	Multiplex PCR	MALDI-TOF	Sequencing
C. albicans (*n* = 128)	*C. albicans* (*n* = 128)	*C. albicans* (*n* = 128)	*C. albicans* (*n* = 128)
C. dubliniensis (*n* = 4)	*C. dubliniensis* (*n* = 4)	*C. dubliniensis* (*n* = 4)	*C. dubliniensis* (*n* = 4)
C. africana (*n* = 3)	*C. africana* (*n* = 3)	*C. albicans* (*n* = 3)	*C. africana* (*n* = 3)[a]
C. glabrata (*n* = 87)	*C. glabrata* (*n* = 87)	*C. glabrata* (*n* = 87)	*C. glabrata* (*n* = 87)
C. nivariensis (*n* = 2)	*C. nivariensis* (*n* = 2)	*C. nivariensis* (*n* = 2)	*C. nivariensis* (*n* = 2)
C. bracarensis (*n* = 2)	*C. bracarensis* (*n* = 2)	*C. bracarensis* (*n* = 2)	*C. bracarensis* (*n* = 2)
C. parapsilosis (*n* = 28)	*C. parapsilosis* (*n* = 28)	*C. parapsilosis* (*n* = 28)	*C. parapsilosis* (*n* = 28)
C. orthopsilosis (*n* = 6)	*C. orthopsilosis* (*n* = 6)	*C. orthopsilosis* (*n* = 6)	*C. orthopsilosis* (*n* = 6)
C. metapsilosis (*n* = 20)	*C. metapsilosis* (*n* = 20)	*C. metapsilosis* (*n* = 20)	*C. metapsilosis* (*n* = 20)

[a] Similarity between *C. albicans* and *C. africana* using sequencing of D1/D2 LSU rDNAwas more than 99%
This library has been enriched with a diverse range of yeast species utilized in brewery

[28]. Consistently, the sequencing of LSU rDNA fragment in *C. africana* showed > 99% similarity with *C. albicans*. Importantly, application of our 9-plex PCR could discriminate these two species. Like DNA microarray [29] and pyrosequencing [30], Sanger sequencing requires highly trained technicians and more turn-around time [8], while our multiplex PCR assay is straightforward and running of the whole application (from master mix preparation to visualization on the gel) only consumes four hours. In terms of expenses, only 0.75–1 euro is enough to finalize the results on the gel electrophoresis, however, sequencing require specific devices and is more expensive. However, in order to resolve the issue of discrepancy between the length of predicted and actual PCR products we suggest to use either our in-house ladder or to run the amplicons of each control species individually in a separate lane.

Our multiplex PCR successfully identified all *C. africana* isolates and, hence, improved the results obtained from MALDI-TOF. Except for *C. africana* strains ($n = 3$), Bruker MALDI-TOF MS could identify the rest of cryptic species complexes, resulting in 98.93% agreement with our multiplex PCR assay. Variability in accuracy of commercial MALDI-TOF MS database for identification of uncommon and cryptic *Candida* species [9, 31, 32], inability of the Bruker MALDI-TOF to distinguish *C. africana* from *C. albicans*, and incompetence of VITEK MS systems for identification of *C. bracarensis*, *C. nivariensis*, and *C. orthopsilosis* and low cut-off value of Bruker MS systems (< 1.700) for identification of *C. bracarensis* complex reinforced the urge for molecular identification tools [22, 33]. On the other hand, unlike the domination of PCR even in developing countries [12, 13], MALDI-TOF is a newer introduced platform, mainly restricted to large or reference laboratories [34–36].

Unlike, AFLP [9] and RFLP [37], there is no need for restriction of the PCR products, several visualization steps and reading of the results are straightforward. Muriel Cornet et al. (2011) used PCR-RFLP, to identify all eight cryptic species except for *C. africana*. However, this method used three primers targeting ribosomal intergenic spacer (IGS), tedious post-PCR restriction and required electrophoretic visualization twice making this experiment daunting, time consuming, and expensive [37]. Additionally, digestion of PCR products with restriction enzymes generated multiple fragments, in turn, makes the interpretation difficult when compared to banding pattern of reference strains.

The successful identification of all nine cryptic species in one tube, complements previous studies identifying members of the species complexes of *Candida albicans* [14], *Candida glabrata* [15], and *Candida parapsilosis* [16] using three separate tubes, and, hence, is time- and cost-saving.

Application of broad diversity of yeast species, five *Aspergillus* species, and human DNA for specificity testing and inclusion of an extensive number of CBS reference strains and clinical isolates, showed that our 9-plex PCR is 100% specific. As a result, our assay circumvents the imperfections of phenotypic assays (CHROMagar, VITEK 2 and ID 32C) that suffer from the lack of specificity [38, 39]. Additionally, subjecting various populations of the same species to phenotypic assay could showed various results [32, 40, 41]. Accordingly, as suggested by Griseo et al. (2015), small clinical laboratories can take advantage of specific phenotypic methods supplemented with easy-to-perform PCR-based approaches to identify and report isolated cryptic *Candia* species [8].

Conclusion

Due to the problems with the identification and discrimination of cryptic *Candida* species from their closest relatives, there is still uncertainty and unclarity about their epidemiology, pathogenicity and antifungal susceptibility pattern [43,44]. Consequently, developing reliable, specific, cost and labor effective methods is necessary. Successful testing of specificity and validation using a broad range of CBS reference strains and clinical isolates, revealed the potential of this assay to be implemented in routine diagnostics and epidemiological studies. As *C. albicans*, *C. glabrata*, and *C. parapsilosis* complex species constitute 80–90% of candidiasis cases, identification of all nine cryptic species within one multiplex PCR assay, could be of a great assistance.

Additional files

Additional file 1: Table S1. CBS reference strains utilized for optimization of 9-plex PCR. (DOCX 20 kb)

Additional file 2: Figure S1. Comparison of home-made ladder and Thermofisher commercial ladder (SM0323). Obviously, amplicons of all target species are distinguished and differentiated from one another. (JPG 79 kb)

Acknowledgements

We would like to Thank Dr. Kamiar Zomorodian, Sadegh Khodavaisy, Hamid Badali, Weiwei Jiang, and Ferry Hagen for kind provision of clinical strains and revision of the manuscript.

Funding

This project has received funding from the European Union's Horizon 2020 research and innovation programme under the Marie Sklodowska-Curie grant agreement No *642095*, National Health Department of China [2018ZX10101003], National Natural Science Foundation of China [31770161], Second Military Medical University [2017JZ47] and Shanghai Science and Technology Committee [14DZ2272900 and 14495800500].

Availability of data and materials

All data are presented in this manuscript.

Authors' contributions

AA and WJF have designed the study participated in study design and practical works, and drafted the manuscript. WHP and TB have contributed

in study design and revision. WL and LY helped with study design, strain provision, drafting and revising manuscript. All authors read and approved the final version.

Ethics approval and consent to participate
Not applicable.

Consent for publication
Not applicable.

Competing interests
Weihua Pan is the editor of BMC Infectious Diseases and we declare that her co-authorship has not influenced the editorial processes.

Publisher's Note

Author details
[1]Westerdijk Fungal Biodiversity Institute, Utrecht 3584, the Netherlands. [2]Department of Dermatology, Shanghai Key Laboratory of Molecular Medical Mycology, Shanghai Institute of Medical Mycology, Shanghai Changzheng Hospital, Second Military Medical University, Shanghai 200003, China. [3]Institute of Biodiversity and Ecosystem Dynamics, University of Amsterdam, Amsterdam 1012 WX, the Netherlands.

Received: 13 February 2018 Accepted: 13 September 2018
Published online: 25 September 2018

References
1. Magill SS, Edwards JR, Bamberg W, Beldavs ZG, Dumyati G, Kainer MA, et al. Multistate point-prevalence survey of health care–associated infections. N Engl J Med. 2014;370:1198–208. https://doi.org/10.1056/NEJMoa1306801.
2. Tietz H-J, Hopp M, Schmalreck a, Sterry W, Czaika V. *Candida africana* sp. nov., a new human pathogen or a variant of *Candida albicans*? Mycoses. 2001;44:437–45. https://doi.org/10.1046/j.1439-0507.2001.00707.x.
3. Sullivan DJ, Westerneng TJ, Haynes KA, Bennett DE, Coleman DC. *Candida dubliniensis* Sp-Nov - phenotypic and molecular characterization of a novel species associated with Oral Candidosis in Hiv-infected individuals. Microbiology-Uk. 1995;141:1507–21.
4. Alcoba-flórez J, Méndez-álvarez S, Guarro J, Pérez-roth E, Arévalo P, Cano J, et al. Phenotypic and molecular characterization of *Candida nivariensis* sp . Nov ., a possible new opportunistic fungus. J Clin Microbiol. 2005;43:4107–11.
5. Bishop JA, Chase N, Magill SS, Kurtzman CP, Fiandaca MJ, Merz WG. *Candida bracarensis* detected among isolates of Candida glabrata by peptide nucleic acid fluorescence in situ hybridization: susceptibility data and documentation of presumed infection. J Clin Microbiol. 2008;46:443–6.
6. Tavanti A, Davidson AD, Gow NAR, MCJ M, Odds FC. *Candida orthopsilosis* and *Candida metapsilosis* spp. nov. to replace *Candida parapsilosis* groups II and III. J Clin Microbiol. 2005;43:284–92.
7. Pryszcz LP, Németh T, Saus E, Ksiezopolska E, Hegedűsová E, Nosek J, et al. The genomic aftermath of hybridization in the opportunistic pathogen *Candida metapsilosis*. PLoS Genet. 2015;11:1–29.
8. Criseo G, Scordino F, Romeo O. Current methods for identifying clinically important cryptic *Candida* species. J Microbiol Methods. 2015;111:50–6. https://doi.org/10.1016/j.mimet.2015.02.004.
9. De Carolis E, Hensgens LAM, Vella A, Posteraro B, Sanguinetti M, Senesi S, et al. Identification and typing of the *Candida parapsilosis* complex: MALDI-TOF MS vs. AFLP. J Music Ther. 2015;52:123–30.
10. Sendid B, Ducoroy P, François N, Lucchi G, Spinali S, Vagner O, et al. Evaluation of MALDI-TOF mass spectrometry for the identification of medically-important yeasts in the clinical laboratories of Dijon and Lille hospitals. Med Mycol. 2013;51:25–32.
11. TM P SP, ID K, GW C. Rapid identification of fungi by sequencing the ITS1 and ITS2 regions using an automated capillary electrophoresis system. Med Mycol. 2003;41:369–81.
12. Ragheb SM, Jimenez L. Polymerase chain reaction/rapid methods are gaining a foothold in developing countries. PDA J Pharm Sci Technol. 2014; 68:239–55.
13. World Health Organization. Establishment of PCR laboratory in developing countries. 2016. http://apps.who.int/iris/bitstream/10665/249549/5/9789290225317-Eng.pdf?ua=1.
14. Romeo O, Criseo G. First molecular method for discriminating between *Candida africana*, *Candida albicans*, and *Candida dubliniensis* by using hwp1 gene. Diagn Microbiol Infect Dis. 2008;62:230–3.
15. Enache-Angoulvant A, Guitard J, Grenouillet F, Martin T, Durrens P, Fairhead C, et al. Rapid discrimination between *Candida glabrata*, *Candida nivariensis*, and *Candida bracarensis* by use of a singleplex PCR. J Clin Microbiol. 2011;49:3375–9.
16. Prandini THR, Theodoro RC, Bruder-Nascimento ACMO, Scheel CM, Bagagli E. Analysis of inteins in the *Candida parapsilosis* complex for simple and accurate species identification. J Clin Microbiol. 2013;51:2830–6.
17. Theelen B, Silvestri M, Guého E, Belkum A, Boekhout T. Identification and typing of *Malassezia* yeasts using amplified fragment length polymorphism (AFLPTm), random amplified polymorphic DNA (RAPD) and denaturing gradient gel electrophoresis (DGGE). FEMS Yeast Res. 2001;1:79–86. https://doi.org/10.1111/j.1567-1364.2001.tb00018.x.
18. Stielow JB, Lévesque CA, Seifert KA, Meyer W, Irinyi L, Smits D, et al. One fungus, which genes? Development and assessment of universal primers for potential secondary fungal DNA barcodes. Persoonia - Mol Phylogeny Evol Fungi. 2015;35:242–63. https://doi.org/10.3767/003158515X689135.
19. Taj-Aldeen SJ, Kolecka A, Boesten R, Alolaqi A, Almaslamani M, Chandra P, et al. Epidemiology of candidemia in Qatar, the Middle East: performance of MALDI-TOF MS for the identification of *Candida* species, species distribution, outcome, and susceptibility pattern. Infection. 2014;42:393–404.
20. Kolecka A, Khayhan K, Groenewald M, Theelen B, Arabatzis M, Velegraki A, et al. Identification of medically relevant species of arthroconidial yeasts by use of matrix-assisted laser desorption ionization-time of flight mass spectrometry. J Clin Microbiol. 2013;51:2491–500.
21. Guinea J. Global trends in the distribution of *Candida* species causing candidemia. Clin Microbiol Infect. 2014;20:5–10. https://doi.org/10.1111/1469-0691.12539.
22. Hou X, Xiao M, Chen SC, Wang H, Yu S, Fan X. Identification and Antifungal Susceptibility Profiles of *Candida nivariensis* and *Candida bracarensis* in a Multi-Center Chinese Collection of Yeasts. 2017;8 January:1–8.
23. Romeo O, Scordino F, Pernice I, Lo Passo C, Criseo G. A multiplex PCR protocol for rapid identification of *Candida glabrata* and its phylogenetically related species *Candida nivariensis* and *Candida bracarensis*. J Microbiol Methods. 2009;79:117–20. https://doi.org/10.1016/j.mimet.2009.07.016.
24. Borman AM, Petch R, Linton CJ, Palmer MD, Bridge PD, Johnson EM. *Candida nivariensis*, an emerging pathogenic fungus with multidrug resistance to antifungal agents. J Clin Microbiol. 2008;46:933–8.
25. Yazdanparast SA, Khodavaisy S, Fakhim H, Shokohi T, Haghani I, Nabili M, et al. Molecular characterization of highly susceptible *Candida africana* from vulvovaginal candidiasis. Mycopathologia. 2015;180:317–23.
26. Gácser A, Schäfer W, Nosanchuk JS, Salomon S, Nosanchuk JD. Virulence of *Candida parapsilosis*, *Candida orthopsilosis*, and *Candida metapsilosis* in reconstituted human tissue models. Fungal Genet Biol. 2007;44:1336–41.
27. Borman AM, Szekely A, Linton CJ, Palmer MD, Brown P, Johnson EM. Epidemiology, antifungal susceptibility, and pathogenicity of *Candida africana* isolates from the United Kingdom. J Clin Microbiol. 2013;51:967–72.
28. Rodríguez-Leguizamón G, Fiori A, López LF, Gómez BL, Parra-Giraldo CM, Gómez-López A, et al. Characterising atypical *Candida albicans* clinical isolates from six third-level hospitals in Bogotá, Colombia. BMC Microbiol 2015;15:1–10. doi:https://doi.org/10.1186/s12866-015-0535-0.
29. Campa D, Tavanti A, Gemignani F, Mogavero CS, Bellini I, Bottari F, et al. DNA microarray based on arrayed-primer extension technique for identification of pathogenic fungi responsible for invasive and superficial mycoses. J Clin Microbiol. 2008;46:909–15.
30. Borman AM, Linton CJ, Oliver D, Palmer MD, Szekely A, Odds FC, et al. Pyrosequencing analysis of 20 nucleotides of internal transcribed spacer 2 discriminates Candida parapsilosis, *Candida metapsilosis*, and *Candida orthopsilosis*. J Clin Microbiol. 2009;47:2307–10.
31. Jamal WY, Ahmad S, Khan ZU, Rotimi VO. Comparative evaluation of two matrix-assisted laser desorption/ionization time-of-flight mass spectrometry (MALDI-TOF MS) systems for the identification of clinically significant yeasts. Int J Infect Dis. 2014;26:167–70. https://doi.org/10.1016/j.ijid.2014.05.031.
32. Kim T-H, Kweon OJ, Kim HR, Lee M-K. Identification of uncommon *Candida* species using commercial identification systems. J Microbiol Biotechnol. 2016;26:2206–13. https://doi.org/10.4014/jmb.1609.09012.

33. Sow D, Fall B, Ndiaye M, Ba BS, Sylla K, Tine R, et al. Usefulness of MALDI-TOF mass spectrometry for routine identification of *Candida* species in a resource-poor setting. Mycopathologia. 2015;180:173–9.
34. Posteraro B, Efremov L, Leoncini E, Amore R, Posteraro P, Ricciardi W, et al. Are the conventional commercial yeast identification methods still helpful in the era of new clinical microbiology diagnostics? A meta-analysis of their accuracy. J Clin Microbiol. 2015;53:2439–50.
35. Posteraro B, De Carolis E, Vella A, Sanguinetti M. MALDI-TOF mass spectrometry in the clinical mycology laboratory: identification of fungi and beyond. Expert Rev Proteomics 2013;10:151–164.
36. Clark AE, Kaleta EJ, Arora A, Wolk DM. Matrix-assisted laser desorption ionization-time of flight mass spectrometry: a fundamental shift in the routine practice of clinical microbiology. Clin Microbiol Rev. 2013;26:547–603.
37. Cornet M, Sendid B, Fradin C, Gaillardin C, Poulain D, Nguyen HV. Molecular identification of closely related *Candida* species using two ribosomal intergenic spacer fingerprinting methods. J Mol Diagnostics. 2011;13:12–22. https://doi.org/10.1016/j.jmoldx.2010.11.014.
38. Bishop JA, Chase N, Lee R, Kurtzman CP, Merz WG. Production of white colonies on CHROMagar Candida medium by members of the *Candida glabrata* clade and other species with overlapping phenotypic traits. J Clin Microbiol. 2008;46:3498–500.
39. Cendejas-Bueno E, Gomez-Lopez A, Mellado E, Rodriguez-Tudela JL, Cuenca-Estrella M. Identification of pathogenic rare yeast species in clinical samples: comparison between phenotypical and molecular methods. J Clin Microbiol. 2010;48:1895–9.
40. Albaina O, Sahand IH, Brusca MI, Sullivan DJ, De Larrinoa IF, Moragues MD. Identification and characterization of nine atypical *Candida dubliniensis* clinical isolates. J Med Microbiol 2015;64:147–156.
41. Romeo O, Criseo G. *Candida africana* and its closest relatives. Mycoses. 2011; 54:475–86.

Received: 1 August 2018 | Revised: 20 September 2018 | Accepted: 14 October 2018

DOI: 10.1111/myc.12863

ORIGINAL ARTICLE

WILEY mycoses Diagnosis, Therapy and Prophylaxis of Fungal Diseases

Genotypic diversity and antifungal susceptibility of *Cryptococcus neoformans* isolates from paediatric patients in China

Nan Hong[1,2] | Min Chen[1,2] | Nan Xu[3] | Abdullah M. S. Al-Hatmi[4,5,6] | Chao Zhang[1,2] | Wei H. Pan[1,2] | Ferry Hagen[4] | Teun Boekhout[1,2,7,8] | Jianping Xu[9] | Xian B. Zou[10] | Wan Q. Liao[1,2]

[1]Department of Dermatology, Changzheng Hospital, Second Military Medical University, Shanghai, China

[2]Shanghai Key Laboratory of Medical Mycology, Changzheng Hospital, Second Military Medical University, Shanghai, China

[3]Department of Dermatology, Shanghai East Hospital, Tongji University School of Medicine, Shanghai, China

[4]Department of Medical Mycology, Westerdijk Fungal Biodiversity Institute, Utrecht, The Netherlands

[5]Centre of Expertise in Mycology, Radboud University Medical Centre/Canisius-Wilhelmina Hospital, Nijmegen, The Netherlands

[6]Ministry of Health, Directorate General of Health Services, Ibri, Oman

[7]Department of Yeast and Basidiomycete Research, Westerdijk Fungal Biodiversity Institute, Utrecht, The Netherlands

[8]Institute of Biodiversity and Ecosystem Dynamics, University of Amsterdam, Amsterdam, The Netherlands

[9]Department of Biology, McMaster University, Hamilton, Ontario, Canada

[10]Department of Dermatology, First Affiliated Hospital of PLA General Hospital, Beijing, China

Correspondence
Wan Q. Liao, Department of Dermatology, Shanghai Key Laboratory of Molecular Medical Mycology, Changzheng Hospital, Second Military Medical University, Shanghai, China.
Email: liaowanqing@smmu.edu.cn
and
Xian B. Zou, Department of Dermatology, First Affiliated Hospital of PLA General Hospital, Beijing, China.
Email: zouxianbiao25@sina.com

Funding information
National Health Department, Grant/Award Number: 2014ZX09J14106-02A and 2018ZX10101003; National Natural Science Foundation of China, Grant/Award Number: 81201269; Shanghai Science and Technology, Grant/Award Number: 14DZ22201000

Abstract

Cryptococcosis is a life-threatening mycosis primarily occurring in adult patients particularly those with immunosuppression such as HIV infection/AIDS. The number of reported cases of paediatric cryptococcosis has increased in the last decade around the world, including China. However, current information on the characteristics of cryptococcosis in children, particularly the genotypic diversity and antifungal susceptibility of the isolates, is limited. In the present study, a total of 25 paediatric isolates of *Cryptococcus neoformans* were genotyped using the ISHAM-MLST scheme. In vitro susceptibility to antifungal agents of the 22 isolates was tested using the CLSI M27-A3 method. Our analyses revealed that the genotypic diversity of *C. neoformans* isolates from Chinese paediatric patients was low, with ST 5 (80%) and ST 31 (12%) being the two major sequence types. Reduced susceptibility to fluconazole (FLU), 5-flucytosine (5-FC) and itraconazole (ITR) was observed among *C. neoformans* isolates from Chinese paediatric patients, particularly among the ST5 isolates, which was similar to observations made on *C. neoformans* isolates from Chinese adult patients. In addition, the majority of isolates (3/4, 75%) obtained from deceased patients showed decreased antifungal susceptibility, which indicates that further monitoring of antifungal susceptibility of *Cryptococcus* isolates is warranted in management of paediatric cryptococcosis.

Nan Hong, Min Chen and Nan Xu contributed equally to this work and share the first co-authorship.

KEYWORDS
antifungal susceptibility, China, *Cryptococcus neoformans*, genotype, paediatric

1 | INTRODUCTION

Cryptococcus neoformans and *Cryptococcus gattii* are two major basidiomycetes yeasts which form a species complex and are associated with cryptococcosis, a life-threatening mycosis involving both immunosuppressed and immunocompetent hosts.[1,2] *Cryptococcus neoformans* has a worldwide distribution, occurring naturally in avian excreta and causing over 80% of cryptococcosis cases each year.[3] *Cryptococcus gattii* is mainly associated with trees and has emerged as a pathogen of immunocompetent humans in temperate regions of North America.[4]

The recent development of molecular techniques, such as multilocus sequence typing (MLST), has improved our understanding of the genetic diversity and taxonomy of *C. neoformans* and *C. gattii* as both are recognised as species complexes.[5-7] *Cryptococcus neoformans* (serotype A) has been divided into three major molecular types, namely AFLP1/VNI, AFLP1A/VNII/VNB and AFLP1B/VNII; molecular type of *Cryptococcus deneoformans* (serotype D) is AFLP2/VNIV; molecular type of the hybrid isolates (serotype AD) is AFLP3/VNIII.[7] In addition, *C. neoformans* and *C. gattii* have two opposite mating types, *MAT*α and *MAT***a**, with *MAT*α being the prevalent mating type of clinical and environmental isolates.[8,9]

The rapid emergence of multidrug-resistant pathogenic fungi has become a major threat to human health.[10] Currently, azoles, particularly fluconazole (FLU), are generally recommended for the treatment of cryptococcosis during the consolidation and maintenance phases.[11] However, cryptococcosis caused by FLU-resistant *Cryptococcus* isolates has recently been reported.[12] Moreover, antifungal susceptibility of *Cryptococcus* isolates has been noted to vary among genotypes and geographic regions.[1,5]

Cryptococcosis is primarily observed in adult patients with HIV/AIDS, while cases involving children are rarely reported.[13-16] It has been documented that paediatric cryptococcosis accounted for 0.9% of all cryptococcosis cases in South Africa.[17] The number of reported cryptococcosis in children, however, has increased worldwide in the last decade, including China.[16,18] A previous study indicated that the majority (approximately 70%) of children (>2 years old) in the Bronx, New York, USA had serologic evidence for *C. neoformans* infection,[19] particularly those older than 5 years old.[20]

To date, data on the characteristics of cryptococcosis in children, particularly the genotypic diversity and antifungal susceptibility of the isolates, are limited. To the best of our knowledge, only one study from South Africa has investigated isolates from paediatric cryptococcosis cases, indicating a high genetic diversity among *C. neoformans* isolates from paediatric patients. Here we report the first genotyping and antifungal susceptibility profiles of paediatric cryptococcosis in China.

2 | MATERIALS AND METHODS

2.1 | Isolates

The paediatric cryptococcosis cases in the present study were all confirmed by a positive culture. Patients whose age at the time of diagnosis was <16 years were included in this study. Twenty-two *C. neoformans* strains isolated from paediatric patients were included in our study. All these isolates were collected from six university hospitals in China namely: Changzheng Hospital (n = 15), Xinhua Hospital (n = 1) and Huashan Hospital (n = 1) in Shanghai; West China Hospital (n = 2) in Chengdu, Sichuan Province; the First Affiliated Hospital of Zhejiang University (n = 2) in Hangzhou, Zhejiang Province; and Guangzhou General Military Hospital (n = 1) in Guangzhou, Guangdong Province. In addition, we also included the MLST sequence and clinical information of three paediatric isolates (PU 18, PU 31 and PU 158) which were reported previously from Beijing[21] for comparison analyses.

2.2 | Mating type

To determine the mating type of the *C. neoformans* isolates, PCRs were performed as previously described.[22] *Cryptococcus neoformans* strains CBS 10512 (*MAT***a**; AFLP1/VNI), CBS10515 (*MAT*α; AFLP1/VNI), and *C. deneoformans* strains CBS 10511 (*MAT***a**; AFLP2/VNIV), CBS 10513 (*MAT*α; AFLP2/VNIV) were used as controls.

2.3 | DNA extraction, PCR and sequencing

DNA extraction of *C. neoformans* isolates was performed following the instructions of the UltraClean® microbial DNA isolation kit (MoBIO Laboratories, Carlsbad, CA, USA). Each locus (*CAP59*, *GPD1*, IGS1, *LAC1*, *PLB1*, *SOD1* and *URA5*) in *C. neoformans* was amplified in a 25 μL PCR volume according to the ISHAM-MLST scheme.[23] PCR products were purified with Sephadex G-50 fine (GE Healthcare Bio-Sciences, Uppsala, Sweden) and were sequenced from both directions. Sequence reads were manually edited using SeqMan v8.0.2 (DNASTAR, Madison, WI, USA) and each MLST sequence was aligned using MUSCLE version 3.8.31[24] and concatenated by the FASconCAT program,[25] and then queried against the online MLST database (http://mlst.mycologylab.org) to assign allele type (AT) for each of the seven loci. The final sequence type (ST) for each isolate was determined based on the combined allelic assignments at the seven sequenced loci.

2.4 | Genotyping

Principal component analysis (PCA) of the sequence data of *C. neoformans* isolates was performed using the Adegenet 2.1.1

TABLE 1 Demographic characteristics of paediatric *C. neoformans* isolates from China

Isolate	Isolated time	Age	Gender	City	Specimen	Underlying diseases	Outcome	Mating type	ST	Ref
SCZ 20079	1998-02	11	Male	Fujian	CSF	None	Alive	α	5	This Study
SCZ 20159	1999-02	8	Male	Shanghai	CSF	None	Alive	α	53	This Study
SCZ 20078	1999-11	4	Male	Henan	CSF	None	Died	α	5	This Study
SCZ 20067	2000-12	12	Female	Shanghai	CSF	None	Alive	α	93	This Study
SCZ 20151	2001-02	14	Male	Shanxi	CSF	None	Alive	α	5	This Study
SCZ 20074	2001-04	14	Male	Sichuan	CSF	None	Alive	α	5	This Study
SCZ 20149	2001-06	8	Female	Anhui	CSF	None	Alive	α	5	This Study
SCZ 20072	2001-06	13	Male	Guangdong	CSF	None	Alive	α	5	This Study
SCZ 20098	2001-11	8	Male	Hunan	Skin	None	Alive	α	5	This Study
SCZ 20145	2003-02	8	Female	Hubei	CSF	None	Alive	α	5	This Study
SCZ 20154	2003-08	3	Male	Henan	CSF	None	Died	α	31	This Study
SCZ 20099	2002-05	8	Male	Sichuan	Skin	None	Alive	α	5	This Study
SCZ 20359	2007-04	12	Female	Jiangsu	CSF	None	Alive	α	5	This Study
SCZ 20126	2007-05	6	Female	Shanghai	CSF	None	Alive	α	5	This Study
SCZ 20361	2009-12	14	Male	Beijing	CSF	None	Alive	α	5	This Study
SCZ 20362	2010-05	13	Female	Hubei	CSF	SLE	Alive	α	5	This Study
SCZ 20363	2010-06	7	Male	Hubei	CSF	None	Alive	α	31	This Study
SCZ 20364	2010-08	8	Female	Beijing	Blood	HIV(+)	Alive	α	5	This Study
SCZ 20321	2010-07	15	Female	Sichuan	Blood	HIV(+)	Died	α	5	This Study
SCZ 20322	2010-11	12	Male	Sichuan	CSF	None	Died	α	31	This Study
SCZ 20161	2015-11	15	Male	Zhejiang	CSF	None	Alive	α	5	This Study
SCZ 20172	2016-07	12	Male	Zhejiang	CSF	None	Alive	α	5	This Study
PU 158	2010-08	8	Female	Hebei	Blood	HIV(+)	Alive	ND	5	21
PU 18	2009-12	14	Male	Hebei	CSF	None	Alive	ND	5	21
PU 31	2010-05	13	Female	Shanxi	CSF	SLE	Alive	ND	5	21

CSF, Cerebrospinal fluids; ST, Sequence type; SLE, Systemic Lupus Erythematosus.

package[26] for software R (version 3.4.4). Moreover, nucleotide diversity (π), number of polymorphic sites (S), average number of nucleotide differences per sequence (k) and average number of nucleotide substitutions per site between populations (D_{xy}) were calculated using DnaSP version 6.10.03.[27] The recent study on paediatric *C. neoformans* isolates from South Africa did not follow the full ISHAM-MLST scheme to analyse genetic diversity. However, among the 11 loci analysed by them, five loci (*GPD1*, *LAC1*, IGS1, *PLB1* and *SOD1*) overlapped with the seven loci used in our study. For comparative analysis of the paediatric *C. neoformans* isolates between China and South Africa, the results of our genetic diversity analysis were all based on the five-locus sequence data. Comparisons of ST distributions between *C. neoformans* isolates from Chinese paediatric cases and that from Chinese adult cases were conducted using Fisher's exact test corrected with the Benjamini-Hochberg method for multiple comparisons. The ST information of *C. neoformans* isolates from 162 Chinese adult cases was collected from two previous studies by Dou et al[21] (n = 77) and Chen et al[28] (n = 85).

2.5 | Phylogenetic analysis

We selected four representative *C. neoformans* isolates from Chinese paediatric patients representing four different STs identified here, five *C. neoformans* isolates from Chinese adult patients with five different STs and twenty-one isolates from paediatric patients in South Africa to show the relationships among the different STs in a phylogenetic tree. Our phylogenetic tree was based on the five-locus sequence data (*GPD1*, *LAC1*, IGS1, *PLB1* and *SOD1*). The sequence data of these five loci were aligned individually using MUSCLE version 3.8.31[24] and concatenated by FASconCAT program.[25] The concatenated alignment was then uploaded into MEGA7.0.9 to construct a phylogenetic tree using maximum likelihood (ML) and maximum parsimony (MP) methods with K2 + G model and 1000-replicate of bootstrap test, respectively.[29]

2.6 | Antifungal susceptibility testing

To assess the in vitro antifungal susceptibility of the isolates, antifungal drugs amphotericin B (AMB), 5-flucytosine (5-FC), fluconazole (FLU), itraconazole (ITR), voriconazole (VOR), posaconazole (POS) and isavuconazole (ISA) were applied to the *Cryptococcus* isolates using the CLST M27-A3 protocol.[30] The minimum inhibitory concentration (MIC) values were determined after 72 hours of incubation at 35°C. *Candida krusei* strain ATCC 6258 and *C. parapsilosis* strain ATCC 22019 were used as quality control (QC) strains. Based on the recommendation of previous studies, the epidemiological cut-off values (ECVs) of *C. neoformans* for 5-FC and FLU used in the present study were 8 mg/L; 0.25 mg/L for ITR, VOR and POS; 1 mg/L for AMB; and 0.12 mg/L for ISA, respectively.[31-33] In this study, isolates with MIC values above the ECVs were considered as non-wild-type (non-WT) isolates and isolates with MIC values equal to the ECVs were considered as having decreased susceptibility to antifungal drugs.

FIGURE 1 Geographical distribution of paediatric *C. neoformans* isolates from China that were included in this study

3 | RESULTS

3.1 | Demographic data of the paediatric isolates

The isolates included in our study were collected from 25 paediatric patients living in 13 different provinces across China as shown in Table 1. The majority of the isolates were obtained from Sichuan (16%, 5/25), followed by Shanghai (12%, 3/25), Hubei (12%, 3/25), Beijing (8%, 2/25), Hebei (8%, 2/25), Henan (8%, 2/25), Shanxi (8%, 2/25), Zhejiang (8%, 2/25), Fujian (4%, 1/25), Anhui (4%, 1/25), Guangdong (4%, 1/25), Hunan (4%, 1/25) and Jiangsu (4%, 1/25). The majority of these isolates were recovered from cerebrospinal fluid (CSF) (80%, 20/25), followed by blood (12%, 3/25), and skin (8%, 2/25). The mean age of these patients was 10.4 ± 3.5 years (range: 3-15 years), with the majority within the age range of 11-15 years (56%, 14/25). The male/female gender ratio was 1.5 (15:10). The majority of the paediatric patients (80%, 20/25) had no underlying diseases. Only three paediatric patients were HIV-infected, and two patients had systematic lupus erythematous (SLE). Patient characteristics are presented in Table 1 and Figure 1.

3.2 | Genotypes and mating types

All of the paediatric isolates from China were identified as *C. neoformans* (AFLP1/VNI, *MAT*α). Among these, four STs were identified with ST5 (80%, 20/25) being predominant, followed by ST31 (12%,

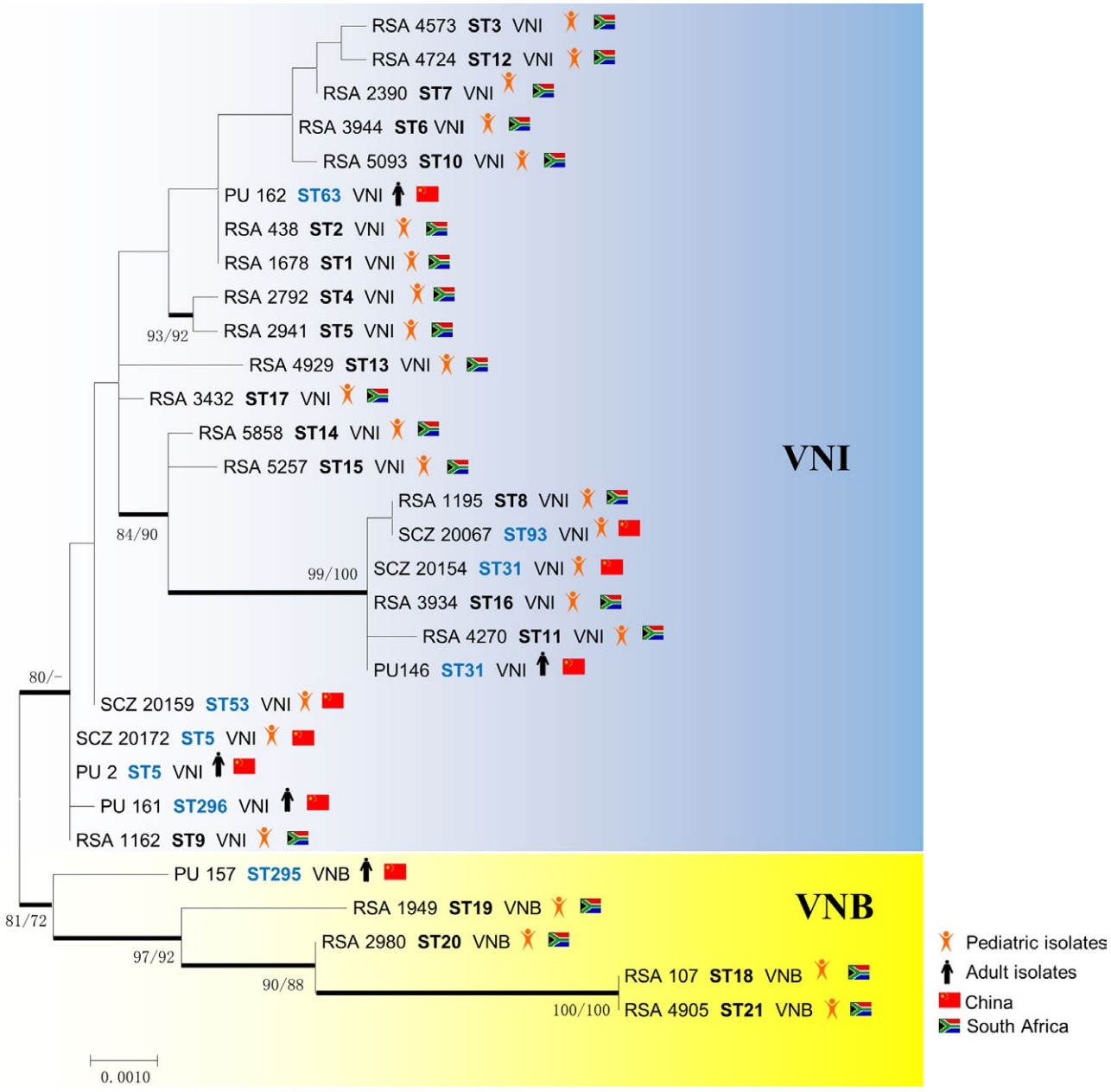

FIGURE 2 A phylogenetic tree for the representative paediatric *C. neoformans* isolates from China and South Africa using ML and MP methods based on the sequences of five loci (*GPD*1, *LAC*1, IGS1, *PLB*1 and *SOD*1). Sequence types in blue derive from the ISHAM-MLST scheme; sequence types in black derive from 11-loci MLST scheme. ST represents sequence type

TABLE 2 Nucleotide polymorphisms in each locus and concatenated sequences of paediatric *C. neoformans* isolates from China and South Africa

	Paediatric isolates from China			Paediatric isolates from South Africa			Paediatric isolates from China and South Africa			
Locus	S	π	*k*	S	π	*k*	S	π	*k*	D_{xy}
PLB1	1	0.00015	0.080	6	0.00208	1.106	6	0.00192	1.021	0.00202
LAC1	1	0.00017	0.333	7	0.00298	1.398	7	0.00288	1.355	0.00315
GPD1	1	0.00054	0.280	6	0.00201	1.044	6	0.00202	1.050	0.00231
IGS1	10	0.00388	2.800	12	0.00654	4.714	12	0.00597	4.307	0.00560
SOD1	0	0	0	1	0.00011	0.059	1	0.00008	0.043	0.00006
Concatenated	13	0.00044	3.493	32	0.00300	8.321	32	0.00280	7.776	0.00282

S, number of polymorphic sites; π, nucleotide diversity; *k*, average number of nucleotide differences per sequence; D_{xy}, average number of nucleotide substitutions per site between populations (paediatric isolates from China vs paediatric isolates from South Africa).

3/25), ST53 (4%, 1/25) and ST93 (4%, 1/25). The details are shown in Table 1.

3.3 | Phylogenetic analysis

The phylogenetic tree revealed that the predominant ST5 isolate (based on the ISHAM-MLST) in Chinese paediatric isolates (represented by strain SCZ 20172) clustered together with a ST9 isolate (based on 11-loci MLST) from the South Africa study (represented by strain RSA 1162). Moreover, the major ST8 isolate (based on 11 loci MLST) from South Africa (represented by strain RSA 1195) clustered together with ST 93 isolate (based on the ISHAM-MLST) from China (represented by strain SCZ 20067). Details of the phylogenetic tree are shown in Figure 2.

3.4 | Comparison of genetic diversity of paediatric isolates between China and South Africa

The PCA was used to assess the genetic structure of the paediatric *C. neoformans* AFLP1/VNI isolates from China and South Africa. The genetic structure captured by the first two principal components showed a combined contribution of 77.8%. The paediatric isolates from China clustered into four groups, whereas the paediatric isolates from South Africa clustered into 10 groups. The PCA results agreed with the results of the phylogenetic analysis, which revealed that the ST5 (based on the ISHAM-MLST) isolates from China were closely related to ST9 (based on 11-loci MLST) isolates from South Africa, and ST93 (based on the ISHAM-MLST) isolates from China were closely related to ST8 (based on 11-loci MLST) isolates from South Africa.

The nucleotide diversity (π) of paediatric isolates from South Africa (π = 0.00300, n = 82) was significantly higher than that from China (π = 0.00044, n = 25). The average number of nucleotide differences per sequence (k-value) of paediatric isolates from South Africa (k = 8.321) was also higher than that of paediatric isolates from China (*k* = 3.493). Together with the paediatric isolates from China and South Africa, the nucleotide sequences of all five loci had polymorphic sites ranging from 1 to 12. Locus IGS1 had the highest nucleotide diversity (π = 0.00597) and the highest average number of nucleotide differences per sequence (*k* = 4.307), followed by *LAC1* (π = 0.00288, *k* = 1.355) and *GPD1* (π = 0.00202, *k* = 1.050). There was a significantly higher percentage of ST31 isolates from Chinese paediatric cases than that from Chinese adult cases (Fisher's Exact test, calibrated *P* = 0.036). However, there was no significant difference in ST5 distribution between *C. neoformans* isolates from Chinese paediatric cases and that from Chines adult cases (calibrated *P* = 0.183). The details are shown in Table 2, Table 3 and Figure 3.

3.5 | In vitro antifungal drug susceptibility

The MIC values of QC strain ATCC 6258 in this study were 1 mg/L for AMB, 16 mg/L for 5-FC, 32 mg/L for FLU, 0.5 mg/L for ITR and POS, 0.25 mg/L for VOR and ISA. The MIC values of QC strain ATCC 22019 in this study were 1 mg/L for AMB, 2 mg/L for FLU, 0.125 mg/L for POS, 0.063 mg/L for VOR, 0.031 mg/L for ISA, 0.25 mg/L for 5-FC and ITR. Our results are consistent with what have been reported for these two strains in CLSI M27-A3 and in previous studies.[31-33] The MIC values of the paediatric isolates of the present study were determined for seven antifungal compounds, namely AMB, 5-FC, FLU, ITR, VOR, POS and ISA. For the 22 isolates, the in vitro antifungal MIC_{90} and susceptibility ranges were 0.5 mg/L (0.25-0.50 mg/L) for AMB, 8 mg/L (2-8 mg/L) for 5-FC, 4 mg/L (0.5-8 mg/L) for FLU, 0.125 mg/L (0.031-0.125 mg/L) for VOR, 0.125 mg/L (0.008-0.125 mg/L) for POS, 0.25 μg/mL (0.031-0.250 mg/L) for ITR and 0.031 mg/L (0.004-0.063 mg/L) for ISA. None of the isolates in this study showed resistance to FLU and 5-FC, which are the two most commonly used antifungal drugs in the treatment of cryptococcosis. Five ST5 isolates from Chinese paediatric patients were observed to have decreased susceptibility to ITR, and seven isolates were found to have decreased susceptibility to 5-FC. One ST5 paediatric isolate (SCZ 20172) was observed to have decreased susceptibility to FLU, 5-FC and ITR. The ST93 and ST53 paediatric isolates in our study were not observed to be resistant or have decreased susceptibility to the

TABLE 3 Comparison of two major ST distributions between paediatric isolates and adult isolates in China

Sequence type	Isolates from paediatric cases (n = 25)	Isolates from adult cases (n = 162)	*P*-value	Calibrated *P*-value
ST 5	20 (0.800)	145 (0.895)	0.183	0.183
ST 31	3 (0.120)	2 (0.012)	0.018	0.036

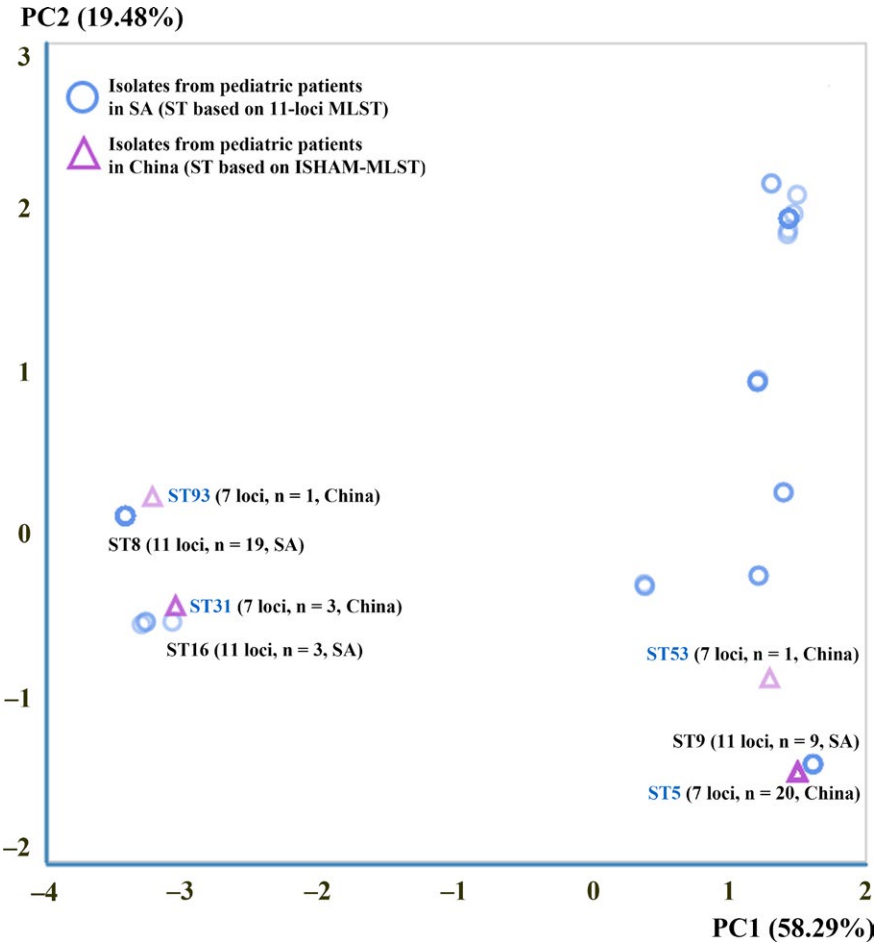

FIGURE 3 Genetic relationships among *C. neoformans* AFLP1/VNI paediatric isolates from China and South Africa by principal component analysis. Circles represent the isolates from South Africa, and triangles represent the isolates from China. Sequence types in blue derive from the ISHAM-MLST scheme; sequence types in black derive from 11-loci MLST scheme. SA represents South Africa

TABLE 4 The MIC range, MIC_{50}, MIC_{90} and geometric mean MIC of seven antifungal agents for paediatric *C. neoformans* isolates from China

Isolates	Antifungal agents	MIC			
		Range	MIC_{50}	Geometric mean MIC	MIC_{90}
This study (*n* = 22)	AMB	0.25-0.5	0.5	0.441	0.5
	5-FC	2-8	4	4.832	8
	FLU	0.25-8	2	2.130	4
	ITR	0.031-0.25	0.125	0.097	0.25
	VOR	0.031-0.125	0.063	0.069	0.125
	POS	<0.008-0.125	<0.008	0.019	0.125
	ISA	<0.004-0.063	0.015	0.012	0.031

seven antifungal compounds. Most paediatric isolates from deceased patients (3/4, 75%) in this study had decreased susceptibility to antifungal compounds. Specifically, two isolates (SCZ 20154 and SCZ 20078) had decreased susceptibility to 5-FC and one isolate had decreased susceptibility to ITR (SCZ 20321). Details are shown in Table 4 and Table S1.

4 | DISCUSSION

Cryptococcosis is a lethal fungal infection that primarily affects adult patients, especially those with AIDS or suffering from other underlying diseases.[3,34] In contrast, cryptococcosis is rare in children, even those who are HIV-infected.[14,35] However, the number of reported cases of cryptococcosis in children has increased in Africa, Europe, South America and Asia, including China.[15,16,18,36-40] Except for the recent study in South Africa,[37] data on the genotypic diversity and antifungal susceptibility of paediatric *Cryptococcus* isolates are limited.

In this study, cryptococcosis mainly occurred in older children with a mean age of 10.4 ± 3.5 years old, which is similar to that of previous studies.[14,37] One possible explanation for the older onset age is that the amount of cryptococcal exposure is important for cryptococcal infection.[20] Repeated exposure of *C. neoformans* in early childhood may be necessary to establish a latent fungal burden which can be reactivated at older age.[20] Sixty per cent of paediatric cryptococcosis patients were male, which is similar to previous studies,[13,14] supporting the theory that *C. neoformans* infections might be gender-related.[40,41] In terms of infection profiles of paediatric cryptococcosis, the most frequent (84%) symptom was *Cryptococcus* meningitis, followed by disseminated cryptococcosis (12%) and skin lesions (4%). The majority of our *C. neoformans* isolates (80.0%) were recovered from apparently immunocompetent children, and this agrees with previous studies in China (83.6%, 92/110),[13,16,18,40] but differs from studies in USA (20.6%, 13/63)[14] and South Africa (4.4%, 2/45).[36] Earlier investigations suggested that cryptococcosis primarily occurs in apparently immunocompetent adults in China.[21,42] However, in China, AIDS patients are generally transferred to special hospitals for treatment and the clinical data of these patients are unavailable. Thus, the incidence of cryptococcosis in HIV-positive patients in China might be underestimated.

A considerable percentage of paediatric cryptococcosis cases caused by members of the *C. gattii* species complex has been reported in Colombia (5.9%),[15] South Africa (7.0%)[43] and Brazil (29.6%).[44] In contrast, cryptococcal isolates from Chinese paediatric patients were all *C. neoformans* genotype AFLP1/VNI and could be divided into four STs (ST5, ST31, ST53 and ST93), with ST5 as the predominant one. This result is not surprising because ST5 isolate is also predominant among cryptococcal isolates from Chinese adult patients.[1,6] This result might also be related to the predominance of *C. neoformans* AFLP1/VNI in China's natural environment.[45] Notably, our study indicated a significant difference in the distribution of ST31 between *C. neoformans* isolates from Chinese paediatric and adult cases (calibrated $P = 0.036$). More studies on the virulence of ST31 isolates are needed to explain the different capability that ST31 isolates showed in infecting Chinese paediatric patients and infecting Chinese adult patients in this study. In addition, all the paediatric isolates were mating type α, which agrees with previous observations that over 90% of both clinical and environmental isolates of *C. neoformans* are mating type α,[8,9] including isolates from China.[42,46] The skewed distribution of *MAT*α isolates might result from clonal expansion by asexual reproduction, self-fruiting, and/or same-sex mating and reproduction among these isolates.[47]

In the present study, low genotypic diversity among isolates obtained from Chinese paediatric patients was observed. Currently, a total of 24 STs of *C. neoformans* have been identified within isolates obtained from Chinese adult patients with predominant sequence type ST5.[6,21,28,46] In our study, only four STs have been identified, and ST5 was also the predominant sequence type (80%, 20/25). This result is reasonable because adult and paediatric patients in China may be exposed to the same natural environment harbouring *C. neoformans* isolates. The genotypic diversity among paediatric isolates in China is lower than that observed in South Africa.[37] Both π and k values of the paediatric isolates from South Africa were higher than those of the isolates from China, which is similar to the results of previous studies.[48,49] Since only five loci sequences were shared between our study and the study from South Africa,[37] phylogenetic analysis and PCA were based on these five shared loci. Phylogenetic analysis suggested that the predominant ST5 (based on the ISHAM-MLST) isolates from China are closely related to ST9 (based on 11-loci MLST) isolates from South Africa, and ST93 (based on the ISHAM-MLST) isolates from China are closely related to the predominant ST8 (based on 11-loci MLST) isolates from South Africa. The PCA results agree with our phylogenetic findings, suggesting significant differences in the population structure of paediatric *Cryptococcus* isolates between China and South Africa. Moreover, we suggest that the ISHAM-MLST scheme should be utilised in investigating the genotypic diversity of more paediatric *C. neoformans* isolates in the future.

The number of reported *C. neoformans* isolates with FLU resistance has increased in the past decade[12] and varies with genotype and geographic region.[31,32] According to the current clinical guidelines for cryptococcosis,[11] AMB and 5-FC were recommended to treat central nervous system (CNS) cryptococcal infection and disseminated cryptococcosis in children and FLU is used in maintenance therapy of cryptococcosis in children. When we apply the recently published ECVs to evaluate the current results, none of the isolates in this study showed resistance to FLU and 5-FC, however, eight ST5 paediatric isolates and two ST31 paediatric isolates showed decreased susceptibility to 5-FC, and/or FLU, and/or ITR. These results agree with the findings of a previous study that showed increasing rates of *C. neoformans* isolates that are resistant to FLU in China, particularly the ST5 isolates.[6] Moreover, most paediatric isolates from deceased patients (3/4, 75%) in this study had decreased susceptibility to antifungal compounds. Two paediatric isolates had decreased susceptibility to 5-FC and one paediatric isolate had decreased susceptibility to ITR, suggesting that decreased susceptibility to antifungal drugs of *C. neoformans* isolates might be related to therapeutic failure. Thus, antifungal drug susceptibility testing of *C. neoformans* isolates should be recommended to improve prognosis of paediatric cryptococcosis patients.

In summary, the genotypic diversity of paediatric *C. neoformans* isolates from China is low, and the two most frequent sequence types were ST5 and ST31. Decreased susceptibility to

FLU, 5-FC and ITR were observed among paediatric *C. neoformans* isolates from China, particularly among the ST5 isolates. Further investigations of paediatric *C. neoformans* isolates from around the world, particularly relating to genotypic diversity and drug resistance, are needed for better prevention and treatment of paediatric cryptococcosis.

ACKNOWLEDGEMENTS

This study was funded in part with the grants from Major National R&D Projects of the National Health Department (2014ZX09J14106-02A), the National Health Department (2018ZX10101003), National Natural Science Foundation of China (No. 81201269) and Shanghai Science and Technology counsel projects of 14DZ22201000 supported this study.

CONFLICT OF INTERESTS

None declared.

AUTHORS' CONTRIBUTIONS

NH, MC and NX participated in laboratory testing, statistical analysis, and drafting of the manuscript. TB, WHP, FH, JPX and AMS participated in designing this study and revising the manuscript. WQL and XBZ conceived and designed the study. All of the authors have read and approved the final manuscript.

ORCID

Min Chen http://orcid.org/0000-0002-0629-9264
Wei H. Pan http://orcid.org/0000-0001-8077-023X
Jianping Xu http://orcid.org/0000-0003-2915-2780

REFERENCES

1. Cogliati M. Global Molecular Epidemiology of *Cryptococcus neoformans* and *Cryptococcus gattii*: an atlas of the molecular types. *Scientifica*. 2013;2013:675213.
2. Hagen F, Lumbsch HT, Arsic Arsenijevic V, et al. Importance of resolving fungal nomenclature: the case of multiple pathogenic species in the Cryptococcus genus. *mSphere*. 2017;2(4):e00238-17.
3. Mitchell TG, Perfect JR. Cryptococcosis in the era of AIDS–100 years after the discovery of *Cryptococcus neoformans*. *Clin Microbiol Rev*. 1995;8(4):515-548.
4. Chen SC, Meyer W, Sorrell TC. *Cryptococcus gattii* infections. *Clin Microbiol Rev*. 2014;27(4):980-1024.
5. Khayhan K, Hagen F, Pan W, et al. Geographically structured populations of *Cryptococcus neoformans* variety *grubii* in Asia correlate with HIV status and show a clonal population structure. *PLoS ONE*. 2013;8(9):e72222.
6. Fan X, Xiao M, Chen S, et al. Predominance of *Cryptococcus neoformans* var. *grubii* multilocus sequence type 5 and emergence of isolates with non-wild-type minimum inhibitory concentrations to fluconazole: a multi-centre study in China. *Clin Microbiol Infect*. 2016;22(10):887-e881.
7. Hagen F, Khayhan K, Theelen B, et al. Recognition of seven species in the *Cryptococcus gattii/Cryptococcus neoformans* species complex. *Fungal Genet Biol*. 2015;78:16-48.
8. Kwon-Chung KJ, Bennett JE. Distribution of alpha and alpha mating types of *Cryptococcus neoformans* among natural and clinical isolates. *Am J Epidemiol*. 1978;108(4):337-340.
9. Campbell LT, Fraser JA, Nichols CB, Dietrich FS, Carter D, Heitman J. Clinical and environmental isolates of *Cryptococcus gattii* from Australia that retain sexual fecundity. *Eukaryot Cell*. 2005;4(8):1410-1419.
10. Bastos RW, Carneiro HCS, Oliveira LVN, et al. Environmental triazole induces cross-resistance to clinical drugs and affects morphophysiology and virulence of *Cryptococcus gattii* and *C. neoformans*. *Antimicrob Agents Chemother*. 2018;62(1):e01179-17.
11. Perfect JR, Dismukes WE, Dromer F, et al. Clinical practice guidelines for the management of cryptococcal disease: 2010 update by the infectious diseases society of america. *Clin Infect Dis*. 2010;50(3):291-322.
12. Cheong JW, McCormack J. Fluconazole resistance in cryptococcal disease: emerging or intrinsic? *Med Mycol*. 2013;51(3):261-269.
13. Yuanjie Z, Jianghan C, Nan X, et al. Cryptococcal meningitis in immunocompetent children. *Mycoses*. 2012;55(2):168-171.
14. Joshi NS, Fisher BT, Prasad PA, Zaoutis TE. Epidemiology of cryptococcal infection in hospitalized children. *Pediatr Infect Dis J*. 2010;29(12):e91-e95.
15. Lizarazo J, Escandon P, Agudelo CI, Castaneda E. Cryptococcosis in Colombian children and literature review. *Mem Inst Oswaldo Cruz*. 2014;109(6):797-804.
16. Luo FL, Tao YH, Wang YM, Li H. Clinical study of 23 pediatric patients with cryptococcosis. *Eur Rev Med Pharmacol Sci*. 2015;19(20):3801-3810.
17. McCarthy KM, Morgan J, Wannemuehler KA, et al. Population-based surveillance for cryptococcosis in an antiretroviral-naive South African province with a high HIV seroprevalence. *AIDS*. 2006;20(17):2199-2206.
18. Liu L, Guo L, Liu Y, et al. Clinical characteristics and prognosis of pediatric cryptococcosis in Beijing Children's Hospital, 2002-2014. *Eur J Pediatr*. 2017;176(9):1235-1244.
19. Goldman DL, Khine H, Abadi J, et al. Serologic evidence for *Cryptococcus neoformans* infection in early childhood. *Pediatrics*. 2001;107(5):E66.
20. Ramsay S. *C neoformans* common in urban children. *Lancet*. 2001;357(9267):1507.
21. Dou HT, Xu YC, Wang HZ, Li TS. Molecular epidemiology of *Cryptococcus neoformans* and *Cryptococcus gattii* in China between 2007 and 2013 using multilocus sequence typing and the DiversiLab system. *Eur J Clin Microbiol Infect Dis*. 2015;34(4):753-762.
22. Chaturvedi S, Rodeghier B, Fan J, McClelland CM, Wickes BL, Chaturvedi V. Direct PCR of *Cryptococcus neoformans MAT*alpha and *MAT*a pheromones to determine mating type, ploidy, and variety: a tool for epidemiological and molecular pathogenesis studies. *J Clin Microbiol*. 2000;38(5):2007-2009.
23. Meyer W, Aanensen DM, Boekhout T, et al. Consensus multilocus sequence typing scheme for *Cryptococcus neoformans* and *Cryptococcus gattii*. *Med Mycol*. 2009;47(6):561-570.
24. Edgar RC. MUSCLE: multiple sequence alignment with high accuracy and high throughput. *Nucleic Acids Res*. 2004;32(5):1792-1797.
25. Kuck P, Longo GC. FASconCAT-G: extensive functions for multiple sequence alignment preparations concerning phylogenetic studies. *Front Zool*. 2014;11(1):81.
26. Jombart T. adegenet: a R package for the multivariate analysis of genetic markers. *Bioinformatics*. 2008;24(11):1403-1405.
27. Rozas J, Ferrer-Mata A, Sanchez-DelBarrio JC, et al. DnaSP 6: DNA sequence Polymorphism analysis of large data sets. *Mol Biol Evol*. 2017;34(12):3299-3302.

28. Chen YH, Yu F, Bian ZY, et al. Multilocus Sequence typing reveals both shared and unique genotypes of *Cryptococcus neoformans* in Jiangxi Province, China. *Sci Rep*. 2018;8(1):1495.
29. Kumar S, Stecher G, Tamura K. MEGA7: Molecular evolutionary genetics analysis version 7.0 for bigger datasets. *Mol Biol Evol*. 2016;33(7):1870-1874.
30. Pan W, Khayhan K, Hagen F, et al. Resistance of Asian *Cryptococcus neoformans* serotype A is confined to few microsatellite genotypes. *PLoS ONE*. 2012;7(3):e32868.
31. Espinel-Ingroff A, Aller AI, Canton E, et al. *Cryptococcus neoformans-Cryptococcus gattii* species complex: an international study of wild-type susceptibility endpoint distributions and epidemiological cutoff values for fluconazole, itraconazole, posaconazole, and voriconazole. *Antimicrob Agents Chemother*. 2012;56(11):5898-5906.
32. Espinel-Ingroff A, Chowdhary A, Cuenca-Estrella M, et al. *Cryptococcus neoformans-Cryptococcus gattii* species complex: an international study of wild-type susceptibility endpoint distributions and epidemiological cutoff values for amphotericin B and flucytosine. *Antimicrob Agents Chemother*. 2012;56(6):3107-3113.
33. Espinel-Ingroff A, Chowdhary A, Gonzalez GM, et al. Multicenter study of isavuconazole MIC distributions and epidemiological cutoff values for the *Cryptococcus neoformans-Cryptococcus gattii* species complex using the CLSI M27-A3 broth microdilution method. *Antimicrob Agents Chemother*. 2015;59(1):666-668.
34. Sloan DJ, Parris V. Cryptococcal meningitis: epidemiology and therapeutic options. *Clin Epidemiol*. 2014;6:169-182.
35. Speed BR, Kaldor J. Rarity of cryptococcal infection in children. *Pediatr Infect Dis J*. 1997;16(5):536-537.
36. Laman M, Hwaihwanje I, Davis TM, Manning L. Cryptococcal meningitis in immunocompetent Papua New Guinean children. *Trop Doct*. 2010;40(1):61-63.
37. Miglia KJ, Govender NP, Rossouw J, Meiring S, Mitchell TG. Analyses of pediatric isolates of *Cryptococcus neoformans* from South Africa. *J Clin Microbiol*. 2011;49(1):307-314.
38. Adonis-Koffy L, Diarrassouba G, Mouba J, et al. Cryptococcal meningitis in two HIV-negative children. *Arch Pediatr*. 2010;17(7):1072-1073.
39. Gupta N, Sachdev A, Gupta D, Radhakrishnan N. Disseminated cryptococcosis in an immunocompetent toddler. *Indian Pediatr*. 2017;54(2):145-146.
40. Guo J, Zhou J, Zhang S, et al. A case-control study of risk factors for HIV-negative children with cryptococcal meningitis in Shi Jiazhuang, China. *BMC Infect Dis*. 2012;12:376.
41. Guess TE, Rosen JA, McClelland EE. An overview of sex bias in *C. neoformans* Infections. *J Fungi (Basel)*. 2018;4(2):49.
42. Chen J, Varma A, Diaz MR, Litvintseva AP, Wollenberg KK, Kwon-Chung KJ. *Cryptococcus neoformans* strains and infection in apparently immunocompetent patients. *China. Emerg Infect Dis*. 2008;14(5):755-762.
43. Meiring ST, Quan VC, Cohen C, et al. A comparison of cases of paediatric-onset and adult-onset cryptococcosis detected through population-based surveillance, 2005-2007. *AIDS*. 2012;26(18):2307-2314.
44. Severo CB, Xavier MO, Gazzoni AF, Severo LC. Cryptococcosis in children. *Paediatr Respir Rev*. 2009;10(4):166-171.
45. Chen M, Xu Y, Hong N, et al. Epidemiology of fungal infections in China. *Front Med*. 2018;12(1):58-75.
46. Wu SY, Lei Y, Kang M, Xiao YL, Chen ZX. Molecular characterisation of clinical *Cryptococcus neoformans* and *Cryptococcus gattii* isolates from Sichuan province. *China. Mycoses*. 2015;58(5):280-287.
47. Sun S, Billmyre RB, Mieczkowski PA, Heitman J. Unisexual reproduction drives meiotic recombination and phenotypic and karyotypic plasticity in *Cryptococcus neoformans*. *PLoS Genet*. 2014;10(12):e1004849.
48. Simwami SP, Khayhan K, Henk DA, et al. Low diversity *Cryptococcus neoformans* variety *grubii* multilocus sequence types from Thailand are consistent with an ancestral African origin. *PLoS Pathog*. 2011;7(4):e1001343.
49. Litvintseva AP, Mitchell TG. Population genetic analyses reveal the African origin and strain variation of *Cryptococcus neoformans* var. *grubii*. *PLoS Pathog*. 2012;8(2):e1002495.

SUPPORTING INFORMATION

Additional supporting information may be found online in the Supporting Information section at the end of the article.

Table S1. Details of the MIC for Chinese pediatric *C. neoformans* isolates for seven antifungals

How to cite this article: Hong N, Chen M, Xu N, et al. Genotypic diversity and antifungal susceptibility of *Cryptococcus neoformans* isolates from paediatric patients in China. *Mycoses*. 2018;00:1–10. https://doi.org/10.1111/myc.12863

Diagnostic Microbiology and Infectious Disease xxx (xxxx) xxx–xxx

Contents lists available at ScienceDirect

Diagnostic Microbiology and Infectious Disease

journal homepage: www.elsevier.com/locate/diagmicrobio

YEAST PANEL multiplex PCR for identification of clinically important yeast species: stepwise diagnostic strategy, useful for developing countries

Amir Arastehfar [a,1,2], Wenjie Fang [a,b,c,2], Weihua Pan [b,c,*], Michaela Lackner [d], Wanqing Liao [b,c], Parisa Badiee [e], Kamiar Zomorodian [f], Hamid Badali [g], Ferry Hagen [a], Cornelia Lass-Flörl [d], Teun Boekhout [a,c,h,**]

[a] Westerdijk Fungal Biodiversity Institute, Utrecht, the Netherlands
[b] Department of Dermatology, Shanghai Changzheng Hospital, Second Military Medical University, Shanghai, China
[c] Shanghai Key Laboratory of Molecular Medical Mycology, Shanghai Institute of Medical Mycology, Shanghai Changzheng Hospital, Second Military Medical University, Shanghai, China
[d] Division of Hygiene and Medical Microbiology, Medical University of Innsbruck, Innsbruck, Austria
[e] Prof. Alborzi Clinical Microbiology Research Center, Shiraz University of Medical Sciences, Shiraz, Iran
[f] Basic Sciences in Infectious Diseases Research Center, and Department of Medical Mycology and Parasitology, School of Medicine, Shiraz University of Medical Sciences, Shiraz, Iran
[g] Department of Medical Mycology and Parasitology, School of Medicine, Mazandaran University of Medical Sciences, Sari, Iran
[h] Institute of Biodiversity and Ecosystem Dynamics, University of Amsterdam, Amsterdam, the Netherlands

ARTICLE INFO

Article history:
Received 24 April 2018
Received in revised form 7 September 2018
Accepted 12 September 2018
Available online xxxx

Keywords:
Developing countries
Yeast infection
Multiplex PCR
Molecular identification
Developing countries

ABSTRACT

Identification of opportunistic yeasts in developing countries is mainly performed by phenotypic assays, which are time-consuming and prone to errors. Wrong species identification may result in suboptimal treatment and inaccurate epidemiological data. To improve rapidity and accuracy of species identification, a diagnostic strategy using a stepwise "YEAST PANEL multiplex PCR assays" targeting 21 clinically important yeast species of *Candida*, *Trichosporon*, *Rhodotorula*, *Cryptococcus*, and *Geotrichum* was designed. Four hundred CBS reference strains were used for optimization and specificity testing. Eight hundred clinical species were prepared in blinded sets for multiplex polymerase chain reaction (PCR) and matrix-assisted laser desorption time of flight mass spectrophotometry (MALDI-TOF MS) investigation. Results obtained from YEAST PANEL multiplex PCR assay were 100% consistent with those of MALDI-TOF MS. Utilization of pure colony testing showed distinct amplicons for each species, thus eliminating the need for DNA extraction. The targeted yeast species of this assay are responsible for 95% of the yeast infections. In conclusion, due to the high accuracy and coverage of a broad range of yeasts, this assay could be useful for identification in routine laboratories and epidemiological studies.

1. Introduction

The number of patients with invasive fungal infections (IFIs) continues to rise (Pfaller and Diekema, 2007), and the majority of the infections are attributable to members of yeast genera, e.g., *Candida*, *Trichosporon, Rhodotorula, Cryptococcus,* and *Geotrichum* (Pappas et al., 2010; Pfaller and Diekema, 2007). *Candida* species account for the majority of candidiasis in patients with a broad range of underlying conditions (Miceli et al., 2011). *Trichosporon* species are the second leading cause of fungemia among patients with hematological disorders (Miceli et al., 2011). *Rhodotorula* species are linked to catheter-related infections (Miceli et al., 2011), while *Cryptococcus* species are more likely to be found in HIV/AIDS-infected patients (Park et al., 2009). *Geotrichum* species are associated with infections in severely immunocompromised patients (Miceli et al., 2011). Depending on the species, mortality of invasive yeast infections ranges from 15 to 80% (Pfaller and Diekema, 2007; Richardson and Lass-Flörl, 2008). Additionally, the growing number of non-*albicans Candida* species that are less susceptible to fluconazole is worrisome (Cleveland et al., 2015; Vallabhaneni et al., 2016).

Historically, phenotypic and biochemical assays are frequently used in developing countries for species identification (Posteraro et al., 2015). However, these assays are time-consuming and prone to error (Kathuria et al., 2015). Despite the rising popularity of matrix-assisted laser desorption time of flight mass spectrophotometry (MALDI-TOF

* Corresponding author. Tel.: +86-2181885494; fax: +86-2181885493.
** Corresponding author. Tel.: +31-30-212-2600; fax: +31-30-21-22-601.
E-mail addresses: panweihua@smmu.edu.cn (W. Pan), t.boekohout@westerdijkinstitute.nl (T. Boekhout).
[1] Present address: Westerdijk Fungal Biodiversity Institute, Utrecht, Netherlands, and Shanghai Changzheng Hospital, Second Military Medical University, Shanghai, China.
[2] AA and WF have equally contributed to this work.

https://doi.org/10.1016/j.diagmicrobio.2018.09.007

MS), this technique is suffering from the limited availability of reference spectra for rare *Candida* species and opportunistic yeast species in general, and the database should be updated regularly (Clark et al., 2013; Posteraro et al., 2013, 2015). Sanger sequencing of so-called DNA barcodes is the gold standard approach in medical mycology; however, the application in developing countries is limited (Clark et al., 2013; Criseo et al., 2015; Posteraro et al., 2013, 2015). Limited usage of MALDI-TOF MS and Sanger sequencing in developing countries is due to high costs (Azim et al., 2015; Criseo et al., 2015; Mathur et al., 2014).

Nowadays, polymerase chain reaction (PCR) is regarded as a standard platform in many clinical laboratories even in developing countries due to its affordability and reproducibility (Ragheb and Jimenez, 2014; World Health Organization, 2016). Herein, we developed a panel of PCR assays, the YEAST PANEL multiplex PCR assay, which identifies the most clinically important yeast species, including the most important species of *Candida*, *Cryptococcus* spp., *Trichosporon asahii*, *Rhodotorula mucilaginosa*, and *Geotrichum* spp.

2. Materials and methods

2.1. Isolates and growth conditions

For the primary validation, our multiplex PCR assay was evaluated using 405 CBS reference strains. In order to optimize and test the specificity of the YEAST PANEL multiplex PCR, 121 CBS reference strains (Supplementary Table A1), including 100 strains of clinically important nontarget fungal species and 21 yeast target species (pooled from the validation test set), were used. Upon optimization and proving specificity, 305 CBS reference strains containing 21 target species were employed for the validation test set. Finally, in order to assess the reproducibility of the multiplex PCR assay, 804 clinical isolates from Austria, Iran, and China were used (Fig. 1). Isolates were grown on Glucose-Yeast Extract-Peptone-Agar (GYPA) media for 48 h at 25 °C. In order to detect mixed colonies and presumptively identify target species, the same copy of strains alternatively was grown on CHROMagar (Chromogenic Technology, Paris, France). Afterward, single pure colonies were subjected to the second round of culture on GYPA media for 48 h at 25 °C.

2.2. Primer design

Target loci for primer design were retrieved from NCBI database (https://www.ncbi.nlm.nih.gov/nucleotide/). Selection criteria for primers were as follows: 1) primers should not cross-react with the other species, 2) compatibility of amplicon sizes of one target species with the rest of target species in the same multiplex PCR, 3) melting temperature compatibility of primers within the same multiplex PCR, 4) LOCATION of primers in the most stable segment of target loci, and 5) in order to prevent cross-reactivity with nontarget species, the gaps and mismatches were positioned in the 3′ end of primers. Online free software of Integrated DNA Technology was used to calculate Tm and Delta G of primers (https://eu.idtdna.com/calc/analyzer). Primers were constructed and shipped by IDT Company (Leuven, Belgium). All employed primers in this study are listed in Supplementary Tables A2-A4.

2.3. DNA extraction

DNA samples were extracted by QIAGEN DNeasy Blood and Tissue Kit (QIAGEN, Hilden, Germany) with slight modifications. One full loop of pure colonies (with the volume of 10 μL) was mixed with 200

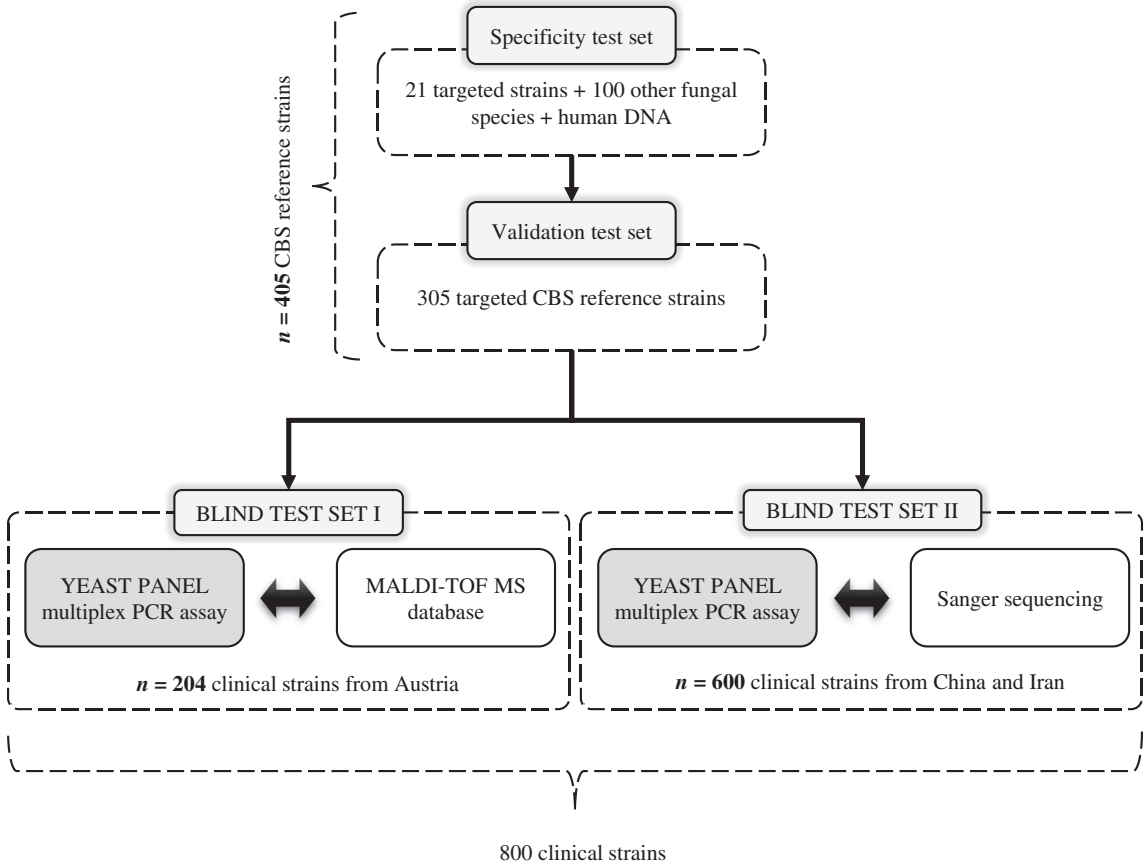

Fig. 1. Workflow chart utilized in this study. After initial optimization, specificity, and validation using CBS reference strains, YEAST PANEL multiplex PCR assay was subjected to reproducibility testing using two blinded test sets containing clinical isolates (204 isolates from Austria and 600 isolates from Iran and China).

Please cite this article as: Arastehfar A, et al, YEAST PANEL multiplex PCR for identification of clinically important yeast species: stepwise diagnostic strategy, useful for devel..., Diagn Microbiol Infect Dis (2018), https://doi.org/10.1016/j.diagmicrobio.2018.09.007

μL of ATL buffer and 20 μL of proteinase K (QIAGEN, Hilden, Germany) and incubated at 56 °C for 30 min. Cell suspensions were bead-beaten for 3 min with the frequency of 30,000 oscillations/min. Subsequently, samples were mixed with 200 μL of AL buffer and incubated at 56 °C for 30 min. The rest of DNA extraction was performed as instructed by manufacturer. Quantity and quality of DNA samples were measured by QuBit dsDNA BR Assay Kit (Thermo Fisher Scientific corporation, Waltham, MA, USA) and NanoDrop™ 2000 (Thermo Fisher Scientific, Waltham, MA), respectively. DNA samples were adjusted at 1 ng/μL, and 1 μL of DNA samples was used as PCR template.

2.4. PCR conditions

The PCR was optimized in a final volume of 50 μL as follows: 5 μL 10× buffer (10× NH4, No $MgCl_2$), 1.5 mM $MgCl_2$, 0.2 mM of mixed dNTP (dNTP mix, 100 Mm, Biolab), 2.5 U of *Taq* enzyme (Bio Taq DNA Polymerase, Biolab), and 1 μL of DNA, and MilliQ water was used to adjust the volume to 50 μL. The quantity of each primer used for each reaction is mentioned in Supplementary Tables A2–A4.

PCR was carried out on Applied Biosystem 2720 Thermal Cycler (Thermo Fisher Scientific, Walham, MA). PCR conditions and programs are mentioned in Supplementary Tables A2–A4. Upon PCR, amplicons were run on a 2% agarose gel for 75 min (8 V/cm), stained with GelRed (BioTium, USA), and visualized using gel documentation (Gel Doc XR^+, BioRad, USA). Species identification was achieved by discrimination of amplicon sizes (Fig. 3).

2.5. Specificity testing and optimization

A test set encompassing closely and distantly related yeast species (CBS reference strains), filamentous fungi (CBS reference strains), and human genomic DNA (Promega Corporation, Madison, WI) was prepared by a first technician in a blinded fashion. Isolates were sequentially ordered from 1 to 121 (Supplementary Table A1). The second technician carried out the PCR as indicated in the workflow (Fig. 2). The results obtained from YEAST PANEL multiplex PCR assay were compared to the species identity as designated by Westerdijk Institute, Utrecht, Netherlands (http://www.westerdijkinstitute.nl/Collections/). For ease of identification and prevention of misidentifications, the following tips are essential: 1) running respective controls along with unidentified isolates to monitor presence of inhibitors or appropriate condition of master mix (inactivity or lack of PCR components) and 2) instead of regular commercial ladders, 15 μL of mixture of PCR products of target species was utilized, which contained 10 μL of PCR product from each target species (70 μL), 10 μL of deionized water, and 16 μL of 10× loading dye.

2.6. Validation of YEAST Panel Multiplex PCR Assay using pure colonies of CBS reference strains

In order to optimize each PCR reactions of YEAST Panel multiplex PCR assay, 305 CBS reference strains were utilized. In this stage, in order to shorten hands-on time, instead of DNA samples, the pure

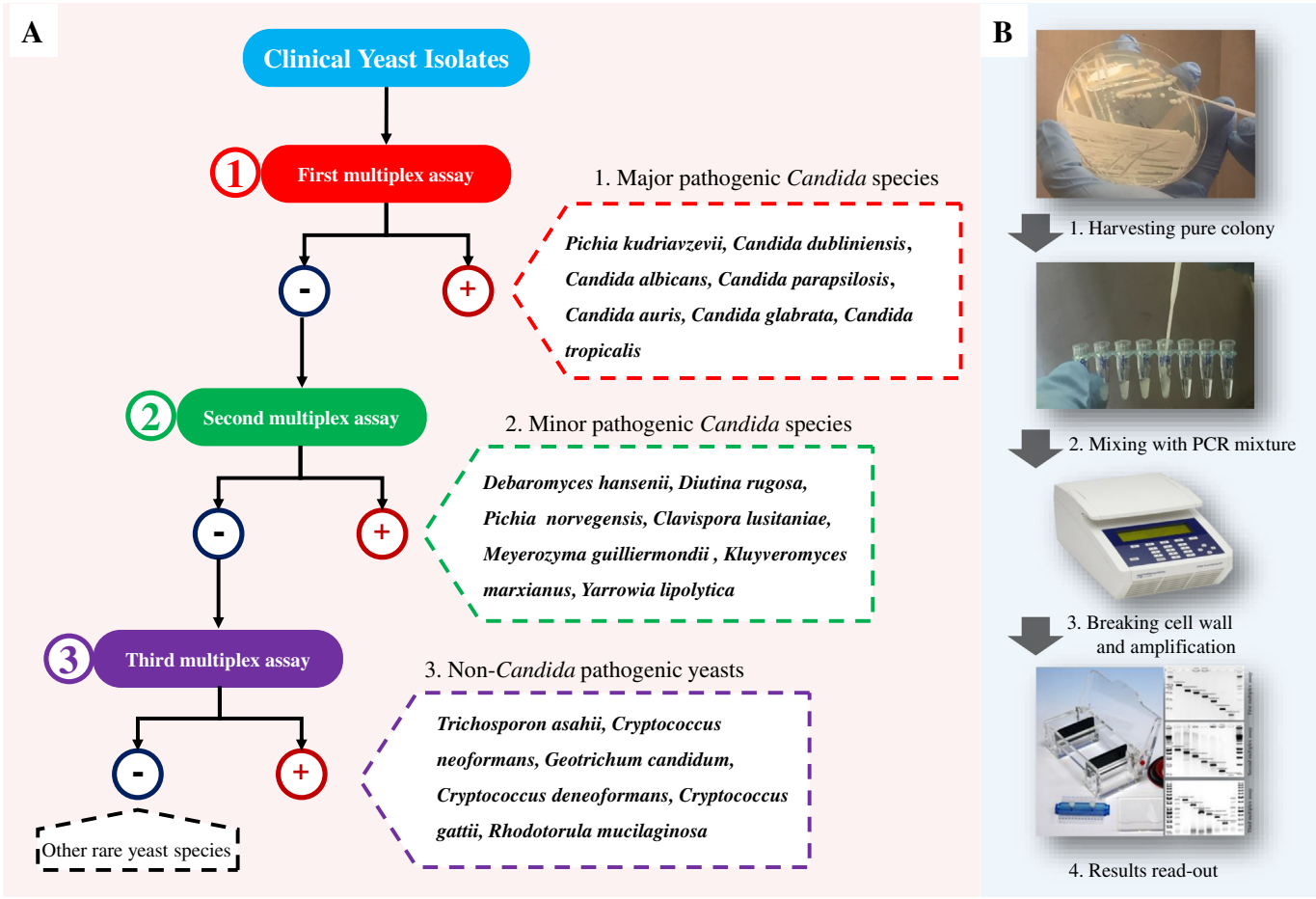

Fig. 2. The workflow of YEAST PANEL. A) The identification strategy used. If the first multiplex PCR is negative, the yeast colony is subjected to the second multiplex PCR. If the result from the second multiplex PCR is negative, a third multiplex PCR is carried out. If the third multiplex PCR is negative, it could be another yeast species not covered by our multiplex PCR. B) Two to 3 small colonies are mixed with the PCR master mix followed by running PCR program. Results are visualized on the gel, and the banding patterns are compared with the respective controls.

Please cite this article as: Arastehfar A, et al, YEAST PANEL multiplex PCR for identification of clinically important yeast species: stepwise diagnostic strategy, useful for devel..., Diagn Microbiol Infect Dis (2018), https://doi.org/10.1016/j.diagmicrobio.2018.09.007

colonies of each target species were utilized. Briefly, one full loop of colonies (1 μL volume, around 1–3 small colonies) was used as the PCR template, and by turning the loop, colonies were completely mixed inside the PCR master mixes (Table 1 and Fig. 1).

2.7. Identification strategy

The identification strategy of YEAST PANEL multiplex PCR assay is summarized in Fig. 2. Initially, pure yeast colonies are obtained, and they were subjected to the first multiplex PCR assay targeting the most clinically encountered *Candida* species. In case of negative results, the pure colonies were employed in the second multiplex PCR targeting less common *Candida* species. If strain identification was not successful, the pure colonies were mixed in the third tube, targeting common basidiomycetous yeast species and *Geotrichum* spp. If identification through the final multiplex was not possible, the yeast species is not present in the panel, and it might be regarded as a rare yeast species.

2.8. Evaluation of YEAST Panel Multiplex PCR assay through MALDI-TOF MS-identified clinical strains (blind test set I)

In order to validate the reproducibility of YEAST Panel multiplex PCR assay, one blind test set from Hygiene and Medical Microbiology Division, Innsbruck, Austria (n=204) was prepared. These isolates were identified by MALDI-TOF MS, and they were serially coded from 1 to 204. Blind test set was prepared as mentioned before. Results obtained from the PCR were compared with those of MALDI-TOF MS. In this experiment, pure colonies were used as template.

2.9. MALDI-TOF MS

Identification by MALDI-TOF MS (Bruker Biotyper, MicroFlex, LT, BRUKER DALTONIOS, Bremen, Germany) was performed by full extraction method (Cassagne et al., 2013).

2.10. Evaluation of YEAST Panel Multiplex PCR assay through Sanger sequencing-identified clinical strains (blind test set II)

In order to validate the reproducibility of the YEAST Panel multiplex PCR assay, a second blind test set from Invasive Fungal Research Center, Sari, Iran, and Shanghai Key Laboratory Molecular Medical Microbiology, Shanghai, China (n=600), was prepared. These isolates were identified by dideoxy-chain termination sequencing using large subunit ribosomal DNA primers and internal transcribed spacer (Stielow et al., 2015). The blind test set was prepared as mentioned before. Results obtained from the PCR were compared with those of Sanger sequencing. In this experiment, except for *Rhodotorula mucilaginosa* (appeared as red colonies), for the rest of isolates, pure colonies were used as PCR template.

3. Results

3.1. Specificity testing

Specificity testing using a wide range of yeast species, 4 filamentous fungi (*Aspergillus* spp.), and human DNA showed no cross-reactivity for the first and third multiplex PCR assay. In the second multiplex PCR, *Meyerozyma caribbica* was identified as *Meyerozyma guilliermondii*. Additionally, in the same reaction, *Candida zeylanoides* was misidentified as *M. guiliermondii*.

3.2. YEAST PANEL Multiplex PCR assay resolution for species identification

Subjecting 305 CBS reference strains to the YEAST PANEL multiplex PCR assay resulted in unequivocal identification of each target species as designated by the Westerdijk Institute (Supplementary Table A1, Fig. 3). Additionally, members of the cryptic species complex of *C. albicans* and *C. africana* were identified as *C. albicans* species complex. *C. parapsilosis*, *C. orthopsilosis*, and *C. metapsilosis* were identified as

Table 1
CBS reference strains utilized for validation of YEAST Panel Multiplex PCR Assay. Species identification was assigned based on distinct PCR products sizes. Identification for all of strains was performed on pure colonies, while for *R. mucilaginosa*, DNA samples extracted were used as PCR template.

Species	PCR ID		PCR results		
		Amplicon Size (bp)	First tube	Second tube	Third tube
Candida albicans (n=38)	*Candida albicans*	606 bp	38/38	0/38	0/38
C. africana (n=1)	*Candida albicans*	606 bp	1/1	NA	NA
C. dubliniensis (n=15)	*C. dubliniensis*	718 bp	15/15	0/15	0/15
C. glabrata (n=20)	*C. glabrata*	212 bp	40/40	0/40	0/40
C. nivarensis (n=1)	NA	NA	0/1	0/1	0/1
C. bracarensis (n=1)	NA	NA	0/1	0/1	0/1
C. parapsilosis (n=26)	*C. parapsilosis* complex	490 bp	44/44	0/44	0/44
C. orthopsilosis (n=1)	*C. parapsilosis* complex	490 bp	1/1	NA	NA
C. metapsilosis (n=1)	*C. parapsilosis* complex	490 bp	1/1	NA	NA
C. auris (n=35)	*C. auris*	331 bp	35/35	0/35	0/35
Pichia kudriavzevii (n=15)	*Pichia kudriavzevii*	1159 bp	15/15	0/15	0/15
C. tropicalis (n=15)	*C. tropicalis*	126 bp	15/15	0/15	0/15
Debaromyces hansenii (n=5)	*Debaromyces hansenii*	818 bp	0/5	5/5	0/5
Meyerozyma guilliermondii (n=8)	*Meyerozyma guilliermondii*	302 bp	0/8	8/8	0/8
Kluyveromyces marxianus (n=2)	*Kluyveromyces marxianus*	203 bp	0/2	2/2	0/2
Yarrowia lipolytica (n=8)	*Yarrowia lipolytica*	149 bp	0/8	8/8	0/8
Clavispora lusitaniae (n=12)	*Clavispora lusitaniae*	377 bp	0/12	12/12	0/12
Pichia norvegensis (n=5)	*Pichia norvegensis*	536 bp	0/5	5/5	0/5
Diutina rugosa (n=13)	*Diutina rugosa*	689 bp	0/13	13/13	0/13
Cryptococcus deneoformans (n=19)	*Cryptococcus deneoformans*	235 bp	0/19	0/19	19/19
Cryptococcus neoformans (n=30)	*Cryptococcus neoformans*	392 bp	0/30	0/30	30/30
Cryptococcus gattii (n=22)	*Cryptococcus gattii*	184 bp	0/22	0/22	22/22
Geotrichum candidum (n=6)	*Geotrichum* spp.	299 bp	0/6	0/6	6/6
Rhodotorula mucilaginosa (n=6)	*Rhodotorula mucilaginosa*	111 bp	0/6	0/6	6/6
Trichosporon asahii (n=10)	*Trichosporon* spp.	483 bp	0/10	0/10	10/10
Trichosporon lactis (n=7)	*Trichosporon* spp.	480 bp	0/7	0/7	7/7

Candida africana was identified as *Candida albicans* (606 bp), *Candida orthopsilsis* and *Candida metapsilosis* were identified as *Candida parapsilosis* (490 bp), and *Candida zeylanoides* was misidentified as *Candida guilliermondii* (302 bp).
NA = not amplified.

Please cite this article as: Arastehfar A, et al, YEAST PANEL multiplex PCR for identification of clinically important yeast species: stepwise diagnostic strategy, useful for devel..., Diagn Microbiol Infect Dis (2018), https://doi.org/10.1016/j.diagmicrobio.2018.09.007

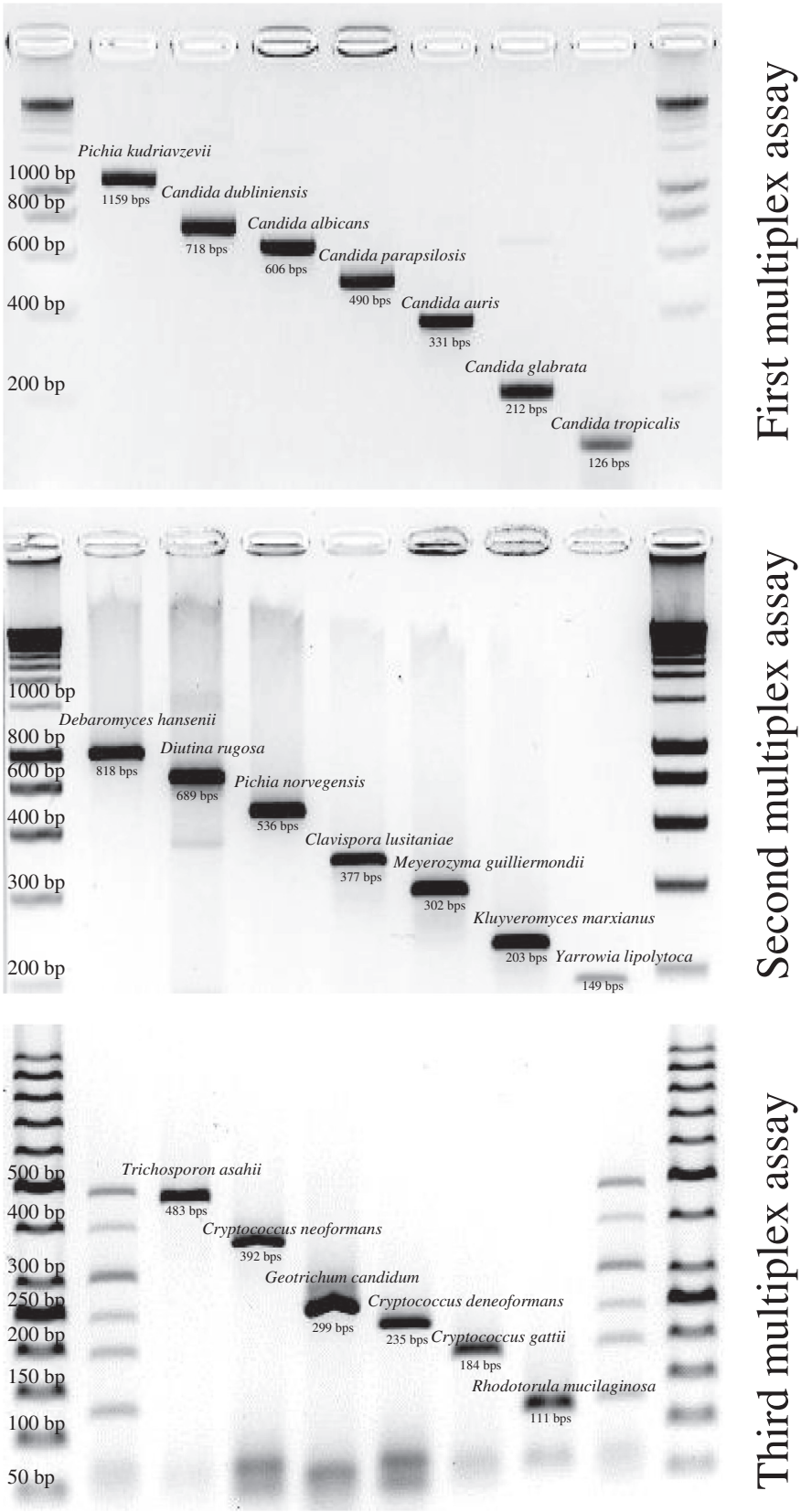

Fig. 3. Banding patterns and the strategy of discrimination of opportunistic yeast species in each multiplex PCR are depicted. Species identification was assigned based on distinct PCR products sizes.

C. parapsilosis. However, the specific primers of *C. glabrata* did not amplify *C. nivariensis* and *C. bracarensis*. Subjecting mixtures of cells of *C. albicans* and *C. glabrata*, *C. albicans* and *C. parapsilosis*, *C. albicans* and *C. tropicalis*, *C. glabrata* and *C. tropicalis*, and *C. glabrata* and *C. parapsilosis* resulted in 2 separate bands in 1 lane corresponding to target species (Supplementary Fig. 1).

Please cite this article as: Arastehfar A, et al, YEAST PANEL multiplex PCR for identification of clinically important yeast species: stepwise diagnostic strategy, useful for devel..., Diagn Microbiol Infect Dis (2018), https://doi.org/10.1016/j.diagmicrobio.2018.09.007

3.3. Comparison of MALDI-TOF MS with YEAST PANEL Multiplex PCR assay

Two hundred isolates from Austria were prepared in a blinded way and identified by MALDI-TOF MS (Table 2). YEAST PANEL multiplex PCR showed 100% consistency with results obtained from MALDI-TOF MS. Nontarget yeast species were not amplified, leading to further proof of specificity.

3.4. Comparison of sequencing with YEAST PANEL Multiplex PCR assay

Testing 600 clinical isolates from Iran and China with the YEAST Panel multiplex PCR assay and its comparison with results obtained from the sequencing of D1/D2 large subunit of rDNA and internal transcribed spacer were fully concordant (Table 3).

3.5. Pure colony testing

The YEAST PANEL multiplex PCR assay, except for *Rhodotorula mucilaginosa*, showed full compatibility with pure colony testing. Of 12 clinical isolates of *Rhodotorula mucilaginosa*, none were amplified using pure colony testing; hence, DNA samples were extracted for these isolates. Subsequently, 12 DNA samples corresponding to 12 clinical isolates of *Rhodotorula mucilaginosa* were all successfully amplified. Failure in amplification of direct colonies of *Rhodotorula mucilaginosa* is linked to its pigments that hamper PCR amplification.

4. Discussion

Due to the worldwide growing incidence of non-*albicans Candida* species and their association with difficulty in treatment (Richardson and Lass-Flörl, 2008), identification to the species level is of great importance. However, hospitals and clinics in developing countries due to limited financial supports are deprived of precise but expensive means of identifications, i.e., DNA sequencing and MALDI-TOF MS (Azim et al., 2015; Mathur et al., 2014), leading to poor infection and mortality control in these regions (Herwaldt et al., 1996). However, because of the affordability of the PCR device even for developing countries (Ragheb and Jimenez, 2014; World Health Organization, 2016), this technique can be successfully employed as a useful identification tool. Hence, we present a YEAST PANEL multiplex PCR assay that can identify and distinguish the most clinically important opportunistic yeast species.

Our assay presents a novel stepwise strategy for identification of the clinically most important yeasts belonging to Ascomycota and Basidiomycota. The ARTEMIS-DISK study has shown that *Candida* and basidiomyceteous yeast species account for 95.8% and 4.2% of episodes of yeast infections, respectively (Pfaller et al., 2009). Although *Geotrichum* spp. was not reported in the ARTEMIS study, other studies conducted in the United States, France, and Denmark showed that this opportunistic pathogen accounts for 4.5% to 10.1% of episodes of non-*Candida* yeast infections (Arendrup et al., 2014). The YEAST PANEL multiplex PCR assay can identify 99.6% of the causative agents of candidiasis, and 95% of infections caused by all yeast pathogens (Pfaller et al., 2009). Additionally, as *C. auris* caused fatal outbreak in 5 continents (Chowdhary et al., 2017) and constitutes 5.2% of nosocomial infections in India (Chakrabarti et al., 2014), this globally emerging multidrug-resistant yeast was included in our multiplex PCR assay.

The consistency between YEAST PANEL multiplex PCR assay and MALDI-TOF MS was 100%. Although MALDI-TOF MS bears a high degree of specificity, misidentification of important *Candida* and other yeast species due to insufficient number of spectra is considered as a deficiency of this platform (Jamal et al., 2014; Kim et al., 2016; Ling et al., 2014). Additionally, despite lower experimental costs of MALDI-TOF MS than conventional phenotypic assays, the purchase and maintenance of a MALDI-TOF MS device are cost-prohibitive, driving developing countries to rely on nonspecific conventional and phenotypic methods (Kim et al., 2016; Mathur et al., 2014; Xiao et al., 2016).

Subjecting a wide range of yeast species to the YEAST PANEL multiplex PCR assay and its comparison with sequencing resulted in 100% agreement with all clinical target strains (n=600). Traditionally, Sanger sequencing is considered as the gold standard approach in medical mycology (Pryce et al., 2003). However, the inevitable requirement for highly trained technicians to run the device, apart from being more time-consuming and expensive, is a deterrent factor for its popularity in routine laboratories (Criseo et al., 2015). However, YEAST PANEL multiplex PCR assay is less expensive and requires less hands-on time when compared to sequencing.

Despite the widespread usage of phenotypic and biochemical assays in routine laboratories, especially in developing countries (Kathuria et al., 2015), a multitude of studies have revealed that commercially routine biochemical assays misidentify uncommon yeast species (de

Table 2
Clinical strains from Austria utilized for validation of YEAST Panel Multiplex PCR assay and its comparison with MALDI-TOF MS. Species identification was assigned based on distinct PCR products sizes.

Species	PCR ID	Amplicon size	PCR results			Concordance with MALDI-TOF MS
			First tube	Second tube	Third tube	
C. albicans (n=84)	*C. albicans*	606 bp	84/84	NA	NA	84/84
C. dubliniensis (n=3)	*C. dubliniensis*	718 bp	3/3	NA	NA	3/3
C. glabrata (n=33)	*C. glabrata*	212 bp	33/33	NA	NA	33/33
C. parapsilosis (n=26)	*C. parapsilosis* complex	490 bp	26/26	NA	NA	26/26
Pichia kudriavzevii (n=17)	*Pichia kudriavzevii*	1159 bp	17/17	NA	NA	17/17
C. tropicalis (n=15)	*C. tropicalis* (n=15)	126 bp	15/15	NA	NA	15/15
Meyerozyma guilliermondii (n=3)	*Meyerozyma guilliermondii*	302 bp	0/3	3/3	NA	3/3
Kluyveromyces marxianus (n=2)	*Kluyveromyces marxianus*	203 bp	0/2	2/2	NA	2/2
Clavispora lusitaniae (n=5)	*Clavispora lusitaniae*	377 bp	0/5	5/5	NA	5/5
Diutina pararugosa (n=5)	NA	NA	0/5	0/5	0/5	0/5
Diutina rugosa (n=1)	*Diutina rugosa*	689 bp	0/1	1/1	NA	1/1
Pichia inconspicua (n=5)	NA	NA	0/5	0/5	0/5	0/5
Cryptococcus neoformans (n=2)	*Cryptococcus neoformans*	392 bp	0/2	0/2	2/2	2/2
Trichosporon asahii (n=1)	*Trichosporon* spp.	483 bp	0/1	0/1	1/1	1/1
Stephanoascus ciferrii (n=1)	NA	NA	0/1	0/1	0/1	0/1
Saccharomyces cerevisiae (n=1)	NA	NA	0/1	0/1	0/1	0/1
Total number (n=204)[a]	n= 192 (94%)		n=178 (100%)	n=11 (100%)	n=3 (100%)	n=192 (94%)

NA = not amplified.
[a] Among total 204 isolates, 12 are nontarget yeast species, while the rest of 192 isolates are among target species.

Please cite this article as: Arastehfar A, et al, YEAST PANEL multiplex PCR for identification of clinically important yeast species: stepwise diagnostic strategy, useful for devel..., Diagn Microbiol Infect Dis (2018), https://doi.org/10.1016/j.diagmicrobio.2018.09.007

Table 3
Clinical strains from Iran and China utilized for validation of YEAST Panel Multiplex PCR assay and its comparison with Sanger sequencing. Species identification was assigned based on distinct PCR products sizes. Identification for all of strains was performed on pure colonies, while for *R. mucilaginosa*, DNA samples extracted were used as PCR template.*a, **b

Species	PCR ID	Amplicon size	PCR results			Concordance with Sanger sequencing
			First tube	Second tube	Third tube	
C. albicans (*n*=156)	*C. albicans*	606 bp	156/156	NA	NA	156/156
C. dubliniensis (*n*=8)	*C. dubliniensis*	718 bp	8/8	NA	NA	8/8
C. glabrata (*n*=140)	*C. glabrata*	212 bp	140/140	NA	NA	140/140
Pichia kudriavzevii (*n*=25)	*Pichia kudriavzevii*	1159 bp	25/25	NA	NA	25/25
C. parapsilosis complex[a] (*n*=80)	*C. parapsilosis* complex	490 bp	80/80	NA	NA	80/80
C. tropicalis (*n*=65)	*C. tropicalis*	126 bp	65/65	NA	NA	65/65
Debaromyces hansenii (*n*=19)	*Debaromyces hansenii*	818 bp	0/19	19/19	NA	19/19
Meyerozyma guilliermondii (*n*=40)	*Meyerozyma guilliermondii*	302 bp	0/40	40/40	NA	40/40
Kluyveromyces marxianus (*n*=17)	*Kluyveromyces marxianus*	203 bp	0/17	17/17	NA	17/17
Yarrowia lipolytica (*n*=3)	*Yarrowia lipolytica*	149 bp	0/3	3/3	NA	5/5
Clavispora lusitaniae (*n*=1)	*Clavispora lusitaniae*	377 bp	0/1	1/1	NA	1/1
Pichia norvegensis (*n*=3)	*Pichia norvegensis*	536 bp	0/3	3/3	NA	5/5
Diutina rugosa (*n*=5)	*Diutina rugosa*	689 bp	0/5	5/5	NA	5/5
Cryptococcus neoformans (*n*=10)	*Cryptococcus neoformans*	392 bp	0/10	0/10	10/10	10/10
Geotrichum silvicola (*n*=9)	*Geotrichum spp.*	299 bp	0/9	0/9	9/9[b]	9/9
Trichosporon asahii (*n*=7)	*Trichosporon* spp.	483 bp	0/7	0/7	7/7	7/7
Rhodotorula mucilaginosa (*n*=12)	*Rhodotorula mucilaginosa*	111 bp	0/12	0/12	12/12	12/12
Total Number (*n*=600)			*n*=474 (100%)	*n*=88 (100%)	*n*=38 (100%)	*n*=600 (100%)

[a] *Candida parapsilosis* complex contained 2 strains of *Candida orthopsilosis* and 2 strains of *Candida metapsilosis* and were identified as *Candida parapsilosis* (490 bp).
[b] *Geotrichum silvicola* is the synonym of *Galactomyces candidum*

Almeida Júnior et al., 2014) and a broad variety of *Candida* species (Keçeli et al., 2016), especially *M. guilliermondii* and *C. auris* (Castanheira et al., 2013; Kathuria et al., 2015). Additionally, delayed and inappropriate identifications are associated with a higher mortality rate and hospitalization costs (Morrell et al., 2005). The turnaround time for identification, another inherent obstacle of conventional biochemical assays (up to 48 h), was improved with the YEAST PANEL multiplex PCR assay since identification was achieved in 3–6 h.

Misidentification of *C. zeylanoides* as *M. guilliermondii* in the second multiplex PCR reaction was the major limitation of our study. However, literatures data revealed that the incidence of *C. zeylanoides* is extremely low (0.01–0.04%) globally. In the same tube, *Meyerozyma caribbica* was misidentified as *Meyerozyma guilliermondii*, which can be explained by their close genetic similarity. Although *Saccharomyces cerevisiae*, *C. nivariensis*, and *C. bracarensis* have been implicated in human infections, they were not included in our multiplex PCR assay (Enache-Angoulvant and Hennequin, 2005; Hou et al., 2017). Direct colony and gel electrophoresis dependence and lack of identification of clinically important molds were among the other limitations to our study. As *Rhodotorula mucilaginosa* contains red-colored pigments, DNA extraction and purification are imperative to obtain successful PCR amplification and subsequently establish the identity of this species.

5. Conclusion

Due to the shortages of systematic epidemiological data in developing countries and the lack of financial supports for high-cost and precise means of identification, such as Sanger sequencing and MALDI-TOF MS, these countries might face difficulties in the establishment of empiric therapies, which cause a higher rate of mortality. However, because of the affordability of PCR devices, the YEAST PANEL multiplex PCR assay has the potential to be integrated in large-scale epidemiological studies. On the other hand, routine laboratories in developing countries can take the advantage of supplementation of biochemical assays with YEAST PANEL multiplex PCR assay.

Supplementary data to this article can be found online at https://doi.org/10.1016/j.diagmicrobio.2018.09.007.

Acknowledgments

Not applicable.

Funding sources

This work was supported by the Major National R&D Projects of the National Health Department (2018ZX10101003), European Union's Horizon 2020 research and innovation program under the Marie Sklodowska-Curie grant agreement no. 64209, National Natural Science Foundation of China (31770161), and Shanghai Science and Technology Committee (grant numbers 14DZ2272900 and 14495800500).

References

de Almeida Júnior JN, Figueiredo DSY, Toubas D, Del Negro GMB, Motta AL, Rossi F, et al. Usefulness of matrix-assisted laser desorption ionisation-time-of-flight mass spectrometry for identifying clinical Trichosporon isolates. Clin Microbiol Infect 2014;20(8):784–90. https://doi.org/10.1111/1469-0691.12502.

Arendrup MC, Boekhout T, Akova M, Meis JF, Cornely OA, Lortholary O, et al. ESCMID and ECMM joint clinical guidelines for the diagnosis and management of rare invasive yeast infections. Clin Microbiol Infect 2014;20(S3):76–98. https://doi.org/10.1111/1469-0691.12360.

Azim A, Baronia A, Marak RK, Gurjar M, Ahmed A. Invasive candidiasis in non neutropenic critically ill—need for region-specific management guidelines. Indian J Crit Care Med 2015;19(6):333. https://doi.org/10.4103/0972-5229.158273.

Cassagne C, Cella AL, Suchon P, Normand AC, Ranque S, Piarroux R. Evaluation of four pretreatment procedures for MALDI-TOF MS yeast identification in the routine clinical laboratory. Med Mycol 2013;51(4):371–7. https://doi.org/10.3109/13693786.2012.720720.

Castanheira M, Woosley LN, Diekema DJ, Jones RN, Pfaller MA. *Candida guilliermondii* and other species of *Candida* misidentified as *Candida famata*: assessment by Vitek 2, DNA sequencing analysis, and matrix-assisted laser desorption ionization-time of flight mass spectrometry in two global antifungal surveillance program. J Clin Microbiol 2013;51(1):117–24. https://doi.org/10.3109/13693786.2012.720720.

Chakrabarti A, Sood P, Rudramurthy SM, Chen S, Kaur H, Capoor M, et al. Incidence, characteristics and outcome of ICU-acquired candidemia in India. Intensive Care Med 2014;41(2):285–95. https://doi.org/10.1007/s00134-014-3603-2.

Chowdhary A, Sharma C, Meis JF. *Candida auris*: a rapidly emerging cause of hospital-acquired multidrug-resistant fungal infections globally. PLoS Pathog 2017;13(5):1–10. https://doi.org/10.1371/journal.ppat.1006290.

Clark AE, Kaleta EJ, Arora A, Wolk DM. Matrix-assisted laser desorption ionization-time of flight mass spectrometry: a fundamental shift in the routine practice of clinical microbiology. Clin Microbiol Rev 2013;26(3):547–603. https://doi.org/10.1128/CMR.00072-12.

Cleveland AA, Harrison LH, Farley MM, Hollick R, Stein B, Chiller TM, et al. Declining incidence of candidemia and the shifting epidemiology of *Candida* resistance in two US metropolitan areas, 2008–2013: results from population-based surveillance. PLoS One 2015;10(3):2008–13. https://doi.org/10.1371/journal.pone.0120452.

Please cite this article as: Arastehfar A, et al, YEAST PANEL multiplex PCR for identification of clinically important yeast species: stepwise diagnostic strategy, useful for devel..., Diagn Microbiol Infect Dis (2018), https://doi.org/10.1016/j.diagmicrobio.2018.09.007

Criseo G, Scordino F, Romeo O. Current methods for identifying clinically important cryptic *Candida* species. J Microbiol Methods 2015;111:50–6. https://doi.org/10.1016/j.mimet.2015.02.004.

Enache-Angoulvant A, Hennequin C. Invasive saccharomyces infection: a comprehensive review. Clin Infect Dis 2005;41(11):1559–68. https://doi.org/10.1086/497832.

Herwaldt LA, McGowan JE, Metchock BG. Basic microbiologic support for hospital epidemiology. Infect Control Hosp Epidemiol 1996;17(5):298–303.

Hou X, Xiao M, Chen SCA, Wang H, Yu SY, Fan X, et al. Identification and antifungal susceptibility profiles of *Candida nivariensis* and *Candida bracarensis* in a multi-center Chinese collection of yeasts. Front Microbiol 2017;8(JAN):1–8. https://doi.org/10.3389/fmicb.2017.00005.

Jamal WY, Ahmad S, Khan ZU, Rotimi VO. Comparative evaluation of two matrix-assisted laser desorption/ionization time-of-flight mass spectrometry (MALDI-TOF MS) systems for the identification of clinically significant yeasts. Int J Infect Dis 2014. https://doi.org/10.1016/j.ijid.2014.05.031.

Kathuria S, Singh PK, Sharma C, Prakash A, Masih A, Kumar A, et al. Multidrug-resistant *Candida auris* misidentified as *Candida haemulonii*: characterization by matrix-assisted laser desorption ionization-time of flight mass spectrometry and DNA sequencing and its antifungal susceptibility profile variability by vitek 2, CLSI Broth Microdilution, and Etest Method. J Clin Microbiol 2015;53(6):1823–30. https://doi.org/10.1128/JCM.00367-15.

Keçeli SA, Dündar D, Tamer GS. Comparison of Vitek matrix-assisted laser desorption/ionization time-of-flight mass spectrometry versus conventional methods in *Candida* identification. Mycopathologia 2016;181(1–2):67–73. https://doi.org/10.1007/s11046-015-9944-8.

Kim T-H, Kweon OJ, Kim HR, Lee M-K. Identification of uncommon *Candida* species using commercial identification systems. J Microbiol Biotechnol 2016;26(12):2206–13. https://doi.org/10.4014/jmb.1609.09012.

Ling H, Yuan Z, Shen J, Wang Z, Xu Y. Accuracy of matrix-assisted laser desorption ionization-time of flight mass spectrometry for identification of clinical pathogenic fungi: a meta-analysis. J Clin Microbiol 2014;52(7):2573–82. https://doi.org/10.1128/JCM.00700-14.

Mathur P, Xess I, Misra M, Rajkumari N. Distribution of different yeasts isolates among trauma patients and comparison of accuracy in identification of yeasts by automated method versus conventional methods for better use in low resource countries. Indian J Med Microbiol 2014;32(4):391. https://doi.org/10.4103/0255-0857.142243.

Miceli MH, Díaz JA, Lee SA. Emerging opportunistic yeast infections. Lancet Infect Dis 2011;11(2):142–51. https://doi.org/10.1016/S1473-3099(10)70218-8.

Morrell M, Fraser VJ, Kollef MH. Delaying the empiric treatment of *Candida* bloodstream infection until positive blood culture results are obtained: a potential risk factor for hospital mortality. Antimicrob Agents Chemother 2005;49(9):3640–5. https://doi.org/10.1128/AAC.49.9.3640–3645.2005.

Pappas PG, Alexander BD, Andes DR, Hadley S, Kauffman CA, Freifeld A, et al. Invasive fungal infections among organ transplant recipients: results of the Transplant-Associated Infection Surveillance Network (TRANSNET). Clin Infect Dis 2010;50(8):1101–11. https://doi.org/10.1086/651262.

Park BJ, Wannemuehler KA, Marston BJ, Govender N, Pappas PG, Chiller TM. Estimation of the current global burden of cryptococcal meningitis among persons living with HIV/AIDS. AIDS 2009;23(4):525–30. https://doi.org/10.1097/QAD.0b013e328322ffac.

Pfaller MA, Diekema DJ. Epidemiology of invasive candidiasis: a persistent public health problem. Clin Microbiol Rev 2007;20(1):133–63. https://doi.org/10.1128/CMR.00029-06.

Pfaller MA, Diekema DJ, Gibbs DL, Newell VA, Bijie H, Dzierzanowska D, et al. Results from the ARTEMIS DISK Global Antifungal Surveillance Study, 1997 to 2007: 10.5-year analysis of susceptibilities of noncandidal yeast species to fluconazole and voriconazole determined by CLSI standardized disk diffusion testing. J Clin Microbiol 2009;47(1):117–23. https://doi.org/10.1128/JCM.01747-08.

Posteraro B, De Carolis E, Vella A, Sanguinetti M. MALDI-TOF mass spectrometry in the clinical mycology laboratory: identification of fungi and beyond. Expert Rev Proteomics 2013;10(2):151–64. https://doi.org/10.1586/epr.13.8.

Posteraro B, Efremov L, Leoncini E, Amore R, Posteraro P, Ricciardi W, et al. Are the conventional commercial yeast identification methods still helpful in the era of new clinical microbiology diagnostics? A meta-analysis of their accuracy. J Clin Microbiol 2015;53(8):2439–50. https://doi.org/10.1128/JCM.00802-15.

Pryce TM, Palladino S, Kay ID, Coombs GW. Rapid identification of fungi by sequencing the ITSI and ITS2 regions using an automated capillary electrophoresis system. Med Mycol 2003;41(5):369–81. [doi: IO.lO8Oll369378O3 1000 1600435].

Ragheb SM, Jimenez L. Polymerase chain reaction/rapid methods are gaining a foothold in developing countries. PDA J Pharm Sci Technol 2014;68(3):239–55. https://doi.org/10.5731/pdajpst.2014.00979.

Richardson M, Lass-Flörl C. Changing epidemiology of systemic fungal infections. Clin Microbiol Infect 2008;14(Suppl. 4):5–24. https://doi.org/10.1111/j.1469-0691.2008.01978.x.

Stielow JB, Lévesque CA, Seifert KA, Meyer W, Irinyi L, Smits D, et al. One fungus, which genes? Development and assessment of universal primers for potential secondary fungal DNA barcodes. Persoonia 2015;35(1):242–63. https://doi.org/10.3767/003158515X689135.

Vallabhaneni S, Mody RK, Walker T, Chiller T. The global burden of fungal diseases. Infect Dis Clin N Am 2016;30(1):1–11. https://doi.org/10.1016/j.idc.2015.10.004.

World Health Organization (WHO). Establishment of PCR laboratory in developing countries. Available from: http://apps.who.int/iris/bitstream/10665/249549/5/9789290225317-Eng.pdf?ua=1, 2016.

Xiao M, Fan X, Chen XX, Wang H, Zhang L, Xu ZP, et al. Misidentification of a rare species, *Cryptococcus laurentii*, by commonly used commercial biochemical methods and matrix-assisted laser desorption ionization-time of flight mass spectrometry systems: challenges for clinical mycology laboratories. J Clin Microbiol 2016;54(1):226–9. https://doi.org/10.1128/JCM.02830-15.

Please cite this article as: Arastehfar A, et al, YEAST PANEL multiplex PCR for identification of clinically important yeast species: stepwise diagnostic strategy, useful for devel..., Diagn Microbiol Infect Dis (2018), https://doi.org/10.1016/j.diagmicrobio.2018.09.007

Unequivocal identification of an underestimated opportunistic yeast species, Cyberlindnera fabianii, and its close relatives using a dual-function PCR and literature review of published cases

Running Head: Identification of *Cyberlindnera fabianii* and literature review

Amir Arastehfar,[a] Wenjie Fang,[b,c] Abdullah M. S. Al-Hatmi,[a,d] Mohammad Hosein Afsarian,[e] Farnaz Daneshnia,[a] Mina Bakhtiari,[f] Sara Khanjari Sadati,[f] Hamid Badali,[g] Sadegh Khodavaysi,[h] Ferry Hagen[a], Wanqing Liao,[b,c] Weihua Pan,[b,c*] Kamiar Zomorodian,[f*] and Teun Boekhout,[a, b, i]

[a] Westerdijk Fungal Biodiversity Institute, Utrecht, the Netherlands

[b] Department of Dermatology, Shanghai Changzheng Hospital, Second Military Medical University, Shanghai, China

[c] Shanghai Key Laboratory of Molecular Medical Mycology, Shanghai Institute of Medical Mycology, Shanghai Changzheng Hospital, Second Military Medical University, Shanghai, China

[d] Ministry of Health, Directorate General of Health Services, Ibri, Oman

[e] Departments of Parasitology & Mycology, Fasa University of Medical Sciences, Fasa, Iran

[f] Basic Sciences in Infectious Diseases Research Center, and Department of Medical Mycology and Parasitology, School of Medicine, Shiraz University of Medical Sciences, Shiraz, Iran

[g] Department of Medical Mycology/Invasive Fungi Research Center (IFRC), School of Medicine, Mazandaran University of Medical Sciences, Sari, Iran

[h] Department of Medical Parasitology and Mycology, School of Public Health, Tehran University of Medical Sciences , Tehran, Iran

[i] Institute of Biodiversity and Ecosystem Dynamics, University of Amsterdam, Amsterdam, the Netherlands

* Correspondence:

Prof. Weihua Pan, panweihua@smmu.edu.cn,

Prof. Kamiar Zomorodian, Zomorodian2@yahoo.com

AA and WF have contributed equally to this work

Key words: *Cy. fabianii*, *Cy. jadinii*, *Cy. mississipiensis*, *W. anomalus*, biochemical assays, multiplex PCR

Abstract

Cyberlindnera fabinaii is rare yeast opportunist, but has ability to cause septicemia, biofilm production, and rapid acquirement of resistance to fluconazole and voriconazole, have made its identification from closely related species important. The urge for reliable means of identification remains unsolved for 28 years, as the biochemical assays misidentify this species as *Cyberlindnera jadinii* or *Wickerhamomyces anomalus*. During six months, six isolates of *Cy. fabianii* (central venous catheter *n*=2 and vaginal swabs *n*=4) and (vaginal swabs n=1) of *Cy. jadinii* from Iranian patients were identified using MALDI-TOF MS and

sequencing. In order to differentiate between *Cy. fabianii*, *Cy. mississipiensis*, *Cy. jadinii*, and *W. anomalus*, we designed a dual-function multiplex PCR assay (conventional and qPCR). Challenging our dual-function multiplex PCR assay with 30 most clinically important yeast species, proved its specificity. Additionally, a literature review of published cases from 1990 to 2017 is reported.

1 Introduction

Candida species are associated with 10-15% causes of nosocomial candiduria (Sobel et al., 2011) and considered as the fourth common cause of nosocomial bloodstream infections (Pfaller et al., 2018). Although *C. albicans* is still the most frequently isolated yeast pathogen, the dynamic nature of epidemiology shows a shift towards a growing number of rare yeast pathogens (Miceli et al., 2011). For instance, recently, *C. auris*, multidrug-resistant yeast has emerged globally as a nosocomial pathogen and its systemic infections have increased significantly (Mohsin et al., 2017).

Cyberlindnera fabianii, the teleomorph of *C. fabianii*, is an uncommon and rare ascomycetous opportunistic yeast species with low virulence attributes (Jindal et al., 2015). However, it has been reported causing invasive bloodstream infections (Bhally et al., 2006; Hamal et al., 2008; Valenza et al., 2006). Another significant factor involved in *Cy. fabianii* virulence is its ability to form antifungal resistant biofilms (Hamal et al., 2008). Previous studies reported that *Cy. fabianii* developed resistance to different antifungals, including fluconazole, voriconazole, caspofungin, and amphotericin B (Hamal et al., 2008; Jindal et al., 2015; Vágvölgyi et al., 2015). Infection with *Cy. fabianii* can lead to a 50% failure outcome with prophylactic and therapeutic treatment with fluconazole (Vágvölgyi et al., 2015), and may cause fatal septicemia (Taj-Aldeen et al., 2014; Valenza et al., 2006; Yun et al., 2013).

Cyberlindnera fabianii is usually misidentified as *Cy. jadinii* or *Wickerhamomyces anomalus* especially when using commercially available biochemical assays (ID-32 C, API 20 C Aux, Vitek2 YST Card, and Vitek2 Compact) (Baghdadi et al., 2015; Jindal et al., 2015; Lee et al., 2015; Svobodova et al., 2016a, 2016b; Valenza et al., 2006). However, using molecular identification, it was found that the prevalence of *Cy. fabainii* was 10 times higher than *W. anomalus* and approximately 37 higher than *Cy. jadinii* (Svobodova et al., 2016b). Because susceptibility testing seems to differ between *Cy. fabianii*, *Cy. jadinii*, and *W. anomalus* species (Svobodova et al., 2016b), a definitive molecular identification to species level is important. Here, we described the first Iranian cases of *Cy. fabianii* from CVC and vagina, performed a systematic review of the literature to identify clinical and mycological features and outcomes of human Cy. *fabainii* infections and designed a dual-function multiplex PCR that can be utilized in both conventional and real-time PCR and that targets *Cy. fabianii*, *Cy. jadinii*, *Cy. mississipiensis*, and *W. anomalus*.

2 Materials and methods

2.1 Epidemiology and clinical profile

A clinical and epidemiology evaluation of global *Cy. fabianii* cases was performed published cases. Cases from the literature were systematically searched from Pubmed and Google scholar (searching date: 08-03-2018). The key words for our search were "*fabianii*" and "infection", without any limitation in language or date. All the titles and abstracts were checked and full-text of related papers were downloaded for further evaluation. All cases have been confirmed by culture, and appropriate diagnostic tools such as MALDI-TOF MS or DNA

sequencing for species identification, except for the first clinically isolated *Cy. fabianii* in 1990, as it was identified by API 20 C and appropriate complementary mating type.

2.2 Isolates and conditions

During six months (01-07-2017 to 31-12-2017), six isolates of *Cy. fabianii* (two from central venous catheter and four from vaginal swabs) and one isolate of *Cy. jadinii* were collected from Iranian patients in Shiraz, and Fasa. In order to check the specificity and sensitivity of our multiplex PCR assay, a panel of 70 strains comprising of 30 clinically important yeast species (40 target and 30 non-target species) were received from the collection of Westerdijk Fungal Biodiversity Institute (formerly known as CBS) (Supplementary Table 1). Strains were cultured on GYPA plates for 48 hours at 25 °C. Central venous catheters and vaginal swabs were streaked on the SDA and Chromagar media, followed by incubation at 37 °C for 24-48 hours. Clinical isolates of *Cy. fabianii* (n=6) and *Cy. jadinii* (n=1) were included in this study. Patients from who the isolates were collected were asked to sign the consent forms for both participation in the study and publishing data derived from their isolates and medical charts.

2.3 MALDI-TOF MS

The initial identification of clinical isolates were carried out by MALDI-TOF MS (Marklein et al., 2009). Scores over two were considered as reliable identification.

2.4 Sequencing

The molecular identification of our strains was carried out using (ITS1 and ITS4) and (LR5 and LROR) primers targeting ITS and LSU of rDNA (Stielow et al., 2015).

2.5 DNA extraction, quality and quantity assessments

One full loop of pure colonies (10 µl) were subjected to the DNeasy Blood and Tissue kit and DNA extraction was performed according to manufacturer's protocol. In the last step of DNA extraction, 70 µl of elution buffer (AE buffer) was added to the columns and they were incubated at room temperature for 15 minutes followed by centrifugation at 10,000 rpm for one minute.

NanoDrop™ 2000 (Thermo Fisher Scientific, Waltham, Massachusetts, USA) and QuBit dsDNA BR Assay Kit (Thermo Fisher Scientific corporation, Waltham, Massachusetts, USA) were used for quality and quantity assessments, respectively. DNA samples were adjusted at one nanogram/µl and utilized as template for PCR reactions.

2.6 Primer design

In order to design specific primers for *Cy. fabianii*, *Cy. mississipiensis*, *W. anomalus*, and *Cy. jadinii*, ITS1-5.8s-ITS2 rDNA loci were obtained from NCBI database (https://blast.ncbi.nlm.nih.gov/Blast.cgi). One universal primer and five species-specific primers were designed (Table 1). The primer properties were evaluated based on the IDT Oligo analyzer on-line software (https://eu.idtdna.com/calc/analyzer) and primers were manufactured by the IDT Company (Integrated DNA Technology, Leuven, Belgium).

2.7 Conventional PCR reactions

The multiplex PCR assay was utilized in both conventional and real-time PCR machines. For the conventional PCR the reactions were adjusted at 50 µl as follows, 39 µL MiliQ water (Merck Millipore, Billerica, Massachusetts, United States), 5 µL 10X buffer, 1.5mM $MgCl_2$, 2.5 units of *Taq* enzyme (Bio Taq DNA Polymerase, Biolab), 0.2mM of mixed dNTP (dNTP mix, 100Mm, Biolab), 5 picomoles of the PR-Ano, PR-Jad, PR-Missi and 10 pM of PF-Universal, PF-Fab and PR-Fab primers, and 1 µL of DNA template.

PCR (2720 Thermal Cycler, , Applied Biosystems, Waltham, Massachusetts, USA) used the following program, pre-denaturation for 5 minutes at 94 ℃, 35 cycles of 94 ℃ for 30 seconds, 65 ℃ for 30 seconds, 72 ℃ for 30 seconds, and final extension at 72 ℃ for 8 minutes. PCR products were run on 2% agarose gel for 45 minutes (8 Volt/cm), stained with GelRed (BioTium Corporation, USA) and visualized using gel documentation with exposure time of 4 seconds (Gel Doc XR^+, BioRad, California, USA).

2.8 Real-time PCR reactions

For real-time PCR (Applied Biosystems® 7500 fast, Thermo Fisher Scientific corporation, Waltham, Massachusetts, USA) The following PCR conditions were used: 10 µl of Power Up SYBR Green Master Mix (Thermo Fisher Scientific corporation, Waltham, Massachusetts, USA) five pM of the PR-Fab, PF-Fab, PR-Ano, PR-Jad, PR-Missi and 10 pM of PF-Universal primer, 1µl of DNA template and Mili-Q water (Merck Millipore, Darmstadt, Germany) to reach the final volume of 20 µl. The PCR program was as following: 50 ℃ for two minutes, 95 ℃ for 3 minutes, followed by 40 cycles of 95 ℃ for 15 seconds and 64 ℃ for 30 seconds. Upon termination of the PCR program, the PCR products were undergone melting curve analysis using continuous heating of 0.5 ℃/second increment from 95 ℃ for 15 seconds, 60 ℃ for one minute, 95 ℃ for 15 seconds and finally 60 ℃ for 15 seconds. Data analysis was carried out using 7500 software version 2.3 (Thermo Fisher Scientific corporation, Waltham, Massachusetts, USA).

2.9 Specificity and sensitivity testing

A panel of 70 CBS reference strains comprising 30 clinically-related yeast species were used for the specificity testing (Supplementary Table 1).

In order to draw the standard curve, 10 log serial dilutions of DNA samples in duplicate starting from 10,000 CFU/µl and ending at 10 CFU/µl were prepared for each target species. Sensitivity, reproducibility, and the efficiency of the multiplex PCR were obtained from the standard curves.

2.10 Antifungal susceptibility testing

Susceptibility testing was assayed for the six identified strains of *Cy. fabianii* and one isolate of *Cy. jadinii* according to the Clinical and Laboratory Standards Institute (CLSI) M27-A3 and M27-S4 documents) (Rex et al., 2008). The following drugs were tested; itraconazole (Janssen Research Foundation, Beerse, Belgium), voriconazole (Pfizer, Central Research, Sandwich, United Kingdom), fluconazole (Pfizer, Groton, CT, USA), anidulafungin (Pfizer, Central Research, Sandwich, United Kingdom), and amphotericin B (Sigma, St. Louis, MO, USA) were obtained as reagent-grade powders from the respective manufacturers for preparation of the CLSI microdilution trays. The minimal inhibitory concentration (MIC) endpoints for amphotericin B and all other agents were determined by 100 and 50% inhibition, respectively. MICs were compared with previously published breakpoints for amphotericin B (≥ 2 µg /ml), itraconazole and voriconazole (≥ 1 µg/ml), fluconazole (≥ 8 µg /ml) and caspofungin (≥ 1 µg/ml) (Pfaller and Diekema, 2012). *Candida krusei* ATCC 6258 and *Candida parapsilosis* ATCC 22019 were used as quality control strains.

2.11 Utilized software

Genious (version 10.2.3) software was used to design the primers. SPSS (version 21, International Business Machines Corporation, New York, U.S.A.) and Graph Pad Prism (version 5, GraphPad Software, Inc. California, U.S.A.) were used for statistical analysis. Mean ±standard deviation (SD) was used for data with normal distribution.

3 Results

3.1 Literature review of cases

Literature review identified 23 detailed cases (Tables 2 and 3). The global distribution of infectious cases is shown in Figure 1. The majority of the cases clustered in Western Europe (Figure 1.). Patient characteristics including demographic, clinical information, and microbiological findings are presented in Tables 2 and 3. The majority of the cases (19/23; 83%) were published after 2010. Small differences in terms of gender were observed (male/female =10/12). A high proportion of patients were neonates (<1 month, *n*=7), infant (> 1 month and <1 year, *n*=2), and children (> 1 year and <18 years, *n*=4). Fungemia is the most common infection caused by *Cy. fabianii* (15/23, 65%), followed by candiduria (*n*=4), prostatitis (*n*=1), endocarditis (*n*=1), meningitis (*n*=1) and peritonitis (*n*=1). Catheter insertion was performed in eight cases and three of them showed growth of *Cy. fabianii* from catheters. For the seven neonates cases, three of them were preterms born after 24, 25^{+3}, 33^{+4} weeks gestation, respectively. Thirteen cases had a history of exposure to antibiotics before

the symptoms of infection. Post-surgery histories were observed among 12 cases. Five cases were reported with cancer . Other risk factors included steroids exposure, dialysis, leukopenia, mechanical ventilation, posterior urethral valve, and malnutrition.

Nineteen cases were not identified correctly, with 17 misidentified and two unidentified. *Cy. fabianii* was most frequently misidentified as *Cy. jadinii* (*n*=10). The most frequently used identification kits were API kits (*n*=9) or the VITEK system (n=4), but they failed in all identification. However, subjecting misidentified cases to either MALDI-TOF or sequencing resulted in accurate identification.

Antifungal susceptibility testing showed 16.7% (3/21), 12.5% (1/11), 8.3% (1/15), 12.5% (2/19) resistant rates for fluconazole, itraconazole, voriconazole and amphotericin B. No resistance to anidulafungin and flucytosine, were observed. The overall mortality for all included cases was 33.4% (7/23).

As *Cy. fabianii, Cy. jadinii,* and *W. anomalus* are easily misidentified by phenotypic and biochemical assays and in order to obtain a clear image about the epidemiology of *Cy. fabianii*, papers that utilized MALDI-TOF and sequencing were investigated, as well (Supplementary Table 2).

3.2 MALDI-TOF and Sanger sequencing results

From July 1st 2017 to December 31st, 2017, six isolates of *Cy. fabianii* and one isolate of *Cy. jadinii* were isolated from central venous catheters and vaginal samples. Sanger sequencing using D1/D2 LSU rDNA domains and MALDI-TOF MS were 100% in agreement with each other. *Cyberlindnera fabianii* were isolated from central venous catheter (*n*=2) and vaginal swabs (*n*=4) and the isolate of *Cyberlindnera jadinii* was isolated from vaginal swab.

3.3 Antifungal susceptibility testing

Supplementary table 3 summarize the MIC values of the tested antifungal drugs against six clinical strains of *Cy. fabiani* and one isolate of *Cy. jadinii*. All strains of *Cy. fabiani* had low MICs for anidulafungin, followed by itraconazole and voriconazole, whereas the least active drug was fluconazole. Among the antifungal drugs, fluconazole exhibited the highest MIC value that ranged from 1 to 8 µg/mL, followed by amphotericin B (MIC range 0.016-2 µg/mL), voriconazole (MIC range 0.016-1 µg/mL), and itraconazole (MIC range 0.063-1 µg/mL. All *Cy. fabianii* and *Cy. jadinii* isolates were susceptible to anidulafungin (MIC=0.006 µg/mL). The MIC value of fluconazole against three isolates of *Cy. fabianii* (two from CVC and one from vagina) was >3 log3 higher than that of the other isolates.

3.4 Conventional multiplex PCR results

Subjecting genomic DNA samples of *Cy. fabianii* (*n*=14), *Cy. jadinii* (*n*=11), *W. anomalus* (*n*=13), *Cy. mississipiensis* (*n*=2) to our multiplex PCR resulted in amplicons of 84bps, 176bps, 235bps, and 320bps, respectively (Figure 2A). All four target species could be distinguished and identified unequivocally. Subjecting CBS 7232 (reference strain of *Cy.*

jadinii) to our multiplex PCR resulted in negative amplification. Further identification by MALDI-TOF and sanger sequencing matched the identity with *Pichia guilliermondii*. As a result, designation of CBS 7232 in the collection department of Westerdijk Institute was corrected. Challenging Our conventional multiplex PCR with DNA samples of 30 clinically important yeast species, revealed 100% specificity.

3.5 Multiplex qPCR

Primers utilized for the conventional multiplex PCR were used for identification using a SYBR Green I-based qPCR assay. Distinctive melt temperatures of 77.62±0.19 ℃, 80.48±0.2 ℃, 81.38±0.23 ℃, and 81.56±0.38 ℃ distinguished *Cy. fabianii* (*n*=14), *W. anomalus* (*n*=13), *Cy. jadinii* (*n*=11), *Cy. mississipiensis* (*n*=2) (Figure 2B). However, the melting Tm of *Cy. jadinii* showed an overlap with that of *Cy. mississipiensis*. As a result, the specific primer of PR-Missi was taken out from the multiplex reaction to unequivocally identify *Cy. jadinii* (as the former species clinically is not important). Challenging our multiplex PCR with a specificity test set, resulted in minor cross-reaction at higher Ct values of 25 and 30 with the DNA of *Pichia kudriavzevii* (*Candida krusei*) and *Pichia guilliermondii* (*Candida guilliermondii*), respectively (Supplementary Figure 1). However, by adjusting the threshold at a Ct of 22, three species of *Cy. fabianii*, *W. anomalus*, *Cy. jadinii* were reliably identified (100 CFU) and cross-reaction with other clinically important yeast pathogens was not observed. Subjecting one ng DNA from the mistakenly designated reference strain of CBS 7232 to our multiplex qPCR resulted in amplification at a Ct value of 30, while the rest of DNA of *Cy. jadinii* were amplified at a Ct value of 14, which was in concordant with results obtained from the conventional multiplex PCR, MALDI-TOF MS and Sanger sequencing. Regarding the reproducibility, five runs in three consecutive days generated an average R^2 value of 0.99 for all target species, which demonstrated the high reproducibility of the qPCR conditions (Supplementary Figure 2).

3.6 Accession numbers

D1/D2 LSU and ITS rDNA sequences obtained for *Cy. fabianii* and *Cy. jadinii* with the accession numbers of MH236225, MH236226, MH236227, MH236228, MH236229, MH236230, MH236231, MH236232, MH236233, MH236234, MH236235, MH236236, and MH236237 were deposited in the GenBank database (https://www.ncbi.nlm.nih.gov/genbank/).

4 Discussion

Cyberlindnera fabianii rarely is involved in human infections and regularly presented in fermented products (Nyanga et al., 2013) and alcoholic beverages (Jeyaram et al., 2008). Up to now multitude of studies in various countries have proved its association with infection in human (Table 3). In 2009, *Pichia fabianii, P. mississipiensis* and *P. jadinii* were transferred into *Cyberlindnera* genus. (D.W. Minter, 2009). Herein, we reported the first Iranian cases of

Cy. fabianii isolated from central venous catheter and vaginal samples and provided a literature review of cases caused by *Cy. fabianii*. Additionally, we designed the first multiplex PCR using the same primers which can be used in both conventional and real-time PCR platforms as a diagnostic tools.

Using MALDI-TOF MS and sequencing of ITS and LSU rDNA, we identified six isolates of *Cy. fabianii* (n=4 from vagina and n=2 from CVC). Two patients (isolates from CVC) had underlying conditions. One suffered from acute myeloid leukemia (AML), end-stage renal diseases, hypertension, and diabetes mellitus, and the other one from accident leading to severe trauma and subsequent surgery. Concordant with previous studies, AML, severe trauma and surgical interventions are risk factors for development of invasive candidiasis (Yapar, 2014). Investigating published case-reports revealed that the main risk factors associated with the acquirement of *Cy. fabianii* infection are attributable to previous exposure with antibiotic therapy (54%) followed by central venous catheter insertion, surgery, and cancer each 34%, neutropenia, chemotherapy, renal failure and low birth weight each 13%. In our study, four patients with vaginitis did not have any underlying diseases and they were all immunocompetent. Literature data revealed that there have been four reported cases of funguria with *Cy. fabaianii*, however, in all cases the patients suffered from underlying conditions, (Jindal et al., 2015; Vágvölgyi et al., 2015). Although it has been thought that infections pertained to *Cy. fabianii* are mainly linked to neonates (Hof et al., 2017b), adults with the age of ≥17 years and the range of 17-87 years, constituted the highest strata of infected individuals (43%) followed by neonates with the age of <1 month (30%), and infants with the age of <1 year (8%). In concordance with these findings, all of our cases were >18 years, which is in agreement with the *Cy. fabianii* isolate (obtained from sputum) previously reported by Karimi *et al*. from Iran, from a 69-year old man (Karimi et al., 2015). No significant difference between males and females in terms of acquiring infection by *Cy. fabianii* was observed, but females showed a slightly higher proportion of infection (1.18/1) than males. However, in our cases the ratio of five female to one male was observed, which is due to the fact that four isolates were obtained from vagina, while CVC-isolated cases equally infected one male and one female with *Cy. fabianii*. Although, *Cy. fabianii* features a wide range of clinical syndromes, ranging fungemia and funguria to meningitis, fungemia with the highest proportion (65.2%), is considered as the most prevalent clinical complication caused by this opportunistic yeast species.

In the current study, antifungal susceptibility pattern of tested isolates exhibited the highest MICs for fluconazole, followed by amphotericin B, which is in agreement with previous reports (Jindal et al., 2015), and even multidrug resistant (fluconazole and voriconazole) *Cy. fabianii* (Hamal et al., 2008). In our study, results showed that 100% of *Cy. fabianii* isolates (n= 5) were susceptible to anidulafungin, which is in agreement with previous study (Lee et al., 2015). It has been shown that *Cy. fabianii* rapidly within 48 hours after treatment with fluconazole acquired resistance against fluconazole and further treatment with voriconazole resulted in emergence of strains resistant to both fluconazole and voriconazole (Hamal et al., 2008). Besides, *Cy. fabianii* can produce biofilm, which is pertained to resistance to antifungal drugs (Hamal et al., 2008). However, no significant differences were found in the activities of tested drugs between *Cy. fabianii* and *Cy. jadinii* ($P > .05$).

For treatment of *Cy. fabianii*, fluconazole was the most widely utilized drug followed by different formulation of amphotericin B, caspofungin, and flucytosine in 14, 10, 7, and 2 studies, respectively. Regarding the efficacy of antifungal drugs for clearance of infection, studies suggest that a combination of fluconazole with liposomal AMB or caspofungin or removal of CVC and urinary tract catheter (Vágvölgyi et al., 2015). In addition, treatment

with anidulafungin (Lee et al., 2015) led to successful outcome for all patients infected with *Cy. fabiani*. In our cases, one of patients died despite of treatment with AMB. However, death could not be linked to failure in treatment as the patient suffered from other serious background diseases. Treatment of the second patient (with trauma and surgery) with AMB resulted in successful outcome. Regarding the patients suffering from vaginitis (n=4) were all successfully treated with topical clotrimazole and fluconazole. Although, studied cases describing infection with *Cy. fabianii* showed the mortality rate of 30.4% (7/23), all of dead individuals suffered from other severe health conditions, including hematological disorders, co-infection with other yeast or bacterial agents, low birth weight, open heart surgery and loss of skin barrier due to burning (Hill and Wittwer, 2010; Hof et al., 2017a; Jindal et al., 2015; Katagiri et al., 2016; Taj-Aldeen et al., 2014; Yun et al., 2013).

In order to overcome the persisting challenge of misidentification of *Cy. fabianii*, we developed a multiplex PCR. Our dual-purpose multiplex PCR showed 100% agreement with sequencing and MALDI-TOF MS. A previous study described a singleplex PCR that could only detect *Cy. fabianii* and utilized limited number of yeast species for specificity testing (Vágvölgyi et al., 2015). However, our assay firstly tested a broad range of yeast species proving its specificity and secondly is a multiplex PCR targeting *Cy. fabianii*, *Cy. mississipiensis* , *Cy. jadinii*, and *W. anomalus*. Although, MALDI-TOF and sequencing can definitively identify these three clinically important yeast species, these devices are usually not available in routine clinical microbiology laboratories and they are either expensive or require highly trained personnel to perform the experiments (Criseo et al., 2015). Currently, PCR as an affordable an reproducible device has been exploited as an supplementary identification tool even in routine laboratories (including developing countries) (World Health Organization, 2016). Our multiplex PCR Compared to time-consuming biochemical assays takes only 2-3.5 hours to report the identification results. Although, biochemical assays are used frequently for identification, especially in developing countries (Kathuria et al., 2015), they do not have enough discriminatory power and frequently misidentify *Cy. fabianii* as *Cy. jadinii* or *W. anomalus* (Svobodova et al., 2016b, 2016a). Consequently, important worldwide studies such as the ARTEMIS DISK global antifungal surveillance over a period of 10.5 years did not identify a single isolate of *Cy. fabianii*, while they could identify 88 and 6 isolates of *W. anomalus* and *Cy. jadinii*, respectively (Pfaller et al., 2010). In contrast, MALDI-TOF MS correctly identified 163 and 222 isolates of *Cy. fabianii* that previously using API ID 32C kit were misidentified as *W. anomalus* and *Cy. jadinii* (Svobodova et al., 2016b, 2016a).

Obtaining these erroneous results can lead to a concealed image of epidemiology for *Cy. fabianii* (Svobodova et al., 2016a). Different epidemiological studies that used either MALDI-TOF MS or sequencing for identification, showed that *Cy. fabianii*, although with a low rate, but consistently is isolated (Fernández-Ruiz et al., 2017; Pongrácz et al., 2015; Won et al., 2013b). From five epidemiological studies, *Cy. fabianii*, *W. anomalus*, and *Cy. jadinii* were identified in five, two, and no cases, respectively (Fernández-Ruiz et al., 2017; Karimi et al., 2015; Pongrácz et al., 2015; Taj-Aldeen et al., 2014; Won et al., 2013a). In our study, we found six isolates of *Cy. fabianii*, one isolate of *Cy. jadinii*, and no *W. anomalus*.

Due to the growing number of infections caused by non-*Candida albicans* yeast species, establishing definitive breakpoints and the development of specific molecular means of identification for these species can contribute to both successful treatment and a better knowledge on the occurrence of uncommon yeast pathogens.

The limitation of our study was that we utilized only 40 reference strains of *Cy. fabianii*, *W.anomalus*, *Cy. jadinii*, and *Cy. mississipiensis* and therefore further experiments in different setups are required.

5 Funding

This work was supported by the Major National R&D Projects of the National Health Department (2018ZX10101003), European Union's Horizon 2020 research and innovation program under the Marie Sklodowska-Curie grant agreement No 642095, National Natural Science Foundation of China (31770161), Shanghai Science and Technology Committee (grant numbers 14DZ2272900 and 14495800500)

6 Conflict of Interest Statement

The authors declare that the research was conducted in the absence of any commercial or financial relationships that could be construed as a potential conflict of interest.

7 Author Contributions Statement

AA, FD, and WJF participated in primer design, PCR optimization, data collection and drafted the manuscript. WHP, KZ and TB participated in designing this study and revising the manuscript. AMH, WL, and FH actively participated in paper revision. HB, SK, MHA, MB, and SKA participated collecting Iranian clinical isolates and associated clinical data. All authors contributed to the revision of the final manuscript.

8 References

Baghdadi, J., Hemarajata, P., Humphries, R., and Kelesidis, T. (2015). First Report of Ventriculoperitoneal Shunt Infection due to Cyberlindnera fabianii. *Case Rep. Infect. Dis.* 2015, 630816. doi:10.1155/2015/630816.

Bhally, H. S., Jain, S., Shields, C., Halsey, N., Cristofalo, E., and Merz, W. G. (2006). Infection in a neonate caused by Pichia fabianii: Importance of molecular identification. *Med. Mycol.* 44, 185–187. doi:10.1080/13693780500160793.

Criseo, G., Scordino, F., and Romeo, O. (2015). Current methods for identifying clinically important cryptic Candida species. *J. Microbiol. Methods* 111, 50–56. doi:10.1016/j.mimet.2015.02.004.

D.W. Minter (2009). Cyberlindnera, a replacement name for Lindnera Kurtzman et al., nom.

409 illegit. *Mycotaxon* 110, 473–476. Available at:
410 http://lacertilia.de/AS/Bibliografie/BIB_5285.pdf#page=15.

411 Dooley, D. P., Beckius, M. L., Mcallister, C. K., and Jeffery, B. S. (1990). Prostatitis Caused
412 by Hansenula fabianii Isolated Meningitis Caused by Blastoschizomyces capitatus.
413 *ournal Infect. Dis.* 161, 1040–1041.

414 Fernández-Ruiz, M., Guinea, J., Puig-Asensio, M., Zaragoza, O., Almirante, B., Cuenca-
415 Estrella, M., et al. (2017). Fungemia due to rare opportunistic yeasts: Data from a
416 population-based surveillance in Spain. *Med. Mycol.* 55, 125–136.
417 doi:10.1093/mmy/myw055.

418 Flores-González, J. C., Guerrero-Lozano, I., Pérez-Guerrero, J. J., Hernández-González, A.,
419 Galán-Sánchez, F., Quintero-Otero, S., et al. (2016). Primer caso de infección fúngica
420 invasora por Candida fabianii en un paciente pediátrico no neonatal. *Rev. Iberoam. Micol.*
421 33, 48–50. doi:10.1016/j.riam.2015.06.003.

422 Gabriel, F., Noel, T., and Accoceberry, I. (2012). Lindnera (Pichia) fabianii blood infection
423 after mesenteric ischemia. *Med. Mycol.* 50, 310–314.
424 doi:10.3109/13693786.2011.587455.

425 Hamal, P., Ostransky, J., Dendis, M., Horvath, R., Ruzicka, F., Buchta, V., et al. (2008). A
426 case of endocarditis caused by the yeast Pichia fabianii with biofilm production and
427 developed in vitro resistance to azoles in the course of antifungal treatment. *Med. Mycol.*
428 46, 601–605. doi:10.1080/13693780802078180.

429 Hill, H. R., and Wittwer, C. T. (2010). Pichia fabianii Fungemia in a Neonate. *Pediatr. Infect.*
430 *Dis. J.* 29, 191.

431 Hof, H., Amann, V., Tauber, C., and Paulun, A. (2017a). Peritonitis in a neonate due to
432 Cyberlindnera fabianii, an ascomycetic yeast. *Infection* 45, 921–924.
433 doi:10.1007/s15010-017-1062-8.

434 Hof, H., Amann, V., Tauber, C., and Paulun, A. (2017b). Peritonitis in a neonate due to
435 Cyberlindnera fabianii, an ascomycetic yeast. *Infection* 45, 921–924.
436 doi:10.1007/s15010-017-1062-8.

437 Jeyaram, K., Singh, W. M., Capece, A., and Romano, P. (2008). Molecular identification of
438 yeast species associated with "Hamei" - A traditional starter used for rice wine
439 production in Manipur, India. *Int. J. Food Microbiol.* 124, 115–125.
440 doi:10.1016/j.ijfoodmicro.2008.02.029.

441 Jindal, N., Arora, S., Dhuria, N., and Arora, D. (2015). Cyberlindnera (Pichia) fabianii
442 infection in a neutropenic child : importance of molecular identification. *JMM Case*
443 *Reports* 1, 2015–2017. doi:10.1099/jmmcr.0.000033.

444 Karimi, L., Mirhendi, H., Khodadadi, H., and Mohammadi, R. (2015). Molecular
445 identification of uncommon clinical yeast species in Iran. *Curr. Med. Mycol.* 1, 1–6.
446 doi:10.18869/acadpub.cmm.1.2.1.

447 Katagiri, S., Gotoh, M., Tone, K., Akahane, D., Ito, Y., Ohyashiki, K., et al. (2016). Fatal
448 Cyberlindnera fabianii fungemia in a patient with mixed phenotype acute leukemia after

umbilical cord blood transplantation. *Int. J. Hematol.* 103, 592–595. doi:10.1007/s12185-016-1953-y.

Kathuria, S., Singh, P. K., Sharma, C., Prakash, A., Masih, A., Kumar, A., et al. (2015). Multidrug-resistant Candida auris misidentified as Candida haemulonii: Characterization by matrix-assisted laser desorption ionization-time of flight mass spectrometry and DNA sequencing and its antifungal susceptibility profile variability by vitek 2, CL. *J. Clin. Microbiol.* 53, 1823–1830. doi:10.1128/JCM.00367-15.

Kim, Y. J., Yang, J. J., and Lee, H. J. (2015). Possibility of Frequent Detection of Invasive Cyberlindera fabianii Infection Using Molecular Method. *Ann. Clin. Microbiol.* 18, 133–134. doi:0.1099/jmmcr.0.000033.3.

Lee, J. I., Yu, S., Park, J. S., Joo, E., Shin, J. H., and Kwon, M. (2015). Successful Treatment of Fungemia Caused by Cyberlindnera fabianii with Anidulafungin : A Case Report. 18, 94–97.

Marklein, G., Josten, M., Klanke, U., Müller, E., Horré, R., Maier, T., et al. (2009). Matrix-assisted laser desorption ionization-time of flight mass spectrometry for fast and reliable identification of clinical yeast isolates. *J. Clin. Microbiol.* 47, 2912–2917. doi:10.1128/JCM.00389-09.

Miceli, M. H., Díaz, J. A., and Lee, S. A. (2011). Emerging opportunistic yeast infections. *Lancet Infect. Dis.* 11, 142–151. doi:10.1016/S1473-3099(10)70218-8.

Nyanga, L. K., Nout, M. J. R., Smid, E. J., Boekhout, T., and Zwietering, M. H. (2013). Fermentation characteristics of yeasts isolated from traditionally fermented masau (Ziziphus mauritiana) fruits. *Int. J. Food Microbiol.* 166, 426–432. doi:10.1016/j.ijfoodmicro.2013.08.003.

Pfaller, M. A., and Diekema, D. J. (2012). Progress in antifungal susceptibility testing of Candida spp. by use of Clinical and Laboratory Standards Institute broth microdilution methods, 2010 to 2012. *J. Clin. Microbiol.* 50, 2846–2856. doi:10.1128/JCM.00937-12.

Pfaller, M. A., Diekema, D. J., Gibbs, D. L., Newell, V. A., Ellis, D., Tullio, V., et al. (2010). Results from the artemis disk global antifungal surveillance study, 1997 to 2007: A 10.5-year analysis of susceptibilities of candida species to fluconazole and voriconazole as determined by CLSI standardized disk diffusion. *J. Clin. Microbiol.* 48, 1366–1377. doi:10.1128/JCM.02117-09.

Pfaller, M. A., Jones, R. N., Messer, S. A., Edmond, M. B., and Wenzel, R. P. (2018). National Surveillance of Nosocomial Blood Stream Infection Due to Species of Candida Other than Candida albicans: Frequency of Occurrence and Antifungal Susceptibility in the SCOPE Program. *Diagn. Microbiol. Infect. Dis.* 30, 121–129. doi:10.1016/S0732-8893(97)00192-2.

Pongrácz, J., Juhász, E., Iván, M., and Kristóf, K. (2015). Significance of yeasts in bloodstream infection: Epidemiology and predisposing factors of Candidaemia in adult patients at a university hospital (2010–2014). *Acta Microbiol. Immunol. Hung.* 62, 317–329. doi:10.1556/030.62.2015.3.9.

Rex, J. H., Alexander, B. D., Andes, D., Arthington-Skaggs, B., Brown, S. D., Chaturvedi, V.,

et al. (2008). Reference method for broth dilution antifungal susceptibility testing of yeasts: approved standard - third edition. *Clin. Lab. Stand. Inst.*, 1–25. doi:10.1007/SpringerReference_5244.

Sobel, J. D., Fisher, J. F., Kauffman, C. A., and Newman, C. A. (2011). Candida urinary tract infections - Epidemiology. *Clin. Infect. Dis.* 52, 433–436. doi:10.1093/cid/cir109.

Stielow, J. B., Lévesque, C. A., Seifert, K. A., Meyer, W., Irinyi, L., Smits, D., et al. (2015). One fungus, which genes? Development and assessment of universal primers for potential secondary fungal DNA barcodes. *Persoonia - Mol. Phylogeny Evol. Fungi* 35, 242–263. doi:10.3767/003158515X689135.

Svobodova, L., Bednarova, D., and Hamal, P. (2016a). [The prevalence of Candida pelliculosa, Candida utilis, and Candida fabianii in the Olomouc University Hospital: epidemiological study]. *Epidemiol. Mikrobiol. Imunol. Cas. Spol. pro Epidemiol. a Mikrobiol. Ces. Lek. Spol. J.E. Purkyne* 65, 34–38.

Svobodova, L., Bednarova, D., Ruzicka, F., Chrenkova, V., Dobias, R., Mallatova, N., et al. (2016b). High frequency of Candida fabianii among clinical isolates biochemically identified as Candida pelliculosa and Candida utilis. *Mycoses* 59, 241–246. doi:10.1111/myc.12454.

Taj-Aldeen, S. J., AbdulWahab, A., Kolecka, A., Deshmukh, A., Meis, J. F., and Boekhout, T. (2014). Uncommon opportunistic yeast bloodstream infections from Qatar. *Med. Mycol.* 52, 552–556. doi:10.1093/mmycol/myu016.

Vágvölgyi, C., Mlinarić-Missoni, E., Kocsubé, S., Hatvani, L., Škarić, I., and Lukić-Grlić, A. (2015). Cyberlindnera fabianii in the neonatal and paediatric intensive care unit: case reports. *JMM Case Reports* 2, 1–7. doi:10.1099/jmmcr.0.000032.

Valenza, G., Valenza, R., Brederlau, J., Frosch, M., and Kurzai, O. (2006). Identification of Candida fabianii as a cause of lethal septicaemia. *Mycoses* 49, 331–334. doi:10.1111/j.1439-0507.2006.01240.x.

Won, E. J., Shin, J. H., Lee, K., Kim, M.-N., Lee, H. S., Park, Y.-J., et al. (2013a). Accuracy of species-level identification of yeast isolates from blood cultures from 10 university hospitals in South Korea by use of the matrix-assisted laser desorption ionization-time of flight mass spectrometry-based Vitek MS system. *J. Clin. Microbiol.* 51, 3063–3065. doi:10.1128/JCM.00945-13.

Won, E. J., Shin, J. H., Lee, K., Kim, M. N., Lee, H. S., Park, Y. J., et al. (2013b). Accuracy of species-level identification of yeast isolates from blood cultures from 10 university hospitals in south korea by use of the matrix-assisted laser desorption ionization-time of flight mass spectrometry-based vitek MS system. *J. Clin. Microbiol.* 51, 3063–3065. doi:10.1128/JCM.00945-13.

World Health Organization (2016). *Establishment of PCR laboratory in developing countries*. Available at: http://apps.who.int/iris/bitstream/10665/249549/5/9789290225317-Eng.pdf?ua=1.

Wu, Y., Wang, J., Li, W., Jia, H., Che, J., Lu, J., et al. (2013). Pichia fabianii blood infection in a premature infant in China: Case report. *BMC Res. Notes* 6, 2–5. doi:10.1186/1756-

0500-6-77.

Yapar, N. (2014). Epidemiology and risk factors for invasive candidiasis. *Ther. Clin. Risk Manag.* 10, 95–105. doi:10.2147/TCRM.S40160.

Yun, J. W., Park, K. S., Ki, C. S., and Lee, N. Y. (2013). Catheter-related bloodstream infection by Lindnera fabianii in a neutropenic patient. *J. Med. Microbiol.* 62, 922–925. doi:10.1099/jmm.0.048306-0.

10 Figures legends

Primer name	Primer sequence	Target Loci	Target species	Melting temperature	PCR product size
PR-Missi	CCATGCTTCAACACTACTGC	ITS2 rDNA	*Cy. mississipiensis*	81.56±0.38	320bps

Figure 1. Geographical distribution of *Cy. fabianii* cases are depicted.

Figure 2. Differentiation of target species using A) conventional PCR through amplicon size polymorphism (M, 100 bps molecular weight, A1-A3, CBS14917, CBS 5481, CBS 5482, A4-A6, CBS1517, CBS1726, CBS 621, A7-A9, CBS 6417, CBS 110, CBS 2870, A10-A12, CBS 7023, CBS 5837, CBS 5837) and B) qPCR through melting temperatures.

11 Tables

Table 1. Information of the primers utilized in this study.

PR-Ano	GCTTATTAGTACACTCTTGCTAAGTCAA	ITS2 rDNA	*W. anomalus*	80.48±0.2	235bps
PR-Jad	ACCAAGTCCCCTAGAGGATC	ITS2 rDNA	*Cy. jadinii*	81.38±0.23	176bps
PF-Universal	CAACGGATCTCTTGGTTCTCG	5.8s rDNA	All except for *Cy. fabianii*	NA	NA
PF-Fab	ACTAGCGCGGCGACTAAAAC	ITS1 rDNA	*Cy. fabianii*	77.62±0.19	84bps
PR-Fab	CGCAGAAAAGCTAGGCTTATTCC	ITS1 rDNA	*Cy. fabianii*	77.62±0.19	84bps

546

548 Table2: Microbiological information obtained from comprehensive review of infections caused by *Cy. Fabianii*

	Identification	Successful method of identification	Morphological signature	AFST protocol	FLU	ITC	VRC	CFG	MIC	AFG	AMB	5-FLC	Reference
1	API 20C combined with appropriate complementary mating types	API 20 C combined with appropriate complementary mating types	hat shaped-ascospore formation	ND	Susceptible	ND	ND	ND	ND	ND	Susceptible	Susceptible	(Dooley et al., 1990)
2	API 20C Aux, D1/D2 sequencing	D1/D2 sequencing	ND	M27-A2	Susceptible	ND	ND	ND	ND	ND	Susceptible	Susceptible	(Bhally et al., 2006)
3	API ID 32C, VITEK-2 YST, and ITS1 and ITS2 sequencing	ITS1 and ITS2	Growth at 40 °C	Commercial YeastOne	Susceptible	Susceptible	Susceptible	ND	ND	ND	Susceptible	Susceptible	(Valenza et al., 2006)
4	API ID 32C and ITS2 sequencing	ITS2	Growth at 42 ℃	E-test strips	Resistant	ND	Resistant	ND	ND	ND	ND	ND	(Hamal et al., 2008)
5	26s and ITS rDNA sequencing	26s and ITS rDNA sequencing	ND	E-test strips	Susceptible	ND	ND	ND	ND	ND	Susceptible	Susceptible	(Hill and Wittwer, 2010)
6	API ID 32C, ITS and 18s rDNA and EF-1α sequencing	ITS and 18s rDNA sequencing	ND	E-test strips	Susceptible	ND	Susceptible	Susceptible	ND	ND	Susceptible	Susceptible	(Gabriel et al., 2012)
7	Vitek-2 YST an d D1/D2 rDNA sequencing	D1/D2 domain of rDNA sequencing	ND	CLSI M27-A3	Susceptible	ND	Susceptible	ND	ND	ND	Susceptible	Susceptible	(Yun et al., 2013)
8	API 20C Aux and D1/D2 and ITS rDNA sequencing	D1/D2 and ITS rDNA sequencing	Growth at 42 ℃	ATB Fungus3 and CLSI	Susceptible	Resistant	Susceptible	ND	ND	ND	Resistant	Susceptible	(Wu et al., 2013)
9	MALDI-TOF and D1/D2 rDNA sequencing	MALDI-TOF and D1/D2 rDNA sequencing	ND	M27-A3	Susceptible	Susceptible	Susceptible	Susceptible	Susceptible	ND	Susceptible	ND	(Taj-Aldeen et al., 2014)
10	ITS rDNA sequencing, PCR-RFLP, and PCR-FSP	ITS rDNA sequencing	ND	ND	ND	ND	ND	ND	ND	ND	ND	ND	(Karimi et al., 2015)
11-16	API ID 32C, ITS rDNA sequencing, and specific PCR	ITS rDNA sequencing and specific PCR	ND	ATB Fungus 3 and Etest (Liofilchem)	Susceptible	Susceptible	Susceptible	Higher** MIC	Highest** MIC	Lowest** MIC	Susceptible	Susceptible	(Vágvölgyi et al., 2015)

17	API 20C Aux, MALDI-TOF MS, and D1/D2 rDNA sequencing	MALDI-TOF MS and D1/D2 rDNA sequencing	ND	CLSI M27-A3	Susceptible	ND	ND	ND	ND	ND	Susceptible	Susceptible	(Baghdadi et al., 2015)
18	Vitek2 YST Card, ITS and D1/D2 rDNA sequencing	ITS and D1/D2 rDNA sequencing	ND	CLSI M27-A3	Susceptible	ND	ND	ND	ND	Susceptible	ND	ND	(Lee et al., 2015)
19	Vitek2 compact and D1/D2 rDNA	D1/D2 rDNA sequencing	ND	ND	Susceptible	ND	Susceptible	Susceptible	ND	ND	Resistant	Susceptible	(Jindal et al., 2015)
20	API 20C Aux and ITS rDNA sequencing	ITS rDNA sequencing	ND	ND	ND	ND	ND	ND	ND	ND	ND	ND	(Kim et al., 2015)
21	MALDI-TOF MS and ITS rDNA sequencing	MALDI-TOF MS and ITS rDNA sequencing	ND	YeastOne	Susceptible	Susceptible	Susceptible	Susceptible	Susceptible	Susceptible	Susceptible	Susceptible	(Flores-González et al., 2016)
22	ITS and D1/D2 rDNA and EF1-α sequencing	ITS and D1/D2 rDNA and EF1-αsequencing	ND	CLSI M27-A3	Susceptible	Susceptible	Susceptible	Susceptible	Susceptible	ND	Susceptible	Susceptible	(Katagiri et al., 2016)
23	MALDI-TOF MS, ITS and 18s rDNA sequencing	MALDI-TOF MS, ITS and 18s rDNA sequencing	ND	Etest and EUCAST	Susceptible	ND	ND	ND	ND	Susceptible	Susceptible	ND	(Hof et al., 2017b)
24	MALDI-TOF MS, D1/D2 rDNA sequencing, multiplex-PCR	MALDI-TOF MS, D1/D2 rDNA sequencing, multiplex-PCR	ND	CLSI M27-A3	high	low	low	ND	ND	low	high	ND	This study
25	MALDI-TOF MS, D1/D2 rDNA sequencing, multiplex-PCR	MALDI-TOF MS, D1/D2 rDNA sequencing, multiplex-PCR	ND	CLSI M27-A3	high	low	low	ND	ND	low	high	ND	This study
26	MALDI-TOF MS, D1/D2 rDNA sequencing, multiplex-PCR	MALDI-TOF MS, D1/D2 rDNA sequencing, multiplex-PCR	ND	CLSI M27-A3	low	low	low	ND	ND	low	low	ND	This study
27	MALDI-TOF MS, D1/D2 rDNA	MALDI-TOF MS, D1/D2 rDNA	ND	CLSI M27-A3	low	low	low	ND	ND	low	low	ND	This study

	sequencing, multiplex-PCR	sequencing, multiplex-PCR											
28	MALDI-TOF MS, D1/D2 rDNA sequencing, multiplex-PCR	MALDI-TOF MS, D1/D2 rDNA sequencing, multiplex-PCR	ND	CLSI M27-A3	high*	low	low	ND	ND	low	low	ND	This study
29	MALDI-TOF MS, D1/D2 rDNA sequencing, multiplex-PCR	MALDI-TOF MS, D1/D2 rDNA sequencing, multiplex-PCR	ND	CLSI M27-A3	low	low	low	ND	ND	low	low	ND	This study

549

550

551

552 Table 3: Clinical information obtained from comprehensive review of infections caused by *Cy. fabianii*

No.	Publication year	Location	Age/Sex	Specimen type	Type of infection	Predisposing factors	Treatment option	Outcome	reference
1	1990	USA	57 years/Male	Urine	Prostatitis	Chronic lymphoytic leukemia, chronic urinary tract infection	Amphotericin B	Survived	(Dooley et al., 1990)
2	2006	USA	5 weeks /Female	Blood (catheter), endotracheal suction	Fungemia	Born after 25^{+3} weeks gestation, multiple antibiotics exposure, steroids exposure, catheter insertion	Amphotericin B, catheter removal	Survived	(Bhally et al., 2006)
3	2006	Germany	46 years /Male	Blood, bronchoalveolar lavage fluid	Fungemia	Multiple antibiotics exposure, cholecystectomy	Fluconazole→caspofungin	Dead (multi-organ failure)	(Valenza et al., 2006)
4	2008	Czech Republic	40 years /Male	Blood, aortic valve	Fungemia, Endocarditis	congenital combined aortic incompetence of the mitral valve, Ischemic stroke, decompressive craniectomy	Fluconazole →Voriconazole→Amphotericin B	Survived with neurological sequelae	(Hamal et al., 2008)
5	2010	France	11 days /Female	Skin, mouth, pleural fluid aspirate, blood	Disseminated Fungemia	Born after 24 weeks gestation, 700g birth weight, poor respiratory effort, APGAR scores were 5 and 7 at one and five minutes	L-Amphotericin B, flucytosine	Dead	(Hill and Wittwer, 2010)
6	2012	France	53 years /Female	Oropharyngeal swab, urine, stool, and blood	Disseminated Fungemia	Mesenteric ischemia, renal failure (continuous dialysis required), enterectomy, antibiotic exposure	caspofungin → Fluconazole	Survived	(Gabriel et al., 2012)
7	2013	South Korea	47 years /Female	Blood and central venous catheter	Fungemia	Plasma cell myeloma, autologous peripheral blood stem cell transplantation, chemotherapy, radiation therapy, respiratory failure, leukopenia, catheter insertion	Amphotericin B → caspofungin	Dead (multi-organ failure, septic shock and lactic acidosis)	(Yun et al., 2013)
8	2013	China	<1 month /Female	Blood	Fungemia	Born after 33^{+4} week of gestation, 1760g birth weight, mild neonatal asphyxia, peripheral venous hyperalimentation, respirator, antibiotic exposure; mother: 33-years-old, hysteromyoma, gestational hypertension.	Fluconazole	Survived	(Wu et al., 2013)
9	2014	Qatar	19 years /Male	Blood	Fungemia	Burn (55% of the body surface area)	Fluconazole	Dead	(Taj-Aldeen et al., 2014)
10	2015	Iran	69 years /Male	Sputum	Suspected infection	ND*	ND	ND	(Karimi et al., 2015)
11	2015	Croatia	3.5 years /Female	Blood, stool	Fungemia	antibiotic exposure, chemotherapy, leukopenia, antibacterial therapy	Fluconazole→L-Amphotericin B	Survived	(Vágvölgyi et al., 2015)
12	2015	Croatia	1.5 months /Male	Urine	Funguria	Posterior urethral valve, hydronephrosis, surgery, antibiotic exposure, catheter insertion	Fluconazole, urinary catheter removal	Survived	(Vágvölgyi et al., 2015)
13	2015	Croatia	<1 month /Female	Urine, nasopharyngeal swab	Funguria	Gastroschisis, surgery, mechanical ventilation, parenteral nutrition, antibiotic exposure, catheter insertion	Fluconazole, urinary catheter removal, central venous catheter removal	Survived	(Vágvölgyi et al., 2015)

14	2015	Croatia	<1 month /Male	Urine, ureostomal swab, wound, stool	Funguria	Hydronephrosis, surgery, parenteral nutrition, antibiotic exposure	Fluconazole→ caspofungin	Survived	(Vágvölgyi et al., 2015)
15	2015	Croatia	<1 month /Female	Blood, stool, gastric content	Fungemia	Intestinal atresia, surgery, parenteral nutrition, antibiotic exposure, catheter insertion	Fluconazole, central venous catheter removal	Survived	(Vágvölgyi et al., 2015)
16	2015	Croatia	<1 month /Female	Blood, tubal aspirate, oropharyngeal swab	Fungemia	Pulmonary cyst, 740 g weight, antibiotic exposure, mechanical ventilation, parenteral nutrition	Fluconazole→ caspofungin	Survived	(Vágvölgyi et al., 2015)
17	2015	USA	49 years /Female	Cerebrospinal fluid	Meningitis	Ventriculoperitoneal shunt	L-Amphotericin B, Flucytosine, Fluconazole	Survived	(Baghdadi et al., 2015)
18	2015	South Korea	87 years /Male	Blood	Fungemia	Obstructive pneumonitis and cancer	Anidulafungin	Survived	(Lee et al., 2015)
19	2015	India	5 years /Male	Urine	Funguria	ventriculoperitoneal shunt, multiple antibiotics exposure (including antitubercular agents), intubation, neutropenia, catheter insertion	Amphotericin B	Dead	(Jindal et al., 2015)
20	2015	South Korea	ND	Blood	Fungemia	Neutropenia, catheter insertion	Fluconazole	ND	(Kim et al., 2015)
21	2016	Spain	2 years /Male	Blood	Fungemia	Short bowel syndrome, hypophosphatemia, severe malnutrition	caspofungin	Survived	(Flores-González et al., 2016)
22	2016	Japan	69 years /Female	Blood (catheter)	Fungemia	Acute leukemia, chemotherapy, umbilical cord blood transplantation, neutropenia, rapid respiratory failure, noninvasive positive pressure ventilation, catheter insertion, hemodiafltration, multiple antibiotics exposure	Micafungin → L-Amphotericin B	Dead	(Katagiri et al., 2016)
23	2017	Germany	<1 month /Female	Dialysis fluid	Peritonitis	Multiple antibiotics exposure, open heart surgery, peritoneal dialysis	Fluconazole→L-Amphotericin B+caspofungin→Fluconazole	Dead (multiorgan failure, irreversible capillary leak syndrome)	(Hof et al., 2017b)
24	2017	Iran	58 years /Female	Central venous catheter	Fungemia	End stage renal disease, diabetes, Acute myeloid leukemia (M5), catheter insertion	Amphotericin B	Dead	This study
25	2017	Iran	17 years /Male	Central venous catheter	Fungemia	Catheter insertion	Amphotericin B	Survived	This study
26	2017	Iran	30/female	Vaginal swab	Vulvovaginitis	Itching	Clotrimazole vaginal / Fluconazole	Survived	This study
27	2017	Iran	56/female	Vaginal swab	Vulvovaginitis	Recurrent vulvovaginal candidiasis/ discharge, pain	Clotrimazole vaginal / Fluconazole	Survived	This study
28	2017	Iran	35/female	Vaginal swab	Vulvovaginitis	discharge/pain	Clotrimazole vaginal / Fluconazole	Survived	This study

29	2017	Iran	60/female	Vaginal swab	Vulvovaginitis	Recurrent vulvovaginal candidiasis/ discharge/pain/itching	Clotrimazole Fluconazole	vaginal	/	Survived	This study

553

554

555

556

Supplementary files

Supplementary Figure 1. Late amplification of *Pichia kudriavzevii* and *Pichia guilliermondii* are depicted. Adjusting Ct value of 22, distinguished target from non-target species.

Supplementary figure 2. Cumulative reproducibility ≥ 0.99 for five runs in three consecutive day for target species.

Supplementary Figure 3. Tm distribution of target species of *Cy. fabianii*, *W. anomalus*, and *Cy. jadinii*.

Supplementary Table 1. Target and non-target species utilized for optimization and specificity testing in this study.

Supplementary table 2. Epidemiological data that utilized MALDI-TOF MS or sequencing as a reliable means of identification of *Cy. fabianii*, *Cy. jadinii*, and *W. anomalus*.

Supplementary table 3. Antifungal susceptibility pattern for *Cy. fabianii* and *Cy. jadinii* isolates in this study.

Research Article

For reprint orders, please contact: reprints@futuremedicine.com

Future MICROBIOLOGY

Novel multiplex real-time quantitative PCR detecting system approach for direct detection of *Candida auris* and its relatives in spiked serum samples

Amir Arastehfar[‡,1], Wenjie Fang[‡,1,2,3], Farnaz Daneshnia[1], Abdullah M S Al-Hatmi[1,4,5], Wanqing Liao[2,3], Weihua Pan*[,2,3], Ziauddin Khan[6], Suhail Ahmad[6], Katharina Rosam[7], Michaela Lackner[7], Cornelia Lass-Flörl[7], Ferry Hagen[1] & Teun Boekhout**[,1,3,8]

[1]Westerdijk Fungal Biodiversity Institute, Utrecht 3584, The Netherlands

[2]Department of Dermatology, Shanghai Changzheng Hospital, Second Military Medical University, Shanghai 200003, PR China

[3]Shanghai Key Laboratory of Molecular Medical Mycology, Shanghai Institute of Mycology, Shanghai Changzheng Hospital, Second Military Medical University, Shanghai 200003, PR China

[4]Center of Expertise in Mycology Radboud University Medical Center, Canisius Wilhelmina Hospital, Nijmegen 6500HB, The Netherlands

[5]Ministry of Health, Directorate General of Health Services, PO Box 393, 100 Muscat, Oman

[6]Department of Microbiology, Faculty of Medicine, Kuwait University, Safat, Kuwait

[7]Division of Hygiene & Medical Microbiology, Medical University of Innsbruck, Innsbruck, Austria

[8]Institute of Biodiversity & Ecosystem Dynamics, University of Amsterdam, Amsterdam 1012 WX, The Netherlands

*Author for correspondence: Tel.: +86 8188 5494; panweihua@smmu.edu.cn

**Author for correspondence: Tel.: +31 62 929 0360; t.boekhout@westerdijkinstitute.nl

[‡]Authors contributed equally

The multidrug-resistant opportunistic yeast species of *Candida auris*, *Candida haemulonii, Candida duobushaemulonii* and *Candida pseudohaemulonii* continue to endanger the healthcare settings around the globe. Due to the lack of a specific qPCR assay for detection of these species from clinical samples, we developed a multiplex qPCR assay. Analytical specificity and sensitivity showed 100% specificity and the sensitivity of up to ten genomes of target species with a high value of reproducibility (R^2 >0.99). Subsequently, from spiked serum samples, our qPCR specifically could detect up to ten genomes of *C. auris* and one genome of *C. haemulonii, C. duobushaemulonii* and *C. pseudohaemulonii* (R^2 >0.98). Lack of cross reaction with the human DNA, a high degree of specificity and sensitivity, showed the potential of our multiplex PCR for direct detection of *C. auris* and closely related species from serum samples of suspected patients. Future studies are warranted to assure its applicability in clinical settings.

First draft submitted: 11 August 2018; Accepted for publication: 20 November 2018; Published online: 12 December 2018

Keywords: bloodstream infection • *Candida auris* • melting curve analysis • qPCR

Nowadays, controlling infections caused by opportunistic yeast species is challenged owing to increasing of immunocompromised population, emerging pathogenic species and increasing prevalence of antifungal-resistant isolates, which potentially lead to diagnostic and therapeutic failures and increased healthcare costs [1–4]. The globally fast-spreading *Candida auris* currently is regarded as one of the most important opportunistic emerging yeast species, which caused a huge concern for healthcare settings [5–7]. Using routine typing protocols, clinical isolates of *C. auris* are clustered in four distinctive clades namely, east Asian, south Asian, South American and African [8]. From 2012 to 2017, >361 isolates of *C. auris* were obtained from blood cultures, accounting for 67.48% of the all recovered isolates from clinical samples, worldwide [9]. On the other hand, the other closely related species of *C. auris* namely, *Candida haemulonii, Candida duobushaemuloni* and *Candida pseudohaemulonii* have been reported to possess a multidrug-resistant profile and all have been isolated from blood samples in various countries [10–12]. *Candida haemulonii,* which was first known as a human pathogen in 1984, is being increasingly reported worldwide [6,10]. Additionally, recent surveillance studies of candidemia conducted in Panama, revealed

Future Medicine

Table 1. Primers and targets used in the qPCR assay.

Target species	Primer name	Primer sequence	Target loci	Product size (bps)
Candida auris	Auris-F	CGGTGGCGTTGCATTCA	Internal Transcribed Spacer 2	244
	Auris-R	CTGCTGCTAGAACACCTCGT	28S rDNA	
Candida haemulonii	Haemu-F	CCGAGGACCGCAGCAAT	28S rDNA	181
	Haemu-R	CCCGTCCGAGCACTTCCA	28S rDNA	
Candida duobushaemulonii	Duobu-F	GAACGCACATTGCGCCTTGG	5.8S rDNA	115
	Duobu-R	GTAGACTTCGCTGCGGATATGTTA	Internal Transcribed Spacer 2	
Candida pseudohaemulonii	Pseud-F	TAACCTGCGGAAGGATCATTAAG	18S rDNA	197
	Pseud-R	AATGTGCGTTCAAAGATTCGATG	5.8S rDNA	

that almost half of 36 isolates primarily identified as *C. auris* were *C. duobushaemulonii* [13], which highlights the importance of correct identification of other closely related species of *C. auris. Candida pseudohaemulonii* that for the first time in 2006 was detected in the blood sample of a Thai patient showing resistance to amphotericin B and azoles [14], was accountable for approximately a third of clinical isolates identified as *C. haemulonii* in a Korean surveillance study and surprisingly all of the isolates were from blood samples [10].

For these multidrug-resistant pathogens, rapid and precise diagnosis is important to initiate appropriate antifungal treatment, prognosis improvement and outbreak control [15–17]. Up to now, >20 identification methods have been published for *C. auris* [9,18–20]. Biochemical assays as one of the most widely used phenotypic approaches, besides of being time consuming and expensive, cannot properly identify these species [21]. Recently, several species-specific PCRs have been established to identify *C. auris* from DNA samples derived from pure colonies or environmental swab samples [18,19]. Although the need for a culture-independent molecular method is urgent, unfortunately, this is still lingering as an unsolved issue.

Herein, we developed the first multiplex qPCR assay for *C. auris,* and its relatives, that is, *C. haemulonii, C. duobushaemulonii* and *C. pseudohaemulonii*, which can detect these opportunistic yeast species directly from spiked serum samples with a clinically relevant limit of detection (LOD).

Materials & methods

Fungal strains

Two hundred and eighty-two reference strains and clinical isolates were used in two different analytical validation test sets. The first test set included 177 reference strains consisted of 33 *C. auris*, 25 *C. haemulonii*, five *C. duobushaemulonii*, three *C. pseudohaemulonii* and 111 fungal strains representing 68 other closely or distantly related species, which were included for testing the analytical sensitivity, reproducibility, specificity and proficiency testing (Supplementary Tables 1 & 2). Reference strains were obtained from Westerdijk Fungal Biodiversity Institute, Utrecht, Netherlands. Human genomic DNA (male, 10 ng/µl, Thermo Fisher Scientific, MA, USA) was also used for specificity testing. The second test set included 105 clinical isolates obtained from Faculty of Medicine, Kuwait University, Kuwait, which were previously identified as *C. auris* by matrix-assisted laser desorption/ionization TOF mass spectrometry (MALDI-TOF MS; Bruker Corporation, MA, USA) [22,23].

Primer design

Sequences of rDNA for *C. auris* (including the isolates of the four clades analyzed by Lockhart *et al.* in 2016 [8] and more isolates after 2016) and its relatives were retrieved from GenBank (www.ncbi.nlm.nih.gov/genbank/) for primer design. We analyzed the rDNA region of 233 global isolates for the reverse primer of *C. auris*, of which 138 of the sequences were from our own database and the rest were from Genbank. Only primers meeting the following criteria were chosen for further optimization: they should cover all the clades of target species; no cross reaction with other clinically and environmentally important fungi and human DNA; production of a single discriminative melting peak for each locus, which is at least 1°C different from the other locus; and being compatible with the rest of primers in the same reaction in terms of primer Tm values and primer homo/heterodimer formations. uMELT (www.dna.utah.edu/umelt/umelt.html) was used to predict PCR products melting temperature. IDT OligoAnalyzer 3.1 (https://eu.idtdna.com/calc/analyzer) was used to predict primer Tm values and homo/heterodimers. Subsequently, oligonucleotides were synthesized by Integrated DNA Technology Company (IDT, Leuven, Belgium). Table 1 shows the primers information used in this study.

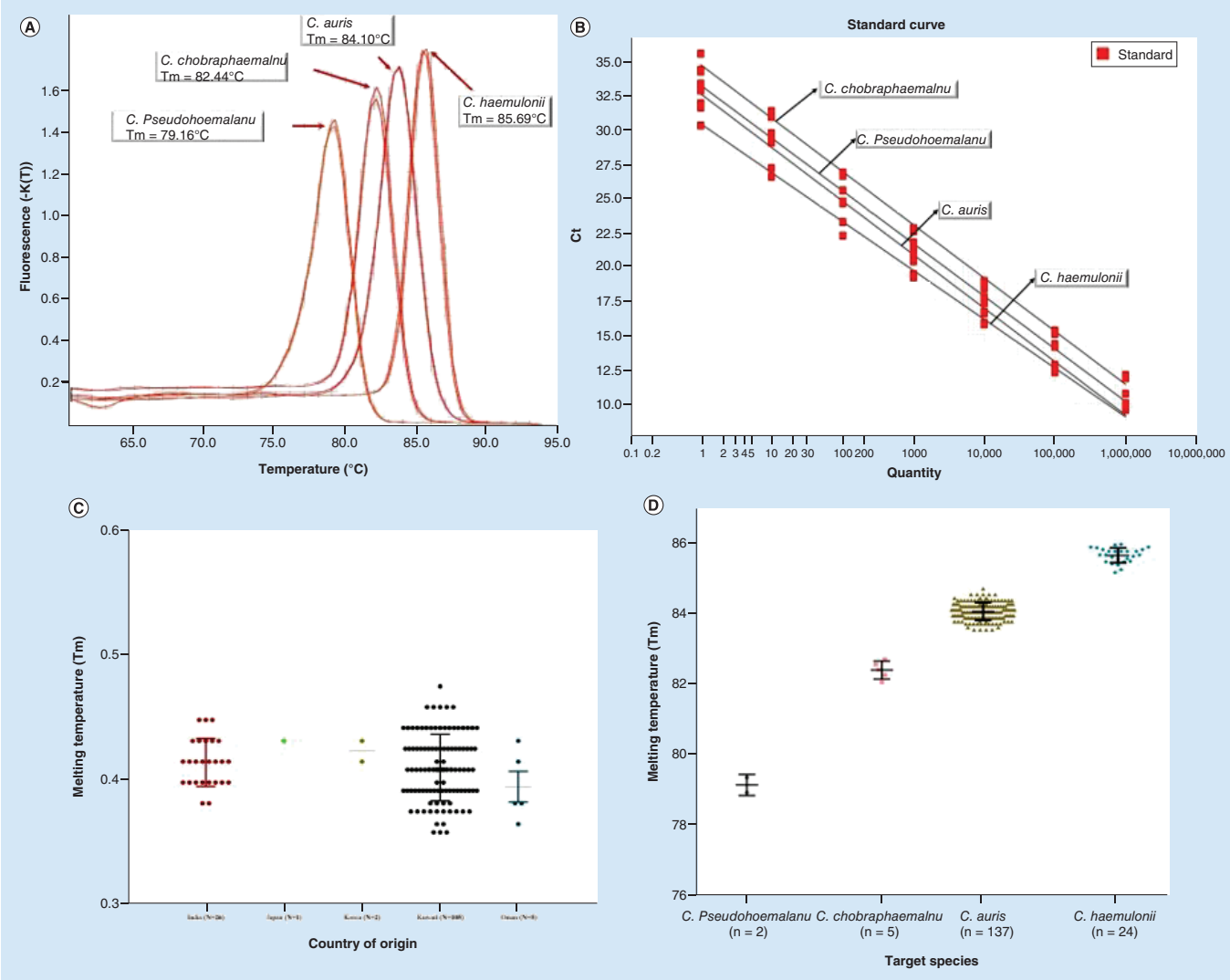

Figure 1. Shows the analytical features obtained for our qPCR assay. (A) Melting profile of target species including *Candida pseudohaemulonii*, *Candida duobushaemulonii*, *Candida auris* and *Candida haemulonii*. **(B)** Standard curves of four target species over seven orders of magnitude. **(C)** Melting temperature distribution of *C. auris* in five countries. **(D)** Shows the Tm distribution of four target species.

Analytical validation

Log-10 serial dilutions (starting from 1 ng/µl) of DNA of all four target species were prepared to find the LOD and the reproducibility of our assay. The analytical specificity was evaluated using 1 ng/µl DNA of diverse range of other yeast species, filamentous fungi and human.

Two technicians ran the proficiency testing in a blind fashion using DNA of eight target strains of *C. auris*, *C. pseudohaemulonii*, *C. duobushaemulonii* and *C. haemulonii* dispersed among 111 nontarget strains representing 68 fungal species (Supplementary Table 3). One technician, who was aware of the identity of each DNA samples, randomly distributed them and provided the second technician with the blinded test set. Besides, single pure colonies of *C. auris*, *C. pseudohaemulonii*, *C. duobushaemulonii* and *C. haemulonii* were subjected to our multiplex PCR.

Institutional ethical committee approval

As clinical validation phase of our study required serum samples, the procedure of serum sampling was reviewed and approved by the ethical committee members of Medical University of Innsbruck.

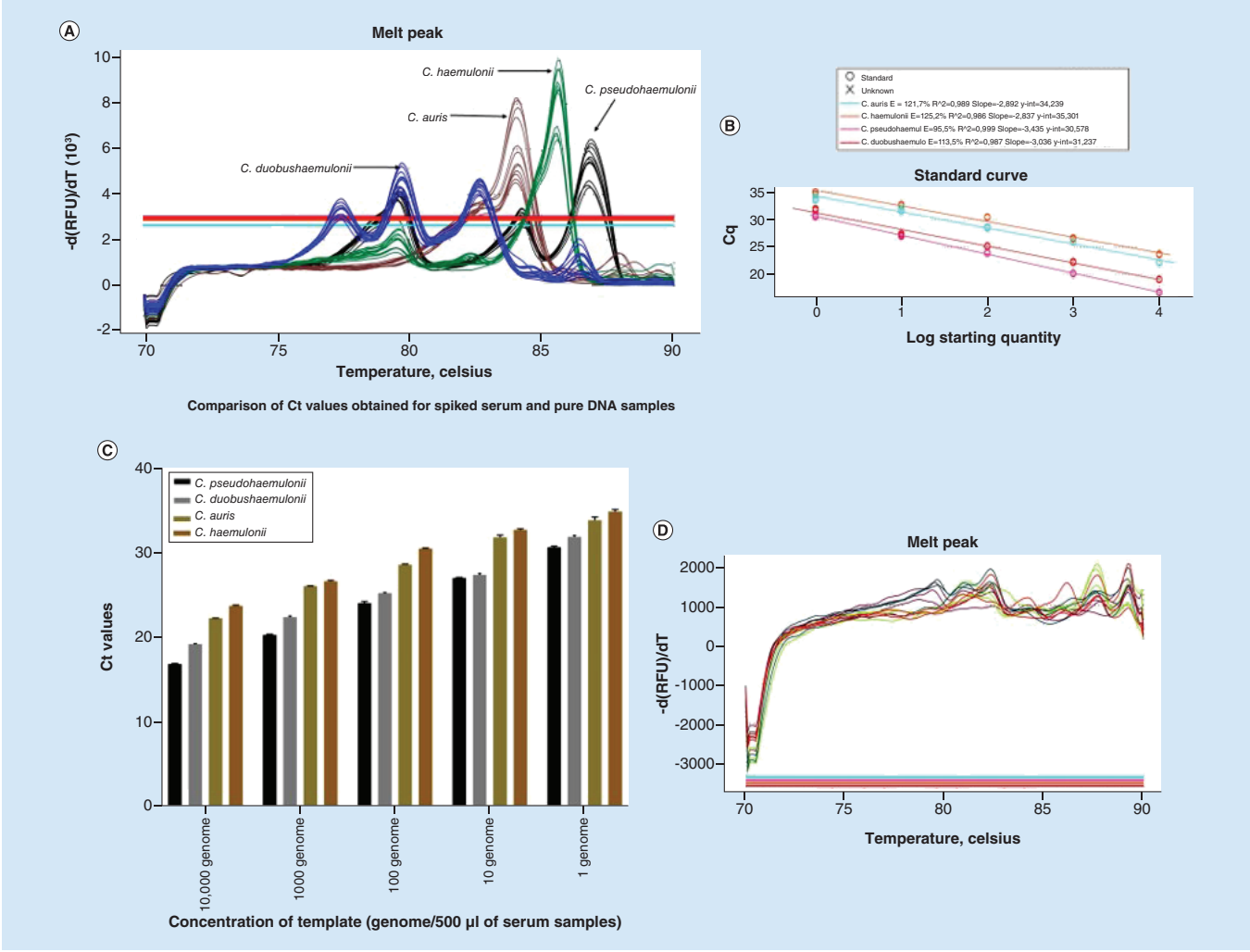

Figure 2. Analytical information derived from spiked serum samples. (A) Serum samples spiked with five orders of magnitude (10^4–10^0) of the DNA of target species. **(B)** The efficiency of target species derived from spiked serum samples (R^2 >0.98). **(C)** Ct values of spiked serum samples with five order of magnitude of DNA (10^4–10^0) of four target species. **(D)** And, the irregular-shaped melting curves obtained from negative serum samples. The data obtained from the standard curves including efficiency, limit of detection and R2 values are automatically calculated by the software installed on the real-time PCR machine and they were not measured manually.

Spiked serum samples

Due to the lack of serum samples of suspected or proven cases, we proceeded with spiking serum samples with the DNA samples obtained from *C. auris* (CBS 10913), *C. haemulonii* (CBS 5149), *C. duobushaemulonii* (CBS 7798) and *C. pseudohaemulonii* (CBS 10004).

For serum preparation, blood clots were subjected to centrifugation with 3000 × *g* for 15 min. Serum samples were distributed in 500 µl aliquots in DNase/RNase sterile 2 ml tubes and stored at -20°C for future uses. Serum samples were collected from two donors.

Five hundred microliters of serum samples were spiked with serially diluted DNA samples (from 10^4 genome to 10^0 genome) obtained from *C. auris* (CBS10913), *C. haemulonii* (CBS5149), *C. duobushaemulonii* (CBS7798) and *C. pseudohaemulonii* (CBS10004). As, 100 pg of DNA of *C. albicans* estimated to be 10^4 genomes [24] and due to the similarity of genome size of the *C. albicans* (14.6 Mb) with those of *C. auris* (12.36 Mb), *C. haemulonii* (13.6 Mb), *C. duobushaemulonii* (12.58 Mb) and *C. pseudohaemulonii* (12.64 Mb), we considered 1 ng DNA of target species as 10^5 genomes.

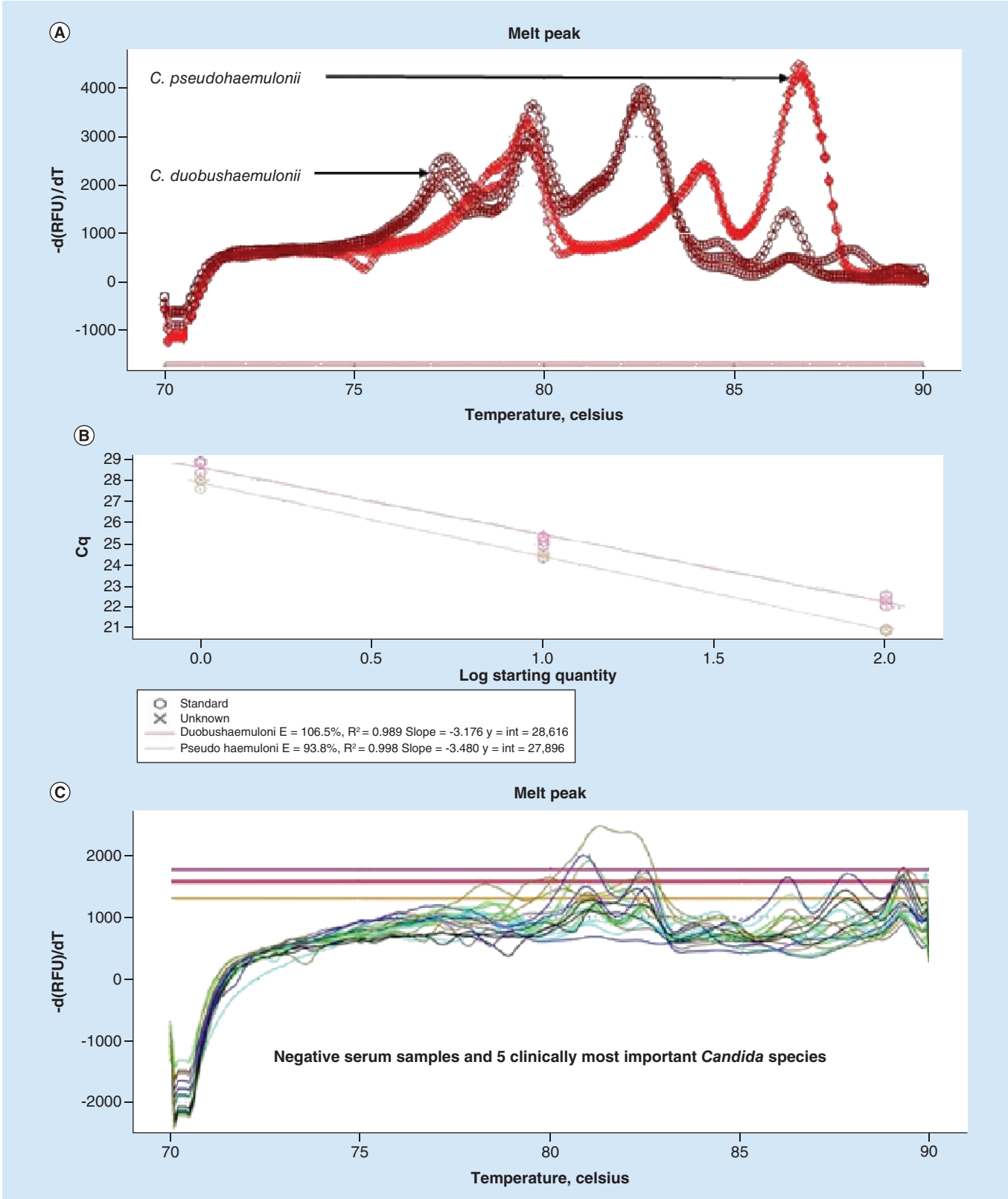

Figure 3. Melting curve analysis for *Candida duobushaemulonii* and *Candida pseudohaemulonii* (102–100 genomes) and negative samples. Shows the melting curve obtained from spiked serum samples with DNA (10^2–10^0 genomes) of *Candida duobushaemulonii* and *Candida pseudohaemulonii* **(A & B)**, and *Candida albicans*, *Candida parapsilosis*, *Candida glabrata*, *Candida tropicalis*, *Candida krusei* and negative serum samples **(C)**. As it is evident from the figure, nontarget *Candida* species and negative serum samples **(C)** generated unusual melt curves that are readily distinguishable from those of target species **(A)**. Although, normal standard curves include at least four concentration points, due to the clinical concentration relevance, only three concentration points (1, 10 and 100 genomes) were used.

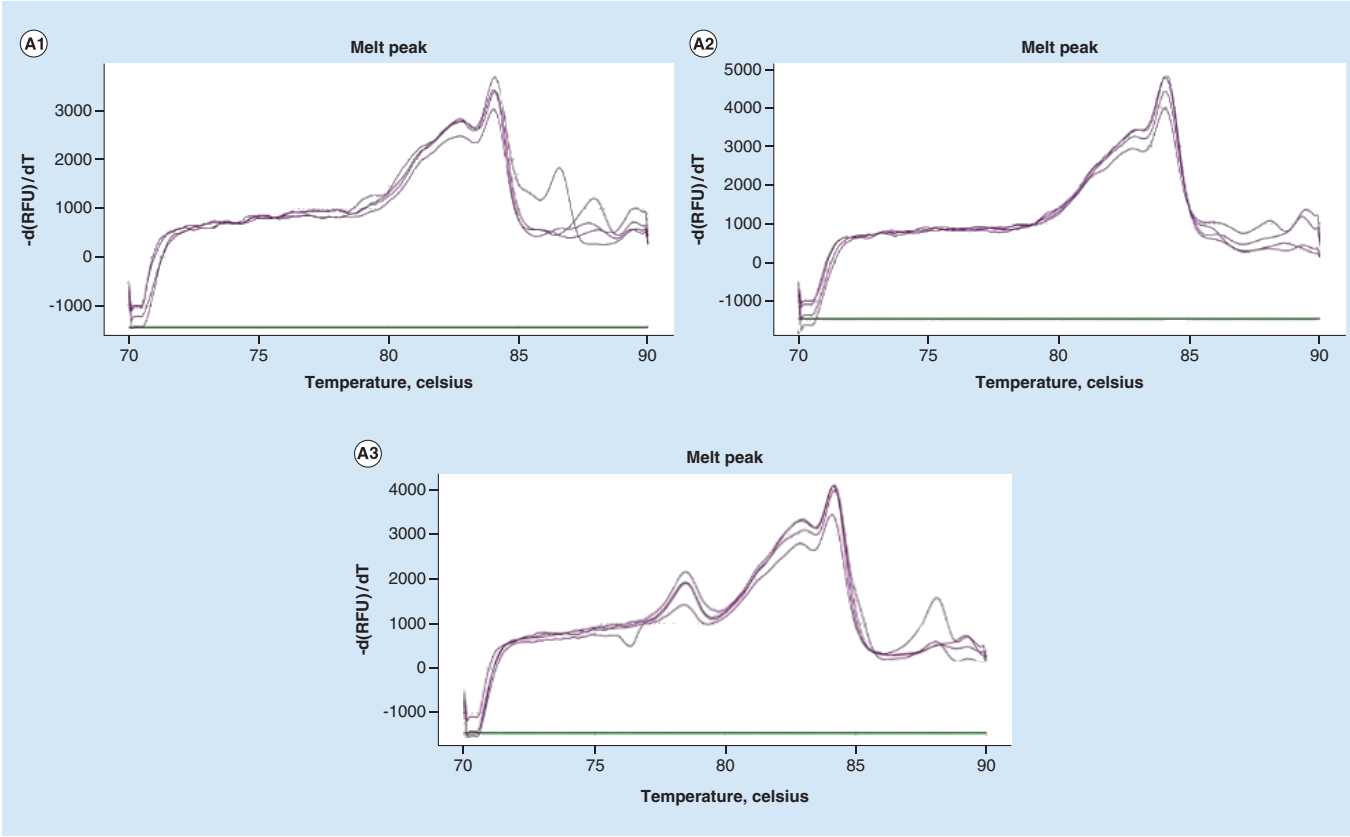

Figure 4. Melt curves obtained from serum samples spiked with mixture of *Candida albicans* and each target species, individually. (A1) A total of 100 genome (Ge) of *Candida albicans*–10 Ge of *Candida auris*; **(A2)** 100 Ge of *C. auris*–10 Ge of *C. albicans*; **(A3)** 10 Ge of *C. auris*–10 Ge of *C. albi cans*; **(B1)** 100 Ge of *C. albicans*–10 Ge of *Candida duobushaemulonii*; **(B2)** 100 Ge of *C. duobushaemulonii*–10 Ge of *C. albicans*; **(B3)** 10 Ge of *C. duobushaemulonii*–10 Ge of *C. albicans*; **(C1)** 100 Ge of *C. albicans*–10 Ge of *Candida haemulonii*; **(C2)** 100 Ge of *C. haemulonii*–10 Ge of *C. albicans*; **(C3)** 10 Ge of *C. haemulonii*–10 Ge of *C. albicans*; **(D1)** 100 Ge of *C. albicans*–10 Ge of *Candida pseudohaemulonii*; **(D2)** 100 Ge of *C. pseudohaemulonii*–10 Ge of *C. albicans*; **(D3)** 10 Ge of *C. pseudohaemulonii*–10 Ge of *C. albicans*.

Simulating mixed infection in spiked serum samples containing the DNA of *C. albicans* & target species

As *C. albicans* shown to be the most predominant isolated species in coinfection cases [25], hence DNA sample of each of target species (100 and 10 genomes) were individually mixed with DNA samples of *C. albicans* (100 and 10 genomes as follows, 100 genome of *C. albicans*–10 genome of target species, 100 genome of target species–10 genome of *C. albicans*, 10 genome of *C. albicans*–10 genome of target species). Twelve serum samples (500 µl) were spiked with the DNA mixtures and the serum samples were subjected to DNA extraction as mentioned in the following.

DNA extraction from fungal cells & simulated serum samples

DNA extraction from pure colonies was performed by cetyltrimethyl ammonium bromide (CTAB) method [26]. The obtained DNA samples were checked for purity by NanoDrop™ 2000 (Thermo Fisher Scientific) and for quantity by QuBit dsDNA BR Assay Kit (Thermo Fisher Scientific Corporation). All the DNA samples were standardized to 1 ng/µl for further checking of sensitivity and specificity.

Serum samples were extracted by QIAamp® UltraSens® Virus kit (QIAGEN, Hilden, Germany) with a slight modification of the manufacturer's protocol. In the last step of elution of DNA samples, instead of two continuous elution stages with 30 µl, the DNA samples were eluted by two steps of 25 and 20 µl. In order to monitor the phenomenon of cross contamination during DNA extraction steps, negative serum samples (without DNA of target species) were included. Eight microliters of each extracted DNA samples were run in the qPCR assays in duplicate.

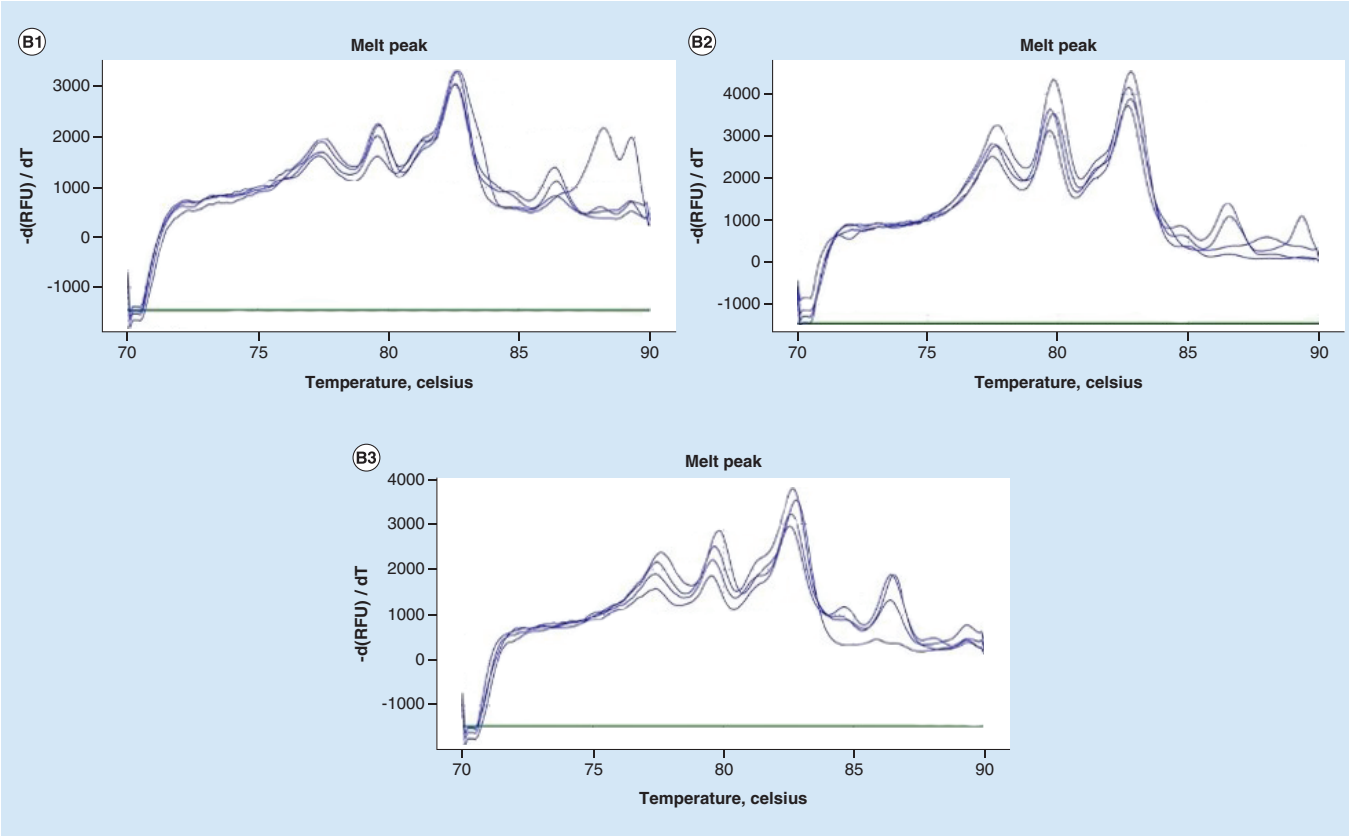

Figure 4. Melt curves obtained from serum samples spiked with mixture of *Candida albicans* and each target species, individually (cont.). (A1) A total of 100 genome (Ge) of *Candida albicans*–10 Ge of *Candida auris*; **(A2)** 100 Ge of *C. auris*–10 Ge of *C. albicans*; **(A3)** 10 Ge of *C. auris*–10 Ge of *C. albi cans*; **(B1)** 100 Ge of *C. albicans*–10 Ge of *Candida duobushaemulonii*; **(B2)** 100 Ge of *C. duobushaemulonii*–10 Ge of *C. albicans*; **(B3)** 10 Ge of *C. duobushaemulonii*–10 Ge of *C. albicans*; **(C1)** 100 Ge of *C. albicans*–10 Ge of *Candida haemulonii*; **(C2)** 100 Ge of *C. haemulonii*–10 Ge of *C. albicans*; **(C3)** 10 Ge of *C. haemulonii*–10 Ge of *C. albicans*; **(D1)** 100 Ge of *C. albicans*–10 Ge of *Candida pseudohaemulonii*; **(D2)** 100 Ge of *C. pseudohaemulonii*–10 Ge of *C. albicans*; **(D3)** 10 Ge of *C. pseudohaemulonii*–10 Ge of *C. albicans*.

PCR conditions

As our study had two phases of optimization (Westerdijk Fungal Biodiversity Institute, Netherlands) and assessment of performance with spiked serum samples (Division of Hygiene and Medical Microbiology/Reference Centre for *Aspergillus* and *Aspergillus* Infections, Austria), hence, two kinds of master mixes and qPCR machines were used.

In the optimization phase, both DNA samples and pure colonies were subjected to qPCR assay (Applied Biosystems® 7500 fast, Thermo Fisher Scientific Corporation). The latter was to check whether our assay is able to detect the signal from pure colonies and, hence, skip the tedious DNA extraction procedures. The following PCR conditions were used for the optimization phase: 10 µl of Power Up SYBR Green Master Mix (A25742 Thermo Fisher Scientific Corporation), 10 pM of Auris-F, Auris-R, Pseud-F and Pseud-R, 8 pM for Haemu-F and Haemu-R, and 5 pM for Duobu-F and Duobu-R, 1 µl of DNA template (or 1 mm^3 of pure colony) and Milli-Q water (Merck Millipore, Darmstadt, Germany) to reach the final volume of 20 µl. The PCR program was as following: 50°C for 2 min, 95°C for 3 min, followed by 40 cycles of 95°C for 15 s and 64°C for 30 s. Melting curves were obtained from 65 to 95°C with the increment of 0.5°C/s, and data analysis was carried out by 7500 software version 2.3 (Thermo Fisher Scientific Corporation).

As for the DNA of the spiked serum samples, qPCR ingredients included 10 µl of SsoFast™ EvaGreen® Supermix with Low ROX (BioRad, CA, USA), 10 pM of Auris-F, Auris-R, Pseud-F and Pseud-R, 8 pM for Haemu-F and Haemu-R, and 5 pM for Duobu-F and Duobu-R, and 8 µl of DNA samples obtained from spiked serum samples in duplicate. The same PCR program (CFX96, Bio-Rad) used as it was optimized, with the exception of limiting melt curve analysis from 70 to 90°C, and the increment of 0.1°C/s. Obtained data were analyzed by Bio-Rad CFX

10.2217/fmb-2018-0227

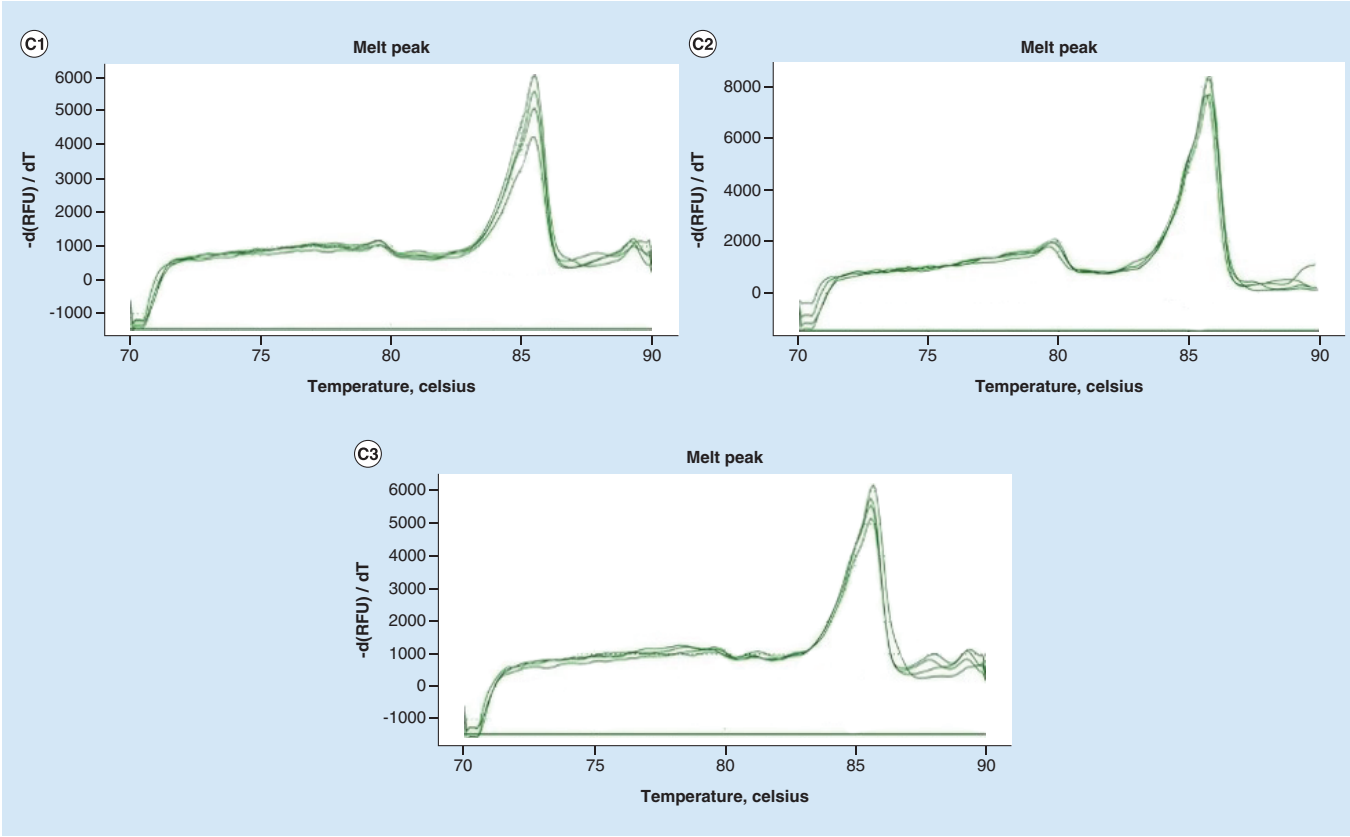

Figure 4. Melt curves obtained from serum samples spiked with mixture of *Candida albicans* and each target species, individually (cont.). (A1) A total of 100 genome (Ge) of *Candida albicans*–10 Ge of *Candida auris*; **(A2)** 100 Ge of *C. auris*–10 Ge of *C. albicans*; **(A3)** 10 Ge of *C. auris*–10 Ge of *C. albi cans*; **(B1)** 100 Ge of *C. albicans*–10 Ge of *Candida duobushaemulonii*; **(B2)** 100 Ge of *C. duobushaemulonii*–10 Ge of *C. albicans*; **(B3)** 10 Ge of *C. duobushaemulonii*–10 Ge of *C. albicans*; **(C1)** 100 Ge of *C. albicans*–10 Ge of *Candida haemulonii*; **(C2)** 100 Ge of *C. haemulonii*–10 Ge of *C. albicans*; **(C3)** 10 Ge of *C. haemulonii*–10 Ge of *C. albicans*; **(D1)** 100 Ge of *C. albicans*–10 Ge of *Candida pseudohaemulonii*; **(D2)** 100 Ge of *C. pseudohaemulonii*–10 Ge of *C. albicans*; **(D3)** 10 Ge of *C. pseudohaemulonii*–10 Ge of *C. albicans*.

Manager Version 3.1 (Bio-Rad). Efficiency of utilized primers, costs and avoiding cross reaction were the most important factors ruling the concentration of primers. *Candida auris* as the main target species had the highest primer concentration (10 pM), while the rest of target species due to possessing higher efficiency (8 and 5 pM) required less amount of respective primers.

Sequencing

Sequencing of D1/D2 domain of large subunit of rDNA was performed for all the 283 strains to explicitly approve the identity of each strain. In order to report the identity of each species, obtained sequences were subjected to BLAST program (https://blast.ncbi.nlm.nih.gov/Blast.cgi).

Statistical analysis

SPSS (version 25, International Business Machines Corporation, NY, USA) was used for statistical analysis. Results were presented as mean ± standard deviation for normal data or median with interquartile ranges for non-normal data.

Results

Analytical sensitivity, reproducibility & specificity

Based on the melting temperature of the target species, the designed primers unequivocally distinguished *C. auris, C. haemulonii*, *C. duobushaemulonii* and *C. pseudohaemulonii.* Melting temperatures for *C. auris, C. haemulonii*, *C. duobushaemulonii* and *C. pseudohaemulonii* were 84.10 ± 0.25°C, 85.69 ± 0.21°C, 82.44 ± 0.25°C and

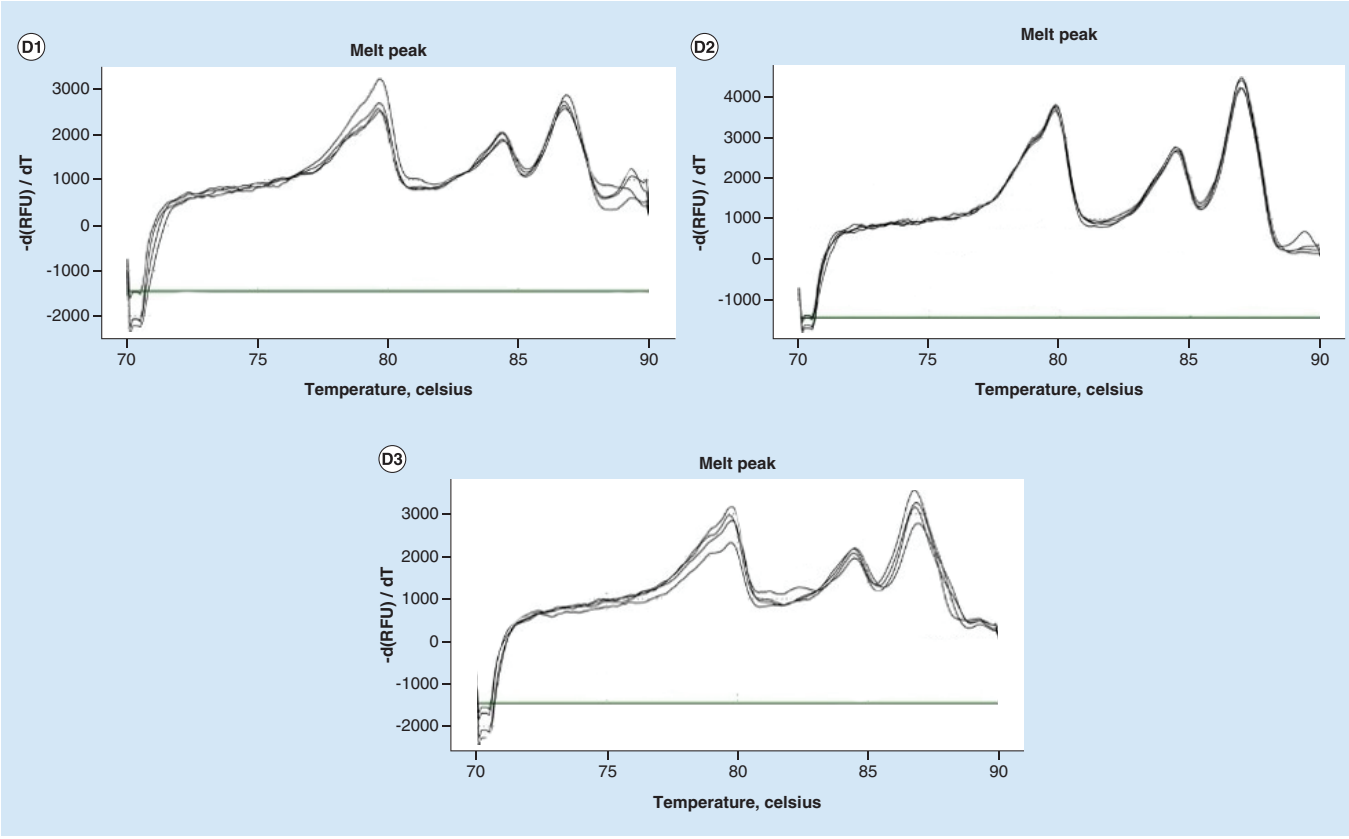

Figure 4. Melt curves obtained from serum samples spiked with mixture of *Candida albicans* and each target species, individually (cont.). (A1) A total of 100 genome (Ge) of *Candida albicans*–10 Ge of *Candida auris*; **(A2)** 100 Ge of *C. auris*–10 Ge of *C. albicans*; **(A3)** 10 Ge of *C. auris*–10 Ge of *C. albi cans*; **(B1)** 100 Ge of *C. albicans*–10 Ge of *Candida duobushaemulonii*; **(B2)** 100 Ge of *C. duobushaemulonii*–10 Ge of *C. albicans*; **(B3)** 10 Ge of *C. duobushaemulonii*–10 Ge of *C. albicans*; **(C1)** 100 Ge of *C. albicans*–10 Ge of *Candida haemulonii*; **(C2)** 100 Ge of *C. haemulonii*–10 Ge of *C. albicans*; **(C3)** 10 Ge of *C. haemulonii*–10 Ge of *C. albicans*; **(D1)** 100 Ge of *C. albicans*–10 Ge of *Candida pseudohaemulonii*; **(D2)** 100 Ge of *C. pseudohaemulonii*–10 Ge of *C. albicans*; **(D3)** 10 Ge of *C. pseudohaemulonii*–10 Ge of *C. albicans*.

79.16 ± 0.18°C, respectively (Figure 1A & D, Supplementary Table 4). No difference in melting temperature ($p > 0.05$) was shown among *C. auris* strains from different countries (Figure 1C). All the target strains were correctly identified except for CBS 12371, which was wrongly designated as *C. pseudohaemulonii*, while our assay in accordance to D1/D2 sequencing and MALDI-TOF MS identified this strain as *C. haemulonii*. When the DNA samples obtained from pure cultures, the LOD for *C. auris*, *C. pseudohaemulonii* and *C. duobushaemulonii* was 10 CFU/PCR with a Cq value of 32, and the LOD for *C. haemulonii* was 10 CFU/PCR with a Cq value of 29. The average of R^2 value for six consecutive runs of qPCR was 0.99, indicating a high degree of reproducibility of this assay (Figure 1B). Specificity tests showed no cross reactivity with the other fungal species and genomic human DNA. Subjecting 105 clinical isolates of *C. auris* from Kuwait to our qPCR gave the same results as those obtained by MALDI-TOF MS and D1/D2 domain of ribosomal large subunit (LSU) rDNA sequencing, resulting in 100% agreement with these methods. Using blinded test set, our qPCR showed 100% accuracy and pure colonies as the pure DNA samples successfully identified target species.

Performance assessment with spiked serum samples

Results obtained from spiked serum samples revealed that our qPCR assay can reliably identify and detect ten genomes of *C. auris* (Cq = 31.75) and one genome of *C. haemulonii* (Cq = 34.82), *C. pseudohaemulonii* (Cq = 34.82) and *C. duobushaemulonii* (Cq = 30.61) (Figure 2A & C), and showed no cross reaction with negative serum samples (Figure 2D). Spiked serum samples with *C. auris* and *C. haemulonii* showed an identical melt curve as what was obtained for the pure DNA of both species (Figure 2A). Unexpectedly *C. duobushaemulonii* and *C. pseudohaemulonii* generated unique triple peaks specific for each species (Figure 2A). Repeated experimentation of

spiking serum samples with *C. pseudohaemulonii* and *C. duobushaemulonii* provided the same results. However, in order to prove that these frequent melting peaks are unique for *C. pseudohaemulonii* and *C. duobushaemulonii*, 500 µl of serum samples were spiked with three orders of magnitude (10^2 genomes to 10^0 genome) DNA of *C. albicans*, *Candida parapsilosis*, *Candida glabrata*, *Candida tropicalis* and *Candida krusei* (Figure 3A & C). As it is shown in the Figure 3, serum samples spiked with the DNA of aforementioned *Candida* species and negative serum samples generated irregular-shaped melt curves, while melt peaks for *C. pseudohaemulonii* and *C. duobushaemulonii* consistently and efficiently resulted in the same melt curve patterns and turned out that those patterns are specific and distinctive fingerprints of these two species (Figure 3A & B). In order to prove that frequent melting peaks were not resulted from serum background, we utilized serum samples from two healthy individuals and both serums resulted in identical and irregular melting peaks. Spiked serum samples with *C. auris*, *C. haemulonii*, *C. pseudohaemulonii* and *C. duobushaemulonii* showed acceptable reproducibility value ($R^2 \geq 0.98$). These observations indicated that serum samples could be a suitable blood fraction for detection and identification of target species when using our multiplex qPCR assay.

In simulated co-infection experiment, serum samples were spiked with DNA mixture of *C. albicans* and each target species individually. Results from the qPCR of simulated co-infection test revealed that regardless of concentration of DNA of *C. albicans* (ten-times more, ten-times less and equal to target species) target species were detected and distinguished unequivocally (Figure 4).

Discussion

The lack of reliable clinical diagnostic tools potentially led to underestimation and neglection of *C. auris* cases [17,27–29]. When facing *C. auris* outbreaks, microbiologists mainly handle cultures, environmental swab or clinical samples (blood, sputum, urine). Using biochemical assays such as VITEK, API20C-AUX, AuxaColor 2, BD Phoenix, MicroScan etc. 90% of the *C. auris* isolates are misidentified as *C. haemulonii* (most commonly), *Candida famata*, *Candida sake*, *Candida lusitaniae*, *Candida catenulata*, *Candida guilliermondii*, *C. parapsilosis*, *C. tropicalis*, *C. albicans*, *Rhodotorula glutinis* and *Saccharomyces cerevisiae* [5].

Detecting *C. auris* directly from clinical or environmental swab samples in a culture-independent manner is essential for outbreak control. For environmental screening purposes, Leach *et al.* (2017) reported the ability of single-plex probe-based qPCR for detection of *C. auris* from environmental swabs [18]. Although, in outbreaks environmental screening is an essential part of infection control, identification of patients suspected with blood-borne infections by *C. auris* and its relatives is of a great importance. Epidemiological studies revealed that *C. auris* can represent up to 5.2% of candidemia cases in India [30], although with a lower prevalence, fatal bloodstream infection due to this pathogen is reported from other countries [9]. Moreover, it is estimated that delay of 1 h in starting immediate appropriate antimicrobial therapy for ICU patients will increase the mortality rate [31]. Thus, the urge for a rapid, specific, reliable and economic molecular means of identification from clinical samples is highly relevant. Herein for the first time, we developed a multiplex PCR assay that can detect *C. auris* and its relatives directly from serum samples in a culture-independent manner. Testing our qPCR with the serum samples spiked with serially diluted DNA of target species, showed an exceptional LOD of one genome for *C. haemulonii, C. pseudohaemulonii* and *C. duobushaemulonii*, and ten genomes for *C. auris.* Moreover, serum due to its applicability for downstream applications such as serology tests and its ease of DNA extraction procedure, has earned reputation for being a suitable blood fraction for identification of fungemia [32]. It has been shown that for identification of invasive candidiasis, serum samples showed the same performance as whole blood samples when subjected to real-time PCR [33]. Additionally, serum has been regarded as a suitable matrix for validation of PCR-based assays meant to detect *Candida* species from infected patients [34–36]. The diagnostic strategy using our assay can dramatically shorten the clinical turn-around time (Supplementary Figure 1). Moreover, our qPCR assay utilizes the most basic and inexpensive qPCR chemistry, that is, SYBR GreenI and EVA Green, and offers the first qPCR assay with the potential clinical utility for identification of *C. auris* and its relatives. Moreover, despite the fact that *C. albicans* accounts for the majority of mixed infections, which could affect the specificity and sensitivity of PCR assays [25], our assay regardless of the DNA concentration of *C. albicans* (ten-times more, ten-times less and equal to target species) readily identified *C. auris*, *C. haemulonii*, *C. pseudohaemulonii* and *C. duobushaemulonii* in serum samples spiked the mixture DNA of target species and *C. albicans.* This observation reinforced the specificity of our qPCR assay in mixed infections.

For specificity testing, our assay was challenged with 111 reference strains representing 68 nontarget yeast and filamentous fungal species, while in the published melting curve-based qPCR, only 19 nontarget species were

tested [37]. Large difference in melting temperature between *C. auris* and its relatives is another advantage of our qPCR, as PCR inhibitors, such as humic acid, melanin, hematin and collagen, are commonly found in the environmental and clinical samples and they can change the melting curve temperature causing melt temperature shift followed by misidentification [38]. In our assay, the difference in average melting temperature between *C. auris* and *C. pseudohaemulonii*, *C. duobushaemulonii*, *C. haemulonii* were 5, 1.7 and 1.6°C, respectively. Additionally, the minimum difference in melting temperature between any two species was 1.1°C. While in the published melting curve qPCR, small differences in melting temperature between *C. auris* and *C. duobushaemulonii* and *C. haemulonii* were observed (0.4 and 1°C, respectively) [37]. On the other hand, despite the presence of heterogeneity in the submitted sequences of *C. haemulonii* complex, that is, *C. haemulonii* var. *vulnera* and *C. haemulonii* (*C. haemulonii* Group I), our assay successfully amplified various strains within this complex [39].

Although, a given developed diagnostic assays should be assessed with the relevant clinical materials obtained from suspected patients, in our situation due to the lack of such clinical sources we had to spike serum samples with the DNA of target species. Hence, clinical performance and utility of our qPCR assay warrants further experimentations in settings where suspected patients exist.

In summary, we developed a novel multiplex qPCR, which can discriminate *C. auris*, from *C. haemulonii, C. duobushaemulonii* and *C. pseudohaemulonii* in one multiplex qPCR reaction. The fact is that our multiplex assay has been validated by using a comprehensive set of reference strains and clinical isolates, and proved to be rapid, specific and sensitive with spiked serum samples, indicating that it might have the applications for environmental screening and diagnostic purposes from clinical samples.

Conclusion

Culture-independent and species-level identification of the multidrug-resistant opportunistic yeast species *Candida auris, C. haemulonii, C. pseudohaemulonii* and *C. duobushaemulonii* is an important clinical practice. Involved healthcare settings of various countries can evaluate the specificity and sensitivity our multiplex qPCR assay in the light of culture as the gold standard technique. If proved to be sensitive and specific, it will show implications in early diagnosis followed by adminstartion of appropriate antifungal drugs. Moreover, its inexpensiveness, rapidity and sensitivity might highlight its applicability for environmental screening.

Summary points

- Based on the simple melt curve technique, our multiplex qPCR can distinguish and identify *Candida auris*, and its relatives, *Candida haemulonii*, *Candida duobushaemulonii* and *Candida pseudohaemulonii.*
- When DNAs obtained from pure colonies were used, the limit of detection for *C. auris*, *C. haemulonii, C. pseudohaemulonii* and *C. duobushaemulonii* was 10 CFU/PCR, with a high degree of reproducibility (R^2 = 0.99).
- Specificity tests showed no cross reactivity with the other fungal species and genomic human DNA.
- Subjecting pure colonies of target strains showed the expected melting temperature, which indicated good compatibility of our assay when using pure colonies without DNA extraction.
- Results obtained from spiked serum samples revealed that our qPCR assay reliably identifies and detects ten genomes of *C. auris* (Ct = 31.75) and one genome of *C. haemulonii* (Ct = 34.82), *C. pseudohaemulonii* (Ct = 34.82) and *C. duobushaemulonii* (Ct = 30.61).
- Spiked serum samples with both *C. auris* and *C. haemulonii* showed acceptable reproducibility value ($R^2 \geq 0.98\%$).
- Simulated co-infection test revealed that regardless of concentration of DNA of *C. albicans*, target species are identified unequivocally.
- Having a high degree of sensitivity and reasonable difference in the melt profile of target species reveals the potential utility of our qPCR assay for both serum samples derived from suspected patients and environmental swab samples for infection control purposes.

Supplementary data

To view the supplementary data that accompany this paper please visit the journal website at: https://www.futuremedicine.com/doi/suppl/10.2217/fmb-2018-0227

Financial & competing interests disclosure

This work was supported by the National Health Department (2018ZX10101003), EU's Horizon 2020 Research and Innovation Program under the Marie Sklodowska-Curie grant (642095), National Natural Science Foundation of China (31770161), Second Military Medical University (2017JZ47) and Shanghai Science and Technology Committee (17DZ2270900 and 14495800500). The authors have no other relevant affiliations or financial involvement with any organization or entity with a financial interest in or financial conflict with the subject matter or materials discussed in the manuscript apart from those disclosed.

No writing assistance was utilized in the production of this manuscript.

References

Papers of special note have been highlighted as: •• of considerable interest

1. Pfaller MA, Diekema DJ, Gibbs DL *et al.* Results from the ARTEMIS DISK Global Antifungal Surveillance Study, 1997 to 2007: 10.5-year analysis of susceptibilities of noncandidal yeast species to fluconazole and voriconazole determined by CLSI standardized disk diffusion testing. *J. Clin. Microbiol.* 47(1), 117–123 (2009).
2. Miceli MH, Diaz JA, Lee SA. Emerging opportunistic yeast infections. *Lancet. Infect. Dis.* 11(2), 142–151 (2011).
3. Jeffery-Smith A, Taori SK, Schelenz S *et al. Candida auris*: a review of the literature. *Clin. Microbiol. Rev* 31(1), pii: e00029–00017 (2017).

•• **Misidentification through routinely used phenotypic and biochemical assays. *Candida auris* is easily misidentified as other yeast species when tested with the routinely used phenotypic and biochemical assays.**

4. Fang W, Zhang L, Liu J *et al.* Tuberculosis/cryptococcosis co-infection in China between 1965 and 2016. *Emerg. Microbes. Infect.* 6(8), e73 (2017).
5. Chowdhary A, Sharma C, Meis JF. *Candida auris*: a rapidly emerging cause of hospital-acquired multidrug-resistant fungal infections globally. *PLoS Pathog.* 13(5), e1006290 (2017).

•• **Persistent colonizer in hospitals. *Candida auris* for a long period of time can stay in the hospitals and clinical settings.**

6. Ben-Ami R, Berman J, Novikov A *et al.* Multidrug-resistant *Candida haemulonii* and *C. auris*, Tel Aviv, Israel. *Emerg. Infect. Dis.* 23(1), 195–203 (2017).
7. Ruiz-Gaitan A, Moret AM, Tasias-Pitarch M *et al.* An outbreak due to *Candida auris* with prolonged colonisation and candidaemia in a tertiary care European hospital. *Mycoses* 61(7), 498–505 (2018).
8. Lockhart SR, Etienne KA, Vallabhaneni S *et al.* Simultaneous emergence of multidrug-resistant *Candida auris* on 3 continents confirmed by whole-genome sequencing and epidemiological analyses. *Clin. Infect. Dis.* 64(2), 134–140 (2017).

•• **Multidrug resistance. Clinical isolates of *C. auris* can show multidrug-resistant nature to two or three classes of antifungals posing a threat to its treatment.**

9. Osei Sekyere J. *Candida auris*: a systematic review and meta-analysis of current updates on an emerging multidrug-resistant pathogen. *Microbiologyopen* doi:10.1002/mbo3.578 (2018) (Epub ahead of print).

•• **Cause of fatal outbreaks. Once established in healthcare settings, it can be easily transferred to the other hospitals in different cities, countries and even continents.**

10. Kim MN, Shin JH, Sung H *et al. Candida haemulonii* and closely related species at 5 university hospitals in Korea: identification, antifungal susceptibility, and clinical features. *Clin. Infect. Dis.* 48(6), e57–e61 (2009).
11. Hou X, Xiao M, Chen SC *et al.* Identification and antifungal susceptibility profiles of *Candida haemulonii* species complex clinical isolates from a multicenter study in China. *J. Clin. Microbiol.* 54(11), 2676–2680 (2016).
12. Khan ZU, Al-Sweih NA, Ahmad S *et al.* Outbreak of fungemia among neonates caused by *Candida haemulonii* resistant to amphotericin B, itraconazole, and fluconazole. *J. Clin. Microbiol.* 45(6), 2025–2027 (2007).
13. Ramos R, Caceres DH, Perez M *et al.* Emerging multidrug-resistant *Candida duobushaemulonii* infections in Panama hospitals: importance of laboratory surveillance and accurate identification. *J. Clin. Microbiol.* 56(7), (2018).

•• **Wrong identification and overestimation in number of *C. auris*. By using reliable means of identification wrongly identified *C. auris* isolates were identified as *Candida duobushaemulonii* leading to revealing of the genuine epidemiology of this species.**

14. Sugita T, Takashima M, Poonwan N, Mekha N. *Candida pseudohaemulonii* Sp. Nov., an amphotericin B-and azole-resistant yeast species, isolated from the blood of a patient from Thailand. *Microbiol. Immunol.* 50(6), 469–473 (2006).

•• **Multidrug resistance nature of its siblings. Species within the *Candida haemulonii* complex, including *Candida haemulonii*, *Candida pseudohaemulonii* and *Candida duobushaemulonii* are multidrug-resistant emerging yeast species that are closely related to *C. auris*. References 10–14**

15. Lepak AJ, Zhao M, Berkow EL, Lockhart SR, Andes DR. Pharmacodynamic optimization for treatment of invasive *Candida auris* infection. *Antimicrob. Agents Chemother.* 61(8), 1–5 (2017).
16. Fakhim H, Chowdhary A. *In vitro* interactions of echinocandins with triazoles against multidrug-resistant *Candida auris*. *Antimicrob. Agents. Chemother.* 61(11), pii: e01056-17 (2017).
17. Mizusawa M, Miller H, Green R *et al.* Can multidrug-resistant *Candida auris* be reliably identified in clinical microbiology laboratories? *J. Clin. Microbiol.* 55(2), 638–640 (2017).
18. Leach L, Zhu Y, Chaturvedi S. Development and validation of a real-time PCR assay for rapid detection of *Candida auris* from surveillance samples. *J. Clin. Microbiol.* 56 2 pii: e01223-17 (2018).
19. Arastehfar A, Fang W, Badali H *et al.* Low-cost tetraplex PCR for the global spreading multi-drug resistant fungus, *Candida auris* and its phylogenetic relatives. *Front. Microbiol.* 9, 1119 (2018).
20. Voelker R. New test identifies *Candida auris*. *JAMA* 319(21), 2164 (2018).
21. Snayd M, Dias F, Ryan RW, Clout D, Banach DB. Misidentification of *Candida auris* by RapID Yeast Plus, a commercial, biochemical enzyme-based manual rapid identification system. *J. Clin. Microbiol.* 56(5), 1–2 (2018).
22. Vlek A, Kolecka A, Khayhan K *et al.* Interlaboratory comparison of sample preparation methods, database expansions, and cutoff values for identification of yeasts by matrix-assisted laser desorption ionization-time of flight mass spectrometry using a yeast test panel. *J. Clin. Microbiol.* 52(8), 3023–3029 (2014).
23. Khan Z, Ahmad S, Benwan K *et al.* Invasive *Candida auris* infections in Kuwait hospitals: epidemiology, antifungal treatment and outcome. *Infection* 46(5), 641–650 (2018).

•• **High mortality rate. The rate of mortality for *C. auris* can go to up to 60%.**

24. Loeffler J, Henke N, Hebart H *et al.* Quantification of fungal DNA by using fluorescence resonance energy transfer and the light cycler system. *J. Clin. Microbiol.* 38(2), 586–590 (2000).
25. Jensen J, Munoz P, Guinea J, Rodriguez-Creixems M, Pelaez T, Bouza E. Mixed fungemia: incidence, risk factors, and mortality in a general hospital. *Clin. Infect. Dis.* 44(12), e109–e114 (2007).
26. Diaz MR, Boekhout T, Kiesling T, Fell JW. Comparative analysis of the intergenic spacer regions and population structure of the species complex of the pathogenic yeast *Cryptococcus neoformans*. *FEMS Yeast Res.* 5(12), 1129–1140 (2005).
27. Chowdhary A, Sharma C, Duggal S *et al.* New clonal strain of *Candida auris*, Delhi, India. *Emerg. Infect. Dis.* 19(10), 1670–1673 (2013).
28. Kathuria S, Singh PK, Sharma C *et al.* Multidrug-resistant *Candida auris* misidentified as *Candida haemulonii*: characterization by matrix-assisted laser desorption ionization-time of flight mass spectrometry and DNA sequencing and its antifungal susceptibility profile variability by Vitek 2, CLSI Broth Microdilution, and Etest Method. *J. Clin. Microbiol.* 53(6), 1823–1830 (2015).
29. Centers for Disease Control and Prevention. Clinical alert to US healthcare facilities – June 2016: global emergence of invasive infections caused by the multidrug-resistant yeast *Candida auris*. Centers for Disease Control and Prevention, Atlanta, GA, USA (2016). www.cdc.gov/fungal/diseases/candidiasis/candida-auris-alert.html
30. Chakrabarti A, Sood P, Rudramurthy SM *et al.* Incidence, characteristics and outcome of ICU-acquired candidemia in India. *Intens. Care Med.* 41(2), 285–295 (2015).
31. Kumar A, Roberts D, Wood KE *et al.* Duration of hypotension before initiation of effective antimicrobial therapy is the critical determinant of survival in human septic shock. *Crit. Care Med.* 34(6), 1589–1596 (2006).
32. White PL, Mengoli C, Bretagne S *et al.* Evaluation of *Aspergillus* PCR protocols for testing serum specimens. *J. Clin. Microbiol.* 49(11), 3842–3848 (2011).
33. Fortun J, Meije Y, Buitrago MJ *et al.* Clinical validation of a multiplex real-time PCR assay for detection of invasive candidiasis in intensive care unit patients. *J. Antimicrob. Chemoth.* 69(11), 3134–3141 (2014).
34. Dunyach C, Bertout S, Phelipeau C, Drakulovski P, Reynes J, Mallie M. Detection and identification of *Candida* spp. in human serum by LightCycler real-time polymerase chain reaction. *Diagn. Micr. Infec. Dis.* 60(3), 263–271 (2008).
35. Ahmad S, Khan Z, Mustafa AS, Khan ZU. Seminested PCR for diagnosis of candidemia: comparison with culture, antigen detection, and biochemical methods for species identification. *J. Clin. Microbiol.* 40(7), 2483–2489 (2002).
36. Mcmullan R, Metwally L, Coyle PV *et al.* A prospective clinical trial of a real-time polymerase chain reaction assay for the diagnosis of candidemia in nonneutropenic, critically ill adults. *Clin. Infect. Dis.* 46(6), 890–896 (2008).
37. Kordalewska M, Zhao Y, Lockhart SR, Chowdhary A, Berrio I, Perlin DS. Rapid and accurate molecular identification of the emerging multidrug resistant pathogen *Candida auris*. *J. Clin. Microbiol.* 55(8), 2445–2452 (2017).
38. Mccord B, Opel K, Funes M, Zoppis S, Jantz LM. An investigation of the effect of DNA degradation and inhibition on PCR amplification of single source and mixed forensic samples. (2011). www.ncjrs.gov/pdffiles1/nij/grants/236692.pdf
39. Cendejas-Bueno E, Kolecka A, Alastruey-Izquierdo A *et al.* Reclassification of the *Candida haemulonii* complex as *Candida haemulonii* (*C. haemulonii* group I), *C. duobushaemulonii* sp. nov. (*C. haemulonii* group II), and *C. haemulonii var. vulnera var. nov.*: three multiresistant human pathogenic yeasts. *J. Clin. Microbiol.* 50(11), 3641–3651 (2012).